



# **Modulatie en Detectie**

-

# **Modulation and Detection**

Prof. Marc Moeneclaey & Dr. Lennert Jacobs  
Universiteit Gent  
Vakgroep Telecommunicatie en Informatieverwerking (TELIN)  
Sint-Pietersnieuwstraat 41  
9000 GENT

# Chapter 1

## Channel models

### 1.1. Representation of bandpass signals and bandpass filters

Let us consider a real-valued bandpass signal  $x_{BP}(t)$ ; its Fourier transform (FT)  $X_{BP}(f)$  satisfies the condition  $X_{BP}(f) = 0$  for  $||f| - f_0| > B$ , where  $f_0$  and  $B_{RF} = 2B$  denote the center frequency and the radio-frequency (RF) bandwidth of the bandpass signal ( $f_0 > B$ , and in many cases  $f_0 \gg B$ ). As  $x_{BP}(t)$  is real-valued, its FT satisfies the symmetry relation  $X_{BP}^*(f) = X_{BP}(-f)$ ; hence, on both the positive and negative frequency axis,  $x_{BP}(t)$  occupies an interval of length  $B_{RF}$ .

We represent the real-valued bandpass signal  $x_{BP}(t)$  by the complex-valued baseband signal ("complex envelope", "complex baseband representation")  $x_{LP}(t)$ , with  $X_{LP}(f) = 0$  for  $|f| > B$  ( $B$  is the bandwidth of the complex baseband signal  $x_{LP}(t)$ ):

$$\begin{aligned} x_{BP}(t) = \sqrt{2} \operatorname{Re}[x_{LP}(t) \exp(j2\pi f_0 t)] &\Leftrightarrow X_{BP}(f) = \frac{\sqrt{2}}{2} X_{LP}(f - f_0) + \frac{\sqrt{2}}{2} X_{LP}^*(-f - f_0) \\ &\quad \Updownarrow \qquad \qquad \qquad \Updownarrow \\ x_{LP}(t) = \{\sqrt{2} x_{BP}(t) \exp(-j2\pi f_0 t)\}_{LP} &\Leftrightarrow X_{LP}(f) = \sqrt{2} X_{BP}(f + f_0) \Pi_{LP}(f) \end{aligned} \quad (1.1-1)$$

where

$$\Pi_{LP}(f) = \begin{cases} 1 & |f| \leq B \\ 0 & \text{otherwise} \end{cases} \quad (1.1-2)$$

is the transfer function of an ideal lowpass filter with gain 1 and bandwidth  $B$ , and  $\{z(t)\}_{LP}$  denotes the components of  $z(t)$  that are in the frequency band  $(-B, B)$ . The bandpass signal  $x_{BP}(t)$  can also be expressed as

$$x_{BP}(t) = \sqrt{2} x_R(t) \cos(2\pi f_0 t) - \sqrt{2} x_I(t) \sin(2\pi f_0 t) \quad (1.1-3)$$

where  $x_R(t) = \operatorname{Re}[x_{LP}(t)]$  and  $x_I(t) = \operatorname{Im}[x_{LP}(t)]$  are the in-phase and quadrature components of  $x_{BP}(t)$ , that have a bandwidth equal to  $B$ .

Similarly, we represent a real-valued bandpass filter with impulse response  $h_{BP}(t)$  ( $H_{BP}(f) = 0$  for  $||f| - f_0| > B$ ) by a complex-valued lowpass filter with impulse response  $h_{LP}(t)$  ( $H_{LP}(f) = 0$  for  $|f| > B$ ):

$$\begin{aligned} h_{BP}(t) = 2 \operatorname{Re}[h_{LP}(t) \exp(j2\pi f_0 t)] &\Leftrightarrow H_{BP}(f) = H_{LP}(f - f_0) + H_{LP}^*(-f - f_0) \\ &\quad \Updownarrow \qquad \qquad \qquad \Updownarrow \\ h_{LP}(t) = \{h_{BP}(t) \exp(-j2\pi f_0 t)\}_{LP} &\Leftrightarrow H_{LP}(f) = H_{BP}(f + f_0) \Pi_{LP}(f) \end{aligned} \quad (1.1-4)$$

Now we apply  $x_{BP}(t)$  to the filter  $h_{BP}(t)$ , and denote the resulting bandpass signal as  $y_{BP}(t)$ . Then the following equivalence holds :

$$\begin{aligned} y_{BP}(t) = \int h_{BP}(u)x_{BP}(t-u)du & \Leftrightarrow Y_{BP}(f) = H_{BP}(f)X_{BP}(f) \\ \Updownarrow & \Updownarrow \\ y_{LP}(t) = \int h_{LP}(u)x_{LP}(t-u)du & \Leftrightarrow Y_{LP}(f) = H_{LP}(f)X_{LP}(f) \end{aligned} \quad (1.1-5)$$

where  $x_{LP}(t)$ ,  $h_{LP}(t)$  and  $y_{LP}(t)$  are the complex baseband representations of  $x_{BP}(t)$ ,  $h_{BP}(t)$  and  $y_{BP}(t)$ . The above frequency-domain relations are illustrated in Fig. 1-1.

In this course we consider the transmission of bandpass signals over bandpass channels. The bandpass channel impulse response and the transmitted and received bandpass signals will be characterized by their baseband representations. Although we will refer to these complex baseband representations as the "channel impulse response", the "transmitted signal" and the "received signal" (unless mentioned otherwise), it should be kept in mind that the physical impulse response and physical signals are real-valued and bandpass.

## 1.2. Additive white Gaussian noise channel

The additive white Gaussian noise (AWGN) channel is described as

$$r(t) = H_{ch}s(t) + w(t) \quad (1.2-1)$$

where  $r(t)$ ,  $H_{ch}$ ,  $s(t)$  and  $w(t)$  are complex-valued :  $s(t)$  is the input signal,  $H_{ch}$  is the channel gain,  $r(t)$  is the output signal, and  $w(t) = w_R(t) + jw_I(t)$  is zero-mean additive white Gaussian noise, with independent real and imaginary parts that each have a power spectral density of  $N_0/2$ . We use the short-hand notation  $w(t) \sim N_c(0, N_0\delta(u))$ , which is explained in more detail in Appendix A.2;  $\delta(u)$  is the Dirac delta function. The effect of the channel gain is to scale (by  $|H_{ch}|$ ) and to rotate (by  $\arg(H_{ch})$ ) the transmitted signal  $s(t)$ . The AWGN channel model corresponding to (1.2-1) is shown in Fig. 1-2. Often the AWGN channel will be normalized (i.e.,  $H_{ch} = 1$ ), so that the useful signals at the input and output have the same energy.

The AWGN channel is *memoryless* : its output at instant  $t$  is determined by its input at instant  $t$  but not at other instants. The AWGN channel does not introduce any signal distortion (apart from scaling and rotation), but only adds noise. It is a convenient model for communication over wired channels when the signal bandwidth is small as compared to the channel bandwidth, so that the channel transfer function is essentially constant over the signal bandwidth (e.g., transmission of a 1MHz bandwidth signal over a coaxial CATV network) and for communication over wireless channels when there is a dominating line-of-sight path (as in satellite communication and radio relay systems).

### 1.3. Linear time-invariant channel

The linear time-invariant (LTI) channel is characterized by its impulse response  $h_{ch}(u)$ , or, equivalently, by its transfer function  $H_{ch}(f)$ . The LTI channel acts as a LTI filter and adds AWGN. The relation between the input  $s(t)$  and the output  $r(t)$  is

$$\begin{aligned} r(t) &= \int h_{ch}(u)s(t-u)du + w(t) \\ &= \int H_{ch}(f)S(f)\exp(j2\pi ft)df + w(t) \end{aligned} \quad (1.3-1)$$

where  $w(t) \sim N_c(0, N_0\delta(u))$ . The LTI channel model is illustrated in Fig. 1-3. Assuming that  $S(f) = 0$  for  $|f| > B$ , the integration interval in the second line of (1.3-1) is  $(-B, B)$ .

The first line in (1.3-1) indicates that the LTI channel has *memory* : its output at instant  $t$  depends on its input at instant  $t$ , but also on its input at past instants (when  $h_{ch}(u) \neq 0$  for  $u > 0$ ) and future instants (when  $h_{ch}(u) \neq 0$  for  $u < 0$ ). The channel memory causes *dispersion* : when the duration of the input signal  $s(t)$  and the impulse response  $h_{ch}(t)$  are  $T_{in}$  and  $T_{ch}$ , the duration of the output signal is  $T_{in} + T_{ch}$ . The second line of (1.3-1) indicates that the LTI channel is *frequency-selective* : when  $H_{ch}(f)$  is not constant over  $(-B, B)$ , the attenuation and phase shift introduced by the channel are frequency-dependent; this introduces *linear distortion* to the signal  $s(t)$ .

When the signal bandwidth  $B$  is so small that the variation of  $H_{ch}(f)$  over  $(-B, B)$  is negligible, the approximation  $H_{ch}(f) \approx H_{ch}(0)$  applies, so that the LTI channel model reduces to the AWGN channel model :  $r(t) = H_{ch}(0)s(t) + w(t)$ .

The LTI channel model is convenient for wired communication where the channel transfer function varies significantly over the bandwidth of the transmitted signal (such as communication over the twisted-pair telephone line : voice-band modem, ADSL, ...).

### 1.4. Linear time-varying channel

A linear time-varying (LTV) channel is characterized by a time-varying impulse response  $h_{ch}(u;t)$ , with  $u$  and  $t$  denoting the "delay variable" and the "time variable", respectively. The time-varying transfer function  $H_{ch}(f;t)$  associated to  $h_{ch}(u;t)$  is defined as :

$$H_{ch}(f;t) = \int h_{ch}(u;t)\exp(-j2\pi fu)du \quad (1.4-1)$$

The LTV channel acts as a LTV filter and adds AWGN. The relation between the input  $s(t)$  and the output  $r(t)$  is

$$\begin{aligned} r(t) &= \int h_{ch}(u;t)s(t-u)du + w(t) \\ &= \int H_{ch}(f;t)S(f)\exp(j2\pi ft)df + w(t) \end{aligned} \quad (1.4-2)$$

where  $w(t) \sim N_c(0, N_0\delta(u))$ . The LTV channel model is illustrated in Fig. 1-4. Assuming that  $S(f) = 0$  for  $|f| > B$ , the integration interval in the second line of (1.3-1) is  $(-B, B)$ .

In order to explain the impact of a LTV filter, we concentrate on the contribution of  $s(t)$  to  $r(t)$ , which we denote as  $s_{out}(t)$  :

$$\begin{aligned} s_{out}(t) &= \int h_{ch}(u;t)s(t-u)du \\ &= \int H_{ch}(f;t)S(f)\exp(j2\pi ft)df \end{aligned} \quad (1.4-3)$$

The case of a LTI filter is obtained when dropping the variable  $t$  in  $h_{ch}(u;t)$  and  $H_{ch}(f;t)$ . Table 1-1 shows the expression for  $s_{out}(t)$  when  $s(t) = \delta(t-t_0)$  and  $s(t) = \exp(j2\pi Ft)$ , both for a LTI and a LTV filter. The following conclusions can be drawn.

- The impulse response  $h_{ch}(u;t)$  can be interpreted as the response of the LTV filter at instant  $t$  to a Dirac delta function applied at instant  $t-u$ . For a LTI filter the corresponding response is  $h_{ch}(u)$ , irrespective of  $t$ . This is illustrated in Fig. 1-5 which shows the response to a sequence of two Dirac delta functions : whereas for the LTI filter the response consists of shifted versions of the response to  $\delta(t)$ , the responses of the LTV filter to the individual Dirac delta functions have different shape.
- For a LTI filter, the response to  $\exp(j2\pi Ft)$  is a complex exponential with an amplitude  $|H_{ch}(F)|$  and a phase  $\arg(H_{ch}(F))$  that do not change with time; the FT of the filter response is given by  $H_{ch}(F)\delta(f-F)$ , which corresponds to a spectral line at  $f = F$ . For a LTV filter, the response is a complex exponential with amplitude  $|H_{ch}(F;t)|$  and phase  $\arg(H_{ch}(F;t))$  that are both time-varying; in this case the response has a nonzero spectral width, that increases when the changes of  $H_{ch}(F;t)$  become faster. This effect is illustrated in Fig. 1-6.

	$s_{out}(t)$	
	LTI	LTV
$s(t) = \delta(t-t_0)$	$h_{ch}(t-t_0)$	$h_{ch}(t-t_0;t)$
$s(t) = \exp(j2\pi Ft)$	$H_{ch}(F)\exp(j2\pi Ft)$	$H_{ch}(F;t)\exp(j2\pi Ft)$

Table 1-1 : responses of LTI and LTV filters

Just like the LTI channel, the LTV channel has memory, because of the nonzero duration of the impulse response  $h_{ch}(u;t)$  when considered as a function of  $u$ . Hence the LTV channel is frequency-selective and introduces linear distortion (dispersion). In addition, the LTV channel is time-selective : denoting the LTV filter response to  $s(t)$  as  $s_{out}(t)$ , the response

to  $s(t-\tau)$  is different from  $s_{\text{out}}(t-\tau)$ , because the LTV filter has changed over a time interval of duration  $\tau$  (i.e.,  $h_{\text{ch}}(u;t) \neq h_{\text{ch}}(u;t+\tau)$ ); this is in contrast to the LTI filter case.

When the signal bandwidth  $B$  is so small that the variation of  $H_{\text{ch}}(f;t)$  for  $f \in (-B, B)$  is negligible, the approximation  $H_{\text{ch}}(f;t) \approx H_{\text{ch}}(0;t)$  applies, so that the LTV channel becomes memoryless ("*frequency-flat*") :  $r(t) = H_{\text{ch}}(0;t)s(t) + w(t)$ .

The LTV channel model is convenient for wireless communication that is subject to fading, caused by multipath propagation and by motion of the transmitter, the receiver or within the channel (mobile radio (GSM), indoor radio (wireless LAN), HF radio communication). The properties of the mobile radio channel will be considered in more detail in the next section.

## 1.5. Mobile radio channel

The LTV channel introduced in section 1.4 will be used as a model for the mobile radio channel. Here we summarize some important properties of the mobile radio channel.

The received power in wireless communications depends on the positions of the transmitter and the receiver.

- When the distance between receiver and transmitter changes over about a wavelength  $\lambda$  of the carrier frequency  $f_0$  ( $\lambda = c/f_0$ , with  $c = 3 \cdot 10^8$  m/s), the *local power* at the receiver can fluctuate over several tens of decibels (dBs). This phenomenon is caused by multipath propagation : the received signal is a sum of many contributions with different phases, that can change by up to  $\pi$  rad when the receiver moves over  $\lambda/2$ . For carrier frequencies of 1 GHz and 10 GHz, the wavelengths are 30 cm and 3 cm, respectively. Because of the small values of  $\lambda$ , this phenomenon is called *small-scale (or short-term) fading*.
- When averaging the local power over an area with dimensions in the order of  $10\lambda$ , the small-scale fading is removed. The resulting *local average power* shows a fluctuation over all locations at a given distance  $d$  from the transmitter, because the topology of buildings, trees, ... that affect the propagation is location-dependent. This phenomenon is called *large-scale (or long-term) fading*, or *shadowing*.
- The median of the distribution of the local averages of the received power, corresponding to locations at a given distance  $d$  from the transmitter, decreases with increasing distance.

This *median power* is determined by the *path loss* over the considered distance.

These three effects are described in more detail below. We consider the case of a transmitter positioned at the origin, and a receiver at (variable) position  $\mathbf{x}$ . We denote by  $P_{\text{loc}}(\mathbf{x})$  and

$P_{\text{loc,avg}}(\mathbf{x})$  the local received power and the average (over an area of size  $10\lambda$ ) local received power at position  $\mathbf{x}$ .

### 1.5.1 Path loss

The median  $P_{50}(d)$  of the distribution of the local average power  $P_{\text{loc,avg}}(\mathbf{x})$  for all positions  $\mathbf{x}$  at distance  $d$  from the transmitter (i.e.,  $|\mathbf{x}| = d$ ) is defined as

$$\Pr[P_{\text{loc,avg}}(\mathbf{x}) > P_{50}(d)] = \Pr[P_{\text{loc,avg}}(\mathbf{x}) < P_{50}(d)] = 1/2 \quad (1.5.1-1)$$

Extensive measurements have indicated that the median powers  $P_{50}(d)$  and  $P_{50}(d_0)$  at distances  $d$  and  $d_0$  from the transmitter are related by

$$P_{50}(d) = P_{50}(d_0) \cdot \left( \frac{d}{d_0} \right)^{-n} \quad (1.5.1-2)$$

where  $n$  is referred to as the *path loss exponent*. According to (1.5.1-2), when  $d$  increases by a factor of 10,  $P_{50}(d)$  decreases by  $10 \cdot n$  dB.

In free space, we have  $n = 2$ . However, in a mobile radio environment where signal reflections occur, the path loss exponent is larger than 2 : it is about 3 to 5 in an urban environment (with  $n = 4$  as typical value) and about 4 to 6 in an indoor environment.

### 1.5.2 Shadowing

The local mean power, expressed in dB with respect to some reference power (e.g., a reference power of 1 mW), has a Gaussian distribution, with mean  $10 \cdot \log(P_{50}(d))$  from (1.5.1-2) and variance  $\sigma_{\text{sh}}^2$ ; in this course we use  $\log(\cdot)$  as short-hand notation for  $\log_{10}(\cdot)$ . The local mean power, expressed on a linear scale, has a lognormal distribution with median value  $P_{50}(d)$ . Denoting the local mean power in dB as  $10 \cdot \log(P_{\text{loc,avg}}(\mathbf{x}))$ , we have

$$10 \cdot \log(P_{\text{loc,avg}}(\mathbf{x})) = 10 \cdot \log(P_{50}(d)) + u_{\text{sh}}, \quad (1.5.2-1)$$

where the random variable  $u_{\text{sh}}$  (in dB) represents the shadowing, with  $u_{\text{sh}} \sim N(0, \sigma_{\text{sh}}^2)$ . Typical values of  $\sigma_{\text{sh}}$  range from 6 dB to 12 dB.

When considering two locations  $\mathbf{x}_1$  and  $\mathbf{x}_2$  at distance  $d$  from the transmitter, that are  $\Delta d$  apart (see Fig. 1-7), their local mean powers are correlated for small  $\Delta d$ . Denoting the shadowing contributions to the local mean power at the two locations as  $u_{\text{sh},1}$  and  $u_{\text{sh},2}$ , measurements have indicated that the *shadowing correlation*  $E[u_{\text{sh},1}u_{\text{sh},2}]$  can be modeled as

$$E[u_{\text{sh},1}u_{\text{sh},2}] = \sigma_{\text{sh}}^2 \exp\left(\frac{-\Delta d}{d_{\text{sh}}}\right) \quad (1.5.2-2)$$

where the *shadowing correlation distance*  $d_{\text{sh}}$  is in the order of 10m (urban area) to 500m (suburban area). When  $\Delta d \ll d_{\text{sh}}$ , the environment that affects the propagation is essentially

the same for the two locations, so the shadowing correlation is large; when  $\Delta d \gg d_{sh}$ , the environments at the two locations are very different, so the shadowing correlation is essentially zero. As the correlation distances are much larger than the wavelength of the carrier frequency, the shadowing is a large-scale effect.

### 1.5.3 Small-scale fading

Because of reflections and scattering on various objects such as buildings, trees, cars, people, ... multipath propagation occurs : the received bandpass signal is a sum of delayed versions of the transmitted bandpass signal  $s_{BP}(t)$ . We denote by  $s(t)$  the baseband representation of  $s_{BP}(t)$  :

$$s_{BP}(t) = \sqrt{2} \operatorname{Re}[s(t) \exp(j2\pi f_0 t)] \quad (1.5.3-1)$$

Similarly, we introduce the bandpass signal  $s_{out,BP}(t; \mathbf{x})$  and its baseband representation  $s_{out}(t; \mathbf{x})$ , received at position  $\mathbf{x}$  (ignoring the AWGN contribution). Taking into account the multipath propagation, one obtains

$$\begin{aligned} s_{out,BP}(t; \mathbf{x}) &= \sum_m \sqrt{2} \operatorname{Re}[A_m(\mathbf{x}) \exp(j\theta_m(\mathbf{x})) s(t - \tau_m(\mathbf{x})) \exp(j2\pi f_0 (t - \tau_m(\mathbf{x})))] \\ &\quad \Downarrow \\ s_{out}(t; \mathbf{x}) &= \sum_m A_m(\mathbf{x}) \exp(j\theta_m(\mathbf{x})) s(t - \tau_m(\mathbf{x})) \exp(-j2\pi f_0 \tau_m(\mathbf{x})) \end{aligned} \quad (1.5.3-2)$$

where  $A_m(\mathbf{x})$ ,  $\theta_m(\mathbf{x})$  and  $\tau_m(\mathbf{x})$  are the gain, phase shift and propagation delay associated with the  $m$ -th propagation path, as observed at the receiver location  $\mathbf{x}$ .

When the receiver location changes from  $\mathbf{x}$  to  $\mathbf{x} + \Delta \mathbf{x}$ , the path parameters change, and this change will affect the received signal. For small  $\Delta \mathbf{x}$ , we ignore the variation of  $A_m$  and  $\theta_m$ , and concentrate on the path delay variation :

$$\tau_m(\mathbf{x} + \Delta \mathbf{x}) = \tau_m(\mathbf{x}) - \frac{\Delta d}{c} \cos(\psi_m) \quad (1.5.3-3)$$

where  $\Delta d = |\Delta \mathbf{x}|$ , and the angle of incidence  $\psi_m$  is determined by the propagation direction of the  $m$ -th path and the direction of motion of the receiver, as indicated in Fig. 1-8 : when the receiver moves towards (away from) the incoming wavefront of the  $m$ -th path, the corresponding path delay decreases (increases). Considering  $\Delta d$  in the order of the wavelength  $\lambda$ , the path delay variation is in the order of  $1/f_0$ , corresponding to 1 ns and 0.1 ns for  $f_0 = 1$  GHz and  $f_0 = 10$  GHz, respectively.



### Effect of path delay variation

Let us first investigate how the path delay variation affects  $s(t-\tau_m)$ . Assuming that  $s(t)$  has a bandwidth  $B$  (i.e.,  $S(f) = 0$  for  $|f| > B$ ), we obtain

$$\begin{aligned} s(t - \tau_m(\mathbf{x} + \Delta\mathbf{x})) &= \int_{-B}^B S(f) \exp(j2\pi f(t - \tau_m(\mathbf{x}))) \exp(j2\pi f \Delta d \cos(\psi_m)/c) df \\ &\approx \int_{-B}^B S(f) \exp(j2\pi f(t - \tau_m(\mathbf{x}))) df = s(t - \tau_m(\mathbf{x})) \end{aligned} \quad (1.5.3-4)$$

The approximation in (1.5.3-4) assumes  $\exp(j2\pi f \Delta d \cos(\psi_m)/c) \approx 1$ , which holds when  $B \ll c/|\Delta d|$ . For  $\Delta d < \lambda$ , this condition becomes  $B \ll f_0$ , which holds for most systems encountered in practice. Hence the small delay variation corresponding to an increment  $\Delta d$  in the order of  $\lambda$  has essentially no effect on  $s(t-\tau_m)$ .

Now we consider the effect of the path delay variation on the phase term  $\exp(-j2\pi f_0 \tau_m)$ . Using (1.5.3-3) we obtain

$$\exp(-j2\pi f_0 \tau_m(\mathbf{x} + \Delta\mathbf{x})) = \exp(-j2\pi f_0 \tau_m(\mathbf{x})) \exp\left(j2\pi \frac{\Delta d}{\lambda} \cos(\psi_m)\right) \quad (1.5.3-5)$$

which indicates that an increment  $\Delta d$  in the order of  $\lambda$  give rise to substantial phase shifts (up to  $2\pi$ ), that depend on the angles  $\psi_m$ . Hence, the effect of the path delay variation on the phase term should not be ignored.

Taking into account the above considerations, the following approximation holds

$$s_{\text{out}}(t; \mathbf{x} + \Delta\mathbf{x}) = \sum_m \alpha_m(\mathbf{x}) s(t - \tau_m(\mathbf{x})) \exp\left(j2\pi \frac{\Delta d}{\lambda} \cos(\psi_m)\right) \quad (1.5.3-6)$$

with  $\alpha_m(\mathbf{x}) = A_m(\mathbf{x}) \exp(j\theta_m(\mathbf{x})) \exp(-j2\pi f_0 \tau_m(\mathbf{x}))$  denoting the complex-valued gain of the  $m$ -th path at position  $\mathbf{x}$ .

### Response to unmodulated carrier

Let us determine the channel response when the transmitted signal  $s_{\text{BP}}(t)$  is a sinusoid with power  $P_{\text{tr}}$ , phase  $\theta$  and frequency  $f_0$  that equals the carrier frequency; the corresponding complex baseband representation  $s(t)$  of the transmitted signal  $s_{\text{BP}}(t)$  is

$$s(t) = \sqrt{P_{\text{tr}}} \exp(j\theta) \quad (1.5.3-7)$$

Substituting (1.5.3-7) into (1.5.3-6), the local power  $P_{\text{loc}}(\mathbf{x} + \Delta\mathbf{x})$  of the received signal  $s_{\text{out}}(t; \mathbf{x} + \Delta\mathbf{x})$  is given by

$$\begin{aligned}
P_{\text{loc}}(\mathbf{x} + \Delta\mathbf{x}) &= |s_{\text{out}}(t; \mathbf{x} + \Delta\mathbf{x})|^2 \\
&= P_{\text{tr}} \sum_m |\alpha_m(\mathbf{x})|^2 + P_{\text{tr}} \sum_{m \neq n} \alpha_m(\mathbf{x}) \alpha_n^*(\mathbf{x}) \exp\left(j2\pi \frac{\Delta d_{m,n}}{\lambda}\right)
\end{aligned} \tag{1.5.3-8}$$

where  $\Delta d_{m,n} = \Delta d(\cos(\psi_m) - \cos(\psi_n))$ . Averaging (1.5.3-8) with respect to  $\Delta\mathbf{x}$  over an area with dimensions in the order of  $10\lambda$  gives rise to the local power mean  $P_{\text{loc,avg}}(\mathbf{x})$ , which is affected by shadowing and path loss, but not by small-scale fading. The small-scale fading is represented by the second term in (1.5.3-8), which exhibits large changes when the variation of  $\Delta d$  is in the order of  $\lambda$ . As the average of  $\exp(j2\pi\Delta d_{m,n}/\lambda)$  over the considered area is essentially zero, we obtain from (1.5.3-8) :

$$P_{\text{loc,avg}}(\mathbf{x}) = P_{\text{tr}} \sum_m |\alpha_m(\mathbf{x})|^2 = P_{\text{tr}} \sum_m A_m^2(\mathbf{x}) \tag{1.5.3-9}$$

which indicates that the local power mean is simply the sum of the powers received from the individual paths. The shadowing models the variation of  $P_{\text{loc,avg}}(\mathbf{x})$  over all locations  $\mathbf{x}$  that are at a distance  $d$  from the transmitter; a substantial variation in  $P_{\text{loc,avg}}(\mathbf{x})$  occurs only when the distance between considered locations is in the order of the shadowing correlation distance  $d_{\text{sh}}$  (which is much larger than  $\lambda$ ).

### Effect of motion

When the receiver is moving at speed  $v$ , we have  $\Delta d = v \cdot t$  (assuming that the receiver is at position  $\mathbf{x}$  at  $t=0$ ). Dropping the dependence of the path parameters on  $\mathbf{x}$  for notational convenience, the corresponding received signal is given by (see (1.5.3-6))

$$s_{\text{out}}(t) = \sum_m \alpha_m s(t - \tau_m) \exp(j2\pi f_{D,m} t) \tag{1.5.3-10}$$

where  $f_{D,m} = f_D \cos(\psi_m)$  is the Doppler frequency shift associated with the  $m$ -th path, and  $f_D = f_0 \cdot v/c$  denotes the *maximum Doppler frequency shift*, that depends on the carrier frequency  $f_0$  and the velocity  $v$ .

The signal  $s_{\text{out}}(t)$  from (1.5.3-10) can be obtained by applying the transmitted signal  $s(t)$  to the cascade of two filters. The first filter has an impulse response  $\delta(u - \tau_0)$ , where  $\tau_0 = \min_m \tau_m$  is the path delay of the shortest path to the receiver; this filter simply accounts for the propagation delay between transmitter and receiver, and is immaterial to the rest of our discussion. The second filter is a LTV filter with impulse response  $h_{\text{ch}}(u; t)$ , given by

$$h_{\text{ch}}(u; t) = \sum_m \alpha_m \delta(u - \Delta\tau_m) \exp(j2\pi f_{D,m} t) \tag{1.5.3-11}$$

where  $\Delta\tau_m = \tau_m - \tau_0$  represents the *delay difference* between the m-th path and the shortest path; note that  $\Delta\tau_0 = 0$  and  $\Delta\tau_m > 0$  for  $m \neq 0$ . The corresponding transfer function  $H_{ch}(f;t)$  is

$$H_{ch}(f;t) = \sum_m \alpha_m \exp(-j2\pi f \Delta\tau_m) \exp(j2\pi f_{D,m} t) \quad (1.5.3-12)$$

From (1.5.3-11)-(1.5.3-12) the following can be observed.

- Because of the nonzero Doppler shifts  $f_{D,m} = f_D \cos(\psi_m)$ , the channel is time-selective : considering the transfer function at two instants  $t$  and  $t+\Delta t$ , we have in general  $H_{ch}(f;t) \neq H_{ch}(f;t+\Delta t)$ . We get  $H_{ch}(f;t) \approx H_{ch}(f;t+\Delta t)$  only when  $\exp(j2\pi f_{D,m} \Delta t) \approx 1$  for all  $m$ , which requires  $|\Delta t| \ll 1/f_D$ . The *coherence time*  $T_{coh}$  of the channel is defined as the inverse of the maximum Doppler shift  $f_D$  :

$$T_{coh} = \frac{1}{f_D} \quad (1.5.3-13)$$

When  $t$  changes by an amount  $T_{coh}$ , the phase of any term in the summation (1.5.3-12) changes by at most  $2\pi$ . In literature, various definitions of  $T_{coh}$  can be found, but they all are of the type  $T_{coh} = C/f_D$ , indicating that the coherence time is inversely proportional to the maximum Doppler shift. When observing the channel at two instants  $t$  and  $t+\Delta t$ , the channel has virtually not changed over  $(t, t+\Delta t)$  provided that  $\Delta t \ll T_{coh}$ ; otherwise, the channel is time-selective over the interval  $(t, t+\Delta t)$ . Table 1-2 shows some values of  $f_D$  and  $T_{coh}$ .

- Considering  $s(t) = \exp(j2\pi Ft)$ , we obtain  $s_{out}(t) = H_{ch}(F;t) \exp(j2\pi Ft)$ . According to (1.5.3-12),  $s_{out}(t)$  is a sum of complex exponentials with frequencies  $F+f_{D,m}$ ; the corresponding power spectra are given by

$$S_s(f) = \delta(f - F) \quad S_{s_{out}}(f) = \sum_m |\alpha_m|^2 \delta(f - F - f_{D,m}) \quad (1.5.3-14)$$

Hence, the nonzero Doppler shifts give rise to a spectral spreading of the output signal  $s_{out}(t)$  as compared to the input signal  $s(t)$ . Each frequency  $F$  of the input signal is spread over the interval  $(F-f_D, F+f_D)$ ; therefore the maximum Doppler shift  $f_D$  is also called the *Doppler spread*.

- Because of the nonzero delay differences  $\Delta\tau_m$ , the channel is frequency-selective : considering the transfer function at two frequencies  $f_1$  and  $f_2$ , we have in general  $H_{ch}(f_1;t) \neq H_{ch}(f_2;t)$ . We get  $H_{ch}(f;t) \approx H_{ch}(0;t)$  only when  $\exp(-j2\pi |f_1-f_2| \Delta\tau_m) \approx 1$ ; this requires  $|f_1-f_2| \ll 1/\Delta\tau_{max}$ , with the *delay spread*  $\Delta\tau_{max} = \max_m \Delta\tau_m$  denoting the path delay difference

between the longest and the shortest path. The coherence bandwidth  $B_{\text{coh}}$  of the channel is defined as the inverse of the delay spread  $\Delta\tau_{\text{max}}$  :

$$B_{\text{coh}} = \frac{1}{\Delta\tau_{\text{max}}} \quad (1.5.3-15)$$

When  $f$  changes by an amount  $B_{\text{coh}}$ , the phase of any term in the summation (1.5.3-12) changes by at most  $2\pi$ . In literature, various definitions of  $B_{\text{coh}}$  can be found, but they all are of the type  $B_{\text{coh}} = C/\Delta\tau_{\text{max}}$ , indicating that the coherence bandwidth is inversely proportional to the delay spread. The channel is frequency-flat over a signal bandwidth  $(-B, B)$  provided that  $2B \ll B_{\text{coh}}$ ; otherwise, the channel is frequency-selective over the considered frequency interval. Table 1-3 shows some values of  $\Delta\tau_{\text{max}}$  and  $B_{\text{coh}}$  for different environments.

		$f_D$	$T_{\text{coh}}$
$f_0 = 1 \text{ GHz}$	$v = 1 \text{ km/h}$	1 Hz	1000 ms
	$v = 10 \text{ km/h}$	10 Hz	100 ms
	$v = 100 \text{ km/h}$	100 Hz	10 ms
$f_0 = 10 \text{ GHz}$	$v = 1 \text{ km/h}$	10 Hz	100 ms
	$v = 10 \text{ km/h}$	100 Hz	10 ms
	$v = 100 \text{ km/h}$	1000 Hz	1 ms

Table 1-2 : relation between carrier frequency, speed, Doppler shift and coherence time

Environment	Delay Spread	Coherence Bandwidth
Rural	200 ns	5 MHz
Hilly Terrain	5–10 $\mu\text{s}$	100–200 kHz
Urban	1–3 $\mu\text{s}$	300 kHz–1 MHz
Indoor	10–50 ns	20–100 MHz

Table 1-3 : delay spread and coherence bandwidth for several environments

### Statistical modelling : Rayleigh fading, Rice fading

The parameters that describe the propagation paths are location-dependent, and their values are unknown to the communication system designer. Therefore, they are considered as *random variables*. Hence, the impulse response  $h_{ch}(u;t)$  and the associated transfer function  $H_{ch}(f;t)$ , when viewed as a function of  $t$ , are random processes. One often makes the assumption of wide-sense stationary uncorrelated scattering (WSSUS), in which case the path gains are modeled as *statistically independent stationary random processes*. Depending on whether a line-of-sight (LOS) path is available between transmitter and receiver, one distinguishes between Rayleigh fading and Rice fading.

#### Rayleigh fading

Rayleigh fading refers to the case where no LOS path is present. The impulse response and transfer function of the multipath fading channel are represented as

$$h_{ch}(u;t) = \sum_{m=0}^{L-1} c_m(t) \delta(u - \Delta\tau_m) \quad H_{ch}(f;t) = \sum_{m=0}^{L-1} c_m(t) \exp(-j2\pi f \Delta\tau_m) \quad (1.5.3-16)$$

where  $\{c_m(t), m = 0, \dots, L-1\}$  are complex-valued *statistically independent zero-mean* stationary Gaussian processes, with  $c_m(t) \sim N_c(0, 2\sigma_m^2 R_D(\Delta t))$  and  $R_D(0) = 1$ , so that  $E[|c_m(t)|^2] = 2\sigma_m^2$ . Usually the impulse response  $h_{ch}(u;t)$  is normalized, meaning that

$$2 \sum_{m=0}^{L-1} \sigma_m^2 = 1 \quad (1.5.3-17)$$

This normalization implies that the signals at the input and output of the LTV filter have the same average (over time) power.

For given  $f$  and  $t$ ,  $H_{ch}(f;t) \sim N_c(0, 1)$  when the normalization (1.5.3-17) holds. The distribution of  $|H_{ch}(f;t)|$  is the so-called Rayleigh distribution, whereas  $|H_{ch}(f;t)|^2$  (which represents the instantaneous power at the output of the channel when the channel input is  $\exp(j2\pi ft)$ ) has a (scaled)  $\chi^2$  distribution with 2 degrees of freedom and mean equal to 1. Hence,  $\Pr[|H_{ch}(f;t)|^2 < \epsilon] = 1 - \exp(-\epsilon) \approx \epsilon$  for  $\epsilon \ll 1$ , so that the probability that  $10 \cdot \log(|H_{ch}(f;t)|^2)$  is less than -20 dB (-30 dB) is about 0.01 (0.001).

The correlation function  $R_D(\Delta t)$  describes the time-selectivity of the channel. The FT of  $R_D(\Delta t)$  is called the *Doppler spectrum*  $S_D(f)$ , with  $S_D(f) = 0$  for  $|f| > f_D$ . When  $|\Delta t| \ll T_{coh} = 1/f_D$ , we have  $R_D(\Delta t) \approx 1$ , which indicates that the channel has virtually not changed over the interval  $(t, t+\Delta t)$ .

The *multipath intensity profile* or *power delay profile*  $\phi_h(u)$  is the average (over the realizations of  $h_{ch}(u;t)$ ) instantaneous power  $E[|s_{out}(t_0+u)|^2]$  at the output of the channel, when the channel input  $s(t)$  is a very narrow unit-energy pulse at  $t = t_0$  (i.e.,  $|s(t)|^2 = \delta(t-t_0)$ ). From (1.5.3-16) we obtain :

$$\phi_h(u) = \sum_{m=0}^{L-1} (2\sigma_m^2) \delta(u - \Delta\tau_m) \quad (1.5.3-18)$$

When for a given delay spread  $\Delta\tau_{max}$  the number of paths is very large, such that a continuum of paths (rather than distinct paths) results, the power delay profile  $\phi_h(u)$  becomes a continuous function of  $u$ .

The corresponding channel model (including path loss and shadowing) is shown in Fig. 1-9. The coefficient  $\gamma(d)$  accounts for path loss and shadowing;  $\gamma(d)$  has a lognormal distribution ( $10 \cdot \log(\gamma^2(d)) \sim N(10 \cdot \log(P_{50}(d)), \sigma_{sh}^2)$ ) and varies slowly with  $d$  (shadowing correlation distance  $d_{sh} \gg \lambda$ , see (1.5-22)).

### Rice fading

Rice fading refers to the case where a LOS path (or *specular* component) is present. The LOS path is not affected by fading, but the other paths (the *diffuse* components) are subjected to Rayleigh fading. The normalized channel impulse response and transfer function are represented as

$$h_{ch}(u;t) = A \exp(j\theta) \exp(j2\pi f_{D,LOS}t) \delta(t) + \sqrt{1-A^2} h_{Rayleigh}(u;t) \quad (1.5.3-19)$$

$$H_{ch}(f;t) = A \exp(j\theta) \exp(j2\pi f_{D,LOS}t) + \sqrt{1-A^2} H_{Rayleigh}(f;t) \quad (1.5.3-20)$$

where  $0 \leq A \leq 1$ , and  $h_{Rayleigh}(u;t)$  and  $H_{Rayleigh}(f;t)$  are the normalized impulse response and transfer function of a Rayleigh fading channel. The quantities  $A \cdot \exp(j\theta)$  and  $f_{D,LOS}$  are the path gain and the Doppler shift of the LOS component; note that the path gain of the LOS component is not time-varying. The carrier-to-multipath (C/M) ratio (which is also called the K factor) is defined as the ratio of specular power to diffuse power :

$$C/M = \frac{A^2}{1-A^2} \Leftrightarrow A^2 = \frac{C/M}{1+(C/M)} \quad 1-A^2 = \frac{1}{1+(C/M)} \quad (1.5.3-19)$$

For given  $f$  and  $t$ , we have  $H_{ch}(f;t) \sim N_c(\mu, 2\sigma^2)$ , with  $|\mu| = A$  and  $2\sigma^2 = 1-A^2$ , so that  $E[|H_{ch}(f;t)|^2] = 1$ . The corresponding distribution of  $|H_{ch}(f;t)|$  is called a Rice distribution.

When  $C/M \rightarrow 0$ , the Rice fading channel becomes a Rayleigh fading channel, because the LOS component can be neglected. When  $C/M \rightarrow \infty$ , the Rice fading channel becomes an

AWGN channel affected by Doppler shift; the Doppler shift can be removed at the receiver by multiplying the received signal with  $\exp(-j2\pi f_{D,LOS}t)$ , in which case an AWGN channel without Doppler shift results.

The resulting Rice fading channel model (including path loss and shadowing) is shown in Fig. 1-10.

#### 1.5.4 Numerical results

In order to illustrate the above results, we present some computer simulations that correspond to the following configuration :

- carrier frequency  $f_0 = 1$  GHz ( $\lambda = 30$  cm)
- path loss exponent = 4
- lognormal shadowing :  $\sigma_{sh} = 6$  dB,  $d_{sh} = 50$  m
- Rayleigh/Rice fading :
  - power delay profile : see Table 1-4
  - Doppler spectrum ( $f_D = 100$  Hz)

$$S_D(f) = \begin{cases} 1/(2f_D) & |f| \leq f_D \\ 0 & \text{otherwise} \end{cases} \Leftrightarrow R_D(\Delta t) = \frac{\sin(2\pi f_D \Delta t)}{2\pi f_D \Delta t} \quad (1.5.4-1)$$

Noting that  $R_c(i/(2f_D)) = 0$  for nonzero  $i$ , it follows that  $c_m(t)$  and  $c_m(t+\Delta t)$  are statistically independent for  $\Delta t = i/(2f_D)$ , or, equivalently, when the distance travelled during  $\Delta t$  is  $i\lambda/2$  (because  $f_D = v/\lambda$ )

delay ( $\mu$ s)	0	0.15	1
$2\sigma^2$	0.5	0.375	0.125

Table 1-4: power delay profile of 3-path channel

Fig. 1-11 illustrates the effect of shadowing, by showing (in dB) the median power  $P_{50}(d)$  and the local average power  $P_{loc,avg}(\mathbf{x})$  of the received signal at distance  $d$  from the transmitter, when transmitting a sinusoidal bandpass signal; we define the 0 dB power level to be  $P_{50}(100)$ . As the path loss exponent equals 4,  $P_{50}(d)$  decreases by 40 dB when  $d$  increases by a factor of 10. Assuming Rayleigh fading, Fig. 1-12 compares the local received power  $P_{loc}(\mathbf{x})$  to the local average power when  $d$  ranges from 925 m to 940 m (i.e.,  $\Delta d = 50\lambda$ ). The fluctuations due to Rayleigh fading are much stronger and much faster than those caused by

shadowing; this indicates that Rayleigh fading has a considerable impact on receiver performance.

Still assuming the transmitted bandpass signal is sinusoidal, the fluctuations of the received power caused by Rayleigh fading and Rice fading are compared in Fig. 1-13 (only fluctuations caused by small-scale fading are shown); the average received power has been set to 0 dB. Note that the smaller C/M, the larger the power fluctuations; hence, the Rayleigh fading case is the most critical one.

Fig. 1-14 shows  $|H_{ch}(f;t)|^2$  (in dB) over a 10MHz interval for two time instants that are separated by  $1/(2f_D)$ ; because of (1.5.4-1), the channel transfer functions at these two instants are statistically independent. Note the frequency-selectivity (variation of  $|H_{ch}(f;t)|^2$  with  $f$ ) and the time-selectivity (variation of  $|H_{ch}(f;t)|^2$  with  $t$ ) of the channel.

## 1.6. Discrete-time channel model

In digital communications we want to transmit a discrete-time sequence  $\{x(k)\}$  (that in some way represents the sequence of bits) rather than a continuous-time signal. However, the physical channel operates in continuous time. The sequence  $\{x(k)\}$  is transformed into a continuous-time signal  $s(t)$  by applying that sequence to a transmit filter with impulse response  $h_{tr}(t)$  and transfer function  $H_{tr}(f)$ . This yields :

$$s(t) = \sum_m x(m)h_{tr}(t - mT) \quad (1.6.0-1)$$

with  $T$  and  $1/T$  denoting the signaling interval and the signaling rate, respectively. The signal  $s(t)$  is fed to the channel. The channel output  $r(t)$  is applied to a receive filter. The receive filter output is sampled at instants  $kT$ , which yields the sequence  $\{y(k)\}$ . In the following we investigate the discrete-time channel model that relates  $\{y(k)\}$  to  $\{x(k)\}$ .

### 1.6.1 LTI channel

When the channel and the receive filter are LTI, they are specified by their impulse responses  $h_{ch}(t)$  and  $h_{rec}(t)$ , or, equivalently, by their transfer functions  $H_{ch}(f)$  and  $H_{rec}(f)$ . From Fig. 1-15 it follows that the continuous-time signal  $y_c(t)$  at the output of the receive filter is given by

$$y_c(t) = \sum_m x(m)g_c(t - mT) + n_c(t) \quad (1.6.1-1)$$

where

$$G_c(f) = H_{tr}(f)H_{ch}(f)H_{rec}(f) \quad (1.6.1-2)$$



and  $n_c(t) \sim N_c(0, R_{n_c}(u))$ , where  $R_{n_c}(u) = E[n_c(t+u)n_c^*(t)]$  is the inverse FT (IFT) of the power spectrum  $S_{n_c}(f)$  of  $n_c(t)$ , with

$$S_{n_c}(f) = N_0 |H_{\text{rec}}(f)|^2 \quad (1.6.1-3)$$

Sampling  $y_c(t)$  at instants  $kT$  yields

$$y(k) = \sum_m x(k-m)g(m) + n(k) \quad (1.6.1-4)$$

where  $y(k) = y_c(kT)$ ,  $g(k) = g_c(kT)$  and  $n(k) = n_c(kT)$ . We have  $\{n(k)\} \sim N_c(0, R_n(m))$ , with  $R_n(m) = R_{n_c}(mT)$ . Hence,  $g(m)$  and  $R_n(m)$  are obtained by sampling the IFTs of the functions  $H_{\text{tr}}(f)H_{\text{ch}}(f)H_{\text{rec}}(f)$  and  $N_0|H_{\text{rec}}(f)|^2$  at instant  $mT$  :

$$g(m) = \int H_{\text{tr}}(f)H_{\text{ch}}(f)H_{\text{rec}}(f)\exp(j2\pi fmT)df \quad (1.6.1-5)$$

$$R_n(m) = N_0 \int |H_{\text{rec}}(f)|^2 \exp(j2\pi fmT)df \quad (1.6.1-6)$$

We observe from (1.6.1-4) that  $\{y(k)\}$  is obtained by applying  $\{x(k)\}$  to a discrete-time LTI channel with impulse response  $\{g(m)\}$ , that adds Gaussian noise  $\{n(k)\}$  with correlation function  $R_n(m)$ . The discrete-time FT (DTFT) of  $\{g(m)\}$  and  $\{R_n(m)\}$  are the channel transfer function  $G(\exp(j2\pi fT))$  and noise spectrum  $S_n(\exp(j2\pi fT))$ . They can be obtained directly from the FT of  $g_c(t)$  and  $R_{n_c}(t)$  as follows :

$$G(\exp(j2\pi fT)) = \{G_c(f); 1/T\}_{\text{fld}} = \{H_{\text{tr}}(f)H_{\text{ch}}(f)H_{\text{rec}}(f); 1/T\}_{\text{fld}} \quad (1.6.1-7)$$

$$S_n(\exp(j2\pi fT)) = \{S_{n_c}(f); 1/T\}_{\text{fld}} = N_0 \{|H_{\text{rec}}(f)|^2; 1/T\}_{\text{fld}} \quad (1.6.1-8)$$

This follows from the identity

$$\sum_m q(mT)\exp(-j2\pi fmT) = \{Q(f); 1/T\}_{\text{fld}} \quad (1.6.1-9)$$

where  $q(t)$  is an arbitrary function with FT  $Q(f)$ , and

$$\{Q(f); F\}_{\text{fld}} = F \sum_{i=-\infty}^{+\infty} Q(f - iF) \quad (1.6.1-10)$$

is the periodic extension of  $F \cdot Q(f)$  with period  $F$ , obtained by "folding"  $Q(f)$ . The LTI discrete-time channel model is shown in Fig. 1-16; Fig. 1-17 details the operations performed by the channel filter ( $z^{-1}$  represents a delay equal to  $T$ ), assuming that  $g(m) = 0$  for  $m \notin (-M_1, M_2)$ . Note that  $(M_1+M_2)T$  is the sum of the individual durations of  $h_{\text{tr}}(u)$ ,  $h_{\text{ch}}(u)$  and  $h_{\text{rec}}(u)$ .

## 1.6.2 LTV channel

Now we consider the case where the channel and the receive filter are LTV (see Fig. 1-18). The signal  $y_c(t)$  at the output of the receive filter is given by

$$y_c(t) = \sum_m x(m)g_c(t - mT; t) + n_c(t) \quad (1.6.2-1)$$

where

$$g_c(u; t) = \iint h_{\text{rec}}(u_1; t) h_{\text{ch}}(u_2; t - u_1) h_{\text{tr}}(u - u_1 - u_2) du_1 du_2 \quad (1.6.2-2)$$

$$n_c(t) = \int h_{\text{rec}}(u_1; t) w(t - u_1) du_1 \quad (1.6.2-3)$$

We have  $n_c(t) \sim N_c(0, R_{n_c}(u, t))$ , with

$$\begin{aligned} R_{n_c}(u, t) &= E[n_c(t + u)n_c^*(t)] \\ &= N_0 \int h_{\text{rec}}(v + u; t + u) h_{\text{rec}}^*(v; t) dv \\ &= N_0 \int H_{\text{rec}}(f; t + u) H_{\text{rec}}^*(f; t) \exp(j2\pi fu) df \end{aligned} \quad (1.6.2-4)$$

From (1.6.2-2) and (1.6.2-4) we note that

- $g_c(u; t)$  is *NOT* the IFT of  $H_{\text{tr}}(f)H_{\text{ch}}(f; t)H_{\text{rec}}(f; t)$ , because the second argument of the channel impulse response in the integrand of (1.6.2-2) is  $t - u_1$  instead of  $t$ , due to the memory of the receive filter.
- the correlation function (1.6.2-4) depends on both  $t$  and  $u$ , instead of just  $u$ : the noise  $n_c(t)$  is *nonstationary* when the receive filter is time-varying.

Sampling  $y_c(t)$  at instants  $kT$  yields

$$y(k) = \sum_m x(k - m)g(m; k) + n(k) \quad (1.6.2-5)$$

where  $y(k) = y_c(kT)$ ,  $g(m; k) = g_c(mT; kT)$  and  $n(k) = n_c(kT)$ , with  $\{n(k)\} \sim N_c(0, R_{n_c}(mT, kT))$ . The resulting discrete-time channel model (1.6.2-5) is dispersive and time-varying. This model is shown in Fig. 1-19, with the transfer function  $G(\exp(j2\pi fT); k)$  denoting the DTFT of  $\{g(m; k)\}$ . Fig. 1-20 illustrates the operation of the LTV filter  $g(m; k)$ , assuming that  $g(m; k) = 0$  for  $m \notin (-M_1, M_2)$ ; according to (1.6.2-2),  $(M_1 + M_2)T$  is the sum of the durations of the pulses  $h_{\text{rec}}(u; t)$ ,  $h_{\text{ch}}(u; t)$  and  $h_{\text{tr}}(u)$ .

In many cases encountered in practice, the fading is *slow*: the coherence times of the channel and of the receive filter are much longer than the duration of the impulse response of the receive filter. For slow fading, the expressions (1.6.2-2) and (1.6.2-4) can be simplified.

- Assuming without loss of generality that  $h_{\text{rec}}(u; t)$  has its center near  $u = 0$  (which is easily accomplished by applying a suitable time-shift), we can use in (1.6.2-2) the approximation  $h_{\text{ch}}(u_2; t - u_1) \approx h_{\text{ch}}(u_2; t)$ ; this is because the coherence time of  $h_{\text{ch}}(u_2; t)$  is much larger than the range of  $u_1$ , which is limited to the duration of  $h_{\text{rec}}(u_1; t)$ . This yields

$$\begin{aligned}
g_c(u;t) &= \iint h_{\text{rec}}(u_1;t)h_{\text{ch}}(u_2;t)h_{\text{tr}}(u-u_1-u_2)du_1du_2 \\
&= \int H_{\text{tr}}(f)H_{\text{ch}}(f;t)H_{\text{rec}}(f;t)\exp(j2\pi fu)df
\end{aligned} \tag{1.6.2-6}$$

which indicates that now  $g_c(u;t)$  is simply the IFT of  $H_{\text{tr}}(f)H_{\text{ch}}(f;t)H_{\text{rec}}(f;t)$ . Hence, the transfer function  $G(\exp(j2\pi fT);k)$  of the discrete-time channel is given by

$$G(\exp(j2\pi fT);k) = \{H_{\text{tr}}(f)H_{\text{ch}}(f;kT)H_{\text{rec}}(f;kT);1/T\}_{\text{fld}} \tag{1.6.2-7}$$

- As the integrand in (1.6.2-4) becomes zero when  $|u|$  exceeds the duration of  $h_{\text{rec}}(u;t)$ , and the coherence time of  $h_{\text{rec}}(u;t)$  is much larger than the duration of  $h_{\text{rec}}(u;t)$ , the approximation  $h_{\text{rec}}(v+u; t+u) \approx h_{\text{rec}}(v+u; t)$  holds. Hence,

$$R_{n_c}(u, t) = N_0 \int |H_{\text{rec}}(f; t)|^2 \exp(j2\pi fu)df \tag{1.6.2-8}$$

The corresponding power spectrum  $S_n(\exp(j2\pi fT);k)$  of the nonstationary noise  $n(k) = n_c(kT)$  is defined as the DTFT (with respect to the variable  $m$ ) of  $R_n(m,k) = R_{n_c}(mT, kT)$ , yielding

$$S_n(\exp(j2\pi fT);k) = \{N_0|H_{\text{rec}}(f;kT)|^2;1/T\}_{\text{fld}} \tag{1.6.2-9}$$

Note that (1.6.2-7) and (1.6.2-9), which hold for the slow fading channel, are very similar to the corresponding equations (1.6.1-7) and (1.6.1-8) for a LTI channel. Hence, for slow fading the computations can be carried out as for a LTI channel.

### Example : slowly fading multipath channel with $\Delta\tau_m = mT$

We consider a slowly fading multipath channel determined by (1.5.3-16), and a time-invariant receive filter with transfer function  $H_{\text{rec}}(f)$ . In this case, (1.6.2-7) becomes

$$G(e^{j2\pi fT};k) = \sum_m c_m(kT) \{H_{\text{tr}}(f)H_{\text{rec}}(f)e^{-j2\pi f\Delta\tau_m};1/T\}_{\text{fld}} \tag{1.6.2-10}$$

In order to simplify (1.6.2-10) we assume that all the path delay differences  $\Delta\tau_m$  are *multiples of the signaling interval  $T$* :  $\Delta\tau_m = mT$  (this is unlikely to occur in practice !). This yields :

$$G(e^{j2\pi fT};k) = \{H_{\text{tr}}(f)H_{\text{rec}}(f);1/T\}_{\text{fld}} \sum_m c_m(kT)e^{-j2\pi mfT} \tag{1.6.2-11}$$

When the transfer functions  $H_{\text{tr}}(f)$  and  $H_{\text{rec}}(f)$  are selected such that  $\{H_{\text{tr}}(f)H_{\text{rec}}(f);1/T\}_{\text{fld}} = 1$ , (1.6.2-11) reduces to the simple expression

$$G(e^{j2\pi fT};k) = \sum_m c_m(kT)e^{-j2\pi mfT} \tag{1.6.2-12}$$

which indicates that  $g(m;k) = c_m(kT)$ .

## 1.7. Implementation aspects

In this section we indicate how the transmitter part and receiver part from Fig. 1-18 can be implemented by means of digital signal processing and simple analog filtering.

### 1.7.1 Transmitter implementation

Fig. 1-18 and eq. (1.6.0-1) suggest that the transmitted signal  $s(t)$  is obtained by simply applying the sequence  $\{x(k)\}$  to a *continuous-time* transmit filter with impulse response  $h_{tr}(t)$ . However, the transmit filter might be very difficult to implement by means of analog components. In this case, we will use digital signal processing to compute samples of  $s(t)$  at a rate  $1/T_s$  that is an integer multiple of the signaling rate  $1/T$  ( $T = N_s T_s$ ), and apply these samples to a simple analog interpolation filter to obtain the transmitted signal  $s(t)$ .

Assuming that  $H_{tr}(f) = 0$  for  $|f| > B$ , we select  $1/T_s = N_s/T > 2B$ , in order that the samples  $s(kT_s)$  contain all information that is present in  $s(t)$  (sampling theorem !). This yields

$$s(kT_s) = \sum_m x(m) h_{tr}(kT_s - mN_s T_s) = \sum_i x_{up}(i) h_{tr}(kT_s - iT_s) \quad (1.7.1-1)$$

where

$$x_{up}(i) = \begin{cases} x(m) & i = mN_s \\ 0 & \text{otherwise} \end{cases} \quad (1.7.1-2)$$

The sequence  $\{x_{up}(i)\}$  is obtained by *upsampling* the sequence  $\{x(m)\}$  by a factor  $N_s$  : this corresponds to inserting  $(N_s-1)$  zeroes between successive elements of  $\{x(m)\}$ . Note that the rates of the sequences  $\{x(m)\}$  and  $\{x_{up}(i)\}$  are  $1/T$  and  $1/T_s$ , respectively. The upsampled sequence  $\{x_{up}(i)\}$  is applied to a discrete-time filter with impulse response  $\{h_{tr}(iT_s)\}$ , which results in the sequence  $\{s(kT_s)\}$ .

Finally, the transmitted signal  $s(t)$  is obtained by applying  $\{s(kT_s)\}$  to a continuous-time *interpolation filter* with impulse response  $h_{int}(t)$  and transfer function  $H_{int}(f)$  :

$$s(t) = \sum_k s(kT_s) h_{int}(t - kT_s) \Leftrightarrow S(f) = H_{int}(f) \{S(f); 1/T_s\}_{fld} \quad (1.7.1-3)$$

The resulting transmitter is shown in Fig. 1-21. In order that (1.7.1-3) holds, the interpolator transfer function must satisfy the following condition :

$$H_{int}(f) = T_s \text{ for } |f| < B \quad H_{int}(f) = 0 \text{ for } |f| > 1/T_s - B \quad (1.7.1-4)$$

which is illustrated in Fig. 1-22. Note that the transition band  $(B, 1/T_s - B)$  can be made very large (so that a simple analog interpolation filter results) by selecting  $1/T_s \gg 2B$ , at the expense of more computations per signaling interval  $T$  in the digital part of the transmitter.

### 1.7.2 Receiver implementation

Fig. 1-18 shows a receiver containing a continuous-time receiver filter with impulse response  $h_{\text{rec}}(u;t)$  and transfer function  $H_{\text{rec}}(f;t)$ . However, when the receiver filter is difficult to implement by means of analog components, we resort to a simple analog filter followed by digital signal processing.

Let us assume that  $H_{\text{rec}}(f;t) = 0$  for  $|f| > B_{\text{rec}}$ . In this case, only the frequency components of  $r(t)$  in  $(-B_{\text{rec}}, B_{\text{rec}})$  are relevant. We apply  $r(t)$  to a continuous-time *anti-aliasing* filter with transfer function  $H_{\text{AA}}(f)$ ; which is selected such that

$$H_{\text{AA}}(f) = 1 \text{ for } |f| < B_{\text{rec}} \quad H_{\text{AA}}(f) = 0 \text{ for } |f| > B_{\text{AA}} \quad (1.7.2-1)$$

with  $B_{\text{AA}} > B_{\text{rec}}$ . The resulting signal  $r_{\text{AA}}(t)$  is sampled at a rate  $1/T_s$ , with  $1/T_s > (B_{\text{rec}} + B_{\text{AA}})$ . The samples  $r_{\text{AA}}(kT_s)$  are applied to a discrete-time filter with impulse response  $h_{\text{rec}}(i;k) = T_s h_{\text{rec}}(iT_s; kT_s)$ , and the filter output is computed only at instants  $mT = mN_s T_s$ , yielding the sequence  $\{y_c(mN_s T_s)\} = \{y(m)\}$  at rate  $1/T$ . Conceptually, this is equivalent to computing the filter output  $\{y_c(kT_s)\}$  at rate  $1/T_s$ , followed by *downsampling* ("decimation") by a factor  $N_s$  to obtain the sequence  $\{y(m)\}$ . The former approach is used in practice because of its smaller (by a factor  $N_s$ ) complexity, whereas the latter is mainly used in block diagrams for its clarity. The corresponding receiver structure is shown in Fig. 1-23. Selecting  $B_{\text{AA}} \gg B_{\text{rec}}$  eases the implementation of the analog anti-aliasing filter (large transition band), but imposes a large value of  $1/T_s$ , which gives increases the number of computations per signaling interval  $T$  in the digital part of the receiver.

Now we verify that the digital filter from Fig. 1-23 indeed provides the samples at  $kT_s$  of the signal  $y_c(t)$  from Fig. 1-18, with

$$y_c(kT_s) = \int h_{\text{rec}}(u; kT_s) r(kT_s - u) du = \int_{-B_{\text{rec}}}^{B_{\text{rec}}} H_{\text{rec}}(f; kT_s) R(f) e^{j2\pi k f T_s} df \quad (1.7.2-2)$$

The discrete-time filter output is given by

$$\begin{aligned} \sum_i T_s h_{\text{rec}}(iT_s; kT_s) r_{\text{AA}}(kT_s - iT_s) &= \int_{-1/(2T_s)}^{1/(2T_s)} \{T_s H_{\text{rec}}(f; kT_s); 1/T_s\}_{\text{fld}} \{T_s R_{\text{AA}}(f); 1/T_s\}_{\text{fld}} e^{j2\pi k f T_s} df \\ &= \int_{-B_{\text{rec}}}^{B_{\text{rec}}} H_{\text{rec}}(f; kT_s) R_{\text{AA}}(f) e^{j2\pi k f T_s} df \end{aligned} \quad (1.7.2-3)$$

where the second line from (1.7.2-3) results from the condition  $1/T_s > B_{\text{rec}} + B_{\text{AA}} > 2B_{\text{rec}}$ , which guarantees that (see Fig. 1-24)

- $\{T_s H_{\text{rec}}(f; kT_s); 1/T_s\}_{\text{fld}} = H_{\text{rec}}(f; kT_s)$  for  $|f| < 1/(2T_s)$
- $\{T_s R_{\text{AA}}(f); 1/T_s\}_{\text{fld}} = R_{\text{AA}}(f)$  for  $|f| < B_{\text{rec}}$  (no aliasing occurs within  $(-B_{\text{rec}}, B_{\text{rec}})$ )

Finally, because of  $H_{AA}(f) = 1$  for  $|f| < B_{rec}$ , we can replace in the second line of (1.7.2-3)  $R_{AA}(f)$  by  $R(f)$ , so that the filter output at instant  $kT_s$  equals  $y_c(kT_s)$ .

## 1.8. Simulation issues

Computer simulation is a useful and flexible tool to investigate the operation and performance of communication systems before actually building the system in hardware.

In a computer simulation, only discrete-time signals can be generated. Hence, the transmitted and received signals (which are in continuous time) must be represented by their samples, taken at a sufficiently high rate  $1/T_s$  so that the information contained in the continuous-time signals is preserved.

Let us consider the simulation of the system from Fig. 1-18. We assume that  $H_{tr}(f) = 0$  for  $|f| > B$  and  $H_{rec}(f;t) = 0$  for  $|f| > B_{rec}$ . We select a sampling frequency  $1/T_s = N_s/T$ , with  $1/T_s > \max(B, B_{rec})$ .

- From Fig. 1-21, it follows that we can simulate  $\{s(kT_s)\}$  by first upsampling  $\{x(m)\}$  by a factor  $N_s$ , and then applying the upsampled sequence to a discrete-time filter with impulse response  $h_{tr}(iT_s)$ .
- We observe from Fig. 1-23 that the noise contribution  $w_{AA}(kT_s)$  to  $r_{AA}(kT_s)$  is obtained by applying white noise  $w(t) \sim N_c(0, N_0\delta(u))$  to the anti-aliasing filter  $H_{AA}(f)$  and sampling the filter output at instants  $kT_s$ . Selecting  $H_{AA}(f) = 1$  for  $|f| < 1/(2T_s)$  and  $H_{AA}(f) = 0$  otherwise, it is easily shown that  $w_{AA}(kT_s) \sim N_c(0, (N_0/T_s)\delta(m))$
- According to Figs. 1-21 and 1-23, the signal contribution  $s_{AA}(kT_s)$  to  $r_{AA}(kT_s)$  results from applying  $\{s(kT_s)\}$  to the cascade of the interpolation filter  $H_{int}(f)$ , the channel filter  $H_{ch}(f;t)$  and the anti-aliasing filter  $H_{AA}(f)$ , and sampling the output of the cascaded filter at  $kT_s$ . Assuming that the channel correlation time is much larger than the duration of the impulse response of the filter  $H_{AA}(f)$ , this is equivalent to applying  $\{s(kT_s)\}$  to  $T_s H_{ch,LP}(f;kT_s) = H_{int}(f)H_{ch}(f;kT_s)H_{AA}(f)$  and sampling at  $kT_s$  :

$$s_{AA}(kT_s) = T_s \sum_i h_{ch,LP}(kT_s - iT_s; kT_s) s(iT_s) \quad (1.8-1)$$

Selecting  $H_{int}(f) = T_s$  for  $|f| < 1/(2T_s)$  and  $H_{int}(f) = 0$  otherwise, we obtain  $H_{ch,LP}(f;kT_s) = H_{ch}(f;kT_s)$  for  $|f| < 1/(2T_s)$  and  $H_{ch,LP}(f;kT_s) = 0$  otherwise.

- After computing  $r_{AA}(kT_s) = s_{AA}(kT_s) + w_{AA}(kT_s)$ , it follows from Fig. 1-23 that we can simulate  $\{y(m)\}$  by first applying  $\{r_{AA}(kT_s)\}$  to a filter with impulse response  $T_s h_{rec}(iT_s; mT_s)$  and then decimating the filter output by a factor  $N_s$ .

The resulting discrete-time simulation model is shown in Fig. 1-25.

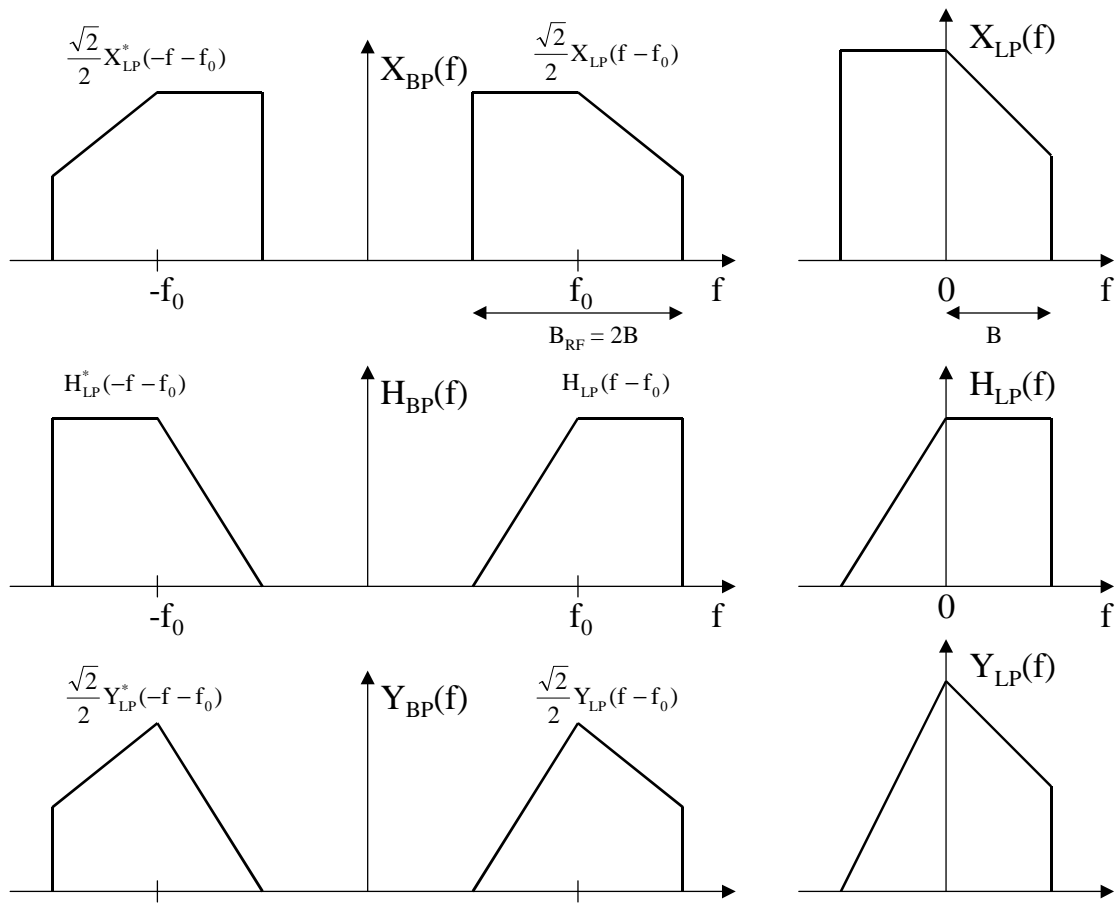


Fig. 1-1 : relation between real-valued bandpass signals and their complex-valued baseband representation

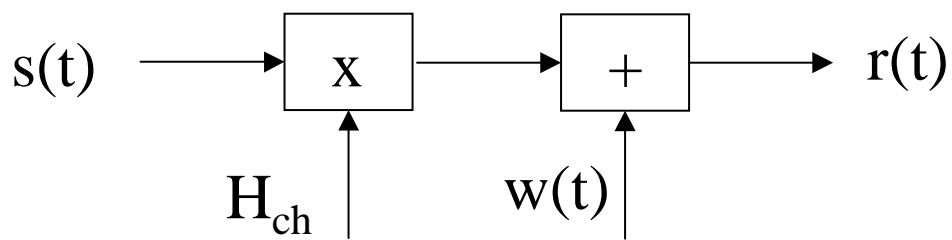


Fig. 1-2 : AWGN channel model

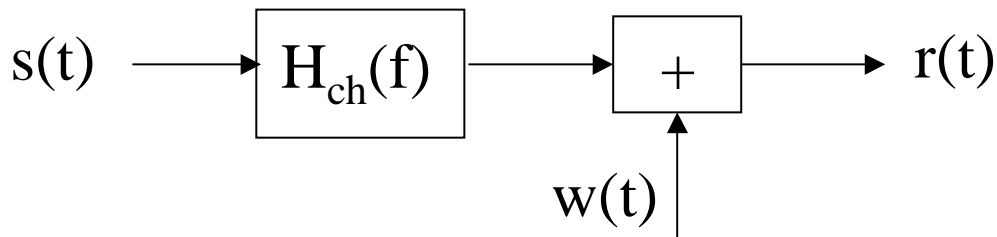


Fig. 1-3 : LTI channel model

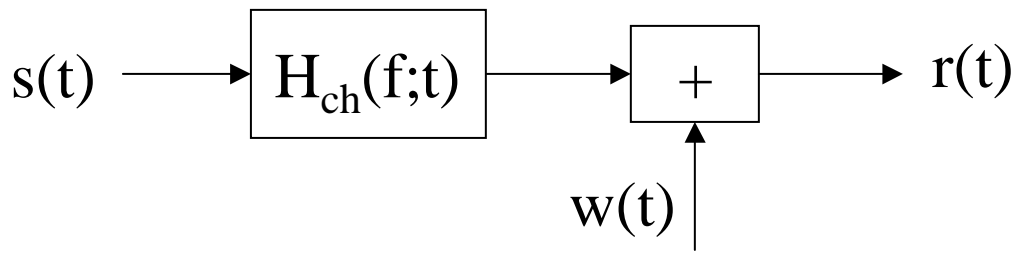


Fig. 1-4 : LTV channel model

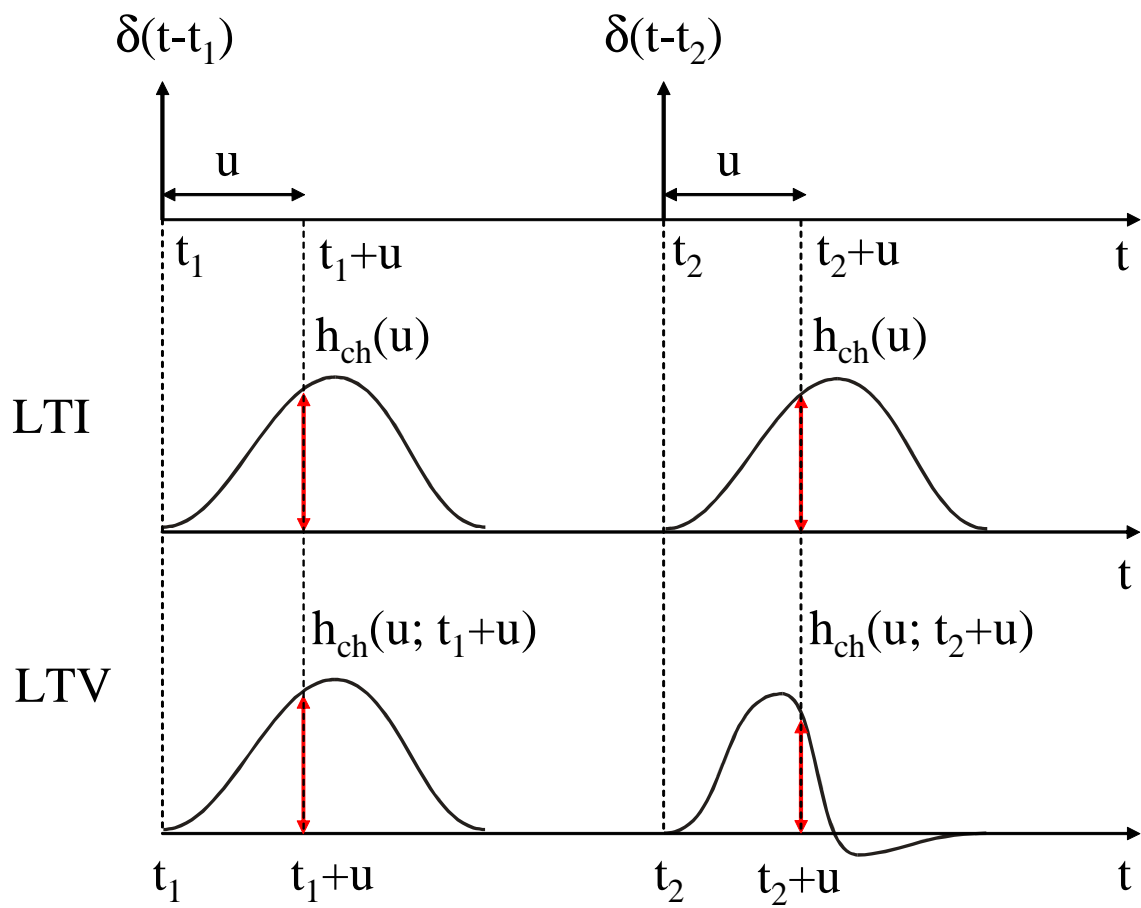


Fig. 1-5 : impulse response of LTI filter and LTV filter



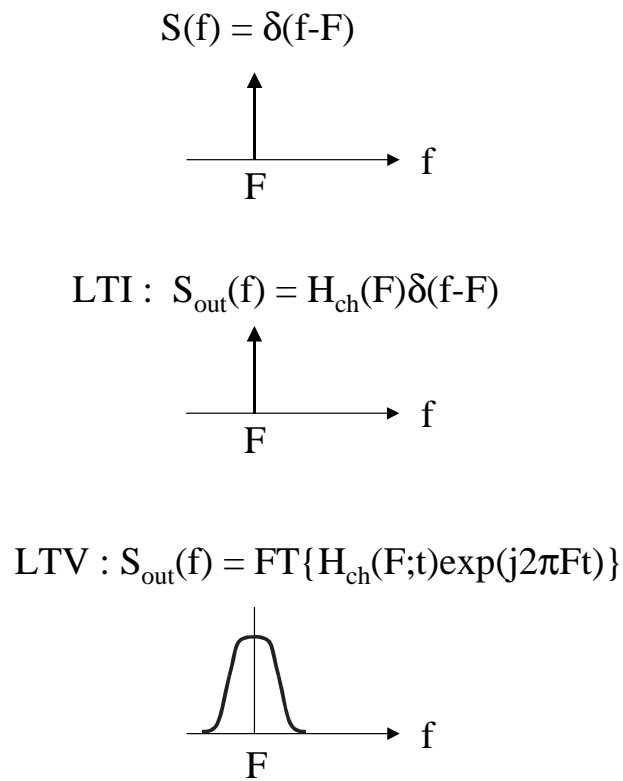


Fig. 1-6 : response of LTI filter and LTV filter to complex exponential

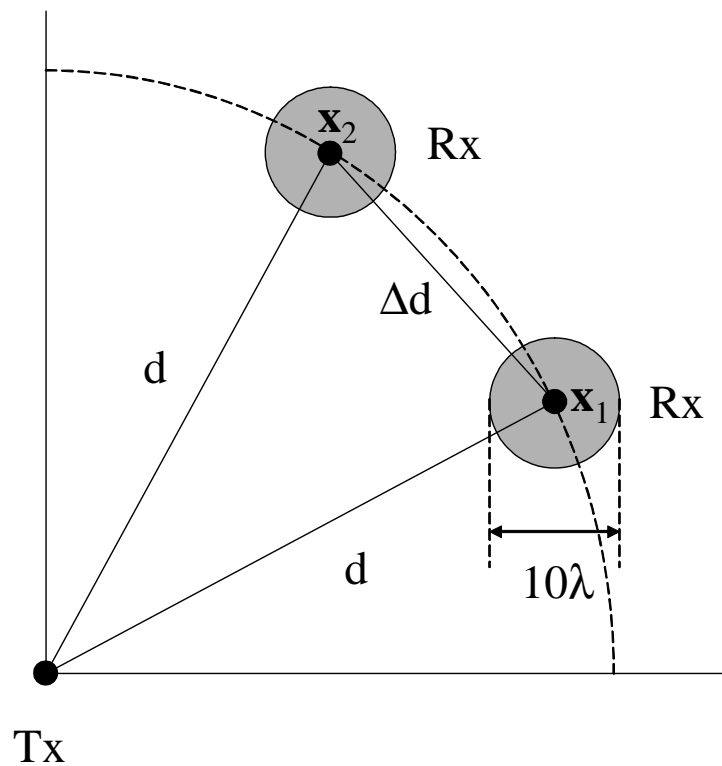


Fig. 1-7 : configuration for shadowing measurement

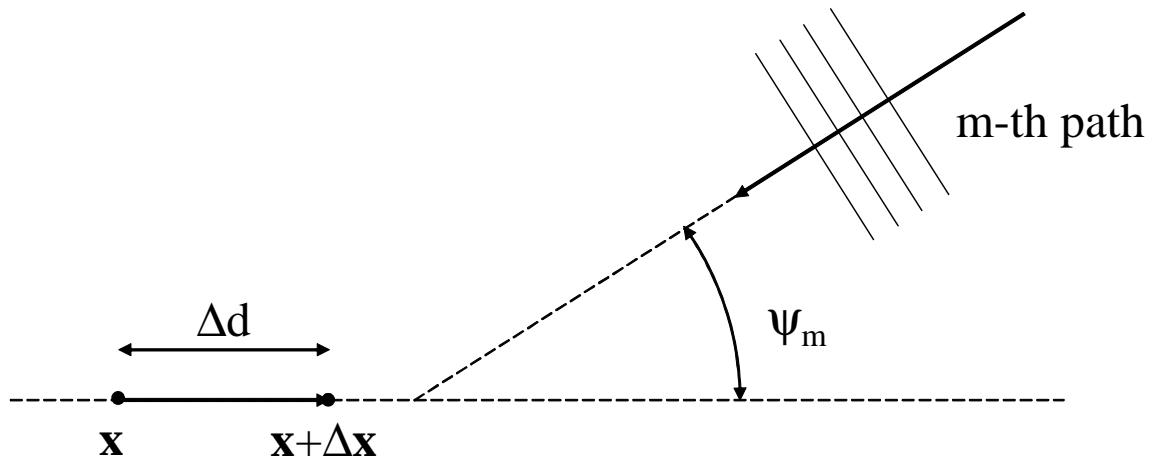
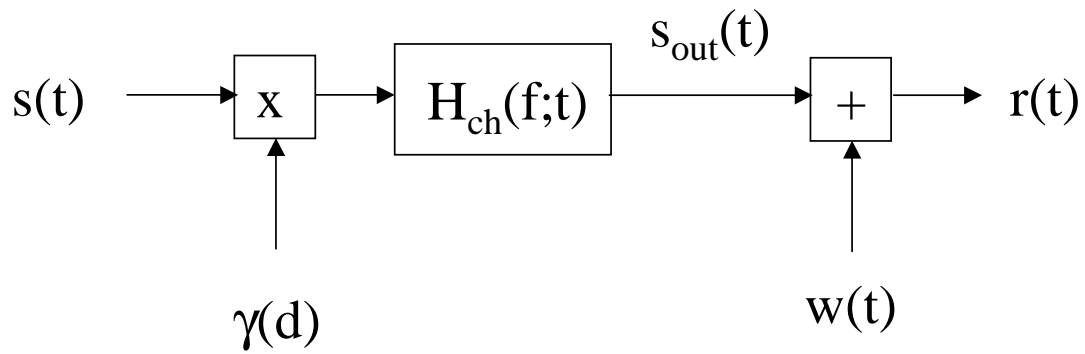
Fig. 1-8 : definition of angle of incidence  $\psi_m$ 

Fig. 1-9 : Rayleigh fading channel model

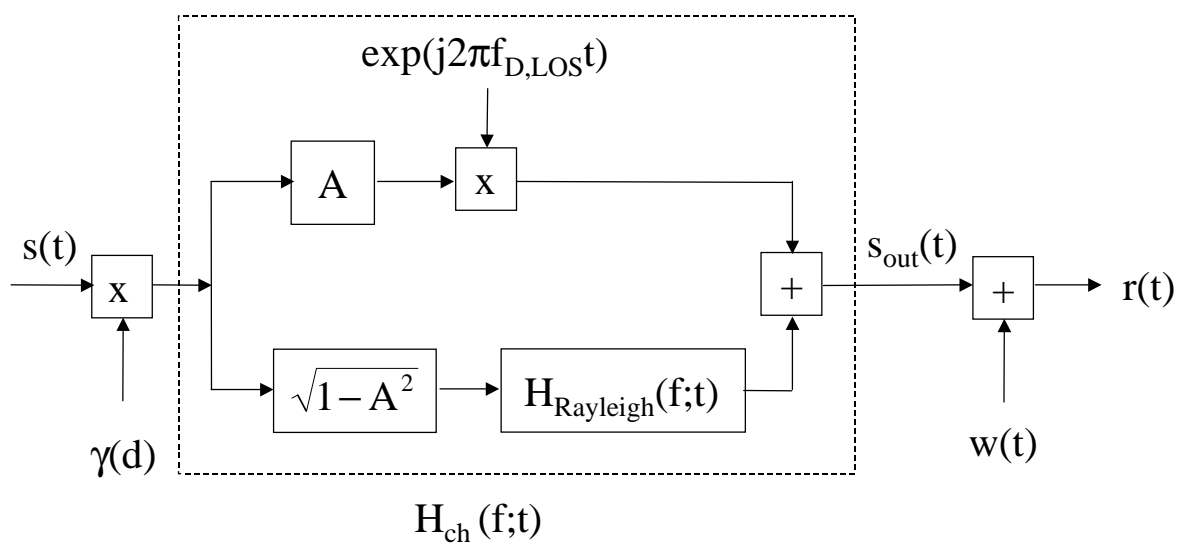


Fig. 1-10 : Rice fading channel model

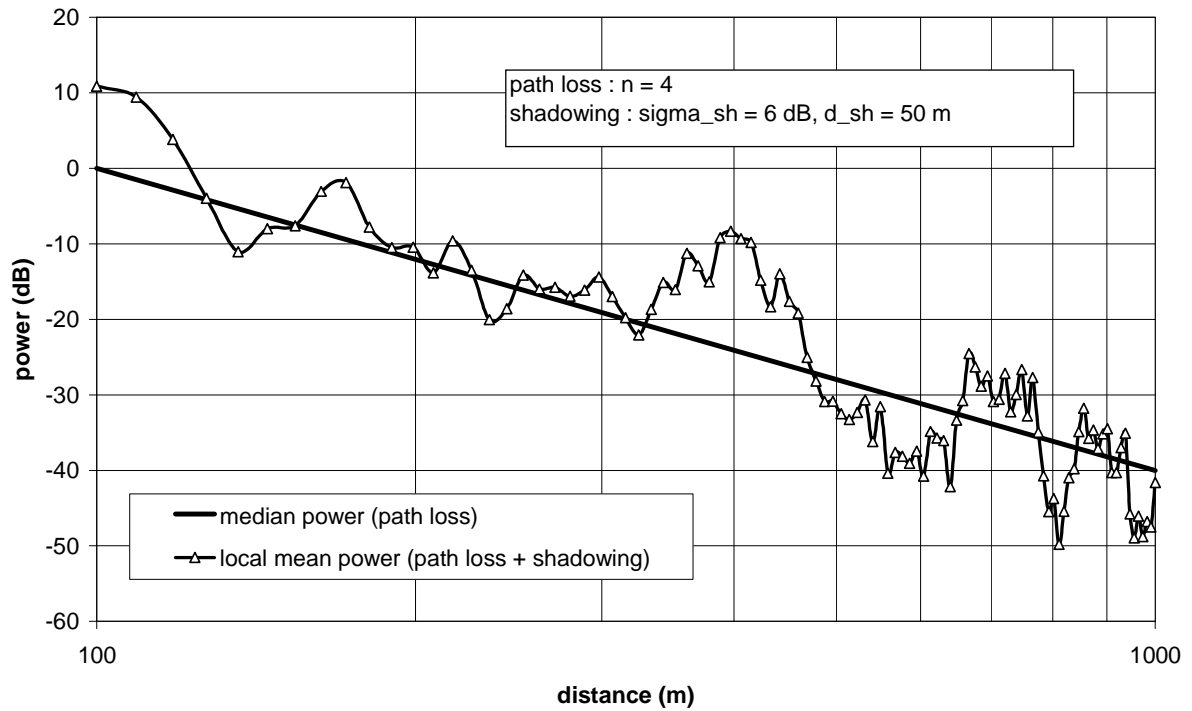


Fig. 1-11 : effect of shadowing

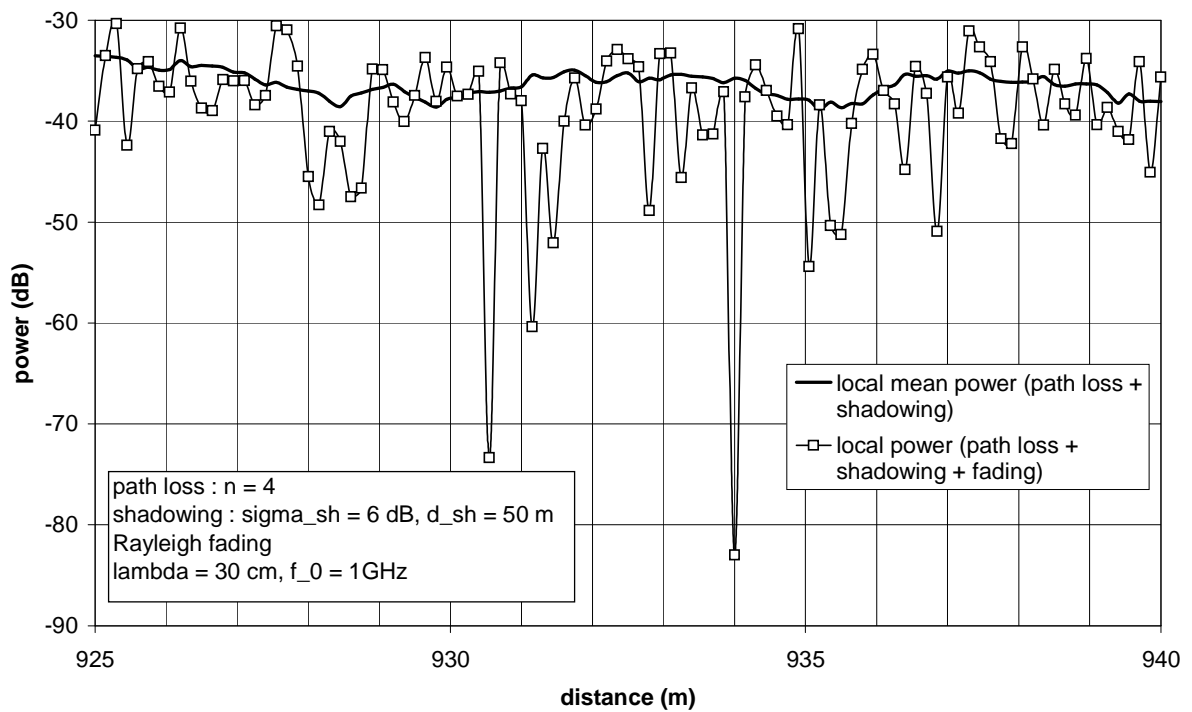


Fig. 1-12 : effect of small-scale fading

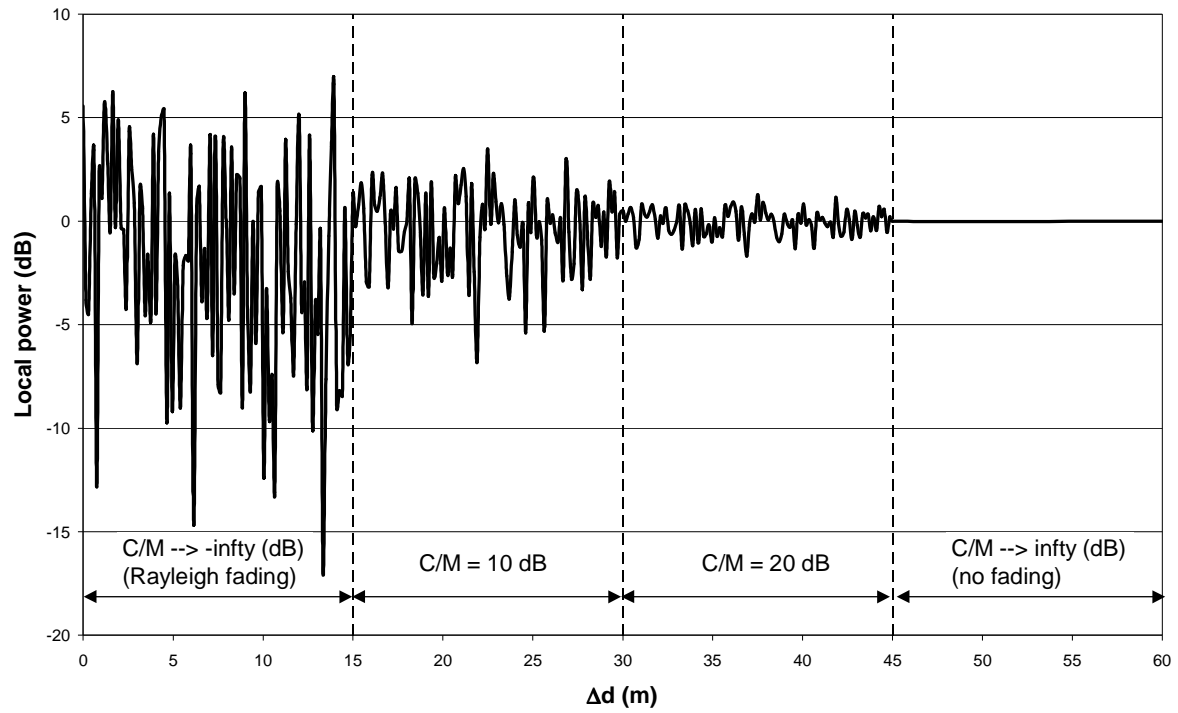


Fig. 1-13 : effect of C/M on Rice fading

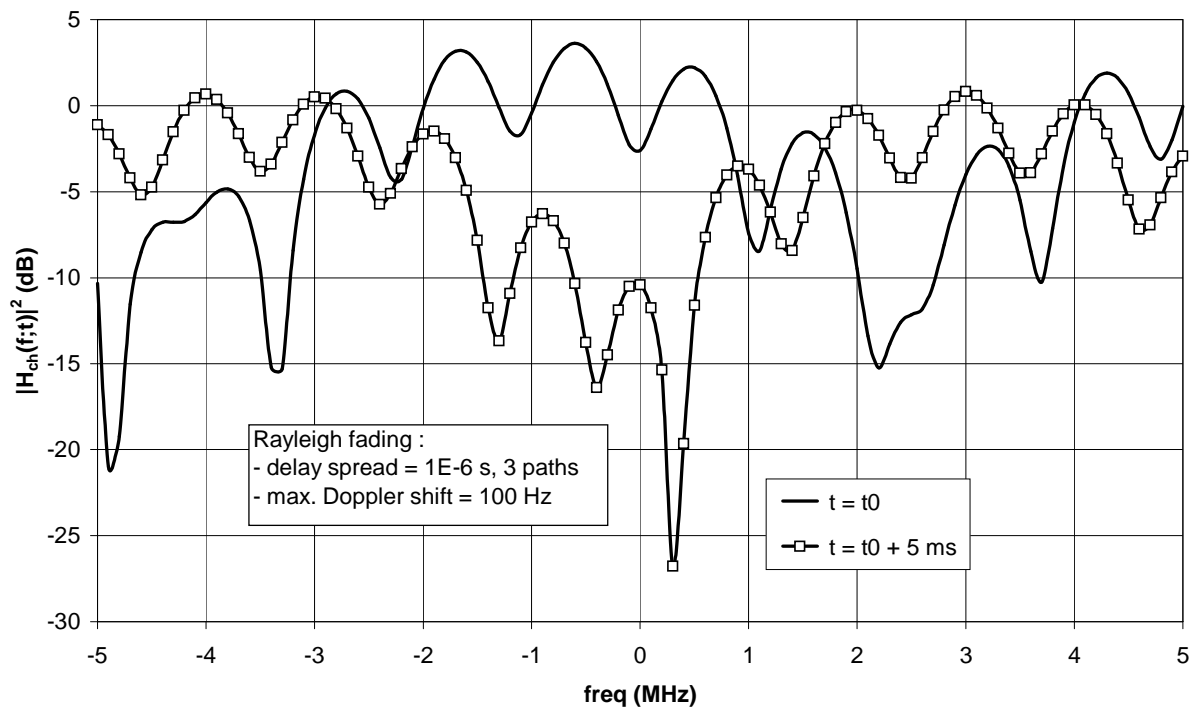


Fig. 1-14 : illustration of frequency selectivity

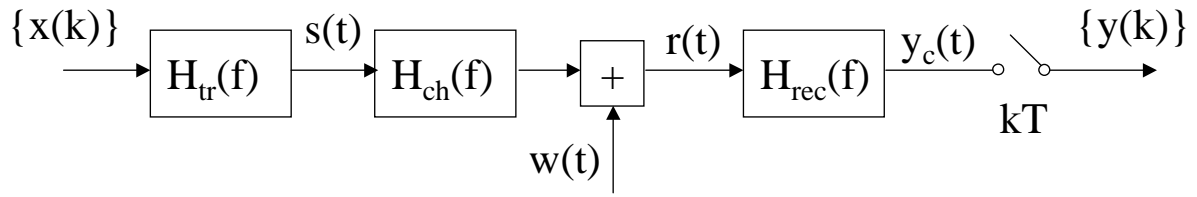


Fig. 1-15 : transmit filter, LTI channel, receive filter and sampling

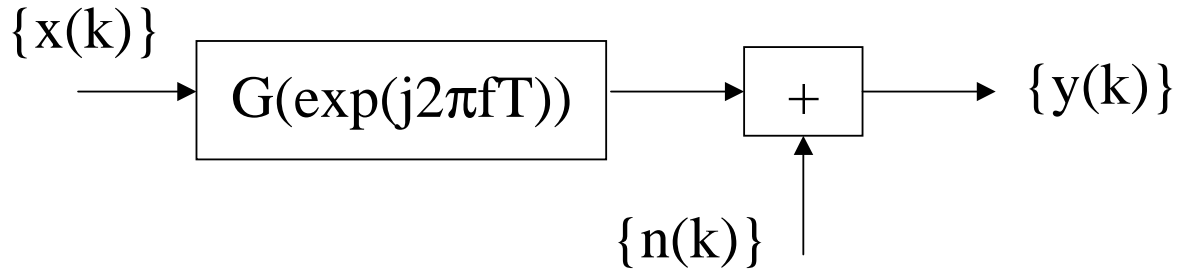


Fig. 1-16 : discrete-time LTI channel model

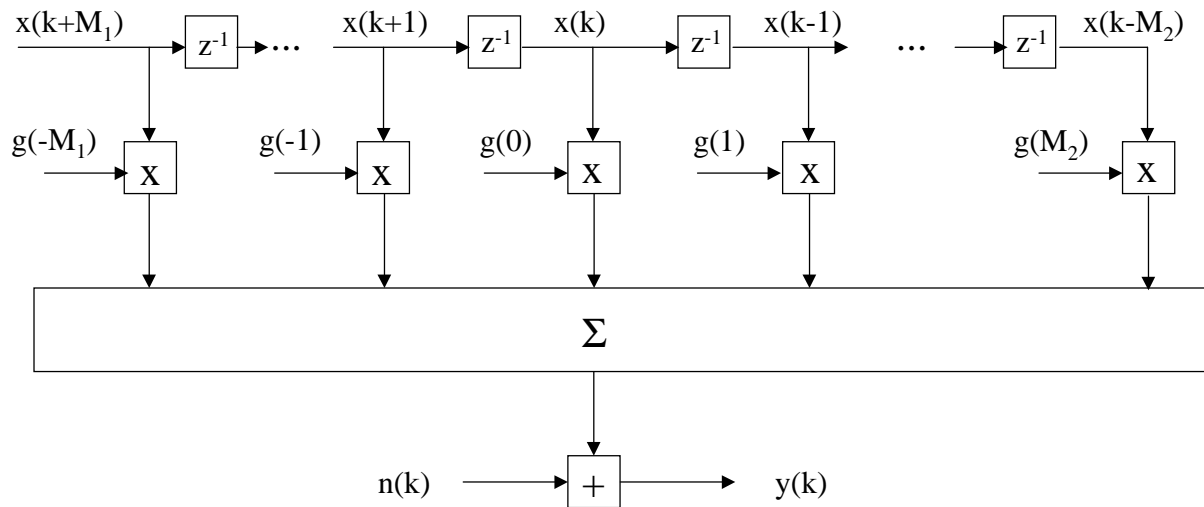


Fig. 1-17 : discrete-time LTI channel model, with detail of LTI filter operation

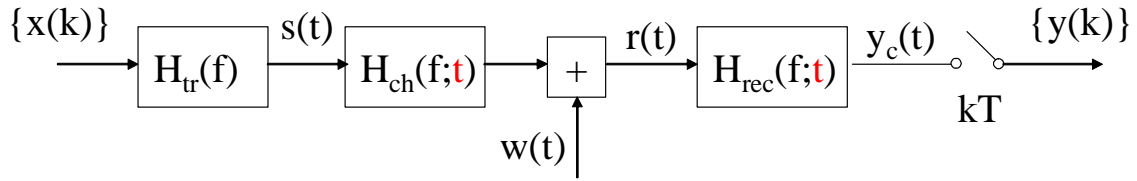


Fig. 1-18 : transmit filter, LTV channel, receive filter and sampling

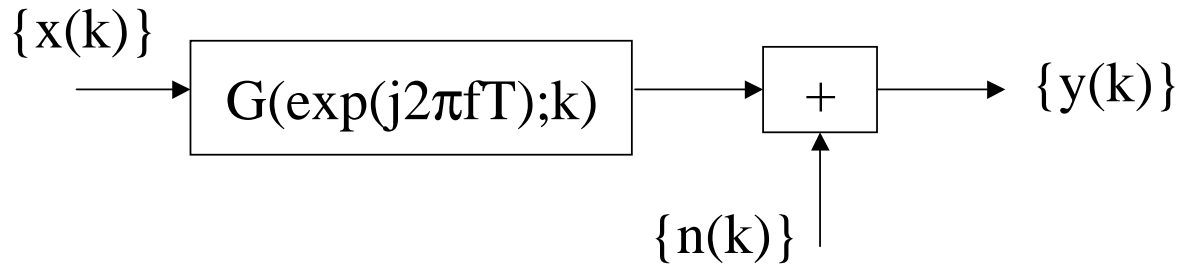


Fig. 1-19 : discrete-time LTV channel model

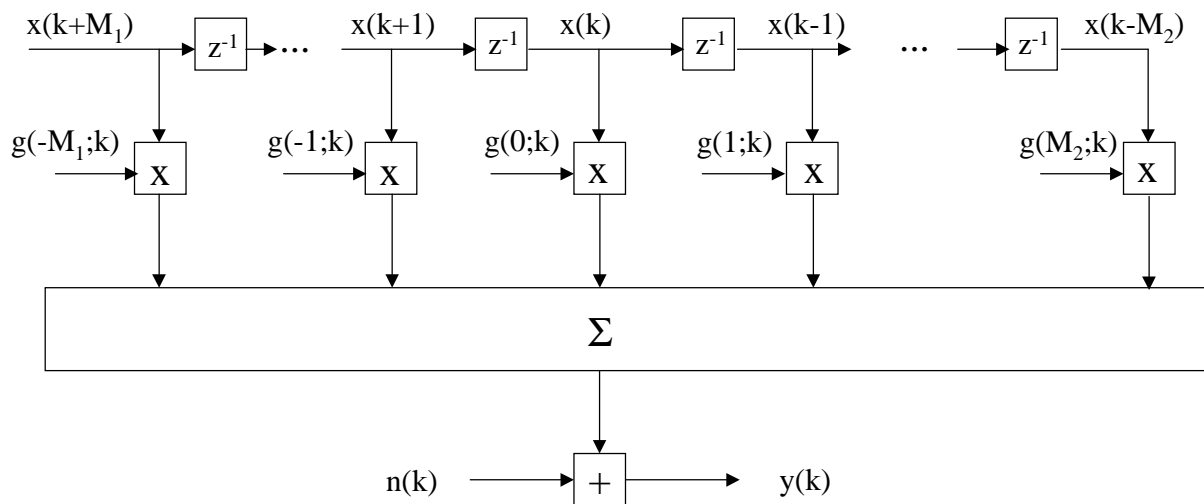


Fig. 1-20 : discrete-time LTV channel model, with detail of LTV filter operation

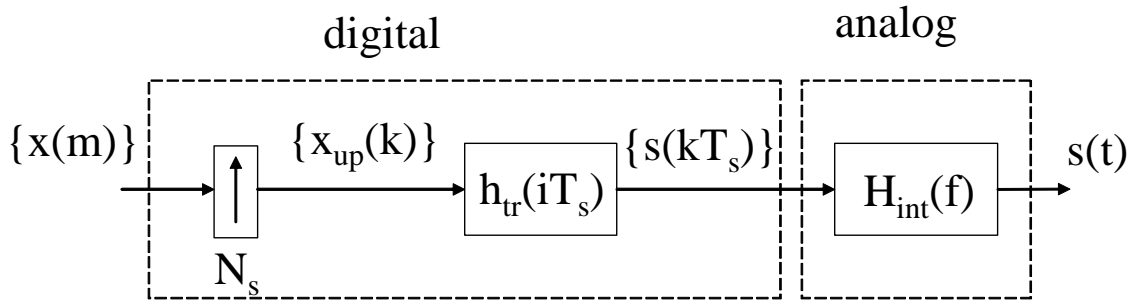


Fig. 1-21 : Practical implementation of transmitter

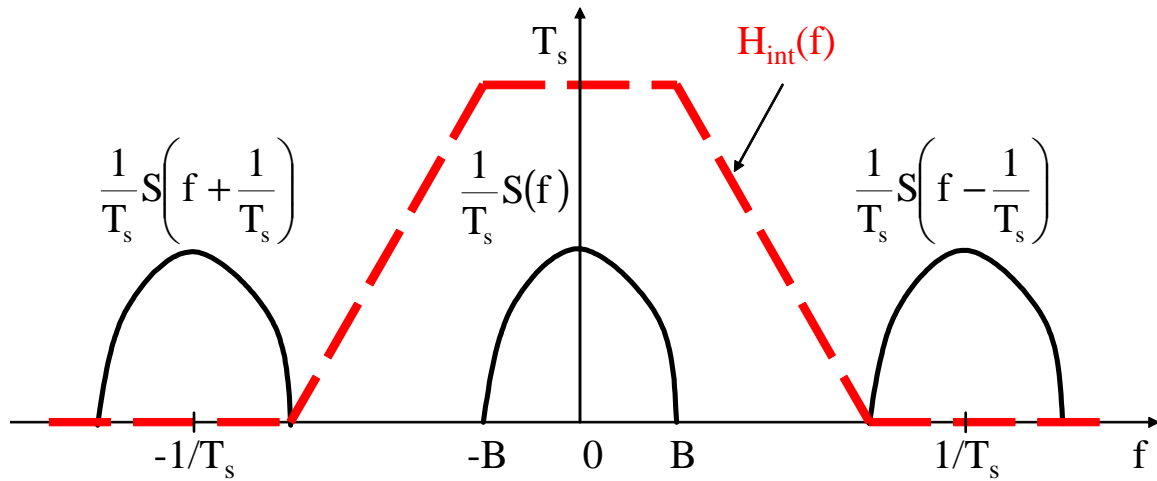


Fig. 1-22 : Conditions on interpolation filter

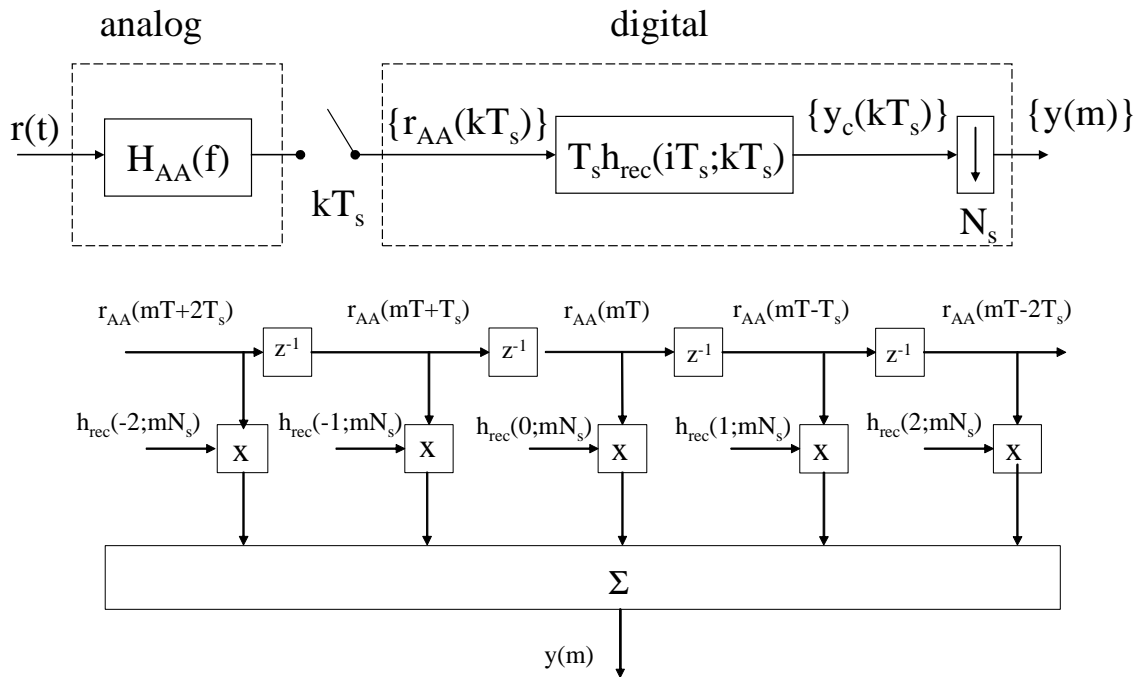


Fig. 1-23 : Practical implementation of receiver (with detail of digital part)

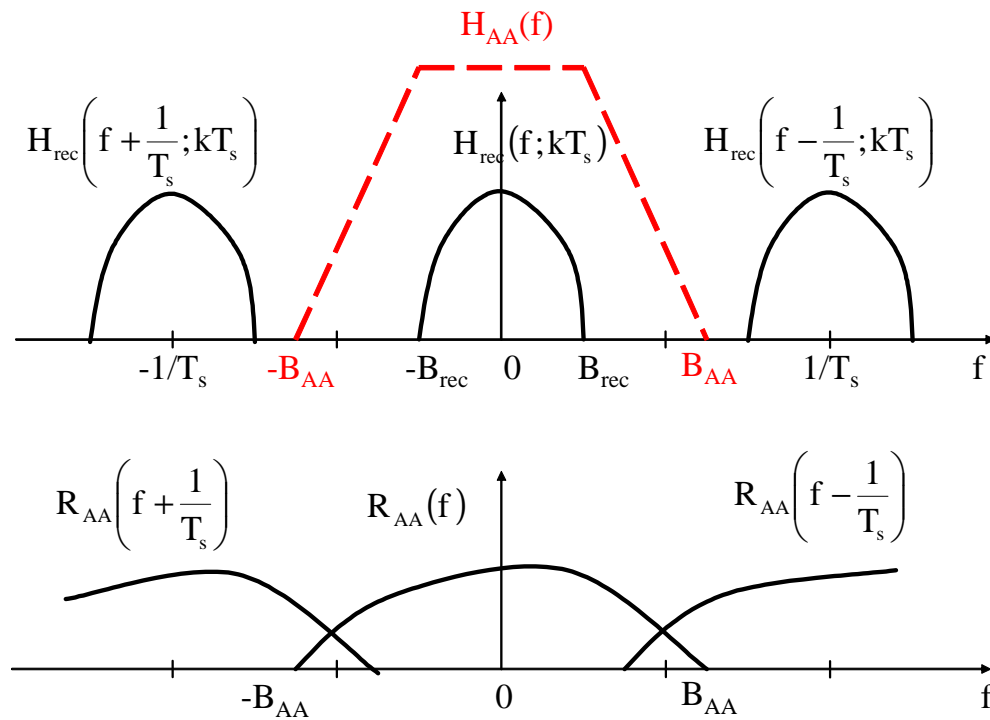
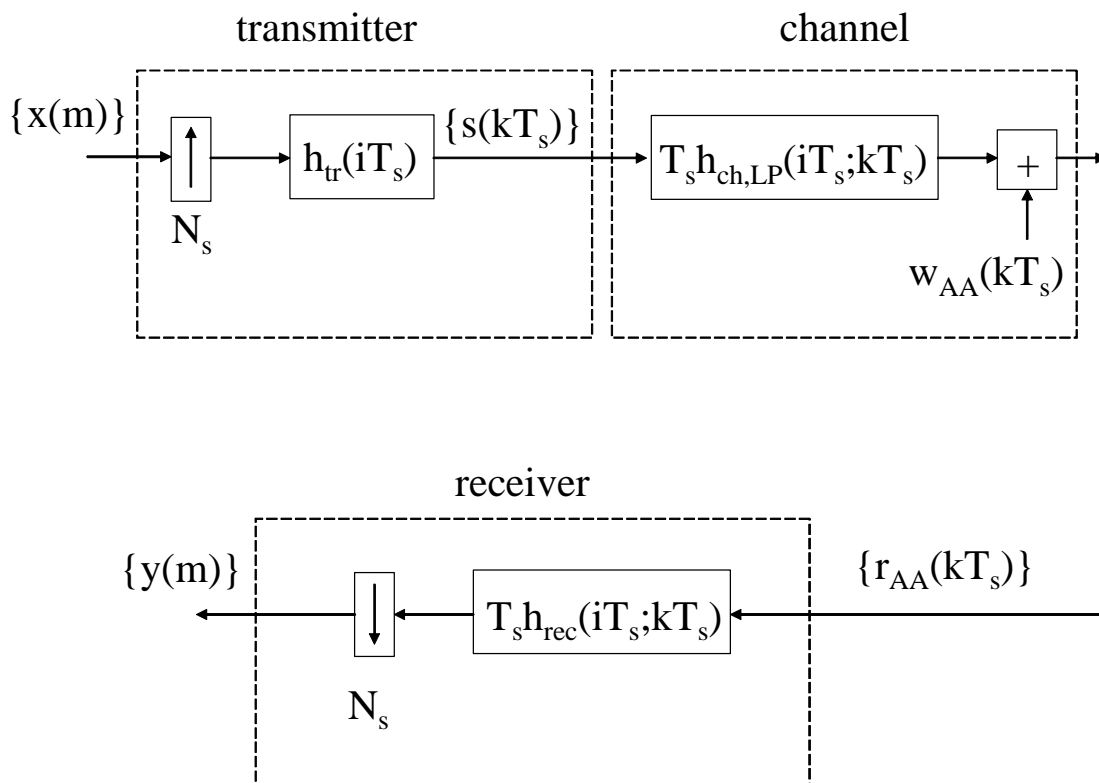
Fig. 1-24 : No aliasing inside  $(-B_{\text{rec}}, B_{\text{rec}})$ 

Fig. 1-25 : Discrete-time simulation model



## Chapter 2

### Notions about estimation and decision theory

In digital communications, the task of the receiver is to extract with high reliability the digital information contained in the received signal. In order to do so, the receiver first needs the value of some unknown parameters of the received signal, such as amplitude and carrier phase. The derivation of receiver algorithms for extracting the digital information and the unknown signal parameters is based on *estimation and decision theory*, which belongs to the field of statistics.

#### 2.1. Definitions

We consider a *probabilistic mapping*  $\mathbf{x} \rightarrow \mathbf{r}$  that transforms a parameter vector  $\mathbf{x}$  into an observation vector  $\mathbf{r}$ . Whereas in a deterministic mapping the observation  $\mathbf{r}$  is fully determined for given  $\mathbf{x}$  (i.e.,  $\mathbf{r}$  is a function of  $\mathbf{x}$ ), in a probabilistic mapping the parameter  $\mathbf{x}$  determines the probability density function (pdf) of  $\mathbf{r}$ , rather than  $\mathbf{r}$  itself. The pdf of  $\mathbf{r}$  that corresponds to a parameter value  $\mathbf{x}$  is denoted  $p(\mathbf{r}|\mathbf{x})$ . In general, it is not possible to determine  $\mathbf{x}$  unambiguously from  $\mathbf{r}$  : when two different parameter values  $\mathbf{x}_1$  and  $\mathbf{x}_2$  yield functions  $p(\mathbf{r}|\mathbf{x}_1)$  and  $p(\mathbf{r}|\mathbf{x}_2)$  with overlapping domains, the value of  $\mathbf{x}$  cannot be derived from the observation when  $\mathbf{r}$  belongs to the intersection of the domains of  $p(\mathbf{r}|\mathbf{x}_1)$  and  $p(\mathbf{r}|\mathbf{x}_2)$ ; this is illustrated in Fig. 2-1, assuming a scalar observation  $r$ . As obtaining  $\mathbf{x}$  from  $\mathbf{r}$  is not possible in general, we instead want to derive from  $\mathbf{r}$  an *estimate*  $\hat{\mathbf{x}}$  of  $\mathbf{x}$ . The estimate  $\hat{\mathbf{x}}$  is a deterministic function of  $\mathbf{r}$ , denoted as  $\hat{\mathbf{x}} = \varepsilon(\mathbf{r})$  : the value of the estimate  $\hat{\mathbf{x}}$  is completely determined by the value of the observation  $\mathbf{r}$ . As  $\mathbf{r}$  is a random variable,  $\hat{\mathbf{x}} = \varepsilon(\mathbf{r})$  is also a random variable.

In order to define the quality of the estimate, we introduce a *cost function*  $C(\hat{\mathbf{x}}, \mathbf{x})$  that has a minimum for  $\hat{\mathbf{x}} = \mathbf{x}$ . The *risk*  $R$ , which is defined as the average of the cost  $C(\hat{\mathbf{x}}, \mathbf{x})$ , serves as quality measure of the estimate  $\hat{\mathbf{x}} = \varepsilon(\mathbf{r})$  :

$$R = E_{\mathbf{r}, \mathbf{x}}[C(\hat{\mathbf{x}}, \mathbf{x})] = \iint C(\varepsilon(\mathbf{r}), \mathbf{x}) p(\mathbf{r}, \mathbf{x}) d\mathbf{r} d\mathbf{x} \quad (2.1-1)$$

where  $E_{\mathbf{r}, \mathbf{x}}[.]$  denotes averaging over  $\mathbf{r}$  and  $\mathbf{x}$ , and  $p(\mathbf{r}, \mathbf{x})$  is the joint pdf of  $\mathbf{r}$  and  $\mathbf{x}$ . The value of the risk  $R$  depends on how we select the function  $\varepsilon(.)$ . The optimum estimate is the function  $\varepsilon(.)$  that minimizes the risk  $R$ .

The joint pdf  $p(\mathbf{r}, \mathbf{x})$ , to be used in (2.1-1), can be factored in the following ways :

$$p(\mathbf{r}, \mathbf{x}) = p(\mathbf{r}|\mathbf{x})p(\mathbf{x}) = p(\mathbf{x}|\mathbf{r})p(\mathbf{r}) \quad (2.1-2)$$

The definition and interpretation of these factors is as follows.

- The pdf  $p(\mathbf{x})$  is the *a priori* distribution of  $\mathbf{x}$  : it indicates what we know about  $\mathbf{x}$  when we have no access to the observation  $\mathbf{r}$ .
- The pdf  $p(\mathbf{r}|\mathbf{x})$ , viewed as a function of  $\mathbf{x}$  for given  $\mathbf{r}$ , is called the *likelihood function* of  $\mathbf{x}$ : it indicates the likelihood of the event that the parameter value  $\mathbf{x}$  gives rise to a given observation  $\mathbf{r}$ ;  $p(\mathbf{r}|\mathbf{x})$  represents the knowledge about  $\mathbf{x}$  we get from the observation  $\mathbf{r}$ . We will often make use of  $\ln(p(\mathbf{r}|\mathbf{x}))$ , which is called the *log-likelihood function*.
- The pdf  $p(\mathbf{r})$  is the marginal distribution of the observation  $\mathbf{r}$  :

$$p(\mathbf{r}) = \int p(\mathbf{r}, \mathbf{x})d\mathbf{x} = \int p(\mathbf{r} | \mathbf{x})p(\mathbf{x})d\mathbf{x} \quad (2.1-3)$$

As  $p(\mathbf{r})$  does not depend on  $\mathbf{x}$ , it provides no information about  $\mathbf{x}$ .

- The pdf  $p(\mathbf{x}|\mathbf{r}) = p(\mathbf{r}|\mathbf{x})p(\mathbf{x})/p(\mathbf{r})$  is the *a posteriori* distribution of  $\mathbf{x}$  : it represents our *total knowledge* about  $\mathbf{x}$ , combining the a priori knowledge  $p(\mathbf{x})$  and the knowledge  $p(\mathbf{r}|\mathbf{x})$  from the observation  $\mathbf{r}$ . Note that  $1/p(\mathbf{r})$  (with  $p(\mathbf{r})$  given by (2.1-3)) is merely a normalization factor yielding  $\int p(\mathbf{x} | \mathbf{r})d\mathbf{x} = 1$ .

### Example

We consider the case of a scalar observation :

$$r = x + w \quad (2.1-4)$$

where  $x$  has a triangular a priori distribution  $p(x)$  given by

$$p(x) = \begin{cases} 2 - 4|x| & |x| < 0.5 \\ 0 & \text{otherwise} \end{cases} \quad (2.1-5)$$

and  $w \sim N(0, \sigma^2)$ . Hence,  $p(r|x)$  is a Gaussian distribution with mean  $x$  and variance  $\sigma^2$ . Figs. 2-2 and 2-3 show, for  $\sigma = 0.1$  and  $\sigma = 0.7$  respectively, the a priori pdf  $p(x)$ , the likelihood function  $p(r|x)$ , and the a posteriori pdf  $p(x|r)$  as a function of  $x$ , for  $r = -0.20$  and  $r = 0.65$ .

- The a priori distribution  $p(x)$  tells that  $x$  is in  $(-1/2, 1/2)$ , with the highest probability occurring at  $x = 0$ .
- The likelihood function  $p(r|x)$  tells that  $x = r$  is the most likely value of  $x$ , even when  $r$  is not in the interval  $(-1/2, 1/2)$  :  $p(r|x)$  is determined by the observation model only, and does *not* take a priori information about  $x$  into account.

- The pdf  $p(x|r)$  combines the information provided by  $p(x)$  and  $p(r|x)$ .
  - For  $\sigma = 0.7$ ,  $p(r|x)$  is much broader than  $p(x)$ , so that  $p(r|x)$  does not change much in the interval  $(-1/2, 1/2)$ . Hence,  $p(x|r)$  and  $p(x)$  are very similar, which indicates that the information  $p(r|x)$  provided by observing  $r$  is not important as compared to the a priori information  $p(x)$ .
  - For  $\sigma = 0.1$ ,  $p(x)$  is much broader than  $p(r|x)$ . When  $r$  is in the interval  $(-1/2, 1/2)$ ,  $p(x)$  does not change much over the interval  $(r-2\sigma, r+2\sigma)$  in which  $p(r|x)$  is concentrated. Hence,  $p(x|r)$  and  $p(r|x)$  are very similar, which indicates that the a priori information  $p(x)$  is not important as compared to the information  $p(r|x)$  provided by observing  $r$ . When  $r$  is not in the interval  $(-1/2, 1/2)$ ,  $p(x|r)$  takes large values near the edge of the interval closest to  $r$  : this is a compromise between  $p(x)$  telling that  $x$  is inside  $(-1/2, 1/2)$  and  $p(r|x)$  telling that  $x$  is likely to equal  $r$  which is outside  $(-1/2, 1/2)$ .

## 2.2. Detection and estimation

Depending on whether  $\mathbf{x}$  is a discrete or a continuous parameter, we distinguish between *detection* and *estimation*.

Suppose  $\mathbf{x}$  is a discrete parameter that can take values from a *finite* (or a countably infinite) set  $X$ . A typical example in the context of digital communications is the parameter  $\mathbf{x}$  representing a string of bits. Estimation of a discrete parameter is called *detection*, and the resulting estimate is called a *decision*. The decision  $\hat{\mathbf{x}} = \varepsilon(\mathbf{r})$  also belongs to the set  $X$ . Hence, a decision rule corresponds to a partitioning of the observation space into *decision regions*, with each region associated to a different element from  $X$ . A convenient performance measure when dealing with a discrete parameter  $\mathbf{x}$  is the *decision error probability*  $P_e = \Pr[\hat{\mathbf{x}} \neq \mathbf{x}]$ ;  $P_e$  is the risk  $R$  that corresponds to the cost function  $C(\hat{\mathbf{x}}, \mathbf{x}) = 0$  for  $\hat{\mathbf{x}} = \mathbf{x}$  and  $C(\hat{\mathbf{x}}, \mathbf{x}) = 1$  for  $\hat{\mathbf{x}} \neq \mathbf{x}$ . It can be shown that the decision error probability  $P_e$  is minimized by the *maximum a posteriori probability* (MAP) detector :

$$\hat{\mathbf{x}} = \varepsilon(\mathbf{r}) = \arg \max_{\tilde{\mathbf{x}} \in X} \Pr[\mathbf{x} = \tilde{\mathbf{x}} | \mathbf{r}] = \arg \max_{\tilde{\mathbf{x}} \in X} \ln \Pr[\mathbf{x} = \tilde{\mathbf{x}} | \mathbf{r}] \quad \text{MAP detector} \quad (2.2-1)$$

In (2.2-1),  $\Pr[\mathbf{x} = \tilde{\mathbf{x}} | \mathbf{r}]$  is the a posteriori probability mass function (pmf) of  $\mathbf{x}$ , i.e., the probability that  $\mathbf{x} = \tilde{\mathbf{x}}$ , conditioned on the value of the observation  $\mathbf{r}$ . The second equality in (2.2-1) holds because  $\ln(\cdot)$  is a monotonically increasing function. Making use of Bayes' rule, we obtain :

$$\Pr[\mathbf{x} = \tilde{\mathbf{x}} | \mathbf{r}] = \frac{p(\tilde{\mathbf{x}}, \mathbf{r})}{p(\mathbf{r})} = \frac{p(\mathbf{r} | \tilde{\mathbf{x}}) \Pr[\mathbf{x} = \tilde{\mathbf{x}}]}{p(\mathbf{r})} \quad (2.2-2)$$

where  $\Pr[\mathbf{x}=\tilde{\mathbf{x}}]$  is the a priori probability mass function of  $\mathbf{x}$ . Taking into account that  $p(\mathbf{r})$  does not depend on  $\tilde{\mathbf{x}}$ , the MAP detector reduces to

$$\begin{aligned}\hat{\mathbf{x}} = \varepsilon(\mathbf{r}) &= \arg \max_{\tilde{\mathbf{x}} \in X} \Pr[\mathbf{x} = \tilde{\mathbf{x}}] p(\mathbf{r} | \tilde{\mathbf{x}}) \\ &= \arg \max_{\tilde{\mathbf{x}} \in X} (\ln \Pr[\mathbf{x} = \tilde{\mathbf{x}}] + \ln p(\mathbf{r} | \tilde{\mathbf{x}}))\end{aligned}\quad \text{MAP detector} \quad (2.2-3)$$

In many cases,  $\mathbf{x}$  is uniformly distributed over the elements of  $X$ , so that  $\Pr[\mathbf{x}=\tilde{\mathbf{x}}]$  does not depend on  $\tilde{\mathbf{x}}$ . For a uniform a priori distribution, the MAP detector reduces to the *maximum-likelihood* (ML) detector, which maximizes the (log-)likelihood function :

$$\hat{\mathbf{x}} = \varepsilon(\mathbf{r}) = \arg \max_{\tilde{\mathbf{x}} \in X} p(\mathbf{r} | \tilde{\mathbf{x}}) = \arg \max_{\tilde{\mathbf{x}} \in X} \ln p(\mathbf{r} | \tilde{\mathbf{x}}) \quad \text{ML detector} \quad (2.2-4)$$

The ML detector can also be used when the a priori distribution of  $\mathbf{x}$  is not known, or when we do not want to take the a priori distribution into account.

We refer to *estimation*, when  $\mathbf{x}$  takes values from a *continuous* set  $X$ . A typical example in the context of digital communications is  $\mathbf{x}$  representing a set of signal parameters, such as amplitude, carrier phase, time delay or frequency offset. The estimate  $\hat{\mathbf{x}} = \varepsilon(\mathbf{r})$  also belongs to the set  $X$ . A convenient performance measure when dealing with a continuous parameter  $\mathbf{x}$  is the *mean square error* (MSE)  $E_{\mathbf{r}, \mathbf{x}}[|\hat{\mathbf{x}} - \mathbf{x}|^2]$ , which is the risk  $R$  corresponding to the cost function  $C(\hat{\mathbf{x}}, \mathbf{x}) = |\hat{\mathbf{x}} - \mathbf{x}|^2$ . It can be shown that the MSE is minimized when  $\hat{\mathbf{x}}(\mathbf{r})$  equals the a posteriori expectation of  $\mathbf{x}$  :

$$\hat{\mathbf{x}} = \int \mathbf{x} p(\mathbf{x} | \mathbf{r}) d\mathbf{x} \quad \text{minimum MSE estimator} \quad (2.2-5)$$

where  $p(\mathbf{x}|\mathbf{r})$  is the a posteriori pdf of  $\mathbf{x}$ . However, in many cases the a posteriori expectation is hard to compute. Therefore, we resort to a simpler estimate, such as the *maximum a posteriori probability* (MAP) estimate :

$$\begin{aligned}\hat{\mathbf{x}} = \varepsilon(\mathbf{r}) &= \arg \max_{\tilde{\mathbf{x}} \in X} p(\tilde{\mathbf{x}} | \mathbf{r}) = \arg \max_{\tilde{\mathbf{x}} \in X} \ln p(\tilde{\mathbf{x}} | \mathbf{r}) \\ &= \arg \max_{\tilde{\mathbf{x}} \in X} p(\tilde{\mathbf{x}}) p(\mathbf{r} | \tilde{\mathbf{x}}) = \arg \max_{\tilde{\mathbf{x}} \in X} (\ln p(\tilde{\mathbf{x}}) + \ln p(\mathbf{r} | \tilde{\mathbf{x}}))\end{aligned}\quad \text{MAP estimator} \quad (2.2-6)$$

When  $\mathbf{x}$  is uniformly distributed over  $X$ ,  $p(\tilde{\mathbf{x}})$  does not depend on  $\tilde{\mathbf{x}}$ . For a uniform a priori distribution, the MAP estimator reduces to the *maximum-likelihood* (ML) estimator, which maximizes the (log-)likelihood function :

$$\hat{\mathbf{x}} = \varepsilon(\mathbf{r}) = \arg \max_{\tilde{\mathbf{x}} \in X} p(\mathbf{r} | \tilde{\mathbf{x}}) = \arg \max_{\tilde{\mathbf{x}} \in X} (\ln p(\mathbf{r} | \tilde{\mathbf{x}})) \quad \text{ML estimator} \quad (2.2-7)$$

The ML estimator can also be used when the a priori distribution of  $\mathbf{x}$  is not known, when we do not want to take the a priori distribution into account, or when  $\mathbf{x}$  is an unknown deterministic parameter.

**Example : estimation**

We consider the case of a scalar real-valued observation :  $r = x + w$ , where  $x$  is uniformly distributed in  $(-1/2, 1/2)$ , and  $w \sim N(0, \sigma^2)$ . As  $p(x)$  is uniform, the ML estimate is the same as the MAP estimate. Taking into account that, for given  $x$ ,  $r \sim N(x, \sigma^2)$ , we obtain

$$\ln p(r | x) = -\ln(\sqrt{2\pi}\sigma) - \frac{(r-x)^2}{2\sigma^2} \propto \frac{-(r-x)^2}{2\sigma^2} \quad (2.2-8)$$

We use the symbol " $\propto$ " to indicate that the expressions on both sides of " $\propto$ " are the same within a term not depending on the parameter to be estimated/detected; in (2.2-8), this parameter is the scalar  $x$ . Hence, the MAP (or ML) estimate is given by

$$\hat{x} = \begin{cases} r & r \in (-1/2, 1/2) \\ -1/2 & r < -1/2 \\ 1/2 & r > 1/2 \end{cases} \quad (2.2-9)$$

**Example : detection**

We consider again the previous example, but now we assume that  $x$  is a discrete parameter with  $\Pr[x=1] = \Pr[x=-1] = 1/2$ . ML detection of  $x$  involves maximizing (2.2-8) over  $x \in \{-1, 1\}$ . As  $x$  has a uniform a priori pmf, ML detection is the same as MAP detection. ML detection yields

$$\ln p(r | x = 1) \underset{\hat{x}=-1}{\overset{\hat{x}=1}{>}} \ln p(r | x = -1) \quad (2.2-10)$$

which according to (2.2-8) reduces to

$$r \underset{\hat{x}=-1}{\overset{\hat{x}=1}{>}} 0 \quad (2.2-11)$$

Hence, the MAP (or ML) decision is given by  $\hat{x} = \text{sgn}(r)$ .

**Example : decoding on the binary symmetric channel (detection)**

A sequence  $\mathbf{b} = (b_1, \dots, b_k)$  of  $k$  information bits ( $b_i \in \{0,1\}$ ) is applied to an encoder for protection against transmission errors. This yields the binary codeword  $\mathbf{c} = (c_1, \dots, c_n)$ , which we denote as  $\chi(\mathbf{b})$ , with  $\chi(\cdot)$  representing the encoding function; the  $2^k$  codewords are a subset of the  $2^n$  binary sequences of length  $n$ . The codeword  $\mathbf{c}$  is transmitted over a binary symmetric

channel (BSC) with error probability  $p$  ( $p < 1/2$ ). The binary channel output  $\mathbf{r} = (r_1, \dots, r_n)$  is characterized by the following likelihood function :

$$\Pr[\mathbf{r} = \boldsymbol{\alpha} | \mathbf{c}] = \prod_{i=1}^n \Pr[r_i = \alpha_i | c_i] \quad (2.2-12)$$

with  $\alpha_i = (\boldsymbol{\alpha})_i \in \{0,1\}$ , and

$$\Pr[r_i = \alpha_i | c_i] = \begin{cases} 1-p & \alpha_i = c_i \\ p & \alpha_i \neq c_i \end{cases} \quad (2.2-13)$$

Assuming that the information bits are statistically independent and  $\Pr[b_i = 0] = \Pr[b_i = 1] = 1/2$ , all  $2^k$  information sequences have the same a priori probability  $2^{-k}$ , so that MAP detection reduces to ML detection. The likelihood function is given by

$$\Pr[\mathbf{r} = \boldsymbol{\alpha} | \tilde{\mathbf{b}}] = \Pr[\mathbf{r} = \boldsymbol{\alpha} | \mathbf{c} = \chi(\tilde{\mathbf{b}})] = (1-p)^{n-d} p^d \propto \left( \frac{1-p}{p} \right)^{-d} \quad (2.2-14)$$

where  $d = d_H(\mathbf{r}, \chi(\tilde{\mathbf{b}}))$  is the Hamming distance between the received sequence  $\mathbf{r}$  and the codeword  $\tilde{\mathbf{c}} = \chi(\tilde{\mathbf{b}})$  that corresponds to the information sequence  $\tilde{\mathbf{b}}$ . For  $p < 1/2$ , we have  $(1-p)/p > 1$ , so that (2.2-14) is a decreasing function of  $d$ . Hence, the ML decoding rule becomes

$$\hat{\mathbf{b}} = \arg \min_{\tilde{\mathbf{b}}} d_H(\mathbf{r}, \chi(\tilde{\mathbf{b}})) \quad (2.2-15)$$

which corresponds to looking for the codeword  $\hat{\mathbf{c}}$  that has the smallest Hamming distance to the received word  $\mathbf{r}$ , and delivering the information word  $\hat{\mathbf{b}} = \chi^{-1}(\hat{\mathbf{c}})$  that corresponds to  $\hat{\mathbf{c}}$ . When a convolutional code is used, (2.2-15) results in the Viterbi algorithm.

### 2.3. Sufficient statistic and reversible transformation

It often turns out that  $\ln(p(\mathbf{r}|\mathbf{x})) \propto g(\boldsymbol{\varphi}(\mathbf{r}), \mathbf{x})$ , with  $\boldsymbol{\varphi}(\mathbf{r})$  denoting a vector function of  $\mathbf{r}$ . When this is the case, it is sufficient to observe  $\mathbf{z} = \boldsymbol{\varphi}(\mathbf{r})$  instead of  $\mathbf{r}$  itself to make an estimate of  $\mathbf{x}$  (or a decision about  $\mathbf{x}$  when  $\mathbf{x}$  is a discrete random variable). We call  $\mathbf{z} = \boldsymbol{\varphi}(\mathbf{r})$  a *sufficient statistic* :  $\mathbf{z} = \boldsymbol{\varphi}(\mathbf{r})$  contains all the information from  $\mathbf{r}$  that is needed to estimate  $\mathbf{x}$ . Usually the dimension of  $\mathbf{z}$  is smaller than the dimension of  $\mathbf{r}$  : the transformation  $\boldsymbol{\varphi}(\cdot)$  is *irreversible*, so it is not possible to reconstruct  $\mathbf{r}$  from  $\mathbf{z}$ . This means that going from  $\mathbf{r}$  to  $\mathbf{z}$  gives rise to some loss of information, but the lost information is irrelevant to the estimation of  $\mathbf{x}$ .

We apply a *reversible* transformation  $T(\cdot)$  to the sufficient statistic  $\mathbf{z}$ , which yields the vector  $\mathbf{u} : \mathbf{u} = T(\mathbf{z})$ ,  $\mathbf{z} = T^{-1}(\mathbf{u})$ . As  $T(\cdot)$  is reversible,  $\mathbf{z}$  and  $\mathbf{u}$  contain the exactly the same information, so  $\mathbf{u}$  is also a sufficient statistic for estimating  $\mathbf{x}$ .

Now we define some cost function  $C(\hat{\mathbf{x}}, \mathbf{x})$ , and consider the three estimators that are represented in Fig. 2-4 :

- The first estimator produces from the observation  $\mathbf{r}$  an estimate  $\hat{\mathbf{x}}_1 = \varepsilon_1(\mathbf{r})$  which minimizes the risk  $E_{\mathbf{r}, \mathbf{x}}[C(\varepsilon_1(\mathbf{r}), \mathbf{x})]$  over all  $\varepsilon_1(\cdot)$ . The resulting minimum risk is denoted  $R_1$ .
- The second estimator first computes from the observation  $\mathbf{r}$  a sufficient statistic  $\mathbf{z} = \varphi(\mathbf{r})$ , and then produces from  $\mathbf{z}$  an estimate  $\hat{\mathbf{x}}_2 = \varepsilon_2(\mathbf{z})$  which minimizes the risk  $E_{\mathbf{z}, \mathbf{x}}[C(\varepsilon_2(\mathbf{z}), \mathbf{x})]$  over all  $\varepsilon_2(\cdot)$ . The resulting minimum risk is denoted  $R_2$ .
- The third estimator first computes from the observation  $\mathbf{r}$  a sufficient statistic  $\mathbf{z} = \varphi(\mathbf{r})$ , then applies to  $\mathbf{z}$  a reversible transformation  $T(\cdot)$  yielding  $\mathbf{u} = T(\mathbf{z})$ , and finally produces from  $\mathbf{u}$  an estimate  $\hat{\mathbf{x}}_3 = \varepsilon_3(\mathbf{u})$  which minimizes the risk  $E_{\mathbf{u}, \mathbf{x}}[C(\varepsilon_3(\mathbf{u}), \mathbf{x})]$  over all  $\varepsilon_3(\cdot)$ . The resulting minimum risk is denoted  $R_3$ .

Because both  $\mathbf{z} = \varphi(\mathbf{r})$  and  $\mathbf{u} = T(\varphi(\mathbf{r}))$  are sufficient statistics for estimating  $\mathbf{x}$ , all three estimators are equivalent : as far as the estimation of  $\mathbf{x}$  is concerned, the likelihood functions  $p(\mathbf{r}|\mathbf{x})$ ,  $p(\mathbf{z}|\mathbf{x})$  and  $p(\mathbf{u}|\mathbf{x})$  provide the same information. Therefore, the three estimators are equivalent : they yield the same estimates ( $\hat{\mathbf{x}}_1 = \hat{\mathbf{x}}_2 = \hat{\mathbf{x}}_3$ ) and, hence, the same optimum performance ( $R_1 = R_2 = R_3$ ).

### Example : data symbol detection

We consider the observation model  $\mathbf{r} = \mathbf{a} \cdot \mathbf{h} + \mathbf{w}$ , where all quantities are real-valued, the vectors have dimension  $K \times 1$ , and  $\mathbf{w} \sim N(0, \sigma^2 \mathbf{I}_K)$ . The data symbol  $a$  belongs to a constellation  $C$ . For given  $a$ , it follows from the observation model that  $\mathbf{r} \sim N(\mathbf{a} \cdot \mathbf{h}, \sigma^2 \mathbf{I}_K)$ , so that

$$\ln p(\mathbf{r} | a) = -K \cdot \ln(\sqrt{2\pi}\sigma) - \frac{|\mathbf{r} - \mathbf{a} \cdot \mathbf{h}|^2}{2\sigma^2} \propto \frac{-1}{2\sigma^2} (\lambda a^2 - 2a \cdot (\mathbf{h}^T \mathbf{r})) \quad (2.3-1)$$

where  $\lambda = |\mathbf{h}|^2 = \mathbf{h}^T \mathbf{h}$ .

We note from (2.3-1) that  $\ln(p(\mathbf{r}|a)) \propto g(\varphi(\mathbf{r}), a)$ , with  $\varphi(\mathbf{r}) = \mathbf{h}^T \mathbf{r}$ . Hence,  $z = \mathbf{h}^T \mathbf{r}$  is a sufficient statistic for detecting  $a$ . From the observation model we get  $z = \mathbf{h}^T \mathbf{r} = \lambda a + n$ , where  $n = \mathbf{h}^T \mathbf{w}$ . The variance of  $n$  is obtained as

$$E[|n|^2] = E[(\mathbf{h}^T \mathbf{w})^2] = \mathbf{h}^T \underbrace{E[\mathbf{w} \mathbf{w}^T]}_{\sigma^2 \mathbf{I}_K} \mathbf{h} = \sigma^2 \mathbf{h}^T \mathbf{h} = \sigma^2 \lambda \quad (2.3-2)$$

Hence,  $n \sim N(0, \sigma^2 \lambda)$ . For given  $a$ ,  $z \sim N(\lambda a, \sigma^2 \lambda)$ , so that

$$\ln p(z|a) \propto \frac{-1}{\sigma^2 \lambda} (z - \lambda \cdot a)^2 \propto \frac{-1}{\sigma^2} (\lambda \cdot a^2 - 2z \cdot a) \quad (2.3-3)$$

As  $z$  is a scalar and the observation  $\mathbf{r}$  is a vector of dimension  $K \times 1$ , the transformation from  $\mathbf{r}$  to  $z$  is irreversible. The information from  $\mathbf{r}$  that is lost in the transformation is the component of  $\mathbf{r}$  that is orthogonal to  $\mathbf{h}$ ; as this orthogonal component contains only noise that is statistically independent of  $n$  and of  $a$ , it is irrelevant for detecting  $a$ .

We consider the reversible transformation  $u = z/\lambda$ . For given  $a$ ,  $u \sim N(a, \sigma^2/\lambda)$ , and

$$\ln p(u|a) \propto \frac{-\lambda}{2\sigma^2} (u - a)^2 \propto \frac{-\lambda}{2\sigma^2} (a^2 - 2u \cdot a) \quad (2.3-4)$$

As  $z$  is a sufficient statistic and  $u$  results from a reversible transformation of  $z$ , we conclude that  $p(\mathbf{r}|a)$ ,  $p(z|a)$  and  $p(u|a)$  provide the same information regarding the estimation of  $a$ .

Let us consider ML detection of  $a$ . The decision  $\hat{a}$  is the value of  $\tilde{a} \in \mathcal{C}$  that maximizes  $p(\mathbf{r}|\tilde{a})$ ,  $p(z|\tilde{a})$  or  $p(u|\tilde{a})$  (all three yield the same decision  $\hat{a}$ ); the easiest is to maximize  $p(u|\tilde{a})$ : from (2.3-4) it follows that

$$\hat{a} = \min_{\tilde{a} \in \mathcal{C}} (u - \tilde{a})^2 \quad (2.3-5)$$

which indicates that  $\hat{a}$  is the constellation point that is closest to  $u$ .

## 2.4. Gaussian observation vector

Let us consider the following observation model :

$$\mathbf{r} = \mathbf{s}(\mathbf{x}) + \mathbf{w} \quad (2.4-1)$$

where  $\mathbf{r}$ ,  $\mathbf{s}(\cdot)$  and  $\mathbf{w}$  are complex-valued column vectors of dimension  $K$  :  $\mathbf{s}(\mathbf{x})$  is a deterministic vector function of the parameter  $\mathbf{x}$ , and  $\mathbf{w} \sim N_c(0, N_0 \mathbf{I}_K)$ . Hence, for given  $\mathbf{x}$ , we have  $\mathbf{r} \sim N_c(\mathbf{s}(\mathbf{x}), N_0 \mathbf{I}_K)$ . Taking into account that the components of  $\mathbf{r}$  are statistically independent, the following expression for the log-likelihood function  $\ln(p(\mathbf{r}|\mathbf{x}))$  is obtained :

$$\begin{aligned} \ln p(\mathbf{r}|\mathbf{x}) &= -K \ln(2\pi\sigma_0^2) - \frac{1}{2\sigma_0^2} \sum_k |r_k - s_k(\mathbf{x})|^2 \\ &= -K \ln(2\pi\sigma_0^2) - \frac{1}{2\sigma_0^2} |\mathbf{r} - \mathbf{s}(\mathbf{x})|^2 \\ &\propto -\frac{1}{2\sigma_0^2} |\mathbf{r} - \mathbf{s}(\mathbf{x})|^2 \end{aligned} \quad (2.4-2)$$

where the squared magnitude operator is defined as  $|\mathbf{u}|^2 = \mathbf{u}^H \mathbf{u}$ , and we have introduced  $\sigma_0^2 = N_0/2$ . As far as the maximization of  $\ln(p(\mathbf{r}|\mathbf{x}))$  (ML detector or ML estimator) or  $(\ln(p(\mathbf{r}|\mathbf{x})) + \ln(p(\mathbf{x})))$  (MAP detector or MAP estimator) over  $\mathbf{x}$  is concerned, the term not depending on



$\mathbf{x}$  is immaterial. It follows from (2.4-2) that maximizing  $\ln(p(\mathbf{r}|\mathbf{x}))$  with respect to  $\mathbf{x}$  is equivalent to minimizing over  $\mathbf{x}$  the squared Euclidean distance  $|\mathbf{r} - \mathbf{s}(\mathbf{x})|^2$  between  $\mathbf{r}$  and  $\mathbf{s}(\mathbf{x})$ .

Expanding the squared magnitude in the last line of (2.4-2) yields

$$\begin{aligned} \ln p(\mathbf{r}|\mathbf{x}) &\propto -\frac{1}{2\sigma_0^2} (|\mathbf{r}|^2 - 2\text{Re}[\mathbf{s}^H(\mathbf{x})\mathbf{r}] + |\mathbf{s}(\mathbf{x})|^2) \\ &\propto \frac{1}{2\sigma_0^2} (2\text{Re}[\mathbf{s}^H(\mathbf{x})\mathbf{r}] - |\mathbf{s}(\mathbf{x})|^2) \end{aligned} \quad (2.4-3)$$

where the term in  $|\mathbf{r}|^2$  has been dropped in the second line because it does not depend on  $\mathbf{x}$ .

When  $\mathbf{r}$ ,  $\mathbf{s}(\mathbf{x})$  and  $\mathbf{w}$  are real-valued (with  $\mathbf{w} \sim N_c(0, \sigma_0^2 \mathbf{I}_K)$ ), the expressions (2.4-2) and (2.4-3) are still valid, with Hermitian conjugate  $(.)^H$  replaced by transpose  $(.)^T$ .

### Example : soft decoding on the AWGN channel

A sequence  $\mathbf{b} = (b_1, \dots, b_k)$  of  $k$  information bits ( $b_i \in \{0,1\}$ ) is applied to a channel encoder for protection against transmission errors. This yields the binary codeword  $\mathbf{c} = (c_1, \dots, c_n)$ . The binary codeword is mapped to a sequence  $\mathbf{a}$  of symbols that belong to an  $M$ -ary constellation  $\mathcal{C}$ . The sequence  $\mathbf{a}$  has  $K = n/\log_2(M)$  components, but only a subset of  $2^k$  symbol sequences from the set  $\mathcal{C}^K$  (which contains  $2^n$  elements) are valid sequences. We denote  $\mathbf{a} = \chi(\mathbf{b})$ , with  $\chi(.)$  representing the concatenation of the encoding and the mapping function. The symbol sequence  $\mathbf{a}$  is transmitted over an AWGN channel, yielding  $\mathbf{r} = \mathbf{a} + \mathbf{w}$  with  $\mathbf{w} \sim N_c(0, \mathbf{I}_K)$ . Assuming that the information bits are statistically independent and  $\Pr[b_i = 0] = \Pr[b_i = 1] = 1/2$ , all  $2^k$  information sequences have the same a priori probability  $2^{-k}$ , so that MAP detection reduces to ML detection. This yields

$$\hat{\mathbf{b}} = \arg \min_{\mathbf{b}} |\mathbf{r} - \chi(\mathbf{b})|^2 \quad (2.4-4)$$

which corresponds to looking for the valid symbol sequence  $\hat{\mathbf{a}}$  that has the smallest Euclidean distance to the received sequence  $\mathbf{r}$ , and delivering the information word  $\hat{\mathbf{b}} = \chi^{-1}(\hat{\mathbf{a}})$  that corresponds to  $\hat{\mathbf{a}}$ . In the case of convolutional encoding and 2-PSK or 4-QAM mapping, (2.4-4) gives rise to the Viterbi algorithm.

## 2.5. Continuous-time Gaussian observation

Let us now consider a continuous-time observation model :

$$\mathbf{r}(t) = \mathbf{s}(t; \mathbf{x}) + \mathbf{w}(t) \quad (2.5-1)$$

where  $\mathbf{r}(t)$ ,  $\mathbf{s}(t; \mathbf{x})$  and  $\mathbf{w}(t)$  are complex-valued, with  $\mathbf{w}(t)$  representing additive white Gaussian noise (AWGN) :  $\mathbf{w}(t) \sim N_c(0, N_0\delta(u))$ . It can be shown that the log-likelihood function corresponding to (2.5-1) is given by

$$\begin{aligned} \ln p(\mathbf{r} | \mathbf{x}) &\propto \frac{-1}{N_0} \int |\mathbf{r}(t) - \mathbf{s}(t; \mathbf{x})|^2 dt \\ &\propto \frac{1}{N_0} \int (2 \operatorname{Re}[\mathbf{r}(t) \mathbf{s}^*(t; \mathbf{x})] - |\mathbf{s}(t; \mathbf{x})|^2) dt \end{aligned} \quad (2.5-2)$$

where  $\mathbf{r}$  denotes a vector representation of  $\mathbf{r}(t)$ , and the squared magnitude operator is defined as  $|\mathbf{u}(t)|^2 = \mathbf{u}(t) \mathbf{u}^*(t)$ . Expression (2.5-2) is the continuous-time equivalent of (2.4-2) and (2.4-3). The computation of the log-likelihood function is illustrated in Fig. 2-5.

In some cases the observation consists of more than one signal. This occurs, for example, when a receiver is equipped with several antennas. Denoting the  $n$ -th received signal by  $\mathbf{r}_n(t)$ , with  $n = 0, \dots, N-1$ , we have

$$\mathbf{r}_n(t) = \mathbf{s}_n(t; \mathbf{x}) + \mathbf{w}_n(t) \quad (2.5-3)$$

with  $\mathbf{w}_n(t) \sim N_c(0, N_{0,n}\delta(u))$ ; further, we assume that  $\mathbf{w}_n(t)$  and  $\mathbf{w}_{n'}(t)$  are statistically independent for  $n \neq n'$ . It can be verified that the corresponding log-likelihood function is obtained as

$$\begin{aligned} \ln p(\mathbf{r} | \mathbf{x}) &\propto \sum_{n=0}^{N-1} \frac{-1}{N_{0,n}} \int |\mathbf{r}_n(t) - \mathbf{s}_n(t; \mathbf{x})|^2 dt \\ &\propto \sum_{n=0}^{N-1} \frac{1}{N_{0,n}} \int (2 \operatorname{Re}[\mathbf{r}_n(t) \mathbf{s}_n^*(t; \mathbf{x})] - |\mathbf{s}_n(t; \mathbf{x})|^2) dt \end{aligned} \quad (2.5-4)$$

which is the extension of (2.5-2) to the case of multiple received signals.

The expressions (2.5-2) and (2.5-4) will be used throughout this course. When all signals are real-valued (with  $\mathbf{w}(t) \sim N(0, (N_0/2)\delta(u))$  and  $\mathbf{w}_n(t) \sim N(0, (N_{0,n}/2)\delta(u))$ ), (2.5-2) and (2.5-4) are still valid, and complex conjugation  $(.)^*$  can be dropped.

## 2.6. Cramer-Rao lower bound

Regarding the estimation of a *real-valued*  $N \times 1$  vector parameter  $\mathbf{x}$ , a fundamental performance bound (*Cramer-Rao lower bound*) can be derived. Although the Cramer-Rao bound (CRB) applies to a general observation model, here we restrict our attention to a Gaussian observation vector :  $\mathbf{r} \sim N_c(\mathbf{s}(\mathbf{x}), 2\sigma^2 \mathbf{I}_N)$ .

The CRB is a lower bound on the mean-square estimation error on the individual components of  $\mathbf{x}$  :

$$E_{\mathbf{r},\mathbf{x}}[(\hat{x}_m - x_m)^2] \geq (\mathbf{J}_T^{-1})_{m,m} \quad (2.6-1)$$

where  $\hat{x}_m = \varepsilon_m(\mathbf{r})$ , and  $\mathbf{J}_T$  is an  $N \times N$  matrix given by

$$\mathbf{J}_T = \mathbf{J}_P + E_{\mathbf{x}}[\mathbf{J}] \quad (2.6-2)$$

In (2.6-2),  $\mathbf{J}_P$  is a contribution from the a priori pdf  $p(\mathbf{x})$ , given by

$$(\mathbf{J}_P)_{m,n} = E_{\mathbf{x}} \left[ \frac{\partial \ln p(\mathbf{x})}{\partial x_m} \cdot \frac{\partial \ln p(\mathbf{x})}{\partial x_n} \right] = -E_{\mathbf{x}} \left[ \frac{\partial^2 \ln p(\mathbf{x})}{\partial x_m \partial x_n} \right] \quad (2.6-3)$$

while  $\mathbf{J}$  denotes the Fisher information matrix, which is related to the log-likelihood function  $\ln(p(\mathbf{r}|\mathbf{x}))$  :

$$(\mathbf{J})_{m,n} = \frac{1}{\sigma^2} \left( \text{Re} \left[ \frac{\partial s^H(\mathbf{x})}{\partial x_m} \cdot \frac{\partial s(\mathbf{x})}{\partial x_n} \right] \right) \quad (2.6-4)$$

In (2.6-1)-(2.6-3),  $E_{\mathbf{r},\mathbf{x}}[\dots]$  and  $E_{\mathbf{x}}[\dots]$  denote expectation w.r.t. to the pdf  $p(\mathbf{r}, \mathbf{x})$  and  $p(\mathbf{x})$ , respectively.

When MAP estimation is performed, it can be shown that, in the limit for  $N \rightarrow \infty$  or  $\sigma^2 \rightarrow 0$ , (2.6-1) holds with equality. Hence, for small  $\sigma^2$  and/or large  $N$ , no estimate performs better than the MAP estimate.

When  $\mathbf{x}$  is a complex-valued vector, we construct a real-valued vector  $\mathbf{x}' = (\mathbf{x}_R^T \ \mathbf{x}_I^T)^T$  by stacking the real part  $\mathbf{x}_R$  and the imaginary part  $\mathbf{x}_I$ , and apply the CRB to  $\mathbf{x}'$ .

In the case of a continuous-time Gaussian observation, the Fisher information matrix  $\mathbf{J}$  is determined by

$$(\mathbf{J})_{m,n} = \frac{2}{N_0} \text{Re} \left[ \int \frac{\partial s^*(t; \mathbf{x})}{\partial x_m} \cdot \frac{\partial s(t; \mathbf{x})}{\partial x_n} dt \right] \quad (2.6-5)$$

which is the continuous-time equivalent of (2.6-4).

**Example**

We consider  $r = x + w$ , with  $x \sim N(0, \sigma_x^2)$  and  $w \sim N(0, \sigma_w^2)$ . The MAP estimate and associated CRB are given by

$$\hat{x} = r \frac{\sigma_x^2}{\sigma_x^2 + \sigma_w^2} \quad E_{r,x}[(\hat{x} - x)^2] \geq \frac{\sigma_w^2 \sigma_x^2}{\sigma_x^2 + \sigma_w^2} \quad (2.6-6)$$

When the a priori information is *not* taken into account, we have

$$\hat{x} = r \quad E_{r,x}[(\hat{x} - x)^2] \geq \sigma_w^2 \quad (2.6-7)$$

which is obtained by taking in (2.6-6) the limit for infinite  $\sigma_x$  (so that the a priori distribution  $p(x)$  becomes uniform over a very large range).

It can be shown that in this example the CRBs hold with equality. The estimate that makes use of a priori information performs better than the estimate that ignores a priori information. However, the performance advantage from exploiting a priori information decreases with decreasing  $(\sigma_w/\sigma_x)^2$ .

**2.7. ML detection from Gaussian observation : BER performance**

We consider the  $K \times 1$  Gaussian observation vector  $\mathbf{r}$  from (2.4-1), with  $\mathbf{x}$  replaced by the  $N \times 1$  data symbol vector  $\mathbf{a}$  :  $\mathbf{r} = \mathbf{s}(\mathbf{a}) + \mathbf{w}$ . We assume that the  $N$  entries of  $\mathbf{a}$  are statistically independent and uniformly distributed over an  $M$ -point constellation  $C = \{\alpha_m, m = 1, \dots, M\}$ . According to (2.4-2), the ML detection of  $\mathbf{a}$  reduces to

$$\hat{\mathbf{a}} = \min_{\tilde{\mathbf{a}} \in C^N} |\mathbf{r} - \mathbf{s}(\tilde{\mathbf{a}})|^2 \quad (2.7.0-1)$$

where  $C^N$  is the set of all  $M^N$  vectors  $\{\alpha_i, i = 1, \dots, M^N\}$  of dimension  $N \times 1$ , with entries  $(\alpha_i)_n$  belonging to the constellation  $C$ .

**2.7.1 General BER expression**

Let us investigate the bit error rate (BER) resulting from the ML decision rule (2.7.0-1). The BER is defined as the ratio of the average number of erroneously detected bits in  $\hat{\mathbf{a}}$  to the number of bits transmitted; the latter equals  $N \log_2(M)$ . As each data symbol represents  $\log_2(M)$  bits, the number of bit errors in a detected data symbol  $\hat{a}_n = (\hat{\mathbf{a}})_n$  is between 0 and  $\log_2(M)$ . The total number of bit errors in  $\hat{\mathbf{a}}$  is obtained as the sum of the number of bit errors associated with the individual symbols.

Denoting by  $N_b(\mathbf{a}_i, \mathbf{a}_j)$  the number of bits in which the symbol sequences  $\mathbf{a}_i$  and  $\mathbf{a}_j$  differ, we obtain

$$N_b(\mathbf{a}_i, \mathbf{a}_j) = \sum_{n=1}^N n_b((\mathbf{a}_i)_n, (\mathbf{a}_j)_n) \quad (2.7.1-1)$$

where  $n_b(\alpha_m, \alpha_{m'})$  is the number of bits in which the symbols  $\alpha_m$  and  $\alpha_{m'}$  differ. Hence, the BER can be expressed as

$$\text{BER} = \frac{E[N_b(\mathbf{a}, \hat{\mathbf{a}})]}{N \cdot \log_2(M)} = \frac{1}{N \cdot \log_2(M)} \sum_{i,j=1}^{M^N} N_b(\mathbf{a}_i, \mathbf{a}_j) \Pr[\mathbf{a} = \mathbf{a}_i, \hat{\mathbf{a}} = \mathbf{a}_j] \quad (2.7.1-2)$$

Taking (2.7.1-1) into account, (2.7.1-2) can be transformed into

$$\text{BER} = \frac{1}{N} \sum_{n=1}^N \text{BER}_n \quad (2.7.1-3)$$

where  $\text{BER}_n$  denotes the contribution from the  $n$ -th data symbol to the BER :

$$\text{BER}_n = \frac{E[n_b(a_n, \hat{a}_n)]}{\log_2(M)} = \frac{1}{\log_2(M)} \sum_{m,m'=1}^M n_b(\alpha_m, \alpha_{m'}) \Pr[a_n = \alpha_m, \hat{a}_n = \alpha_{m'}] \quad (2.7.1-4)$$

As (2.7.1-2) and (2.7.1-4) involve the joint probability of two symbol vectors and two symbols, respectively, (2.7.1-4) appears to be simpler than (2.7.1-2); however, it should be noted that the evaluation of  $\Pr[a_n = \alpha_m, \hat{a}_n = \alpha_{m'}]$  requires the summation of  $\Pr[\mathbf{a} = \mathbf{a}_i, \hat{\mathbf{a}} = \mathbf{a}_j]$  over all  $(\mathbf{a}_i, \mathbf{a}_j)$  for which  $((\mathbf{a}_i)_n, (\mathbf{a}_j)_n) = (\alpha_m, \alpha_{m'})$ . Hence, in both cases we need to compute the joint probability of the symbol vectors  $\mathbf{a}$  and  $\hat{\mathbf{a}}$ .

## 2.7.2 BER upper bound

In general, the evaluation of the joint probability  $\Pr[\mathbf{a} = \mathbf{a}_i, \hat{\mathbf{a}} = \mathbf{a}_j]$  turns out to be very difficult, if not impossible. Therefore, we will resort to a simple approximation that provides an upper bound on the BER. First, we write

$$\Pr[\mathbf{a} = \mathbf{a}_i, \hat{\mathbf{a}} = \mathbf{a}_j] = \Pr[\hat{\mathbf{a}} = \mathbf{a}_j | \mathbf{a} = \mathbf{a}_i] \Pr[\mathbf{a} = \mathbf{a}_i] = M^{-N} \Pr[\hat{\mathbf{a}} = \mathbf{a}_j | \mathbf{a} = \mathbf{a}_i] \quad (2.7.2-1)$$

The second equality in (2.7.2-1) reflects that all symbol vectors  $\mathbf{a}_i$  have the same a priori probability  $M^{-N}$ . Next, we denote by  $E_{j,\ell}$  the event that  $\mathbf{a}_j$  has higher likelihood than  $\mathbf{a}_\ell$ , or, equivalently, that  $\mathbf{a}_j$  has the smaller squared Euclidean distance to  $\mathbf{r}$  :

$$E_{j,\ell} = "|\mathbf{r} - \mathbf{s}(\mathbf{a}_j)|^2 < |\mathbf{r} - \mathbf{s}(\mathbf{a}_\ell)|^2" \quad (2.7.2-2)$$

The ML detector selects the symbol vector with the highest likelihood; therefore,

$$\Pr[\hat{\mathbf{a}} = \mathbf{a}_j | \mathbf{a} = \mathbf{a}_i] = \Pr\left[\bigcap_{\ell \neq j} E_{j,\ell} | \mathbf{a} = \mathbf{a}_i\right] \quad (2.7.2-3)$$

As the probability of the intersection of events is less than the probability of a single event, the following upper bound is obtained :

$$\Pr[\hat{\mathbf{a}} = \mathbf{a}_j | \mathbf{a} = \mathbf{a}_i] \leq \Pr[E_{j,i} | \mathbf{a} = \mathbf{a}_i] = \Pr[|\mathbf{r} - \mathbf{s}(\mathbf{a}_j)|^2 < |\mathbf{r} - \mathbf{s}(\mathbf{a}_i)|^2 | \mathbf{a} = \mathbf{a}_i] \quad (2.7.2-4)$$

Hence, we have upper bounded the probability, that  $\mathbf{a}_j$  has the highest likelihood, by the probability, that  $\mathbf{a}_j$  has a higher likelihood than the symbol vector  $\mathbf{a}_i$  actually transmitted. The rightmost probability in (2.7.2-4) is called the pairwise error probability (PEP), and will be denoted  $\text{PEP}_{ji}$ , where the indices  $i$  and  $j$  refer to the transmitted vector  $\mathbf{a}_i$  and to the vector  $\mathbf{a}_j$  with the higher likelihood, respectively :

$$\text{PEP}_{ji} = \Pr[|\mathbf{r} - \mathbf{s}(\mathbf{a}_j)|^2 < |\mathbf{r} - \mathbf{s}(\mathbf{a}_i)|^2 | \mathbf{a} = \mathbf{a}_i] \quad (2.7.2-5)$$

So the upper bound on the BER (2.7.1-2) becomes  $\text{BER} \leq \text{BER}_{\text{up}}$ , with

$$\text{BER}_{\text{up}} = \frac{M^{-N}}{N \cdot \log_2(M)} \sum_{i,j=1}^{M^N} N_b(\mathbf{a}_i, \mathbf{a}_j) \text{PEP}_{ji} \quad (2.7.2-6)$$

Now we derive a simple expression for  $\text{PEP}_{ji}$ . Taking into account that  $\mathbf{r} = \mathbf{s}(\mathbf{a}_i) + \mathbf{w}$  when  $\mathbf{a} = \mathbf{a}_i$ , we obtain from (2.7.2-5) :

$$\begin{aligned} \text{PEP}_{ji} &= \Pr[|\mathbf{r} - \mathbf{s}(\mathbf{a}_j)|^2 < |\mathbf{r} - \mathbf{s}(\mathbf{a}_i)|^2 | \mathbf{a} = \mathbf{a}_i] \\ &= \Pr[|\Delta_{i,j} + \mathbf{w}|^2 < |\mathbf{w}|^2] \end{aligned} \quad (2.7.2-7)$$

where we have introduced

$$\Delta_{i,j} = \mathbf{s}(\mathbf{a}_i) - \mathbf{s}(\mathbf{a}_j) \quad (2.7.2-8)$$

Taking into account that

$$|\Delta_{i,j} + \mathbf{w}|^2 = |\Delta_{i,j}|^2 + 2\text{Re}[\Delta_{i,j}^H \mathbf{w}] + |\mathbf{w}|^2 \quad (2.7.2-9)$$

(2.7.2-5) reduces to

$$\text{PEP}_{ji} = \Pr[2\text{Re}[\Delta_{i,j}^H \mathbf{w}] < -|\Delta_{i,j}|^2] \quad (2.7.2-10)$$

Taking into account that  $\mathbf{w} \sim \mathcal{N}_c(0, 2\sigma_0^2 \mathbf{I}_K)$ , it follows that  $\Delta_{i,j}^H \mathbf{w}$  is a zero-mean circularly symmetric complex-valued Gaussian random variable; its variance is given by

$$E[|\Delta_{i,j}^H \mathbf{w}|^2] = E[\Delta_{i,j}^H \mathbf{w} \mathbf{w}^H \Delta_{i,j}] = 2\sigma_0^2 |\Delta_{i,j}|^2 \quad (2.7.2-11)$$

Consequently,  $2\text{Re}[\Delta_{i,j}^H \mathbf{w}]$  is a zero-mean Gaussian random variable with variance equal to  $4\sigma_0^2 |\Delta_{i,j}|^2$ . When  $x \sim N(0, \sigma)$ , then  $\Pr[x > x_0] = \Pr[x < -x_0] = Q(x_0/\sigma)$ , where the function  $Q(v)$  is defined as

$$Q(v) = \int_v^{+\infty} \frac{1}{\sqrt{2\pi}} \exp\left(-\frac{u^2}{2}\right) du \quad (2.7.2-12)$$

Therefore,  $\text{PEP}_{ji}$  from (2.7.2-10) simply reduces to

$$\text{PEP}_{ji} = Q\left(\frac{d_{i,j}}{2\sigma_0}\right) \quad (2.7.2-13)$$

where  $d_{i,j}^2 = |\Delta_{i,j}|^2 = |\mathbf{s}(\mathbf{a}_i) - \mathbf{s}(\mathbf{a}_j)|^2$  denotes the squared Euclidean distance between  $\mathbf{s}(\mathbf{a}_i)$  and  $\mathbf{s}(\mathbf{a}_j)$ . Using (2.7.2-13) in (2.7.2-6), the BER upper bound becomes

$$\text{BER}_{\text{up}} = \frac{M^{-N}}{N \cdot \log_2(M)} \sum_{i,j=1}^{M^N} N_b(\mathbf{a}_i, \mathbf{a}_j) Q\left(\frac{d_{i,j}}{2\sigma_0}\right) \quad (2.7.2-14)$$

For high signal-to-noise ratio (SNR), i.e., for small  $\sigma_0^2$ , the summation in (2.7.2-14) is dominated by the terms for which the argument of  $Q(\cdot)$  is minimum. Defining

$$d_{\min} = \min_{i \neq j} d_{i,j} \quad (2.7.2-15)$$

as the minimum Euclidean distance between any  $\mathbf{s}(\mathbf{a}_i)$  and  $\mathbf{s}(\mathbf{a}_j)$ , we get

$$\text{BER}_{\text{up}} = C \cdot Q\left(\frac{d_{\min}}{2\sigma_0}\right) + \text{smaller terms} \quad (2.7.2-16)$$

where

$$C = \frac{M^{-N}}{N \cdot \log_2(M)} \sum_{i=1}^{M^N} \sum_{\mathbf{a}_j \in A_i} N_b(\mathbf{a}_i, \mathbf{a}_j) \quad (2.7.2-17)$$

and  $A_i$  is the set of vectors  $\mathbf{a}_j$  for which the Euclidean distance between  $\mathbf{s}(\mathbf{a}_i)$  and  $\mathbf{s}(\mathbf{a}_j)$  equals  $d_{\min}$ . The "smaller terms" correspond to Euclidean distances larger than  $d_{\min}$ , and become negligible for large SNR. It can be shown that the bound becomes very tight at large SNR. It follows from (2.7.2-16) that (the upper bound on) the BER is mainly determined by the ratio of the minimum Euclidean distance  $d_{\min}$  between transmitted vectors to the standard deviation  $\sigma_0$  of the noise.

The same reasoning applies to the case of a continuous-time Gaussian observation, where the received signal is given by  $r(t) = s(t; \mathbf{a}) + w(t)$ , with  $w(t) \sim N_c(0, N_0 \delta(u))$ . The resulting BER upper bound is still given by (2.7.2-14), with  $\sigma_0^2$  replaced by  $N_0/2$ , and

$$d_{i,j}^2 = \int |s(t; \mathbf{a}_i) - s(t; \mathbf{a}_j)|^2 dt \quad (2.7.2-18)$$

denoting the squared Euclidean distance between the transmitted signals  $s(t; \mathbf{a}_i)$  and  $s(t; \mathbf{a}_j)$ .

### 2.7.3 Example

In order to illustrate the accuracy of the BER upper bound, we consider a simple example for which the exact BER is easily obtained. The observation model is given by  $\mathbf{r} = \mathbf{a} + \mathbf{w}$ , where  $\mathbf{w} \sim N_c(0, N_0 \mathbf{I}_N)$  and  $a_n \in \{-1, 1\}$ ,  $n = 1, \dots, N$ .

Let us compute the upper bound  $\text{BER}_{\text{up}}$  from (2.7.2-14). Considering two vectors  $\mathbf{a}_i$  and  $\mathbf{a}_j$  that differ in  $m$  positions, it is easily verified that  $N_b(\mathbf{a}_i, \mathbf{a}_j) = m$  and  $d_{i,j}^2 = 4m$ , so that  $d_{\min} = 2$ ; For given  $\mathbf{a}_i$ , the number of vectors  $\mathbf{a}_j$  that differ from  $\mathbf{a}_i$  in  $m$  positions equals  $C_N^m = \frac{N!}{m!(N-m)!}$ . Hence, we obtain

$$\text{BER}_{\text{up}} = \frac{1}{N} \sum_{m=1}^N C_N^m m Q\left(\frac{\sqrt{m}}{\sigma_0}\right) = Q\left(\frac{1}{\sigma_0}\right) + \text{smaller terms} \quad (2.7.3-1)$$

where "smaller terms" contains the terms with  $m > 1$  from the summation in (2.7.3-1).

As the observation model yields  $r_n = a_n + w_n$ , it follows that the detection of  $a_n$  is based solely on the observation  $r_n$ . Denoting the actual value of  $a_n$  by  $\alpha \in \{-1, 1\}$ , the probability that a bit error occurs during the detection of  $a_k$  is given by

$$\begin{aligned} \Pr[|r_n + \alpha|^2 < |r_n - \alpha|^2 | a_n = \alpha] &= \Pr[|2\alpha + w_n|^2 < |w_n|^2] \\ &= \Pr[4\alpha \text{Re}[w_n] < -4] \\ &= Q\left(\frac{1}{\sigma_0}\right) \end{aligned} \quad (2.7.3-2)$$

Hence, the exact BER is given by  $Q(1/\sigma_0)$ , which equals the dominant term in the upper bound (2.7.3-1).

The BER upper bound (2.7.3-1) and the exact BER (2.7.3-2) are shown in Fig. 2.6 (with  $E_b/N_0 = 1/(2\sigma_0^2)$ ) for different values of  $N$ ; we observe that the bound is very tight at large SNR.



## 2.8. Linear digital modulation

Linear digital modulation refers to the case where the transmitted signal is linear in the transmitted data symbols. In the case of a vector observation model, this means that

$$\mathbf{s}(\mathbf{a}) = \mathbf{H}\mathbf{a} = \sum_{n=1}^N a_n \mathbf{h}_n = a_1 \mathbf{h}_1 + a_2 \mathbf{h}_2 + \cdots + a_N \mathbf{h}_N \quad (2.8.0-1)$$

where  $\mathbf{a}$  is a  $N \times 1$  data symbol vector with entries belonging to a constellation  $\mathcal{C}$ ,  $\mathbf{s}(\mathbf{a})$  is a  $K \times 1$  signal vector,  $\mathbf{H}$  is a  $K \times N$  matrix, and  $\mathbf{h}_n$  denotes the  $n$ -th column of  $\mathbf{H}$ . We consider the vectors  $\mathbf{h}_n$  to be unit vectors :  $\|\mathbf{h}_n\| = 1$ ; hence, the energy associated with the transmission of the symbol  $a_n$  is given by  $E_s = E[|a_n|^2]$ . We restrict our attention to the case where the columns of  $\mathbf{H}$  are linearly independent, so that different symbol vectors  $\mathbf{a}_i$  and  $\mathbf{a}_j$  always give rise to different signal vectors  $\mathbf{s}(\mathbf{a}_i)$  and  $\mathbf{s}(\mathbf{a}_j)$ ; this implies that the number ( $K$ ) of rows cannot be less than the number ( $N$ ) of columns :  $K \geq N$ .

The continuous-time equivalent of (2.8.0-1) is

$$s(t; \mathbf{a}) = \sum_{n=1}^N a_n h_n(t) = a_1 h_1(t) + a_2 h_2(t) + \cdots + a_N h_N(t) \quad (2.8.0-2)$$

with  $h_n(t)$  denoting the unit-energy pulse that "carries" the symbol  $a_n$ ; the pulses  $\{h_n(t), n = 1, \dots, N\}$  are assumed to be linearly independent.

### 2.8.1 ML detector

We consider the observation  $\mathbf{r} = \mathbf{H}\mathbf{a} + \mathbf{w}$ , where  $\mathbf{w} \sim \mathcal{N}_c(0, N_0 \mathbf{I}_K)$  and the entries of  $\mathbf{a}$  are statistically independent. According to (2.7.0-1), ML detection of  $\mathbf{a}$  reduces to

$$\hat{\mathbf{a}} = \arg \min_{\tilde{\mathbf{a}} \in \mathcal{C}^N} \|\mathbf{r} - \mathbf{H}\tilde{\mathbf{a}}\|^2 = \arg \min_{\tilde{\mathbf{a}} \in \mathcal{C}^N} (\tilde{\mathbf{a}}^H \mathbf{H}^H \mathbf{H} \tilde{\mathbf{a}} - 2 \operatorname{Re}[\tilde{\mathbf{a}}^H \mathbf{H}^H \mathbf{r}]) \quad (2.8.1-1)$$

which can be transformed into

$$\begin{aligned} \hat{\mathbf{a}} &= \arg \min_{\tilde{\mathbf{a}} \in \mathcal{C}^N} (\tilde{\mathbf{a}}^H \mathbf{G} \tilde{\mathbf{a}} - 2 \operatorname{Re}[\tilde{\mathbf{a}}^H \mathbf{z}]) \\ &= \arg \min_{\tilde{\mathbf{a}} \in \mathcal{C}^N} \left( \sum_{n,n'=1}^N \tilde{a}_n^* G_{n,n'} \tilde{a}_{n'} - 2 \operatorname{Re} \left[ \sum_{n=1}^N \tilde{a}_n^* z_n \right] \right) \end{aligned} \quad (2.8.1-2)$$

where the  $N \times 1$  vector  $\mathbf{z} = \mathbf{H}^H \mathbf{r}$  is a sufficient statistic, and  $\mathbf{G} = \mathbf{H}^H \mathbf{H}$  is an  $N \times N$  positive definite Hermitian matrix. We have

$$z_n = (\mathbf{z})_n = \mathbf{h}_n^H \mathbf{r} = \sum_{k=1}^K h_{k,n}^* r_k \quad (2.8.1-3)$$

$$G_{n,n'} = (\mathbf{G})_{n,n'} = \mathbf{h}_n^H \mathbf{h}_{n'} = \sum_{k=1}^K h_{k,n}^* h_{k,n'} \quad (2.8.1-4)$$

with  $\mathbf{h}_{k,n} = (\mathbf{H})_{k,n}$ ; note that  $|\mathbf{h}_n| = 1$  implies that the diagonal entries of  $\mathbf{G}$  equal 1 :  $G_{n,n} = 1$ .

The sufficient statistic  $\mathbf{z}$  can be decomposed as

$$\mathbf{z} = \mathbf{H}^H \mathbf{r} = \mathbf{H}^H \mathbf{H} \mathbf{a} + \mathbf{H}^H \mathbf{w} = \mathbf{G} \mathbf{a} + \mathbf{n} \quad (2.8.1-5)$$

where  $\mathbf{n} = \mathbf{H}^H \mathbf{w} \sim N_c(0, N_0 \mathbf{G})$ .

When  $\mathbf{G}$  is non-diagonal, the function to be minimized contains cross-terms of the type  $\tilde{a}_n^* G_{n,n'} \tilde{a}_{n'}$ , involving symbols with different indices. Then, in general, the minimization requires the evaluation of the function for all  $M^N$  possible symbol vectors; hence, the computational complexity of the ML detector increases exponentially with the number (N) of symbols transmitted. Note from (2.8.1-5) that a non-diagonal matrix  $\mathbf{G}$  implies that the entries of  $\mathbf{z}$  are affected by inter-symbol interference (ISI) :  $z_n$  depends not only on the symbol  $a_n$ , but also on other symbols  $a_{n'}$  with  $n' \neq n$ ; also, the entries of the noise vector  $\mathbf{n}$  are correlated.

No such cross-terms occur when  $\mathbf{G}$  is diagonal; according to (2.8.1-4), this happens when the columns of  $\mathbf{H}$  are orthonormal : when

$$\mathbf{h}_n^H \mathbf{h}_{n'} = \sum_{k=1}^K \mathbf{h}_{k,n}^* \mathbf{h}_{k,n'} = \delta_{n-n'} \quad (2.8.1-6)$$

we get  $\mathbf{G} = \mathbf{I}_N$ . When (2.8.1-6) holds, the ML decision rule reduces to

$$\hat{\mathbf{a}} = \arg \min_{\tilde{\mathbf{a}} \in \mathbb{C}^N} \sum_{n=1}^N \left( |\tilde{a}_n|^2 - 2 \operatorname{Re}[\tilde{a}_n^* z_n] \right) \quad (2.8.1-7)$$

As (2.8.1-7) contains no cross-terms, each term in the summation depends on one data symbol only. Hence, the sum is minimized by minimizing each term individually. This yields :

$$\hat{a}_n = \arg \min_{\tilde{a} \in \mathbb{C}} \left( |\tilde{a}|^2 - 2 \operatorname{Re}[\tilde{a}^* z_n] \right) = \arg \min_{\tilde{a} \in \mathbb{C}} |z_n - \tilde{a}|^2, \quad n = 1, 2, \dots, N \quad (2.8.1-8)$$

The ML detection now has become a simple symbol-by-symbol detection rule :  $\hat{a}_n$  is the constellation point closest to  $z_n$ ; the associated computational complexity is linear (rather than exponential) with the number (N) of transmitted data symbols. Note from (2.8.1-5) that a diagonal matrix  $\mathbf{G}$  implies that the entries of  $\mathbf{z}$  are not affected by ISI :  $z_n$  depends on the symbol  $a_n$ , but not on other symbols  $a_{n'}$  with  $n' \neq n$ ; also, the entries of the noise vector  $\mathbf{n}$  are statistically independent.

The above also applies to the continuous-time observation  $r(t) = s(t; \mathbf{a}) + w(t)$ , with  $s(t; \mathbf{a})$  given by (2.8.0-2) and  $w(t) \sim N_c(0, N_0 \delta(u))$ . In this case,  $z_n$  and  $G_{n,n'}$  are obtained as

$$z_n = \int \mathbf{h}_n^*(t) r(t) dt \quad (2.8.1-9)$$

$$G_{n,n'} = \int \mathbf{h}_n^*(t) \mathbf{h}_{n'}(t) dt \quad (2.8.1-10)$$

while the orthogonality condition (2.8.1-6) becomes

$$\int h_n^*(t)h_n(t)dt = \delta_{n-n}, \quad (2.8.1-11)$$

Note that  $z_n$  can be interpreted as the output, at  $t=0$ , of a filter *matched* to  $h_n(t)$  (such filter has an impulse response  $h_n^*(-t)$  and transfer function  $H_n^*(f)$ ) when the filter input equals  $r(t)$ . Similarly,  $G_{n,n'}$  can be considered as the output, at  $t=0$ , of the filter matched to  $h_n(t)$ , when  $h_{n'}(t)$  is applied to the input of the filter.

## 2.8.2 BER performance for diagonal G

First, we consider the standard problem of detecting a data symbol  $a$  from an observation  $r = a + n$ , where  $n \sim N_c(0, N_0)$  and  $a$  belongs to an  $M$ -point constellation  $C$  with equally probable constellation points;  $E[|a|^2] = E_s$  denotes the energy per symbol. The ML decision  $\hat{a}$  is the constellation point that is closest to  $r$ . The resulting BER is a function of the ratio  $E_s/N_0$ , which we denote  $BER_C(E_s/N_0)$ , with the subscript  $C$  referring to the constellation type. For various constellations,  $BER_C(E_s/N_0)$  is well documented in the literature; for 2-PSK (or 2-PAM) and 4-PSK (or 4-QAM) we get

$$\begin{aligned} BER_{2-PAM}\left(\frac{E_s}{N_0}\right)_{E_s=E_b} &= BER_{2-PSK}\left(\frac{E_s}{N_0}\right)_{E_s=E_b} = Q\left(\sqrt{\frac{2E_b}{N_0}}\right) \\ BER_{4-PSK}\left(\frac{E_s}{N_0}\right)_{E_s=2E_b} &= BER_{4-QAM}\left(\frac{E_s}{N_0}\right)_{E_s=2E_b} = Q\left(\sqrt{\frac{2E_b}{N_0}}\right) \end{aligned} \quad (2.8.2-1)$$

where  $E_b = E_s \log_2(M)$  denotes the energy per bit. Applying the reasoning from section 2.7.2 to the observation model  $r = a + n$ , for any constellation we obtain

$$BER_C\left(\frac{E_s}{N_0}\right) \leq \frac{1}{\log_2(M)} \cdot \frac{1}{M} \sum_{m,m'=1}^M n_b(\alpha_m, \alpha_{m'}) Q\left(\sqrt{\frac{e_{m,m'}^2}{2N_0}}\right) \quad (2.8.2-2)$$

where  $e_{m,m'} = |\alpha_m - \alpha_{m'}|$  is the Euclidean distance between the constellation points  $\alpha_m$  and  $\alpha_{m'}$ . Hence, for large SNR (such that the upper bound (2.8.2-2) is tight), we obtain

$$BER_C\left(\frac{E_s}{N_0}\right) \approx C \cdot Q\left(\sqrt{\frac{e_{\min}^2}{2N_0}}\right) + \text{smaller terms} \quad (2.8.2-3)$$

where  $e_{\min}$  is the minimum Euclidean distance between constellation points, and

$$C = \frac{1}{\log_2(M)} \cdot \frac{1}{M} \sum_{m=1}^M \sum_{\alpha_{m'} \in A_m} n_b(\alpha_m, \alpha_{m'}) \quad (2.8.2-4)$$

where  $A_m$  is the set of constellation points that are at distance  $e_{\min}$  from  $\alpha_m$ .

Now we concentrate on the sufficient statistic  $\mathbf{z}$  from (2.8.1-5), associated with the observation  $\mathbf{r} = \mathbf{H}\mathbf{a} + \mathbf{w}$ . For diagonal  $\mathbf{G}$ ,  $\mathbf{z}$  reduces to

$$z_n = a_n + (\mathbf{n})_n \quad n = 1, \dots, N \quad (2.8.2-5)$$

where  $(\mathbf{n})_n \sim N_c(0, N_0)$ . Hence, the BER related to the  $n$ -th symbol  $a_n$  is given by

$$\text{BER}_n = \text{BER}_c\left(\frac{E_s}{N_0}\right) \quad (2.8.2-6)$$

Then the average BER (2.7.1-3) becomes

$$\text{BER} = \frac{1}{N} \sum_{n=1}^N \text{BER}_n = \text{BER}_c\left(\frac{E_s}{N_0}\right) \quad (2.8.2-7)$$

Note that for diagonal  $\mathbf{G}$ , i.e., for orthonormal vectors  $\mathbf{h}_n$ , the BER depends only on the data symbol energy, but not on the specific vectors  $\mathbf{h}_n$ .

### 2.8.3 BER upper and lower bound for non-diagonal $\mathbf{G}$

When  $\mathbf{G}$  is non-diagonal, the BER performance resulting from the ML detection cannot be obtained analytically in general.

The BER is upper bounded by  $\text{BER}_{\text{up}}$  from (2.7.2-14), where in the case of linear modulation the Euclidean distance  $d_{i,j}$  is determined by

$$\begin{aligned} d_{i,j}^2 &= |\mathbf{H}(\mathbf{a}_i - \mathbf{a}_j)|^2 = \boldsymbol{\varepsilon}_{i,j}^H \mathbf{H}^H \mathbf{H} \boldsymbol{\varepsilon}_{i,j} \\ &= \boldsymbol{\varepsilon}_{i,j}^H \mathbf{G} \boldsymbol{\varepsilon}_{i,j} = \sum_{n,n'=1}^N (\boldsymbol{\varepsilon}_{i,j})_n^* G_{n,n'} (\boldsymbol{\varepsilon}_{i,j})_n \end{aligned} \quad (2.8.3-1)$$

with  $\boldsymbol{\varepsilon}_{i,j} = \mathbf{a}_i - \mathbf{a}_j$  denoting the symbol error vector. For large SNR, the BER performance is determined by the minimum squared Euclidean distance, given by

$$d_{\min}^2 = \min_{\boldsymbol{\varepsilon}_{i,j} \neq 0} \boldsymbol{\varepsilon}_{i,j}^H \mathbf{G} \boldsymbol{\varepsilon}_{i,j} \quad (2.8.3-2)$$

Let us consider a symbol error vector  $\boldsymbol{\varepsilon}_{i,j}$  which has only one nonzero entry, say, at position  $n$ . This yields a squared Euclidean distance  $d_{i,j}^2 = |(\boldsymbol{\varepsilon}_{i,j})_n|^2$ , which equals the squared Euclidean distance between the constellation points  $(\mathbf{a}_i)_n$  and  $(\mathbf{a}_j)_n$ . Selecting these constellation points such that their squared Euclidean distance is minimum, we obtain

$$d_{\min}^2 \leq e_{\min}^2 \quad (2.8.3-3)$$

where  $e_{\min}$  denotes the minimum Euclidean distance between constellation points.

Let us derive a lower bound on the BER resulting from any receiver operating on  $\mathbf{r} = \mathbf{H}\mathbf{a} + \mathbf{w}$ , by lower bounding in (2.7.1-3) each of the quantities  $\text{BER}_n$ . A simple lower bound on  $\text{BER}_n$  is obtained by considering a "genie"-aided receiver which has been told the values of all data symbols  $a_{n'}$  with  $n' \neq n$ . The BER associated with the ML detection of  $a_n$  by the genie-aided receiver is smaller than  $\text{BER}_n$  for any receiver to which all entries of  $\mathbf{a}$  are unknown.

The genie-aided ML receiver first constructs a vector  $\mathbf{r}'$  by subtracting from  $\mathbf{r}$  the contributions from the known data symbols  $a_{n'}$  with  $n' \neq n$  :

$$\mathbf{r}' = \mathbf{r} - \sum_{n' \neq n} a_{n'} \mathbf{h}_{n'} \quad (2.8.3-4)$$

It follows from (2.8.0-1) that  $\mathbf{r}' = a_n \mathbf{h}_n + \mathbf{w}$ . Hence,

$$\begin{aligned} \ln p(\mathbf{r}' | a_n) &\propto \frac{-1}{2\sigma_0^2} |\mathbf{r}' - a_n \mathbf{h}_n|^2 \\ &\propto \frac{-1}{2\sigma_0^2} (|a_n|^2 - 2\operatorname{Re}[a_n^* z'_n]) \\ &\propto \frac{-1}{2\sigma_0^2} |z'_n - a_n|^2 \end{aligned} \quad (2.8.3-5)$$

where  $z'_n = \mathbf{h}_n^H \mathbf{r}'$ . The ML detection performed by the genie-aided receiver yields for  $\hat{a}_n$  the constellation point that is closest to  $z'_n$ . As  $z'_n \sim N_c(a_n, N_0)$ , the BER resulting from the genie-aided receiver equals  $\operatorname{BER}_C(E_s/N_0)$ . Therefore,  $\operatorname{BER}_C(E_s/N_0) \leq \operatorname{BER}_n$ , with  $\operatorname{BER}_n$  denoting the BER related to the detection of  $a_n$  by any receiver that does not know  $a_{n'}$  with  $n' \neq n$ . This yields

$$\operatorname{BER}_C(E_s/N_0) \leq \operatorname{BER} \quad (\text{genie-based lower bound})$$

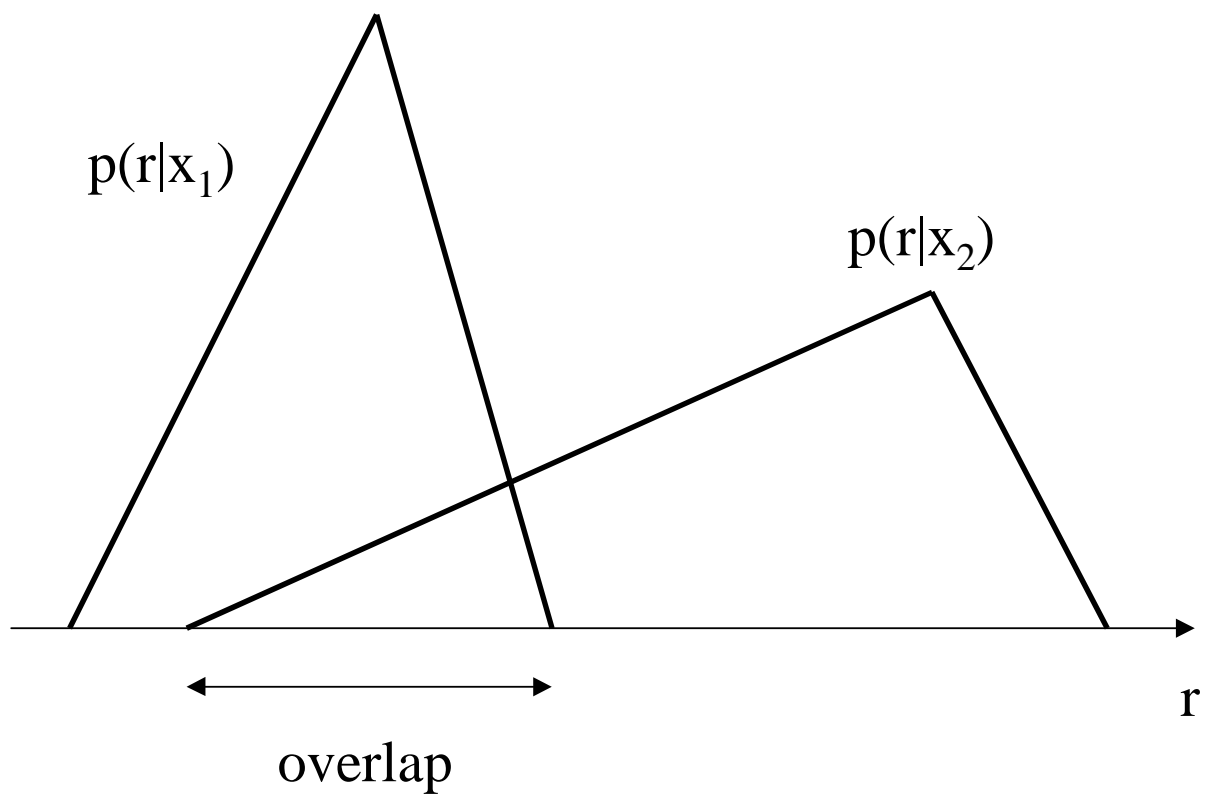
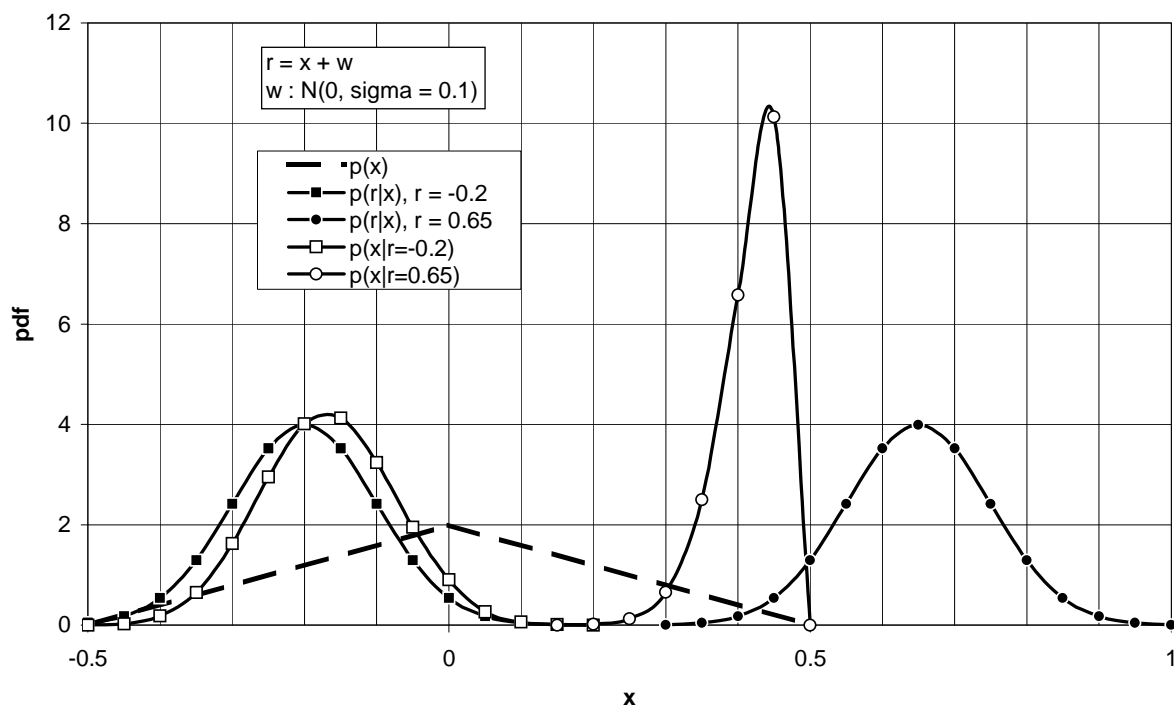
For large SNR, the lower bound  $\operatorname{BER}_C(E_s/N_0)$  is mainly determined by the minimum Euclidean distance  $e_{\min}$  between constellation points (see (2.8.2-3)).

Based on the above, the following important conclusions can be drawn regarding linear digital modulation.

- The BER performance of the ML receiver is determined by the minimum Euclidean distance  $d_{\min}$  between transmitted signal vectors. In general, the computational complexity of the ML detector increases exponentially with the number (N) of symbols transmitted.
- The minimum Euclidean distance ( $d_{\min}$ ) between transmitted symbol vectors cannot exceed the minimum Euclidean distance ( $e_{\min}$ ) between constellation points.
- The genie-based lower bound on the BER for any receiver is determined by  $e_{\min}$
- When the columns of  $\mathbf{H}$  are orthonormal, the BER resulting from ML detection equals the genie-based lower bound. Hence, a system with non-orthogonal columns cannot perform better than a system with orthonormal columns.
- When the columns of  $\mathbf{H}$  are orthonormal, the ML detector reduces to symbol-by-symbol detection. The resulting complexity increases linearly (rather than exponentially) with the number (N) of symbols transmitted.

#### 2.8.4 Symbol-by-symbol receiver for non-diagonal $\mathbf{G}$

see slides ...

Fig. 2-1 :  $p(r|x_1)$  and  $p(r|x_2)$  with overlapping domainsFig. 2-2 : illustration of  $p(x)$ ,  $p(r|x)$  and  $p(x|r)$  for  $\sigma = 0.1$

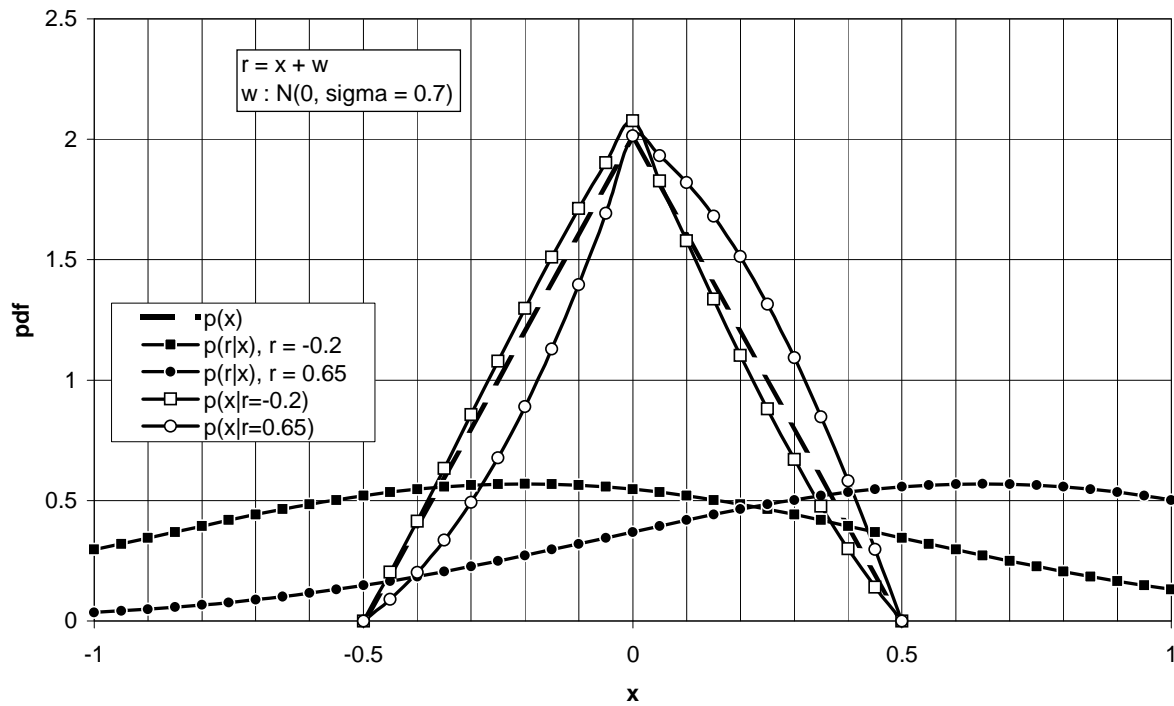
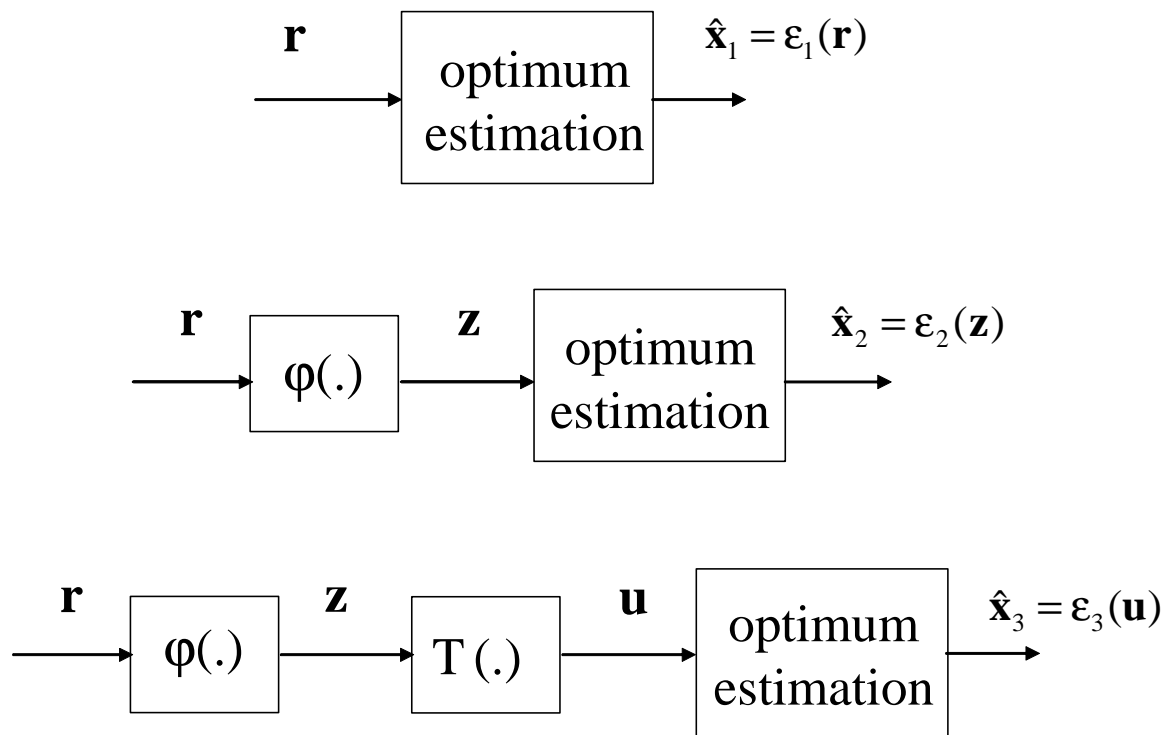
Fig. 2-3 : illustration of  $p(x)$ ,  $p(r|x)$  and  $p(x|r)$  for  $\sigma = 0.1$ 

Fig. 2-4 : equivalent optimum estimators

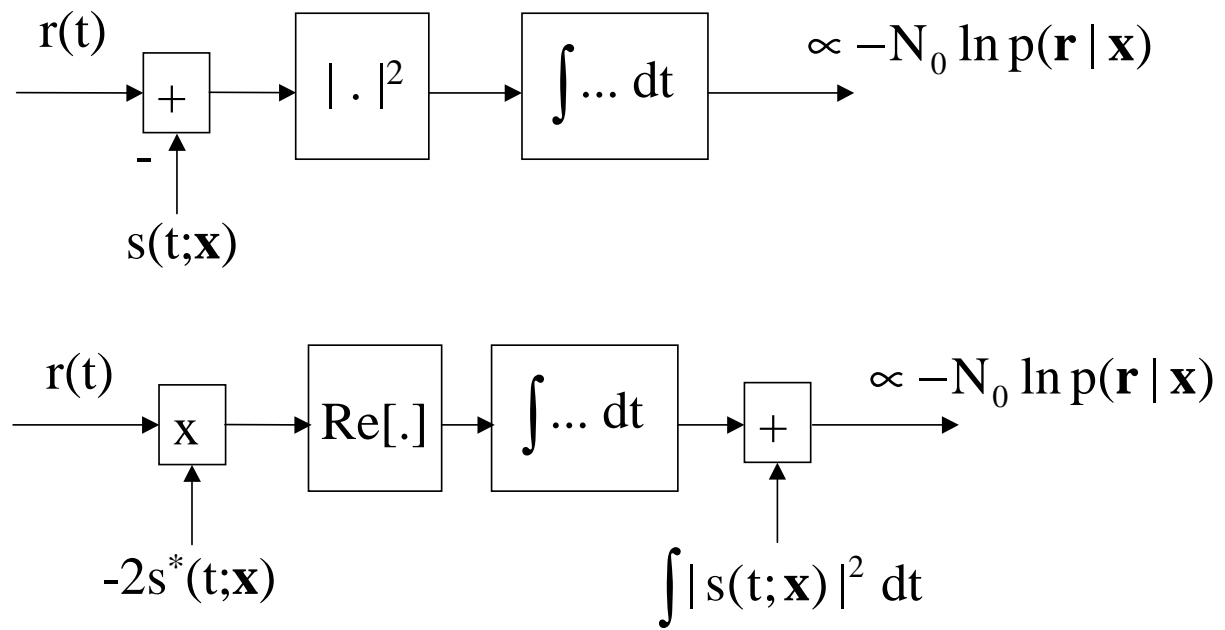
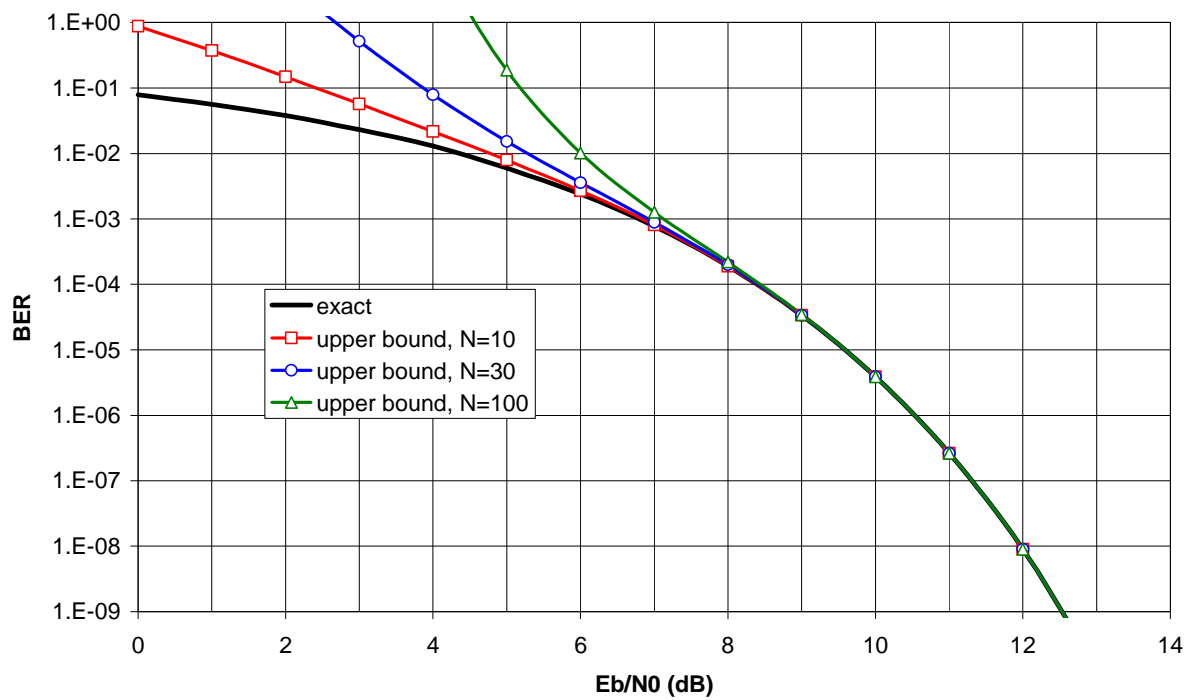
Fig. 2-5 : computation of log-likelihood function from  $r(t)$ 

Fig. 2-6 : comparison of exact BER with BER upper bound



## Chapter 3

### Digital transmission over the AWGN channel

#### 3.1. Transmitter and channel description

We consider the transmission of a sequence  $\mathbf{a}$  of complex-valued data symbols by means of *linear digital modulation*. The data symbols are independent identically distributed (i.i.d.), and take values from an  $M$ -point constellation  $\mathcal{C}$ . Each constellation point represents  $\log_2(M)$  bits, and has a probability of occurrence equal to  $1/M$ . Denoting the  $n$ -th data symbol by  $a(n)$ , we assume that  $E[|a(n)|^2] = \sigma_a^2$  for all  $n$ .

The transmitted signal  $s(t; \mathbf{a})$  is a linear function of the data symbols. In its most general form, this means

$$s(t; \mathbf{a}) = \sum_n a(n) h_{\text{tot},n}(t) \quad (3.1-1)$$

where  $h_{\text{tot},n}(t)$  denotes the symbol pulse associated to the  $n$ -th data symbol.

We will mainly restrict our attention to a special case of (3.1-1). First, the symbol sequence  $\mathbf{a}$  is transformed into a transmitted sequence  $\mathbf{x} = \mathbf{T} \cdot \mathbf{a}$ . The transform matrix  $\mathbf{T}$  has dimensions  $K \times N$ , with  $K$  and  $N$  denoting the number of components in  $\mathbf{x}$  and  $\mathbf{a}$ , respectively. In order to avoid that different sequences  $\mathbf{a}$  are transformed into the same sequence  $\mathbf{s}$  (which would make these symbol sequences indistinguishable at the receiver), the columns of  $\mathbf{T}$  need to be linearly independent; this requires  $K \geq N$ . Then the components of  $\mathbf{s}$  are transmitted sequentially at a signaling rate  $1/T$ , using a transmit filter with impulse response  $h(t)$  and transfer function  $H(f)$ : the transmitted signal is given by

$$s(t; \mathbf{a}) = \sum_m x(m) h(t - mT) = \sum_{m,n} T_{m,n} a(n) h(t - mT) \quad (3.1-2)$$

with  $T_{m,n} = (\mathbf{T})_{m,n}$ . Note that (3.1-2) is obtained from (3.1-1) by taking

$$h_{\text{tot},n}(t) = \sum_m T_{m,n} h(t - mT) \quad (3.1-3)$$

The resulting data symbol rate is given by  $R_s = (N/K)/T \leq 1/T$ .

We assume that  $h(t)$  has unit energy :

$$\int |h(t)|^2 dt = 1 \quad (3.1-4)$$

The contribution from the symbol  $a(n)$  to the transmitted signal  $s(t;\mathbf{a})$  equals  $a(n)h_{\text{tot},n}(t)$ . The energy  $E_s(n)$  associated to the transmission of the symbol  $a(n)$  is the energy of  $a(n)h_{\text{tot},n}(t)$ . Hence,  $E_s(n) = \lambda_n \sigma_a^2$ , with  $\lambda_n$  denoting the energy of  $h_{\text{tot},n}(t)$  :

$$\lambda_n = \int |h_{\text{tot},n}(t)|^2 dt \quad (3.1-5)$$

In most cases of practical interest we select  $h(t)$  and  $\mathbf{T}$  such that  $\lambda_n = 1$  for all  $n$ . This yields  $E_s(n) = \sigma_a^2$  for all  $n$ , in which case  $E_s = \sigma_a^2$  denotes the energy per symbol (irrespective of the symbol index).

The signal  $s(t;\mathbf{a})$  is transmitted over an additive white Gaussian noise (AWGN) channel, yielding the received signal  $r(t)$  :

$$r(t) = s(t;\mathbf{a}) + w(t) \quad (3.1-6)$$

where  $w(t) \sim N_c(0, N_0\delta(u))$ . The transmitter and the channel are shown in Fig. 3-1; the block "P/S" stands for parallel-to-serial conversion.

### Example : conventional linear digital modulation

In the case of conventional linear digital modulation, the data symbols are applied directly to the transmit filter. The transmitted signal is given by

$$s(t;\mathbf{a}) = \sum_m a(m)h(t - mT) \quad (3.1-7)$$

This corresponds to  $\mathbf{T}$  being the  $N \times N$  identity matrix  $\mathbf{I}_N$  (with  $N$  denoting the number of transmitted symbols), yielding  $\mathbf{x} = \mathbf{a}$ . The resulting symbol rate is given by  $R_s = 1/T$ . The energy  $E_s(n)$  in (3.1-5) equals  $E_s = \sigma_a^2$  for any unit-energy transmit pulse  $h(t)$ .

### Example : block transform linear digital modulation

In the case of block transform linear digital modulation, the data symbols are grouped in blocks of  $N_s$  symbols;  $\mathbf{a}(i)$  is the vector of  $N_s$  symbols contained in the  $i$ -th block, the  $n$ -th component of  $\mathbf{a}(i)$  is denoted  $a_n(i)$ , with  $n = 0, \dots, N_s-1$ . The  $i$ -th block  $\mathbf{a}(i)$  is transformed into  $\mathbf{x}(i) = \mathbf{T}(i)\mathbf{a}(i)$ , where  $\mathbf{T}(i)$  is a  $N_t \times N_s$  matrix with  $N_s$  linearly independent columns (this requires  $N_t \geq N_s$ ). The  $m$ -th component of  $\mathbf{s}(i)$  is denoted  $s_m(i)$ ,  $m = 0, \dots, N_t-1$ , with

$$x_m(i) = \sum_{n=0}^{N_s-1} T_{m,n}(i) a_n(i) \quad (3.1-8)$$

Hence, a single symbol  $a_n(i)$  is transformed into a sequence  $\{T_{0,n}a_n(i), T_{1,n}a_n(i), \dots, T_{N_t-1,n}a_n(i)\}$  of  $N_t$  components. Fig. 3-2 shows how  $\mathbf{x}(i)$  is obtained from  $\mathbf{a}(i)$  according to

(3.1-8) : the symbols  $a_n(i)$  are applied to the input with index  $n$  at a rate  $R_s/N_s$  (yielding a total symbol rate of  $R_s$  when summed over all  $N_s$  inputs), which implies that for given  $i$  each symbol  $a_n(i)$  is present at the input during an interval of length  $N_s/R_s$ ; during this interval,  $a_n(i)$  is multiplied with the coefficients  $T_{m,n}(i)$  for  $m = 0, \dots, N_t-1$ , and summation over  $n$  yields the outputs  $s_m(i)$  for  $m = 0, \dots, N_t-1$ ; hence, for given  $n$  the coefficients  $T_{m,n}(i)$  are applied at a rate  $1/T = (N_t/N_s)R_s$ , yielding components  $x_m(i)$  at a rate  $1/T$ . Stacking the vectors  $\mathbf{a}(i)$  and  $\mathbf{x}(i)$  yields the sequences  $\mathbf{a}$  and  $\mathbf{x}$ , respectively :  $a(iN_s+n) = a_n(i)$ ,  $x(iN_t+m) = x_m(i)$ . Fig. 3-3 illustrates the relation between the symbol sequence  $\mathbf{a}$  and the transmitted sequence  $\mathbf{x}$ . The components of  $\mathbf{x}$  are transmitted sequentially, using the transmit filter  $h(t)$ ; this yields

$$\begin{aligned} s(t; \mathbf{a}) &= \sum_i \sum_{m=0}^{N_t-1} x_m(i) h(t - (iN_t + m)T) \\ &= \sum_i \sum_{m=0}^{N_t-1} \sum_{n=0}^{N_s-1} (\mathbf{T}(i))_{m,n} a_n(i) h(t - (iN_t + m)T) \end{aligned} \quad (3.1-9)$$

Eq. (3.1-9) corresponds to taking for  $\mathbf{T}$  in (3.1-2) a block-diagonal matrix  $\mathbf{T} = \text{diag}(\{\mathbf{T}(i)\})$ ; for example, when transmitting 3 blocks we get

$$\underbrace{\begin{pmatrix} \mathbf{x}(1) \\ \mathbf{x}(2) \\ \mathbf{x}(3) \end{pmatrix}}_{\mathbf{x}} = \underbrace{\begin{pmatrix} \mathbf{T}(1) & & \\ & \mathbf{T}(2) & \\ & & \mathbf{T}(3) \end{pmatrix}}_{\mathbf{T}} \underbrace{\begin{pmatrix} \mathbf{a}(1) \\ \mathbf{a}(2) \\ \mathbf{a}(3) \end{pmatrix}}_{\mathbf{a}} \quad (3.1-10)$$

The resulting symbol rate is given by  $R_s = (N_s/N_t)/T \leq 1/T$ . When  $\mathbf{T}(i)$  is independent of the block index  $i$ , we write  $\mathbf{T}(i) = \mathbf{T}_{\text{block}}$  for all  $i$ .

Block transform modulation has a complexity advantage over the general linear modulation  $\mathbf{x} = \mathbf{T}\mathbf{a}$  : in the general case where  $\mathbf{T}$  is not block-diagonal, the computation of each component of  $\mathbf{s}$  may require up to  $N$  multiplications (with  $N$  denoting the number of transmitted symbols, which might be very large), whereas the number of multiplications per element of  $\mathbf{s}$  is limited to  $N_s$  in the block transform modulation case. Several modern communication systems use modulation formats (such as CDMA, multicarrier modulation, ...) that can be described as block transform linear digital modulation. These modulation formats will be discussed in later chapters.

Conventional modulation can be viewed as a special case of block transform modulation : (3.1-9) reduces to (3.1-7) when  $\mathbf{T}(i)$  is a scalar equal to 1 ( $N_s = N_t = 1$ ).

### 3.2. ML receiver

As all allowed data sequences have the same a priori probability, the decision error probability  $\Pr[\hat{\mathbf{a}} \neq \mathbf{a}]$  is minimized by the ML detector. This detector maximizes the log-likelihood function  $\ln p(\mathbf{r} | \tilde{\mathbf{a}})$  over  $\tilde{\mathbf{a}} \in C^N$ , where  $C^N$  is the Cartesian product of  $N$  times the constellation set  $C$ , and  $N$  denotes the number of transmitted data symbols. The log-likelihood function is determined by

$$N_0 \ln p(\mathbf{r} | \tilde{\mathbf{a}}) \propto -\int \left( |s(t; \tilde{\mathbf{a}})|^2 - 2 \operatorname{Re}[r(t)s^*(t; \tilde{\mathbf{a}})] \right) dt \quad (3.2-1)$$

Taking (3.1-1) into account, we obtain

$$\int (-2 \operatorname{Re}[r(t)s^*(t; \tilde{\mathbf{a}})]) dt = -2 \operatorname{Re} \left[ \sum_n \tilde{a}^*(n) \int r(t) h_{\text{tot},n}^*(t) dt \right] = -2 \operatorname{Re}[\tilde{\mathbf{a}}^H \mathbf{z}] \quad (3.2-2)$$

$$\int |s(t; \tilde{\mathbf{a}})|^2 dt = \sum_{n_1, n_2} \tilde{a}^*(n_1) \tilde{a}(n_2) \int h_{\text{tot},n_1}^*(t) h_{\text{tot},n_2}(t) dt = \tilde{\mathbf{a}}^H \mathbf{G}_{\text{tot}} \tilde{\mathbf{a}} \quad (3.2-3)$$

where

$$(\mathbf{z})_n = \int r(t) h_n^*(t) dt \quad (3.2-4)$$

$$(\mathbf{G}_{\text{tot}})_{n_1, n_2} = \int h_{\text{tot},n_1}^*(t) h_{\text{tot},n_2}(t) dt \quad (3.2-5)$$

It can be verified that  $\mathbf{G}_{\text{tot}}$  is a positive definite Hermitian matrix; it follows from (3.1-5) that  $\lambda_n = (\mathbf{G}_{\text{tot}})_{n,n}$ . Taking (3.2-2) and (3.2-3) into account, we have

$$N_0 \ln(p(\mathbf{r} | \tilde{\mathbf{a}})) \propto 2 \operatorname{Re}[\tilde{\mathbf{a}}^H \mathbf{z}] - \tilde{\mathbf{a}}^H \mathbf{G}_{\text{tot}} \tilde{\mathbf{a}} \quad (3.2-6)$$

from which we conclude that  $\mathbf{z}$  is a sufficient statistic for detecting  $\mathbf{a}$ .

In general,  $\mathbf{G}_{\text{tot}}$  is non-diagonal. The presence of non-zero off-diagonal elements gives rise to *crossterms* in (3.2-6) that contain two data symbols with different indices. Because of these crossterms, the ML detection involves computing the log-likelihood function for *all*  $M^N$  possible data sequences, and picking the sequence that yields the maximum value. Clearly, this is not feasible in practice because of the high computational complexity, which is exponentially increasing with the total number  $N$  of data symbols transmitted.

Let us investigate the statistical properties of the sufficient statistic  $\mathbf{z}$ . From (3.1-6), (3.1-1) and (3.2-4) we obtain

$$z(k) = \sum_n a(n) \underbrace{\int h_{\text{tot},n}(t) h_{\text{tot},k}^*(t) dt}_{(\mathbf{G}_{\text{tot}})_{k,n}} + n(k) \quad (3.2-7)$$

with

$$\mathbf{n}(k) = \int w(t) h_{\text{tot},k}^*(t) dt \quad (3.2-8)$$

Hence,  $\mathbf{z} = \mathbf{G}_{\text{tot}} \mathbf{a} + \mathbf{n}$  with  $\mathbf{n} \sim N_c(0, N_0 \mathbf{G}_{\text{tot}})$ . When  $\mathbf{G}_{\text{tot}}$  is non-diagonal, we observe that

- the signal component of the sufficient statistic  $\mathbf{z}$  is affected by intersymbol interference (ISI) :  $z(k)$  contains contributions not only from  $a(k)$ , but also from  $a(n)$  with  $n \neq k$ .
- the noise component  $\mathbf{n}$  of  $\mathbf{z}$  is colored.

Let us assume that  $\mathbf{G}_{\text{tot}} = \mathbf{I}_N$  (in section 3.4 we will show how this can be achieved), which, according to (3.2-5), implies that the symbol pulses  $h_{\text{tot},k}(t)$  and  $h_{\text{tot},n}(t)$  are orthogonal when  $k \neq n$ . In this case the sufficient statistic  $\mathbf{z}$  is given by  $\mathbf{z} = \mathbf{a} + \mathbf{w}$ , with  $\mathbf{w} \sim N_c(0, N_0 \mathbf{I}_N)$  :  $\mathbf{z}$  is not affected by ISI, and the noise term  $\mathbf{w}$  is white. This yields

$$N_0 \ln p(\mathbf{z} | \tilde{\mathbf{a}}) \propto -|\mathbf{z} - \tilde{\mathbf{a}}|^2 = -\sum_n |z(n) - \tilde{a}(n)|^2 \quad (3.2-9)$$

As  $\mathbf{z}$  is a sufficient statistic, ML detection of  $\mathbf{a}$  is equivalent to the maximization of (3.2-9). Noting that (3.2-9) consists of a sum of terms with each term depending on a different data symbol, this corresponds to maximizing each term individually. Hence, ML detection now reduces to symbol-by-symbol detection : the decision  $\hat{a}(n)$  is simply the constellation point that is closest to  $z(n)$ . The complexity of the ML receiver is linear (rather than exponential) in the data symbol length  $N$ .

In obtaining the above results, we have not made use of the assumption that  $h_{\text{tot},n}(t)$  satisfies (3.1-3); hence, the above results are very general. Substituting (3.1-3) into (3.2-4) and (3.2-5) yields

$$(\mathbf{z})_n = \sum_m T_{m,n}^* v_m = (\mathbf{T}^H \mathbf{v})_n \quad (3.2-10)$$

$$(\mathbf{G}_{\text{tot}})_{n_1, n_2} = \sum_{m_1, m_2} T_{m_1, n_1}^* T_{m_2, n_2} \int h^*(t - m_1 T) h(t - m_2 T) dt = (\mathbf{T}^H \mathbf{G} \mathbf{T})_{n_1, n_2} \quad (3.2-11)$$

where

$$(\mathbf{v})_m = v(m) = \int r(t) h^*(t - mT) dt \quad (3.2-12)$$

$$\mathbf{G}_{m_1, m_2} = g(m_1 - m_2) = \int h^*(t - m_1 T) h(t - m_2 T) dt \quad (3.2-13)$$

Note that (3.1-4) implies  $g(0) = 1$ . It follows from (3.2-13) that  $\mathbf{G}$  is a Toeplitz matrix (i.e., all elements on the same from left to right descending diagonal are identical). According to (3.2-12),  $v(m)$  is obtained by applying  $r(t)$  to a receive filter with impulse response  $h^*(-t)$  and transfer function  $H^*(f)$  (i.e., the receive filter is *matched* to the transmit filter  $h(t)$ ), and then

sampling the matched filter output at instant  $t = mT$ . Fig. 3-4 shows how to obtain  $\mathbf{z}$  from  $\mathbf{r}(t)$ ; the block "S/P" stands for serial-to-parallel conversion. Note that  $\mathbf{v}$  and  $\mathbf{z}$  have the same dimension as  $\mathbf{s}$  and  $\mathbf{a}$ , respectively. It can be verified from (3.2-12) that  $\mathbf{v} = \mathbf{GTa} + \mathbf{n}_v$  with  $\mathbf{n}_v \sim N_c(0, N_0\mathbf{G})$ . This yields  $\mathbf{z} = \mathbf{T}^H\mathbf{v} = \mathbf{T}^H\mathbf{GTa} + \mathbf{n}$  with  $\mathbf{n} \sim N_c(0, N_0\mathbf{T}^H\mathbf{GT})$ . Fig. 3-5 shows the discrete-time model that relates the quantities  $\mathbf{a}$ ,  $\mathbf{n}$  and  $\mathbf{z}$ .

When  $\mathbf{T}^H\mathbf{GT} = \mathbf{I}_N$ , we get  $\mathbf{z} = \mathbf{a} + \mathbf{w}$ , with  $\mathbf{w} \sim N_c(0, N_0\mathbf{I}_N)$ . The corresponding discrete-time model relating  $\mathbf{a}$ ,  $\mathbf{w}$  and  $\mathbf{z}$  is shown in Fig. 3-6. The resulting ML receiver reduces to symbol-by-symbol detection, as shown in Fig. 3-7.

### Remark

It is important to note that the maximization of (3.2-9) reduces to a symbol-by-symbol decision rule because we have assumed that the data symbols are statistically independent : the symbols independently take values from the constellation  $\mathcal{C}$ . In the case of channel coding, the data symbols are no longer independent; maximizing (3.2-9) is then equivalent to looking for the coded symbol sequence that is closest to  $\mathbf{z}$  in terms of Euclidean distance (same reasoning as for obtaining (2.3-4) in chapter 2).

## 3.3. BER performance

The receiver performance is measured in terms of the bit error rate (BER), which is the ratio of the average number of erroneous bit detections to the number of bits transmitted :

$$\text{BER} = \frac{E[\text{\# bit errors}]}{\text{\# transmitted bits}} \quad (3.3-1)$$

The BER for linear digital modulation is hard to compute for arbitrary  $\mathbf{T}$  and  $\mathbf{G}$ . Fortunately we can derive a simple lower bound on the BER.

We consider a data symbol sequence  $\mathbf{a}$  of  $N$  components, so that the number of transmitted bits equals  $N \cdot \log_2(M)$ . A data symbol  $a(k)$  represents  $\log_2(M)$  bits, and we introduce the random variable  $e(k)$  that indicates how many of these  $\log_2(M)$  bits are detected in error. This yields

$$\text{BER} = \frac{1}{N} \sum_{k=0}^{N-1} \text{BER}(k) \quad (3.3-2)$$

where

$$\text{BER}(k) = \frac{E[e(k)]}{\log_2(M)} \quad (3.3-3)$$

is the BER associated with the transmission of the symbol  $a(k)$ .

Let us consider the case of a *genie* receiver to which the values of all data symbols, except the symbol  $a(k)$ , have been told in advance. Because of this additional information, the genie receiver that detects  $a(k)$  performs not worse than the regular receiver that does not know any symbol in advance. Knowing all  $a(n)$  with  $n \neq k$ , the genie receiver subtracts from the received signal  $r(t)$  (see (3.1-1)) the contributions from the symbols  $a(n)$  with  $n \neq k$ , yielding

$$r'(t) = r(t) - \sum_{n \neq k} a(n) h_{\text{tot},n}(t) = a(k) h_{\text{tot},k}(t) + w(t) \quad (3.3-4)$$

with  $w(t) \sim N_c(0, N_0 \delta(u))$ . Note that  $r'(t)$  corresponds to the received signal in a scenario where only  $a(k)$  is transmitted, and all other symbols are set to zero. The associated log-likelihood function is determined by

$$N_0 \ln p(\mathbf{r}' | a(k)) \propto 2 \operatorname{Re}[a^*(k) z'(k)] - \lambda_k |a(k)|^2 \quad (3.3-5)$$

where  $\lambda_k$  is the energy of  $h_{\text{tot},k}(t)$ , and  $z'(k)$  is a sufficient statistic, obtained by sampling at  $t=0$  the output of a filter that is matched to  $h_{\text{tot},k}(t)$  and driven by  $r'(t)$  :

$$z'(k) = \int r'(t) h_{\text{tot},k}^*(t) dt \quad (3.3-6)$$

For given  $a(k)$ , we obtain  $z'(k) \sim N_c(\lambda_k a(k), N_0 \lambda_k)$ . Considering the transformation  $u'(k) = z'(k)/\lambda_k$ , we have  $u'(k) \sim N_c(a(k), N_0/\lambda_k)$ , yielding

$$N_0 \ln p(u'(k) | \tilde{a}(k)) \propto -\lambda_k |u'(k) - \tilde{a}(k)|^2 \quad (3.3-7)$$

Hence, the genie receiver computes  $u'(k)$  by scaling the matched filter output sample  $z'(k)$  by a factor  $1/\lambda_k$ , and delivers for  $\hat{a}(k)$  the constellation point that is closest to  $u'(k)$ .

Following the same reasoning as in the example from section 2.8, we obtain that the BER of the genie receiver associated with the detection of  $a(k)$  from  $u'(k)$  is given by  $\text{BER}_C(\lambda_k \sigma_a^2 / N_0) = \text{BER}_C(E_s(k) / N_0)$ , with  $E_s(k)$  denoting the energy associated to the transmission of the symbol  $a(k)$ . Hence, the BER performance of the regular receiver associated with the detection of  $a(k)$  is bounded by

$$\text{BER}(k) \geq \text{BER}_c \left( \frac{E_s(k)}{N_0} \right) \quad (3.3-8)$$

which yields the following bound on the overall BER :

$$\text{BER} \geq \frac{1}{N} \sum_k \text{BER}_c \left( \frac{E_s(k)}{N_0} \right) \quad (3.3-9)$$

The bound (3.3-8) is called the *matched filter bound*. This simple lower bound depends only on the ratio  $E_s(k)/N_0$  and on the constellation type.

In the case of conventional modulation ( $\mathbf{T} = \mathbf{I}_N$ ), we obtain  $\lambda_k = g(0) = 1$  for all  $k$ , yielding  $E_s(k) = \sigma_a^2 = E_s$ . Hence, the matched filter bound (3.3-8) reduces to

$$\text{BER}(k) \geq \text{BER}_C\left(\frac{E_s}{N_0}\right) \quad \text{for } \lambda_k = 1 \quad (3.3-10)$$

We observe that the matched filter bound for conventional modulation does not depend on the symbol index  $k$ , so that the average BER (3.3-2) is also lower bounded by  $\text{BER}_C(E_s/N_0)$ . Further, the matched filter bound does not depend on the shape of the unit-energy transmit pulse  $h(t)$ .

Let us consider the case where  $\mathbf{G}_{\text{tot}} = \mathbf{I}_N$ . As  $\lambda_k = 1$  for all  $k$ , the matched filter bound is given by (3.3-10). We have shown in section 3.2 that when  $\mathbf{G}_{\text{tot}} = \mathbf{I}_N$  the detection of  $a(k)$  consists of looking for the constellation point that is closest to  $z(k)$ , with  $z(k) \sim N_c(a(k), N_0)$ . Hence, the actual BER associated with the detection of  $a(k)$  is given by

$$\text{BER}(k) = \text{BER}_C\left(\frac{E_s}{N_0}\right) \quad \text{for } \mathbf{G}_{\text{tot}} = \mathbf{I}_N \quad (3.3-11)$$

which indicates that the matched filter bound holds *with equality* and the BER is the same for all symbols transmitted. Hence, when we want the same BER performance for each symbol transmitted, the minimum BER is achieved when  $\mathbf{G}_{\text{tot}} = \mathbf{I}_N$ . Note that the resulting BER on the AWGN channel does not depend on the specific selection of  $\mathbf{T}$  and  $h(t)$ , as long as the condition  $\mathbf{T}^H \mathbf{G} \mathbf{T} = \mathbf{I}_N$  is fulfilled; in later chapters we will show that for frequency-selective channels the BER does depend on  $\mathbf{T}$  and  $h(t)$ .



### 3.4. How to achieve $\mathbf{G}_{\text{tot}} = \mathbf{I}_N$ ?

We have shown that when  $\mathbf{G}_{\text{tot}} = \mathbf{I}_N$ , not only the ML detection reduces to simple symbol-by-symbol detection, but also the resulting BER is the same for all transmitted symbols and assumes the lowest possible value. In the following we investigate how the condition  $\mathbf{G}_{\text{tot}} = \mathbf{I}_N$  can be achieved for practical systems, i.e., conventional modulation and block transform modulation, in which case  $\mathbf{G}_{\text{tot}} = \mathbf{T}^H \mathbf{G} \mathbf{T}$  (see (3.2-11)). Finally we will show that the available bandwidth must be sufficiently large in order to meet the condition  $\mathbf{G}_{\text{tot}} = \mathbf{I}_N$ .

#### 3.4.1 Conventional linear digital modulation

In conventional linear digital modulation, the data symbols are applied to the transmit filter directly, which corresponds to  $\mathbf{T} = \mathbf{I}_N$ . Hence, the condition  $\mathbf{T}^H \mathbf{G} \mathbf{T} = \mathbf{I}_N$  reduces to  $\mathbf{G} = \mathbf{I}_N$ , or, equivalently,  $g(m) = \delta(m)$  for all  $m$ . Let us define

$$g_c(t) = \int h(t+u)h^*(u)du \Leftrightarrow G_c(f) = |H(f)|^2 \quad (3.4.1-1)$$

which indicates that  $g_c(t)$  is the response of the matched filter  $h^*(-t)$  to the transmit pulse  $h(t)$ . Comparing (3.4.1-1) to (3.2-13), it follows that  $g_c(mT) = g(m)$ . Hence, the condition  $g(m) = \delta(m)$  is equivalent to

$$g_c(mT) = \delta(m) \Leftrightarrow \{G_c(f); 1/T\}_{\text{fld}} = \{|H(f)|^2; 1/T\}_{\text{fld}} = 1 \quad (3.4.1-2)$$

Assuming  $H(f) = 0$  for  $|f| > B$ , a necessary condition to satisfy (3.4.1-2) is  $B \geq 1/(2T) = R_s/2$  (*Nyquist criterion for zero ISI*). A pulse  $g_c(t)$  satisfying (3.4.1-2) is called a *Nyquist pulse* or *interpolation pulse*; the corresponding  $h(t)$  that satisfies (3.4.1-2) is called a *square-root Nyquist pulse*. Taking (3.2-13) into account, the condition (3.4.1-2) can be transformed into

$$\int h^*(t - mT)h(t)dt = \delta(m) \quad (3.4.1-3)$$

which states that  $h(t)$  must be orthogonal to  $h(t-mT)$  for any nonzero integer  $m$ .

Obviously, in order to satisfy (3.4.1-3) we can select  $h(t)$  to have a duration not exceeding  $T$ . However, such pulses need a large (theoretically infinite) bandwidth. In practice we often take for  $h(t)$  a "square-root cosine rolloff pulse" (also called "square-root raised cosine pulse") with  $B = (1+\beta)/(2T)$ , where the rolloff factor  $\beta$  is between 0 and 1; the corresponding  $H(f)$  equals  $\sqrt{G_c(f)}$ , with

$$G_c(f) = \begin{cases} T & |fT| \leq (1-\beta)/2 \\ \frac{T}{2} \left( 1 + \cos \left( \frac{\pi}{\beta} \left( |fT| - \frac{1-\beta}{2} \right) \right) \right) & (1-\beta)/2 < |fT| \leq (1+\beta)/2 \\ 0 & |fT| > (1+\beta)/2 \end{cases} \quad (3.4.1-4)$$

The pulse  $g(t)$  corresponding to (3.4.1-4) is a "cosine rolloff" (or "raised cosine") pulse. Figs. 3-8 and 3-9 show  $G_c(f)$  and  $g_c(t)$  for various values of the rolloff factor  $\beta$ . It is easily verified from Figs. 3-8 and 3-9 that  $\{G_c(f); 1/T\}_{\text{fld}} = 1$  and  $g_c(mT) = \delta(m)$ .

When (3.4.1-2) holds, the log-likelihood function is determined by

$$N_0 \ln p(\mathbf{r} | \tilde{\mathbf{a}}) \propto \sum_n \left( 2 \operatorname{Re}[\tilde{\mathbf{a}}^*(n)z(n)] - |\tilde{\mathbf{a}}(n)|^2 \right) = 2 \operatorname{Re}[\tilde{\mathbf{a}}^H \mathbf{z}] - \tilde{\mathbf{a}}^H \tilde{\mathbf{a}} \quad (3.4.1-5)$$

The ML receiver reduces to symbol-by-symbol decision. Fig. 3-10 shows the transmitter, channel and ML receiver.

### 3.4.2 Block transform linear digital modulation

Block transform modulation is characterized by a block-diagonal  $\mathbf{T}$  :  $\mathbf{T} = \operatorname{diag}(\{\mathbf{T}(i)\})$ . In order that  $\mathbf{z}$  contains no interblock interference (i.e., interference between data symbols from *different* blocks should be zero), irrespective of  $\{\mathbf{T}(i)\}$ ,  $\mathbf{G}$  should be block-diagonal as well. Taking into account that  $\mathbf{G}$  is Toeplitz with  $g(0) = 1$ , this requires  $\mathbf{G} = \mathbf{I}_K$ , which is achieved by selecting  $h(t)$  to satisfy (3.4.1-3); this requires  $B \geq 1/(2T) = (K/N)R_s/2$ . Let us group the elements of  $\mathbf{v}$  and  $\mathbf{z}$  into blocks of sizes  $N_t$  and  $N_s$ , respectively. Denoting the  $i$ -th blocks by  $\mathbf{v}(i)$  and  $\mathbf{z}(i)$ , we have  $(\mathbf{v}(i))_m = v(iN_t+m)$  and  $(\mathbf{z}(i))_n = z(iN_s+n)$ . When  $\mathbf{G} = \mathbf{I}_K$ , it follows from the block-diagonal nature of  $\mathbf{T}$  that  $\mathbf{v}(i)$  and  $\mathbf{z}(i)$  depend only on the symbols contained in  $\mathbf{a}(i)$  :

$$\mathbf{v}(i) = \mathbf{s}(i) + \mathbf{w}_v(i) = \mathbf{T}(i)\mathbf{a}(i) + \mathbf{w}_v(i) \quad (3.4.2-1)$$

$$\mathbf{z}(i) = \mathbf{T}^H(i)\mathbf{T}(i)\mathbf{a}(i) + \mathbf{n}(i) \quad (3.4.2-2)$$

where  $\mathbf{w}_v(i) \sim N_c(0, N_0 \mathbf{I}_{N_t})$  and  $\mathbf{n}(i) \sim N_c(0, N_0 \mathbf{T}^H(i)\mathbf{T}(i))$ . In order to eliminate in  $\mathbf{z}$  the intrablock interference between symbols from a *same* block  $\mathbf{a}(i)$ , we select  $\mathbf{T}(i)$  such that  $\mathbf{T}^H(i)\mathbf{T}(i) = \mathbf{I}_{N_s}$  for all  $i$  : the  $N_s$  columns of  $\mathbf{T}(i)$  must be *orthonormal*. This yields  $\mathbf{z}(i) = \mathbf{a}(i) + \mathbf{w}(i)$ , with  $\mathbf{w}(i) \sim N_c(0, N_0 \mathbf{I}_{N_s})$ . Fig. 3-11 shows the corresponding transmitter, channel and ML receiver. Fig. 3-12 details the computation of  $\mathbf{z}(i)$  from  $\mathbf{r}(t)$ .

According to the transmitter from Fig. 3-11, block transform modulation can be interpreted as conventional modulation with "symbols"  $\mathbf{x}$  instead of  $\mathbf{a}$ . Hence, when  $h(t)$  is a square-root Nyquist pulse, it follows from (3.4.1-5) that the log-likelihood function is determined by

$$N_0 \ln p(\mathbf{r} | \tilde{\mathbf{a}}) \propto 2 \operatorname{Re}[\mathbf{x}^H \mathbf{v}] - \mathbf{x}^H \mathbf{x} = \sum_i \left( 2 \operatorname{Re}[\mathbf{x}(i)^H \mathbf{v}(i)] - \mathbf{x}^H(i)\mathbf{x}(i) \right) \quad (3.4.2-3)$$

Substituting in (3.4.2-3)  $\mathbf{x}(i) = \mathbf{T}(i)\tilde{\mathbf{a}}(i)$ , we obtain

$$\begin{aligned}
N_0 \ln p(\mathbf{r} | \tilde{\mathbf{a}}) &\propto \sum_i \left( 2 \operatorname{Re}[\tilde{\mathbf{a}}(i)^H \mathbf{T}^H(i) \mathbf{v}(i)] - \tilde{\mathbf{a}}^H(i) \mathbf{T}^H(i) \mathbf{T}(i) \tilde{\mathbf{a}}(i) \right) \\
&= \sum_i \left( 2 \operatorname{Re}[\tilde{\mathbf{a}}(i)^H \mathbf{z}(i)] - \tilde{\mathbf{a}}^H(i) \tilde{\mathbf{a}}(i) \right)
\end{aligned} \tag{3.4.2-4}$$

where we have used  $\mathbf{z}(i) = \mathbf{T}^H(i) \mathbf{v}(i)$  and  $\mathbf{T}^H(i) \mathbf{T}(i) = \mathbf{I}_{N_s}$ . Note that (3.4.2-4) is the same as (3.4.1-5).

### Example : Walsh-Hadamard transform

A Hadamard matrix  $\mathbf{H}_L$  is an  $L \times L$  orthogonal matrix with components from the set  $\{-1, 1\}$ . For example, the rows of  $\mathbf{H}_4$  are (1, 1, 1, 1), (1, -1, 1, -1), (1, 1, -1, -1) and (1, -1, -1, 1). In the case of the Walsh-Hadamard (WH) transform,  $\mathbf{T}_{\text{block}}$  consists of  $N_s$  columns of  $(L)^{-1/2} \mathbf{H}_L$ , with  $(L)^{-1/2}$  a normalization factor yielding unit-norm columns; this yields  $N_t = L$  and  $N_s \leq L$ . The WH transform is used in orthogonal CDMA.

### Example : Discrete Fourier transform

The discrete Fourier transform (DFT) matrix  $\mathbf{F}_L$  is an  $L \times L$  orthogonal matrix with  $(\mathbf{F}_L)_{m,n} = \exp(-j2\pi mn/N)$ . In the case of the DFT,  $\mathbf{T}_{\text{block}}$  consists of  $N_s$  columns of  $(L)^{-1/2} \mathbf{F}_L$ , with  $(L)^{-1/2}$  a normalization factor yielding unit-norm columns; this yields  $N_t = L$  and  $N_s \leq L$ . The DFT is used in multicarrier systems (OFDM).

### 3.5. Requirement on available channel bandwidth

From section 3.2 we know that the symbol pulses  $h_{\text{tot},k}(t)$  and  $h_{\text{tot},n}(t)$  must be orthogonal in order that the ML receiver reduces to symbol-by-symbol detection (which corresponds to a sufficient statistic  $\mathbf{z}$  with a signal component without ISI and a noise component that is white). This orthogonality condition can be met only when the available channel bandwidth is sufficiently large.

It has been shown in Appendix A.3 that the signal space consisting of complex baseband signals, that occupy a frequency interval  $(-B, B)$  and are approximately time-limited to an interval of duration  $T_0$ , has a dimension of  $2BT_0$ .

Let us consider the transmission of  $N$  data symbols at a rate  $R_s$ . Hence, in an interval of duration  $T_0 = N/R_s$ ,  $N$  orthogonal pulses  $h_n(t)$  must be transmitted, so the dimension of the signal space must be at least  $N$ . This yields the necessary condition  $2BN/R_s \geq N$ , or  $B \geq R_s/2$ . Taking into account that complex baseband signals with bandwidth  $B$  correspond to real-valued bandpass signals with RF-bandwidth  $B_{\text{RF}} = 2B$ , we obtain the necessary condition

$$B_{\text{RF}} \geq R_s \quad (3.5-1)$$

which is a fundamental lower bound on the required channel bandwidth.

Let us construct the pulses  $h_{\text{tot},n}(t)$  according to (3.1-3), where  $h(t)$  satisfies the orthogonality condition (3.4.1-3) and  $\mathbf{T}$  is a  $K \times N$  matrix with orthogonal columns (hence,  $K \geq N$ ). The transmission of  $N$  data symbols now requires  $K$  orthogonal pulses  $h(t-mT)$ , which yields the necessary condition  $2BN/R_s \geq K$ , or

$$B_{\text{RF}} \geq (K/N)R_s \quad (h_{\text{tot},n}(t) \text{ according to (3.2-1)}) \quad (3.5-2)$$

The following cases are distinguished :

- When  $K=N$  (conventional modulation, or block modulation with square matrix  $\mathbf{T}$ ) this condition is the same as (3.5-1).
- When  $K>N$ , more bandwidth is needed than is strictly necessary according to (3.5-1). Hence, the case  $K>N$  is not useful on an AWGN channel. We will show later that "spread spectrum" communication systems use  $K \gg N$  in order to achieve some robustness against frequency-selective channels.

Communication systems that occupy a bandwidth  $B_{\text{RF}}$  between  $R_s$  and  $2R_s$  are said to be *bandwidth efficient*.

The pulse construction from section 3.4 indicates that the necessary conditions (3.5-1) and (3.5-2) are also sufficient to obtain orthogonal pulses  $h_{\text{tot},n}(t)$ .

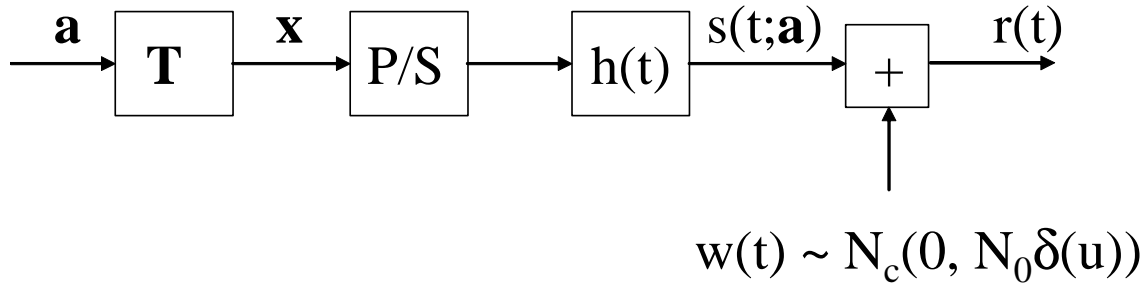
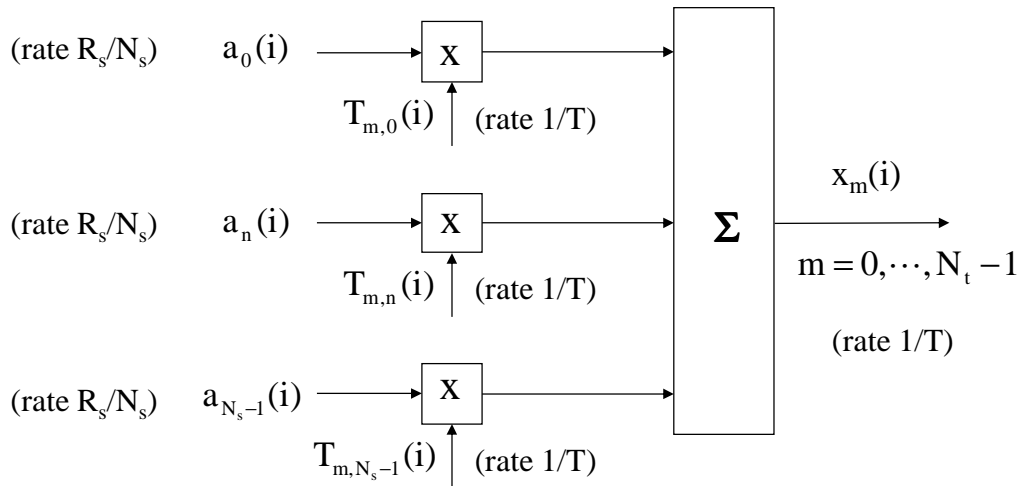
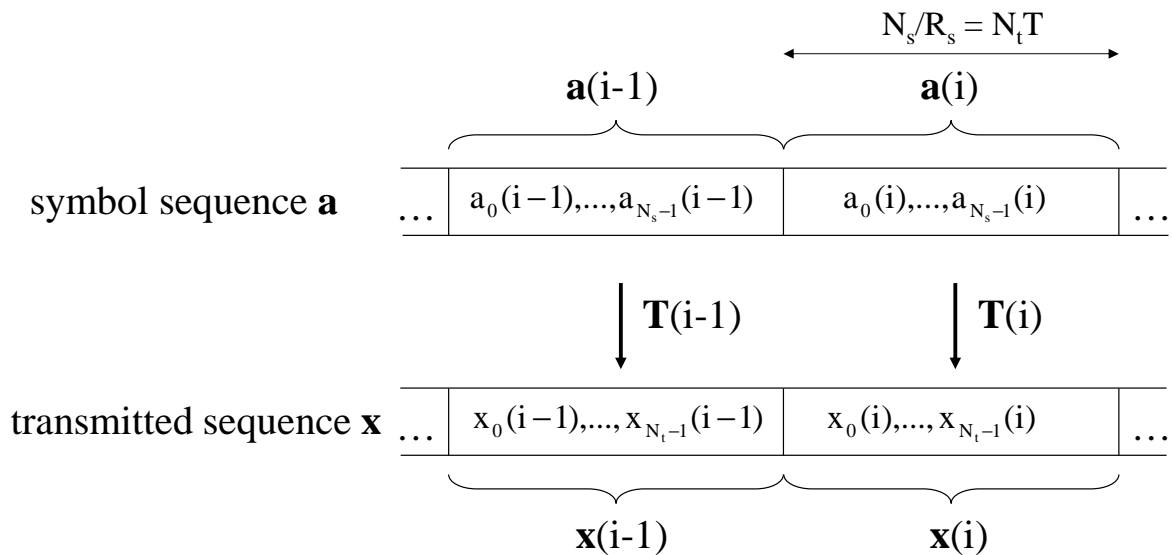
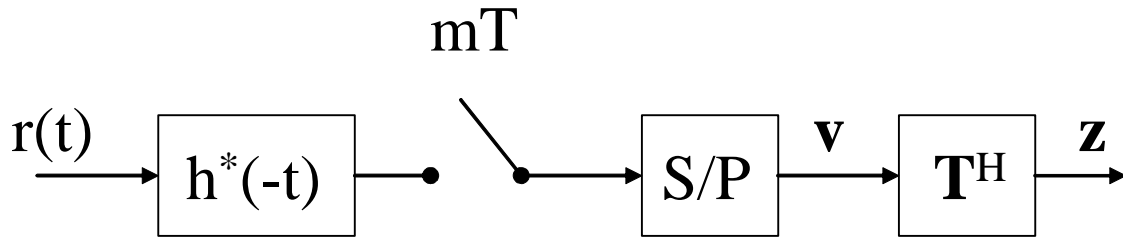
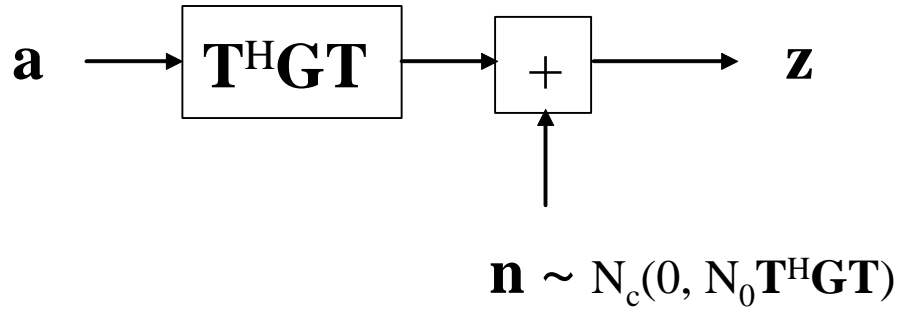
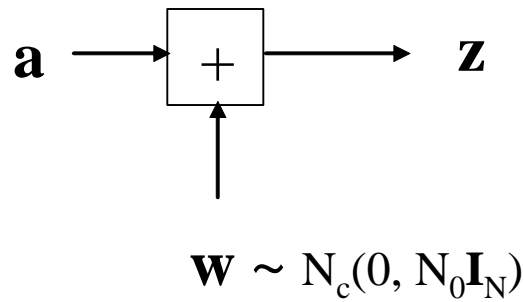
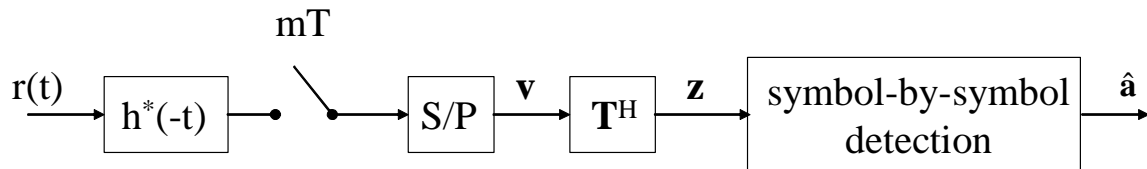
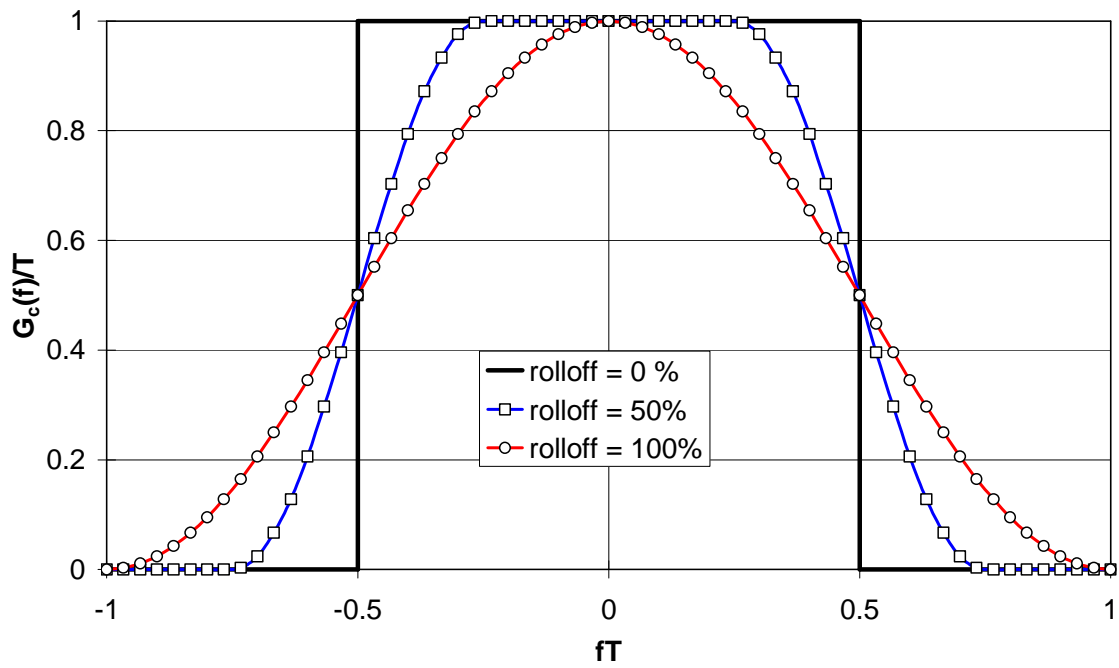
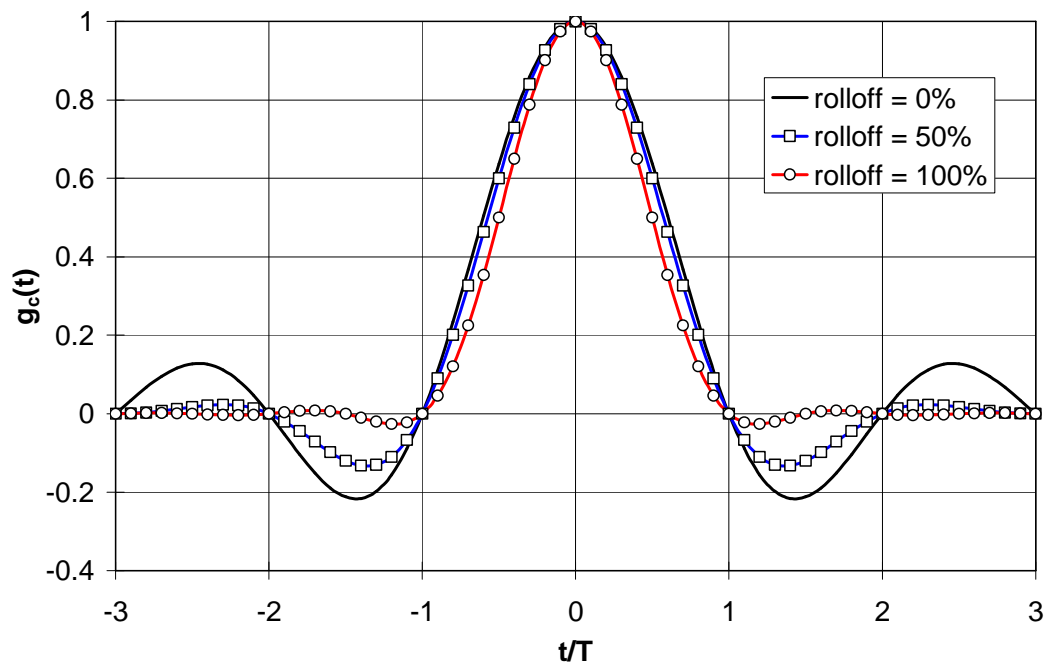
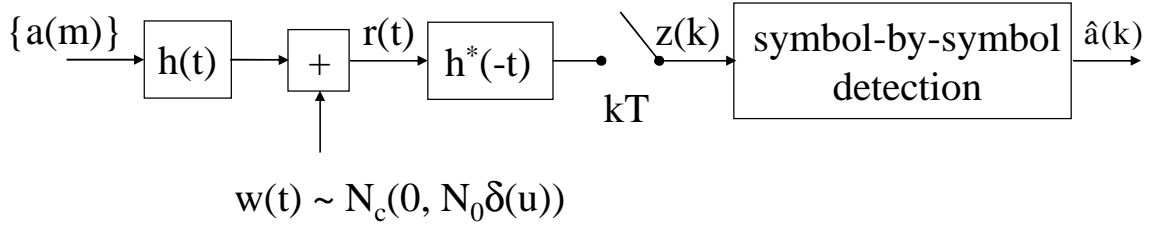
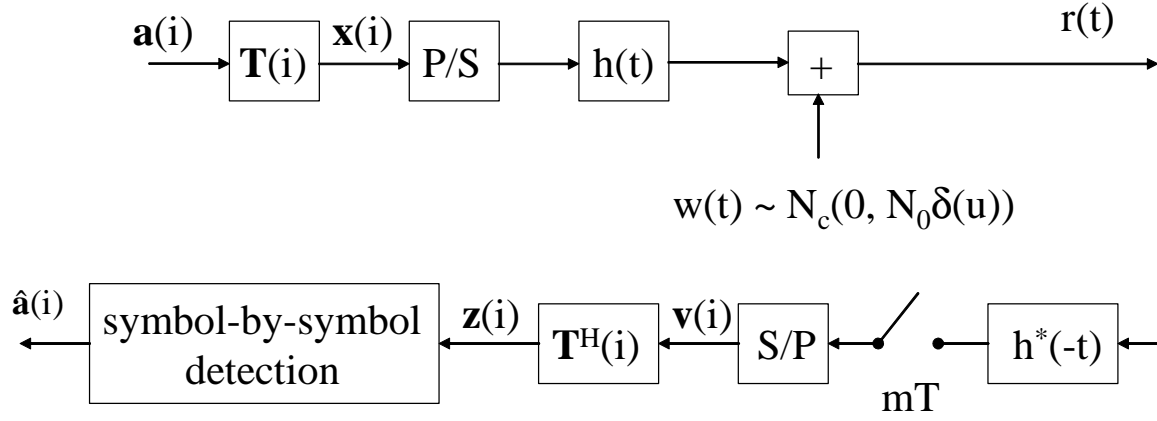
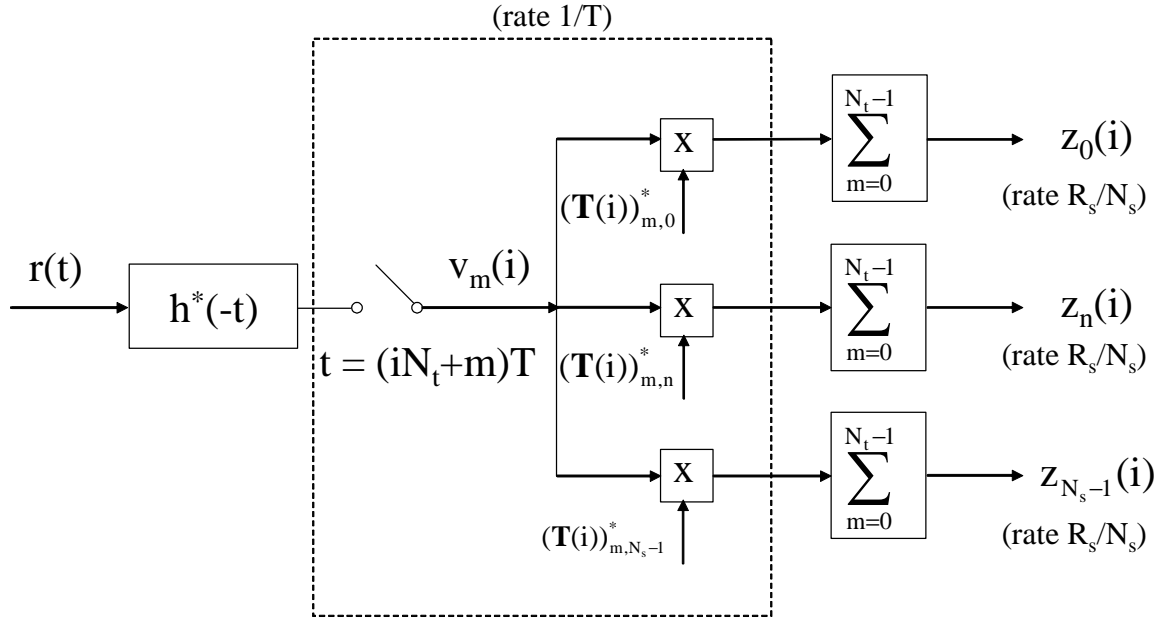


Fig. 3-1 : Linear digital modulation : transmitter and AWGN channel

Fig. 3-2 : Block transform modulation : computing  $\mathbf{x}(i)$  from  $\mathbf{a}(i)$ Fig. 3-3 : Block transform linear digital modulation : relation between  $\mathbf{a}$  and  $\mathbf{x}$

Fig. 3-4 : Computation of sufficient statistic  $\mathbf{z}$  from  $r(t)$ Fig. 3-5 : Discrete-time model relating  $\mathbf{a}$ ,  $\mathbf{n}$  and  $\mathbf{z}$ Fig. 3-6 : Discrete-time model relating  $\mathbf{a}$ ,  $\mathbf{w}$  and  $\mathbf{z}$  when  $\mathbf{T}^H \mathbf{G} \mathbf{T} = \mathbf{I}_N$ Fig. 3-7 : ML receiver when  $\mathbf{T}^H \mathbf{G} \mathbf{T} = \mathbf{I}_N$

Fig. 3-8 : Fourier transform  $G_c(f)$  of cosine-rolloff pulse  $g_c(t)$ Fig. 3-9 : Cosine-rolloff pulse  $g_c(t)$

Fig. 3-10 : Conventional modulation : transmitter, AWGN channel, ML receiver ( $\mathbf{G} = \mathbf{I}_K$ )Fig. 3-11 : Block transform modulation : transmitter, AWGN channel, ML receiver  
( $\mathbf{G} = \mathbf{I}_K$ ,  $\mathbf{T}^H(i)\mathbf{T}(i) = \mathbf{I}_{N_s}$ )Fig. 3-12 : Block transform modulation : computation of  $\mathbf{z}(i)$  from  $r(t)$



## Chapter 4

### Diversity transmission over parallel frequency-flat time-flat fading channels

#### 4.1. Transmitter and channel description

We consider block transform linear digital modulation (which includes conventional linear digital modulation as a special case). The transmitted signal  $s(t; \mathbf{a})$  is given by

$$s(t; \mathbf{a}) = \sum_i \sum_{m=0}^{N_t-1} x_m(i) h(t - (iN_t + m)T) \quad (4.1-1)$$

where  $1/T$  is the signaling rate,  $x_m(i)$  is the  $m$ -th component of  $\mathbf{x}(i)$ , and  $\mathbf{x}(i) = \mathbf{T}(i)\mathbf{a}(i)$ . The transmit pulse  $h(t)$  is a square-root Nyquist pulse :

$$\int h^*(t - mT)h(t)dt = \delta(m) \quad (4.1-2)$$

The transform matrix  $\mathbf{T}(i)$  has dimensions  $N_t \times N_s$ , and has orthonormal columns :  $\mathbf{T}^H(i)\mathbf{T}(i) = \mathbf{I}_{N_s}$ . The data symbols  $a_n(i) = (\mathbf{a}(i))_n$  are statistically independent and equiprobable, with  $E_s = E[|a_n(i)|^2]$ . Because of the above properties of  $h(t)$  and  $\mathbf{T}(i)$ ,  $E_s$  denotes the energy per symbol at the transmitter, irrespective of the symbol index.

For the transmission of  $s(t; \mathbf{a})$  we make use of  $D$  parallel fading channels, with impulse responses  $h_{ch,d}(u;t)$  and transfer functions  $H_{ch,d}(f;t)$ ,  $d = 0, \dots, D-1$ . At the input of the channel with index  $d$  we apply the signal  $\sqrt{\alpha_d} s(t; \mathbf{a})$ , with  $s(t; \mathbf{a})$  given by (4.1-1) and

$$\sum_{d=0}^{D-1} \alpha_d = 1 \quad (4.1-3)$$

Hence, a fraction  $\alpha_d$  of the transmit power is sent over the channel with index  $d$ , and the total transmit power equals the power of  $s(t; \mathbf{a})$ , i.e.,  $E_s R_s$  with  $R_s$  denoting the symbol rate ( $R_s = (N_s/N_t)/T$ ). Transmitting the same data symbol sequence over multiple parallel channels is called *diversity*.

We denote the bandwidth of  $s(t; \mathbf{a})$  by  $B$  (i.e.,  $S(f; \mathbf{a}) = 0$  for  $|f| > B$ ). Assuming that  $2B$  is much less than the coherence bandwidth of each of the channels, the transfer functions  $H_{ch,d}(f;t)$  can be approximated by  $H_{ch,d}(0;t)$  : the channels are *frequency-flat* over the signal bandwidth. The resulting signal  $r_d(t)$  at the output of the channel with index  $d$  is given by

$$r_d(t) = H_{ch,d}(0;t)\sqrt{\alpha_d}s(t; \mathbf{a}) + w_d(t) \quad (4.1-4)$$

with  $w_d(t) \sim N_c(0, N_0\delta(u))$ . The AWGN contributions  $w_d(t)$  on different channels are assumed to be statistically independent. Fig. 4-1 shows the transmitter and channel model.

In the following we will assume that fading is so slow, that the coherence time of the channels  $H_{ch,d}(0;t)$  is much larger than the duration  $N_t T$  of a transmitted block. This yields the following approximation :

$$\begin{aligned} r_d(t) &= H_{ch,d}(0;t) \underbrace{\sqrt{\alpha_d} \sum_i \sum_{m=0}^{N_t-1} x_m(i) h(t - (iN_t + m)T)}_{s(t;\mathbf{a})} + w_d(t) \\ &\approx \sqrt{\alpha_d} \sum_i H_{ch,d}(i) \sum_{m=0}^{N_t-1} x_m(i) h(t - (iN_t + m)T) + w_d(t) \end{aligned} \quad (4.1-5)$$

where  $H_{ch,d}(i) = H_{ch,d}(0; iN_t T)$ . The approximation in (4.1-5) expresses that each of the  $N_t$  pulses  $h(t - (iN_t + m)T)$  with  $m = 0, \dots, N_t-1$  experiences the same fading. The fading channel is said to be *time-flat* over a transmitted block.

## 4.2. ML receiver

As the symbols are i.i.d., the decision error probability is minimized by the ML detector. The noise contributions on the  $D$  channels are statistically independent, so the relevant log-likelihood function to be maximized is given by

$$\ln p(\mathbf{r} | \tilde{\mathbf{a}}) = \sum_{d=0}^{D-1} \ln p(\mathbf{r}_d | \tilde{\mathbf{a}}) \quad (4.2-1)$$

where  $\ln p(\mathbf{r}_d | \tilde{\mathbf{a}})$  denotes the log-likelihood function corresponding to the received signal  $\mathbf{r}_d(t)$  only.

It follows from the second line of (4.1-5) that  $\mathbf{r}_d(t)$  can be interpreted as the signal received on an AWGN channel, when using block modulation with "symbol" blocks  $\mathbf{a}_d(i) = \sqrt{\alpha_d} H_{ch,d}(i) \mathbf{a}(i)$ . Hence, according to (3.4.2-4),  $\ln p(\mathbf{r}_d | \tilde{\mathbf{a}})$  is determined by

$$\begin{aligned} N_0 \ln p(\mathbf{r}_d | \tilde{\mathbf{a}}) &\propto \sum_i \left( 2 \operatorname{Re}[\tilde{\mathbf{a}}_d^H(i) \mathbf{z}_d(i)] - \tilde{\mathbf{a}}_d^H(i) \tilde{\mathbf{a}}_d(i) \right) \\ &= \sum_i \left( 2 \operatorname{Re}[\sqrt{\alpha_d} H_{ch,d}^*(i) \tilde{\mathbf{a}}^H(i) \mathbf{z}_d(i)] - \alpha_d |H_{ch,d}(i)|^2 \tilde{\mathbf{a}}^H(i) \tilde{\mathbf{a}}(i) \right) \end{aligned} \quad (4.2-2)$$

where  $\mathbf{z}_d(i) = \mathbf{T}^H(i) \mathbf{v}_d(i)$  and  $\mathbf{v}_d(i)$  consists of matched filter output samples :

$$(\mathbf{v}_d(i))_m = \int r_d(t) h^*(t - (iN_t + m)T) dt \quad m = 0, \dots, N_t-1 \quad (4.2-3)$$

Fig. 4-2 shows how  $\mathbf{z}_d(i)$  is computed from  $\mathbf{r}_d(t)$ . From (4.2-1) and (4.2-2) we obtain

$$N_0 \ln p(\mathbf{r} | \tilde{\mathbf{a}}) \propto \sum_i \left( 2 \operatorname{Re}[\tilde{\mathbf{a}}^H(i) \mathbf{z}(i)] - \left( \sum_{d=0}^{D-1} \alpha_d |H_{ch,d}(i)|^2 \right) \tilde{\mathbf{a}}^H(i) \tilde{\mathbf{a}}(i) \right) \quad (4.2-4)$$

where  $\mathbf{z}(i)$ , given by

$$\mathbf{z}(i) = \sum_{d=0}^{D-1} \sqrt{\alpha_d} \mathbf{H}_{ch,d}^*(i) \mathbf{z}_d(i) \quad (4.2-5)$$

is a sufficient statistic for detecting  $\mathbf{a}(i)$ . For given  $\mathbf{a}(i)$ , the statistical properties of  $\mathbf{z}_d(i)$  and  $\mathbf{z}(i)$  are

$$\mathbf{z}_d(i) \sim N_c \left( \sqrt{\alpha_d} \mathbf{H}_{ch,d}(i) \mathbf{a}(i), N_0 \mathbf{I}_{N_s} \right) \quad (4.2-6)$$

$$\mathbf{z}(i) \sim N_c \left( \left( \sum_{d=0}^{D-1} \alpha_d |\mathbf{H}_{ch,d}(i)|^2 \right) \mathbf{a}(i), N_0 \left( \sum_{d=0}^{D-1} \alpha_d |\mathbf{H}_{ch,d}(i)|^2 \right) \mathbf{I}_{N_s} \right) \quad (4.2-7)$$

Note that these statistics do not depend on the specific  $h(t)$  and  $\mathbf{T}(i)$  (as long as  $h(t)$  is a square-root Nyquist pulse and the columns of  $\mathbf{T}(i)$  are orthonormal). Let us consider a scaled version  $\mathbf{u}(i)$  of  $\mathbf{z}(i)$  :

$$\mathbf{u}(i) = \left( \sum_{d=0}^{D-1} \alpha_d |\mathbf{H}_{ch,d}(i)|^2 \right)^{-1} \mathbf{z}(i) \quad (4.2-8)$$

This yields  $\mathbf{u}(i) \sim N_c(\mathbf{a}, N_{0,eq}(i) \mathbf{I}_{N_s})$ , with

$$N_{0,eq}(i) = N_0 \left( \sum_{d=0}^{D-1} \alpha_d |\mathbf{H}_{ch,d}(i)|^2 \right)^{-1} \quad (4.2-9)$$

Hence, we obtain

$$\ln p(\mathbf{u} | \tilde{\mathbf{a}}) \propto - \sum_i \frac{1}{N_{0,eq}(i)} |\mathbf{u}(i) - \tilde{\mathbf{a}}(i)|^2 = - \sum_i \frac{1}{N_{0,eq}(i)} \sum_{n=0}^{N_s-1} |u_n(i) - \tilde{a}_n(i)|^2 \quad (4.2-10)$$

We conclude from (4.2-10) that ML detection reduces to symbol-by-symbol detection :  $\hat{a}_n(i)$  is the constellation point that is closest to  $u_n(i)$ . Fig. 4-3 shows how the symbol decisions are obtained from  $\{\mathbf{z}_0(i), \dots, \mathbf{z}_{D-1}(i)\}$ .

We observe from Fig. 4-3 that the receiver makes a linear combination of the quantities  $(\mathbf{z}_d(i))_n$  to construct the  $z_n(i)$  which is a sufficient statistic for detecting  $a_n(i)$ . The SNR associated with  $(\mathbf{z}(i))_n$  is given by (see (4.2-7))

$$\text{SNR}(i) = \frac{E[|a_n(i)|^2]}{\text{Var}[z_n(i)]} = \frac{E_s}{N_{0,eq}(i)} = \sum_{d=0}^{D-1} \text{SNR}_d(i) \quad (4.2-11)$$

where

$$\text{SNR}_d(i) = \frac{|\mathbf{H}_{ch,d}(i)|^2 \alpha_d E[|a_n(i)|^2]}{\text{Var}[(\mathbf{z}_d(i))_n]} = \frac{|\mathbf{H}_{ch,d}(i)|^2 \alpha_d E_s}{N_0} \quad (4.2-12)$$

is the SNR associated with  $(\mathbf{z}_d(i))_n$  (see (4.2-6)). It can be verified that no linear combination gives rise to a SNR that is larger than  $E_s/N_{0,eq}(i)$ ; this is a consequence of the optimality of the

ML detector. Therefore, the receiver operating according to Fig. 4-3 is called a *maximum ratio combining* receiver (with "ratio" to be understood as the SNR resulting from the linear combination).

### 4.3. BER performance

For given  $\{H_{ch,d}(i), d = 0, \dots, D-1\}$ , it follows from the statistics of  $\mathbf{u}(i)$  that the BER associated to any symbol from the  $i$ -th block is given by

$$BER(i) = BER_c \left( \frac{E_s}{N_{0,eq}(i)} \right) \quad (4.3.0-1)$$

which in the case of 2-PAM, 2-PSK, 4-PSK or 4-QAM becomes

$$BER(i) = Q \left( \sqrt{\frac{2E_b}{N_{0,eq}(i)}} \right) \quad (2-PAM, 2-PSK, 4-PSK, 4-QAM) \quad (4.3.0-2)$$

Because of fading,  $N_{0,eq}(i)$  changes from one block to the next. We are interested in the average BER, which is obtained by averaging (4.3.0-1) over the statistics of  $\{H_{ch,d}(i), d = 0, \dots, D-1\}$ .

#### 4.3.1 AWGN channels

Before discussing the BER performance on the  $D$  parallel fading channels, we first consider the simpler case where the  $D$  channels are non-fading AWGN channels : the channel with index  $d$  is characterized by  $H_{ch,d}$  (which does not depend on the block index  $i$ ) and  $N_0$ . The resulting  $N_{0,eq}(i)$  depends no longer on the index  $i$ , and will be denoted  $N_{0,eq}$ . We obtain :

$$\frac{E_s}{N_{0,eq}} = \frac{E_s}{N_0} \sum_{d=0}^{D-1} |H_{ch,d}|^2 \alpha_d \quad (4.3.1-1)$$

Obviously,  $E_s/N_{0,eq}$  depends on the coefficients  $\alpha_d$ , i.e., on how the available transmit power is split over the  $D$  available channels. The optimum allocation of the transmit power consists of sending all power over the channel that has the largest gain  $|H_{ch,d}|$ , and not using any of the other channels. This results in

$$\frac{E_s}{N_{0,eq}} = \frac{E_s}{N_0} \cdot \max_d |H_{ch,d}|^2 \quad (4.3.1-2)$$

When all channels have the same gain,  $E_s/N_{0,eq}$  does not depend on how the transmit power is allocated to the different channels; in this case the transmitter can simply pick any channel and use all transmit power on the selected channel. Hence, splitting the transmit power over more than one AWGN channel does not provide any benefit in BER performance.

### 4.3.2 Rayleigh fading channels

Now we concentrate on the case where the channels are time-varying because of fading. In principle, we could make the allocation of the transmit power to the  $D$  channels time-varying as well (this would imply replacing  $\alpha_d$  by  $\alpha_d(i)$ ), in which case  $E_s/N_{0,eq}(i)$  is maximized by sending during the  $i$ -th block all transmit power over the channel for which  $|H_{ch,d}(i)|$  is maximum. However, such solution is feasible only when the transmitter knows for each block which channel has the largest gain. The transmitter could send a test signal over each of the  $D$  channels, on the basis of which the receiver measures the gain for each channel; then the receiver would communicate to the transmitter which of the  $D$  channels to use. The disadvantage of this approach is that a feedback channel from receiver to transmitter is needed. Moreover, the channel coherence time (say, in the order of 10 ms) might be too small for this approach to work : by the time the transmitter gets information from the receiver about which channel to use, it is possible that this information is no longer relevant, because the channels have changed considerably since the measurement at the receiver was made. Therefore, we limit our attention to a fixed allocation of the transmit power to the  $D$  channels, that does not change with time.

Let us consider the transmission of symbols from a 2-PAM, 2-PSK, 4-PSK or 4-QAM constellation. In all these cases, the BER related to block  $i$  is given by (4.3.0-2) and depends on the instantaneous values of  $H_{ch,d}(i)$  that are contained in  $N_{0,eq}(i)$ ; hence,  $BER(i)$  is a random variable. The average BER is obtained as  $E[BER(i)]$ , with  $E[.]$  denoting averaging over the channel statistics. This averaging is complicated by the presence of the function  $Q(x)$ , which is not well suited for mathematical manipulations. Therefore, we will use a simple upper bound on  $Q(x)$ , i.e.,  $Q(x) \leq (1/2)\exp(-x^2/2)$ , which we derive in section 4.6.1. In the case of transmission over an AWGN channel, this bound yields

$$BER_{AWGN} = Q\left(\sqrt{\frac{2E_b}{N_0}}\right) \leq BER_{up,AWGN} = \frac{1}{2}\exp\left(\frac{-E_b}{N_0}\right) \quad (4.3.2-1)$$

The correct  $BER_{AWGN}$  and the upper bound  $BER_{up,AWGN}$  are compared in Fig. 4-4; note that the bound is tighter than 1dB for  $BER < 10^{-4}$ . Using this bound in (4.3.0-2) and averaging yields

$$\begin{aligned}
E[\text{BER}(i)] &\leq \frac{1}{2} E \left[ \exp \left( \frac{-E_b}{N_{0,\text{eq}}(i)} \right) \right] \\
&= \frac{1}{2} E \left[ \exp \left( -\frac{E_b}{N_0} \sum_{d=0}^{D-1} \alpha_d |H_{\text{ch},d}(i)|^2 \right) \right] \\
&= \frac{1}{2} E \left[ \prod_{d=0}^{D-1} \exp \left( -\alpha_d |H_{\text{ch},d}(i)|^2 \frac{E_b}{N_0} \right) \right]
\end{aligned} \tag{4.3.2-2}$$

Assuming that the coefficients  $H_{\text{ch},d}(i)$  that belong to different channels are *statistically independent*, (4.3.2-2) reduces to

$$E[\text{BER}(i)] \leq \frac{1}{2} \prod_{d=0}^{D-1} E \left[ \exp \left( -\alpha_d |H_{\text{ch},d}(i)|^2 \frac{E_b}{N_0} \right) \right] \tag{4.3.2-3}$$

Let us consider the case of Rayleigh fading :  $H_{\text{ch},d}(i) \sim N_c(0, 2\sigma_d^2)$ , with all  $D$  channels having a nonzero r.m.s. gain  $\sigma_d$ . In this case we obtain (see section 4.6.2) :

$$E \left[ \exp \left( -\alpha_d |H_{\text{ch},d}(i)|^2 \frac{E_b}{N_0} \right) \right] = \left( 1 + 2\sigma_d^2 \alpha_d \frac{E_b}{N_0} \right)^{-1} \tag{4.3.2-4}$$

which yields

$$E[\text{BER}(i)] \leq \text{BER}_{\text{up}} = \frac{1}{2} \prod_{d=0}^{D-1} \left( 1 + 2\sigma_d^2 \alpha_d \frac{E_b}{N_0} \right)^{-1} \tag{4.3.2-5}$$

In principle, the transmit power allocation  $\{\alpha_d, d = 0, \dots, D-1\}$  can be optimized such that  $\text{BER}_{\text{up}}$  from (4.3.2-5) is minimized. The optimum fixed allocation is such that the channels with larger r.m.s gain  $\sigma_d$  get a higher fraction  $\alpha_d$  of the available power. The transmitter needs to know  $\{\sigma_d, d = 0, \dots, D-1\}$  in order to carry out the optimization. When all  $D$  channels have the same  $\sigma_d$ , the optimum allocation is to split the transmit power evenly over all channels, i.e.,  $\alpha_d = 1/D$  irrespective of  $E_b/N_0$ .

For increasing  $E_b/N_0$  the optimum allocation tends to  $\alpha_d = 1/D$ . It can be verified that using  $\alpha_d = 1/D$  at any  $E_b/N_0$  gives rise to only a very small performance loss as compared to the optimum allocation. Therefore we will consider only the case of *evenly split transmit power*.

When the transmit power is evenly split among all  $D$  channels, (4.3.2-5) yields

$$\text{BER}_{\text{up}} = \frac{1}{2} \prod_{d=0}^{D-1} \left( 1 + \frac{2\sigma_d^2}{D} \cdot \frac{E_b}{N_0} \right)^{-1} \tag{4.3.2-6}$$

Let us consider the situation where all  $D$  channels have the same statistical properties, i.e.  $2\sigma_d^2 = 2\sigma^2$  for  $d = 0, \dots, D-1$ . As we will indicate in section 4.4, this is often the case when diversity is realised in practice. Moreover, we normalize the channels ( $2\sigma^2 = 1$ ), so that the energy per bit at the channel output (sum over all  $D$  channels) is the same as the energy per bit at the channel input. This yields (see (4.3.2-6))

$$\text{BER}_{\text{up}} = \frac{1}{2} \left( 1 + \frac{E_b}{N_0} \cdot \frac{1}{D} \right)^{-D} \quad (4.3.2-7)$$

Fig. 4-5 shows  $\text{BER}_{\text{up}}$  from (4.3.2-7) as a function of  $E_b/N_0$ , for various values of  $D$ , along with the upper bound (4.3.2-1) for the AWGN channel; for all these cases, the energy per bit at the receiver is equal to  $E_b$ . For given  $D$  and increasing  $E_b/N_0$ ,  $\text{BER}_{\text{up}}$  is proportional to  $(E_b/N_0)^{-D}$ , as can be verified from (4.3.2-7). For  $D = 1$ , the BER performance is much worse than for the AWGN channel; when  $D$  is increased, the BER performance improves : this is called *diversity gain*. The diversity gain increases with  $D$ , but the largest increase occurs for small  $D$ ; for large  $D$ , the additional gain when going from  $D$  to  $D+1$  is small. Hence, when a number of fading channels is available, one might decide to use only a subset of the available channels, basically to limit the implementation complexity at the transmitter and the receiver.

The reason why a diversity gain occurs can be understood from (4.3.0-2), which in our case of equally split transmit power reduces to

$$\text{BER}(i) = Q \left( \sqrt{\frac{2E_b}{N_0} \cdot X(i)} \right) \quad (4.3.2-8)$$

where

$$X(i) = \frac{1}{D} \sum_{d=0}^{D-1} |H_{\text{ch},d}(i)|^2 \quad (4.3.2-9)$$

with  $H_{\text{ch},d}(i) \sim N_c(0, 1)$  for channels with identical statistics. It can be verified that

$$E[X(i)] = E[|H_{\text{ch},d}(i)|^2] = 1 \quad (4.3.2-10)$$

$$\text{Var}[X(i)] = \frac{1}{D} \text{Var}[|H_{\text{ch},d}(i)|^2] = \frac{1}{D} \quad (4.3.2-11)$$

Hence, increasing  $D$  reduces the variance of  $X(i)$  (so that the fluctuation of  $X(i)$  around its mean  $E[X(i)] = 1$  gets smaller), and decreases the probability that  $X(i)$  assumes very small values. Therefore, for given  $E_b/N_0$ ,  $E[\text{BER}(i)]$  decreases when  $D$  gets larger. When  $D \rightarrow \infty$ , we get  $X(i) \rightarrow 1$ , so that

$$\lim_{D \rightarrow \infty} \text{BER}(i) = Q\left(\sqrt{\frac{2E_b}{N_0}}\right) = \text{BER}_{\text{AWGN}} \quad (4.3.2-12)$$

This is confirmed by considering the following limit of  $\text{BER}_{\text{up}}$  from (4.3.2-7) :

$$\lim_{D \rightarrow \infty} \frac{1}{2} \left(1 + \frac{E_b}{N_0} \cdot \frac{1}{D}\right)^{-D} = \lim_{D \rightarrow \infty} \frac{1}{2} \exp\left(-D \ln\left(1 + \frac{E_b}{N_0} \cdot \frac{1}{D}\right)\right) = \frac{1}{2} \exp\left(\frac{-E_b}{N_0}\right) \quad (4.3.2-13)$$

In arriving at (4.3.2-13), we have made use of the fact that  $\ln(1+\epsilon) \rightarrow \epsilon$  when  $\epsilon \rightarrow 0$ . Note that the limit in (4.3.2-13) corresponds to the upper bound (4.3.2-1) for the BER on the AWGN channel. However, in order that  $\text{BER}_{\text{up}}$  gets close to  $\text{BER}_{\text{up,AWGN}}$ , Fig. 4-5 indicates that quite large values of  $D$  are needed.

In Figs. 4-6 to 4-8 we show 100 independent realizations of the random variable  $X(i)$  from (4.3.2-9), for  $D = 1, 3$  and  $5$ , respectively; Figs. 4-9 to 4-11 show the corresponding  $\text{BER}(i)$ , computed from (4.3.2-8) at  $E_b/N_0 = 15$  dB, along with the average  $E[\text{BER}(i)]$ . For  $D = 1$  we observe that  $X(i)$  occasionally assumes very small values ("deep fades") that are 20 dB to 30 dB below the average level of 0 dB ( $E[X(i)] = 1$ ). These deep fades give rise to large instantaneous BER values, that have a dominant contribution to the average  $E[\text{BER}(i)]$ . For  $D = 3$ , the fluctuation of  $X(i)$  around its 0 dB mean value is smaller than for  $D = 1$ ; consequently, the deep fades and the resulting high instantaneous BER values are much less frequent, and the resulting  $E[\text{BER}]$  is smaller than for  $D = 1$ . This improvement is even more pronounced for  $D = 5$ .

Finally, we mention that an exact expression for  $E[\text{BER}(i)]$  can be derived. Fig. 4-12 compares the exact expression with the simple upper bound (4.3.2-7). We observe that for large  $E_b/N_0$ , the exact BER exhibits the same degree of diversity as the upper bound.



## 4.4. Practical realizations of diversity transmission

Common realizations of diversity transmission are : frequency diversity, time diversity and antenna diversity.

### 4.4.1 Frequency diversity

In the case of frequency diversity,  $D$  parallel channels are created by transmitting the same signal  $s(t;\mathbf{a})/\sqrt{D}$  over  $D$  different frequency bands. In order that the  $D$  diversity channels be frequency-flat, the width of each frequency band must be considerably less than the coherence bandwidth of the physical transmission channel. The spacing between the frequency bands must be larger than the coherence bandwidth, so that the  $D$  diversity channels are statistically independent.

Denoting the transfer function of the dispersive channel as  $H_{ch}(f;t)$ , and the center frequencies of the  $D$  diversity channels as  $F_d$  ( $d=0, \dots, D-1$ ), the diversity channel with index  $d$  is characterized by a channel gain  $H_{ch}(F_d; t_i)$ , with  $t_i$  referring to the transmission instant of the  $D$  copies of the symbol block  $\mathbf{a}(i)$ . Using the WSSUS channel model

$$H_{ch}(f;t) = \sum_{n=0}^{L-1} c_n(t) \exp(-j2\pi f \Delta \tau_n) \quad (4.4.1-1)$$

with  $c_n(t) \sim N_c(0, 2\sigma_n^2 R_c(u))$  and  $R_c(0) = 1$ , it is easily verified that

$$E[|H_{ch}(F_d; t_i)|^2] = \sum_{n=0}^{L-1} (2\sigma_n^2) \quad (4.4.1-2)$$

which indicates that the statistics of a diversity channel does not depend on its center frequency. Hence, all  $D$  diversity channels have the same statistical properties.

Fig. 4-13 shows the transmitter, the channel and part of the receiver. Assuming that  $S(f;\mathbf{a}) = 0$  for  $|f| > B$ ,  $\Pi_{LP}(f)$  refers to a lowpass filter with a passband  $(-B, B)$ . The total (non-contiguous) RF bandwidth occupied by the transmitted signal equals  $2B \cdot D$ . Fig. 4-14 shows the power spectrum of the transmitted signal, with  $S_s(f)$  denoting the power spectrum of  $s(t;\mathbf{a})$ .

### 4.4.2 Time diversity

In the case of time diversity,  $D$  copies of each symbol block  $\mathbf{a}(i)$  are transmitted over the physical channel at  $D$  different instants; each copy yields an energy  $N_s E_s / D$  (with  $N_s$  denoting the number of symbols per block), so that the total energy per symbol equals  $E_s$ . The instants at which these copies are transmitted must be separated in time by more than the channel coherence time, in order that the  $D$  copies from the same symbol block experience

independent fading. When the symbol rate equals  $R_s$ , the transmitter must transmit copies of symbols at a rate  $D \cdot R_s$  in the case of diversity of order  $D$ . Hence, application of time diversity increases the bandwidth by a factor  $D$ . In contrast with frequency diversity, the band occupied in case of time diversity is a contiguous frequency band. In order that the physical transmission channel be frequency-flat over the signal bandwidth, this band must be considerably less than the channel coherence bandwidth.

Denoting by  $\Delta t$  the spacing between copies of a same symbol block  $\mathbf{a}(i)$ , these copies are affected by channel coefficients  $H_{ch}(0; t_i + d\Delta t)$ ,  $d = 0, \dots, D-1$ , where  $t_i$  denotes the transmission instant of the first copy of  $\mathbf{a}(i)$ . As  $H_{ch}(0; t)$  is a stationary process, the channel coefficients have identical statistics.

At the transmitter,  $D$  copies from each block  $\mathbf{x}(i) = \mathbf{T}(i)\mathbf{a}(i)$  are generated, and *interleaving* is applied to the stream of blocks to provide a sufficient time interval  $\Delta t$  between copies of the same symbol block. The interleaver is a memory consisting of  $K_r$  rows and  $D$  columns, with each memory cell containing one block (see Fig. 4-15). The  $D$  copies of a block are written in a row of the memory; the  $k$ -th row contains  $D$  copies of the block  $\mathbf{x}(jK_r+k)$ ,  $k = 0, \dots, K_r-1$ . The copies are read out column by column from the memory. This yields the following sequence at the output of the interleaver :

$$\underbrace{\underbrace{\mathbf{x}(jK_r), \dots, \mathbf{x}(jK_r + K_r - 1)}_{K_r \text{ blocks}}, \dots, \underbrace{\mathbf{x}(jK_r), \dots, \mathbf{x}(jK_r + K_r - 1)}_{K_r \text{ blocks}}}_{D \cdot K_r \text{ blocks}}$$

Note that the spacing between copies of a same block equals  $K_r$  positions;  $K_r$  is called the interleaver depth. The interleaved sequence of blocks is applied to the transmit filter with impulse response  $h(t)$ ; the pulses  $h(t)$  satisfy the orthogonality condition (4.1-2), but with  $1/T$  given by  $D \cdot (N_t/N_s)R_s$  instead of  $(N_t/N_s)R_s$ . The resulting transmitter is shown in Fig. 4-16.

The received signal  $r(t)$  is applied to a matched filter with impulse response  $h^*(-t)$ , and the matched filter output is sampled at rate  $1/T$  (see Fig. 4-17). We denote by  $\mathbf{v}_d(jK_r+k)$  the block of matched filter output samples that corresponds to the  $d$ -th copy of  $\mathbf{a}(jK_r+k)$ . The sequence of blocks  $\mathbf{v}_d(jK_r+k)$  is fed to a *deinterleaver* : the blocks are written column by column into a memory consisting of  $K_r$  rows and  $D$  columns, and read out row by row (see Fig. 4-18). At the output of the deinterleaver, the following sequence appears :

$$\underbrace{\mathbf{v}_0(jK_r), \dots, \mathbf{v}_{D-1}(jK_r)}_{\text{set 0}}, \underbrace{\mathbf{v}_0(jK_r+1), \dots, \mathbf{v}_{D-1}(jK_r+1)}_{\text{set 1}}, \dots, \underbrace{\mathbf{v}_0(jK_r+K_r-1), \dots, \mathbf{v}_{D-1}(jK_r+K_r-1)}_{\text{set } K_r-1}$$

This sequence consists of  $K_r$  sets of  $D$  blocks, with each block in the set with index  $jK_r+k$  being a noisy version of  $\mathbf{x}(jK_r+k)$ . The  $D$  blocks  $\mathbf{v}_d(jK_r+k)$ ,  $d = 0, \dots, D-1$ , are applied to the

transformation  $\mathbf{T}^H(jK_r+k)$ . This yields the blocks  $\mathbf{z}_d(jK_r+k)$ ,  $d = 0, \dots, D-1$  that are noisy versions of the block  $\mathbf{a}(jK_r+k)$ ; the  $D$  blocks  $\mathbf{z}_d(jK_r+k)$  with index  $jK_r+k$  are combined (maximum ratio combining) at the receiver, after which the symbol block  $\mathbf{a}(jK_r+k)$  is detected by means of symbol-by-symbol decision.

As the  $D$  copies of  $\mathbf{a}(i)$  are transmitted at rate  $D \cdot R_s$ , after interleaving the spacing between the start of copies of the same block  $\mathbf{a}(i)$  equals  $\Delta t = K_r N_s / (D \cdot R_s)$ . For given  $D$  and  $R_s$ , the interleaver depth  $K_r$  should be selected such that  $\Delta t$  exceeds the channel coherence time  $T_{\text{coh}}$ , in order to provide statistically independent fading to all  $D$  copies. An important drawback of the use of interleaving is the introduction of delay (latency) :

- the time that elapses between the reception of the start of the first copy and the end of the last copy of a symbol block  $\mathbf{a}(i)$  equals  $((D-1)K_r + 1)N_s / (R_s D)$ , or about  $(D-1)T_{\text{coh}}$ ;
- when no time diversity is used (i.e.,  $D=1$ ), this time is only  $N_s / R_s$ .

Hence the latency introduced by the interleaving amounts to  $(K_r-1)(D-1)N_s / (R_s D)$ , or about  $(D-1)T_{\text{coh}}$ . When the communication between two users is highly interactive, the latency should be kept small; in such applications, the limit on allowable latency might prevent the use of interleaving.

#### 4.4.3 Antenna diversity

In antenna diversity (also called *spatial* diversity), one distinguishes between receive antenna diversity and transmit antenna diversity.

In the case of *receive antenna diversity*, the transmitter has one antenna and the receiver has  $D$  antennas. When the spacing between the receive antennas is in the order of the wavelength  $\lambda$  of the carrier frequency, the propagation paths from the transmit antenna to each of the receive antennas can be considered as statistically independent. We assume that the channel coherence bandwidth is much larger than the bandwidth of the transmitted signal, so that the fading can be considered as frequency-flat. Note that applying receive antenna diversity does NOT increase the bandwidth occupied by the transmitted signal (this is unlike frequency diversity and time diversity). Fig. 4-19 shows part of the transmitter and receiver, along with the equivalent channel model.

In our investigation of diversity transmission, we have assumed so far that a constant transmit power is *split* over  $D$  diversity channels, so that the total received power does not depend on the number of diversity channels. However, in the case of receive antenna diversity we are in the fortunate situation that for a given transmit power the total received power is

proportional to the number of receive antennas ! This is called the *array gain* : when the transmitted energy per bit is denoted  $E_b$ , and the channels are normalized so that the energy per bit per receive antenna is also  $E_b$ , the total received energy per bit equals  $D \cdot E_b$  when  $D$  receive antennas are present. In order to take the array gain into account, we have to replace in (4.3.2-7)  $E_b$  by  $D \cdot E_b$ , which yields

$$\text{BER}_{\text{up}} = \frac{1}{2} \left( 1 + \frac{E_b}{N_0} \right)^{-D} \quad (\text{receive antenna diversity}) \quad (4.4.3-1)$$

Fig. 4-20 shows the corresponding BER curves; note the spectacular performance improvement due to the array gain, as compared to Fig. 4-5.

Receive antenna diversity is quite attractive : as compared to frequency diversity and time diversity, receive antenna diversity benefits from an array gain and uses a bandwidth that does not increase with the diversity order. However, the implementation of receive antenna diversity involves a high hardware complexity at the receiver, because we need  $D$  separate downconverters.

In the case of *transmit antenna diversity*, the transmitter has  $D$  antennas, and the receiver has one antenna. Transmit power is evenly split over the  $D$  antennas. Assuming that the transmit antenna spacing is in the order of the wavelength  $\lambda$ , the fading channels from each transmit antenna to the receive antenna can be considered as statistically independent. We assume that the signal bandwidth is much smaller than the coherence bandwidth of each of the  $D$  channels, so the fading on each channel is frequency-flat. Fig. 4-21 shows the transmitter and part of the receiver, along with the equivalent channel model. The received signal is the sum of contributions from each of the  $D$  transmit antenna signals :

$$r(t) = \frac{1}{\sqrt{D}} \sum_{d=0}^{D-1} H_{\text{ch},d}(0,t) s(t - \tau_d; \mathbf{a}) + w(t) \quad (4.4.3-2)$$

where  $H_{\text{ch},d}(0;t)$  is the channel gain from the  $d$ -th transmit antenna to the receive antenna, and  $\tau_d$  is a delay that is intentionally applied to the signal at the  $d$ -th transmit antenna. Strictly speaking,  $\tau_d$  also includes the propagation delay of the channel with index  $d$ , but as the propagation delay differences between the channels are very small (in the order of  $1/f_0$ , which corresponds to 1 ns for  $f_0 = 1$  GHz) they can be ignored as compared to the intentional delays. The model (4.4.3-2) is equivalent to transmitting the signal  $s(t; \mathbf{a})$  over a frequency-selective channel with transfer function  $H_{\text{ch}}(f;t)$ , given by

$$H_{ch}(f;t) = \frac{1}{\sqrt{D}} \sum_{d=0}^{D-1} H_{ch,d}(0;t) \exp(-j2\pi f\tau_d) \quad (4.4.3-3)$$

Hence, transmit antenna diversity is different from the previous types of diversity, as it does not provide separate received signals; rather, it turns a frequency-flat channel into a frequency-selective channel, of which the delay spread is controlled by proper selection of the delays  $\tau_d$ . Transmission over frequency-selective channels will be discussed in later chapters. In contrast to receive antenna diversity, transmit antenna diversity does not provide array gain.

## 4.5. Remarks

### 4.5.1 Rice fading

Till now, we have considered Rayleigh fading, which corresponds to a situation without LOS component. When a LOS component is present, the Rice fading model applies. Assuming  $D$  statistically identical Rice fading channels, and allocating a fraction  $1/D$  of the total transmit power to each channel, we obtain

$$BER_{up} = \frac{1}{2} \left( 1 + \frac{E_b}{N_0} \cdot \frac{1}{D} \cdot 2\sigma^2 \right)^{-D} \exp \left( \frac{-E_b}{N_0} \cdot \frac{A^2}{1 + \frac{E_b}{N_0} \cdot \frac{1}{D} \cdot 2\sigma^2} \right) \quad (4.5.1-1)$$

with  $A^2 = (C/M)/(1+(C/M))$  and  $2\sigma^2 = 1/(1+(C/M))$ . Figs. 4-22 to 4-24 show  $BER_{up}$  for  $D = 1, 2, 3$ , and various values of  $C/M$ . We observe that for given  $D$  and given  $E_b/N_0$ ,  $BER_{up}$  decreases with increasing  $C/M$ ; in the limit for  $C/M \rightarrow \infty$ , the same performance as for the AWGN channel is obtained. For given  $D$  and  $C/M$ ,  $BER_{up}$  is inversely proportional to  $(E_b/N_0)^D$  when  $E_b/N_0$  gets large.

### 4.5.2 Correlated Rayleigh fading

*Correlated* fading occurs when the spacing between antennas, the time interval between copies of the same block or the frequency spacing between diversity channels is too small, in the cases of antenna diversity, time diversity and frequency diversity, respectively. Let us briefly investigate how correlation of the fading channels affects the performance. We consider two statistically identical Rayleigh fading channels. Assuming that  $E[H_{ch,0}^*(0;i)H_{ch,1}(0;i)] = 2\sigma^2\rho$ , with  $\rho$  denoting the correlation between the channel coefficients, we obtain

$$\text{BER}_{\text{up}} = \frac{1}{2} \left( 1 + \frac{E_b}{N_0} + (1 - \rho^2) \left( \frac{E_b}{2N_0} \right)^2 \right)^{-1} \quad (4.5.2-1)$$

Fig. 4-25 shows  $\text{BER}_{\text{up}}$  for various values of  $\rho$ . We observe that the performance gets worse with increasing  $|\rho|$ ; for  $|\rho| = 1$  the same performance as for one channel is obtained. The results indicate that even for rather high correlation it is better to split the transmit power equally over two correlated channels than to use only one channel.

### 4.5.3 Use of error-correcting codes

The transmission of  $D$  copies of each symbol can be interpreted as transmitting a codeword of a repetition code. When performing soft decoding of the repetition code on the AWGN channel, no coding gain is achieved : this is consistent with the observation that diversity gives no performance advantage on the AWGN channel. Instead of a repetition code, we might envisage using a code that does provide a coding gain on the AWGN channel, and investigate the performance when transmitting the coded bits over independent fading channels and performing soft decoding at the receiver. Fig. 4-26 considers 2-PSK modulation, and compares the decoding error probability for the following scenarios :

- (i) Transmission of a codeword from an extended Hamming code with  $(n, k, d) = (8, 4, 4)$  over the AWGN channel.
- (ii) Transmission of 4 codewords from a  $(2, 1, 2)$  repetition code over the AWGN channel.
- (iii) Transmission of a codeword from an extended Hamming code with  $(n, k, d) = (8, 4, 4)$  over 8 Rayleigh fading diversity channels (one channel per bit of the codeword)
- (iv) Parallel transmission of 4 codewords from a  $(2, 1, 2)$  repetition code over 8 Rayleigh fading diversity channels (one channel per coded bit).

In all scenarios, the energy per coded bit is  $E_b/2$ , with  $E_b$  denoting the energy per *information* bit. The rate of the coded bits is  $2R_b$ , with  $R_b$  denoting the *information* bitrate; hence, all scenarios require the same bandwidth. In the case of fading, the rate of coded bits per diversity channel is  $R_b$ . We observe from Fig. 4-26 that the extended Hamming code provides a coding gain with respect to the repetition code, both on the AWGN channel and on the fading diversity channels : this is because the Hamming code yields the larger Hamming distance (4 instead of 2). For large  $E_b/N_0$ , the decoding error probability in the case of Rayleigh fading is inversely proportional to  $(E_b/N_0)^{-2}$  and  $(E_b/N_0)^{-4}$ , for the repetition code and the extended Hamming code, respectively; this indicates that the extended Hamming code provides more diversity than the repetition code.

## 4.6. Appendix : BER computation

### 4.6.1 Upper bound on $Q(x)$

For  $x \geq 0$ , the function  $Q(x)$  can be expressed as

$$Q(x) = \iint_{\substack{u > x \\ -\infty < v < +\infty}} \frac{1}{2\pi} \exp\left(-\frac{u^2 + v^2}{2}\right) du dv \quad (4.6.1-1)$$

This integral can be upper bounded by integrating over a larger area (see Fig. 4-27):

$$Q(x) \leq \iint_{\substack{u^2 + v^2 > x^2 \\ u > 0}} \frac{1}{2\pi} \exp\left(-\frac{u^2 + v^2}{2}\right) du dv = \frac{1}{2} \int_x^\infty \exp\left(-\frac{r^2}{2}\right) r dr = \frac{1}{2} \int_{x^2/2}^\infty e^{-t} dt = \frac{1}{2} e^{-x^2/2} \quad (4.6.1-2)$$

### 4.6.2 Computation of $E[\exp(-(E_b/N_0)\alpha_d |H_{ch,d}(i)|^2)]$

Taking into account that  $H_{ch,d}(i) \sim N_c(0, 2\sigma_d^2)$ , we obtain

$$\begin{aligned} E\left[\exp\left(-\alpha_d |H_{ch,d}(i)|^2 \frac{E_b}{N_0}\right)\right] &= \frac{1}{2\pi\sigma_d^2} \iint \exp\left(-\frac{E_b\alpha_d}{N_0}(x^2 + y^2)\right) \exp\left(-\frac{1}{2\sigma_d^2}(x^2 + y^2)\right) dx dy \\ &= \left( \frac{1}{\sqrt{2\pi}\sigma_d} \int \exp\left(-\frac{x^2}{2} \left(\frac{2E_b\alpha_d}{N_0} + \frac{1}{\sigma_d^2}\right)\right) dx \right)^2 \\ &= \left( \underbrace{\frac{1}{\sqrt{2\pi}\sigma_{eq}} \int \exp\left(-\frac{x^2}{2\sigma_{eq}^2}\right) dx}_{=1} \right)^2 \left( \frac{\sigma_d^2}{\sigma_{eq}^2} \right)^{-1} = \left( \frac{\sigma_d^2}{\sigma_{eq}^2} \right)^{-1} \end{aligned} \quad (4.6.2-1)$$

with

$$\frac{1}{\sigma_{eq}^2} = \frac{2E_b\alpha_d}{N_0} + \frac{1}{\sigma_d^2} \quad (4.6.2-2)$$

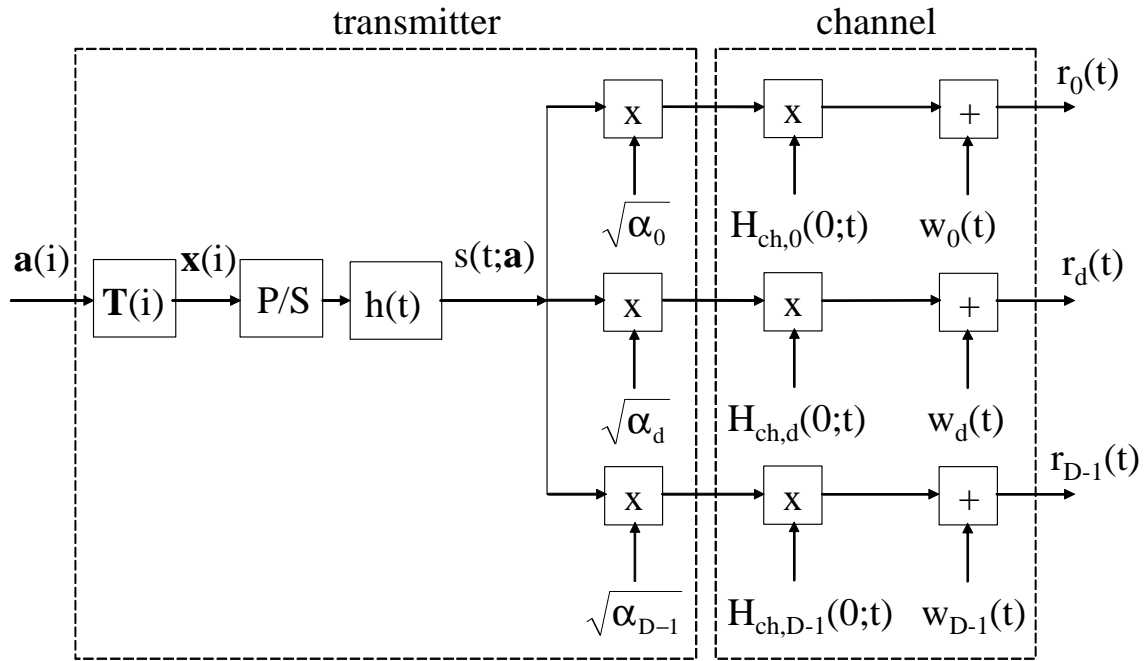
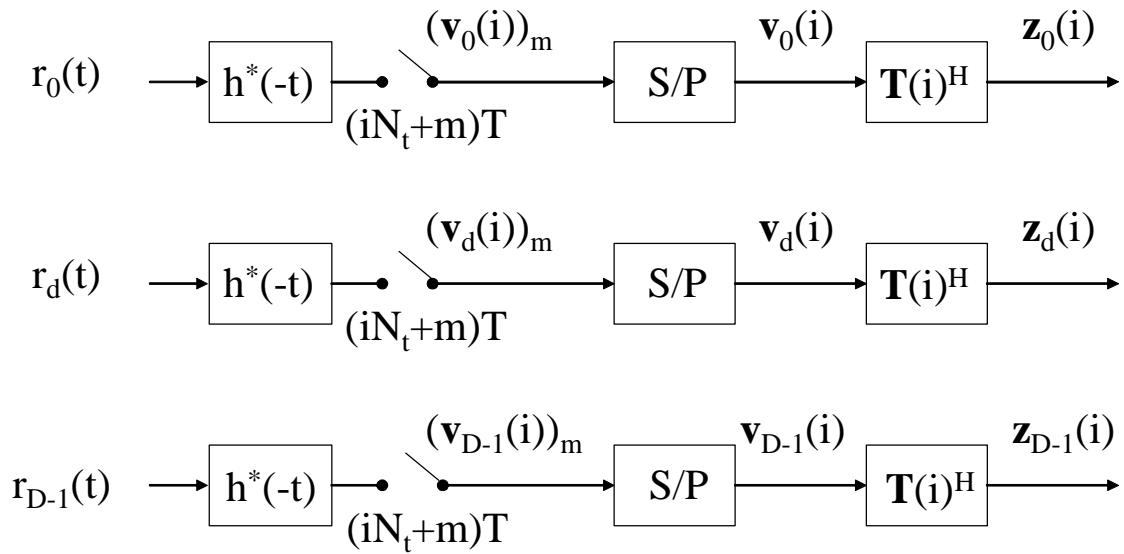


Fig. 4-1 : Transmitter and channel model for diversity transmission


 Fig. 4-2 : Computation of  $z_d(i)$  from  $r_d(t)$ ,  $d = 0, \dots, D-1$



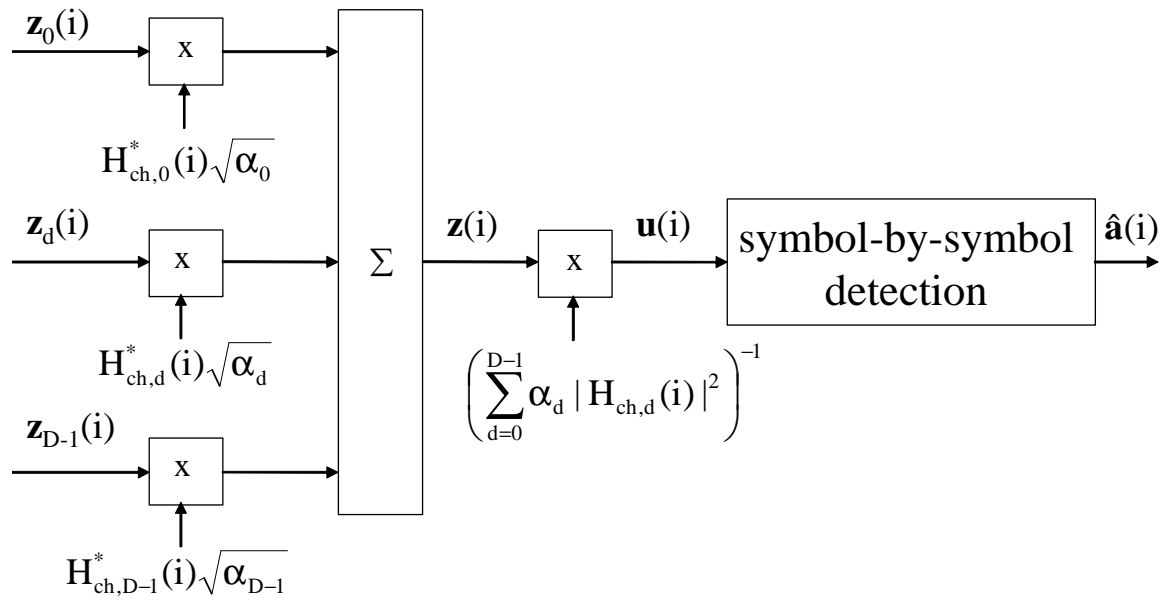
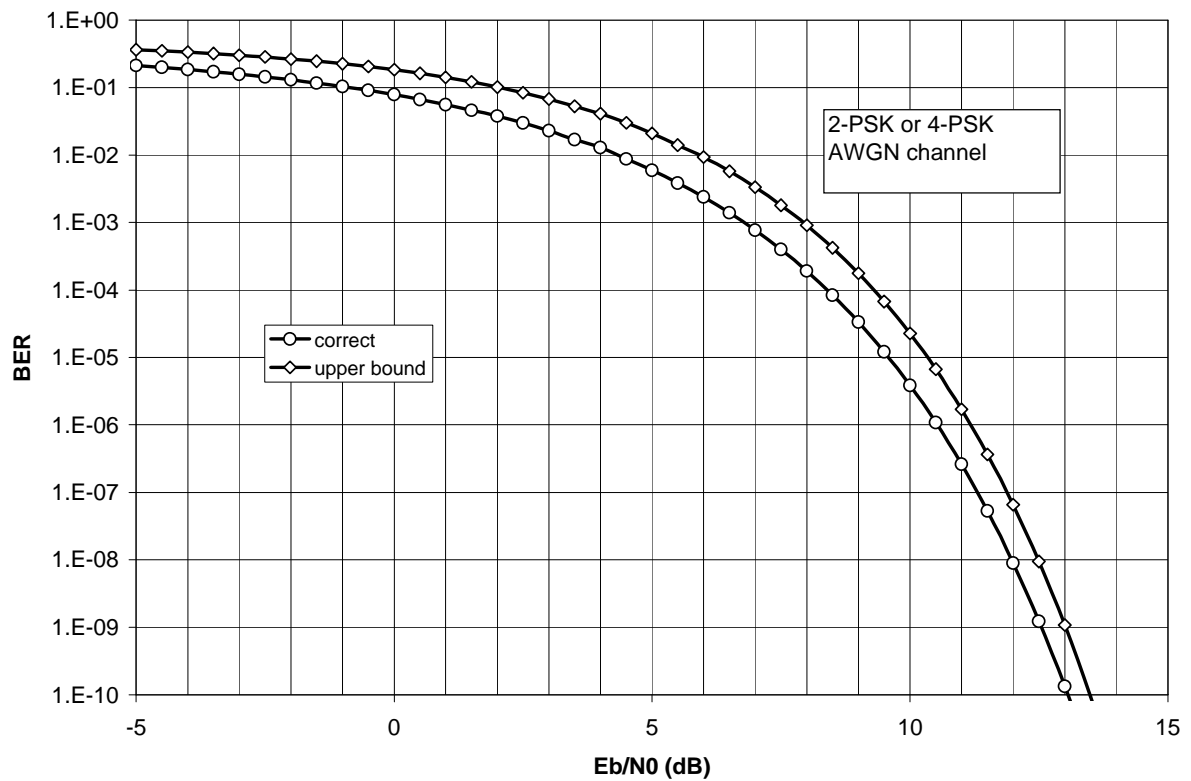

 Fig. 4-3 : ML detection from  $\mathbf{z}_d(i)$ ,  $d = 0, \dots, D-1$ 


Fig. 4-4 : correct BER and upper bound on BER for transmission over AWGN channel

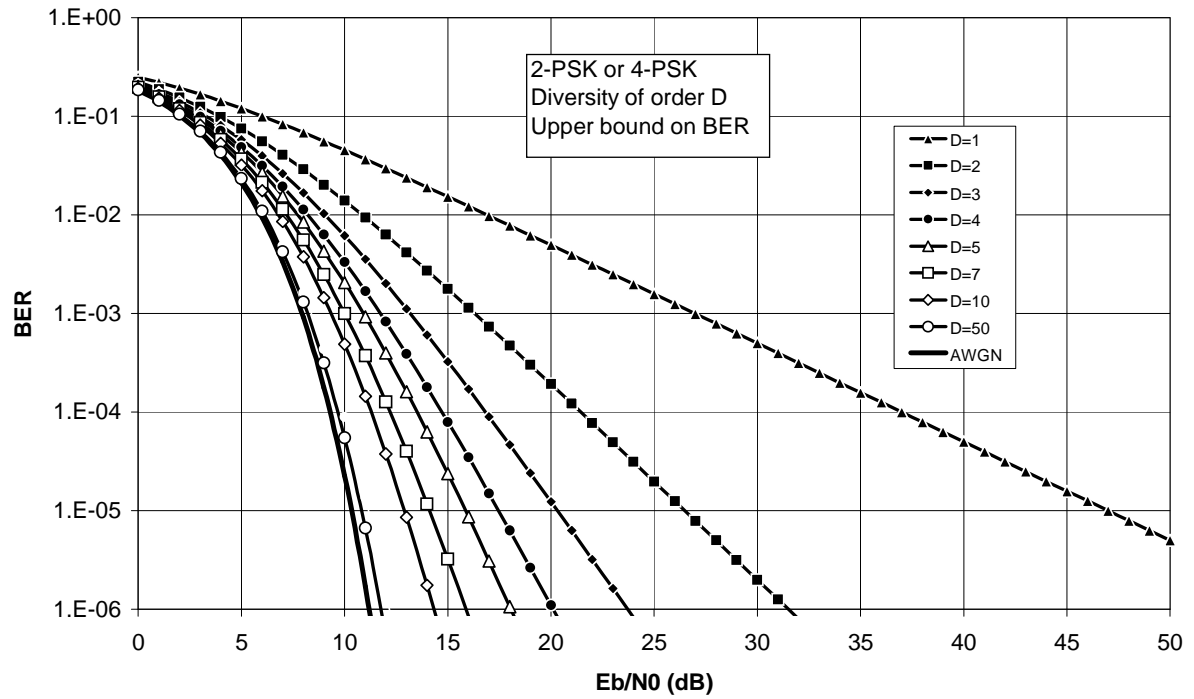


Fig. 4-5 :  $BER_{up}$  for statistically identical channels

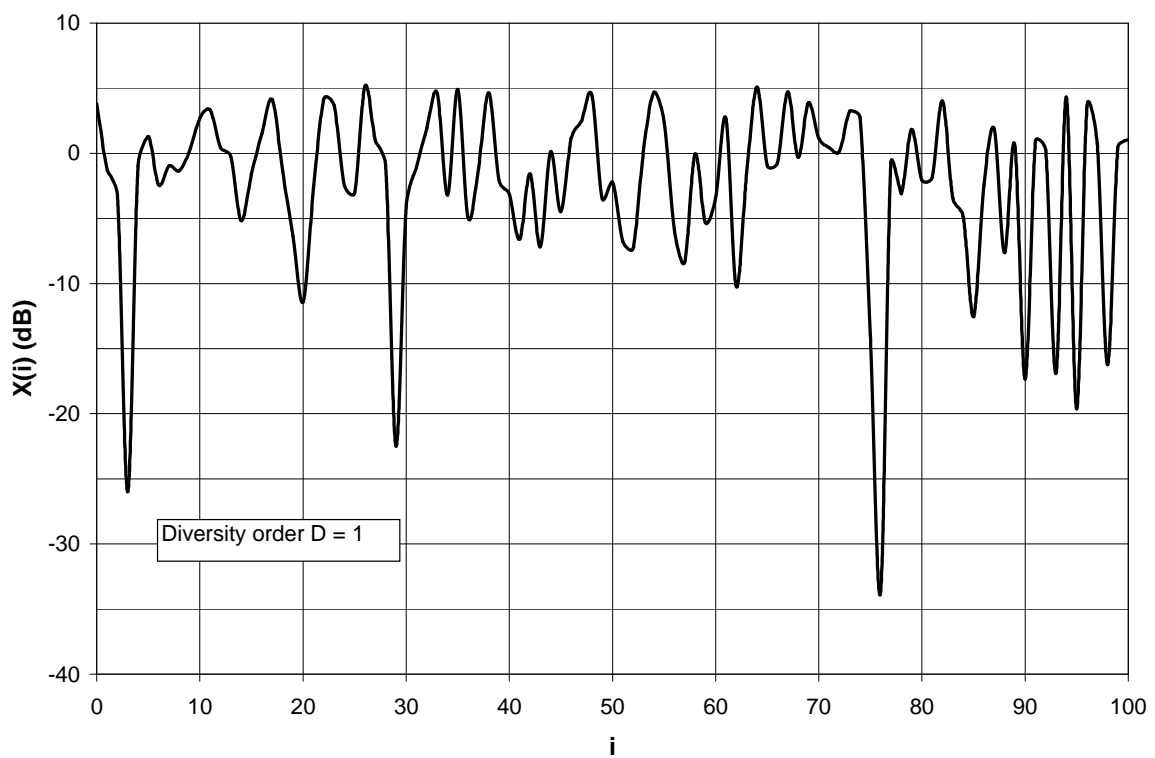


Fig. 4-6 : 100 independent realizations of  $X(i)$ , for  $D = 1$

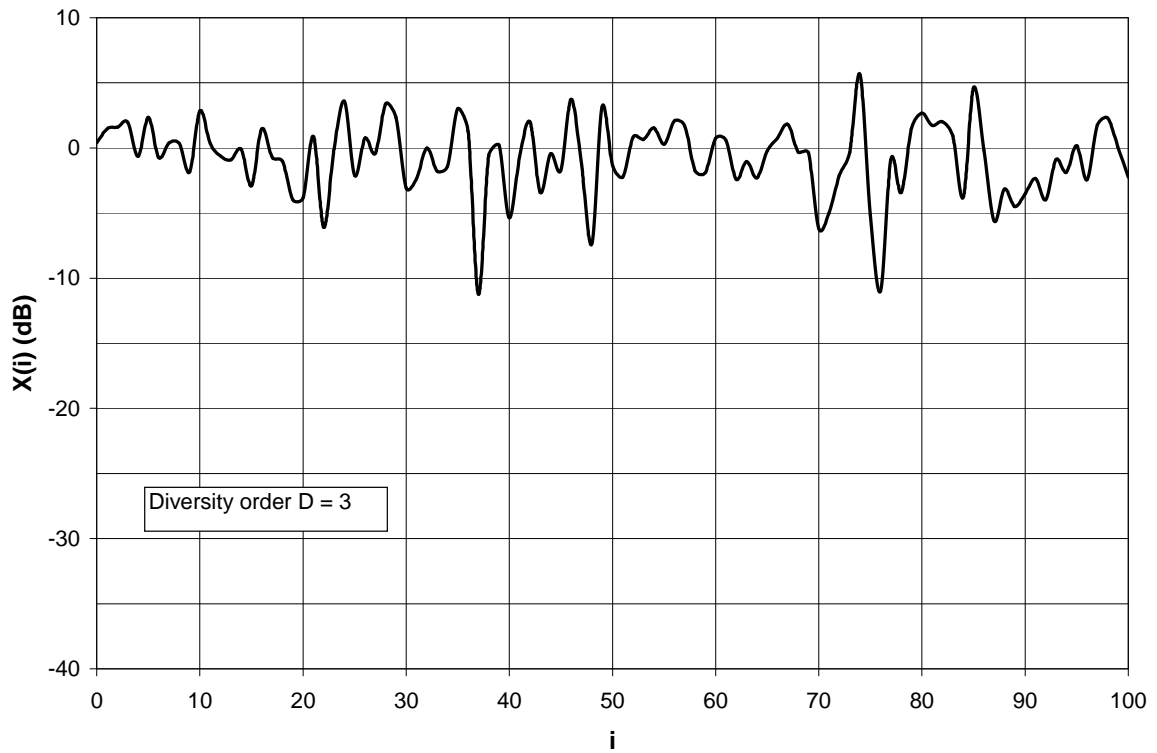


Fig. 4-7 : 100 independent realizations of  $X(i)$ , for  $D = 3$

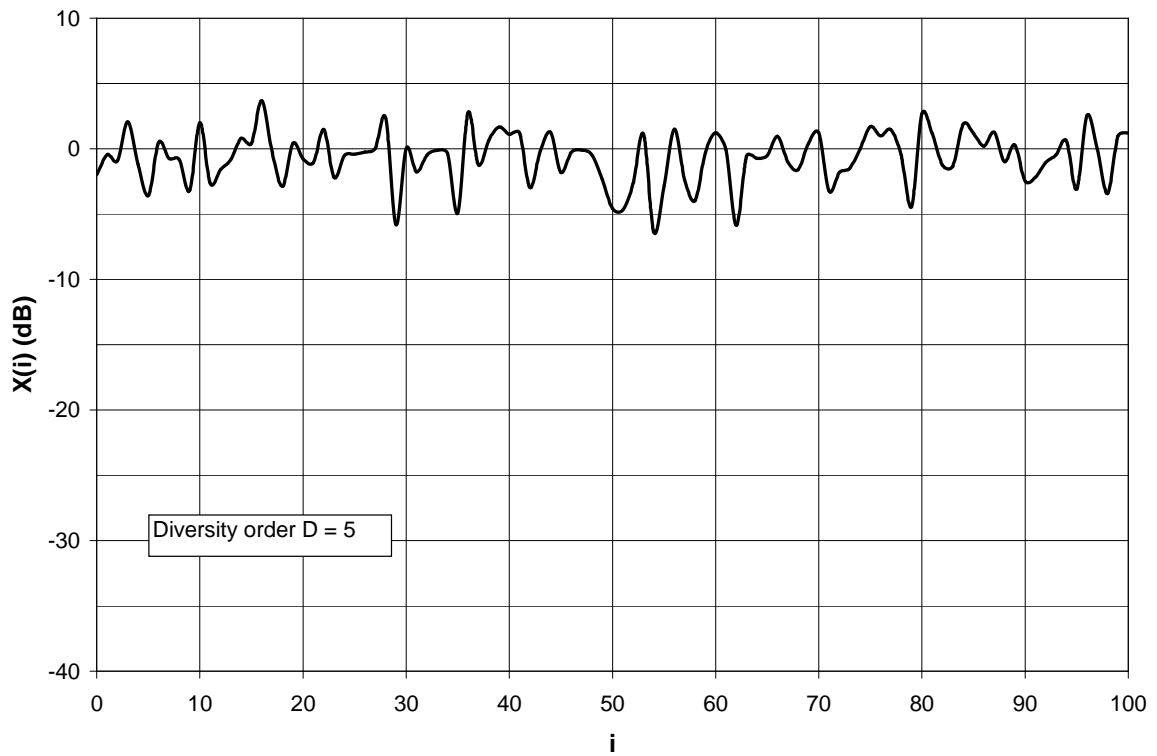


Fig. 4-8 : 100 independent realizations of  $X(i)$ , for  $D = 5$

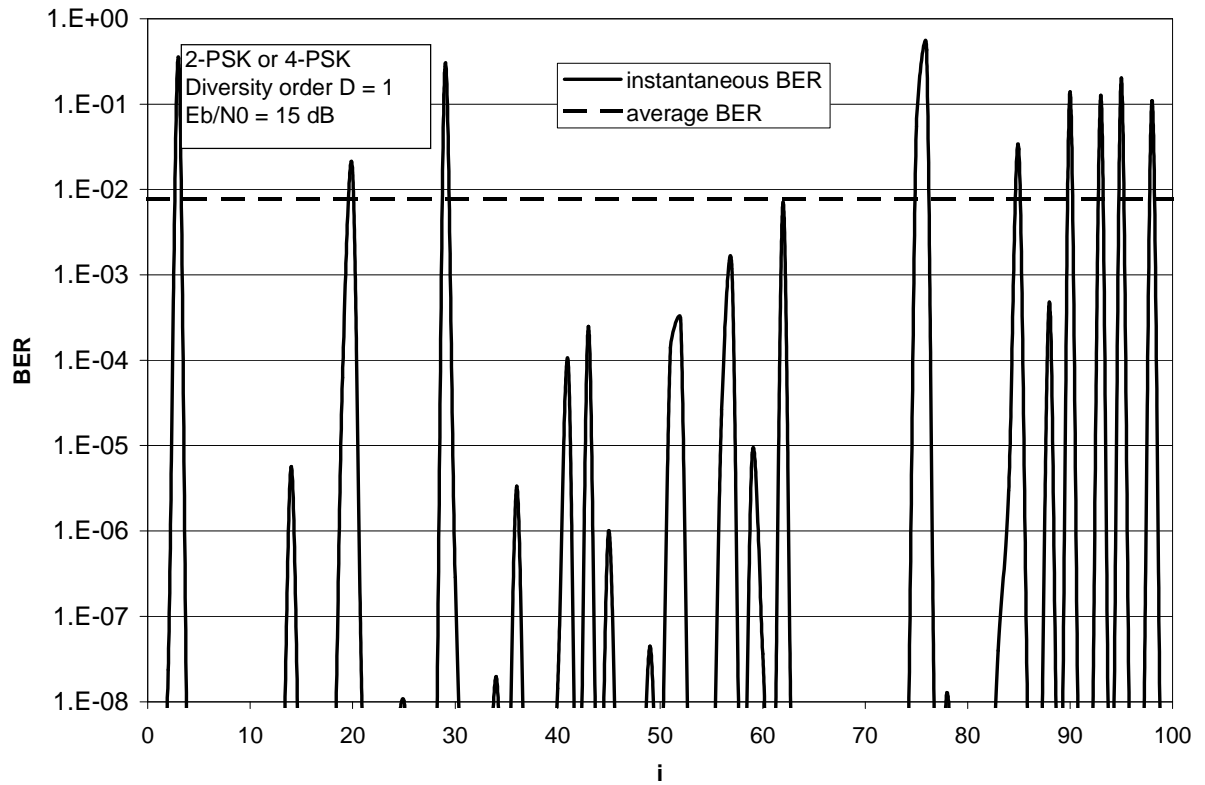


Fig. 4-9 : instantaneous and average BER for  $D = 1$

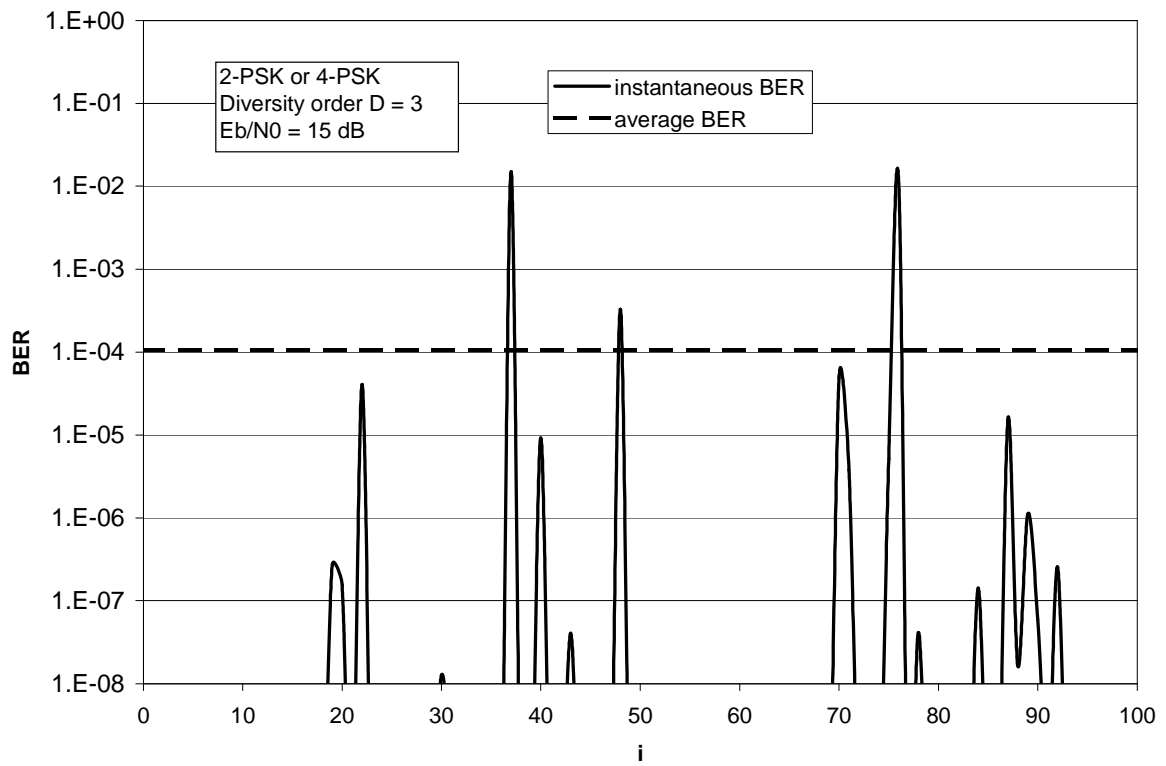


Fig. 4-10 : instantaneous and average BER for  $D = 3$

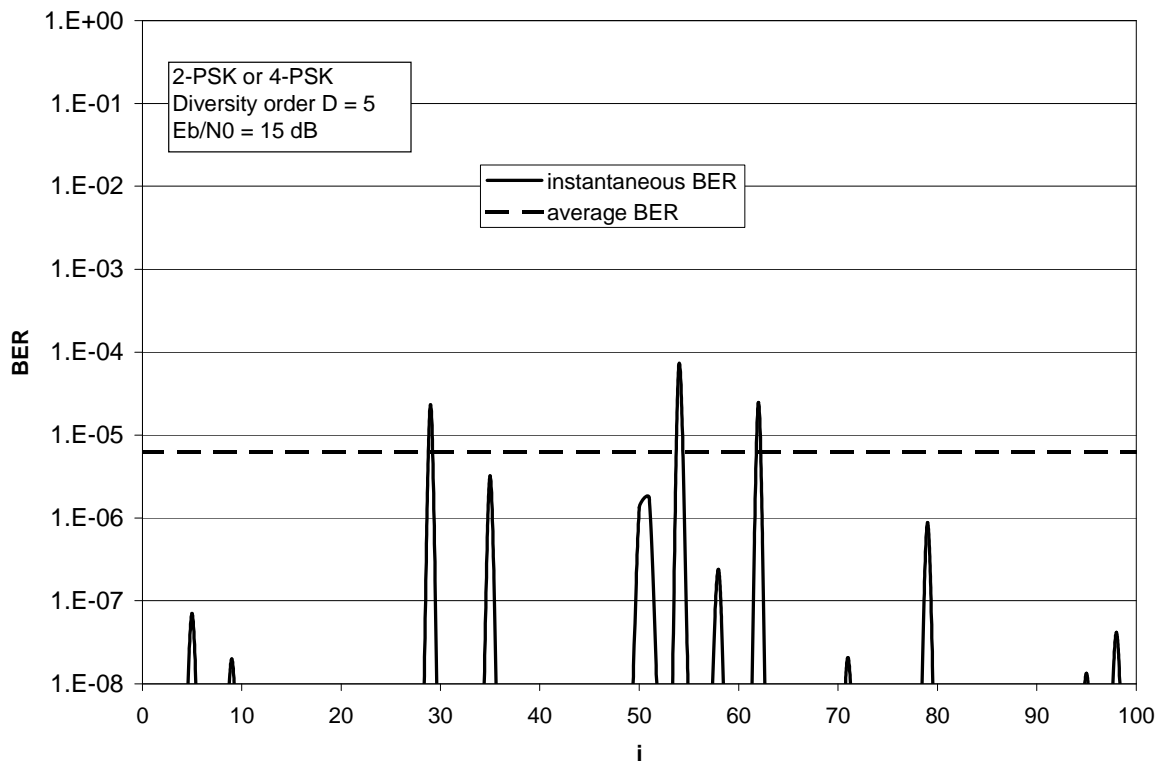


Fig. 4-11 : instantaneous and average BER for  $D = 5$

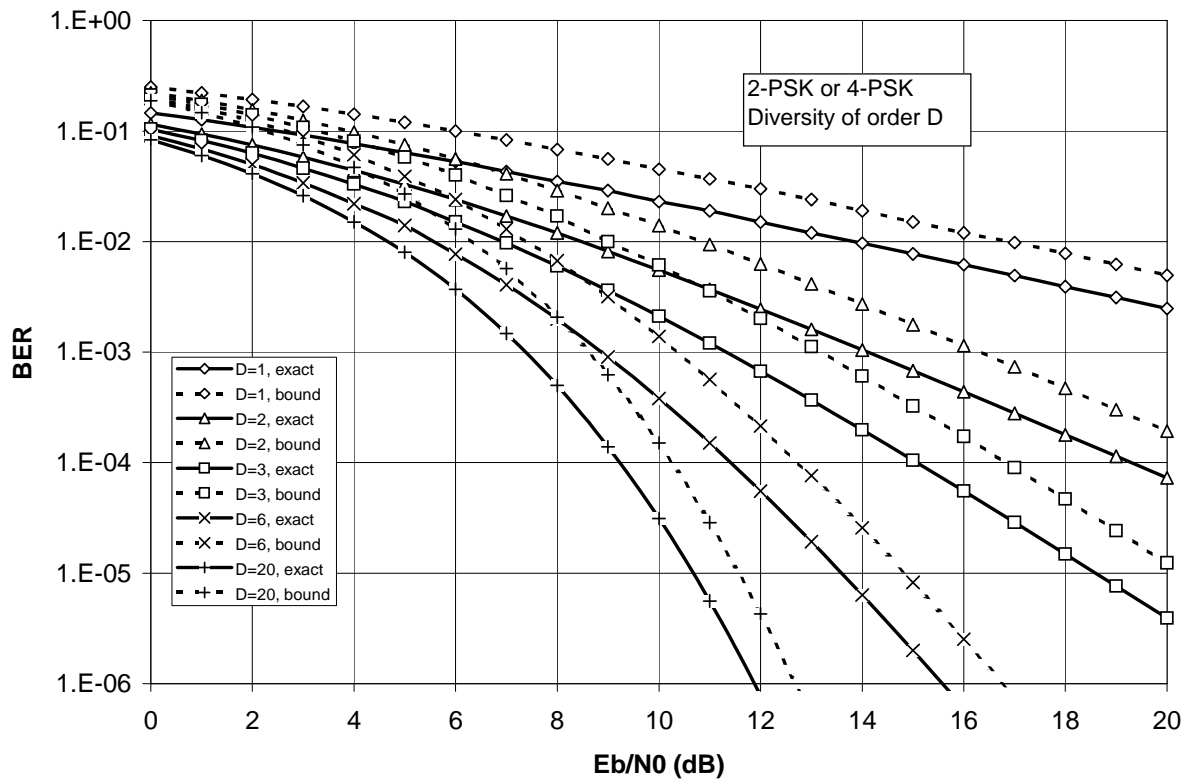


Fig. 4-12 : comparison of exact BER and upper bound on BER

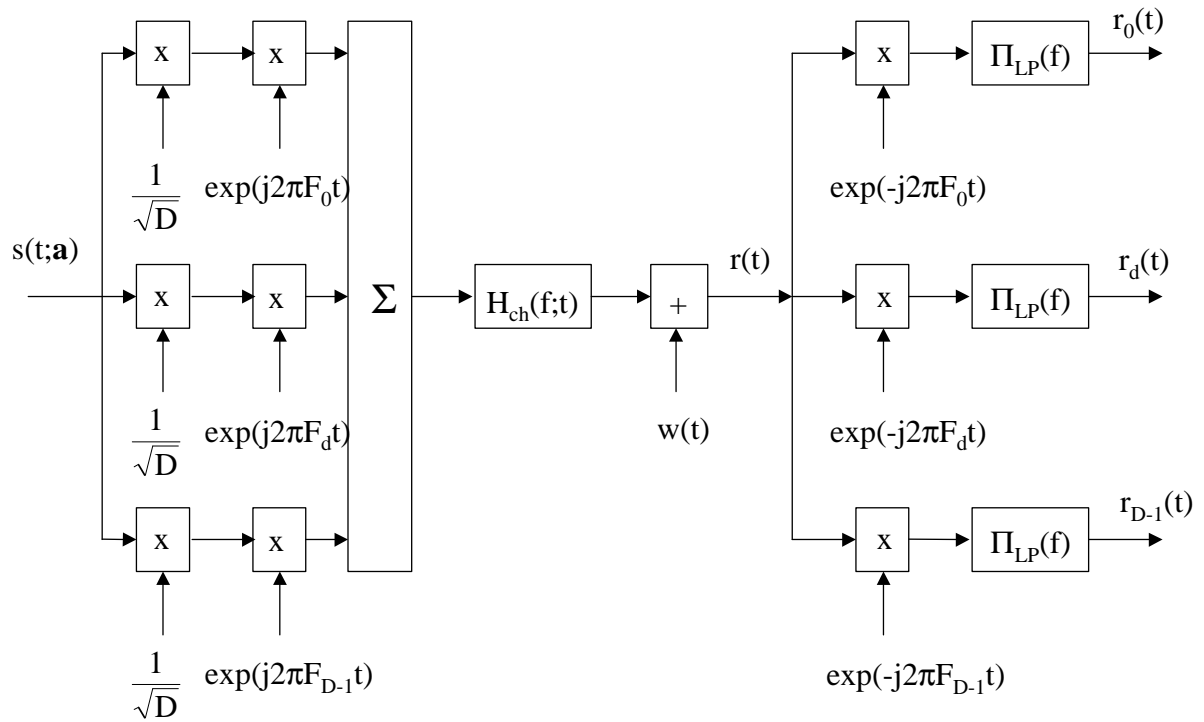


Fig. 4-13 : frequency diversity : transmitter, channel and part of receiver

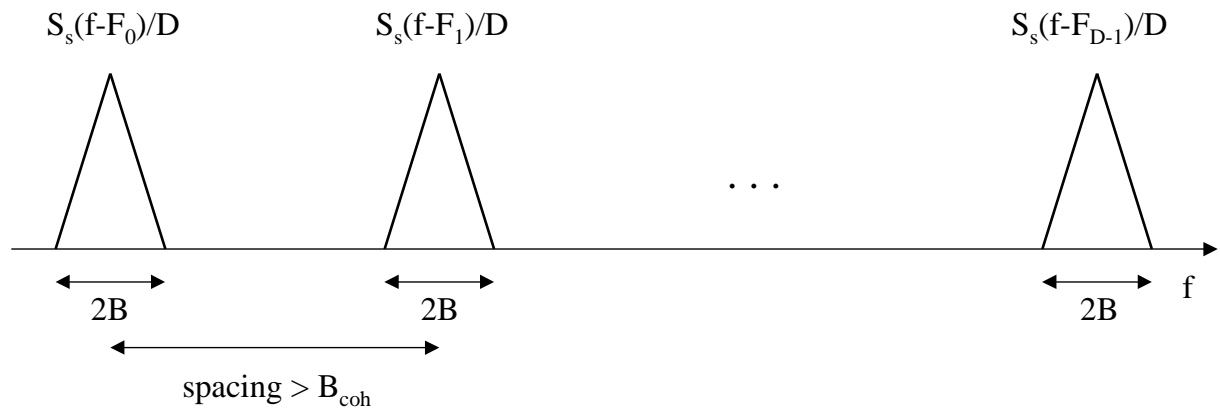


Fig. 4.14 : frequency diversity : power spectrum of transmitted signal

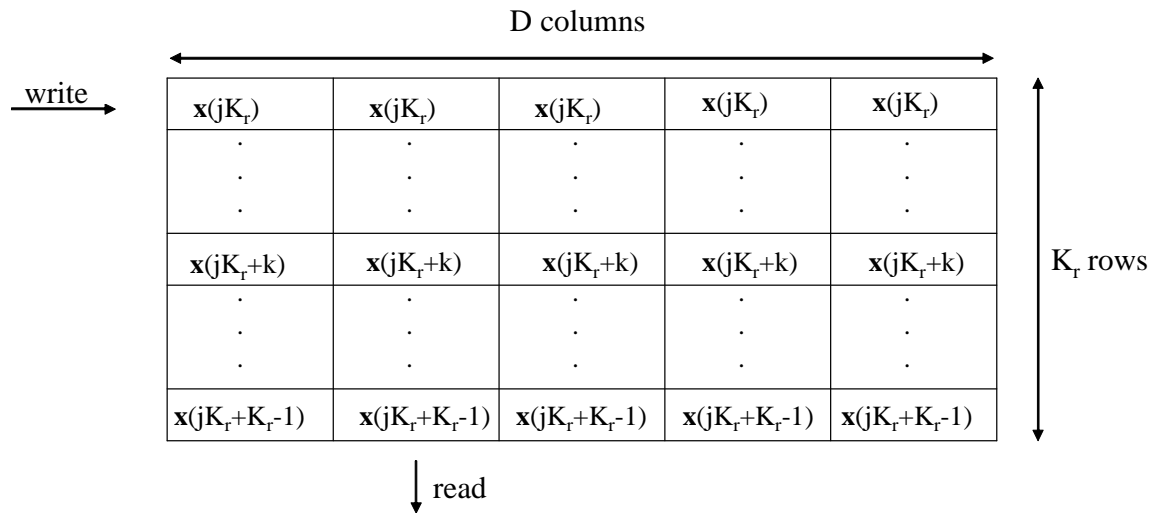


Fig. 4-15 : time diversity : interleaver

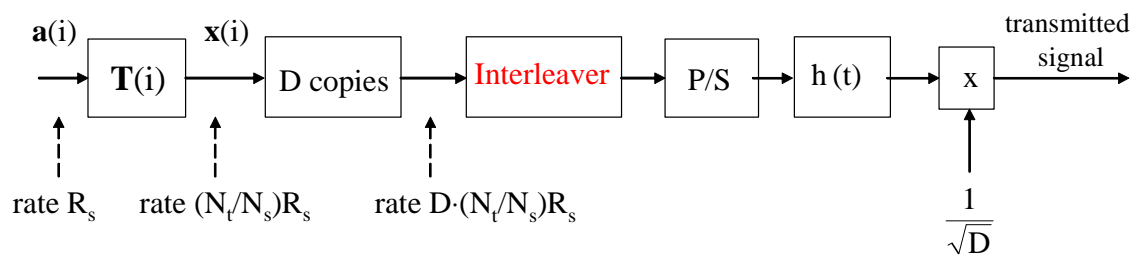


Fig. 4-16 : time diversity : transmitter

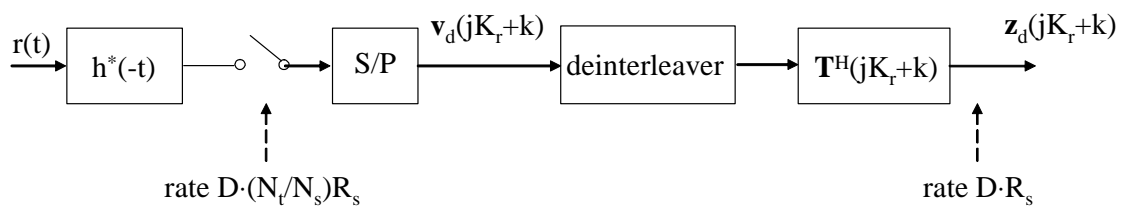


Fig. 4-17 : time diversity : receiver

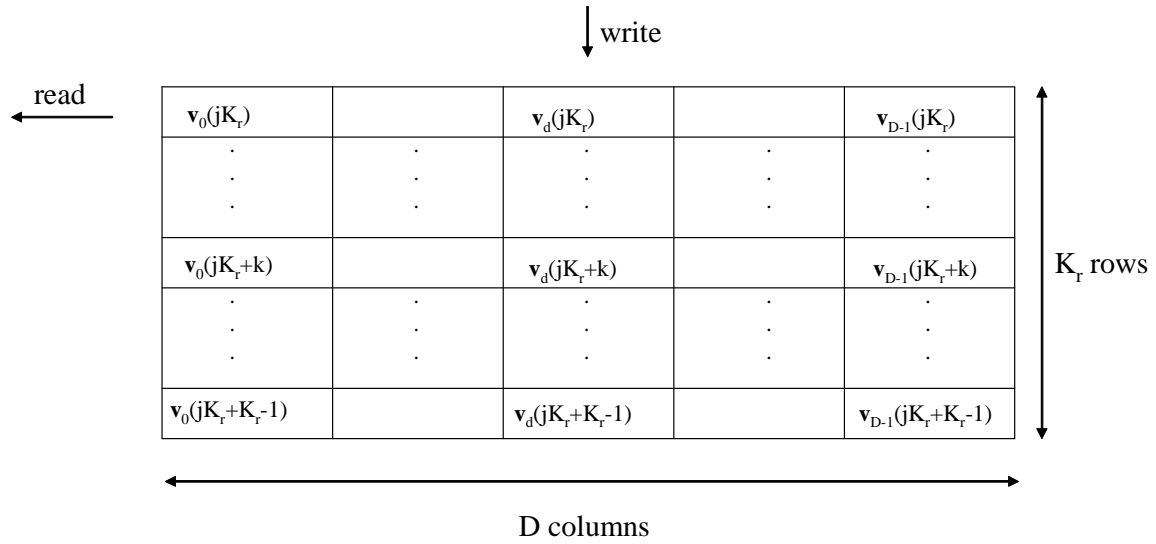


Fig. 4-18 : time diversity : deinterleaver

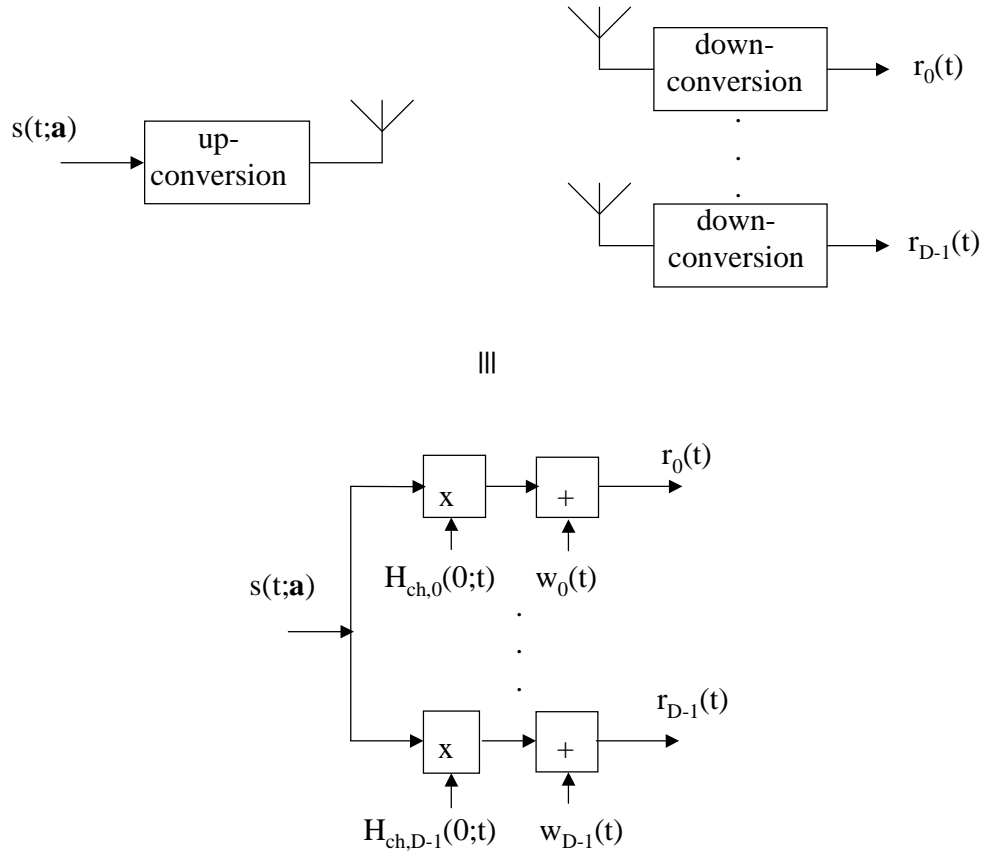


Fig. 4-19 : receive antenna diversity : transmitter, part of receiver, equivalent channel model



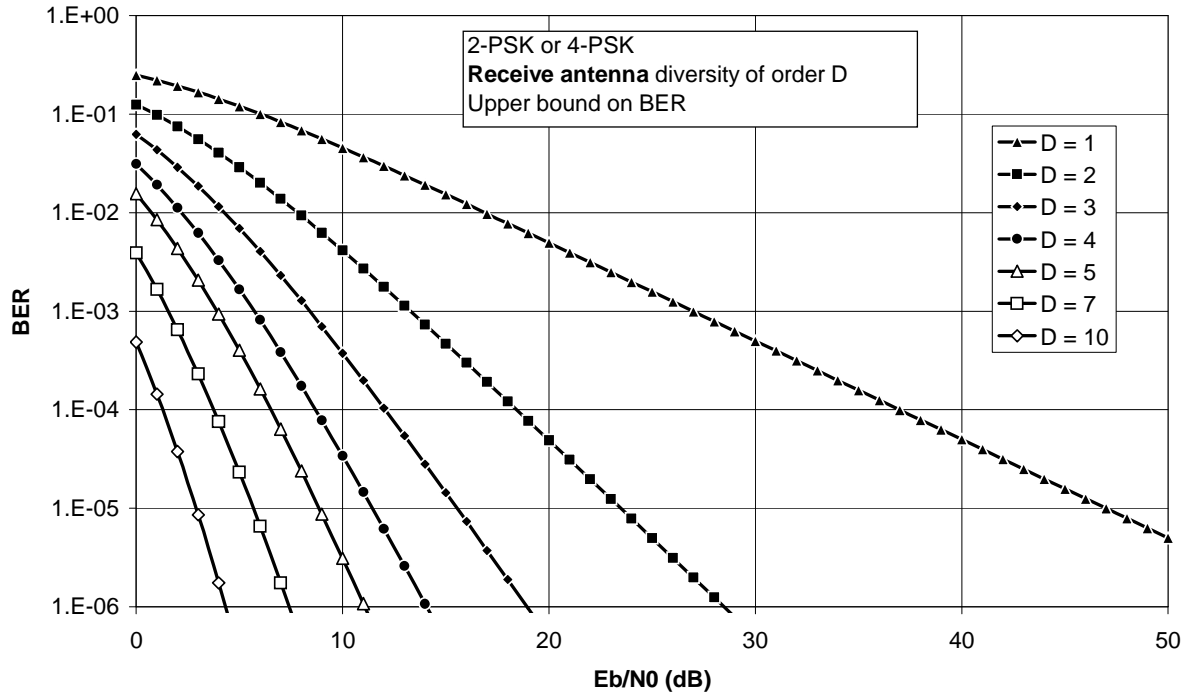
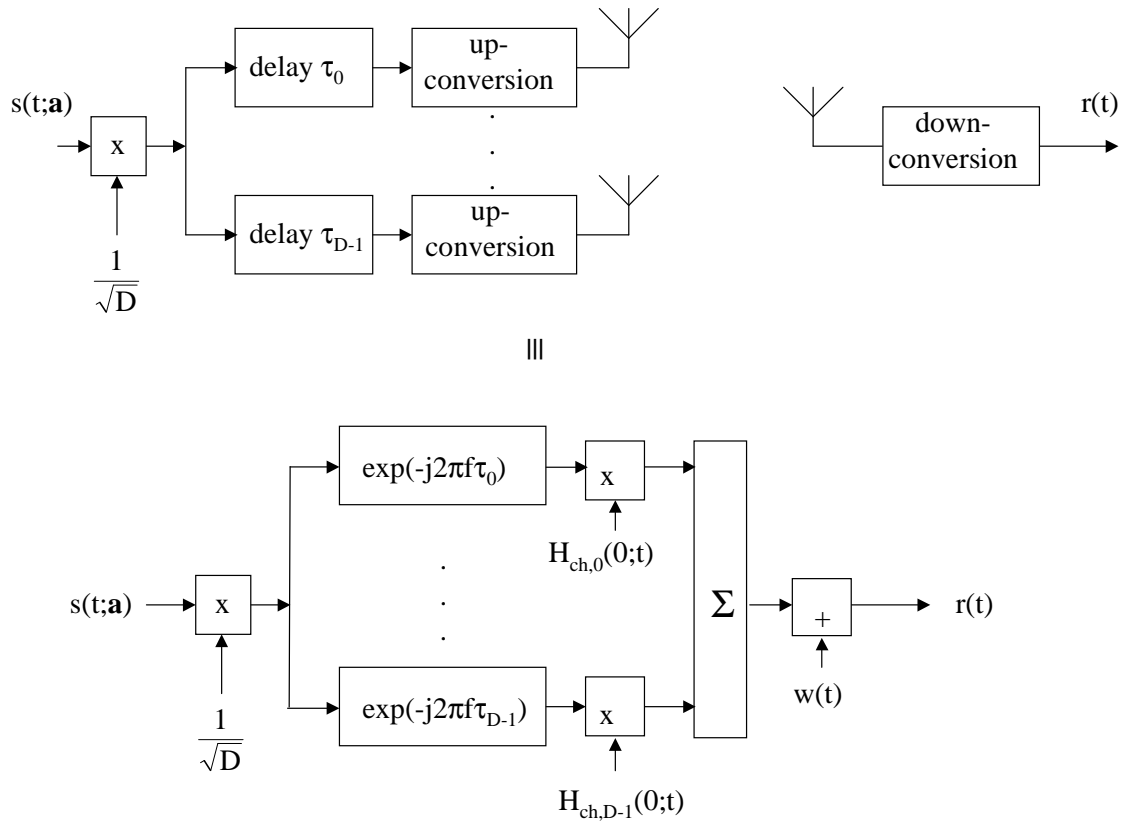

 Fig. 4-20 : receive antenna diversity :  $BER_{up}$ , including array gain


Fig. 4-21 : transmit antenna diversity : transmitter, part of receiver, equivalent channel model

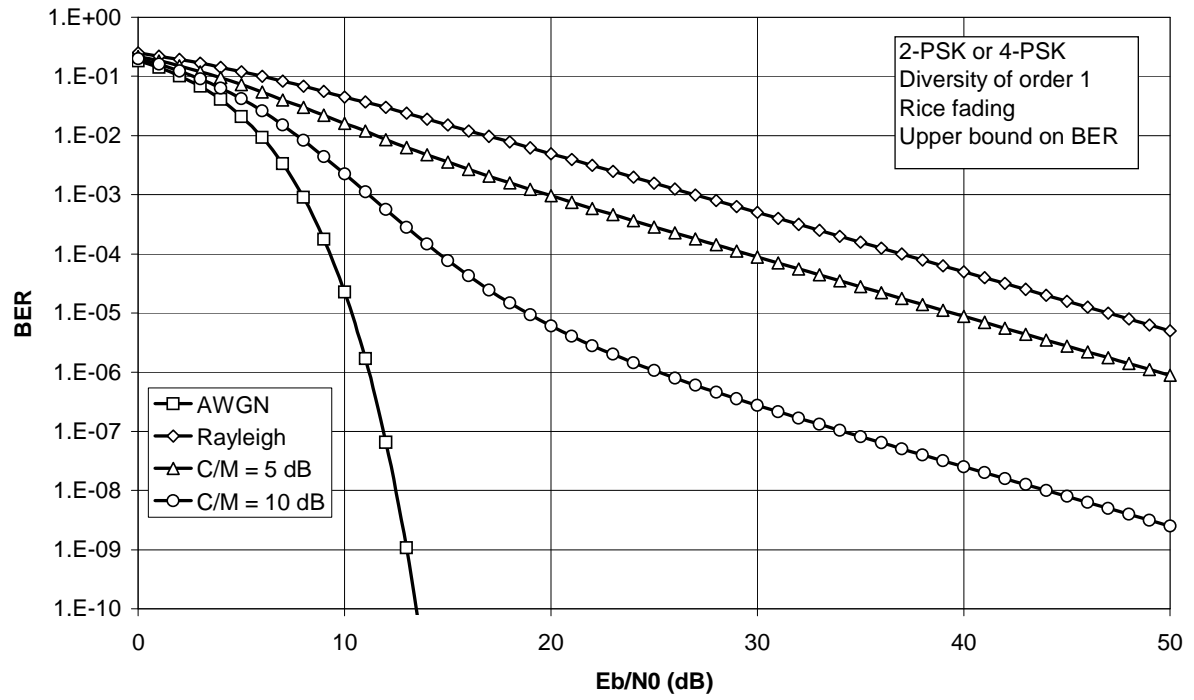


Fig. 4-22 : Rice fading, diversity order = 1

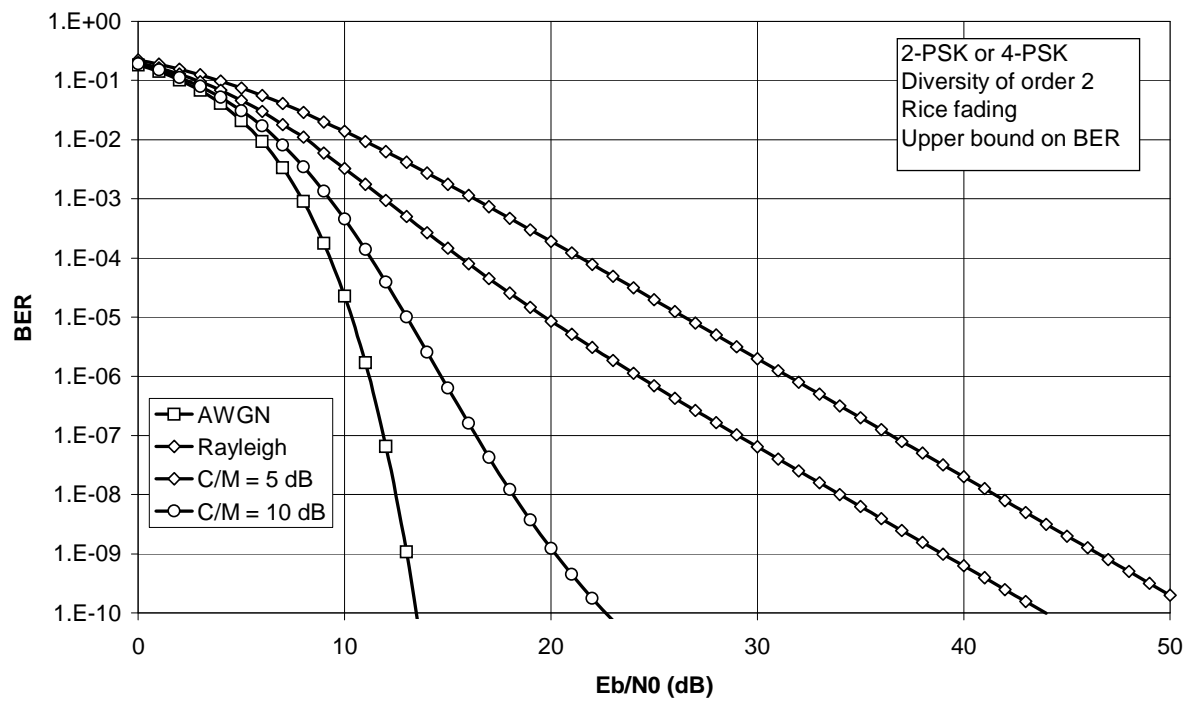


Fig. 4-23 : Rice fading, diversity order = 2

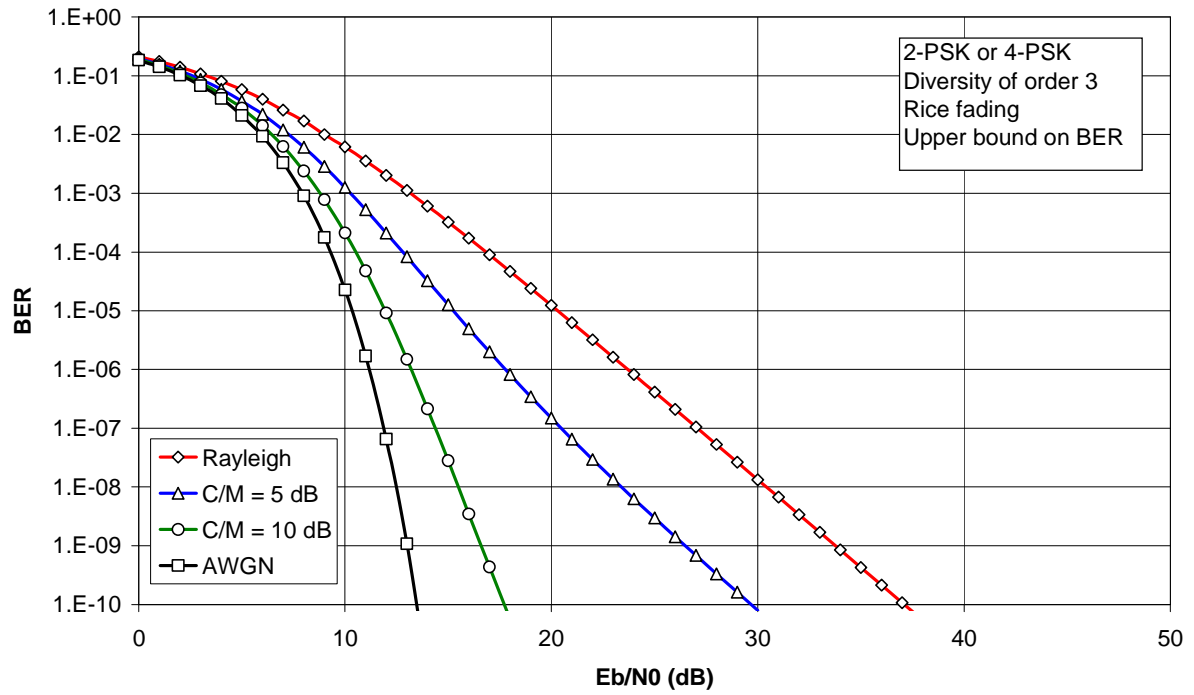


Fig. 4-24 : Rice fading, diversity order = 3

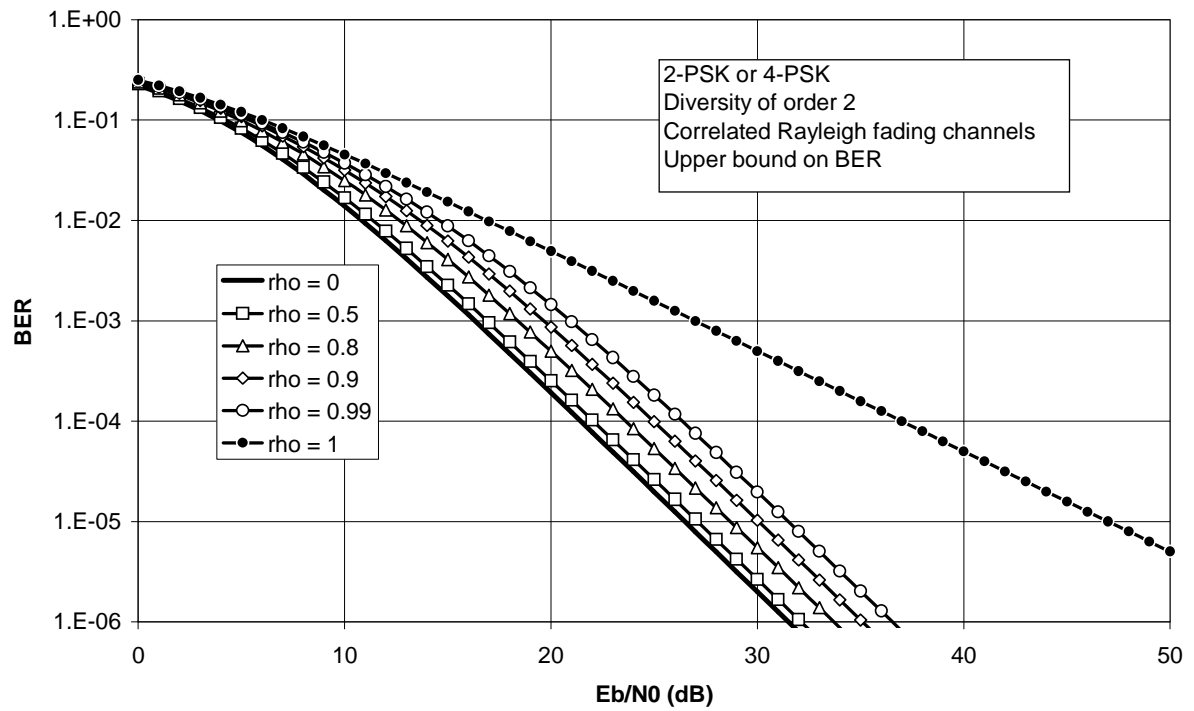


Fig. 4-25 : correlated Rayleigh fading

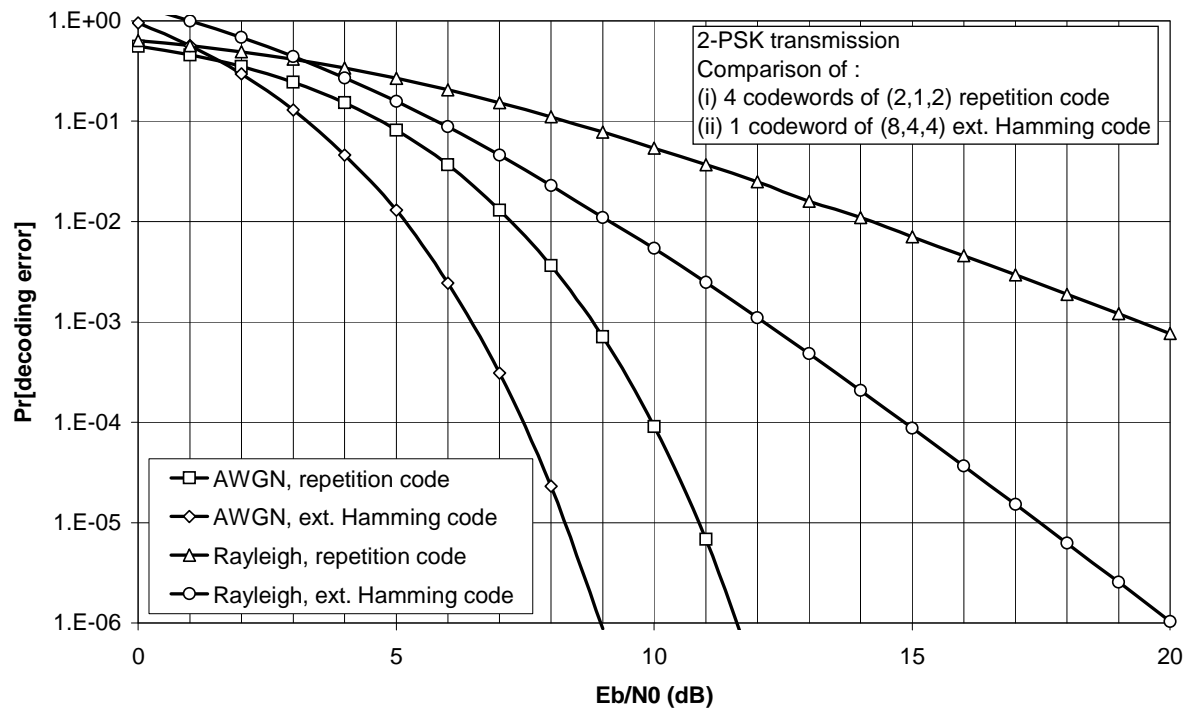


Fig. 4-26 : comparison of repetition code and extended Hamming code

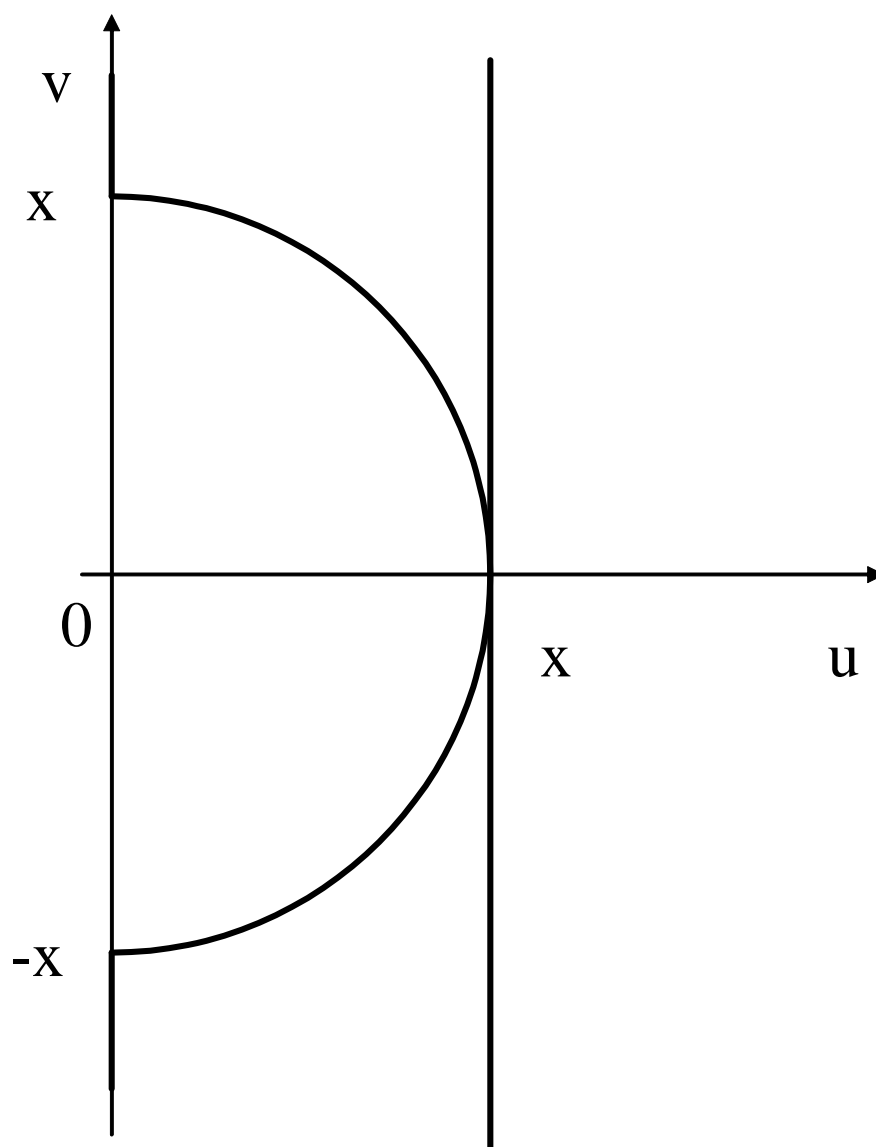


Fig. 4-27 : indication of integration areas

## Chapter 5

### Multiuser communication on the AWGN channel

#### 5.1. Definitions and terminology

In most communication systems, the available channel bandwidth must be shared among different users. Some examples are : radio and TV broadcasting (wireless or via coaxial cable), satellite communication, mobile radio communication (GSM, ...), indoor radio communication (wireless LAN, ...), ...

We consider multi-user communication, where each user terminal (UT) is equipped with a transmitter and a receiver, and is able to send to and receive from a base station (BS). Communication is organized in the following way :

- Upstream communication (uplink communication, communication over the reverse link) : each UT sends a signal to the BS; this is multipoint-to-point communication. The BS has to detect the data transmitted by each of the individual UTs.
- Downstream communication (downlink communication, communication over the forward link) : the BS transmits a sum of signals, with each signal intended to a particular UT; this is point-to-multipoint communication (broadcasting). From the received sum signal, each UT detects only the data intended to that particular UT.

Note that the users do not communicate directly with each other : when user A wants to send a message to user B, the UT of user A first sends the message to the BS, and then the BS sends the message to the UT of user B.

Taking into account that the communication channel must accommodate both the upstream signals and the downstream signals, the reception of one signal can be disturbed by the presence of the other signals. Hence, some measures must be taken to limit the mutual interference between these signals.

- The *multiplexing* scheme describes how to organize the transmission at the BS, so as to avoid interference between the individual downstream signals at the receivers of the UTs.
- The *multiple access* scheme describes how to organize the transmissions at the UTs, so as to avoid interference between the individual upstream signals at the BS receiver.
- The *duplexing* scheme describes how to avoid interference between the group of upstream signals and the group of downstream signals.

## 5.2. Multiuser system description

We assume that the multiuser system consists of one BS and  $N_u$  UTs; hence, the system can accommodate up to  $N_u$  users.

Let us consider a received signal given by

$$r(t) = \underbrace{\sum_{n=0}^{2N_u-1} s_n(t; \mathbf{a}_n)}_{s(t; \mathbf{a})} + w(t) \quad (5.2-1)$$

The noise contribution  $w(t)$  in (5.2-1) is complex-valued white Gaussian noise ( $w(t) \sim N_c(0, N_0\delta(u))$ ). The signals  $\{s_n(t; \mathbf{a}_n), n = 0, \dots, 2N_u-1\}$  represent the set of  $N_u$  upstream signals and  $N_u$  downstream signals; in case some users are not active, the corresponding signals  $s_n(t; \mathbf{a}_n)$  sent to and sent by these users are set to zero. The data symbol sequence contained in  $s_n(t; \mathbf{a}_n)$  is denoted  $\mathbf{a}_n$ , where  $(\mathbf{a}_n)_i = a_n(i)$  and  $i$  is the symbol index. We define  $\mathbf{a}(i)$  as the symbol vector containing the  $2N_u$  data symbols  $\{a_n(i), n = 0, \dots, 2N_u-1\}$  having the same symbol index  $i$ ; all symbol vectors  $\mathbf{a}(i)$  are stacked into the vector  $\mathbf{a}$  :  $a(2N_u i + n) = a_n(i)$ . The symbols  $a(k)$  are i.i.d. and take values from an  $M$ -point constellation. For each signal  $s_n(t; \mathbf{a}_n)$  the average symbol rate equals  $R_s$  : over a long time interval  $T_0$ ,  $s_n(t; \mathbf{a}_n)$  "carries"  $T_0 R_s$  symbols.

The signal (5.2-1) can represent the signal received by the BS or by a UT.

- When  $r(t)$  is the signal received by the BS, we are interested only in detecting the  $N_u$  symbol vectors  $\mathbf{a}_n$  that correspond to the upstream signals transmitted by the UTs.
- When  $r(t)$  is the signal received by a UT, we are interested only in detecting the symbol vector  $\mathbf{a}_n$  that corresponds to the downstream signal intended for the considered UT.

Note that the signal (5.2-1) received by a UT (or by the BS) also contains the signal transmitted by the considered UT (or by the BS). This models the unwanted feedthrough of the transmitted signal to the receiver input that is connected to the same antenna. Although the UT (the BS) knows its transmitted signal and therefore could subtract this feedthrough signal from the received signal, we will assume that such cancellation is not carried out : the feedthrough signal is to be considered as potentially interfering to the receiver.

We will consider linear digital modulation. In its most general form, this means that

$$s(t; \mathbf{a}) = \sum_k a(k) h_k(t) = \sum_{n=0}^{2N_u-1} \underbrace{\sum_i a_n(i) h_{2iN_u+n}(t)}_{s_n(t; \mathbf{a}_n)} \quad (5.2-2)$$

Hence,  $h_{2N_u i + n}(t)$  is the pulse assigned to the  $i$ -th symbol from user signal  $s_n(t; \mathbf{a}_n)$ . We assume that all pulses have a bandwidth not exceeding  $B$  :  $H_k(f) = 0$  for  $|f| > B$ . The shape of the pulses  $h_k(t)$  depends on the type of duplexing, multiplexing and multiple access.

### 5.3. ML detection for orthogonal user signals

From (5.2-1), the log-likelihood function is determined by :

$$N_0 \ln p(\mathbf{r} | \tilde{\mathbf{a}}) \propto 2 \operatorname{Re} \left[ \sum_{n=0}^{2N_u-1} \int r(t) s_n^*(t; \tilde{\mathbf{a}}_n) dt \right] - \sum_{n_1, n_2=0}^{2N_u-1} \int s_{n_1}^*(t; \tilde{\mathbf{a}}_{n_1}) s_{n_2}(t; \tilde{\mathbf{a}}_{n_2}) dt \quad (5.3-1)$$

Assuming all data symbol sequences  $\mathbf{a}$  are equally likely, the decision error probability is minimized by maximizing (5.3-1) over  $\tilde{\mathbf{a}}$  (ML decision rule). However, this maximization is complicated by the fact that the double summation in (5.3-1) contains crossterms involving sequences  $\tilde{\mathbf{a}}_{n_1}$  and  $\tilde{\mathbf{a}}_{n_2}$  with  $n_1 \neq n_2$ . In this case, the likelihood function must be evaluated for all  $M^{2N_u N}$  symbol sequences  $\tilde{\mathbf{a}}$  of length  $2N_u N$ , with  $N$  denoting the number of symbols contained in each signal  $s_n(t; \mathbf{a}_n)$  : the complexity is exponential in the number  $2N_u$  of user signals and in the number  $N$  of symbols per user signal. Even when the BS and the UTs are interested in only a subset of the  $2N_u$  symbol vectors  $\mathbf{a}_n$ , they each must detect all  $2N_u$  symbol vectors, because of the crossterms in (5.3-1).

The crossterms in (5.3-1) disappear when the following orthogonality condition holds :

$$\int s_{n_1}^*(t; \tilde{\mathbf{a}}_{n_1}) s_{n_2}(t; \tilde{\mathbf{a}}_{n_2}) dt = 0 \quad \text{for } n_1 \neq n_2 \text{ and all } (\tilde{\mathbf{a}}_{n_1}, \tilde{\mathbf{a}}_{n_2}) \quad (5.3-2)$$

Using Parseval's relation, (5.3-2) is equivalent to

$$\int S_{n_1}^*(f; \tilde{\mathbf{a}}_{n_1}) S_{n_2}(f; \tilde{\mathbf{a}}_{n_2}) df = 0 \quad \text{for } n_1 \neq n_2 \text{ and all } (\tilde{\mathbf{a}}_{n_1}, \tilde{\mathbf{a}}_{n_2}) \quad (5.3-3)$$

where  $S_n(f; \tilde{\mathbf{a}}_n)$  is the Fourier transform of  $s_n(t; \tilde{\mathbf{a}}_n)$ . Assuming that (5.3-2) holds, (5.3-1) reduces to a sum of  $2N_u$  terms, with each term depending on only one symbol sequence  $\tilde{\mathbf{a}}_n$  :

$$N_0 \ln p(\mathbf{r} | \tilde{\mathbf{a}}) \propto \sum_{n=0}^{2N_u-1} \left( 2 \operatorname{Re} \left[ \int r(t) s_n^*(t; \tilde{\mathbf{a}}_n) dt \right] - \int |s_n(t; \tilde{\mathbf{a}}_n)|^2 dt \right) \quad (5.3-4)$$

Hence, the symbol vectors  $\mathbf{a}_n$  can be detected independently of each other :

$$\hat{\mathbf{a}}_n = \arg \max_{\tilde{\mathbf{a}}_n} \left( 2 \operatorname{Re} \left[ \int r(t) s_n^*(t; \tilde{\mathbf{a}}_n) dt \right] - \int |s_n(t; \tilde{\mathbf{a}}_n)|^2 dt \right) \quad (5.3-5)$$

Note that the same ML decision rule would have been obtained if only the signal  $s_m(t; \mathbf{a}_m)$  were transmitted, i.e.,  $r(t) = s_n(t; \mathbf{a}_n) + w(t)$ .

Substituting (5.2-1) in the first integral in (5.3-5) we obtain

$$\begin{aligned} \int r(t) s_n^*(t; \tilde{\mathbf{a}}_n) dt &= \int \left( \sum_{n_1=0}^{2N_u-1} s_{n_1}(t; \mathbf{a}_{n_1}) + w(t) \right) s_n^*(t; \tilde{\mathbf{a}}_n) dt \\ &= \int (s_n(t; \mathbf{a}_n) + w(t)) s_n^*(t; \tilde{\mathbf{a}}_n) dt \end{aligned} \quad (5.3-6)$$



where the second line of (5.3-6) follows from the orthogonality condition (5.3-2). Hence, the ML decision (5.3-5) and the associated BER performance are not affected by whether or not the terms with  $n_1 \neq n_2$  are present in (5.3-1). This indicates that there is no interference among the different user signals when the orthogonality condition (5.3-2) holds. As the derivation of (5.3-2) does not exploit the fact that linear modulation is used, this condition holds for arbitrary modulation formats.

The complexity of the decision rule (5.3-5) is in general exponential in the number  $N$  of symbols per user signal. This decision rule must be carried out once for each UT and  $N_u$  times (once for each upstream signal) for the BS. Hence the total complexity is linear in  $2N_u$  and exponential in  $N$ .

We know from Chapter 3 that selecting in (5.2-2) the pulses  $h_k(t)$  to be orthogonal gives rise to a ML receiver that reduces to symbol-by-symbol decision. In this case the complexity at the BS and each UT becomes linear in  $N_u N$  and  $N$ , respectively, yielding a total complexity that is proportional to  $2N_u N$ . The resulting BER performance coincides with the matched filter bound, which does not depend on the specific shape of the pulses  $h_k(t)$  (as long as they are orthogonal). Note that these results assume transmission over a frequency-flat channel (such that the orthogonality of the received pulses is preserved).

The selection of orthogonal pulses  $h_k(t)$  is possible only when the available channel bandwidth is sufficiently large. A similar reasoning as in section 3.5 regarding the required bandwidth yields

$$B_{RF} \geq 2N_u R_s \quad (5.3-7)$$

for a multiuser system that accommodates up to  $N_u$  users (i.e.,  $2N_u$  user signals, each with symbol rate  $R_s$ ). Eq. (5.3-7) is the extension of (3.5-1) from the single-user case to the multi-user case.

## 5.4. Basic duplexing, multiplexing and multiple access schemes

Let us formulate some sufficient conditions that yield orthogonal user signals.

- User signals that do not overlap in time are orthogonal (see (5.3-2)).
- User signals that do not overlap in frequency are orthogonal (see (5.3-3)).
- Orthogonal signals that overlap in time and frequency can be generated by assigning orthogonal pulses to the symbols contained in these signals (linear modulation).

The following schemes for duplexing, multiplexing and multiple access, based on these simple sufficient conditions, are frequently encountered in practical systems.

### Duplexing schemes

- Frequency-division duplexing (FDD)

The total bandwidth available is split into two non-overlapping frequency bands, i.e., the *upstream band* and the *downstream band*, which contain the upstream signals and the downstream signals, respectively. The upstream and downstream signals are simultaneously active.

- Time-division duplexing (TDD)

Time is divided into non-overlapping *upstream frames* and *downstream frames* that are alternating, and during which are transmitted the upstream and downstream signals, respectively. Both the set of upstream signals and the set of downstream signals occupy the entire channel bandwidth.

### Multiplexing schemes

- Frequency-division multiplexing (FDM)

The bandwidth available for downstream transmission is split into non-overlapping frequency bands, that each contain one of the downstream signals. The downstream signals are active the whole time that is available for downstream transmission.

- Time-division multiplexing (TDM) :

The time available for downstream transmission is divided into non-overlapping frames, and each such frame is subdivided into non-overlapping slots. A downstream signal is assigned one slot in each frame, and is active only during the assigned slots. Each downstream signal occupies the entire bandwidth that is available for downstream communication.

- Code-division multiplexing (CDM) :

The downstream signals occupy the entire bandwidth and time that are available for downstream communication, but are orthogonal due to user-specific orthogonal "codes" (to be explained in section 5.5).

### Multiple access schemes

For each of the multiplexing schemes defined above, a similar multiple access scheme exists.

- Frequency-division multiple access (FDMA) : the upstream signals occupy non-overlapping frequency bands, and are active the whole time that is available for upstream communication
- Time-division multiplexing (TDMA) : the upstream signals are located in non-overlapping time slots, and each signal occupies the entire bandwidth that is available for upstream communication.
- Code-division multiple access (CDMA) : the upstream signals are orthogonal due to user-specific orthogonal codes, and occupy the entire bandwidth and time that are available for upstream communication

The above schemes for duplexing, multiplexing and multiple access can be visualized by representing them in a time-frequency diagram, showing which signals are active during which time slots and in which frequency bands. The time-frequency diagrams are shown for FDD/FDM/FDMA (Fig. 5-1), FDD/TDM/TDMA (Fig. 5-2), FDD/CDM/CDMA (Fig. 5-3), TDD/FDM/FDMA (Fig. 5-4), TDD/TDM/TDMA (Fig. 5-5), and TDD/ CDM/CDMA (Fig. 5-6). In these cases, the multiplexing and multiple access schemes are of the same type. Fig. 5-7 shows the case of FDD/TDM/CDMA, where the multiplexing and multiple access scheme are of a different type.

The schemes for duplexing, multiplexing and multiple access can be combined with any type of digital modulation. Moreover, they are not restricted to digital modulation : FDD/FDM/FDMA has first been introduced in the context of analog modulation, e.g., for broadcasting radio and TV signals. Here we will focus on linear digital modulation :

- FDM(A) and TDM(A) : conventional modulation with square-root transmit pulse and matched receive filter;
- CDM(A) : block transform modulation, to be explained in section 5.5.

## 5.5. Description of the BS and the UT

Let us consider *upstream communication in case of FDD*, with  $N_u$  upstream signals that use linear digital modulation. Assuming an average transmit power  $P$  and average symbol rate  $R_s$ , the corresponding energy per symbol is  $E_s = P/R_s$ .

- In the case of FDD/FDMA, each upstream signal is permanently active, and occupies a fraction  $1/N_u$  of the upstream bandwidth. Symbols are transmitted by the UT at rate  $R_s$  using transmit power  $P$ . As shown in Fig. 5-8, this transmission involves applying the data symbols to a transmit filter, and upconverting the resulting complex-valued baseband signal to the frequency band assigned to the considered upstream signal. Fig. 5-9 shows the baseband signal, assuming BPSK modulation and a rectangular symbol pulse, corresponding to the symbol sequence  $\{1, -1, 1, 1, -1, 1\}$ . At the BS, the received bandpass signal is applied to a bank of parallel bandpass filters to separate the upstream signals, that occupy different frequency bands (see Fig. 5-10). The  $n$ -th bandpass filter has a passband corresponding to the frequency band occupied by the  $n$ -th upstream signal, and rejects the signals outside this band. Each of the bandpass filter outputs is downconverted to a complex-valued baseband signal, which is applied to a lowpass receive filter and sampled at a rate  $R_s$  in order to detect the data symbols. The hardware cost associated with the BS is rather high, because separate downconverters must be used.
- In the case of FDD/TDMA, each upstream signal occupies the full upstream bandwidth, but is active in only one slot per frame, which corresponds to a fraction  $1/N_u$  of the time. In order to achieve an average symbol rate of  $R_s$ , the symbol rate during the active periods of an upstream signal must equal  $N_u R_s$ . The UT transmitter is shown in Fig. 5-11 : the incoming data symbols (rate  $R_s$ ) are stored in a buffer, which is read at a speed  $N_u R_s$  during the active slots (fraction  $1/N_u$  of the time). The data symbols are applied to a transmit filter, and the resulting complex-valued baseband signal is upconverted to the upstream frequency band. Fig. 5-12 shows the baseband signal, assuming BPSK modulation and a rectangular symbol pulse, corresponding to the symbol sequence  $\{1, -1, 1, 1, -1, 1\}$ . It is important to note that the transmit power during active periods must be  $N_u P$ , in order to achieve a symbol energy  $E_s = (N_u P)/(N_u R_s) = P/R_s$ . Hence, during active periods, the UT transmitter must operate at a rate and a power that are  $N_u$  times larger than the average rate and average power; this of course affects the dimensioning of the associated hardware. At the BS, the received bandpass signal is downconverted from the upstream frequency band to baseband (see Fig. 5-13). The resulting baseband signal is

applied to a receive filter, and sampled at rate  $N_u R_s$  in order to detect the data symbols from all UTs. The detected symbol sequence (rate  $N_u R_s$ ) is demultiplexed into  $N_u$  sequences (each at rate  $R_s$ ) that correspond to the  $N_u$  upstream signals.

- In the case of FDD/CDMA, each upstream signal occupies the full upstream bandwidth and is active all the time. The  $n$ -th upstream signal  $s_n(t; \mathbf{a}_n)$  is given by

$$\begin{aligned} s_n(t; \mathbf{a}_n) &= \sum_i \sum_{m=0}^{N_u-1} T_{m,n}(i) a_n(i) h(t - (iN_u + m)T) \\ &= \sum_k s_n(k) h(t - kT) \end{aligned} \quad n = 0, \dots, N_u-1 \quad (5.5-1)$$

where  $h(t)$  is a square-root Nyquist pulse,  $\{T_{0,n}(i), T_{1,n}(i), \dots, T_{N_u-1,n}(i)\}$  is a "code" used by the  $n$ -th UT during the  $i$ -th symbol interval, and  $s_n(iN_u + m) = T_{m,n}(i) a_n(i)$ . In CDM(A) terminology,  $T_{m,n}(i)$  is the  $m$ -th "chip" in the  $i$ -th symbol interval from the  $n$ -th user, and  $h(t)$  is the "chip pulse". The representation (5.5-1) corresponds to block transform modulation, and is obtained by replacing in (5.2-2) the symbol pulse  $h_{2N_u i+n}(t)$  by

$$h_{2N_u i+n}(t) = \sum_{m=0}^{N_u-1} T_{m,n}(i) h(t - (iN_u + m)T) \quad n = 0, \dots, N_u-1 \quad (5.5-2)$$

From Chapter 3 we know that these  $N_u$  symbol pulses are orthogonal when  $\mathbf{T}^H(i)\mathbf{T}(i) = \mathbf{I}_{N_u}$ , where  $\mathbf{T}(i)$  is the  $N_u \times N_u$  matrix defined as  $(\mathbf{T}(i))_{m,n} = T_{m,n}(i)$ . The signaling rate  $1/T$  (at which the quantities  $s_n(k)$  are transmitted) is related to the symbol rate  $R_s$  by  $1/T = N_u R_s$ . The transmit power equals  $P = E_s R_s$ . The corresponding transmitter of the  $n$ -th UT is shown in Fig. 5-14. The incoming data symbols are multiplied with the user-specific code, the resulting sequence  $s_n(k)$  is applied to the transmit filter (with impulse response  $h(t)$ ), and the transmit filter output signal is upconverted to the upstream frequency band. Fig. 5-15 shows the baseband signal, assuming BPSK modulation and a rectangular chip pulse, corresponding to the symbol sequence  $\{1, 1, -1, 1, -1\}$ . According to Chapter 3, the receiver's decision about the symbol  $a_n(i)$  is the constellation point that is closest to  $z_n(i)$ , where

$$z_n(i) = \sum_{m=0}^{N_u-1} T_{m,n}^*(i) v_m(i) = (\mathbf{T}^H(i) \mathbf{v}(i))_n \quad (5.5-3)$$

and  $v_m(i) = (\mathbf{v}(i))_m$  is obtained by applying the received signal  $r(t)$  to a filter matched to the pulse  $h(t)$ , and sampling the matched filter output at instant  $(iN_u + m)T$ . At the BS, the received upstream bandpass signal is downconverted to baseband, applied to the receive filter and sampled at rate  $N_u R_s$  (see Fig. 5-16). From these samples  $\mathbf{v}(i)$ , the appropriate

linear combinations (5.5-3) are made in order to detect the data symbols from all UTs. Observe the similarity with Fig. 3-2 and Fig. 3-12 (with  $N_s = N_t = N_u$ , and the symbol rate per branch replaced by  $R_s$ ): the UT transmitter implements one branch of the structure from Fig. 3-2 (other branches are implemented by the other UTs), the BS receiver implements the structure from Fig. 3-12.

Still assuming *FDD*, similar considerations are valid for the *downstream communication*. The BS transmitters and UT receivers for FDM, TDM and CDM are described below.

- In the case of FDD/FDM, the BS transmitter (see Fig. 5-17) consists of  $N_u$  parallel branches, with each branch being similar to a UT transmitter for FDMA; the associated hardware cost is rather high, as separate upconverters must be used. The UT receiver (see Fig. 5-18) is similar to a single branch of the BS receiver for FDD/FDMA.
- In the case of FDD/TDM, the BS transmitter (see Fig. 5-19) multiplexes the  $N_u$  incoming data symbol sequences (individual rates  $R_s$ ) into a single data symbol sequence of rate  $N_u R_s$ , such that the symbols to be transmitted to the  $n$ -th UT are in the  $n$ -th slot of each frame. This symbol sequence is applied to the transmit filter, and the resulting signal is upconverted to the downstream frequency band. The UT receiver (see Fig. 5-20) is similar to the BS receiver for FDD/TDMA, but only the receive filter output samples corresponding to the active slots of the corresponding downstream signal (fraction  $1/N_u$ ) are used.
- In the case of FDM/CDM, the BS transmitter (see Fig. 5-21) multiplies each incoming data symbol sequence  $a_n(i)$  (individual data rates  $R_s$ ) with the corresponding code (rate  $N_u R_s$ ), and adds the resulting sequences  $s_n(k)$ ; the sum sequence is applied to the transmit filter, and the resulting signal is upconverted to the downstream frequency band. The UT receiver (see Fig. 5-22) is similar to one branch of the BS receiver for FDD/CDMA. Observe the similarity with Fig. 3-2 and Fig. 3-12 (with  $N_s = N_t = N_u$ , and the symbol rate per branch replaced by  $R_s$ ): the UT receiver implements one branch of the structure from Fig. 3-12 (other branches are implemented by the other UTs), the BS transmitter implements the structure from Fig. 3-2.

In the case of *TDD*, we must take into account that upstream signals and downstream signals are active *only half of the time*. Hence, in order to achieve for each upstream or downstream signal an average power  $P$  and average symbol rate  $R_s$ , for both TDD/FDM(A) and TDD/CDM(A) the transmit power and symbol rate during active frames are  $2P$  and  $2R_s$ ,

whereas for TDD/TDM(A) the transmit power and symbol rate during active slots are  $2N_uP$  and  $2N_uR_s$ . Consequently, the transmitter signaling rate and receiver sampling rate during active periods are equal to  $2R_s$  for TDD/FDM(A) and to  $2N_uR_s$  for both TDD/TDM(A) and TDD/CDM(A).

The above signal properties related to FDM(A), TDM(A) and CDM(A) are summarized in Table 5-1.

	Average power during active period		Signaling rate during active period	
	FDD	TDD	FDD	TDD
FDM(A)	P	2P	$R_s$	$2R_s$
TDM(A)	$N_uP$	$2N_uP$	$N_uR_s$	$2N_uR_s$
CDM(A)	P	2P	$N_uR_s$	$2N_uR_s$

Table 5-1 : Properties of a single signal with average power P and average symbol rate  $R_s$

## 5.6. Requirements on signal coordination

In the case of FDM(A), interference between signals in adjacent frequency bands can occur when their carrier frequencies deviate from their nominal values. In order to reduce this interference, a small guard band is introduced between adjacent frequency bands. In this case, no interference occurs when the carrier frequency deviations are less than the width of the guard band. Interference between signals in adjacent frequency bands can also be caused by a receive filter that is not sufficiently selective to suppress adjacent signals; the introduction of a guard band relaxes the requirements on receive filter selectivity. For similar reasons, a guard band is introduced also between the upstream and downstream frequency bands in FDD.

In the case of TDM(A), the instants at which the different signals are transmitted must be carefully synchronized, in order to avoid the interference that occurs when signals from different transmitters overlap in time when arriving at the receiver. In the case of downstream transmission, synchronization of the transmission instants is easily achieved, because all downstream signals are generated at the same location, i.e., at the BS transmitter. However, in upstream transmission such synchronization is more difficult to achieve, because the UT transmitters are at different locations; in this case, the ideal transmission instants of the individual user signals depend on the propagation delay from the considered UT to the BS (see Fig. 5-23). In order to reduce this interference, a small guard time between adjacent slots

is introduced; in this case, no interference occurs when the deviation of the transmission instants from their nominal values is less than the guard time.

In the case of TDD, the upstream and downstream signals are in different frames. As for TDM and TDMA, transmission instants at the UTs must be synchronized, in order that the upstream signals arrive aligned with the upstream frame at the BS receiver. The propagation delay from the UT to BS gives rise to a "dead zone" between transmission and reception at the BS, the size of which is determined by the maximum propagation delay (see Fig. 5-24).

In the case of CDM(A), the different signals can be separated at the receiver because of their orthogonality. However, when two CDM(A) signals are slightly delayed with respect to each other, they are no longer orthogonal, and give rise to mutual interference. Hence, the transmission instants must be tightly controlled in order to avoid interference. Such accurate synchronization can be realized at the BS transmitter for downstream transmission, but is very hard to achieve in upstream transmission because the UTs are at different locations. Hence, the BS receiver must cope with some amount of interference, caused by transmitter synchronization imperfections at the UTs.

## 5.7. Peak power considerations

Let us consider a number of statistically independent complex-valued signals that are simultaneously active. The sum of these signals, denoted  $s_{\text{sum}}(t)$ , has an average power  $P_{\text{sum}}$  (averaged over their active period). However, occasionally the instantaneous power  $|s_{\text{sum}}(t)|^2$  can be considerably larger than  $P_{\text{sum}}$ . When transmitting or receiving a sum of simultaneously active signals, the statistics of the peaks of  $|s_{\text{sum}}(t)|^2$  should be taken into account when dimensioning the hardware, in order to avoid nonlinear distortion. When the number of signals is large,  $s_{\text{sum}}(t)$  can be approximated by a zero-mean complex-valued Gaussian process with  $E[|s_{\text{sum}}(t)|^2] = P_{\text{sum}}$ . In this case, the instantaneous power  $|s_{\text{sum}}(t)|^2$  has an exponential distribution, determined by

$$\Pr[|s_{\text{sum}}(t)|^2 > P_D] = \exp\left(\frac{-P_D}{P_{\text{sum}}}\right) \quad (5.7-1)$$

Suppose that the hardware has been dimensioned such that no noticeable signal distortion occurs when the instantaneous power  $|s_{\text{sum}}(t)|^2$  of the sum signal is less than  $P_D$ , and we allow  $|s_{\text{sum}}(t)|^2 > P_D$  for only 1% (0.1%) of the time. In order that  $\Pr[|s_{\text{sum}}(t)|^2 > P_D] = 1\%$  (0.1%), we need  $P_D = 4.6 \cdot P_{\text{sum}}$  ( $P_D = 6.9 \cdot P_{\text{sum}}$ ), which implies that the hardware must be designed taking into account a power level  $P_D$  of 6.6 dB (8.4 dB) above the average power  $P_{\text{sum}}$ .



The above considerations apply to FDM(A) and CDM(A), but not to TDM(A). In the case of TDM(A), the user signals are not simultaneously active, so that the peak power of an *individual* signal must be taken into account when dimensioning the hardware. The ratio of peak power to average power (over the active period) for TDM(A) depends on the symbol constellation and the shape of the transmit pulse; for M-PSK with rectangular pulses, this ratio equals 1.

The above peak power considerations related to FDM(A) and CDM(A) are summarized in Table 5-2.

	P <sub>sum</sub> during active period	
	FDD	TDD
FDM(A), CDM(A)	N <sub>u</sub> P	2N <sub>u</sub> P

Table 5-2 : average sum power of N<sub>u</sub> signals, each having average power P

## 5.8. Accommodating variable symbol rates.

A communication system might need some flexibility to accommodate users with different, possibly time-varying, requirements about their symbol rate for transmission or reception.

- In the case of FDM(A), fixed-width frequency bands are available for communication. In principle more than one frequency band could be assigned to some user, but this would imply that the corresponding UT needs a number of parallel transmitters or receivers in order to simultaneously utilize the multiple frequency bands. To avoid the associated hardware complexity, in FDM and FDMA each user is assigned only one frequency band. Hence, FDM and FDMA are suited only for users with fixed symbol rate.
- In the case of TDM(A), more than one time slot can be assigned to a user that requires a higher symbol rate. Besides the fact that the UT must then be active during more than one time slot per frame, the hardware consequences are minor.
- In the case of CDM(A), more than one orthogonal code can be assigned to a user that requires a higher symbol rate. The UT must be able to transmit or receive more than one signal. Besides the fact that the UT transmitter must cope with a higher transmit power, the hardware consequences are minor.

## 5.9. The effect of channel dispersion

In the above discussions, we have ignored the distortion caused by the channel. In several practical situations the channel is dispersive : its transfer function is not constant over the frequency band of interest. Hence, signal components at different frequencies are affected differently by the channel, which causes linear distortion. The signal at the channel output is the convolution of the channel impulse response and the channel input signal. Hence, when the duration of the channel input signal, the channel impulse response and the channel output signal are  $T_{in}$ ,  $T_{ch}$  and  $T_{out}$ , we have  $T_{out} = T_{in} + T_{ch}$ . Let us consider the effect of channel dispersion on the duplexing, multiplexing and multiple access schemes.

- For a linear time-invariant channel, the received signals are in exactly the same frequency bands as the corresponding transmitted signals. Hence, when transmitted signals are in non-overlapping frequency bands (FDD, FDM, FDMA), channel dispersion causes no interference between the received signals. In spite of the linear distortion, the received signals are still orthogonal, so the receiver must cope only with the linear distortion of the useful signal.
- When the transmitted signals are in different time intervals (TDD, TDM, TDMA), the corresponding *received* signals might overlap, because their duration is increased by the channel impulse response duration  $T_{ch}$ . Interference between signals in adjacent time intervals is avoided, by introducing between adjacent intervals a guard time with a duration of at least  $T_{ch}$ . In this case the received signals are still orthogonal, so the receiver must cope only with the linear distortion of the useful signal. As the bandwidth of a TDM(A) signal is larger than the bandwidth of an FDM(A) signal, the linear distortion in TDM(A) is usually larger than in FDM(A).
- In the cases of CDM and CDMA, the transmitted signals occupy the same frequency interval and the same time interval. The channel dispersion destroys their orthogonality, which causes *multiuser interference* at the receiver. The receiver must cope with both the linear distortion of the useful signal and the interference caused by the other signals.

In the cases of FDM and FDMA, the available frequency bands are affected differently by the dispersive channel, so that the BER performance is not the same for all users. In order to provide the same BER quality to all users, *frequency hopping* can be introduced. The assignment of frequency bands to users changes from one hopping interval to the next, such that on average each of the frequency bands has been assigned the same number of times to

each user. Note that for upstream transmission the boundaries of the hopping intervals must be synchronized among the users, so that they are properly aligned when arriving at the BS receiver. (see Fig. 5-25).

## 5.10. The cellular radio concept

Considering a wireless communication system that accommodates a large number of users, it follows from (5.3-7) that huge bandwidths are needed to avoid interference among users : taking  $N_u = 10^6$  and  $R_s = 1$  kbaud, we obtain  $B_{RF,tot} > 2$  GHz ! Clearly, a more practical solution should be found.

The practical solution consists in dividing the geographical area to be served into a number of hexagonal cells. Each cell has one BS at the center, that communicates with  $N_{cell}$  users that are located in the considered cell; BSs can communicate with each other through a wired communication network. The RF-bandwidth  $B_{RF,cell}$  needed to support the wireless upstream and downstream communication within a cell satisfies  $B_{RF,cell} \geq 2N_{cell}R_s$ , with  $R_s$  denoting the symbol rate of each individual user. In order to avoid interference, neighboring cells operate in different frequency bands. Taking into account that path loss increases with distance, frequency bands can be *reused* in sufficiently distant cells. This means that each cell must cope with inter-cell (or "co-channel") interference that is caused by signals in (distant) cells that operate in the same frequency band as the considered cell; the inter-cell interference level experienced by a UT receiver depends on the position of the UT within the cell. Assuming that in total  $N_{re}$  different frequency bands are used, the whole cellular system requires an RF-bandwidth given by

$$B_{RF,tot} = N_{re} B_{RF,cell} \geq 2N_{re}N_{cell}R_s \quad (5.10-1)$$

$N_{re}$  is called the *frequency reuse factor*. Cellular configurations with  $N_{re} = 3, 4, 7$  are shown in Figs. 5-26, 5-27 and 5-28 (cells with the same label operate in the same frequency band). The larger  $N_{re}$ , the more distant the cells that operate in the same frequency band and the less co-channel interference, but the larger the total bandwidth  $B_{RF,tot}$ .

In systems that make use of CDM(A), we usually have  $N_{re} = 1$  : all cells operate in the same frequency band. How to limit the co-channel interference from adjacent cells will be discussed in a later chapter.

### 5.11. Upstream power control

The path loss of the upstream signals in cellular radio depends strongly on the distance of the UTs to the BS. Hence, when all UTs transmit at the same power, the signals received by the BS might have drastically different power levels. When two upstream signals interfere (e.g., this might happen in FDMA when the receive filters are not sufficiently selective, in CDMA when orthogonality is affected by channel dispersion, and in TDMA when the UTs' transmitters are not properly synchronized), the interference caused by the stronger signal (from a nearby user) can be much larger than the useful weaker signal (from a far away user), in which case the data from the weaker user signal cannot be detected reliably. This is called the *near-far problem*.

Even when upstream signals do not interfere at all, it is better that they are received at approximately the same power level, in order to limit the requirements on the dynamic range of the BS receiver hardware.

In order to avoid the near-far problem, upstream power control is introduced : UTs at larger distance from the BS are allowed to transmit more power than those that are close to the BS. This way, each upstream signal is received at the BS at approximately the same power level. In addition, power control reduces the power consumption at the UT transmitter. Power control can be achieved by the BS monitoring the received signal strength of each upstream signal, and sending control signals to the UTs for adjusting their transmit power.

#### Example

Consider two UTs at 0.1 km and 1 km from the BS, respectively. When their transmit powers are the same, the (median) power levels received at the BS are different by 40 dB (for a path loss coefficient  $n = 4$ ). Assuming that each signal is affected by an interference power that is 0.1% of (or 30 dB below) the power of the other signal, the weak signal experiences an interference power that is 10 times (or 10 dB above) its own power. The strong signal, on the other hand, experiences an interference power that is 70 dB below its own power.

In order to avoid the near-far problem, the transmit power of the UT at 1 km from the BS must be 40 dB above the transmit power of the UT at 0.1 km from the BS. When this is the case, both signals experience an interference power at the BS receiver that is 30 dB below their own power.

## 5.12. Downstream power control

When the BS transmits all downstream signals at the same power, a given UT receives the downstream signals at the same strength. However, this strength decreases with increasing distance between the BS and the considered UT. Hence, as each UT receiver also suffers from about the same AWGN level, the ratio of useful received signal power to the power of interference plus noise (this is called the signal to interference plus noise ratio, SINR) decreases with the distance to the BS. Moreover, different UTs might experience different interference levels (e.g., inter-cell interference), according to their position within the cell. Hence, the SINR is user-dependent. The BS adjusts the transmit power of the individual downstream signals in order that all UTs have approximately the same SINR. Note that increasing the power of the downstream signal intended for a particular UT gives rise to an increase of the SINR at that UT, but yields a reduction of the SINR at the other UTs.

Downstream power control can be achieved by the UTs monitoring link quality (e.g., by counting errors when using an error detecting code, or by measuring signal power and interference power), and forwarding link quality to the BS; the BS then adjusts its downstream transmit power levels based on the received link qualities.

## 5.13. Cell sizes

In cellular radio, the symbol rate  $R_s$  per user and the RF bandwidth  $B_{\text{RF,cell}}$  containing the upstream and downstream signals determines the number of users that can be accommodated per cell :  $B_{\text{RF,cell}} \geq 2N_{\text{cell}}R_s$ . Hence, in areas with high user density (number of users per unit area) cell sizes are small, and the transmit power of the BSs is small because distances between BS and UTs are small. The opposite holds in low user density areas : the cell size is large, and the BSs have high transmit power. The following cases are usually distinguished :

- Macrocells have a radius from 1 km to 30 km. They are used in rural areas and suburbs with low user density
- Microcells have a radius from 100 m to 1 km. They are used in areas with high user densities, such as city center or highway
- Picocells have a radius from 10 m to 100 m. They are used for indoor communication in office buildings, airport terminals, shopping centers, ... where user densities are high.

### 5.14. A few current standards

Here we give a short description of a few current standards : GSM, DECT and IS-95. Typical of these systems is that they use a combination of techniques for separating the individual user signals : GSM and DECT make use of FDM(A) and TDM(A), whereas IS-95 makes use of FDM(A) and CDM(A). Such combination is a tradeoff between pure FDM(A), which requires the implementation at the BS of a large number of parallel transmitters and receivers that each operate at the individual user data rate, and pure TDM(A) or CDM(A), which requires the implementation at the BS and the UT of a transmitter and receiver operating at a speed equal to the total data rate.

#### European GSM standard for digital cellular radio

Global System for Mobile Communications (*GSM*) is a standard for digital cellular radio, that covers a large area by means of cells with a radius from 500 m to 30 km. Both digitized voice and data can be transmitted. User mobility up to 200 km/h is supported.

Upstream and downstream signals are separated by means of FDD. Individual user signals are separated by a combination of FDM(A) and TDM(A) : the upstream and downstream bandwidths are divided into "channels" of 200 kHz, and each such channel is shared by 8 users by utilizing TDM(A) frames containing 8 slots. The bitrate during a slot is 270.8 kbit/s. Taking into account the overhead in each slot (guard time, startbits and stopbits, training bits, control information, ...) and the number of slots per frame, the net average bitrate per user is 22.8 kbit/s; these bits consist of information bits (digitized and compressed voice at 13 kbit/s, or data at 9.6 kbit/s) and redundant bits for error control. GSM allows frequency hopping; the hopping interval is one frame and the hopping frequencies are 200 kHz apart.

#### European standard DECT for cordless telephony

DECT is a system for digital cordless telephony, serving small areas (office building, station, airport, ...) by means of cells with a radius from 50 to 500 m. De DECT users can transmit digitized voice, and their mobility is limited to speeds of 6 km/h.

Upstream and downstream signals are separated by means of TDD. Like with GSM, the individual user signals are separated by combining FDM(A) with TDM(A) : the available bandwidth is divided into channels of 1728 kHz, and each channel is shared by 12 user that utilize TDM(A). The bitrate in a slot is 1.152 Mbit/s. These bits consist of digitized and compressed voice (32 kbit/s), to which redundant bits for error control are added.

Compared to GSM, the DECT UT has lower transmit power because of the smaller cell size. The smaller cell size gives rise to less channel dispersion; combining this with the smaller user mobility, it follows that the DECT system environment is less hostile. Therefore, the DECT system can do with less powerful coding than in GSM.

	<b>GSM</b>	<b>DECT</b>
Duplexing	FDD	TDD
Frequency band	890-915 MHz (upstr.) 935-960 MHz (downstr.)	1880-1900 MHz
Number of FDM(A) channels	124 (upstr.) 124 (downstr.)	10
Carrier spacing	200 kHz	1728 kHz
Frame length	4.615 ms	5 ms (upstr.) 5 ms (downstr.)
Number slots/frame	8	12 (upstr.) 12 (downstr.)
Composition of slot : - infobits + redundant bits : - overhead - total : - efficiency :	114 bits 42.25 bits 156.25 bits $73\% \times 24/26 = 67\% (*)$	320 infobits + 16 redund. bits 144 bits 480 bits 70%
Bitrate during burst	270.8 kbit/s	1.152 Mbit/s
Modulation	GMSK (BT = 0.3)	GMSK (BT = 0.3)
Average bitrate per user (infobits + redundant bits)	22.8 kbit/s	33.6 kbit/s
Transmit power UT - peak - average	0.8-20 W 0.1-2.5 W	250 mW 10 mW
Delay spread	up to about 10 $\mu$ s	up to about 100 ns
Doppler spread	about 200 Hz (v = 250 km/h)	about 10 Hz (v = 6 km/h)

(\*) only 24 frames out of 26 frames are used for voice or data

#### **US standard IS-95 for ‘digital cellular radio’ by means of CDMA.**

- Duplexing : FDD (upstream : 824-849 MHz, downstream : 869-894 MHz)
- Information bitrate per user : 9.6 kbit/s
- Chiprate : 1.2288 Mchips/s (= 128 x 9.6 kbit/s)
- Upstream and downstream frequency bands contain several carriers, with a spacing of (at least) 1.25 MHz
- Modulation : BPSK

- Receiver : RAKE
- Transmit power  $U_T$  : 0.6 – 3 W
- Downstream communication
  - A rate 1/2 convolutional code is used for error correction. The resulting rate of coded bits is  $2 \times 9.6 \text{ kbit/s} = 19.2 \text{ kbit/s}$ .
  - Each coded bit is multiplied with a user-specific Walsh-Hadamard (WH) sequence with 64 chips per coded bit, so that the different user signals are orthogonal. The resulting chiprate is 1.2288 Mchips/s.
  - Each chip of the WH sequence is multiplied with one chip of a BS-specific "short" complex PN sequence with period  $2^{15}$ . The PN sequences corresponding to the different BSs are delayed versions of each other (delay = multiple of 64 chips).
- Upstream communication
  - A rate 1/3 convolutional code is used for error correction. The resulting rate of coded bits is  $3 \times 9.6 \text{ kbit/s} = 28.8 \text{ kbit/s}$ .
  - The sequence of coded bits is divided into blocks of 6 bits, and each block is mapped to one of  $2^6 = 64$  orthogonal codewords. These codewords are the 64 orthogonal WH sequences of length 64. This operation is in fact an inner error correcting code (rate 64/6), that is cascaded with the outer convolutional code (rate 1/3) for increased robustness against noise and interference. The resulting rate of WH bits equals  $(64/6) \times 28.8 \text{ kbit/s} = 307.2 \text{ kbit/s}$ .
  - Each WH bit is multiplied with 4 chips of a complex-valued PN sequence, yielding a chiprate of  $4 \text{ chips/bit} \times 307.2 \text{ kbit/s} = 1.2288 \text{ Mchip/s}$ . This operation reduces the multi-user interference by  $10\log(4) = 6 \text{ dB}$ . The complex-valued PN sequence is obtained by multiplying each chip of a real-valued user-specific "long" PN sequence (period of  $2^{42}-1$ ) with a chip of a "short" complex-valued cell-specific sequence (period of  $2^{15}$ ).



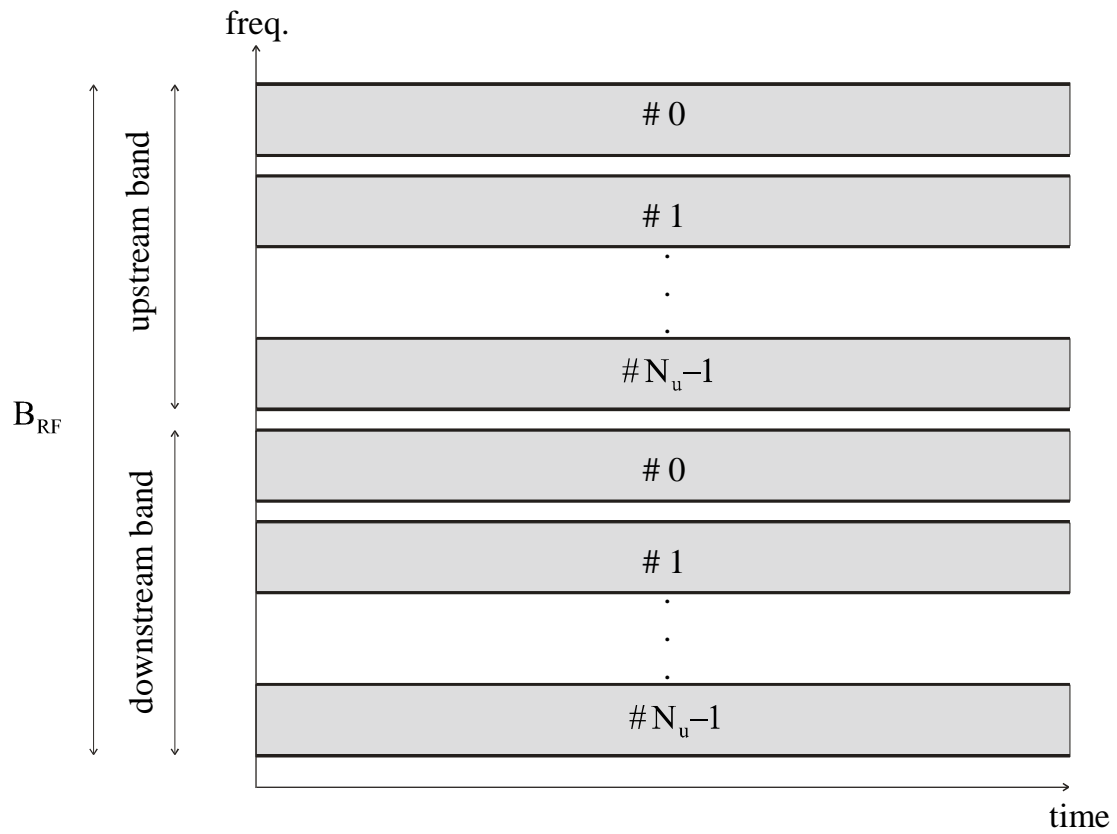


Fig. 5-1 : FDD/FDM/FDMA

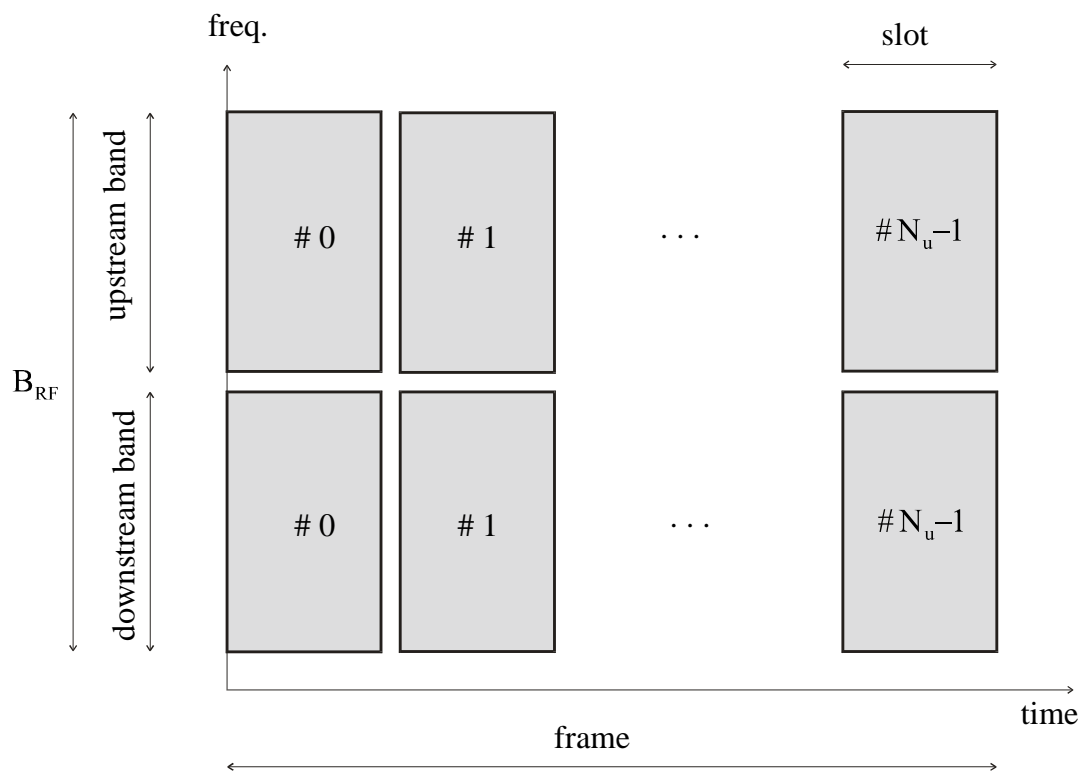


Fig. 5-2 : FDD/TDM/TDMA

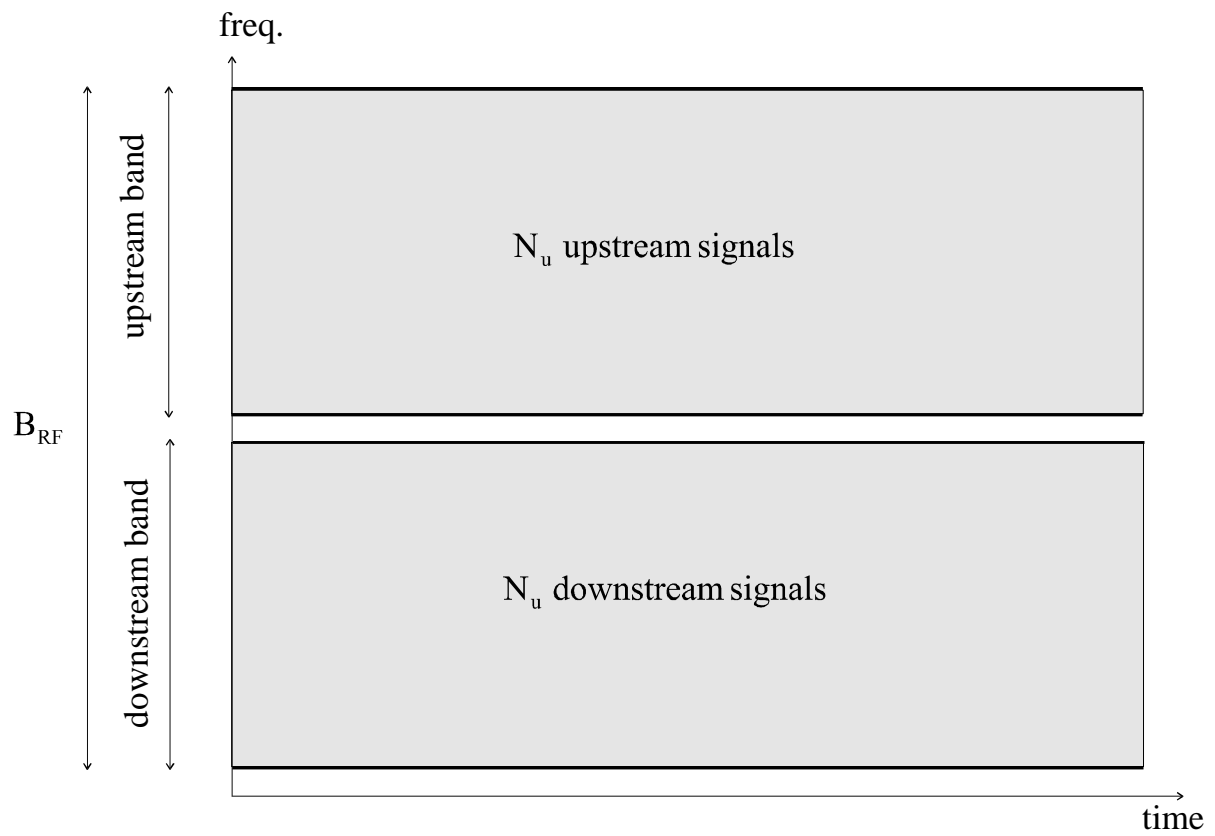


Fig. 5-3 : FDD/CDM/CDMA

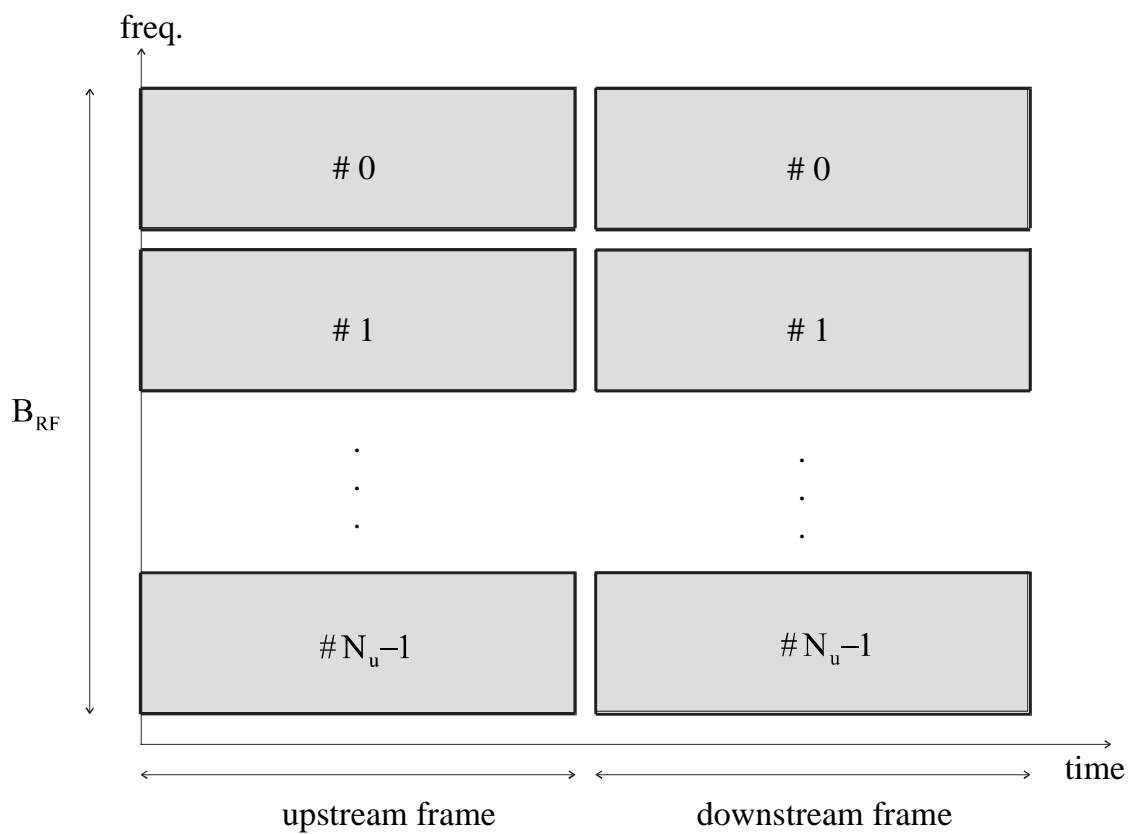


Fig. 5-4 : TDD/FDM/FDMA

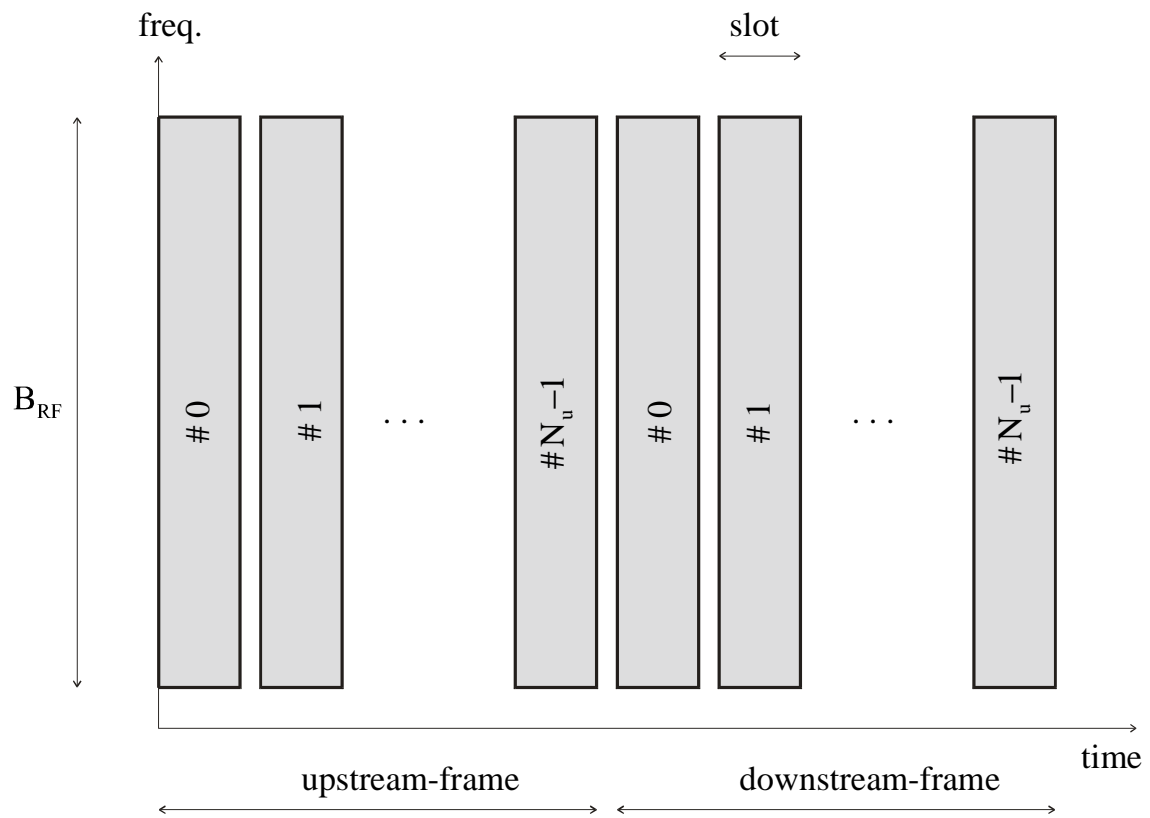


Fig. 5-5 : TDD/TDM/TDMA

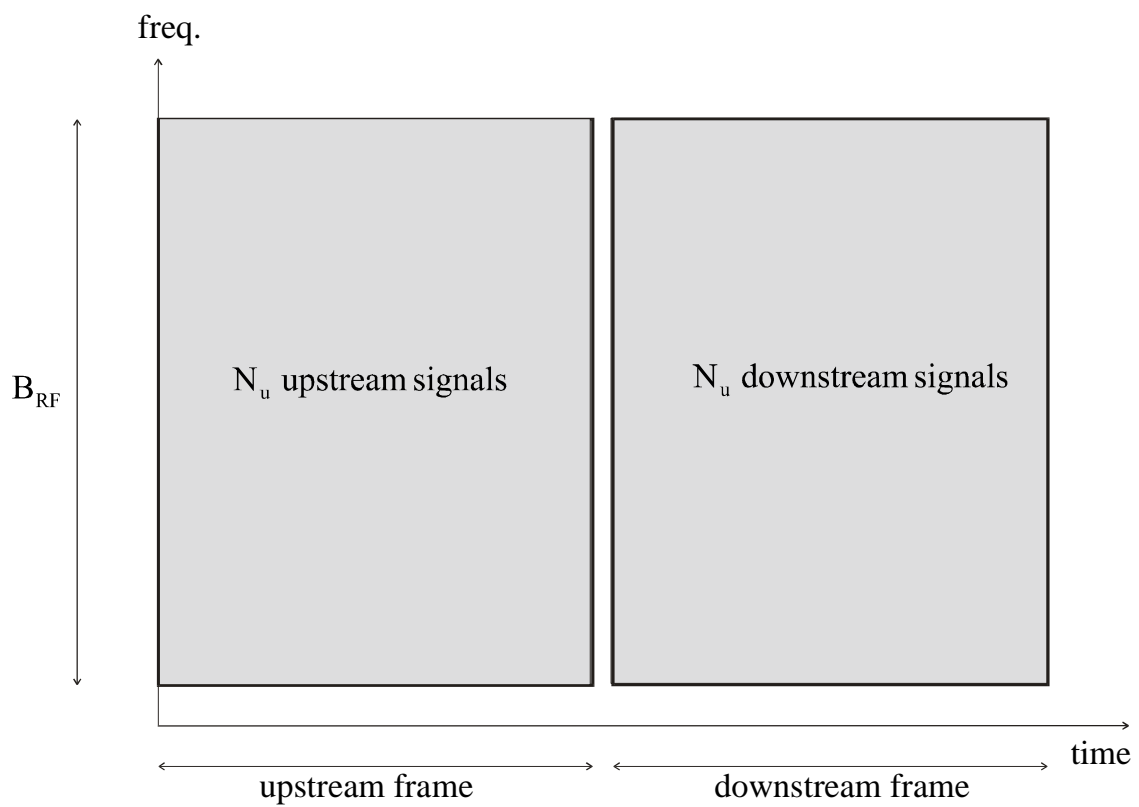


Fig. 5-6 : TDD/CDM/CDMA

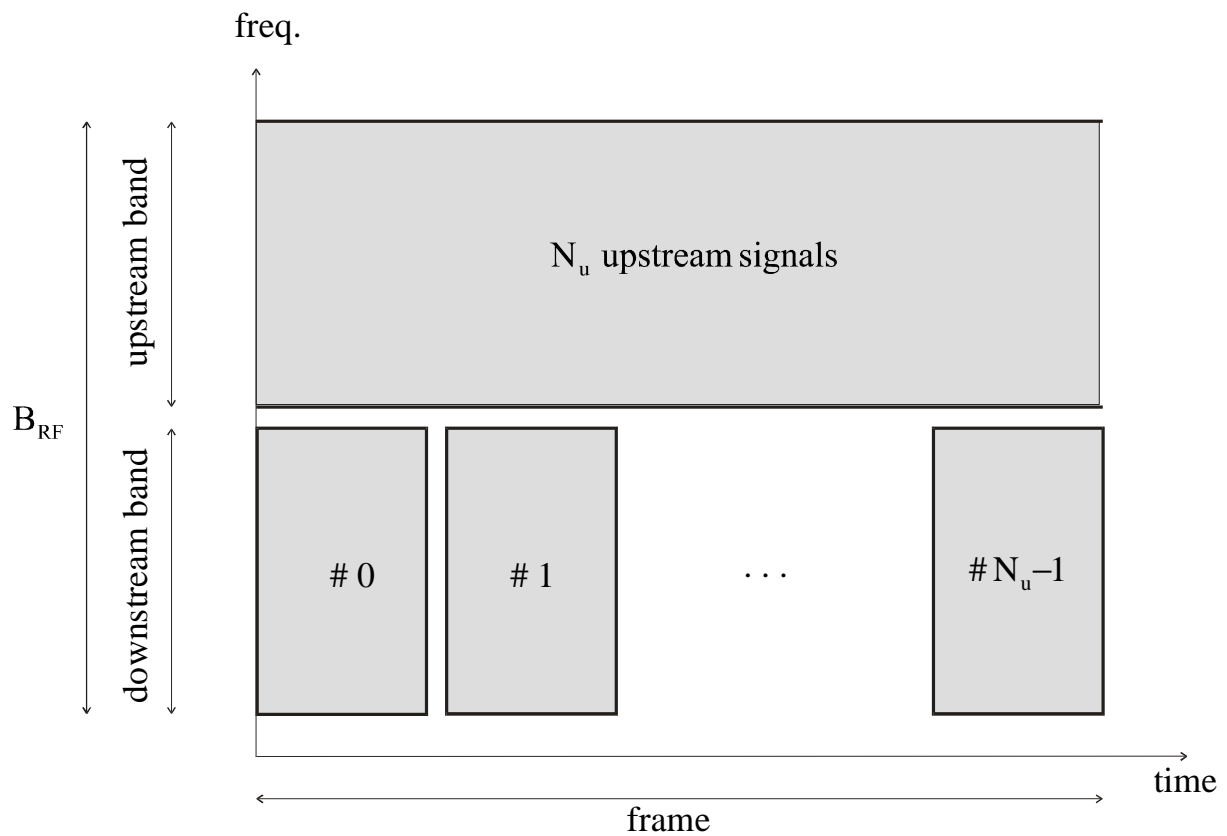


Fig. 5-7 : FDD/TDM/CDMA

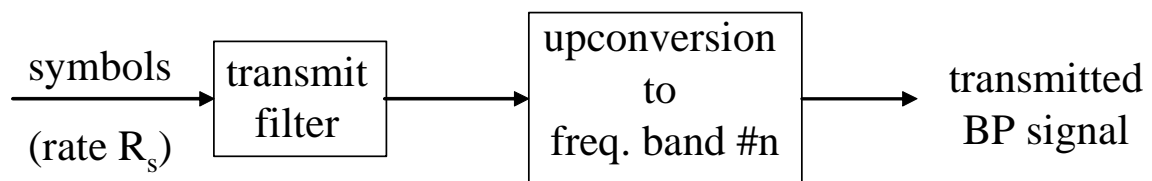


Fig. 5-8 : UT transmitter for FDD/FDMA

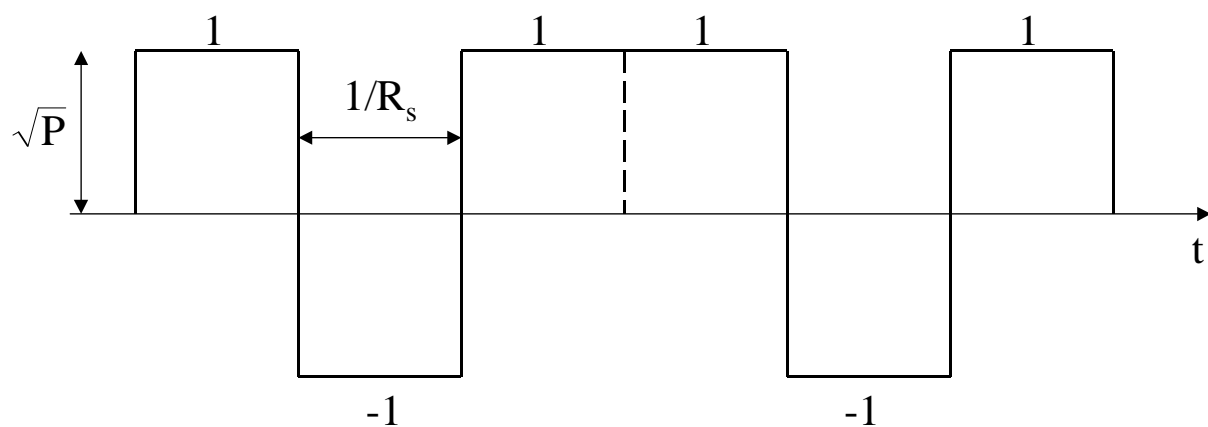


Fig. 5-9 : baseband representation of upstream transmit signal in FDD/FDMA

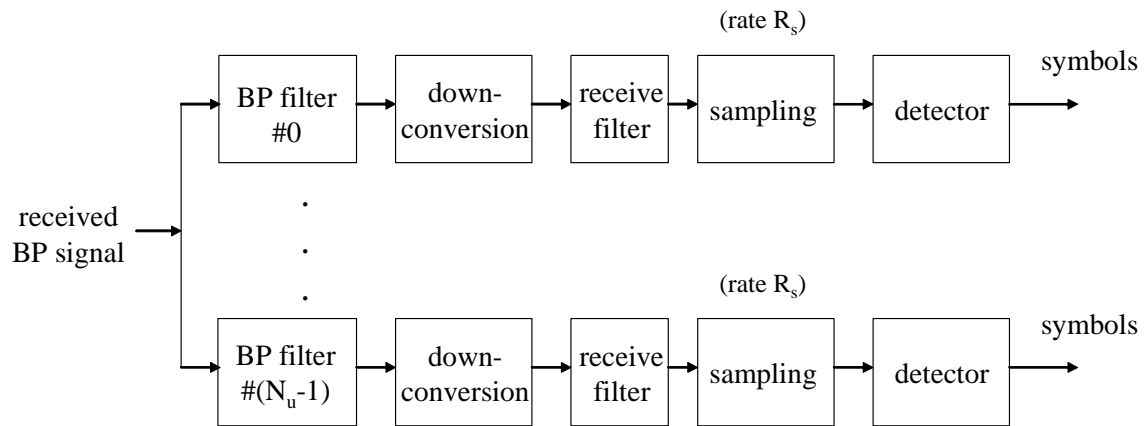


Fig. 5-10 : BS receiver for FDD/FDMA

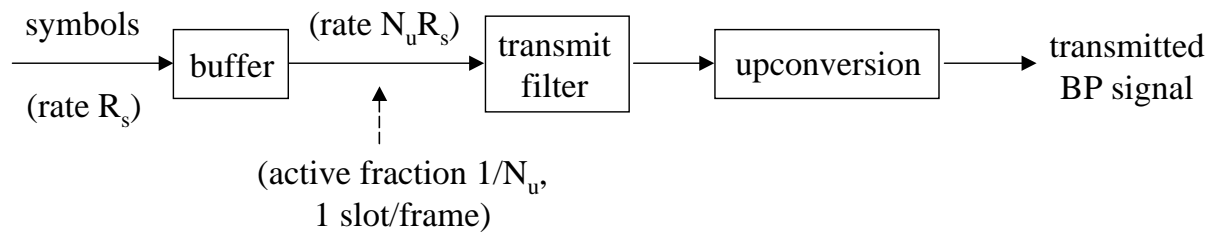


Fig. 5-11 : UT transmitter for FDD/TDMA

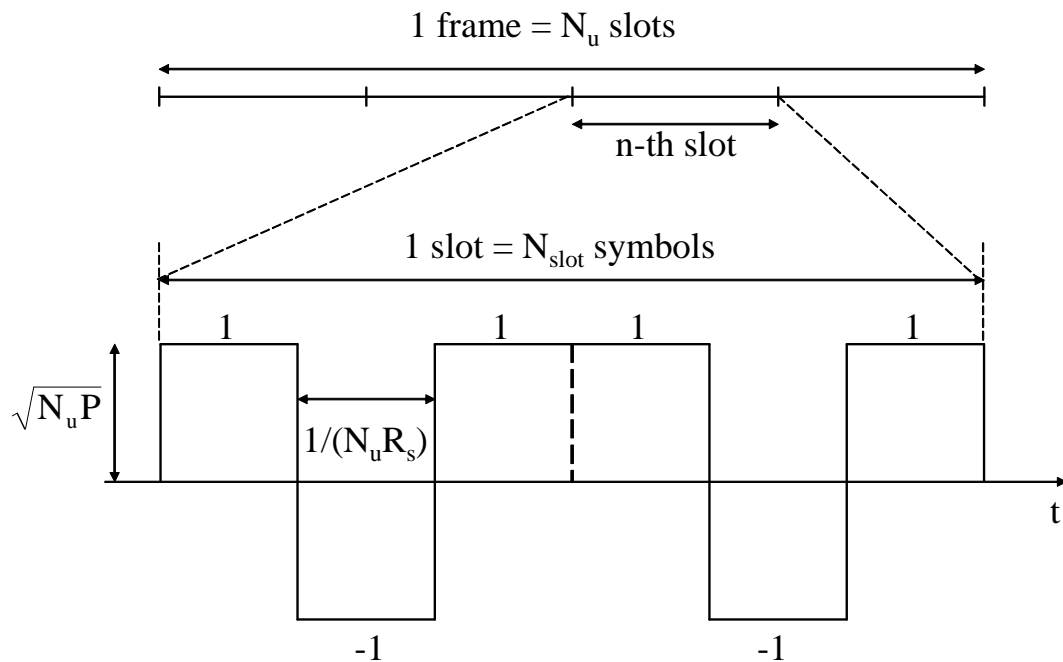


Fig. 5-12 : baseband representation of upstream transmit signal in FDD/TDMA

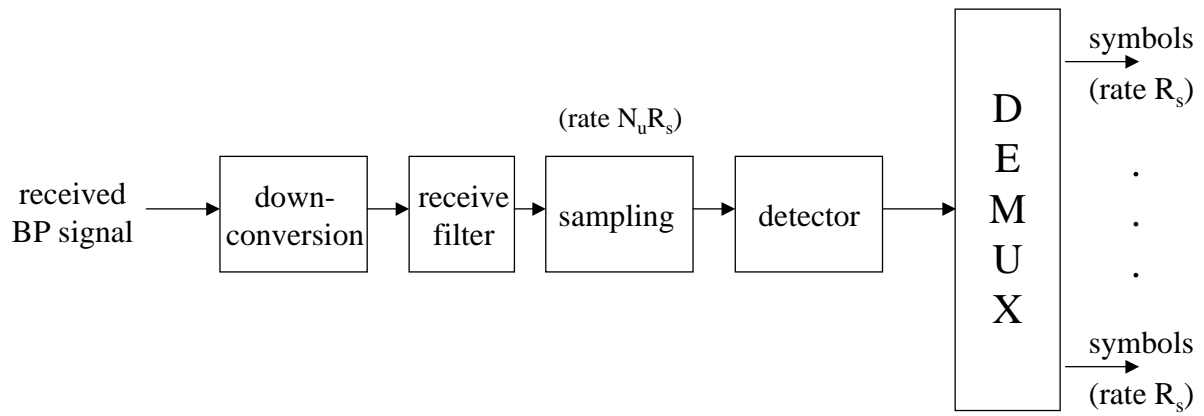


Fig. 5-13 : BS receiver for FDD/TDMA

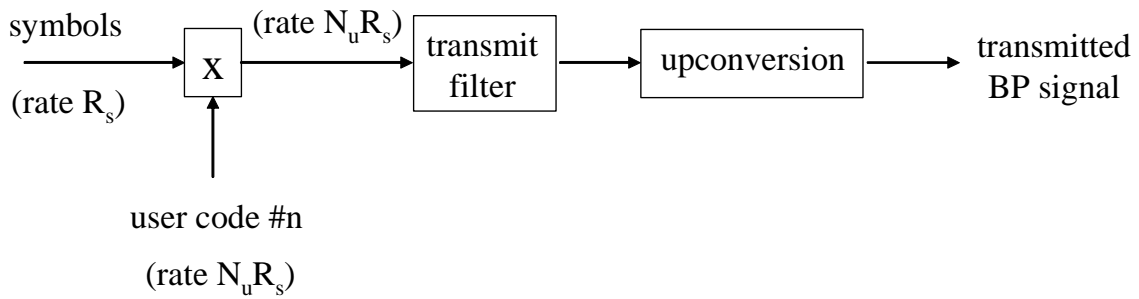


Fig. 5-14 : UT for FDD/CDMA

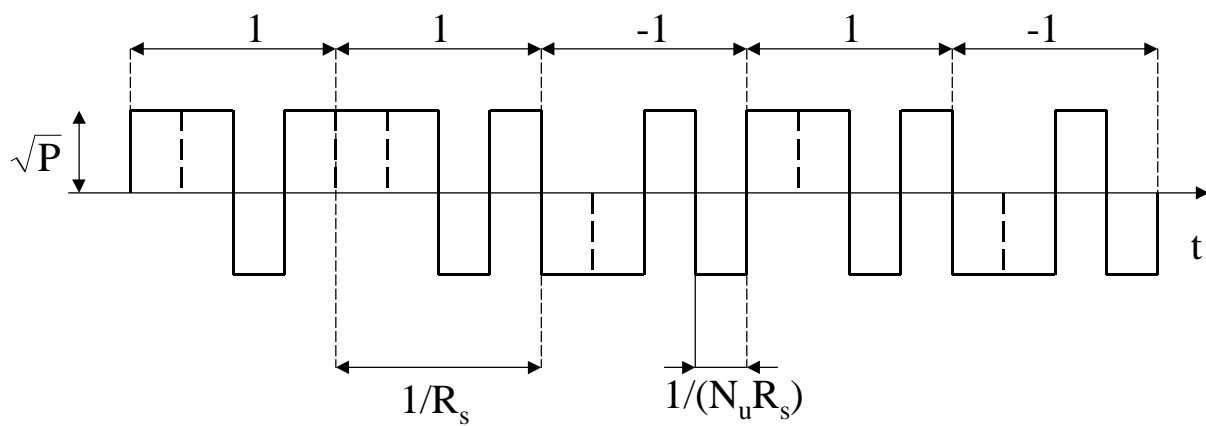


Fig. 5-15 : baseband representation of upstream transmit signal in FDD/CDMA

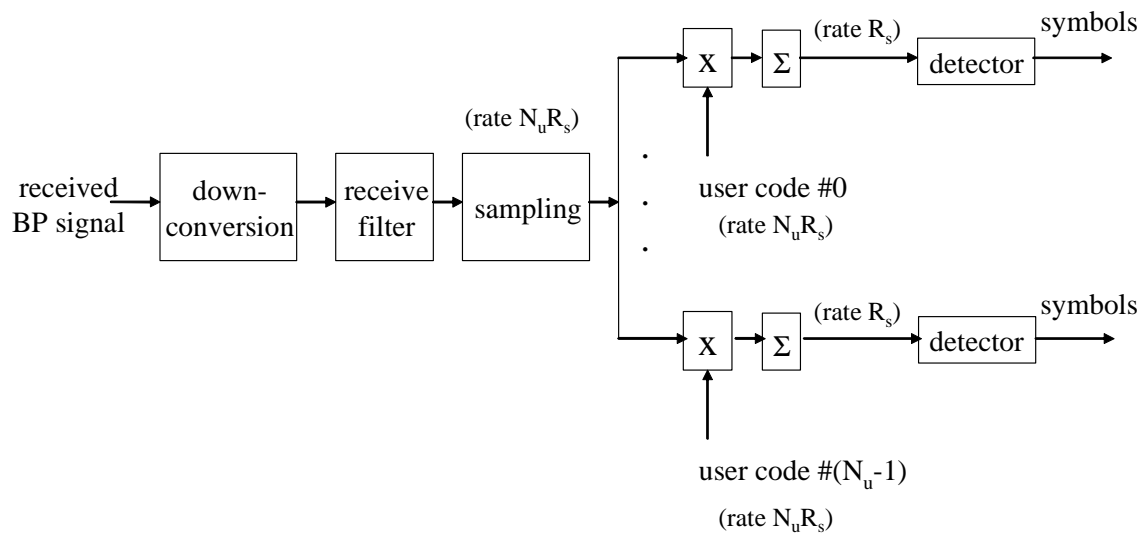


Fig. 5-16 : BS receiver for FDD/CDMA

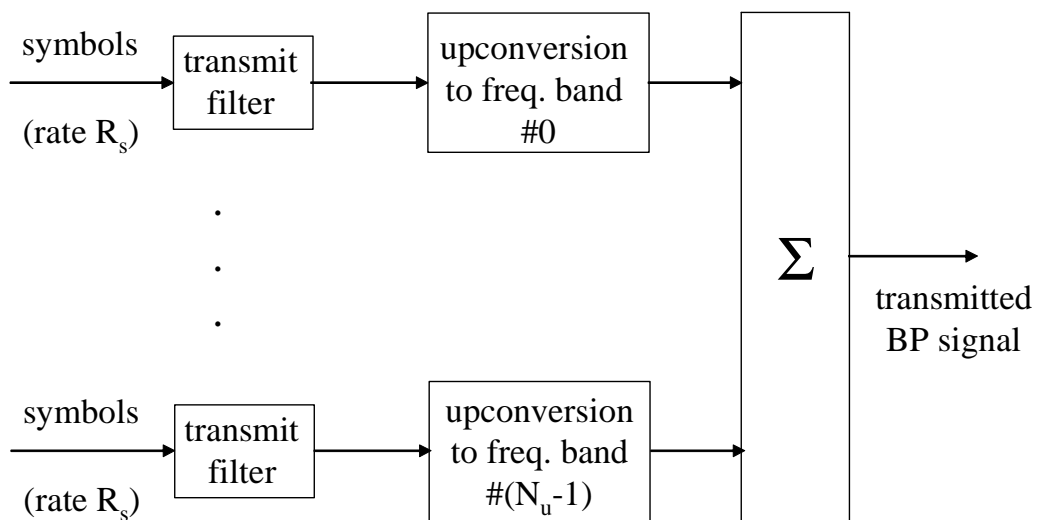


Fig. 5-17 : BS transmitter for FDD/FDM

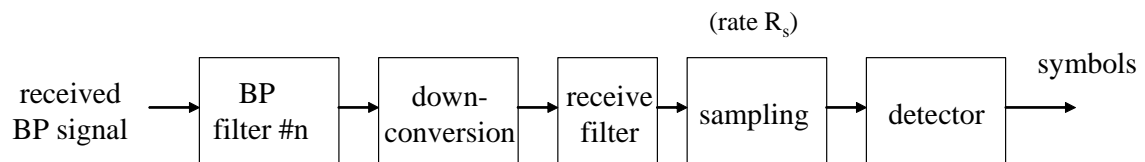


Fig. 5-18 : UT receiver for FDD/FDM

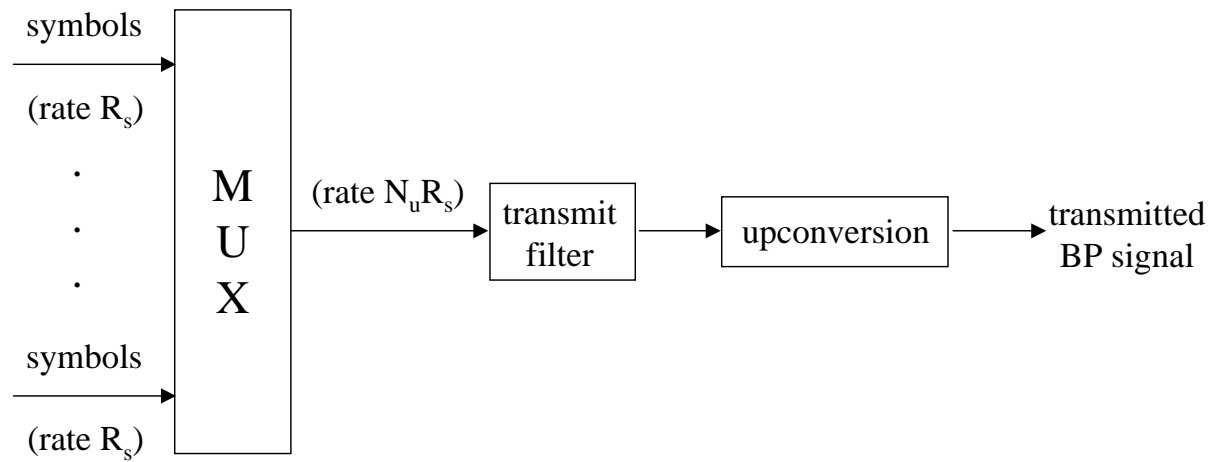


Fig. 5-19 : BS transmitter for FDD/TDD

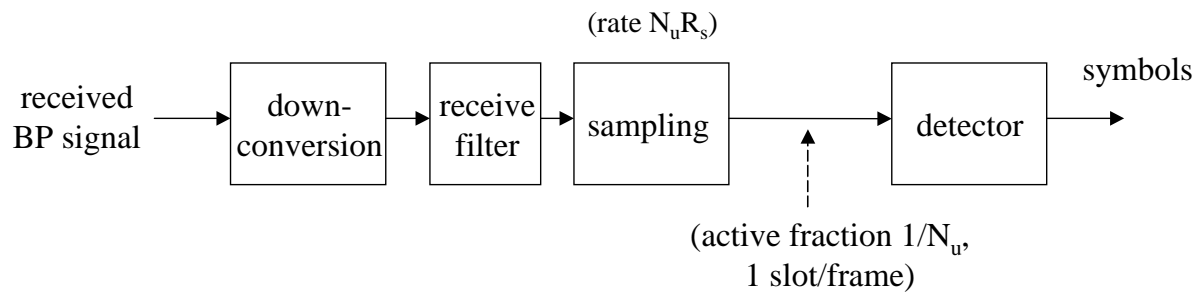


Fig. 5-20 : UT receiver for FDD/TDD

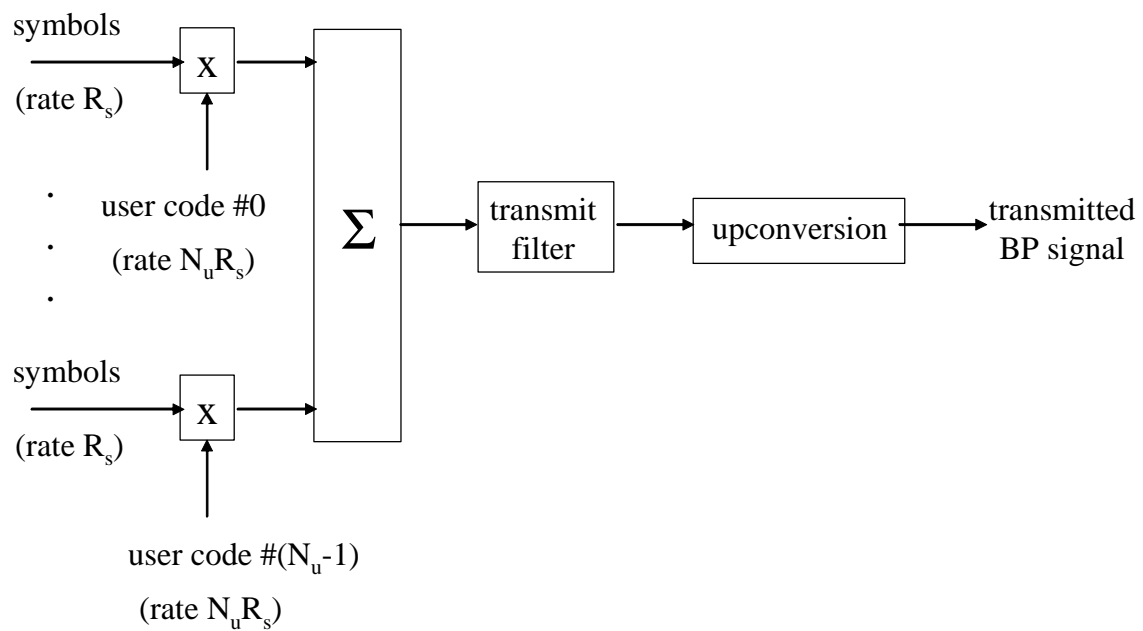


Fig. 5-21 : BS transmitter for FDD/CDD



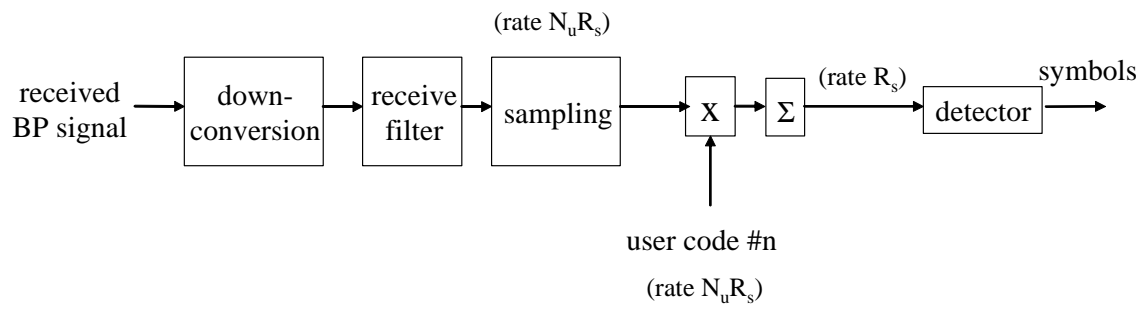


Fig. 5-22 : UT receiver for FDD/CDD

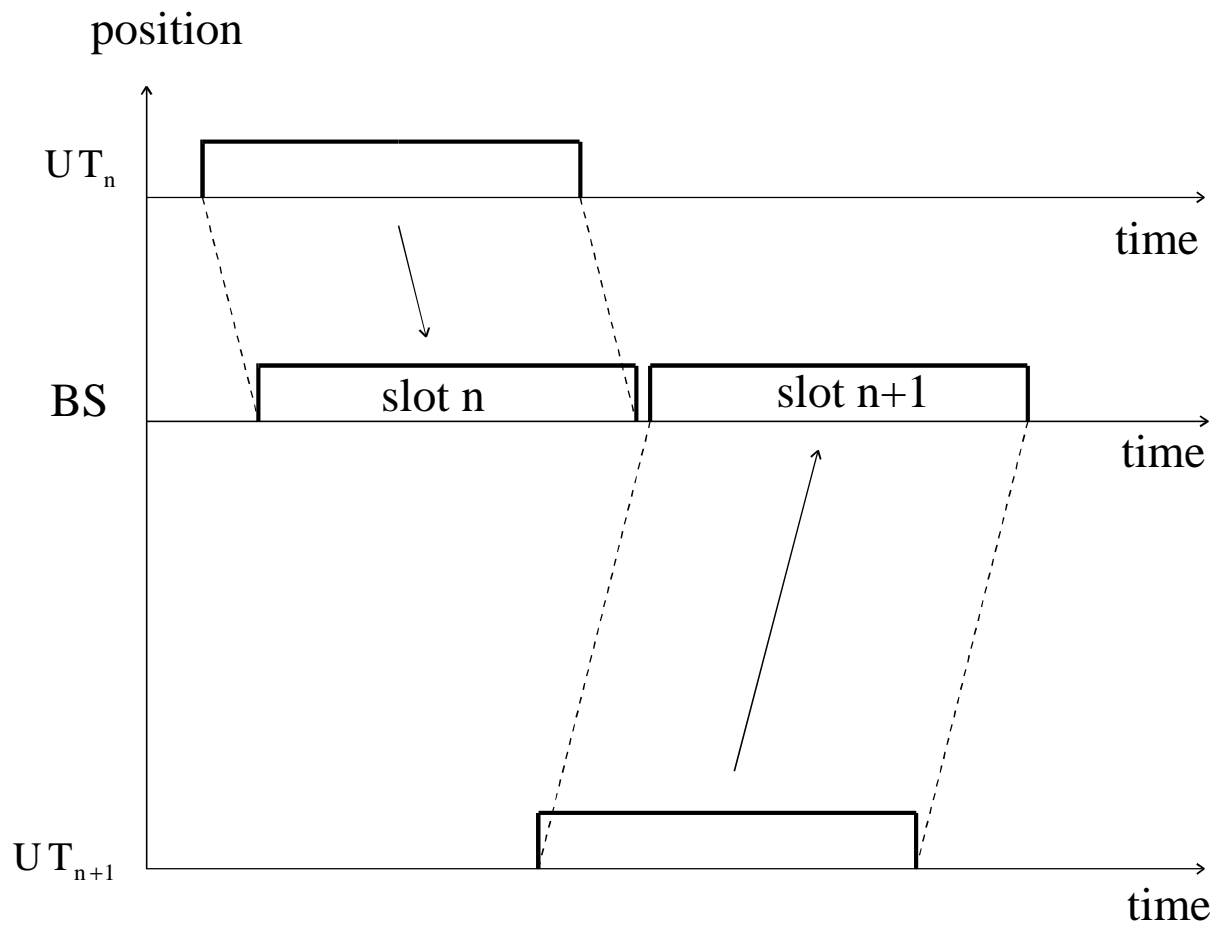


Fig. 5-23 : UT transmitter synchronization for TDMA

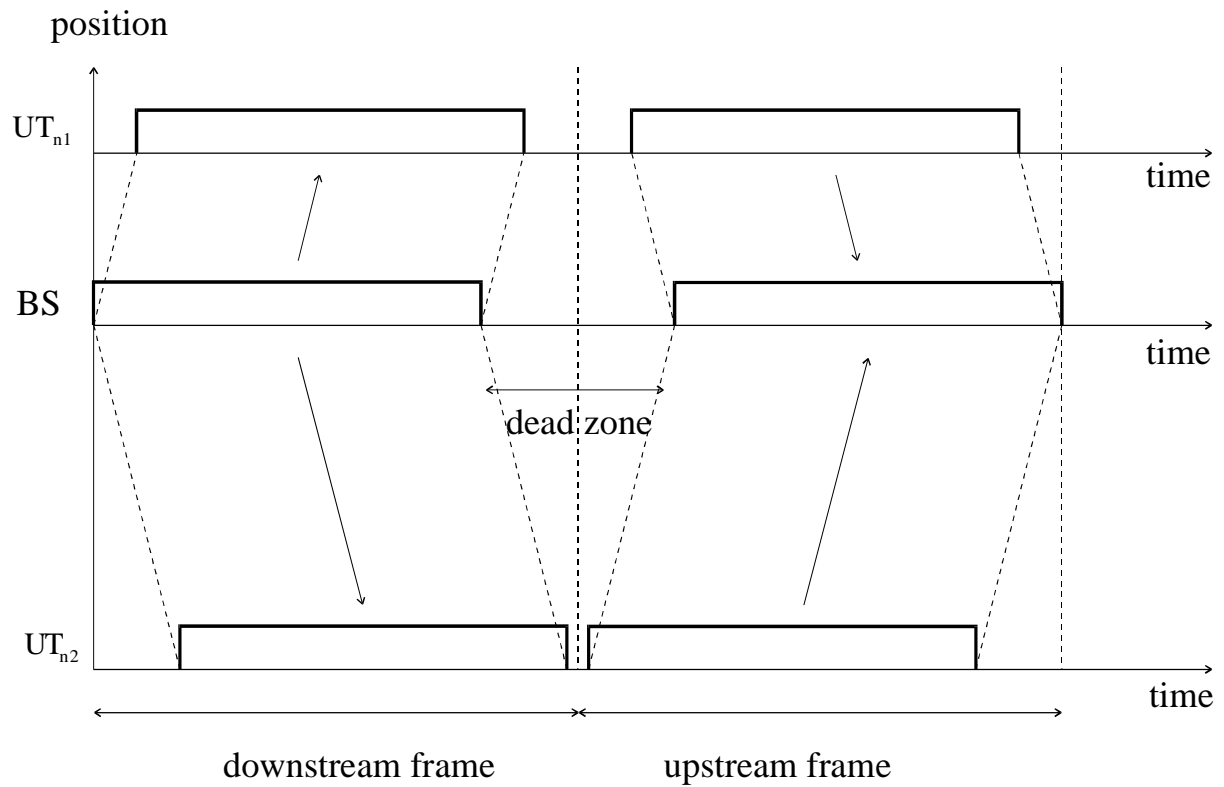


Fig. 5-24 : occurrence of dead time in case of TDD

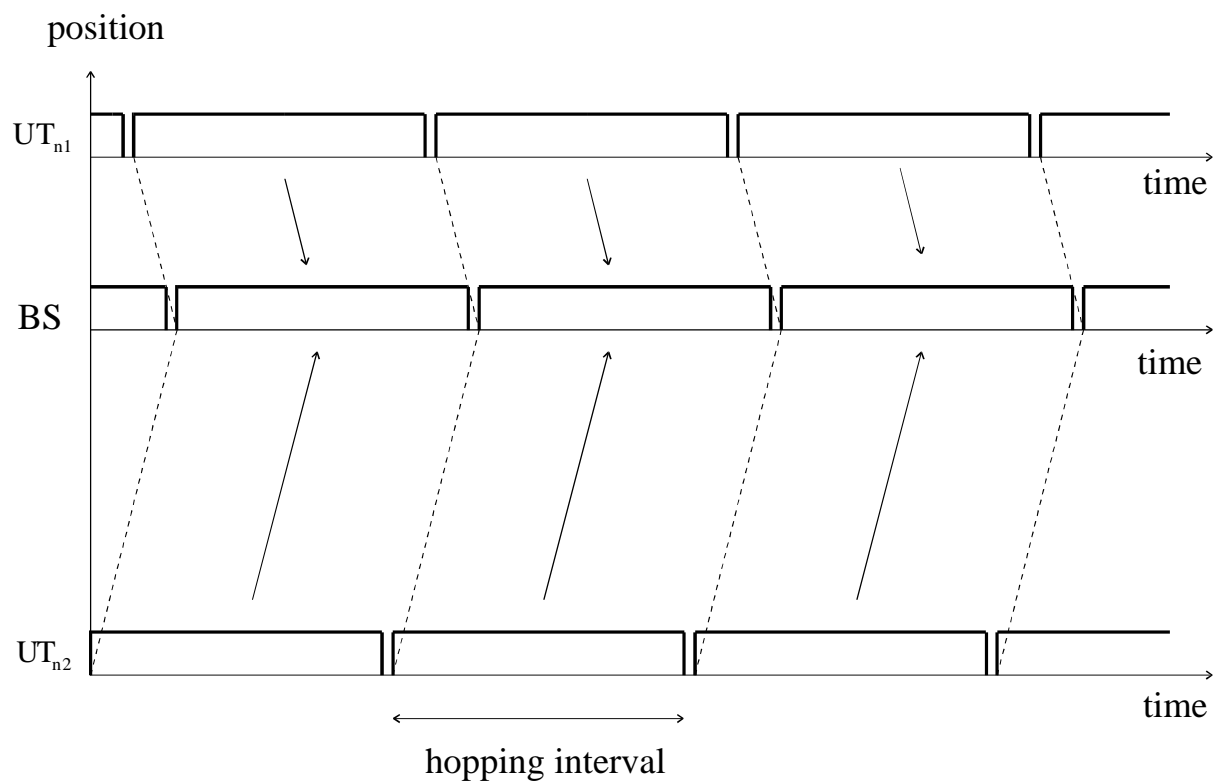
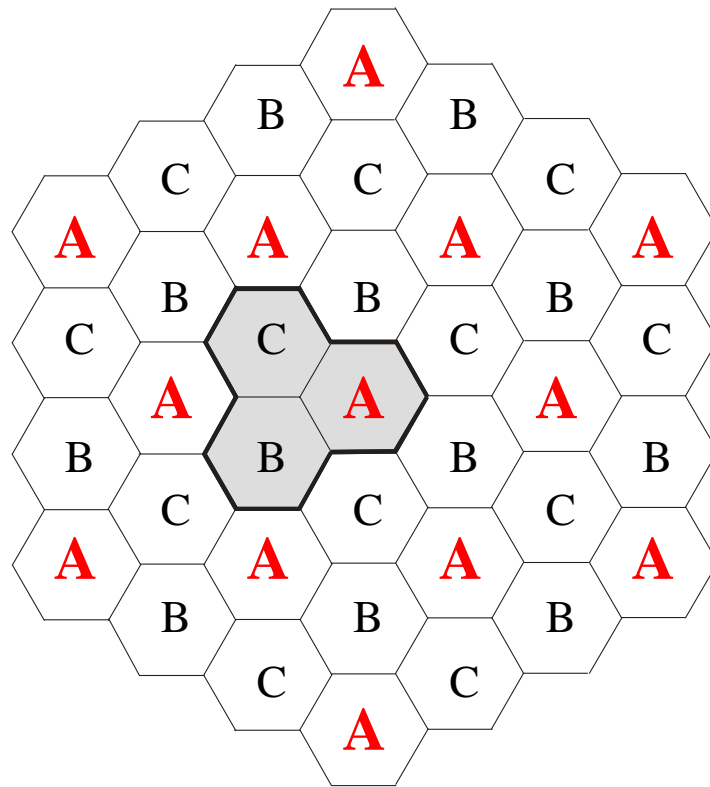
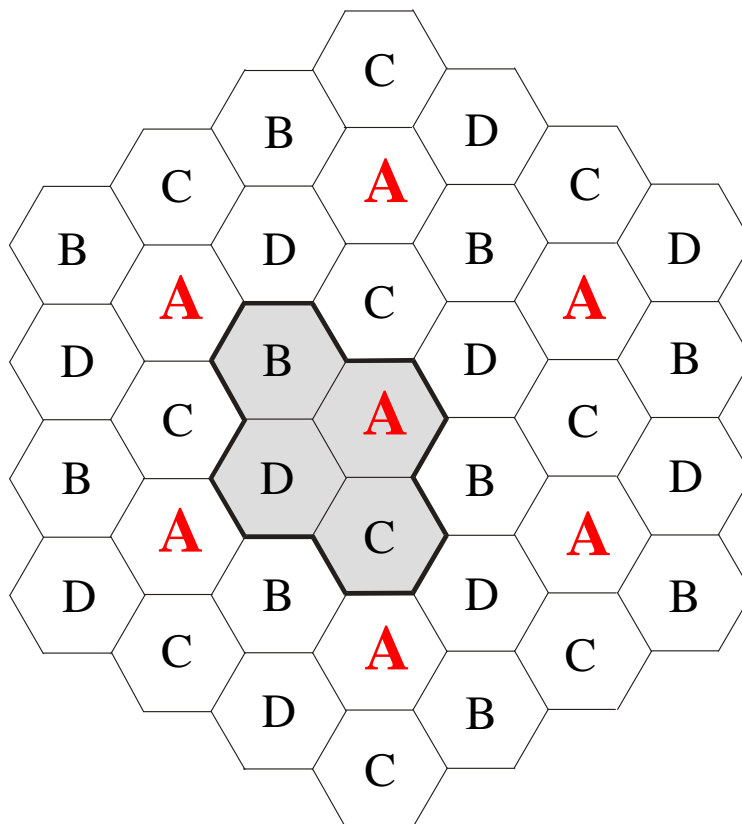
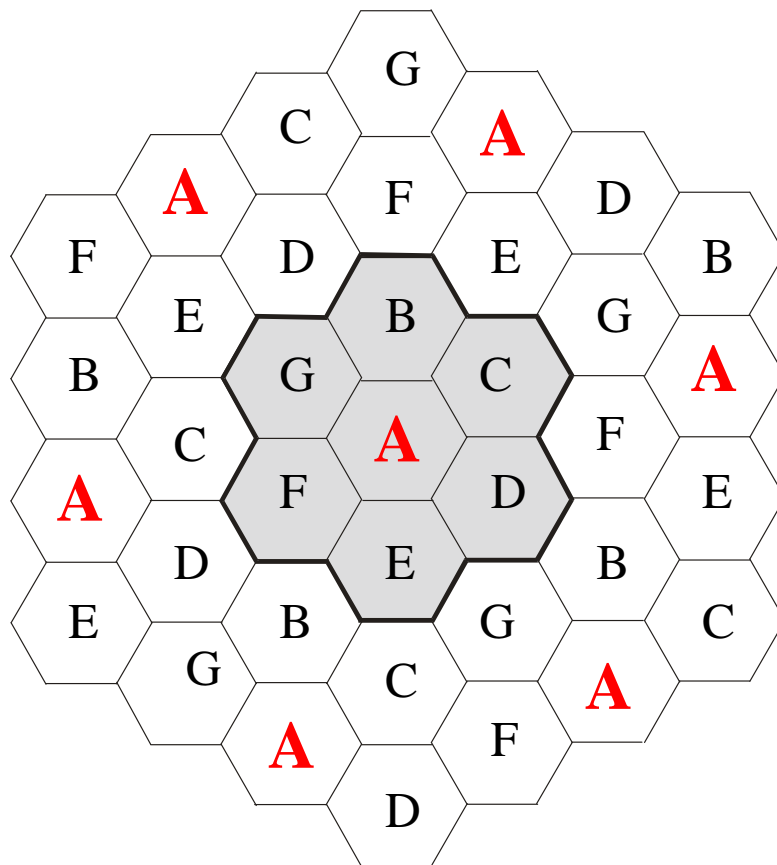


Fig. 5-25 : synchronization of transmission instants in case of FH

Fig. 5-26 : cell structure with  $N_{re} = 3$ Fig. 5-27 : cell structure with  $N_{re} = 4$

Fig. 5-28 : cell structure with  $N_{re} = 7$

## Chapter 6

### Conventional digital modulation on dispersive channels

In this chapter we consider transmission over dispersive channels. We will mainly deal with time-invariant channels with impulse response  $h_{ch}(u)$  and transfer function  $H_{ch}(f)$ , but in section 6.10 the results will be extended to slowly fading multipath channels.

#### 6.1. Transmitter and channel model

By means of conventional linear digital modulation, we transmit a sequence  $\{a(k)\}$  of i.i.d. data symbols belonging to an  $M$ -point constellation  $C$  with  $E[|a(k)|^2] = E_s$ . The resulting transmitted signal  $s(t)$  is given by

$$s(t) = \sum_m a(m)h_{tr}(t - mT) \quad (6.1-1)$$

where  $h_{tr}(t)$  is a unit-energy transmit pulse (so that  $E_s$  is the energy per symbol at the transmitter) and  $R_s = 1/T$  is the symbol rate.

The signal  $s(t)$  is applied to a channel with LTI impulse response  $h_{ch}(u)$  and transfer function  $H_{ch}(f)$ . The channel also adds AWGN  $w(t)$ , where  $w(t) \sim N_c(0, N_0\delta(u))$ . The resulting received signal  $r(t)$  is

$$r(t) = \sum_m a(m)h(t - mT) + w(t) \quad (6.1-2)$$

where  $h(t)$  is the pulse at the input of the receiver :

$$h(t) = \int h_{tr}(t - u)h_{ch}(u)du = \int h_{ch}(t - u)h_{tr}(u)du \Leftrightarrow H(f) = H_{tr}(f)H_{ch}(f) \quad (6.1-3)$$

Fig. 6-1 shows the model of the received signal  $r(t)$ .

#### 6.2. The matched filter and the whitened matched filter

The log-likelihood function  $\ln p(\mathbf{r} | \tilde{\mathbf{a}})$  corresponding to (6.1-2) is determined by

$$N_0 \ln p(\mathbf{r} | \tilde{\mathbf{a}}) \propto 2 \sum_m \text{Re}[\tilde{\mathbf{a}}^*(m)z(m)] - \sum_{m,n} \tilde{\mathbf{a}}^*(m)g(m-n)\tilde{\mathbf{a}}(n) = 2 \text{Re}[\tilde{\mathbf{a}}^H \mathbf{z}] - \tilde{\mathbf{a}}^H \mathbf{G} \tilde{\mathbf{a}} \quad (6.2-1)$$

where  $z(m) = (\mathbf{z})_m$  and  $g(m-n) = (\mathbf{G})_{m,n}$  are given by

$$z(m) = \int r(t)h^*(t - mT)dt \quad (6.2-2)$$

$$g(m-n) = \int h^*(t - mT)h(t - nT)dt = \int h^*(t)h(t + mT - nT)dt = g^*(n - m) \quad (6.2-3)$$

Note that  $g(0)$  equals the energy of  $h(t)$  :

$$\int |h(t)|^2 dt = g(0) \quad (6.2-4)$$

Hence, the energy per symbol at the input of the receiver is  $E_s g(0)$ ; often the channel transfer function  $H_{ch}(f)$  is normalized such that  $g(0) = 1$ . It follows from (6.2-2) that  $z(m)$  is obtained by applying  $r(t)$  to a filter (with impulse response  $h^*(-t)$  and transfer function  $H^*(f)$ ) matched to  $h(t)$ , and sampling the matched filter output at the instant  $mT$ .

The expression (6.2-1) indicates that the sequence of matched filter output samples is a sufficient statistic of  $r(t)$ . This means that no relevant information is lost when observing  $\mathbf{z}$  instead of  $r(t)$ . Hence, irrespective of the criterion for detecting  $\mathbf{a}$  and without loss of optimality, we can use the matched filter as a first stage in the receiver, that converts the continuous-time received signal  $r(t)$  into a sequence of matched filter output samples  $\mathbf{z}$ .

The matched filter output  $z(k)$  can be decomposed as

$$z(k) = \sum_m a(k-m)g(m) + n(k) = \underbrace{a(k)g(0)}_{\text{useful}} + \underbrace{\sum_{m \neq 0} a(k-m)g(m)}_{\text{ISI}} + \underbrace{n(k)}_{\text{noise}} \quad (6.2-5)$$

with  $n(k) \sim N_c(0, N_0 g(m))$ . We introduce the discrete-time FT (DTFT) of  $g(m)$  :

$$\begin{aligned} G(\exp(j2\pi fT)) &= \sum_m g(m) \exp(-j2\pi f m T) \\ &\Downarrow \\ g(m) &= \langle G(\exp(j2\pi fT)) \exp(j2\pi f m T) \rangle_f = T \int_{1/T} G(\exp(j2\pi fT)) \exp(j2\pi f m T) df \end{aligned} \quad (6.2-6)$$

where  $\langle \dots \rangle_f$  denotes averaging over  $f$ , and  $G(\exp(j2\pi fT))$  is periodic in  $f$  with period  $1/T$ . The discrete-time channel model corresponding to (6.2-5) is shown in Fig. 6-2; note that both the channel impulse response and noise correlation are determined by  $\{g(m)\}$  or  $G(\exp(j2\pi fT))$ . Unless  $g(m) = g(0)\delta(m)$  or, equivalently,  $G(\exp(j2\pi fT)) = g(0)$ ,  $z(k)$  is affected by inter-symbol interference (ISI), and the noise terms  $n(k)$  and  $n(k+m)$  are correlated. As  $g(m) = g^*(-m)$ , the ISI in  $z(k)$  is caused by both past and future symbols. Considering (6.2-3), the condition  $g(m) = g(0)\delta(m)$  holds only when  $h(t)$  and  $h(t-mT)$  are orthogonal for all  $m \neq 0$ . However, as the transmitter usually does not know the channel transfer function, we cannot expect the received pulse  $h(t)$  to satisfy this orthogonality condition; hence, in general the matched filter output samples are affected by ISI when the channel is dispersive.

Taking into account that

$$\langle |G(\exp(j2\pi fT))|^2 \rangle_f = \sum_m |g(m)|^2 \quad \langle G(\exp(j2\pi fT)) \rangle_f = g(0) \quad (6.2-7)$$

the ratio of ISI power to useful power in (6.2-5) can be expressed as

$$\begin{aligned}
\frac{\sum_{m \neq 0} |g(m)|^2}{|g(0)|^2} &= \frac{\langle |G(\exp(j2\pi fT))|^2 \rangle_f - |\langle G(\exp(j2\pi fT)) \rangle_f|^2}{|\langle G(\exp(j2\pi fT)) \rangle_f|^2} \\
&= \frac{\langle |G(\exp(j2\pi fT)) - \langle G(\exp(j2\pi fT)) \rangle_f|^2 \rangle_f}{|\langle G(\exp(j2\pi fT)) \rangle_f|^2}
\end{aligned} \tag{6.2-8}$$

It follows from (6.2-8) that the ISI power is proportional to the mean-square fluctuation of  $G(\exp(j2\pi fT))$  w.r.t. its mean  $\langle G(\exp(j2\pi fT)) \rangle_f$ . Hence, there is no ISI in  $z(k)$  when  $G(\exp(j2\pi fT))$  is flat, i.e., when  $G(\exp(j2\pi fT)) = g(0)$ , or, equivalently,  $g(m) = g(0)\delta(m)$ .

In some cases we will find it convenient to apply the matched filter output samples  $z(k)$  to a discrete-time filter  $H_w(\exp(j2\pi fT))$  which is selected such that the noise at the output of the filter is white; the resulting filter is a *whitening filter*, and the cascade of the matched filter and the whitening filter is called the *whitened matched filter*. Taking into account that the noise power spectrum at the output of the matched filter equals  $N_0 G(\exp(j2\pi fT))$ , the whitening filter must satisfy the following condition :

$$N_0 G(\exp(j2\pi fT)) |H_w(\exp(j2\pi fT))|^2 = \text{constant} \tag{6.2-9}$$

with the left-hand side of (6.2-9) denoting the power spectrum of the noise at the output of the whitening filter. The whitening filter satisfying (6.2-9) is not unique, as (6.2-9) imposes no condition on its phase characteristic. In order that no information is lost by applying the whitening filter to the matched filter output samples, the whitening operation must be *reversible*, i.e.,  $1/H_w(\exp(j2\pi fT))$  must exist. In this case, the sequence at the output of the whitening filter is also a sufficient statistic, and no information is lost when operating on the whitening filter output rather than the matched filter output samples.

Using the spectral factorization technique outlined in section 6.11.1,  $G(z)$  can be uniquely decomposed as

$$G(z) = A^2 F_+(z) F_-(z) \tag{6.2-10}$$

where  $A^2 > 0$ , and

- The power series expansion of  $F_+(z)$  contains only powers  $z^n$  with  $n \leq 0$ ; hence it is the transfer function of a *causal* filter. The poles and zeroes of  $F_+(z)$  are the poles and zeroes of  $G(z)$  that are *inside* the unit circle; hence,  $F_+(z)$  is the transfer function of a *stable* causal filter. Further,  $F_+(z)$  is *monic*, meaning that the coefficient  $f_+(0)$  of  $z^0$  is 1. It follows that also  $1/F_+(z)$  is monic, causal and stable.
- The power series expansion of  $F_-(z)$  contains only powers  $z^n$  with  $n \geq 0$ ; hence it is the transfer function of a *anti-causal* filter. The poles and zeroes of  $F_-(z)$  are the poles and zeroes of  $G(z)$  that are *outside* the unit circle; hence,  $F_-(z)$  is the transfer function of a

stable anti-causal filter. Further,  $F_-(z)$  is *monic*, meaning that the coefficient  $f_-(0)$  of  $z^0$  is 1.

It follows that also  $1/F_-(z)$  is monic, anti-causal and stable.

Hence,

$$F_+(z) = 1 + \sum_{m>0} f_+(m)z^{-m} \quad F_-(z) = 1 + \sum_{m<0} f_-(m)z^{-m}$$

It can be verified that  $F_-(\exp(j2\pi fT)) = (F_+(\exp(j2\pi fT)))^*$ , so that  $f_-(m) = (f_+(-m))^*$ ,  $m \leq 0$ . Fig. 6-3 illustrates the properties of the impulse responses  $f_+(m)$  and  $f_-(m)$ . Now  $G(\exp(j2\pi fT))$  can be represented as

$$G(\exp(j2\pi fT)) = A^2 |F_+(\exp(j2\pi fT))|^2 = A^2 |F_-(\exp(j2\pi fT))|^2 \quad (6.2-11)$$

From (6.2-11), we obtain

$$g(0) = \langle G(\exp(j2\pi fT)) \rangle_f = A^2 \langle |F_+(\exp(j2\pi fT))|^2 \rangle_f = A^2 \left( 1 + \sum_{m>0} |f_+(m)|^2 \right) \quad (6.2-12)$$

from which we easily derive the inequality  $g(0) \geq A^2$ .

Now we select  $H_w(z) = 1/(A^2 F_-(z))$  :  $H_w(z)$  is anticausal, stable and reversible. The resulting configuration is shown in Fig. 6-4. The cascade of the filters  $G(z)$  and  $H_w(z)$  yields

$$G(z)H_w(z) = \frac{A^2 F_+(z)F_-(z)}{A^2 F_-(z)} = F_+(z) \quad (6.2-13)$$

The spectrum of the noise at the output of the filter  $H_w(z)$  is given by

$$N_0 G(\exp(j2\pi fT)) |H_w(\exp(j\pi fT))|^2 = N_0 \frac{A^2 |F_+(\exp(j\pi fT))|^2}{A^4 |F_-(\exp(j\pi fT))|^2} = \frac{N_0}{A^2} \quad (6.2-14)$$

As the resulting noise spectrum is constant,  $H_w(z)$  is indeed a whitening filter. Using (6.2-13) and (6.2-14), the output  $u(k)$  of the whitened matched filter can be decomposed as

$$u(k) = a(k) + \sum_{m>0} f_+(m)a(k-m) + w(k) \quad (6.2-15)$$

with  $\{w(k)\} \sim N_c(0, (N_0/A^2)\delta(m))$ . The corresponding model is shown in Fig. 6-4. Noting that  $F_+(z)$  is a causal filter, it follows that the ISI in  $u(k)$  is caused by past symbols only.

When  $G(z)$  is constant ( $G(z) = g(0)$ ), we get  $F_-(z) = F_+(z) = 1$  and  $A^2 = g(0)$ , so that  $H_w(z) = 1/g(0)$  : in this case the noise  $n(k)$  at the matched filter output happens to be white already (so that the whitening filter is only a scaling factor  $1/g(0)$ ), and ISI is absent.



### 6.3. The matched filter bound on the BER performance

According to section 3.3, the BER of any receiver operating on  $r(t)$  from (6.1-2) is lower bounded by the matched filter bound, which is the BER of the genie receiver which operates on the observation  $r'(t) = a(k)h(t-kT) + w(t)$ . Taking into account that the symbol energy at the receiver equals  $E_s g(0)$ , the matched filter bound yields

$$\text{BER} \geq \text{BER}_{\text{MF}} = \text{BER}_{\text{C}}(\text{SNR}_{\text{MF}}) \quad (6.3-1)$$

where

$$\text{SNR}_{\text{MF}} = g(0) \frac{E_s}{N_0} = \frac{E_s A^2}{N_0} \left( 1 + \sum_{m>0} |f_+(m)|^2 \right) \quad (6.3-2)$$

is the SNR at instant  $kT$  at the output of the matched filter  $h^*(-t)$  of the genie receiver.

In the case of 2-PSK and 2-PAM, or 4-PSK and 4-QAM with Gray mapping, the matched filter bound on the BER reduces to

$$\text{BER} \geq \text{BER}_{\text{MF}} = Q \left( \sqrt{\frac{2E_b g(0)}{N_0}} \right) = Q \left( \sqrt{\frac{2E_b A^2}{N_0} \left( 1 + \sum_{m>0} |f_+(m)|^2 \right)} \right) \quad (6.3-3)$$

with  $E_b g(0)$  denoting the energy per bit at the input of the receiver, and  $E_b = E_s / \log_2(M)$  is the energy per bit at the transmitter. For other constellations with Gray mapping, the following approximation holds for large  $g(0)E_s/N_0$ :

$$\text{BER} \geq \text{BER}_{\text{MF}} \approx \frac{N_b}{\log_2 M} Q \left( \sqrt{\frac{g(0)e_{\min}^2}{2N_0}} \right) \quad (6.3-4)$$

where  $e_{\min}$  is the minimum Euclidean distance between constellation points (with  $E[|a(k)|^2] = E_s$ ), and  $N_b$  is the average number of neighboring constellation points at distance  $e_{\min}$ . Note that (6.3-4) reduces to (6.3-3) for 2-PSK and 2-PAM, or 4-PSK and 4-QAM with Gray mapping.

### 6.4. ML sequence detection : Viterbi equalization

ML detection of the transmitted sequence  $\mathbf{a}$  involves the maximization of the log-likelihood function  $\ln p(\mathbf{r} | \tilde{\mathbf{a}})$  over all possible symbol sequences  $\tilde{\mathbf{a}}$ . It follows from (6.2-1) that in general this maximization is quite complex when  $\mathbf{G}$  is nondiagonal : when  $K$  symbols are transmitted,  $\ln p(\mathbf{r} | \tilde{\mathbf{a}})$  must be evaluated for all  $M^K$  symbol sequences, in which case ML sequence detection has a complexity that increases exponentially with the sequence length. Only when  $G(\exp(j2\pi fT))$  is flat,  $\mathbf{G}$  becomes diagonal and the ML detection reduces to simple symbol-by-symbol detection.

In section 6.2, we have shown that the sequence  $\{u(k)\}$  at the output of the whitened matched filter is a sufficient statistic for detecting  $\mathbf{a}$ . Hence, ML detection is equivalent to the maximization of  $\ln p(\mathbf{u} | \tilde{\mathbf{a}})$ . Let us assume that  $f_+(m) = 0$  for  $m > L$  :  $F_+(z)$  and  $F_-(z)$  have  $L+1$  coefficients, and the corresponding  $G(z)$  has  $2L+1$  coefficients. The assumption that  $f_+(m)$  is time-limited will yield an ML receiver having a complexity that is linear (rather than exponential) with  $K$ . As the noise in  $u(k)$  is white, we get

$$-\frac{N_0}{A^2} \ln p(\mathbf{u} | \tilde{\mathbf{a}}) = \sum_{k=0}^{K-1} \left| u(k) - \tilde{a}(k) - \sum_{m=1}^L f_+(m) \tilde{a}(k-m) \right|^2 \quad (6.4-1)$$

where  $K$  is the number of observed whitened matched filter outputs, and we have taken into account the time-limited nature of  $f_+(m)$ .

When  $f_+(m)$  has only  $L+1$  coefficients, it follows from Fig. 6-5 that the useful component  $u_0(k)$  is determined by the current symbol  $a(k)$  and  $L$  previous symbols ( $a(k-1)$ , ...,  $a(k-L)$ ). Hence,  $u_0(k)$  can be considered as the output of a *finite state machine* (FSM) with input  $a(k)$  and state  $S(k) = (a(k-1), \dots, a(k-L))$ . The operation of a FSM is completely described by the output equation  $u_0(k) = \Psi_{\text{out}}(a(k), S(k))$  and the state transition equation  $S(k+1) = \Psi_{\text{st}}(a(k), S(k))$ , as indicated in Fig. 6-6. Selecting

$$\Psi_{\text{out}}(a(k), S(k)) = a(k) + \sum_{m=1}^L a(k-m) f_+(m) \quad (6.4-2)$$

$$\Psi_{\text{st}}(a(k), S(k)) = (a(k), \dots, a(k-L+1)) \quad (6.4-3)$$

the FSM produces the output  $u_0(k)$  from Fig. 6-5.

The evolution of the states with time is visualized by means of the trellis diagram. The trellis diagram shows at each instant  $k$  the  $M^L$  possible states as nodes. Branches between nodes at instant  $k$  and nodes at instant  $k+1$  indicate which state transitions are possible at instant  $k$ . Each state has  $M$  incoming branches and  $M$  outgoing branches. Each branch can be

given the label " $a(k), u_0(k)$ ", denoting the symbol  $a(k)$  that causes the specific state transition from  $S(k)$  to  $S(k+1)$ , and the output  $u_0(k)$  resulting from this transition. As the FSM is time-invariant, the trellis consists of a repetition of  $K$  identical sections. Fig. 6-7 shows such a section for  $L = 2$ , a constellation  $C = \{-1, 1\}$ , and  $(f_+(0), f_+(1), f_+(2)) = (1, 1, 1/2)$ ; the corresponding  $F_+(z)$  has zeroes  $(-1 \pm j)/2$  which are both inside the unit circle. The branch labels  $a(k), u_0(k)$  of the trellis are derived in Table 6-1.

$S(k) =$ $(a(k-1), a(k-2))$	$a(k)$	$S(k+1) =$ $(a(k), a(k-1))$	$u_0(k)$
(1,1)	1	(1,1)	$f_+(0) + f_+(1) + f_+(2) \quad (= 2.5)$
(1,1)	-1	(-1,1)	$-f_+(0) + f_+(1) + f_+(2) \quad (= 0.5)$
(1,-1)	1	(1,1)	$f_+(0) + f_+(1) - f_+(2) \quad (= 1.5)$
(1,-1)	-1	(-1,1)	$-f_+(0) + f_+(1) - f_+(2) \quad (= -0.5)$
(-1,1)	1	(1,-1)	$f_+(0) - f_+(1) + f_+(2) \quad (= 0.5)$
(-1,1)	-1	(-1,-1)	$-f_+(0) - f_+(1) + f_+(2) \quad (= -1.5)$
(-1,-1)	1	(1,-1)	$f_+(0) - f_+(1) - f_+(2) \quad (= -0.5)$
(-1,-1)	-1	(-1,-1)	$-f_+(0) - f_+(1) - f_+(2) \quad (= -2.5)$

Table 6-1 : determining the branch labels  $a(k), u_0(k)$ 

An initial state  $\tilde{S}(0)$  and a symbol sequence  $\tilde{\mathbf{a}}(k) = (\tilde{a}(0), \dots, \tilde{a}(k))$  give rise to a specific path in the trellis that ends in some state at instant  $k+1$ . According to (6.4-1), the log-likelihood (multiplied by  $-N_0/A^2$ ) of this path, given the observations  $(u(0), \dots, u(k))$ , equals the following the *path metric*  $\Lambda(\tilde{\mathbf{a}}(k), \tilde{S}(0))$  :

$$\Lambda(\tilde{\mathbf{a}}(k), \tilde{S}(0)) = \sum_{m=0}^k \lambda(\tilde{a}(m), \tilde{S}(m)) \quad (6.4-4)$$

where the *branch metric*  $\lambda(\tilde{a}(m), \tilde{S}(m))$  is defined as

$$\lambda(\tilde{a}(m), \tilde{S}(m)) = |u(m) - \Psi_{\text{out}}(\tilde{a}(m), \tilde{S}(m))|^2 \quad (6.4-5)$$

The branch metric (6.4-5) is a measure of the difference between the noisy observation  $u(m)$  and the FSM output  $u_0(m)$  that results from the state  $\tilde{S}(m)$  and the input symbol  $\tilde{a}(m)$ . The path metric  $\Lambda(\tilde{\mathbf{a}}(k), \tilde{S}(0))$  is the squared Euclidean distance between the noisy observation sequence  $(u(0), \dots, u(k))$  and the FSM output sequence  $(u_0(0), \dots, u_0(k))$  corresponding to the considered path. ML sequence detection based on  $(u(0), \dots, u(K-1))$  consists of finding the path in the trellis that minimizes the path metric  $\Lambda(\tilde{\mathbf{a}}(K-1), \tilde{S}(0))$ . We denote by  $\{\hat{a}(k)\}$  and  $\{\hat{S}(k)\}$  the ML symbol sequence and the associated state sequence that correspond to this

path. In the following, we use short-hand notations  $\Lambda(k+1) = \Lambda(\tilde{\mathbf{a}}(k), \tilde{\mathbf{S}}(0))$  and  $\lambda(m) = \lambda(\tilde{\mathbf{a}}(m), \tilde{\mathbf{S}}(m))$ .

Finding the path with the smallest metric is a dynamic programming problem, which is solved by means of the *Viterbi algorithm*. For further use, we define the *surviving path* at state  $\mathbf{S}(k)$  as the path with the minimum path metric among all paths originating at  $k=0$  and terminating in  $\mathbf{S}(k)$ . The Viterbi algorithm operates as follows.

- For each of the  $M^L$  initial states ( $k=0$ ), we compute the branch metrics  $\lambda(0)$  of the  $M$  outgoing branches. Each of the  $M^L$  states at  $k=1$  has  $M$  incoming branches. For each of these states, we keep only the surviving path (which at this stage has only one branch), i.e., the incoming branch with the smallest branch metric. We associate the path metric  $\Lambda(1) = \lambda(0)$  of the surviving path to the corresponding terminating state. Hence, from all  $M.M^L$  paths going from a state at  $k=0$  to a state at  $k=1$ , we keep only  $M^L$  surviving paths, i.e., one path for every state at  $k=1$ , and associate the surviving path metric to that state.
- Now we move from  $k=1$  to  $k=2$ . For each state at  $k=1$ , we compute the branch metrics  $\lambda(1)$  of the  $M$  outgoing branches. For each state at  $k=2$ , we keep only the branch for which the sum  $\Lambda(2)$ , of the branch metric  $\lambda(1)$  and the path metric  $\Lambda(1)$  associated to the originating state of that branch, is the smallest. The surviving path at the considered state (at  $k=2$ ) consists of the branch ending in that state, and the surviving path that terminates in the state (at  $k=1$ ) from which that branch originates. The surviving path metric  $\Lambda(2)$  is associated to the corresponding state at  $k=2$ .
- Continuing this procedure, we determine at each instant  $k$  the surviving path and the associated path metric for every state at instant  $k$ . After observing the  $K$  whitened matched filter outputs ( $u(0), \dots, u(K-1)$ ), the procedure stops at  $k=K$ . Each ending state at  $k=K$  has a surviving path and a corresponding path metric  $\Lambda(K)$ . We look for the ending state with the minimum path metric  $\Lambda(K)$ ; the corresponding surviving path is the ML solution.

In some applications, the initial state and/or the ending state are known (when the data symbols that determine these states are known a priori to the receiver). In this case, the Viterbi algorithm is slightly modified.

- When the initial state is known, only branches originating from this initial state are considered at  $k=0$ . For  $k = 1, \dots, L$ , all states have only one incoming branch, so that determining the surviving path is trivial. For  $k > L$ , all states have  $M$  incoming branches, and determining the surviving path is as described above.

- When the ending state  $S(K)$  is known, the ML solution corresponds to the surviving path ending at  $S(K)$ .

The computational complexity of the Viterbi algorithm is proportional to  $M^L K$ , i.e. linear in the sequence length  $K$  but exponential in the memory  $L$  of the filter  $F_+(\exp(j2\pi fT))$ .

### Example

We consider the trellis from Fig. 6-7, and assume that the whitened matched filter outputs are  $(u(0), u(1), u(2), u(3)) = (0.5, -0.5, 2, 0.5)$ . The corresponding branch metrics (which we have multiplied by 4 in order to avoid fractional numbers) are given in Table 6-2. We assume that the initial state is unknown. The computations according to the Viterbi algorithm are illustrated in Fig. 6-8 to Fig. 6-11, which show the surviving paths and their path metric at  $k = 1, \dots, 4$ . At  $k = 4$ , the most likely path has a metric (after multiplication by 4) of 5, and corresponds to the ML state sequence  $(\hat{S}(0), \dots, \hat{S}(4)) = ((1,1), (-1,1), (1,-1), (1,1), (-1,1))$  and output sequence  $(\hat{u}_0(0), \dots, \hat{u}_0(3)) = (0.5, 0.5, 1.5, 0.5)$ ; the ML symbol sequence that causes these state transitions is  $(\hat{a}_0(0), \dots, \hat{a}_3(0)) = (-1, 1, 1, -1)$ . Note that a receiver performing symbol-by-symbol detection on  $(u(0), u(1), u(2), u(3)) = (0.5, -0.5, 2, 0.5)$  would yield the symbol decisions  $(1, -1, 1, 1)$ , which is different from the ML symbol sequence  $(-1, 1, 1, -1)$ .

$S(k) = (a(k-1), a(k-2))$	$a(k)$	$S(k+1) = (a(k), a(k-1))$	$u_0(k)$	$4\lambda(0)$	$4\lambda(1)$	$4\lambda(2)$	$4\lambda(3)$
(1,1)	1	(1,1)	2.5	16	36	1	16
(1,1)	-1	(-1,1)	0.5	0	4	9	0
(1,-1)	1	(1,1)	1.5	4	16	1	4
(1,-1)	-1	(-1,1)	-0.5	4	0	25	4
(-1,1)	1	(1,-1)	0.5	0	4	9	0
(-1,1)	-1	(-1,-1)	-1.5	16	4	49	16
(-1,-1)	1	(1,-1)	-0.5	4	0	25	4
(-1,-1)	-1	(-1,-1)	-2.5	36	16	81	36

Table 6-2 : determining the branch metrics for  $(u(0), u(1), u(2), u(3)) = (0.5, -0.5, 2, 0.5)$

## 6.5. BER performance of the ML sequence detector

Typically, the correct path (corresponding to the symbols actually transmitted) and the detected path (corresponding to the detected symbols) are coincident for most of the time, but occasionally the detected path diverges from the true path and remerges after a while. We say that an *error event* starts at time  $k_1$  and ends at time  $k_2$ , when the detected state is correct at  $k=k_1$  and at  $k=k_2$ , but incorrect for  $k_1 < k < k_2$  : this corresponds to the detected path diverging from the correct path at  $k = k_1$  and remerging with the correct path at  $k = k_2$  (for the first time since  $k = k_1$ ).

An error event starting at  $k_1$  and ending at  $k_2$  is fully characterized by the correct state sequence  $\alpha = (S(k_1), S(k_1+1), \dots, S(k_2))$  and the ML state sequence  $\hat{\alpha} = (\hat{S}(k_1), \hat{S}(k_1+1), \dots, \hat{S}(k_2))$  that have a common starting and ending state ( $\hat{S}(k_1) = S(k_1)$ ,  $\hat{S}(k_2) = S(k_2)$ ), and no common state in between. The transmitted and detected data symbols that give rise to this error event are  $(a(k_1-L), \dots, a(k_2-1))$  and  $(\hat{a}(k_1-L), \dots, \hat{a}(k_2-1))$ , with

$$(\hat{a}(k_1-L), \dots, \hat{a}(k_1-1)) = (a(k_1-L), \dots, a(k_1-1)) \Leftrightarrow \hat{S}(k_1) = S(k_1)$$

$$(\hat{a}(k_2-L), \dots, \hat{a}(k_2-1)) = (a(k_2-L), \dots, a(k_2-1)) \Leftrightarrow \hat{S}(k_2) = S(k_2)$$

$$\hat{a}(k_1) \neq a(k_1), \text{ because } \hat{S}(k_1) = S(k_1) \text{ and } \hat{S}(k_1+1) \neq S(k_1+1)$$

$$\hat{a}(k_2-L-1) \neq a(k_2-L-1), \text{ because } \hat{S}(k_2) = S(k_2) \text{ and } \hat{S}(k_2-1) \neq S(k_2-1)$$

Hence, the first and the last symbol error associated with the error event  $(\alpha, \hat{\alpha})$  occur at  $k=k_1$  and  $k=k_2-L-1$ , and in between there is no occurrence of  $L$  successive correct decisions. Note that the smallest possible value of  $k_2$  is  $k_1+L+1$ , which corresponds to the case where only the symbol  $a(k_1)$  is detected in error.

Error events starting at different instants are said to be of *the same type*, when their correct paths and detected paths correspond to the same correct state sequence and the same ML state sequence. Considering the trellis from Fig. 6-7, Fig. 6-12 shows two error events that are of the same type, starting at  $k$  and  $k'$ , respectively. Their correct paths go through the states  $\alpha = ((-1,1), (-1,-1), (1,-1), (1,1))$  and their ML paths go through the states  $\hat{\alpha} = ((-1,1), (1,-1), (1,1), (1,1))$ . The corresponding symbol sequences that cause these state transitions are  $(-1, 1, 1)$  for the correct path and  $(1, 1, 1)$  for the ML path.

Let us consider the bit error rate (BER) resulting from ML sequence detection. Whenever an error event of type  $(\alpha, \hat{\alpha})$  occurs,  $n_b(\alpha, \hat{\alpha})$  bit errors result :  $n_b(\alpha, \hat{\alpha})$  is obtained by comparing the *bit sequences* that give rise to the state sequences  $\alpha$  and  $\hat{\alpha}$ , and counting in

how many positions these bit sequences are different. For both error events shown in Fig. 6-12 we get  $n_b(\alpha, \hat{\alpha}) = 1$ . Let us denote by  $P_e(\alpha, \hat{\alpha})$  the probability that an error event of type  $(\alpha, \hat{\alpha})$  starts at  $k=0$ . Assuming a (long) sequence of  $K$  transmitted symbols (which corresponds to  $K \cdot \log_2(M)$  transmitted bits), the average number of occurrences of an error event of type  $(\alpha, \hat{\alpha})$  equals  $K \cdot P_e(\alpha, \hat{\alpha})$ . The resulting BER is given by

$$\begin{aligned} \text{BER} &= \frac{1}{\log_2(M)} \sum_{\alpha} \sum_{\hat{\alpha} \in D(\alpha)} n_b(\alpha, \hat{\alpha}) P_e(\alpha, \hat{\alpha}) \\ &= \frac{1}{\log_2(M)} \sum_{\alpha} \sum_{\hat{\alpha} \in D(\alpha)} n_b(\alpha, \hat{\alpha}) P_e(\hat{\alpha} | \alpha) \Pr[\alpha] \end{aligned} \quad (6.5-1)$$

where the outer sum is over all state sequences  $\alpha$  that start at  $k=0$  and end at  $k=i$ , with  $L+1 \leq i \leq K$ , and  $D(\alpha)$  is the set of state sequences with the same starting and ending state as  $\alpha$  and not merging with  $\alpha$  in between. In the second line of (6.5-1),  $P_e(\hat{\alpha} | \alpha)$  is the probability that the ML detector outputs the state sequence  $\hat{\alpha}$  when  $\alpha$  is the correct state sequence, and  $\Pr[\alpha]$  is the probability of occurrence of the correct state sequence  $\alpha$ .

The exact computation of  $P_e(\hat{\alpha} | \alpha)$  in general is not feasible, but fortunately we can provide accurate upper and lower bounds.

### Upper bound on BER

The ML detector selects  $\hat{\alpha}$  instead of the correct  $\alpha$  when  $\hat{\alpha}$  has the highest likelihood among the set of state sequences consisting of  $\alpha$  and of all state sequences from  $D(\alpha)$ . Hence,  $P_e(\hat{\alpha} | \alpha)$  is upper bounded by the probability that the likelihood of  $\hat{\alpha}$  is larger than the likelihood of  $\alpha$ . This yields

$$P_e(\hat{\alpha} | \alpha) \leq \Pr \left[ \sum_{k=0}^{i-1} \left| u(k) - \sum_{m=0}^L f_+(m) a(k-m) \right|^2 > \sum_{k=0}^{i-1} \left| u(k) - \sum_{m=0}^L f_+(m) \hat{a}(k-m) \right|^2 \right] \quad (6.5-2)$$

where  $\{a(k), k = -L, \dots, i-1\}$  and  $\{\hat{a}(k), k = -L, \dots, i-1\}$  refer to the symbol sequences that correspond to  $\alpha$  and  $\hat{\alpha}$ . Taking the decomposition (6.2-15) of  $u(k)$  into account, the bound (6.5-2) becomes

$$\begin{aligned} P_e(\hat{\alpha} | \alpha) &\leq \Pr \left[ \sum_{k=0}^{i-1} |w(k)|^2 > \sum_{k=0}^{i-1} |w(k) - \Delta(k)|^2 \right] \\ &= \Pr \left[ \sum_{k=0}^{i-1} 2 \operatorname{Re}[w^*(k) \Delta(k)] > \sum_{k=0}^{i-1} |\Delta(k)|^2 \right] \end{aligned} \quad (6.5-3)$$

where

$$\Delta(k) = \sum_{m=0}^L f_+(m) e(k-m) \quad (6.5-4)$$

and  $e(k) = \hat{a}(k) - a(k)$ ,  $k = -L, \dots, i-1$ . We stack the quantities  $e(k)$  into the vector  $\mathbf{e}$ , with  $(\mathbf{e})_k = e(k)$ . When we want to emphasize that  $\mathbf{e}$  depends on  $(\alpha, \hat{\alpha})$ , we will use the notation  $\mathbf{e}(\alpha, \hat{\alpha})$ . Taking into account that  $2\text{Re}[w(k)\Delta^*(k)] \sim N(0, 2(N_0/A^2)|\Delta(k)|^2\delta(m))$ , we obtain

$$P_e(\hat{\alpha} | \alpha) \leq Q\left(\sqrt{\frac{d^2(\mathbf{e})A^2}{2N_0}}\right) \quad (6.5-5)$$

with  $d^2(\mathbf{e})$  denoting the squared Euclidean distance between the FSM outputs that correspond to the state sequences  $\alpha$  and  $\hat{\alpha}$  :

$$d^2(\mathbf{e}) = \sum_{k=0}^{i-1} |\Delta(k)|^2 = \sum_{k=0}^{i-1} \left| \sum_{m=0}^L f_+(m) e(k-m) \right|^2 \quad (6.5-6)$$

As the starting and ending states of  $\alpha$  and  $\hat{\alpha}$  are the same, we have  $\mathbf{e} = (e(0), \dots, e(i-L-1))$  with  $e(0) \neq 0$  and  $e(i-L-1) \neq 0$ , and  $e(k) = 0$  for  $k = -L, \dots, -1$  and  $k = i-L, \dots, i-1$  in (6.5-6). Using (6.5-5) in (6.5-1) yields the BER upper bound :

$$\text{BER} \leq \frac{1}{\log_2(M)} \sum_{\alpha} \sum_{\hat{\alpha} \in D(\alpha)} Q\left(\sqrt{\frac{d^2(\mathbf{e})A^2}{2N_0}}\right) n_b(\alpha, \hat{\alpha}) \Pr[\alpha] \quad (6.5-7)$$

The function  $Q(\cdot)$  decreases rapidly when its argument increases. Hence, the most probable error events are those with the smallest  $d^2(\mathbf{e})$ . We define :

$$d_{\min}^2 = \min_{\mathbf{e}} d^2(\mathbf{e}) \quad (6.5-8)$$

and denote by  $A_{\min}$  the set of state sequence pairs  $(\alpha, \hat{\alpha})$  for which  $d^2(\mathbf{e}(\alpha, \hat{\alpha})) = d_{\min}^2$ . For small enough  $N_0$ , the contribution from error events with  $d^2(\mathbf{e}) > d_{\min}^2$  becomes negligible. Hence,

$$\text{BER} \leq K_{\text{up}} Q\left(\sqrt{\frac{d_{\min}^2 A^2}{2N_0}}\right) + \text{other terms} \quad (6.5-9)$$

where

$$K_{\text{up}} = \frac{1}{\log_2(M)} \sum_{(\alpha, \hat{\alpha}) \in A_{\min}} n_b(\alpha, \hat{\alpha}) \Pr[\alpha] \quad (6.5-10)$$

and "other terms" are negligibly small (as compared to the first term) for small  $N_0$ .



**Lower bound on BER**

Now we derive a lower bound on the BER. As  $n_b(\alpha, \hat{\alpha}) \geq 1$ , we get from (6.5-1) the following lower bound :

$$\frac{1}{\log_2(M)} \sum_{\alpha} \left( \sum_{\hat{\alpha} \in D(\alpha)} P_e(\hat{\alpha} | \alpha) \right) \Pr[\alpha] \leq \text{BER} \quad (6.5-11)$$

Let us consider the set  $B_{\min}$  of state sequences  $\alpha$  such that at least one other state sequence  $\alpha'$  from  $D(\alpha)$  yields  $d^2(e(\alpha, \hat{\alpha})) = d_{\min}^2$ . The left-hand side of (6.5-11) can be further lower bounded by summing only over the sequences  $\alpha$  that are contained in the set  $B_{\min}$ . The inner summation in (6.5-11) is the probability that *any* error event occurs at  $k=0$ , when the correct state sequence is  $\alpha$ . This summation equals the probability that  $\alpha$  does not have the highest likelihood among the set of state sequences consisting of  $\alpha$  and of all state sequences from  $D(\alpha)$ . This probability is lower bounded by the probability that the likelihood of  $\alpha$  is smaller than the likelihood of a particular state sequence  $\alpha'$  from  $D(\alpha)$ ; we select  $\alpha'$  such that the resulting  $d^2(e)$  equals  $d_{\min}^2$ . This yields

$$K_{\text{low}} Q \left( \sqrt{\frac{d_{\min}^2 A^2}{2N_0}} \right) \leq \text{BER} \quad (6.5-12)$$

where

$$K_{\text{low}} = \frac{1}{\log_2(M)} \sum_{\alpha \in B_{\min}} \Pr[\alpha] \quad (6.5-13)$$

Combining (6.5-9) and (6.5-12), we obtain

$$K_{\text{low}} Q \left( \sqrt{\frac{d_{\min}^2 A^2}{2N_0}} \right) \leq \text{BER} \leq K_{\text{up}} Q \left( \sqrt{\frac{d_{\min}^2 A^2}{2N_0}} \right) + \text{other terms} \quad (6.5-14)$$

which indicates that the BER is roughly proportional to  $Q(\sqrt{d_{\min}^2 A^2 / (2N_0)})$  for small  $N_0$ .

**Minimum Euclidean distance  $d_{\min}$** 

From the above discussion we conclude that the BER performance is mainly determined by the minimum squared Euclidean distance  $d_{\min}^2$ , defined by (6.5-8). A simple upper bound on  $d_{\min}^2$  is obtained by observing that  $d_{\min}^2$  cannot be larger than  $d^2(\mathbf{e})$  that results from  $\mathbf{e}(k) = e(0)\delta(k)$ , i.e., when  $\mathbf{e}$  has only one nonzero component  $e(0)$ . In this case, the ending state of the error event is at  $k = L+1$ . This yields

$$\Delta(k) = e(0) \sum_{m=0}^L f_+(m) \delta(k-m) = \begin{cases} e(0)f_+(k) & k = 0, \dots, L \\ 0 & \text{otherwise} \end{cases} \quad (6.5-15)$$

The resulting squared Euclidean distance is given by :

$$d^2(\mathbf{e}) = \sum_{k=0}^L \left| \sum_{m=0}^L f_+(m) e(0) \delta(k-m) \right|^2 = |e(0)|^2 \sum_{k=0}^L |f_+(k)|^2 = |e(0)|^2 \frac{g(0)}{A^2} \quad (6.5-16)$$

Now  $d^2(\mathbf{e})$  can be minimized over  $e(0)$ , yielding

$$d^2(\mathbf{e}) = e_{\min}^2 \sum_{k=0}^L |f_+(k)|^2 = e_{\min}^2 \frac{g(0)}{A^2} \quad (6.5-17)$$

where  $e_{\min}^2$  is the minimum squared Euclidean distance between different constellation points.

Hence, the following upper bound is obtained :

$$d_{\min}^2 \leq e_{\min}^2 \sum_{k=0}^L |f_+(k)|^2 = e_{\min}^2 \frac{g(0)}{A^2} \quad (6.5-18)$$

Comparing the matched filter bound (6.3-4) with (6.5-14) and taking (6.5-18) into account, it follows that the ML sequence detector cannot do better than the matched filter bound (this is no surprise, as no receiver can perform better than the matched filter bound). However, in case (6.5-18) holds with equality, the ML sequence detector is able to overcome the presence of ISI, and performs nearly as well as the matched filter bound.

The minimum squared Euclidean distance  $d_{\min}^2$  can be obtained by applying the Viterbi algorithm to a trellis with states  $S'(k) = (e(k-1), \dots, e(k-L))$  and branch metrics  $\lambda'(e(k), S'(k)) = |\Delta(k)|^2$ , with  $\Delta(k)$  given by (6.5-4). We consider only paths with  $(e(-1), \dots, e(-L)) = (0, \dots, 0)$  as starting state, and  $e(0) \neq 0$ ; paths reaching the state  $(0, \dots, 0)$  at  $k > 0$  are not further extended. The metric of such a path equals  $d^2(\mathbf{e})$  from (6.5-6), with  $\mathbf{e}$  denoting the sequence  $(e(0), e(1), \dots)$  corresponding to the considered path. Hence, the paths with the smallest metric correspond to the error sequence  $\mathbf{e}$  yielding the minimum squared Euclidean distance  $d_{\min}^2$ . The Viterbi algorithm can be stopped when at least one path has reached the state  $(0, \dots, 0)$ ,

and the metrics of the paths that have not yet reached the state  $(0, \dots, 0)$  are larger than the minimum metric of the paths that have already reached the state  $(0, \dots, 0)$ .

### Example

We consider the case where the constellation is given by  $C = \{-1, 1\}$  and  $(f_+(0), f_+(1), f_+(2)) = (1, 1, 1/2)$ . As  $e(k) \in \{2, 0, -2\}$  and the channel memory is  $L = 2$ , there are  $3^2 = 9$  possible states  $S'(k)$ . A section of the corresponding trellis is shown in Fig. 6-13, and the associated branch metrics are given in Table 6-3, with  $\lambda'(k) = |e(k) + e(k-1) + (1/2)e(k-2)|^2$ ; the entries  $+$  and  $-$  refer to 2 and -2, respectively. Now the Viterbi algorithm is applied to find the paths that yield  $d_{\min}^2$ . As the paths resulting from  $(e(0), e(1), \dots, e(k))$  and  $(-e(0), -e(1), \dots, -e(k))$  yield the same path metric, we consider only paths with  $e(0) = 2$ .

Fig. 6-14 shows the result of the above procedure. The dashed path corresponds to the state sequence  $((0,0), (0,0), \dots, (0,0))$ ; whenever a path merges with the dashed path, the former path is not further extended. The minimum Euclidean distance path reaches the state  $(00)$  at  $k=4$ , yielding  $d_{\min}^2 = 6$ . The corresponding state sequence and error sequence are  $((00), (+0), (-+), (0-), (00))$  and  $(+, -, 0, 0)$ , respectively; because of symmetry, also the state sequence  $((00), (-0), (+-), (0+), (00))$  and the error sequence  $(-, +, 0, 0)$  give rise to  $d_{\min}^2 = 6$ .

$S'(k) = (e(k-1), e(k-2))$	$e(k)$	$S'(k+1)$	$\lambda'(k)$
(++)	+	(++)	25
(++)	0	(0+)	9
(++)	-	(-+)	1
(+0)	+	(++)	16
(+0)	0	(0+)	4
(+0)	-	(-+)	0
(+-)	+	(++)	9
(+-)	0	(0+)	1
(+-)	-	(-+)	1
(0+)	+	(+0)	9
(0+)	0	(00)	1
(0+)	-	(-0)	1
(00)	+	(+0)	4
(00)	0	(00)	0
(00)	-	(-0)	4

$S'(k) = (e(k-1), e(k-2))$	$e(k)$	$S'(k+1)$	$\lambda'(k)$
(0-)	+	(+0)	1
(0-)	0	(00)	1
(0-)	-	(-0)	9
(-+)	+	(+-)	1
(-+)	0	(0-)	1
(-+)	-	(--)	9
(-0)	+	(+-)	0
(-0)	0	(0-)	4
(-0)	-	(--)	16
(--)	+	(+-)	1
(--)	0	(0-)	9
(--)	-	(--)	25

Table 6-3 : branch metrics for determining minimum distance

Now we compute  $K_{up}$  and  $K_{low}$  from (6.5-10) and (6.5-13). As each error sequence  $\mathbf{e}$  yielding  $d(\mathbf{e}) = d_{min}$  has 4 components ( $e(0), \dots, e(3)$ ), the state sequence  $\alpha$  has 5 components ( $S(0), \dots, S(4)$ ), and is determined by a sequence of 6 data symbols ( $a(-2), \dots, a(3)$ ). Hence,

$$\Pr[\alpha] = \Pr[S(0), S(1), S(2), S(3), S(4)] = \Pr[a(-2), a(-1), a(0), a(1), a(2), a(3)] = \frac{1}{64}$$

As the errors  $e(k) = 2$  and  $e(k') = -2$  are possible only when  $a(k) = -1$  and  $a(k') = 1$ , and  $e(k'') = 0$  is possible irrespective of  $a(k'')$ , it follows that the error sequences  $(+, -, 0, 0)$  and  $(-, +, 0, 0)$  can occur only when  $(a(0), a(1)) = (-1, 1)$  and  $(a(0), a(1)) = (1, -1)$ , respectively, while there are no restrictions on  $(a(-2), a(-1), a(2), a(3))$ . Hence, from all 64 symbol sequences  $(a(-2), \dots, a(3))$ , 32 of them are compatible with an error sequence  $(+, -, 0, 0)$  or  $(-, +, 0, 0)$ , so that the set  $B_{min}$  contains 32 state sequences  $\alpha$ . This yields  $K_{low} = 32/64 = 1/2$ . For each state sequence  $\alpha$  from  $B_{min}$ , there is only one state sequence  $\hat{\alpha}$  giving rise to  $d_{min}^2$ , and the resulting number of symbol errors is 2. Hence, the set  $A_{min}$  has 32 elements  $(\alpha, \hat{\alpha})$ , yielding  $K_{up} = 2 \times 32/64 = 1$ .

The squared Euclidean distance related to the matched filter bound corresponds to the error sequences  $(+, 0, 0)$  and  $(-, 0, 0)$ ; these error sequences yields a path that merges with the dashed path at  $k = 3$ , and have a path metric equal to 9 ( $= e_{min}^2 \sum_{k \geq 0} |f_+(k)|^2$ ). Hence, the ISI caused by the channel dispersion gives rise to a degradation of the ML sequence detector as compared to the matched filter bound of about  $10 \cdot \log(9/6) \approx 1.8$  dB.

## 6.6. Linear equalization

When the channel memory  $L$  is large, the computational complexity of the Viterbi equalizer, which is proportional to  $M^L$ , becomes prohibitively large. In this case, we have to look for suboptimum receivers with reduced complexity. One of the possibilities is to use a *linear equalizer*, followed by symbol-by-symbol detection. The task of the linear equalizer is to reduce the ISI at the input of the symbol-by-symbol detector by means of linear filtering.

Let us consider the receiver structure from Fig. 6-15. The received signal  $r(t)$  from (6.1-2) is applied to the matched filter  $H^*(f)$ , whose output is sampled at instants  $kT$ . The resulting samples  $\{z(k)\}$  are a sufficient statistic for detecting the data symbols. The samples  $\{z(k)\}$  are fed to a discrete-time equalization filter  $H_{LE}(z)$ . The resulting output sequence  $\{u(k)\}$  is applied to a symbol-by-symbol detector, that outputs the constellation point  $\hat{a}(k)$  that is closest to  $u(k)$ .

Taking into account the discrete-time model of  $z(k)$  (see Fig. 6-2), the discrete-time model for the equalizer output  $u(k)$  is shown in Fig. 6-16, with

$$G_{LE}(z) = G(z)H_{LE}(z) \quad (6.6.0-1)$$

The power spectral density  $S_n(\exp(j2\pi fT))$  of the noise  $n'(k)$  at the equalizer output is given by

$$S_n(\exp(j2\pi fT)) = N_0 G(\exp(j2\pi fT)) |H_{LE}(\exp(j2\pi fT))|^2 \quad (6.6.0-2)$$

The equalizer output  $u(k)$  can be represented as

$$u(k) = \underbrace{a(k)g_{LE}(0)}_{\text{useful}} + \underbrace{\sum_{m \neq 0} a(k-m)g_{LE}(m)}_{\text{residual ISI}} + \underbrace{n'(k)}_{\text{noise}} \quad (6.6.0-3)$$

where  $g_{LE}(m)$  is the IDTFT of  $G_{LE}(\exp(j2\pi fT))$ .

Based on (6.6.0-3), several performance measures of the linear equalizer can be defined.

- Defining  $\varepsilon(k) = u(k) - a(k)$ , the normalized mean-square error (MSE) of the linear equalizer is defined as  $MSE_{LE} = E[|\varepsilon(k)|^2]/E_s$ ;  $MSE_{LE}$  is a measure of the difference between the equalizer output  $u(k)$  and the correct data symbol  $a(k)$ . From (6.6.0-3) we obtain

$$MSE_{LE} = |g_{LE}(0) - 1|^2 + \sum_{m \neq 0} |g_{LE}(m)|^2 + \frac{E[|n'(k)|^2]}{E_s} \quad (6.6.0-4)$$

where the noise power  $E[|n'(k)|^2]$  can be computed as

$$E[|n'(k)|^2] = T \int_{-1/T}^{1/T} S_n(\exp(j2\pi fT)) df = \langle S_n(\cdot) \rangle_f \quad (6.6.0-5)$$

and  $S_n(\cdot)$  is given by (6.6.0-2), and we dropped the argument  $\exp(j2\pi fT)$ .

- The signal-to-interference-plus-noise ratio (SINR) is the ratio of the useful signal power in (6.6.0-3) to the power of the ISI and the noise in (6.6.0-3) :

$$SINR_{LE} = \frac{|g_{LE}(0)|^2}{\sum_{m \neq 0} |g_{LE}(m)|^2 + \frac{E[|n'(k)|^2]}{E_s}} \quad (6.6.0-6)$$

Note that SINR is upper bounded by the signal-to-noise ratio SNR, which is the ratio of the useful signal power in (6.6.0-3) to the noise power in (6.6.0-3) :

$$SINR_{LE} \leq SNR_{LE} = \frac{E_s |g_{LE}(0)|^2}{E[|n'(k)|^2]} \quad (6.6.0-7)$$

In (6.6.0-6) and (6.6.0-7), the noise power  $E[|n'(k)|^2]$  is given by (6.6.0-5).

In the following, two types of linear equalization are considered : the zero-forcing linear equalizer (ZF-LE) and the minimum mean-square error linear equalizer (MMSE-LE)

### 6.6.1 Zero-forcing linear equalizer

In the case of ZF-LE, the equalizer  $H_{LE}(z) = H_{ZF-LE}(z)$  is selected such that  $g_{LE}(m) = \delta(m)$ , i.e., no ISI arises at the output of the equalizer, and the useful component in (6.6.0-3) has a coefficient equal to 1. This condition requires  $G_{LE}(z) = 1$ , or, using (6.6.0-1),

$$H_{ZF-LE}(z) = \frac{1}{G(z)} \quad (6.6.1-1)$$

When (6.6.1-1) holds, the noise spectrum  $S_n(\exp(j2\pi fT))$  from (6.6.0-2) reduces to

$$S_n(\exp(j2\pi fT)) = \frac{N_0}{G(\exp(j2\pi fT))} = N_0 H_{ZF-LE}(\exp(j2\pi fT)) \quad (\text{ZF-LE}) \quad (6.6.1-2)$$

Hence, we obtain

$$u(k) = a(k) + n'(k) \quad (6.6.1-3)$$

which is illustrated in Fig. 6-17. From (6.6.1-3) and (6.6.1-2), the SNR and the MSE at the input of the decision device are determined by

$$\text{SNR}_{ZF-LE} = \frac{1}{\text{MSE}_{ZF-LE}} = \frac{E_s}{N_0} \left( \left\langle \frac{1}{G(\cdot)} \right\rangle_f \right)^{-1} = \frac{E_s}{N_0} \cdot \frac{1}{h_{ZF-LE}(0)} \quad (6.6.1-4)$$

where  $\{h_{ZF-LE}(m)\}$  is the impulse response of the ZF-LE filter (6.6.1-1).

As  $n'(k)$  in (6.6.1-3) is circular Gaussian noise, the BER corresponding to the ZF-LE is obtained as  $\text{BER}_C(\text{SNR}_{ZF-LE})$ . The BER corresponding to the matched filter bound is given by  $\text{BER}_C(\text{SNR}_{MF})$ , with (see (6.3-2))

$$\text{SNR}_{MF} = \frac{E_s}{N_0} g(0) = \frac{E_s}{N_0} \langle G(\cdot) \rangle_f \quad (6.6.1-5)$$

Hence, we obtain

$$\frac{\text{SNR}_{MF}}{\text{SNR}_{ZF-LE}} = g(0)h_{ZF-LE}(0) = \langle G(\cdot) \rangle_f \cdot \left\langle \frac{1}{G(\cdot)} \right\rangle_f \geq 1 \quad (6.6.1-6)$$

The inequality in (6.6.1-6) is a special case of the more general inequality

$$E[F(x)] \geq F(E[x]) \quad (6.6.1-7)$$

where  $F(x)$  is an upward convex function of  $x$ . The inequality (6.6.1-6) results from (6.6.1-7) when taking  $F(x) = 1/x$ ,  $x = G(\exp(j2\pi fT))$ , and interpreting  $E[\cdot]$  as averaging over the variable  $f$  which is uniformly distributed over an interval of length  $1/T$ . The inequality (6.6.1-6) is no surprise, as no receiver can do better than the matched filter bound. As compared to the matched filter bound, the degradation (in dB) of the ZF-LE amounts to  $10 \cdot \log(\text{SNR}_{MF}/\text{SNR}_{ZF-LE})$ . This degradation reflects the *noise enhancement* caused by the equalizer : as the matched filter operating on  $r(t)$  maximizes the SNR without constraints on

the ISI, and the cascade of matched filter and ZF-LE operating on  $r(t)$  maximizes the SNR under the restriction of zero ISI, the SNR at the equalizer output cannot exceed the SNR at the matched filter output. The noise enhancement becomes very large when  $G(\exp(j2\pi fT))$  approaches zero for some value of  $f$  (say, at  $f = f_n$ ) : according to (6.6.1-1) and (6.6.1-2), both the equalizer transfer function  $H_{LE}(\exp(j2\pi fT))$  and the noise spectrum  $S_n(\exp(j2\pi fT))$  become very large near  $f = f_n$ .

### Example

We consider the case where

$$G(z) = (1 + \gamma z^{-1})(1 + \gamma^* z) = \gamma^* z + (1 + |\gamma|^2) + \gamma z^{-1} \quad (6.6.1-8)$$

with  $|\gamma| < 1$ . From (6.6.1-8) we get  $g(0) = 1 + |\gamma|^2$ . Applying a partial fraction expansion to  $H_{ZF-LE}(z) = 1/G(z)$ , we obtain

$$\begin{aligned} H_{ZF-LE}(z) &= \frac{1}{G(z)} = \frac{z}{(z + \gamma)(1 + \gamma^* z)} = \frac{\alpha}{z + \gamma} + \frac{\beta}{1 + \gamma^* z} = \frac{\alpha z^{-1}}{1 + \gamma z^{-1}} + \frac{\beta}{1 + \gamma^* z} \\ &= \alpha z^{-1}(1 - \gamma z^{-1} + \dots) + \beta(1 - \gamma^* z + \dots) \end{aligned} \quad (6.6.1-9)$$

with

$$\alpha = \frac{-\gamma}{1 - |\gamma|^2} \quad \beta = \frac{1}{1 - |\gamma|^2} \quad (6.6.1-10)$$

The power series expansion in the last line of (6.6.1-9) is valid because  $|\gamma| < 1$ . It follows from (6.6.1-9) that the coefficient of  $z^0$  in the power series expansion of  $H_{ZF-LE}(z)$  equals  $\beta$ ; hence,  $h_{ZF-LE}(0) = \beta$ . The resulting degradation (in dB) of the ZF-LE as compared to the matched filter bound equals  $10 \cdot \log((1 + |\gamma|^2)/(1 - |\gamma|^2))$ , which becomes infinitely large when  $|\gamma|$  approaches 1. Note that  $G(\exp(j2\pi fT)) = |1 + \gamma \exp(-j2\pi fT)|^2$  has a minimum value of  $(1 - |\gamma|)^2$  for  $2\pi fT = \pi + \arg(\gamma)$ ; hence, when  $|\gamma|$  approaches 1, the minimum of  $G(\exp(j2\pi fT))$  is close to zero, and the resulting noise enhancement becomes very large.

The ZF-LE can also be applied to the samples (at rate  $1/T$ ) at the output of a continuous-time filter that is different from the matched filter. However, unless these samples are a sufficient statistic, the resulting performance is worse. Therefore, the ZF-LE preceded by the matched filter is called the *optimum* ZF-LE.

### 6.6.2 Minimum mean-square error linear equalizer

The ZF-LE has the following drawbacks :

- The noise enhancement becomes very large when  $G(\exp(j2\pi fT))$  approaches zero for some value(s) of  $f$ .
- In general, the equalizer filter that eliminates the ISI has an infinite number of taps.

Hence, an equalizer that is practically implementable usually cannot eliminate the ISI.

Rather than eliminating the ISI, the MMSE-LE allows some residual ISI at the equalizer output, which will lead to less noise enhancement than with the ZF-LE. The equalizer filter  $H_{LE}(z) = H_{MMSE-LE}(z)$  is selected such that the (normalized) mean-square error between the equalizer output  $u(k)$  and the actual data symbol  $a(k)$  is minimum. Fig. 6-18 shows how  $\epsilon(k) = u(k) - a(k)$  depends on the data symbol sequence  $\{a(k)\}$  and the noise sequence  $\{n(k)\}$ . Taking into account that the power spectra of these sequences are  $E_s$  and  $N_0G(\exp(j2\pi fT))$ , respectively, it follows from Fig. 6-18 that

$$MSE = \frac{E[|\epsilon(k)|^2]}{E_s} = \left\langle |G(\cdot) \cdot H_{LE}(\cdot) - 1|^2 + \mu G(\cdot) \cdot |H_{LE}(\cdot)|^2 \right\rangle_f \quad (6.6.2-1)$$

where  $\mu = N_0/E_s$ , and we have dropped the argument  $\exp(j2\pi fT)$  of the functions in the integrand for notational convenience. In order to minimize MSE, we select  $H_{LE}(\exp(j2\pi fT))$  such that for each value of  $f$ , the function inside  $\langle \dots \rangle_f$  in (6.6.2-1) is minimum. Taking into account that  $G(\cdot)$  is real-valued, the function inside  $\langle \dots \rangle_f$  in (6.6.2-1) can be transformed as follows :

$$\begin{aligned} & |G(\cdot)H_{LE}(\cdot) - 1|^2 + \mu G(\cdot) |H_{LE}(\cdot)|^2 \\ &= (G(\cdot) + \mu)G(\cdot)H_{LE}(\cdot)H_{LE}^*(\cdot) - G(\cdot)H_{LE}^*(\cdot) - G(\cdot)H_{LE}(\cdot) + 1 \\ &= (G(\cdot) + \mu)G(\cdot) \left( H_{LE}(\cdot)H_{LE}^*(\cdot) - \frac{H_{LE}^*(\cdot)}{G(\cdot) + \mu} - \frac{H_{LE}(\cdot)}{G(\cdot) + \mu} + \frac{1}{(G(\cdot) + \mu)^2} \right) + \left( 1 - \frac{G(\cdot)}{G(\cdot) + \mu} \right) \\ &= (G(\cdot) + \mu)G(\cdot) \left| H_{LE}(\cdot) - \frac{1}{G(\cdot) + \mu} \right|^2 + \frac{\mu}{G(\cdot) + \mu} \end{aligned} \quad (6.6.2-2)$$

Hence, we see from (6.6.2-2) that MSE is minimum when

$$H_{LE}(z) = H_{MMSE-LE}(z) = \frac{1}{G(z) + \frac{N_0}{E_s}} \quad (6.6.2-3)$$

so that the first term in the last line of (6.6.2-2) becomes zero, and the integrand in (6.6.2-1) equals the last term in the last line of (6.6.2-2). The corresponding minimum MSE is given by



$$\text{MSE}_{\min, \text{LE}} = \mu \left\langle \frac{1}{G(z) + \mu} \right\rangle_f = \frac{N_0}{E_s} h_{\text{MMSE-LE}}(0) \quad (\text{MMSE-LE}) \quad (6.6.2-4)$$

Equivalently,  $\text{MSE}_{\min, \text{LE}}$  is the coefficient of  $z^0$  in the power series expansion of  $\mu/(G(z)+\mu)$ . From (6.6.2-3) and (6.6.0-1) we get  $G_{\text{LE}}(z) = G_{\text{MMSE-LE}}(z)$ , with

$$G_{\text{MMSE-LE}}(z) = \frac{G(z)}{G(z) + \frac{N_0}{E_s}} = 1 - \frac{N_0}{E_s} \cdot \frac{1}{G(z) + \frac{N_0}{E_s}} \quad (6.6.2-5)$$

Fig. 6-19 shows the discrete-time model for the output  $u(k)$  of the MMSE-LE.

Let us derive a relation between the MSE and the SINR that result from the MMSE-LE. Equating the coefficients of  $z^0$  from both sides of (6.6.2-5) yields

$$g_{\text{MMSE-LE}}(0) = 1 - \text{MSE}_{\min, \text{LE}} \quad (6.6.2-6)$$

Considering (6.6.0-4) and (6.6.0-6) with  $G_{\text{LE}}(z)$  substituted by  $G_{\text{MMSE-LE}}(z)$  and taking (6.6.2-6) into account, we obtain

$$\text{MSE}_{\min, \text{LE}} = \text{MSE}_{\min, \text{LE}}^2 + \sum_{m \neq 0} |g_{\text{MMSE-LE}}(m)|^2 + \frac{E[|n'(k)|^2]}{E_s} \quad (6.6.2-7)$$

$$\text{SINR}_{\text{MMSE-LE}} = \frac{(1 - \text{MSE}_{\min, \text{LE}})^2}{\sum_{m \neq 0} |g_{\text{MMSE-LE}}(m)|^2 + \frac{E[|n'(k)|^2]}{E_s}} \quad (6.6.2-8)$$

Hence, the SINR at the output of the MMSE-LE is given by

$$\text{SINR}_{\text{MMSE-LE}} = \frac{1 - \text{MSE}_{\min, \text{LE}}}{\text{MSE}_{\min, \text{LE}}} \quad (6.6.2-9)$$

Eq. (6.6.2-9) will be used to obtain an approximation of the BER that results from the MMSE-LE.

The symbol-by-symbol detector provides the constellation point  $\hat{a}(k)$  that is closest to the output  $u(k)$  of the MMSE-LE. The exact computation of the BER is quite complicated, because  $u(k)$  contains residual ISI and the coefficient  $g_{\text{MMSE-LE}}(0)$  of the useful component is different from 1 (see (6.6.2-6)). A convenient approximation is  $\text{BER} \approx \text{BER}_C(\text{SINR}_{\text{MMSE-LE}})$ . This approximation is accurate at large  $g(0)E_s/N_0$ , where the MSE is dominated by the noise contribution  $n'(k)$  : in this case, the sum of noise and ISI in  $u(k)$  is approximately Gaussian, and  $g_{\text{MMSE-LE}}(0) \approx 1$  (see further). The BER corresponding to the matched filter bound is given by  $\text{BER}_C(\text{SNR}_{\text{MF}})$ . As compared to the matched filter bound, the degradation (in dB) of the MMSE-LE amounts to  $10 \cdot \log(\text{SNR}_{\text{MF}}/\text{SINR}_{\text{MMSE-LE}})$ .

The MMSE-LE can also be applied to the samples (at rate  $1/T$ ) at the output of a continuous-time filter that is different from the matched filter. However, unless these samples are a sufficient statistic, the resulting performance is worse. Therefore, the MMSE-LE preceded by the matched filter is called the *optimum* MMSE-LE.

### 6.6.3 Comparison of ZF-LE and MMSE-LE

Comparing (6.6.2-4) and (6.6.1-4), we obtain

$$\text{MSE}_{\min, \text{LE}} < \text{MSE}_{\text{ZF-LE}} = \frac{1}{\text{SNR}_{\text{ZF-LE}}} \quad (6.6.3-1)$$

which indicates that  $E[|\epsilon(k)|^2]$  is smaller for the MMSE-LE than for the ZF-LE. This is no surprise, as the MMSE-LE has been designed to minimize  $E[|\epsilon(k)|^2]$ .

Let us define  $G_{\max}$  and  $G_{\min}$  as the maximum and minimum of  $G(\exp(j2\pi fT))$  :

$$G_{\max} = \max_f G(\exp(j2\pi fT)) \quad G_{\min} = \min_f G(\exp(j2\pi fT)) \quad (6.6.3-2)$$

According to the value of  $E_s/N_0$ , we distinguish between different operating regions.

- The condition  $N_0/E_s \gg G_{\max}$ , corresponds to the region of very low SNR. In this region, we have  $H_{\text{MMSE-LE}}(\exp(j2\pi fT)) \approx E_s/N_0$  (see 6.6.2-3), so that the equalizer output  $u(k)$  is essentially proportional to the matched filter output  $z(k)$ . This can be explained in the following way : as the noise at the matched filter output is much larger than the ISI, the equalizer mainly avoids noise enhancement, by providing to the detector the sequence  $\{u(k)\}$  that is proportional to the matched filter output samples  $\{z(k)\}$ . Hence,

$$\text{SINR}_{\text{MMSE-LE}} \approx \text{SNR}_{\text{MF}} = \frac{E_s}{N_0} g(0) \ll 1 \quad (6.6.3-3)$$

because the ISI in  $u(k)$  can be neglected as compared to the noise  $n'(k)$ . This operating region is not of practical interest, as the very low SNR gives rise to a large BER.

- The condition  $N_0/E_s \ll G_{\min}$  corresponds to the region of very high SNR. In this region, (6.6.2-3) yields  $H_{\text{MMSE-LE}}(\exp(j2\pi fT)) \approx 1/G(\exp(j2\pi fT)) = H_{\text{ZF-LE}}(\exp(j2\pi fT))$ , so that the MMSE-LE behaves essentially as a ZF-LE. This is explained in the following way : as the noise at the matched filter output is much smaller than the ISI, the equalizer mainly combats the ISI by providing to the detector the sequence  $\{u(k)\}$  that contains no ISI. We obtain  $\text{SINR}_{\text{MMSE-LE}} \approx \text{SNR}_{\text{ZF-LE}}$ .

- When not operating in the regions of very low or very high SNR, the MMSE-LE makes a compromise between reducing the ISI and keeping the noise enhancement small. By allowing a small residual ISI, the BER performance is better than with the ZF-LE.

### Example

We illustrate the above results considering a dispersive channel with  $G(z)$  given by

$$G(z) = (1.49^{-1}) \cdot (1 + 0.7z^{-1}) \cdot (1 + 0.7z) = 0.47z + 1 + 0.47z^{-1}. \quad (6.6.3-4)$$

For this channel we have  $g(0) = 1$ ,  $G_{\max} = 1.94$  and  $G_{\min} = 0.06$ .

- Fig. 6-20 shows  $G(\exp(j2\pi fT))$ , along with the equalizer transfer functions for the ZF-LE and for the MMSE-LE. The equalizer transfer function of the ZF-LE is  $1/G(\exp(j2\pi fT))$  : it compensates for the variation of  $G(\exp(j2\pi fT))$  over the frequency band, yielding  $G_{LE}(\exp(j2\pi fT)) = 1$ . The equalizer transfer function of the MMSE-LE depends on  $E_s/N_0$ . For very small  $E_b/N_0$ , the equalizer acts as an attenuator with gain  $E_s/N_0$  ( $\ll 1$ ). When  $E_s/N_0$  increases, the MMSE-LE transfer function converges to the ZF-LE transfer function.
- In Fig. 6-21, we compare the different contributions to  $MSE_{\min,LE}$ . For small  $E_s/N_0$ , the MMSE-LE strongly attenuates the matched filter output samples, yielding  $|u(k)| \ll |a(k)|$  and  $MSE_{\min,LE} = E[|u(k) - a(k)|^2]/E_s \approx E[|a(k)|^2]/E_s = 1$ ; in this case, the main contribution to  $MSE_{\min,LE}$  comes from  $|1 - g_{MMSE-LE}(0)|^2 \approx 1$ . For large  $E_s/N_0$ ,  $MSE_{\min,LE}$  approaches  $1/SNR_{ZF-LE}$ ; in this case, the largest contribution comes from the Gaussian noise at the equalizer output.
- The ratios  $SNR_{ZF-LE}/SNR_{MF}$  and  $SINR_{MMSE-LE}/SNR_{MF}$  illustrate the noise enhancement (see Fig. 6-22). The ratio  $SNR_{ZF-LE}/SNR_{MF}$  does not depend on  $E_s/N_0$ , and amounts to -4.7 dB for the considered channel. The ratio  $SINR_{MMSE-LE}/SNR_{MF}$  is a decreasing function of  $E_s/N_0$ , evolving from 1 (for  $E_s/N_0 \ll 1$ ) to  $SNR_{ZF-LE}/SNR_{MF}$  (for  $E_s/N_0 \gg 1$ ).
- Fig. 6-23 shows the BER corresponding to the matched filter bound, the ZF-LE and the MMSE-LE. As compared to the matched filter bound, the performance of the ZF-LE is degraded by 4.7 dB (which corresponds to the ratio  $SNR_{ZF-LE}/SNR_{MF}$ ). As  $SINR_{MMSE-LE}$  is larger than  $SNR_{ZF-LE}$ , the MMSE-LE performs better than the ZF-LE.

Now we consider the case

$$G(z) = (1.81^{-1}) \cdot (1 + 0.9z^{-1}) \cdot (1 + 0.9z) = 0.497z + 1 + 0.497z^{-1}. \quad (6.6.3-5)$$

For this channel, we have  $g(0) = 1$ ,  $G_{\max} = 1.994$  and  $G_{\min} = 5.5 \cdot 10^{-3}$ ; observe that  $G_{\min}$  is substantially smaller than for the previously considered channel. In Fig. 6-24, we show the

BER corresponding to the matched filter bound, the ZF-LE and the MMSE-LE. As compared to the matched filter bound, the BER performance of the ZF-LE is degraded by 9.79 dB, and the performance of the MMSE-LE is between the matched filter bound and the ZF-LE. Comparing to Fig. 6-23, we observe that a smaller value of  $G_{\min}$  gives rise to a larger degradation of the BER resulting from ZF-LE and MMSE-LE, but that the advantage of the MMSE-LE as compared to the ZF-LE is larger when  $G_{\min}$  gets smaller.

## 6.7. Decision-feedback equalization

We have seen that the linear equalizer may give rise to a considerable noise enhancement, as a side-effect of the elimination (or substantial reduction) of the ISI. In the case of a decision feedback equalizer (DFE), the matched filter output samples are applied to a feedforward equalizer filter that reduces only the *precursor* ISI, that is caused by future symbols; the *postcursor* ISI, caused by past symbols, is cancelled by subtracting from the output of the feedforward equalizer a linear combination of past symbol decisions. As the feedforward equalizer reduces only precursor ISI and the cancellation of postcursor ISI does not affect the noise level, the DFE yields less noise enhancement than the linear equalizer.

The structure of the DFE is shown in Fig. 6-25. The transfer function of the forward filter is denoted  $H_{FF}(z)$ . The transfer function of the feedback filter is

$$H_{FB}(z) = \sum_{m>0} h_{FB}(m)z^{-m} \quad (6.7.0-1)$$

Note that the summation interval in (6.7.0-1) is restricted to  $m>0$ , because for reasons of causality only *past* symbol decisions can be fed back. Taking into account the model of the matched filter output samples  $z(k)$  from Fig. 6-2, and assuming that the past symbol decisions are correct, the discrete-time model describing the DFE output  $u(k)$  is given in Fig. 6-26, with

$$G_{DFE}(z) = G'_{DFE}(z) - H_{FB}(z) \quad (6.7.0-2)$$

and

$$G'_{DFE}(z) = G(z)H_{FF}(z) \quad (6.7.0-3)$$

The power spectrum  $S_n(\exp(j2\pi fT))$  of the noise  $n'(k)$  at the output of the forward filter is given by

$$S_n(\exp(j2\pi fT)) = N_0 G(\exp(j2\pi fT)) |H_{FF}(\exp(j2\pi fT))|^2 \quad (6.7.0-4)$$

Let us denote by  $g'_{DFE}(m)$  and  $g_{DFE}(m)$  the IDTFT of  $G'_{DFE}(\exp(j2\pi fT))$  and  $G_{DFE}(\exp(j2\pi fT))$ ; it follows from (6.7.0-2) that  $g'_{DFE}(m)$  and  $g_{DFE}(m)$  are related by

$$g_{DFE}(m) = \begin{cases} g'_{DFE}(m) & m \leq 0 \\ g'_{DFE}(m) - h_{FB}(m) & m > 0 \end{cases} \quad (6.7.0-5)$$

Hence, according to Fig. 6-26 we obtain

$$\begin{aligned}
 u(k) &= a(k)g_{\text{DFE}}(0) + \sum_{m \neq 0} a(k-m)g_{\text{DFE}}(m) + n'(k) \\
 &= \underbrace{a(k)g'_{\text{DFE}}(0)}_{\text{useful}} + \underbrace{\sum_{m < 0} a(k-m)g'_{\text{DFE}}(m)}_{\text{precursor ISI}} + \underbrace{\sum_{m > 0} a(k-m)(g'_{\text{DFE}}(m) - h_{\text{FB}}(m))}_{\text{postcursor ISI}} + \underbrace{n'(k)}_{\text{noise}} \quad (6.7.0-6)
 \end{aligned}$$

From (6.7.0-6), we define the normalized MSE and the SINR of the DFE as follows :

$$\begin{aligned}
 \text{MSE}_{\text{DFE}} &= \frac{E[|u(k) - a(k)|^2]}{E_s} \\
 &= |g'_{\text{DFE}}(0) - 1|^2 + \sum_{m < 0} |g'_{\text{DFE}}(m)|^2 + \sum_{m > 0} |g'_{\text{DFE}}(m) - h_{\text{FB}}(m)|^2 + \frac{E[|n'(k)|^2]}{E_s} \quad (6.7.0-7)
 \end{aligned}$$

$$\text{SINR}_{\text{DFE}} = \frac{|g'_{\text{DFE}}(0)|^2}{\sum_{m < 0} |g'_{\text{DFE}}(m)|^2 + \sum_{m > 0} |g'_{\text{DFE}}(m) - h_{\text{FB}}(m)|^2 + \frac{E[|n'(k)|^2]}{E_s}} \quad (6.7.0-8)$$

where  $E[|n'(k)|^2] = \langle S_n(\cdot) \rangle_f$ , with  $S_n(\cdot)$  given by (6.7.0-4). The SINR is upper bounded by the SNR :

$$\text{SINR}_{\text{DFE}} \leq \text{SNR}_{\text{DFE}} = \frac{E_s |g'_{\text{DFE}}(0)|^2}{E[|n'(k)|^2]} \quad (6.7.0-9)$$

$\text{SNR}_{\text{DFE}}$  is upper bounded by  $\text{SNR}_{\text{MF}}$  from (6.6.1-5).

We observe from (6.7.0-6) that the postcursor ISI at the output of the feedforward filter can be cancelled by selecting  $h_{\text{FB}}(m) = g'_{\text{DFE}}(m)$  for  $m > 0$ . This yields :

$$\text{MSE}_{\text{DFE}} = |g'_{\text{DFE}}(0) - 1|^2 + \sum_{m < 0} |g'_{\text{DFE}}(m)|^2 + \frac{E[|n'(k)|^2]}{E_s} \quad (6.7.0-10)$$

$$\text{SINR}_{\text{DFE}} = \frac{|g'_{\text{DFE}}(0)|^2}{\sum_{m < 0} |g'_{\text{DFE}}(m)|^2 + \frac{E[|n'(k)|^2]}{E_s}} \quad (6.7.0-11)$$

Moreover, as the spectrum of  $n'(k)$  is not affected by  $\{h_{\text{FB}}(m)\}$  (see (6.7.0-4)), the elimination of postcursor ISI does not give rise to noise enhancement.

When we select  $h_{\text{FB}}(m) = 0$  for  $m > 0$ , the DFE reduces to the linear equalizer. Hence, when the DFE is optimized over  $\{h_{\text{FB}}(m)\}$  the resulting performance cannot be worse than with the linear equalizer.

### 6.7.1 Zero-forcing decision-feedback equalizer

In the case of the zero-forcing DFE (ZF-DFE), the feedforward and feedback filters are selected such that  $g_{\text{DFE}}(m) = \delta(m)$  (meaning that all precursor and postcursor ISI is eliminated) and the noise variance at the output of the feedforward filter is minimum.

For given  $H_{\text{FB}}(z)$ , it follows from (6.7.0-2) and (6.7.0-3) that the condition  $g_{\text{DFE}}(m) = \delta(m)$  (or, equivalently,  $G_{\text{DFE}}(z) = 1$ ) is achieved by selecting

$$H_{\text{FF}}(z) = \frac{1}{G(z)} (1 + H_{\text{FB}}(z)) \quad (\text{ZF-DFE}) \quad (6.7.1-1)$$

Hence, the feedforward filter can be interpreted as the cascade of the ZF-LE filter  $1/G(z)$  that eliminates all ISI, and a causal filter that is selected to reduce the noise variance but inevitably introduces postcursor ISI. The postcursor ISI is eliminated by the feedback filter  $H_{\text{FB}}(z)$ , so that the benefit of the ZF-DFE over the ZF-LE is a reduced noise variance.

Now we select  $H_{\text{FB}}(z) = H_{\text{ZF-FB}}(z)$  such that the noise variance at the feedforward filter output is *minimized*. The solution follows from section 6.11.2 :  $1 + H_{\text{ZF-FB}}(z)$  is the monic causal and stable filter that whitens the noise  $n'(k)$  at the output of the feedforward filter. Let us consider the factorization (6.2-10) :

$$G(z) = A^2 F_+(z) F_-(z) \quad (6.7.1-2)$$

Now we select

$$1 + H_{\text{ZF-FB}}(z) = F_+(z) \quad (\text{ZF-DFE}) \quad (6.7.1-3)$$

which yields  $H_{\text{FF}}(z) = H_{\text{ZF-FF}}(z)$ , with

$$H_{\text{ZF-FF}}(z) = \frac{F_+(z)}{G(z)} = \frac{1}{A^2 F_-(z)} \quad (6.7.1-4)$$

indicating that the feedforward filter is anti-causal. Note that the feedforward filter  $H_{\text{ZF-DFE}}(z)$  is the same as the noise-whitening filter introduced in section 6.2. The resulting noise spectrum is

$$\begin{aligned} S_{n'}(\exp(j2\pi fT)) &= \frac{N_0 |1 + H_{\text{ZF-FB}}(\exp(j2\pi fT))|^2}{G(\exp(j2\pi fT))} \\ &= \frac{N_0 |F_+(\exp(j2\pi fT))|^2}{A^2 |F_+(\exp(j2\pi fT))|^2} \\ &= \frac{N_0}{A^2} \end{aligned} \quad (6.7.1-5)$$

which indicates that the noise at the output of the feedforward filter is white. This yields the model shown in Fig. 6-27.

The SNR at the input of the symbol-by symbol detector is given by

$$\text{SNR}_{\text{ZF-DFE}} = \frac{1}{\text{MSE}_{\text{ZF-DFE}}} = \frac{E_s}{N_0} A^2 \quad (6.7.1-6)$$

According to (6.11.2-12),  $\text{SNR}_{\text{ZF-DFE}}$  can be expressed directly in terms of  $G(z)$  :

$$\text{SNR}_{\text{ZF-DFE}} = \frac{E_s}{N_0} \exp(\langle \ln G(\cdot) \rangle_f) \quad (6.7.1-7)$$

Taking into account that

$$\text{SNR}_{\text{MF}} = \frac{E_s}{N_0} g(0) = \frac{E_s}{N_0} A^2 \left( 1 + \sum_{m>0} |f_+(m)|^2 \right) \quad (6.7.1-8)$$

it follows that  $\text{SNR}_{\text{MF}} \geq \text{SNR}_{\text{ZF-DFE}}$ , so that the ZF-DFE performance is degraded as compared to the matched filter bound. Comparing (6.7.1-6) and (6.7.1-8), we see that the ZF-DFE exploits only the energy of the signal component  $a(k)f_+(0) = a(k)$ , whereas the matched filter bound takes the energy of all components  $a(k)f_+(m)$  into account. The noise enhancement of the ZF-DFE as compared to the matched filter bound amounts to  $10 \cdot \log \left( 1 + \sum_{m>0} |f_+(m)|^2 \right)$  (in dB). The BER resulting from the ZF-DFE is  $\text{BER} = \text{BER}_C(\text{SNR}_{\text{ZF-DFE}})$

The ZF-DFE can also be applied to the samples (at rate  $1/T$ ) at the output of a continuous-time filter that is different from the matched filter. However, unless these samples are a sufficient statistic, the resulting performance is worse. Therefore, the ZF-DFE preceded by the matched filter is called the *optimum* ZF-DFE.

### Example

We consider again  $G(z)$  given by (6.6.1-8) with  $|\gamma| < 1$ . We have  $F_+(z) = 1 + \gamma z^{-1}$ ,  $A^2 = 1$  and  $g(0) = 1 + |\gamma|^2$ . Hence, the degradation of the ZF-DFE as compared to the matched filter bound is  $10 \cdot \log(1 + |\gamma|^2)$  dB; as  $|\gamma| < 1$ , this degradation is limited to 3 dB. Recall that in the case of the ZF-LE, the degradation is  $10 \cdot \log((1 + |\gamma|^2)/(1 - |\gamma|^2))$ , which becomes infinitely large when  $|\gamma|$  approaches 1. This illustrates the advantage of the ZF-DFE over the ZF-LE.

### 6.7.2 Minimum mean-square error decision-feedback equalizer

In general, the feedforward and feedback filters must have an infinite number of coefficients in order to eliminate all ISI. Hence the ZF criterion is not appropriate when the filters have only a finite number of coefficients, as is always the case in practice. In this case, a minimum mean-square error criterion is more convenient to determine the filter coefficients.

The feedforward and feedback filters of the minimum mean-square error DFE (MMSE-DFE) are selected such that the (normalized) mean-square error  $MSE_{DFE}$  is minimized. Fig. 6-28 indicates how  $\epsilon(k) = u(k) - a(k)$  is obtained in terms of  $a(k)$  and  $n(k)$ ; recall from (6.7.0-2) and (6.7.0-3) that  $G_{DFE}(z) - 1 = G(z)H_{FF}(z) - (1 + H_{FB}(z))$ .

The MSE to be minimized is given w.r.t.  $H_{FF}(z)$  and  $H_{FB}(z)$  is given by

$$MSE = \frac{E[|\epsilon(k)|^2]}{E_s} = \left\langle |G(.)H_{FF}(.) - (1 + H_{FB}(.))|^2 + \mu G(.)|H_{FF}(.)|^2 \right\rangle_f \quad (6.7.2-1)$$

where  $\mu = N_0/E_s$ . First, we minimize MSE w.r.t.  $H_{FF}(z)$  for given  $H_{FB}(z)$ ; using a similar approach as for the MMSE-LE, we obtain

$$H_{FF}(z) = \frac{1 + H_{FB}(z)}{G(z) + \mu} \quad (6.7.2-2)$$

Substituting (6.7.2-2) into (6.7.2-1) yields

$$MSE = \frac{E[|\epsilon(k)|^2]}{E_s} = \left\langle \frac{\mu}{G(.) + \mu} \cdot |1 + H_{FB}(.)|^2 \right\rangle_f \quad (6.7.2-3)$$

which is still to be minimized w.r.t.  $H_{FB}(z)$ . As  $1 + H_{FB}(z)$  is a monic causal filter, MSE from (6.7.2-3) is minimized when  $1 + H_{FB}(z)$  whitens the spectrum  $\mu/(G(z) + \mu)$ . Considering the following spectral decomposition

$$G(z) + \frac{N_0}{E_s} = B^2 F'_+(z) F'_-(z) \quad (6.7.2-4)$$

the MSE is minimized when  $H_{FB}(z) = H_{MMSE-FB}(z)$ , with

$$1 + H_{MMSE-FB}(z) = F'_+(z) \quad (\text{MMSE-DFE}) \quad (6.7.2-5)$$

The corresponding minimum value of the MSE is given by

$$MSE_{\min, DFE} = \frac{N_0}{E_s} \cdot \frac{1}{B^2} \quad (6.7.2-6)$$

According to (6.11.2-12),  $MSE_{\min, DFE}$  can be expressed directly in terms of  $G(z)$  :

$$MSE_{\min-DFE} = \frac{N_0}{E_s} \exp \left( - \left\langle \ln \left( G(.) + \frac{N_0}{E_s} \right) \right\rangle_f \right) \quad (6.7.2-7)$$



Using (6.7.2-2) and (6.7.2-5), the forward filter  $H_{FF}(z)$  reduces to  $H_{FF}(z) = H_{MMSE-FF}(z)$ , with

$$H_{MMSE-FF}(z) = \frac{F'_+(z)}{G(z) + \mu} = \frac{1}{B^2 F'_-(z)} \quad (6.7.2-8)$$

which is anti-causal. This yields  $G'_{DFE}(z) = G'_{MMSE-DFE}(z)$ , with

$$\begin{aligned} G'_{MMSE-DFE}(z) &= G(z)H_{MMSE-FF}(z) \\ &= ((G(z) + \mu) - \mu) \frac{1}{B^2 F'_-(z)} \\ &= F'_+(z) - \frac{\mu}{B^2 F'_-(z)} \end{aligned} \quad (6.7.2-9)$$

Finally, we get  $G_{DFE}(z) = G_{MMSE-DFE}(z)$ , with

$$\begin{aligned} G_{MMSE-DFE}(z) &= G'_{MMSE-DFE}(z) - H_{MMSE-FB}(z) \\ &= \left( F'_+(z) - \frac{\mu}{B^2 F'_-(z)} \right) - (1 - F'_+(z)) \\ &= 1 - \frac{\mu}{B^2 F'_-(z)} \end{aligned} \quad (6.7.2-10)$$

As  $1/F'_-(z)$  is monic and anti-causal,  $G_{MMSE-DFE}(z)$  is anti-causal too, which indicates that the residual ISI at the output of the equalizer is precursor ISI; this is not surprising, as all postcursor ISI is cancelled by the feedback filter.

Now we will relate  $SINR_{MMSE-DFE}$  to  $MSE_{min,DFE}$ , and present an approximation of the BER resulting from the MMSE-DFE. As the coefficient  $g_{MMSE-DFE}(0)$  of the useful component at output of the equalizer is obtained as the coefficient of  $z^0$  in  $G_{MMSE-DFE}(z)$ , we get from (6.7.2-10) :

$$g_{MMSE-DFE}(0) = 1 - \frac{N_0}{E_s} \cdot \frac{1}{B^2} = 1 - MSE_{min,DFE} \quad (6.7.2-11)$$

Substituting (6.7.2-11) in (6.7.0-10) and (6.7.0.11), with  $G_{DFE}(z) = G_{MMSE-DFE}(z)$ , yields

$$MSE_{min,DFE} = MSE_{min,DFE}^2 + \sum_{m<0} |g_{MMSE-DFE}(m)|^2 + \frac{E[|n'(k)|^2]}{E_s} \quad (6.7.2-12)$$

$$SINR_{MMSE-DFE} = \frac{(1 - MSE_{min,DFE})^2}{\sum_{m<0} |g_{MMSE-DFE}(m)|^2 + \frac{E[|n'(k)|^2]}{E_s}} \quad (6.7.2-13)$$

Consequently,  $SINR_{MMSE-DFE}$  is obtained as

$$SINR_{MMSE-DFE} = \frac{1 - MSE_{min,DFE}}{MSE_{min,DFE}} \quad (6.7.2-14)$$

Using a similar reasoning as for the MMSE-LE, the BER resulting from the MMSE-DFE will be approximated as  $\text{BER} \approx \text{BER}_C(\text{SINR}_{\text{MMSE-DFE}})$ .

The MMSE-DFE can also be applied to the samples (at rate  $1/T$ ) at the output of a continuous-time filter that is different from the matched filter. However, unless these samples are a sufficient statistic, the resulting performance is worse. Therefore, the MMSE-DFE preceded by the matched filter is called the *optimum* MMSE-DFE.

### 6.7.3 Comparison of ZF-DFE and MMSE-DFE

Comparing (6.7.2-10) and (6.7.1-7), we obtain

$$\text{MSE}_{\text{min,DFE}} < \text{MSE}_{\text{ZF-DFE}} = \frac{1}{\text{SNR}_{\text{ZF-DFE}}} \quad (6.7.3-1)$$

which indicates that  $E[|\epsilon(k)|^2]$  is smaller for the MMSE-DFE than for the ZF-DFE. This is no surprise, as the MMSE-DFE has been designed to minimize  $E[|\epsilon(k)|^2]$ .

As with the linear equalizer, we distinguish between different operating regions.

- The condition  $N_0/E_s \gg G_{\text{max}}$ , corresponds to the region of very low SNR. In this region, we have  $G(z) + N_0/E_s \approx N_0/E_s$ , so that  $F'_+(z) \approx F'_-(z) \approx 1$ ,  $B^2 \approx N_0/E_s$ ,  $H_{\text{FF-MMSE}}(z) \approx E_s/N_0$ ,  $H_{\text{FB-MMSE}} \approx 1$ . The equalizer output  $u(k)$  is essentially proportional to the matched filter output  $z(k)$  : as the noise at the matched filter output is much larger than the ISI, the equalizer mainly avoids noise enhancement. We obtain

$$\text{SINR}_{\text{MMSE-DFE}} \approx \frac{E_s}{N_0} g(0) = \text{SNR}_{\text{MF}} \ll 1 \quad (6.7.3-2)$$

This operating region is not of practical interest, as the very low SNR gives rise to a large BER.

- The condition  $N_0/E_s \ll G_{\text{min}}$  corresponds to the region of very high SNR. In this region, we have  $G(z) + N_0/E_s \approx G(z)$ , so that the MMSE-DFE behaves essentially as a ZF-DFE : as the noise at the matched filter output is much smaller than the ISI, the equalizer mainly combats the ISI. We obtain  $\text{SINR}_{\text{MMSE-DFE}} \approx \text{SNR}_{\text{ZF-DFE}}$ .
- When not operating in the regions of very low or very high SNR, the MMSE-DFE makes a compromise between reducing the ISI and keeping the noise enhancement small. By allowing a small residual ISI, the BER performance is better than with the ZF-DFE.

**Example**

We illustrate the above results considering a dispersive channel with  $G(z)$  given by (6.6.3-5). For this channel, we have  $g(0) = 1$ ,  $G_{\max} = 1.994$  and  $G_{\min} = 5.5 \cdot 10^{-3}$ .

- In Fig. 6-29, we compare the different contributions to  $\text{MSE}_{\min, \text{DFE}}$ . For small  $E_s/N_0$ , the MMSE-DFE strongly attenuates the matched filter output samples, yielding  $|u(k)| \ll |a(k)|$  and  $\text{MSE}_{\min, \text{DFE}} = E[|u(k) - a(k)|^2]/E_s \approx E[|a(k)|^2]/E_s = 1$ ; in this case, the main contribution to  $\text{MSE}_{\min, \text{DFE}}$  comes from  $|1 - g_{\text{MMSE-LE}}(0)|^2 \approx 1$ . For large  $E_s/N_0$ ,  $\text{MSE}_{\min, \text{DFE}}$  approaches  $1/\text{SNR}_{\text{ZF-DFE}}$ ; in this case, the largest contribution comes from the Gaussian noise at the equalizer output.
- The ratios  $\text{SNR}_{\text{ZF-DFE}}/\text{SNR}_{\text{MF}}$  and  $\text{SINR}_{\text{MMSE-DFE}}/\text{SNR}_{\text{MF}}$  are displayed in Fig. 6-30. The ratio  $\text{SNR}_{\text{ZF-DFE}}/\text{SNR}_{\text{MF}}$  does not depend on  $E_s/N_0$ , and amounts to -2.6 dB for the considered channel. The ratio  $\text{SINR}_{\text{MMSE-DFE}}/\text{SNR}_{\text{MF}}$  is a decreasing function of  $E_s/N_0$ , evolving from 1 (for  $E_s/N_0 \ll 1$ ) to  $\text{SNR}_{\text{ZF-DFE}}/\text{SNR}_{\text{MF}}$  (for  $E_s/N_0 \gg 1$ ).
- Fig. 6-31 shows the BER corresponding to the matched filter bound, the ZF-DFE and the MMSE-DFE. As compared to the matched filter bound, the performance of the ZF-DFE is degraded by 2.6 dB (which corresponds to the ratio  $\text{SNR}_{\text{ZF-DFE}}/\text{SNR}_{\text{MF}}$ ). As  $\text{SINR}_{\text{MMSE-DFE}}$  is larger than  $\text{SNR}_{\text{ZF-DFE}}$ , the MMSE-DFE performs better than the ZF-DFE.

## 6.8. Comparison between LE and DFE performance

Here we compare the DFE and the LE in terms of BER performance. Fig. 6-32 collects the BER results for the channel determined by (6.6.3-5). As compared to the LE, we observe that the DFE yields a substantially smaller noise enhancement; this is because the feedforward filter of the DFE has to reduce only the precursor ISI (the feedback filter of the DFE removes the postcursor ISI without additional noise enhancement), whereas the filter of the LE has to reduce both the precursor ISI and the postcursor ISI. It can be verified that, for the considered channel, the ML sequence detector yields a BER that is very close to the matched filter bound, because the smallest Euclidean distance is achieved for an error event with  $e(k) = e(0)\delta(k)$  (see section 6.5).

Till now we have assumed that the symbol decisions, that are used to cancel the precursor ISI, are correct. However, in practice occasional decision errors occur because of the noise, in which case part of the postcursor ISI is not cancelled. Let us consider the case where the constellation is  $\{-1, 1\}$  and the symbol  $a(k)$  is to be detected : when a decision error has occurred at instant  $k-m$ , the ISI component  $a(k-m)g_{DFE}(m)$  in the DFE output  $u(k)$  is not reduced to zero but is increased to  $2a(k-m)g_{DFE}(m)$ , which increases the probability of a decision error for the symbol  $a(k)$ . This mechanism can give rise to *error propagation* : a decision error gives rise to an increase of the postcursor ISI, which in turn gives rise to more symbol errors. Because of error propagation, the BER resulting from the DFE is somewhat worse than the BER that is obtained under the assumption that the correct symbols are applied to the feedback filter. However, even in the presence of error propagation, the DFE still performs better than the LE on strongly dispersive channels.

## 6.9. Finite-complexity equalizers

We have pointed out that practical filters have a finite number of coefficients, and therefore in general cannot totally eliminate the ISI that affects the matched filter output samples. Hence, for designing practical equalizers a minimum mean-square error criterion is more convenient than a zero-forcing criterion. In sections 6.7.2 and 6.8.2 we have considered the equalization filters that minimize the mean-square error, both for the LE and the DFE. These optimum filters again have in general an infinite number of coefficients. Consequently, the resulting minimum mean-square error is a lower bound on the mean-square error that can be achieved with filters that have a finite number of coefficients.

The continuous-time matched filter and the discrete-time filter(s) of the (linear or decision-feedback) equalizer all depend on the channel transfer function, and therefore must be made adjustable : when the channel transfer function changes, the filters must be modified accordingly. While adjusting a discrete-time filter is easily achieved by changing its coefficient values, a controlled modification of the transfer function of a continuous-time filter is a much more difficult task. In practice this problem is circumvented by applying the received signal  $r(t)$  to a *fixed* (rather than adjustable) continuous-time *anti-aliasing* filter that does not distort the useful signal component, and approximating the cascade of the continuous-time matched filter and the discrete-time equalizer filter (LE) or feedforward filter (DFE) as a discrete-time filter with a finite number of coefficients, that operates at a multiple of the symbol rate. The resulting discrete-time filter is called a *fractionally spaced* (as opposed to symbol-spaced) equalizer. When the channel transfer function changes, the coefficients of the discrete-time fractionally spaced equalizer are adjusted accordingly, but the continuous-time anti-aliasing filter is unaltered.

In order to explain the operation of the fractionally spaced equalizer, we first consider the DFE equalizer from Fig. 6-25; results for a LE are obtained by simply removing the feedback filter. As indicated in Fig. 6-33, the matched filter  $H^*(f) = H_{tr}^*(f)H_{ch}^*(f)$  and the feedforward filter  $H_{FF}(z)$  of the DFE can be combined into a single continuous-time filter  $H_{rec}(f)$ , with

$$H_{rec}(f) = H^*(f)H_{FF}(\exp(j2\pi fT)) = H^*(f) \sum_m h_{FF}(m) \exp(-j2\pi mfT) \quad (6.9-1)$$

Indeed, sampling the output of the filter  $H_{rec}(f)$  at instants  $kT$  yields

$$\int R(f)H_{rec}(f)e^{j2\pi kfT}df = \sum_m h_{FF}(m) \underbrace{\int R(f)H^*(f)e^{j2\pi(k-m)fT}df}_{z(k-m)} = u'(k) \quad (6.9-2)$$

Now we assume that  $H_{tr}(f) = 0$  for  $|f| > B$ ; consequently,  $H_{rec}(f) = 0$  for  $|f| > B$ . Hence, according to section 1.7.2, applying  $r(t)$  to the filter  $H_{rec}(f)$  and sampling the filter output at instants  $kT$  is equivalent to applying  $r(t)$  to an anti-aliasing filter  $H_{AA}(f)$ , sampling the filter output at a rate  $1/T_s = N_s/T$ , applying these samples to a discrete-time filter (i.e., the fractionally spaced equalizer) with impulse response  $h_{eq}(i) = T_s h_{rec}(iT_s)$ , and downsampling the equalizer output by a factor  $N_s$  to obtain the sequence  $\{u'(k)\}$  at a rate  $1/T$  (see Fig. 6-33) :

$$u'(k) = \sum_i h_{eq}(i) r(kN_s - i) \quad (6.9-3)$$

The anti-aliasing filter satisfies the condition  $H_{AA}(f) = 1$  for  $|f| < B$  and  $H_{AA}(f) = 0$  for  $|f| > B_{AA}$ , with  $B_{AA} > B$ ; the sampling rate  $1/T_s$  must be selected such that  $1/T_s > B + B_{AA}$ .

Considering the above, we arrive at the fractionally spaced DFE from Fig. 6-34. In a practical situation, there are only a *finite* number of feedforward coefficients  $h_{eq}(i)$  and feedback coefficients  $h_{FB}(i)$ . These coefficients will be selected such that  $MSE = E[|\varepsilon(k)|^2]/E_s$  is minimized, with  $\varepsilon(k) = u(k) - a(k)$ . We consider the case where the forward filter has  $K_{FF1} + 1 + K_{FF2}$  coefficients  $h_{eq}(i)$  with  $i = -K_{FF1}, \dots, K_{FF2}$ , and the feedback filter has  $K_{FB}$  feedback coefficients  $h_{FB}(m)$  with  $m = 1, \dots, K_{FB}$ . The samples at the output of the anti-aliasing filter are given by

$$r(i) = \sum_m a(m) h(iT_s - mT) + n_{AA}(i) \quad (6.9-4)$$

As  $H_{AA}(f) = 1$  for  $|f| < B$ ,  $h(t)$  is the pulse at the receiver input ( $H(f) = H_{tr}(f)H_{ch}(f)$ ). Further,  $\{n_{AA}(i)\} \sim N_c(0, N_0 R_{AA}(m))$ , with

$$R_{AA}(n) = \int |H_{AA}(f)|^2 \exp(j2\pi f n T_s) df \quad (6.9-5)$$

The spectrum of  $n_{AA}(i)$  is white over  $(-B, B)$ . The input  $u(k)$  to the symbol-by-symbol detector is

$$u(k) = \sum_{i=-K_{FF1}}^{K_{FF2}} h_{eq}(i) r(kN_s - i) - \sum_{m=1}^{K_{FB}} h_{FB}(m) \hat{a}(k - m) \quad (6.9-6)$$

Substituting (6.9-4) in (6.9-6) and assuming that the past decisions are correct, we obtain

$$u(k) = a(k) g'_{eq}(0) + \sum_{m \notin (0, K_{FB})} a(k - m) g'_{eq}(m) + \sum_{m=1}^{K_{FB}} a(k - m) (g'_{eq}(m) - h_{FB}(m)) + n'(k) \quad (6.9-7)$$

which has a similar structure as (6.7.0-6). In (6.9-7),  $g'_{eq}(m)$  and  $n'(k)$  are given by

$$g'_{eq}(m) = \sum_{i=-K_{FF1}}^{K_{FF2}} h_{eq}(i) h(mT - iT_s) \quad (6.9-8)$$

$$n'(k) = \sum_{i=-K_{FF1}}^{K_{FF2}} h_{eq}(i) n_{AA}(kN_s - i) \quad (6.9-9)$$

The resulting MSE is obtained as

$$\text{MSE} = |1 - g'_{\text{eq}}(0)|^2 + \sum_{m \notin (0, K_{\text{FB}})} |g'_{\text{eq}}(m)|^2 + \sum_{m=1}^{K_{\text{FB}}} |g'_{\text{eq}}(m) - h_{\text{FB}}(m)|^2 + E[|n'(k)|^2] \quad (6.9-10)$$

where

$$E[|n'(k)|^2] = \mu \sum_{i, i'=-K_{\text{FF1}}}^{K_{\text{FF2}}} h_{\text{eq}}^*(i) R_{\text{AA}}(i-i') h_{\text{eq}}(i') \quad (6.9-11)$$

with  $\mu = N_0/E_s$ . When minimizing MSE over  $\{h_{\text{FB}}(m)\}$ , it is obvious that the solution is  $h_{\text{FB}}(m) = g'_{\text{eq}}(m)$ , so that the second summation in (6.9-10) becomes zero : this eliminates the ISI caused by the symbols  $(a(k-1), \dots, a(k-K_{\text{FB}}))$ . The resulting MSE, given by

$$\begin{aligned} \text{MSE} &= |1 - g'_{\text{eq}}(0)|^2 + \sum_{m \notin (0, K_{\text{FB}})} |g'_{\text{eq}}(m)|^2 + \mu \sum_{i, i'=-K_{\text{FF1}}}^{K_{\text{FF2}}} h_{\text{eq}}^*(i) R_{\text{AA}}(i-i') h_{\text{eq}}(i') \\ &= \sum_{m \notin (1, K_{\text{FB}})} |g'_{\text{eq}}(m)|^2 - g'_{\text{eq}}(0) - g_{\text{eq}}^*(0) + \mu \sum_{i, i'=-K_{\text{FF1}}}^{K_{\text{FF2}}} h_{\text{eq}}^*(i) R_{\text{AA}}(i-i') h_{\text{eq}}(i') + 1 \end{aligned} \quad (6.9-12)$$

must now be minimized over  $\{h_{\text{eq}}(i), i = -K_{\text{FF1}}, \dots, K_{\text{FF2}}\}$ .

Introducing the vectors  $\mathbf{h}_{\text{eq}} = (h_{\text{eq}}(-K_{\text{FF1}}), \dots, h_{\text{eq}}(K_{\text{FF2}}))^T$  and  $\mathbf{h}_m = (h(mT + K_{\text{FF1}}T_s), \dots, h(mT - K_{\text{FF2}}T_s))^T$ , (6.9-8) is reduced to  $g'_{\text{eq}}(m) = \mathbf{h}_{\text{eq}}^T \mathbf{h}_m = \mathbf{h}_m^T \mathbf{h}_{\text{eq}}$ . Hence, (6.9-12) can be transformed into

$$\begin{aligned} \text{MSE} &= \mathbf{h}_{\text{eq}}^H \mathbf{M} \mathbf{h}_{\text{eq}} - \mathbf{h}_{\text{eq}}^H \mathbf{h}_0^* - \mathbf{h}_0^T \mathbf{h}_{\text{eq}} + 1 \\ &= (\mathbf{h}_{\text{eq}} - \mathbf{h}_{\text{eq, opt}})^H \mathbf{M} (\mathbf{h}_{\text{eq}} - \mathbf{h}_{\text{eq, opt}}) + (1 - \mathbf{h}_{\text{eq, opt}}^H \mathbf{M} \mathbf{h}_{\text{eq, opt}}) \end{aligned} \quad (6.9-13)$$

where  $\mathbf{M}$  is a positive semi-definite Hermitian matrix, given by

$$\mathbf{M} = \mu \mathbf{R}_{\text{AA}} + \sum_{m \notin (1, K_{\text{FB}})} \mathbf{h}_m^* \mathbf{h}_m^T \quad (6.9-14)$$

As  $h(t)$  is essentially time-limited in practice, the sum in (6.9-14) contains only a finite number of terms. Identification of the first and second line of (6.9-13) yields

$$\mathbf{M} \mathbf{h}_{\text{eq, opt}} = \mathbf{h}_0^* \Leftrightarrow \mathbf{h}_{\text{eq, opt}} = \mathbf{M}^{-1} \mathbf{h}_0^* \quad (6.9-15)$$

As  $\mathbf{M}$  is a positive definite matrix, MSE becomes minimum when  $\mathbf{h}_{\text{eq}} = \mathbf{h}_{\text{eq, opt}}$ ; the resulting minimum value  $\text{MSE}_{\min}$  is given by

$$\text{MSE}_{\min} = 1 - \mathbf{h}_{\text{eq, opt}}^H \mathbf{M} \mathbf{h}_{\text{eq, opt}} = 1 - (\mathbf{M} \mathbf{h}_{\text{eq, opt}})^H \mathbf{h}_{\text{eq, opt}} = 1 - \mathbf{h}_0^T \mathbf{h}_{\text{eq, opt}} = 1 - g'_{\text{eq, opt}}(0) \quad (6.9-16)$$

Finally, using a similar reasoning as for the MMSE-LE and MMSE-DFE, it can be verified that for the optimized finite-complexity equalizer we obtain

$$\text{SINR} = \frac{1 - \text{MSE}_{\min}}{\text{MSE}_{\min}} \quad (6.9-17)$$

and the associated BER is approximated as  $\text{BER} \approx \text{BER}_C(\text{SINR})$ .

**Example**

We consider the case where the transmit pulse is a square-root cosine rolloff pulse with a 50% excess bandwidth; as  $B = 3/(4T) < 1/T$ , we select  $N_s = 2$  : the equalizer operates at twice the symbol rate ( $1/T_s = 2/T$ ). The channel transfer function  $H_{ch}(f)$  is given by

$$H_{ch}(f) = h_{ch}(0) + h_{ch}(1)\exp(-j2\pi fT) \quad (6.9-18)$$

with  $h_{ch}(0) = 1/(1.49^{1/2})$  and  $h_{ch}(1) = 0.7/(1.49^{1/2})$ , so that  $(h_{ch}(0))^2 + (h_{ch}(1))^2 = 1$ . The anti-aliasing filter  $H_{AA}(f)$  is an ideal lowpass filter that suppresses all frequencies  $f$  with  $|f| > N_s/(2T)$ . This yields  $\{n_{AA}(i)\} \sim N_c(0, (N_0/T_s)\delta(m))$ . Fig. 6-35 shows the resulting MSE, corresponding to various combinations of  $K_{FF1}$ ,  $K_{FF2}$  and  $K_{FB}$ . When  $K_{FB} = 0$  and both  $K_{FF1}$  and  $K_{FF2}$  increase, the MSE converges to  $MSE_{min,LE}$  of the MMSE-LE, derived in section 6.7-2; in order to get close to this asymptote, we need  $K_{FF1} = 1$  and  $K_{FF2} = 15$ , in which case the linear equalizer has 17 taps with spacing  $T/2$ . When  $K_{FB}$ ,  $K_{FF1}$  and  $K_{FF2}$  increase, the MSE converges to  $MSE_{min,DFE}$  of the MMSE-DFE, derived in section 6.8-2; in order to get close to this asymptote, we need  $K_{FB} = K_{FF1} = 1$  and  $K_{FF2} = 2$ , in which case the feedforward filter has 4 taps with spacing  $T/2$ , and the feedback filter has 1 tap. This example illustrates that the performance of the optimum (infinite length) equalizers can be closely approximated by means of fractionally-spaced equalizers with *limited complexity*.

**6.10. Multipath fading channels**

When the received signal is affected by fading, the channel can be modeled as a linear time-varying (LTV) filter. In order to cope with the time-variations of the channel, the receiver must be time-varying as well.

Assuming that the fading is *slow*, the theory developed in the previous sections is still valid, provided that an argument "k", referring to the index of the symbol to be detected, is added to the impulse responses and transfer functions. Basically, this means that we consider a specific realization (denoted by the index k) of the channel impulse response, and apply the theory developed in the previous sections to this particular realization, as if the channel were time-invariant. This approach is valid when the coherence times of the multipath fading channel and the corresponding receive filter (which includes the time-varying equalizer) is much longer than the duration of the impulse response of the receive filter (see section 1.6.2). For example, in the case of a fractionally-spaced DFE, the input  $u(k)$  to the symbol-by-symbol detector is given by

$$u(k) = \sum_{i=-K_{FF1}}^{K_{FF2}} h_{eq}(i;k)r(kN_s - i) - \sum_{m=1}^{K_{FB}} h_{FB}(m;k)\hat{a}(k - m) \quad (6.10-1)$$



The corresponding receiver structure is shown in Fig. 6-36. The coefficients  $\{h_{eq}(i;k)\}$  and  $\{h_{FB}(m;k)\}$  are updated once per symbol interval.

The multipath fading channel provides *multipath diversity*. We illustrate the multipath diversity by means of the following simple example. We consider a square-root Nyquist transmit pulse  $h_{tr}(t)$ , i.e.,

$$\int h_{tr}^*(t-nT)h_{tr}(t-n'T)dt = \int |H_{tr}(f)|^2 \exp(j2\pi f(n-n')T)df = \delta(n-n') \quad (6.10-2)$$

and a channel impulse response  $h_{ch}(u;k)$ , given by

$$h_{ch}(u;k) = \sum_{n=0}^{L-1} c_n(k)\delta(u-nT) \quad (6.10-3)$$

with  $c_n(k) \sim N_c(0, 2\sigma_n^2)$  and

$$\sum_{n=0}^{L-1} \sigma_n^2 = \frac{1}{2} \quad (6.10-4)$$

The coefficients  $c_n(k)$  and  $c_{n'}(k)$  are statistically independent when  $n \neq n'$ . The channel impulse response  $h_{ch}(u;k)$  corresponds to multipath Rayleigh fading, with path delay differences that are multiples of the symbol interval  $T$ . Let us derive the matched filter bound that corresponds to the channel (6.10-3). For a given realization of the coefficients  $c_n(k)$ , we obtain (see (6.3-2))

$$SNR_{MF}(k) = \frac{E_s}{N_0} g(0;k) \quad (6.10-5)$$

where

$$\begin{aligned} g(0;k) &= \int |H_{tr}(f)|^2 |H_{ch}(f;k)|^2 df \\ &= \sum_{n,n'=0}^{L-1} c_n^*(k)c_{n'}(k) \underbrace{\int |H_{tr}(f)|^2 \exp(j2\pi f(n-n')T)df}_{=\delta(n-n')} \\ &= \sum_{n=0}^{L-1} |c_n(k)|^2 \end{aligned} \quad (6.10-6)$$

Assuming a 4-QAM constellation, the matched filter bound on the BER for a particular realization of the channel impulse response becomes

$$BER(k) \geq BER_{MF}(k) = Q\left(\sqrt{\frac{2E_b}{N_0} \sum_{n=0}^{L-1} |c_n(k)|^2}\right) \quad (6.10-7)$$

Averaging over the statistics of the channel coefficients yields

$$BER \geq BER_{MF} = E\left[Q\left(\sqrt{\frac{2E_b}{N_0} \sum_{n=0}^{L-1} |c_n(k)|^2}\right)\right] \quad (6.10-8)$$

Note that  $\text{BER}_{\text{MF}}$  is the BER that would be obtained when transmitting the data symbols over  $L$  parallel frequency-flat fading channels, with coefficients  $c_0(k), \dots, c_{L-1}(k)$ . Hence, a diversity order of  $L$  is achieved : for large  $E_b/N_0$ ,  $\text{BER}_{\text{MF}}$  is proportional to  $(E_b/N_0)^{-L}$ . Increasing the number of paths gives rise to a smaller  $\text{BER}_{\text{MF}}$ .

However, the matched filter bound does not take into account the ISI that is caused by the multipath channel. Actual receivers have to cope with the ISI, so their performance is worse than the matched filter bound. The larger the number of paths, the stronger the ISI, and the more the performance of the actual receiver is degraded as compared to the matched filter bound. In Fig. 6-37 we display the matched filter bound and the performance of the optimum MMSE-DFE, assuming a channel impulse response given by (6.10-3), with  $L$  paths of equal strength ( $2\sigma_n^2 = 1/L$ ); the BER curves are obtained by averaging over 5000 independent realizations of the channel impulse response. We make the following observations :

- For  $L = 1$ , the channel is frequency-flat, so there is no ISI. Hence, the performance of the MMSE-DFE coincides with the matched filter bound.
- For  $L > 1$ , the channel is frequency-selective, and gives rise to ISI. Hence, the MMSE-DFE performs worse than the matched filter bound. The degradation of the MMSE-DFE as compared to the matched filter bound is about 1.5 dB for  $L = 3$  and 2 dB for  $L = 5$ .
- The matched filter bound on the BER is considerably reduced (especially at high  $E_b/N_0$ ) when  $L$  gets larger, because of the diversity of order  $L$ . For large  $E_b/N_0$ , the BER curves for the MMSE-DFE are essentially parallel with their corresponding matched filter bound; this indicates that the MMSE-DFE also benefits from a diversity of order  $L$ .

From these observations we conclude that the MMSE-DFE benefits from the presence of multiple paths, in spite of the occurrence of ISI. The same conclusion must hold for the ML sequence detector (Viterbi algorithm), because this detector has a BER that is lower bounded by the matched filter bound and upper bounded by the BER of the MMSE-DFE.

When the channel is frequency-flat, the performance can be improved by means of transmit antenna diversity (see section 4.4.3), which creates a multipath fading channel. The receiver then must cope with the ISI, by applying ML sequence detection (Viterbi algorithm) or by applying some form of equalization (LE or DFE).

## 6.11. Appendix

### 6.11.1 Spectral factorization

Consider a complex-valued stationary discrete-time process  $\{x(m)\}$  with autocorrelation function  $R_x(k) = E[x^*(m)x(k+m)]$ . We denote by  $S_x(z)$  the z-transform of  $R_x(k)$  :

$$S_x(z) = \sum_{k=-\infty}^{+\infty} R_x(k)z^{-k} \quad (6.11.1-1)$$

We assume that  $\sum_{k=-\infty}^{+\infty} |R(k)|$  converges, so that the unit circle  $|z| = 1$  belongs to the convergence area of  $S_x(z)$ . The power spectral density of  $\{x(m)\}$  is given by  $S_x(\exp(j2\pi fT))$ , which is nonnegative. Noting that  $R_x(k) = (R_x(-k))^*$ , we obtain  $S_x(\exp(j2\pi fT)) = (S_x(\exp(j2\pi fT)))^*$ , or  $S_x(z) = (S_x(1/z^*))^*$ . Hence, the poles and zeroes of  $S_x(z)$  appear in pairs :

- When  $z_p$  is a pole of  $S_x(z)$ ,  $1/(z_p)^*$  is also a pole of  $S_x(z)$ . The product of the magnitudes of these poles is given by  $|z_p|/|(z_p)^*| = 1$ , which indicates that one of the poles is inside the unit circle and the other pole is outside the unit circle. We will denote the pole inside the unit circle by  $z_p$  (i.e.,  $|z_p| < 1$ ), and the pole outside the unit circle by  $1/(z_p)^*$ .
- Similarly, when  $z_n$  is a zero of  $S_x(z)$ ,  $1/(z_n)^*$  is also a zero of  $S_x(z)$ . One of these zeroes is inside the unit circle and the other zero is outside the unit circle. We will denote the zero inside the unit circle by  $z_n$  (i.e.,  $|z_n| < 1$ ), and the zero outside the unit circle by  $1/(z_n)^*$ .

Considering the above,  $S_x(z)$  can be uniquely factored as follows :

$$S_x(z) = A^2 \cdot F_+(z) \cdot F_-(z) \quad (6.11.1-2)$$

where  $A^2$  is a positive scaling factor,  $F_+(z)$  contains all poles and zeroes of  $S_x(z)$  that are located *inside* the unit circle, and  $F_-(z) = F_+^*(1/z^*)$  contains the poles and zeroes of  $S_x(z)$  that are located *outside* the unit circle :

$$F_+(z) = \frac{\prod_{i=1}^{N_z} (1 - z_{n,i} z^{-1})}{\prod_{j=1}^{N_p} (1 - z_{p,j} z^{-1})} \quad F_-(z) = F_+^*(1/z^*) = \frac{\prod_{i=1}^{N_z} (1 - z_{n,i}^* z)}{\prod_{j=1}^{N_p} (1 - z_{p,j}^* z)} \quad (6.11.1-3)$$

where  $2N_p$  and  $2N_z$  denote the numbers of poles and zeroes of  $S_x(z)$ . The z-transforms  $F_+(z)$  and  $F_-(z) = F_+^*(1/z^*)$  have the following properties :

- The power series expansions of  $F_+(z)$  and  $1/F_+(z)$  consist of powers  $z^{-k}$  ( $k = 0, 1, 2, \dots$ ) with coefficients that vanish with increasing  $k$ . Hence, they can be interpreted as the z-

transforms of impulse responses of *causal*, stable and invertible filters. Both z-transforms are monic : the coefficient of  $z^0$  in their power series expansion is equal to 1.

- The power series expansions of  $F_-(z) = F_+^*(1/z^*)$  and  $1/F_-(z) = 1/F_+^*(1/z^*)$  consist of powers  $z^k$  ( $k = 0, 1, 2, \dots$ ) with coefficients that vanish with increasing  $k$ . Hence, they can be interpreted as the z-transforms of impulse responses of *anti-causal*, stable and invertible filters. Both z-transforms are monic.

Hence, as far as the power spectral density  $S_x(\exp(j2\pi fT)) = A^2 |F_+(\exp(j2\pi fT))|^2$  or the autocorrelation  $R_x(m)$  is concerned, the discrete-time process  $x(k)$  can be considered as the output of stable causal and monic filter  $F_+(z)$ , driven by a white sequence  $w(k)$  with  $E[w^*(k)w(k+m)] = A^2\delta(m)$ . The white sequence  $w(k)$  can be obtained from  $x(k)$ , by applying  $x(k)$  to the filter  $1/F_+(z)$ .

### Examples

1) We consider

$$R_x(k) = e^{-\alpha|k|} \text{ (with } \alpha > 0, \text{ so that } R_x(k) \text{ vanishes for large } |k| \text{)} \quad (6.11.1-4)$$

The corresponding z-transform is given by

$$\begin{aligned} S_x(z) &= \sum_{k=-\infty}^{-1} e^{\alpha k} z^{-k} + 1 + \sum_{k=1}^{+\infty} e^{-\alpha k} z^{-k} = \sum_{k=1}^{+\infty} e^{-\alpha k} z^k + 1 + \sum_{k=1}^{+\infty} e^{-\alpha k} z^{-k} \\ &= \frac{1 - e^{-2\alpha}}{(1 - e^{-\alpha}z)(1 - e^{-\alpha}z^{-1})} \end{aligned} \quad (6.11.1-5)$$

$S_x(z)$  has two poles,  $e^{-\alpha}$  (inside unit circle) and  $e^{\alpha}$  (outside unit circle). Spectral factorization of  $S_x(z)$  yields :

$$A^2 = 1 - e^{-2\alpha} \quad (6.11.1-6)$$

$$F_+(z) = \frac{1}{1 - e^{-\alpha}z^{-1}} = \sum_{k=0}^{+\infty} e^{-\alpha k} z^{-k} \quad \frac{1}{F_+(z)} = 1 - e^{-\alpha}z^{-1} \quad (6.11.1-7)$$

$$F_-(z) = F_+^*(1/z^*) = \frac{1}{1 - e^{-\alpha}z} = \sum_{k=0}^{+\infty} e^{-\alpha k} z^k \quad \frac{1}{F_-(z)} = 1 - e^{-\alpha}z \quad (6.11.1-8)$$

2) We consider

$$R_x(0) = 1, R_x(1) = R_x(-1) = \gamma \text{ (}\gamma \text{ real)}, R_x(m) = 0 \text{ for } |m| > 1 \quad (6.11.1-9)$$

The corresponding z-transform is given by

$$S_x(z) = \gamma z + 1 + \gamma z^{-1} \quad (6.11.1-10)$$

In order that  $S_x(\exp(j2\pi fT))$  be nonnegative for all  $f$ , it is required that  $|\gamma| \leq 1/2$ .  $S_x(z)$  has two real-valued zeroes, which we denote as  $\alpha$  and  $1/\alpha$  (with  $-1 < \alpha < 1$ );  $\alpha$  is given by

$$\alpha = \frac{-1 + \sqrt{1 - 4\gamma^2}}{2\gamma} \quad (6.11.1-11)$$

Note that the condition  $|\gamma| \leq 1/2$  makes  $\alpha$  real-valued. Spectral factorization yields

$$F_+(z) = 1 - \alpha z^{-1} \quad \frac{1}{F_+(z)} = \frac{1}{1 - \alpha z^{-1}} = \sum_{k=0}^{+\infty} \alpha^k z^{-k} \quad (6.11.1-12)$$

$$F_-(z) = F_+^*(1/z^*) = 1 - \alpha z \quad \frac{1}{F_-(z)} = \frac{1}{1 - \alpha z} = \sum_{k=0}^{+\infty} \alpha^k z^k \quad (6.11.1-13)$$

$$F_+(z)F_-(z) = -\alpha z + (1 + \alpha^2) - \alpha z^{-1} \Rightarrow A^2 = \frac{1}{1 + \alpha^2} = \frac{1 + \sqrt{1 - 4\gamma^2}}{2} \quad (6.11.1-14)$$

### 6.11.2 Linear prediction

Consider a complex-valued stationary discrete-time process  $\{x(m)\}$  with autocorrelation function  $R_x(k) = E[x^*(m)x(k+m)]$  and power spectral density  $S_x(\exp(j2\pi fT))$ . Based on the observation of the infinite past  $x(k-1), x(k-2), \dots$  we want to produce an estimate (prediction)  $\hat{x}(k)$  of  $x(k)$ , that is a linear combination of the observations  $x(k-1), x(k-2), \dots$ :

$$\hat{x}(k) = -\sum_{m=1}^{+\infty} h_{pr}(m)x(k-m) \quad (6.11.2-1)$$

For convenience, the coefficient of  $x(k-m)$  in the linear combination is denoted  $-h_{pr}(m)$  instead of  $h_{pr}(m)$ . The prediction  $\hat{x}(k)$  is the output of a filter  $-H_{pr}(z)$ , driven by  $\{x(m)\}$ , with

$$H_{pr}(z) = \sum_{k=1}^{+\infty} h_{pr}(k)z^{-k} \quad (6.11.2-2)$$

The resulting prediction error  $e(k)$  is defined as :

$$e(k) = x(k) - \hat{x}(k) \quad (6.11.2-3)$$

The prediction error can be interpreted as the output of a filter  $1 + H_{pr}(z)$ , with input  $\{x(m)\}$ .

Our aim is to select the predictor coefficients  $-h_{pr}(m)$  such that the mean square prediction error  $E[|e_k|^2]$  is minimum. These coefficients satisfy a set of equations, that can be obtained by equating to zero the derivatives of  $E[|e_k|^2]$  with respect to the real and imaginary parts of the predictor coefficients. This yields, for  $i = 1, 2, \dots$  :

$$0 = \frac{\partial E[e(k)e^*(k)]}{\partial \text{Re}[h_{pr}(i)]} = 2 \text{Re} \left[ E \left[ e(k) \frac{\partial e^*(k)}{\partial \text{Re}[h_{pr}(i)]} \right] \right] = 2 \text{Re} [E[e(k)x^*(k-i)]] \quad (6.11.2-4)$$

$$0 = \frac{\partial E[e(k)e^*(k)]}{\partial \text{Im}[h_{pr}(i)]} = 2 \text{Re} [-jE[e(k)x^*(k-i)]] = 2 \text{Im} [E[e(k)x^*(k-i)]] \quad (6.11.2-5)$$

Combining the two equations above, we obtain

$$E[e(k)x^*(k-i)] = 0 \quad (i = 1, 2, \dots) \quad (6.11.2-6)$$

which expresses that the prediction error  $e(k)$  is uncorrelated with all *past* observations  $x(k-1)$ ,  $x(k-2)$ , .... A crucial step towards the solution of the equations is the observation that the prediction error  $e(k)$  is uncorrelated with past prediction errors  $e(k-1)$ ,  $e(k-2)$ , ..., because the past prediction errors are linear combinations of past observations :

$$R_e(i) = E[e(k)e^*(k-i)] = 0 \quad \text{for } i = 1, 2, \dots \quad (6.11.2-7)$$

However, as  $R_e(i)$  exhibits conjugate symmetry ( $R_e(i) = R_e^*(-i)$ ), it follows that  $R_e(i)$  must be zero for *all* nonzero  $i$  :

$$R_e(i) = E[e(k)e^*(k-i)] = 0 \quad \text{for } i \neq 0 \quad (6.11.2-8)$$

This indicates that sequence  $\{e(k)\}$  of prediction errors is *white* : as  $S_e(z)$ , which is the  $z$ -transform of  $R_e(i) = R_e(0)\delta(i)$ , does not depend on  $z$ , the power spectral density  $S_e(\exp(j2\pi fT))$  is constant as a function of  $f$ . Taking into account that  $e(k)$  is obtained by applying  $x(k)$  to the filter  $(1+H_{pr}(z))$ ,  $S_e(z)$  is given by

$$\begin{aligned} S_e(z) &= S_x(z)(1+H_{pr}(z))(1+H_{pr}^*(1/z^*)) \\ &= \underbrace{A^2 \cdot F_+(z)F_+^*(1/z^*)}_{S_x(z)}(1+H_{pr}(z))(1+H_{pr}^*(1/z^*)) \end{aligned} \quad (6.11.2-9)$$

In order that  $S_e(z)$  be independent of  $z$ , and  $1+H_{pr}(z)$  be causal and monic, we select

$$1+H_{pr}(z) = 1/F_+(z) \quad (6.11.2-10)$$

This yields

$$S_e(z) = A^2, \quad E[|e(k)|^2]_{\min} = A^2 \quad (6.11.2-11)$$

It can be shown that  $E[|e(k)|^2]_{\min}$  from (6.11.2-11) can be expressed directly in terms of  $S_x(z)$  :

$$E[|e(k)|^2]_{\min} = \exp\left(\int_{1/T} \ln S_x(e^{j2\pi fT}) dfT\right) = \exp(\langle \ln S_x(\cdot) \rangle_f) \quad (6.11.2-12)$$

## Examples

1) We consider

$$R_x(k) = e^{-\alpha|k|} \quad (\alpha > 0) \quad (6.11.2-13)$$

Taking (6.11.1-7) into account, we obtain

$$1+H_{pr}(z) = 1 - e^{-\alpha}z^{-1} \quad (6.11.2-14)$$

such that  $-H_{pr}(z) = e^{-\alpha}z^{-1}$ . Hence, the prediction  $\hat{x}(k)$  and prediction error  $E[|e(k)|^2]_{\min}$  are given by

$$\hat{x}(k) = e^{-\alpha}x(k-1) \quad E[|e(k)|^2]_{\min} = 1 - e^{-2\alpha} \quad (6.11.2-15)$$

2) We consider

$$R_x(0) = 1, R_x(1) = R_x(-1) = \gamma \text{ (}\gamma \text{ real, and } |\gamma| < 1/2\text{), } R_x(m) = 0 \text{ for } |m| > 1 \quad (6.11.2-16)$$

Taking (6.11.1-12) into account, we obtain

$$1 + H_{pr}(z) = \frac{1}{1 - \alpha z^{-1}} \Rightarrow -H_{pr}(z) = \frac{-\alpha z^{-1}}{1 - \alpha z^{-1}} \quad (6.11.2-17)$$

Hence, the prediction  $\hat{x}(k)$  and the prediction error  $E[|e(k)|^2]_{\min}$  are given by

$$\hat{x}(k) = -\sum_{m=1}^{+\infty} \alpha^m x(k-m) \quad E[|e(k)|^2]_{\min} = 1/(1+\alpha^2) \quad (6.11.2-18)$$

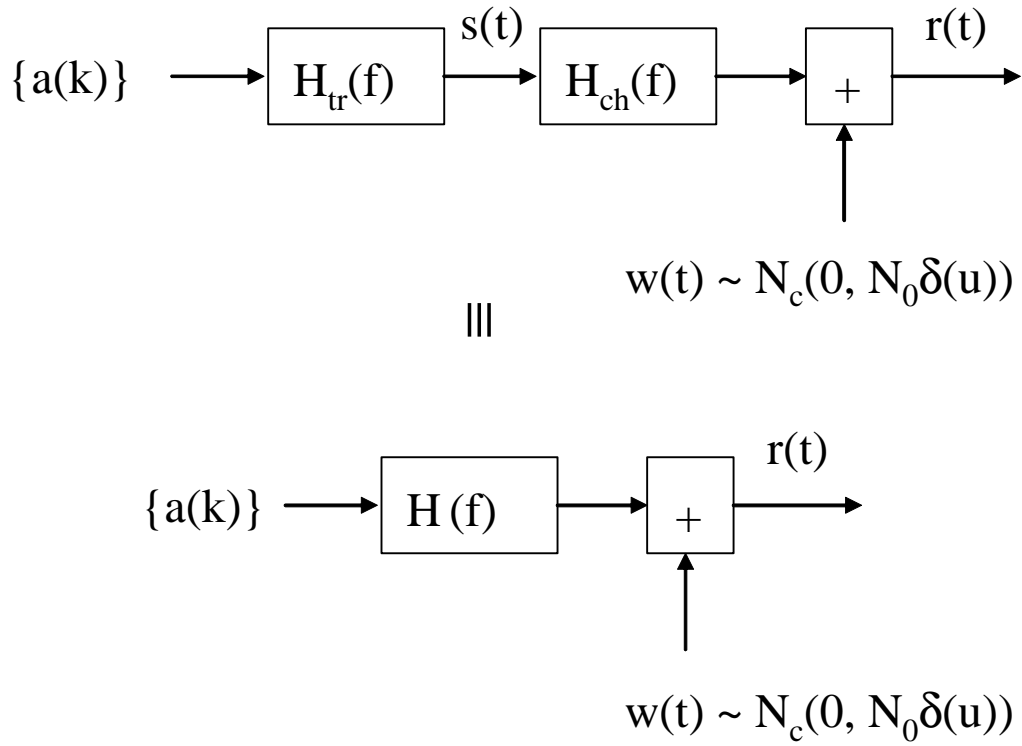


Fig. 6-1 : transmitter and channel model

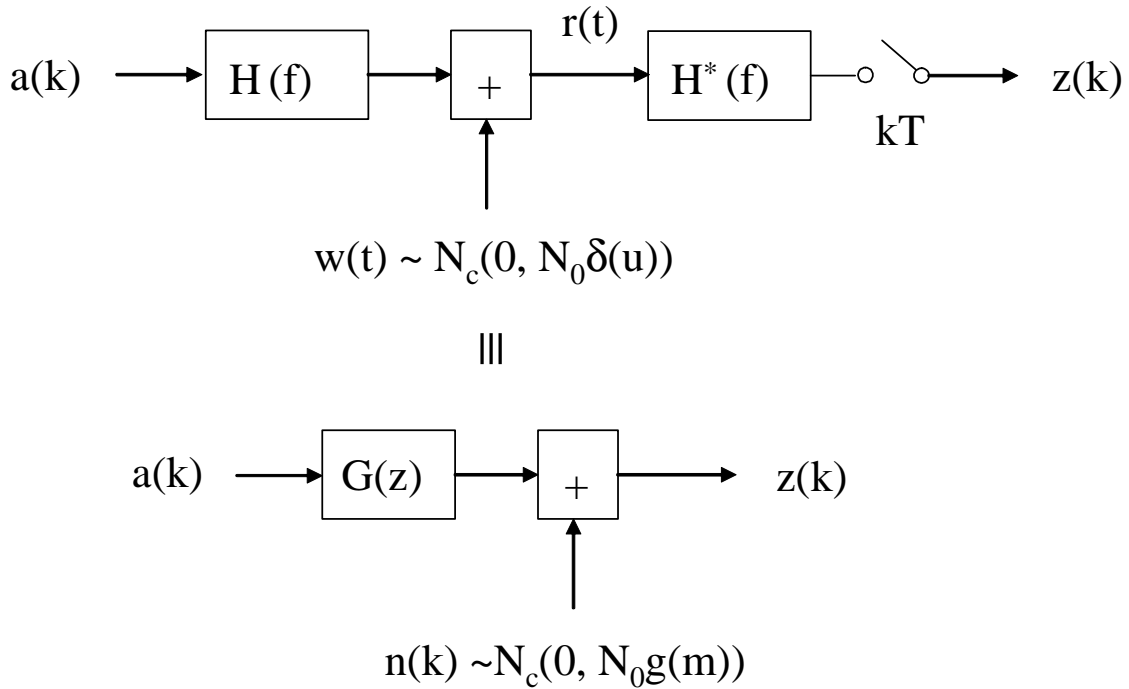


Fig. 6-2 : model of matched filter output samples



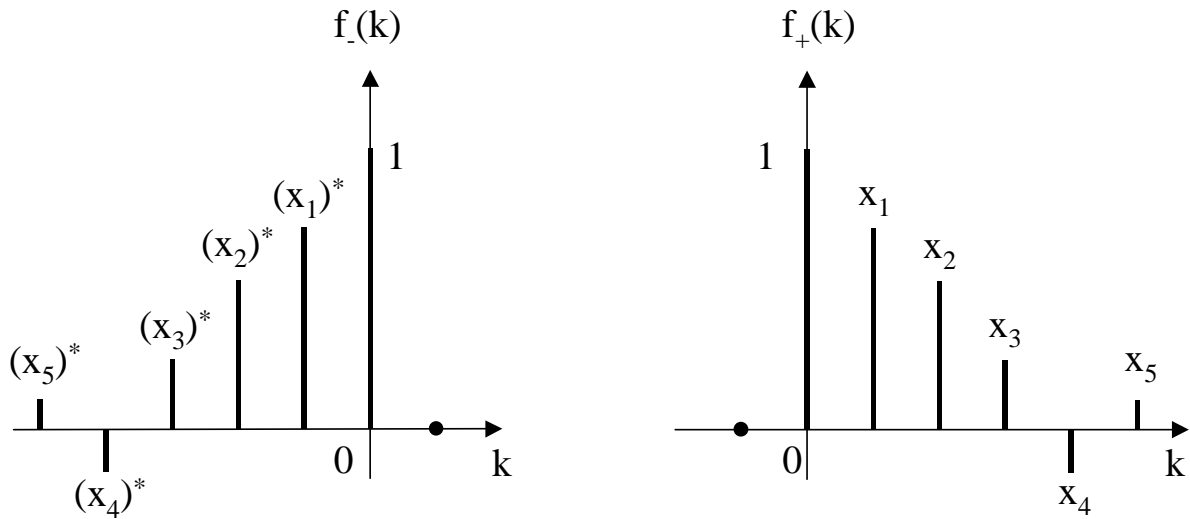
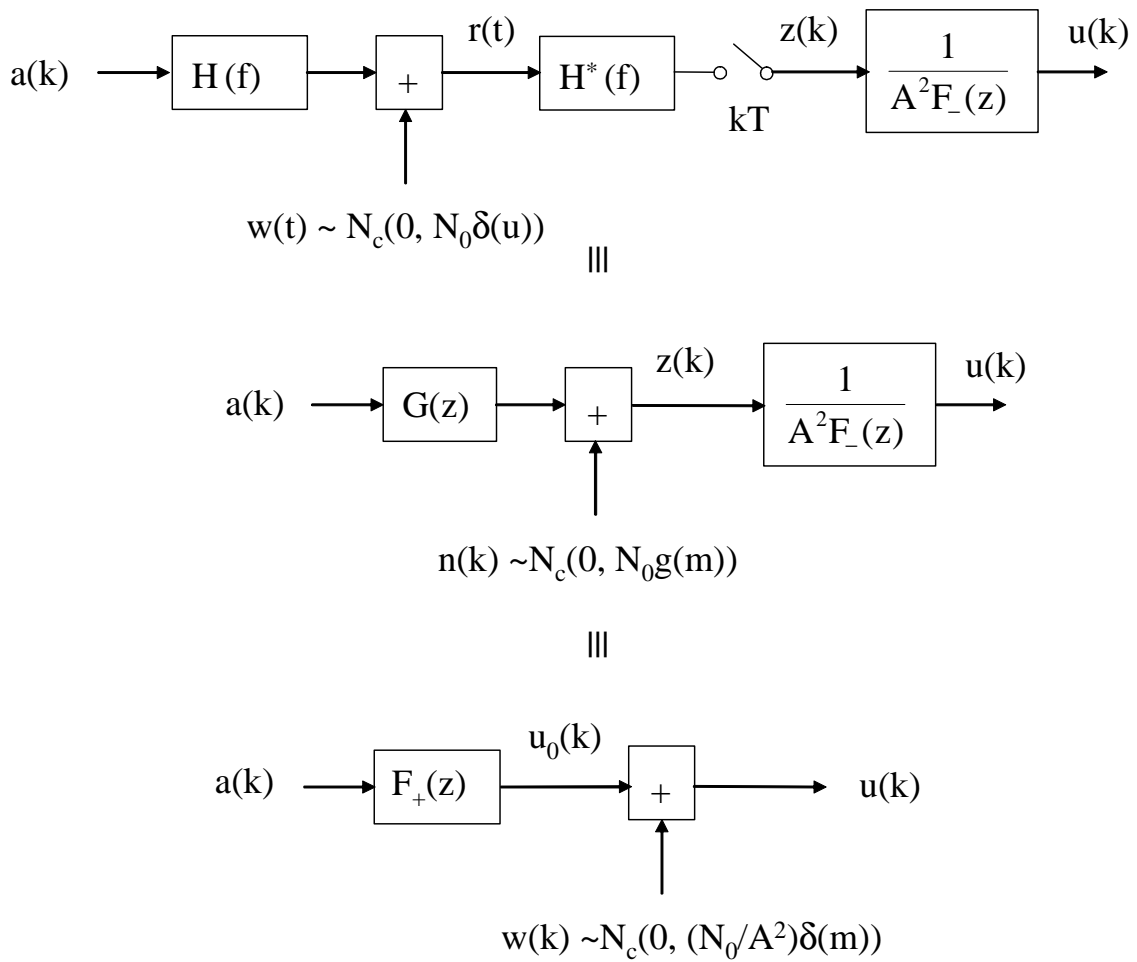
Fig. 6-3 : impulse responses  $\{f_-(k)\}$  and  $\{f_+(k)\}$ 

Fig. 6-4 : configuration with whitened matched filter

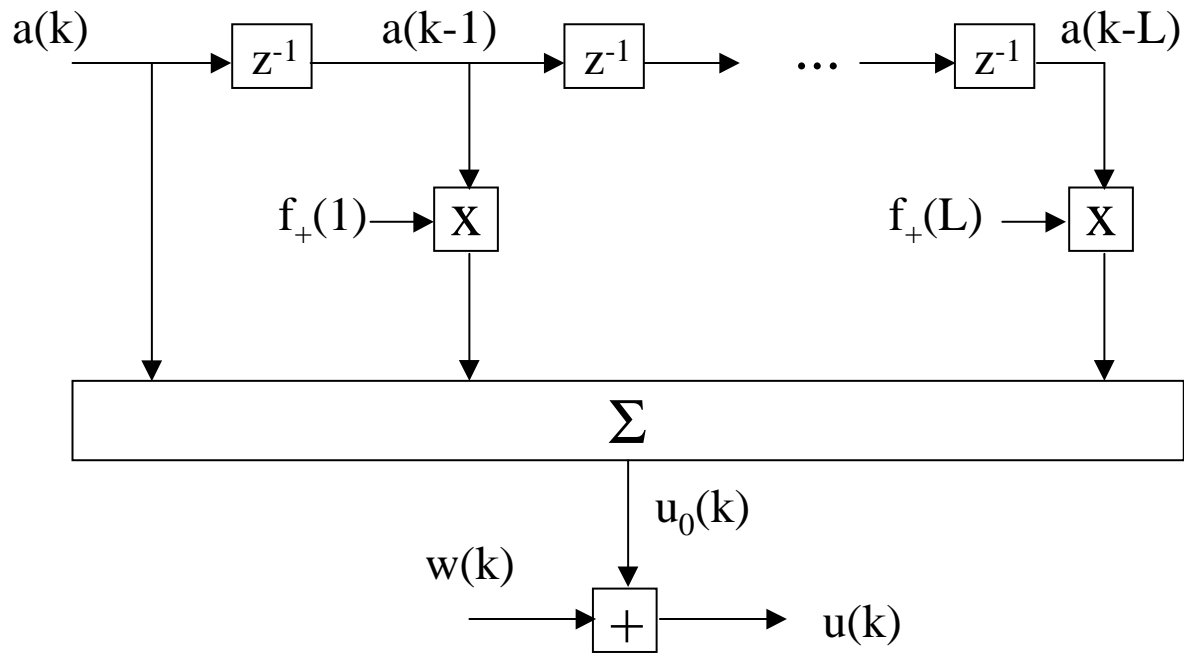
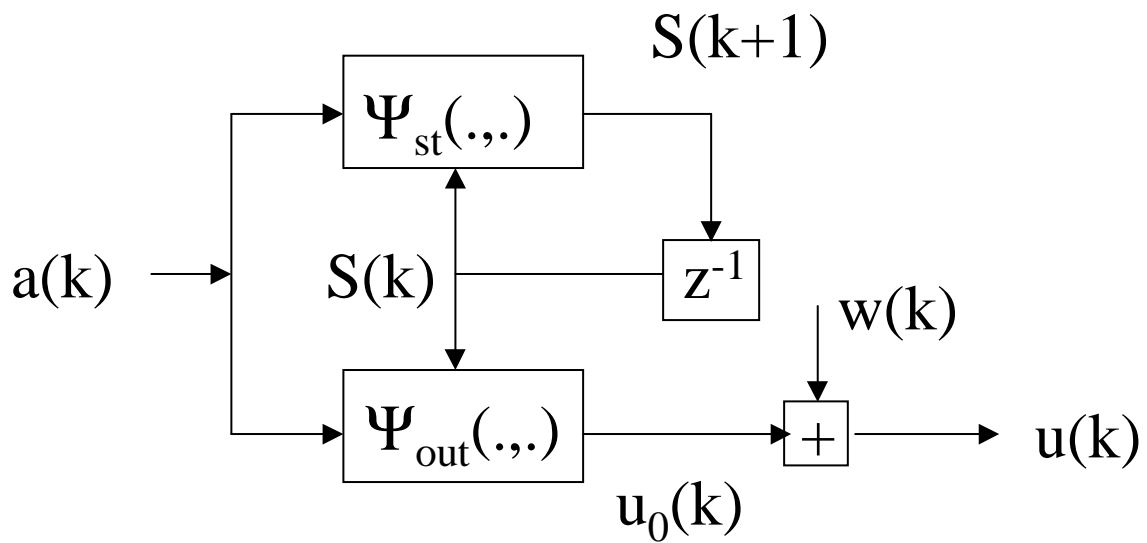
Fig. 6-5 : details of the filter  $F_+(z)$ 

Fig. 6-6 : finite-state machine

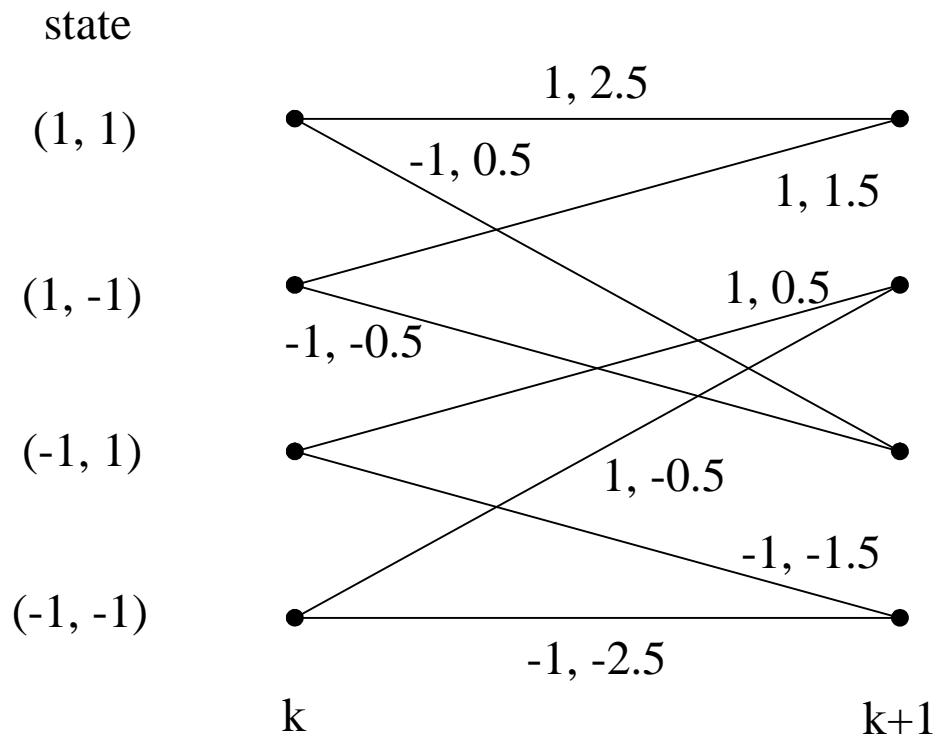
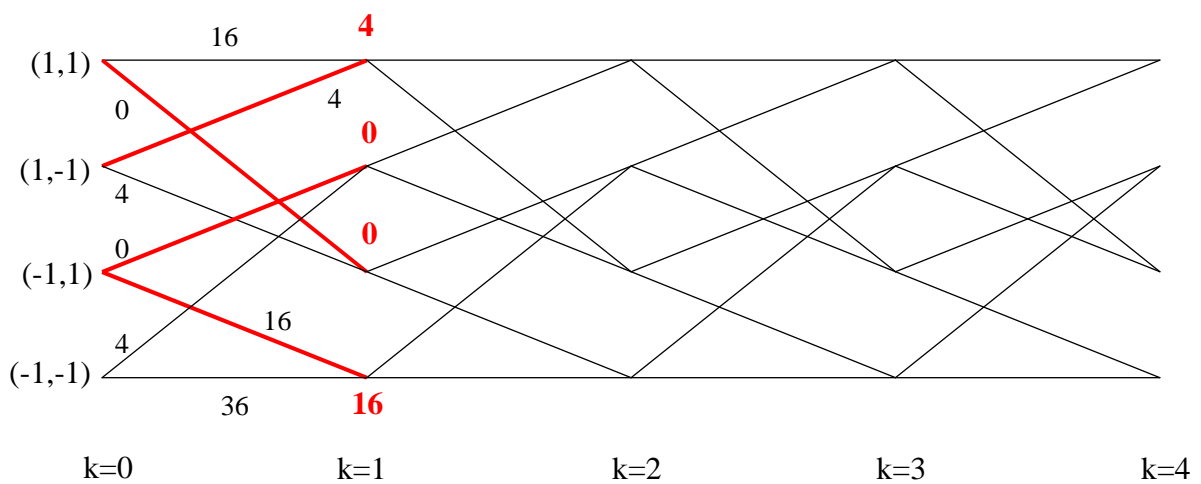
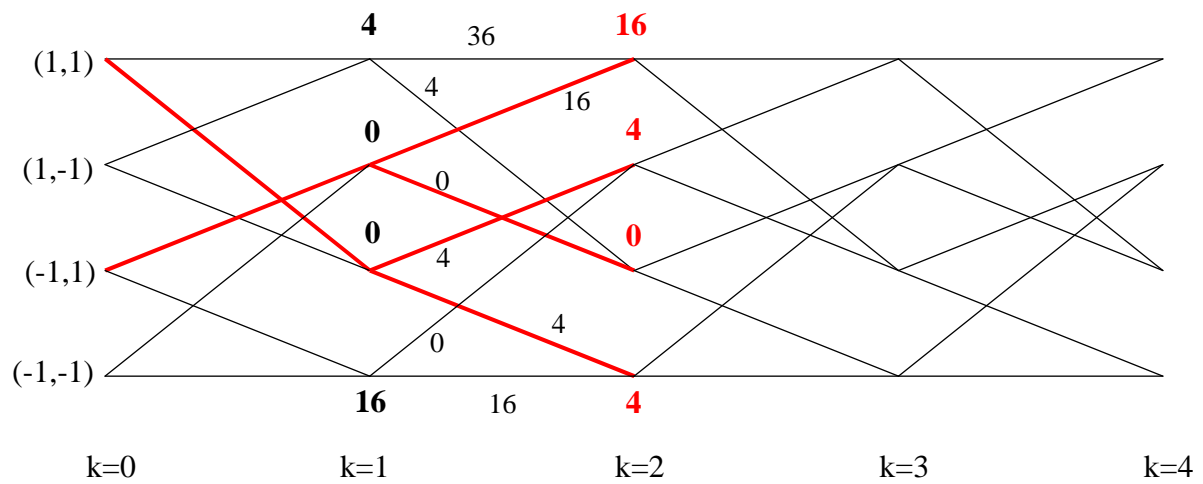
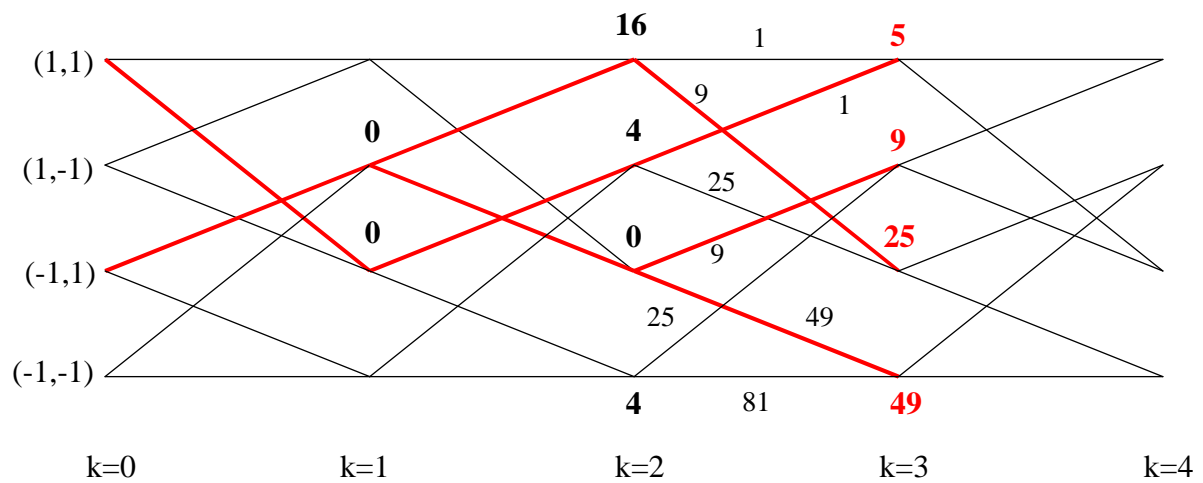
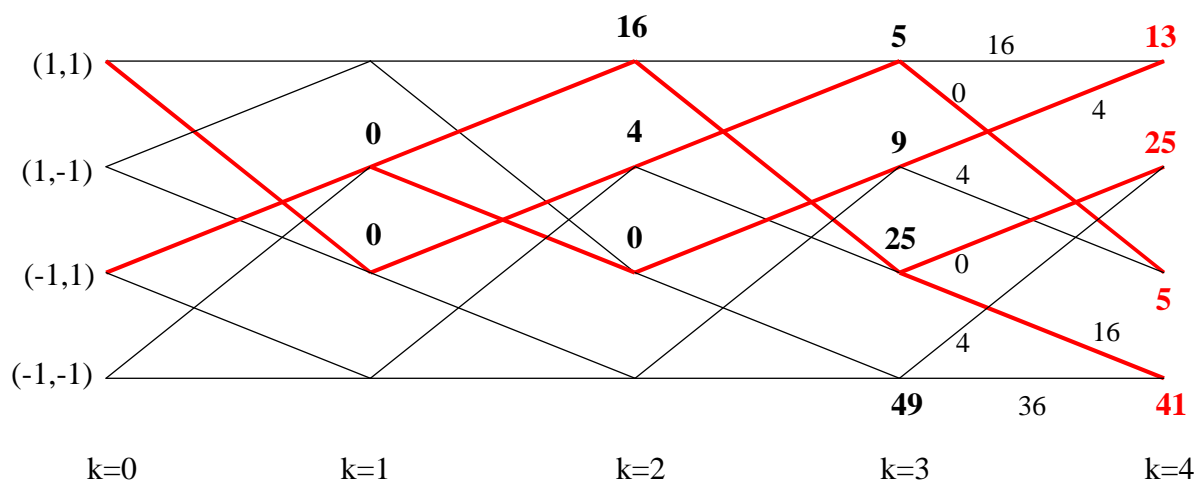


Fig. 6-7 : section of trellis

Fig. 6-8 : surviving paths at  $k = 1$

Fig. 6-9 : surviving paths at  $k = 2$ Fig. 6-10 : surviving paths at  $k = 3$ Fig. 6-11 : surviving paths at  $k = 4$

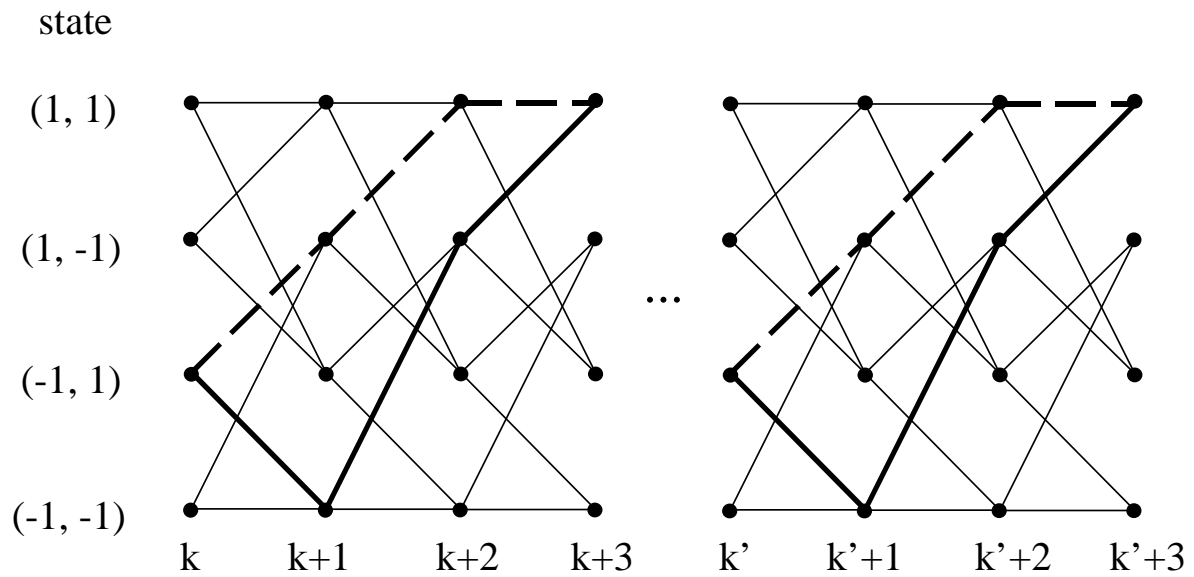


Fig. 6-12 : two error events of the same type  
(solid line : correct path; dashed line : erroneous path)

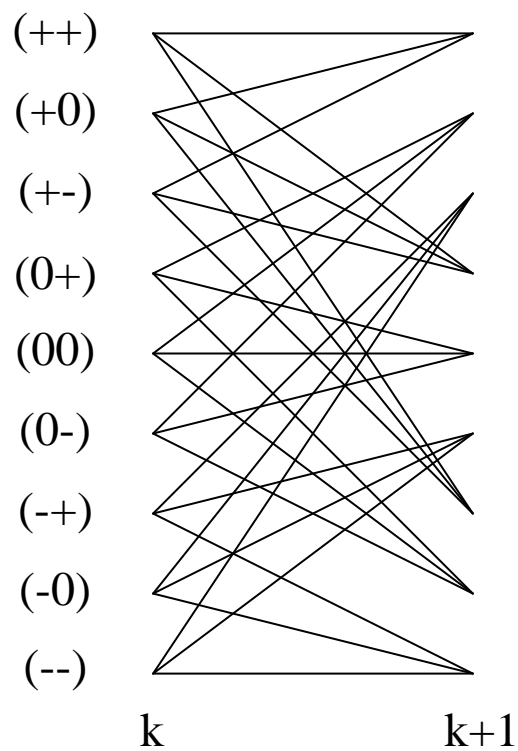


Fig. 6-13 : section of trellis for determining minimum distance

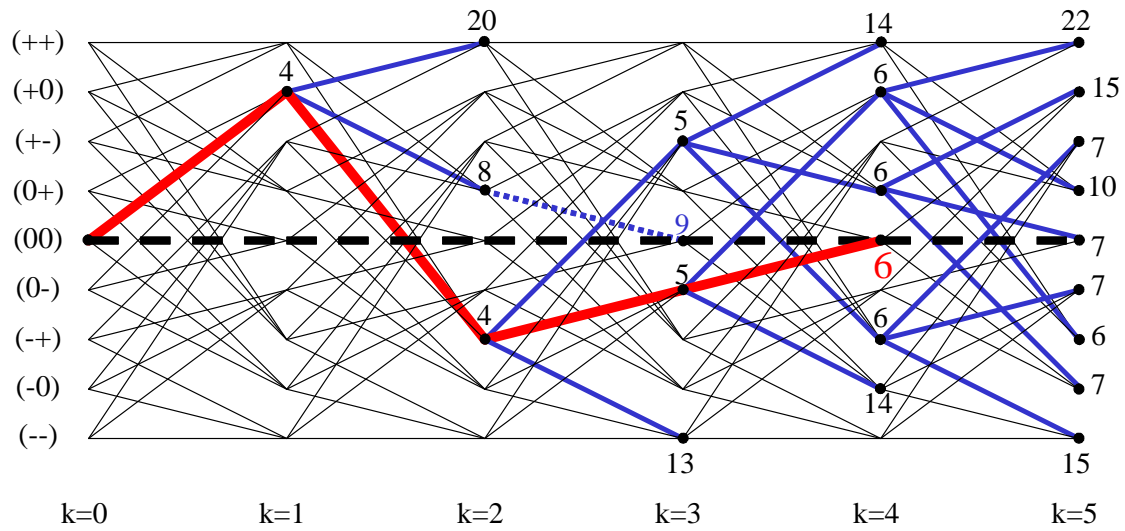


Fig. 6-14 : determining minimum distance by means of Viterbi algorithm

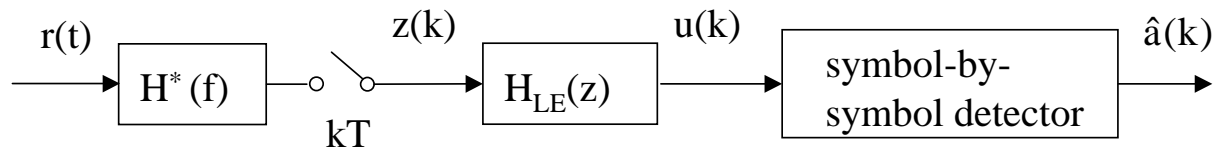


Fig. 6-15 : receiver with linear equalizer

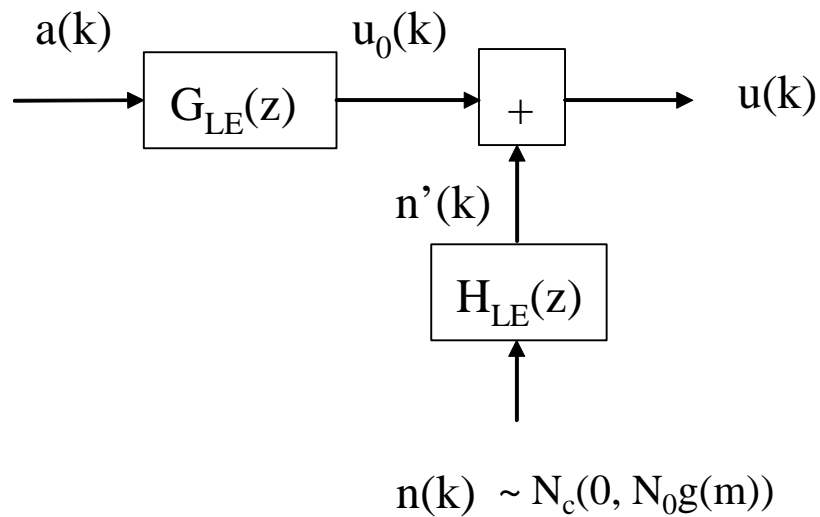


Fig. 6-16 : model for output of linear equalizer

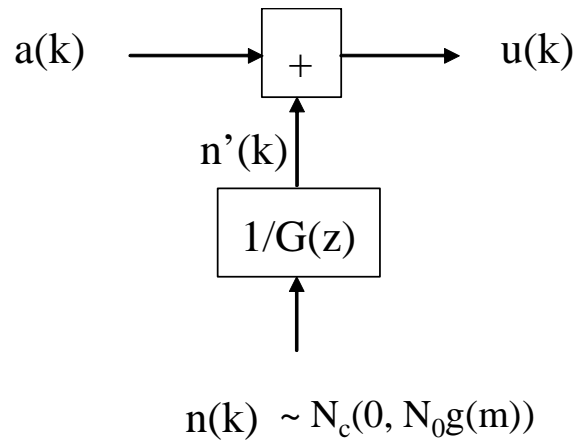


Fig. 6-17 : model for output of ZF-LE

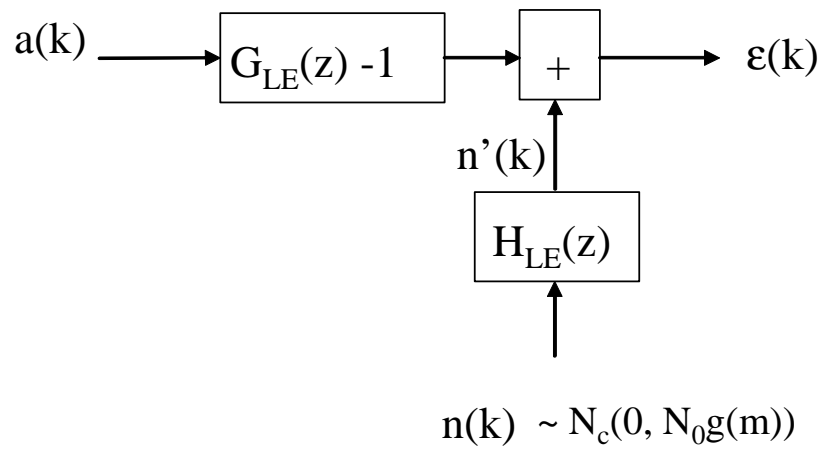
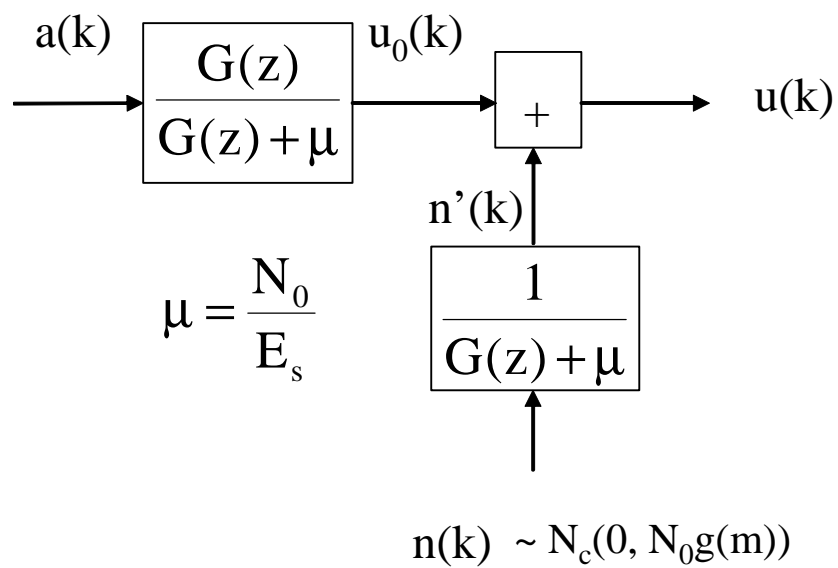
Fig. 6-18 : model for error signal  $\epsilon(k)$ 

Fig. 6-19 : model for output of MMSE-LE

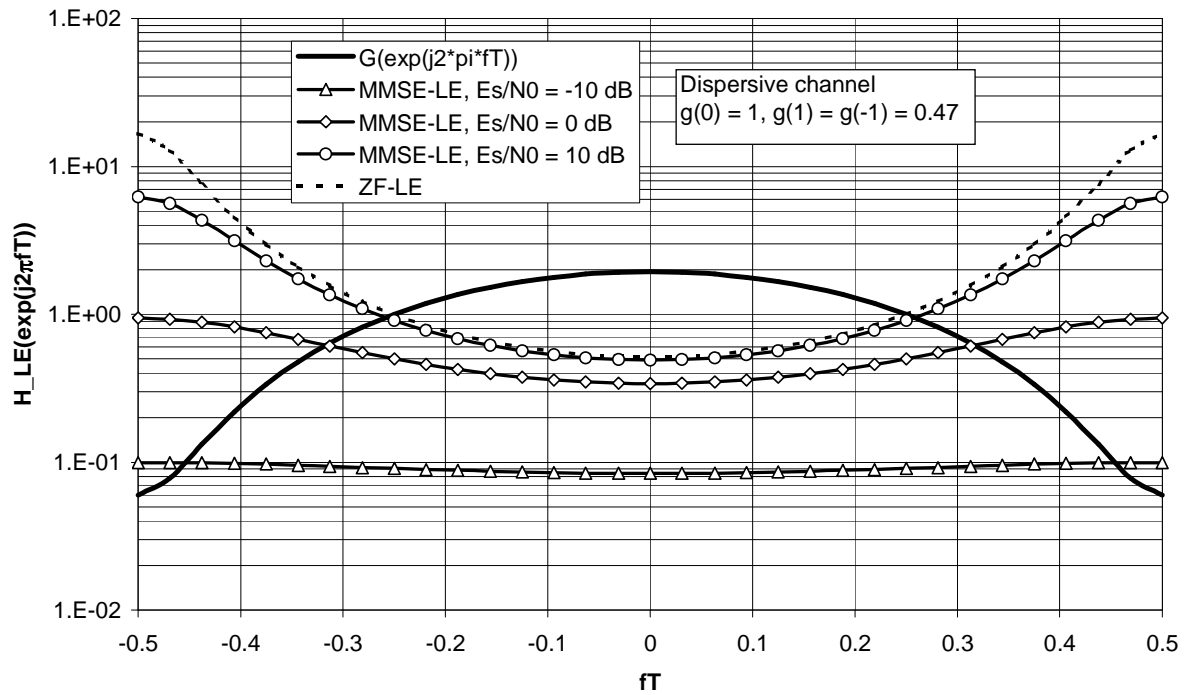
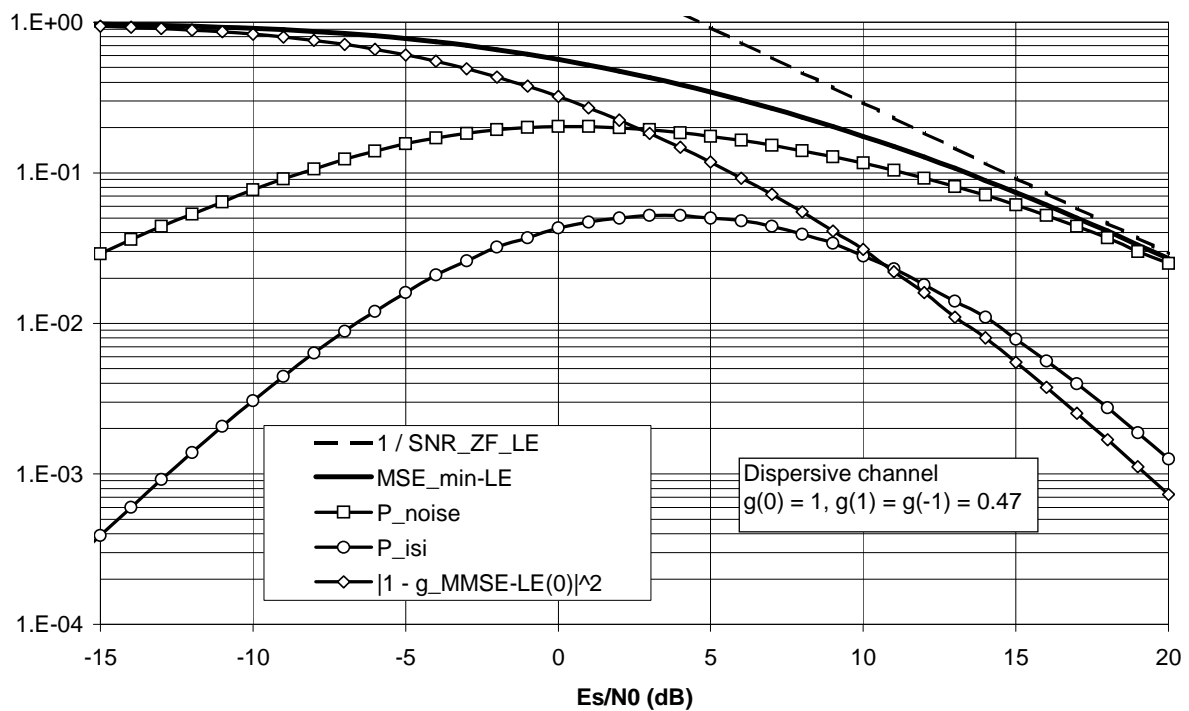


Fig. 6-20 : equalizer transfer functions

Fig. 6-21 : contributions to  $MSE_{min\_LE}$



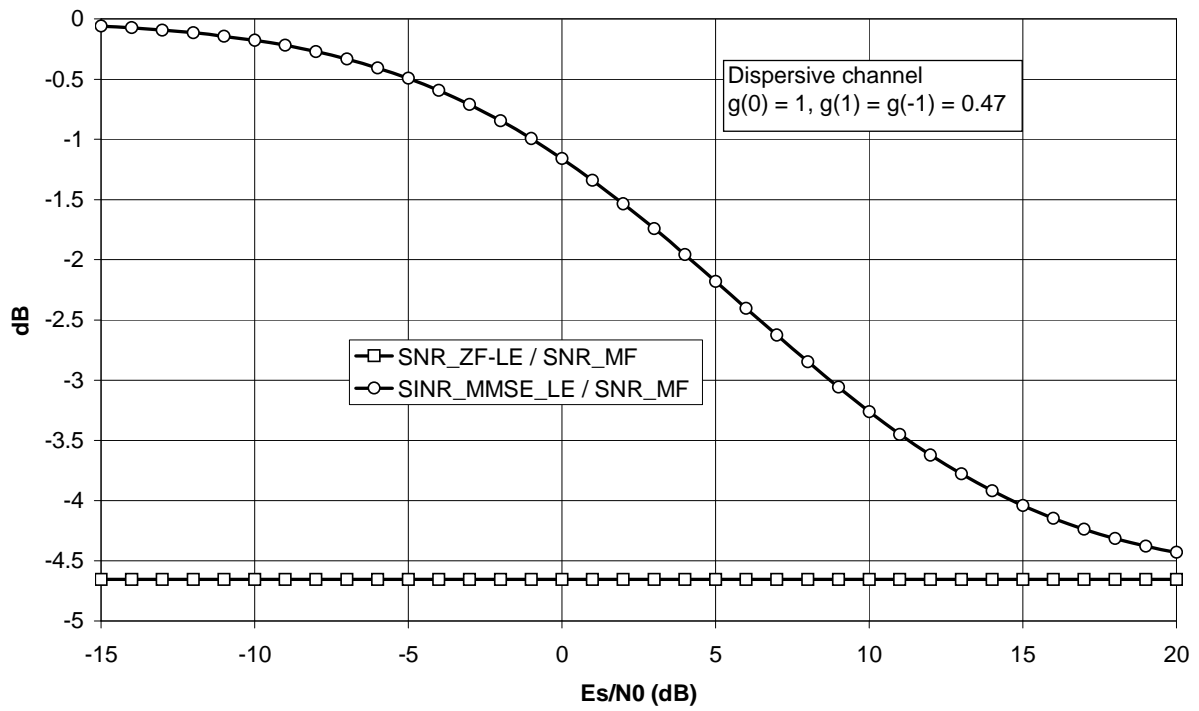
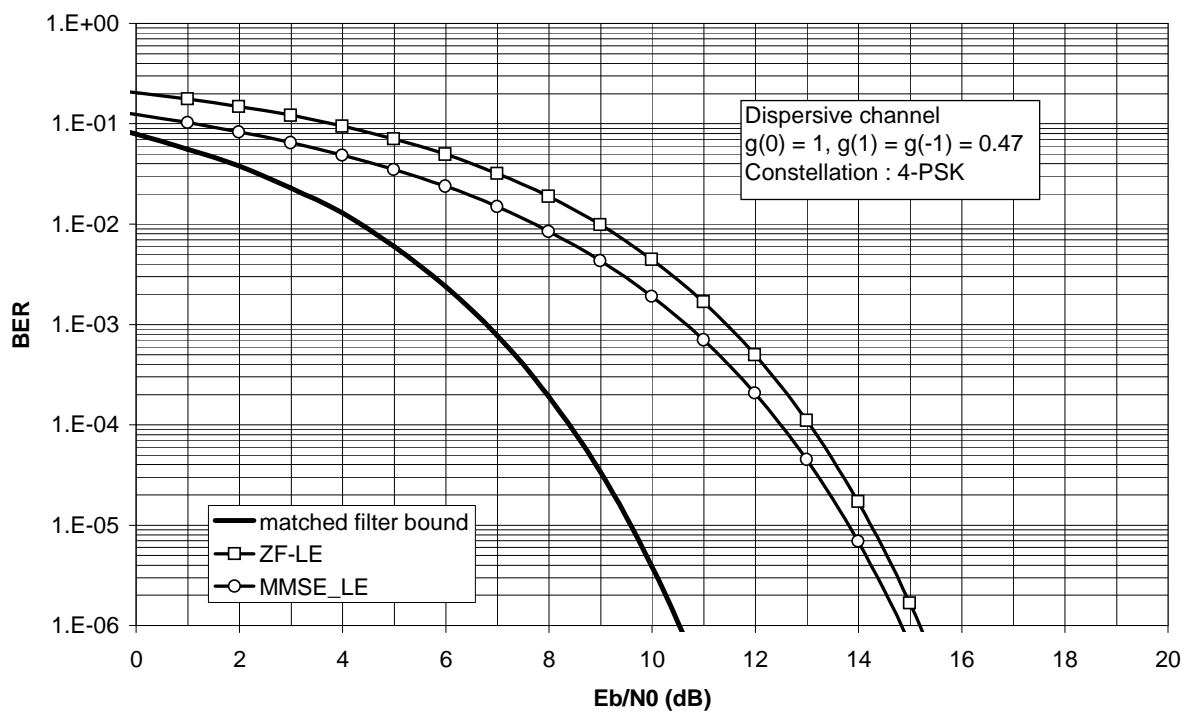
Fig. 6-22 : ratios  $\text{SNR}_{\text{ZF-LE}}/\text{SNR}_{\text{MF}}$  and  $\text{SINR}_{\text{MMSE-LE}}/\text{SNR}_{\text{MF}}$ 

Fig. 6-23 : BER performance

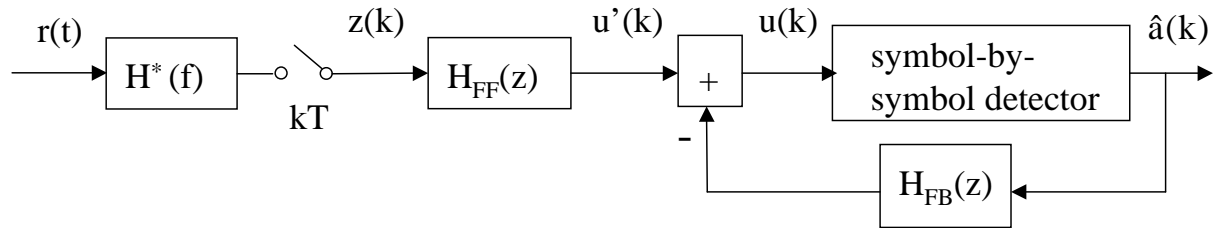
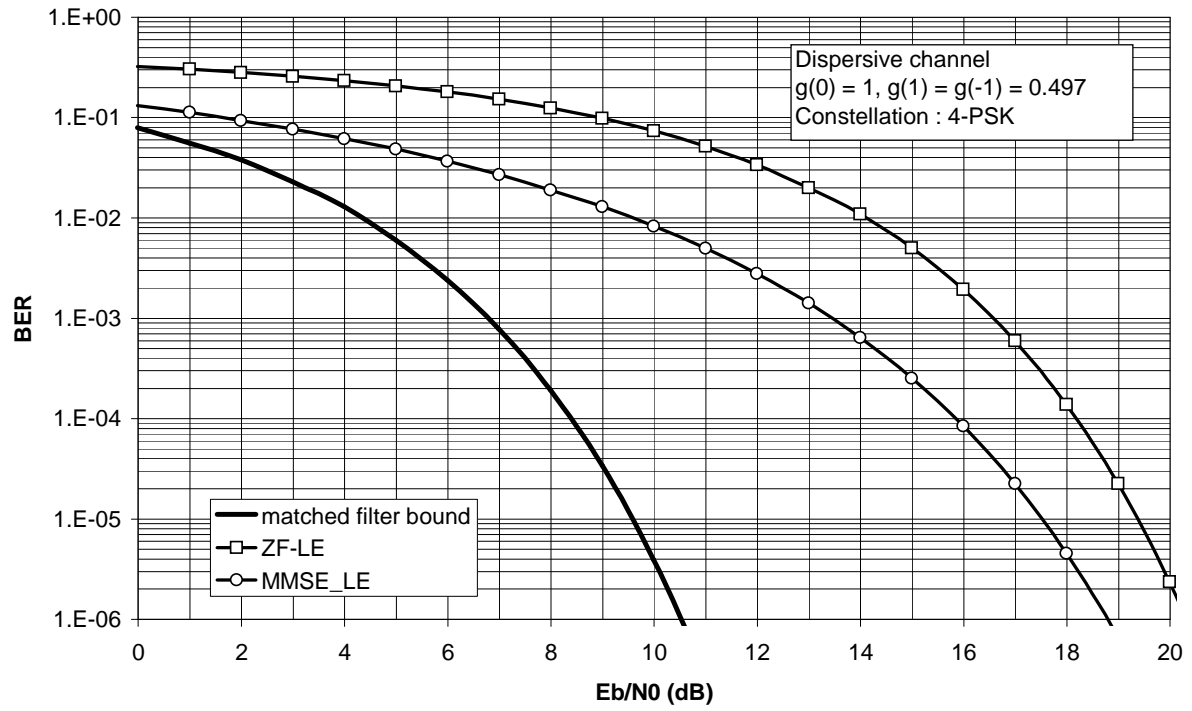
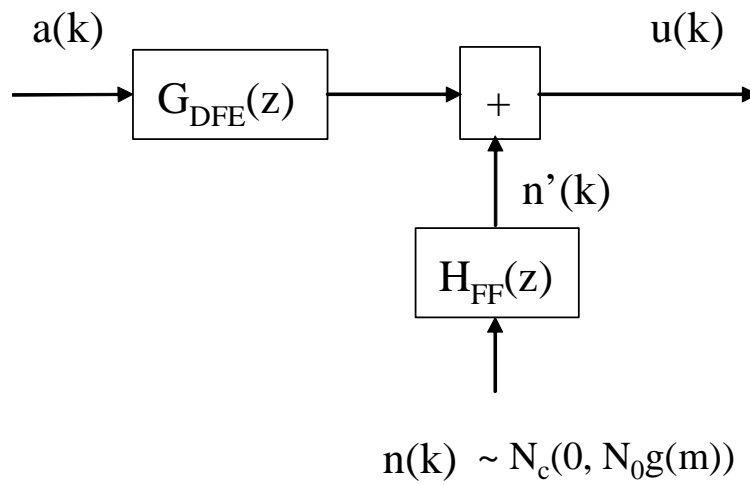


Fig. 6-25 : receiver with decision-feedback equalizer

Fig. 6-26 : model of DFE output  $u(k)$

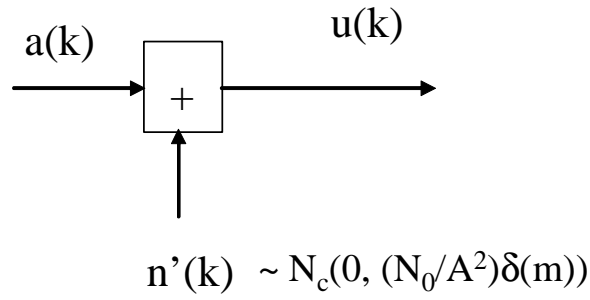
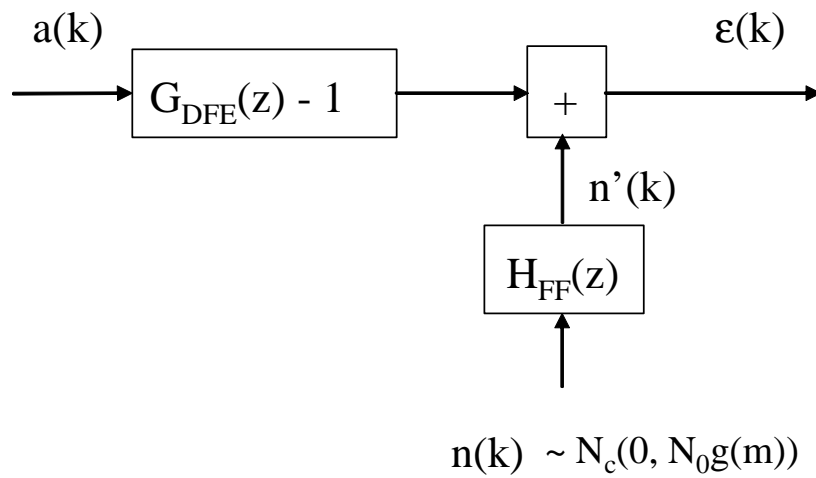
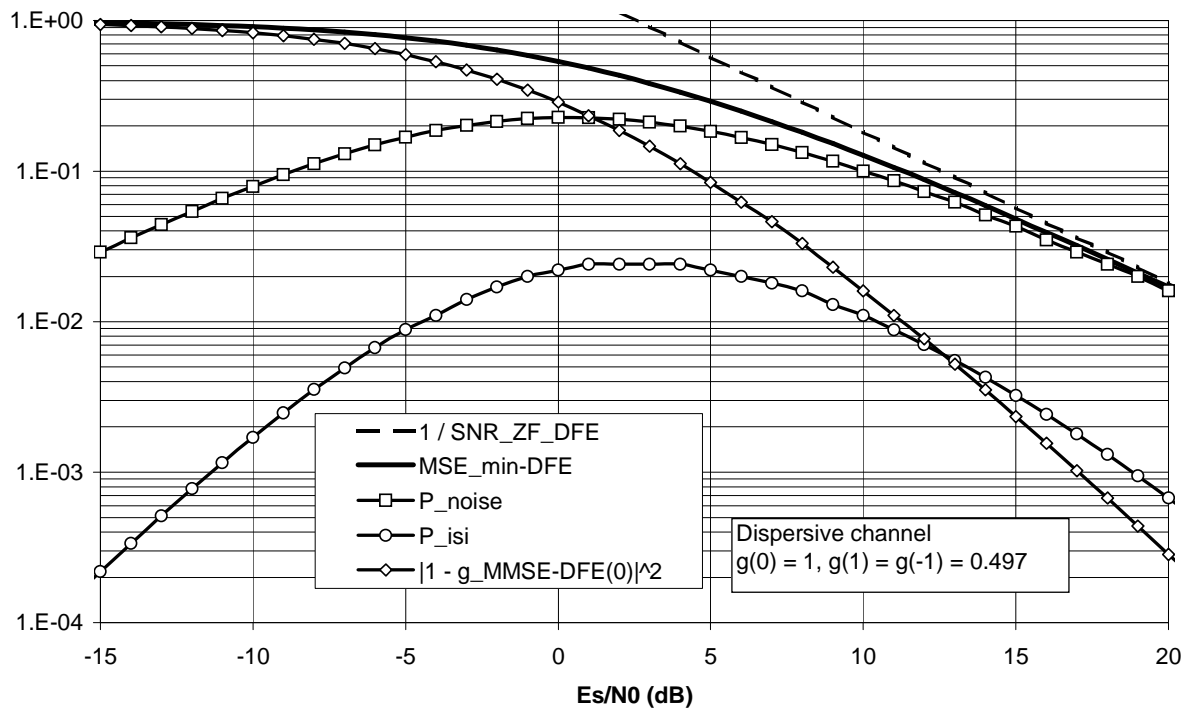


Fig. 6-27 : model for ZF-DFE

Fig. 6-28 : model for error signal  $\varepsilon(k)$ Fig. 6-29 : contributions to  $MSE_{\min-DFE}$

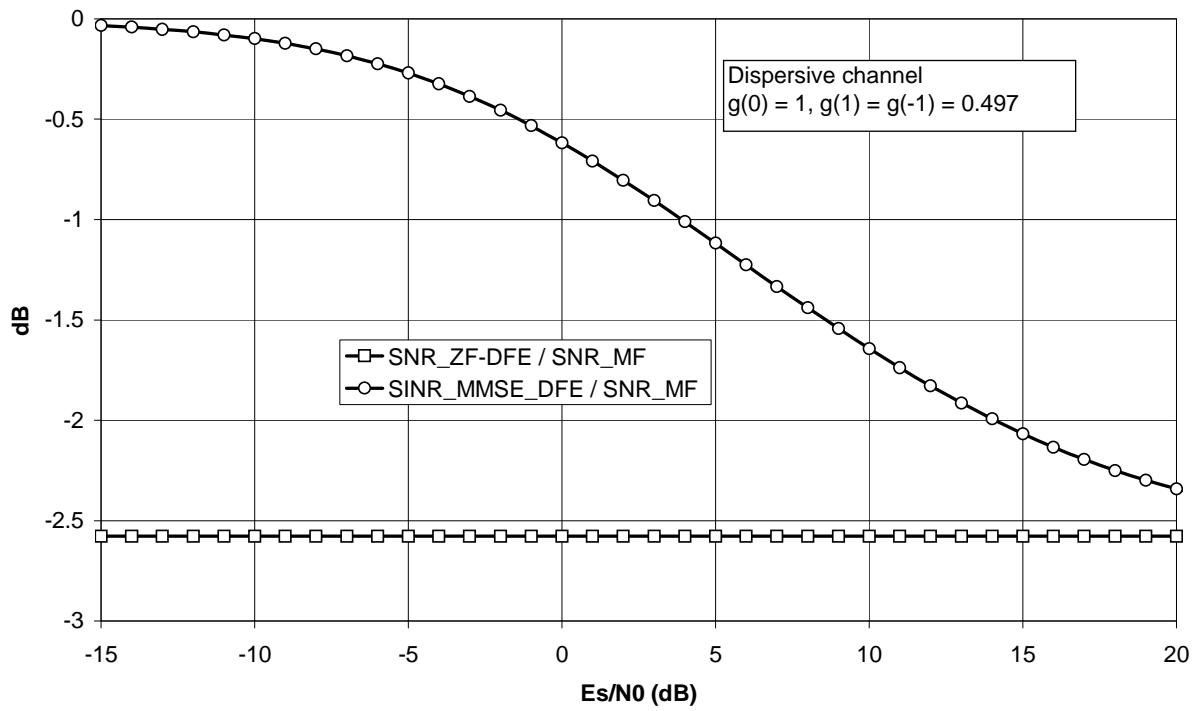
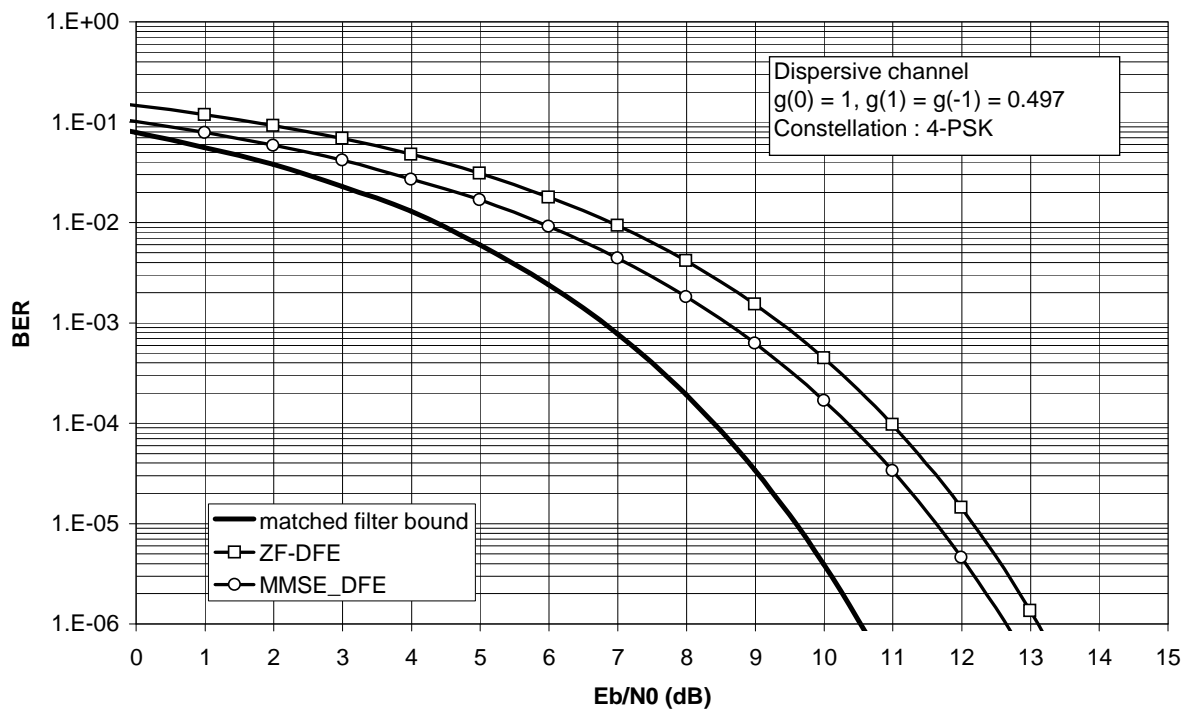
Fig. 6-30 : ratios  $\text{SNR}_{\text{ZF-DFE}}/\text{SNR}_{\text{MF}}$  and  $\text{SINR}_{\text{MMSE-DFE}}/\text{SNR}_{\text{MF}}$ 

Fig. 6-31 : BER performance

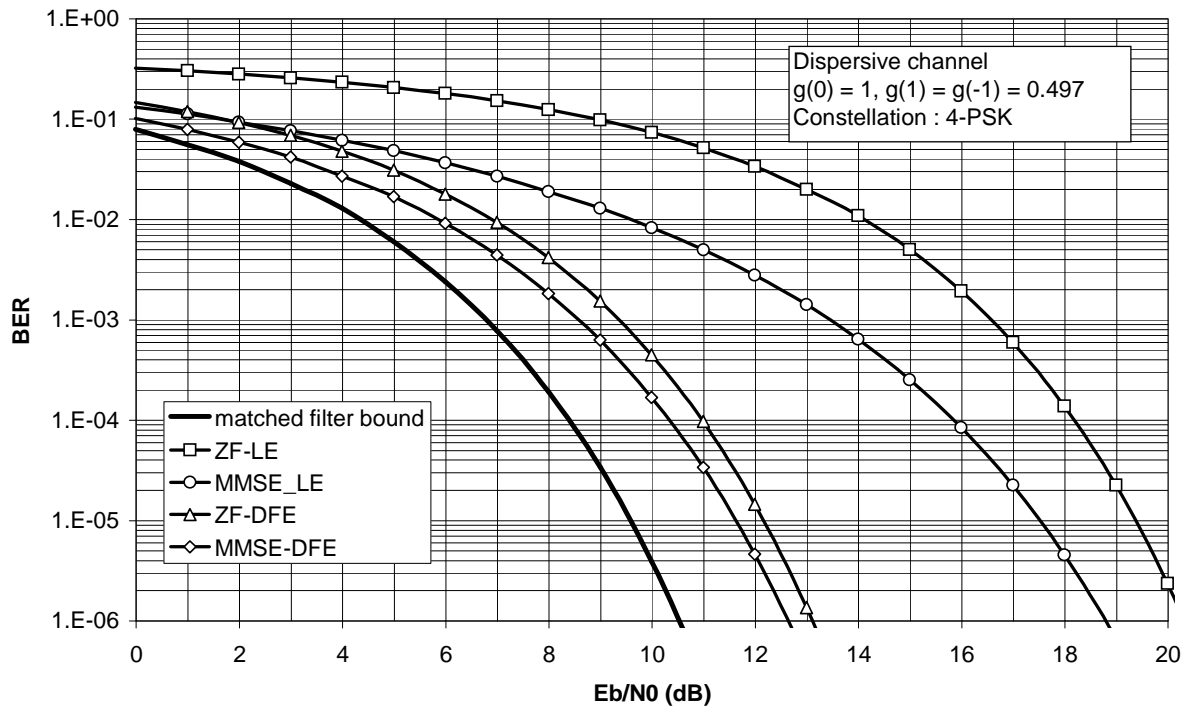


Fig. 6-32 : comparison of BER performances

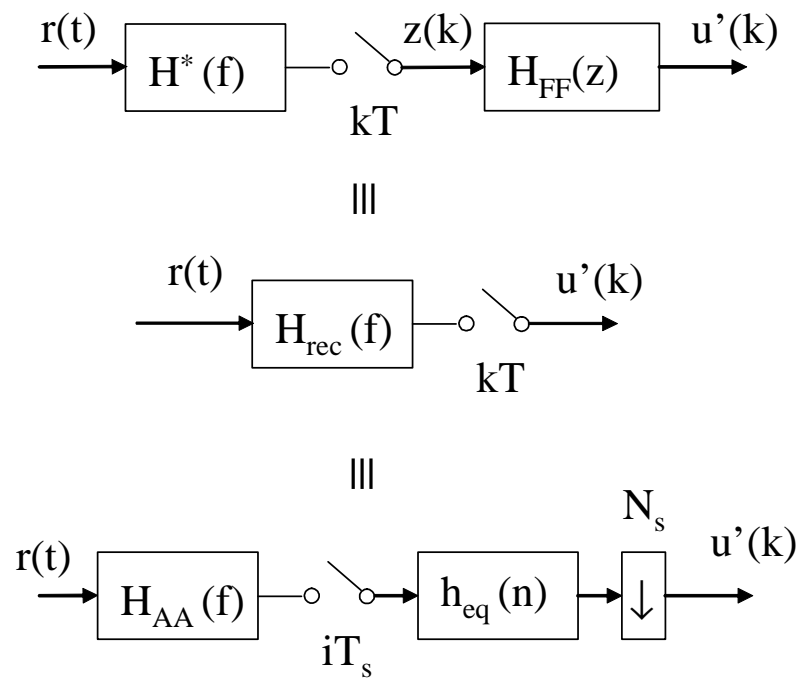


Fig. 6-33 : fractionally-spaced equalizer

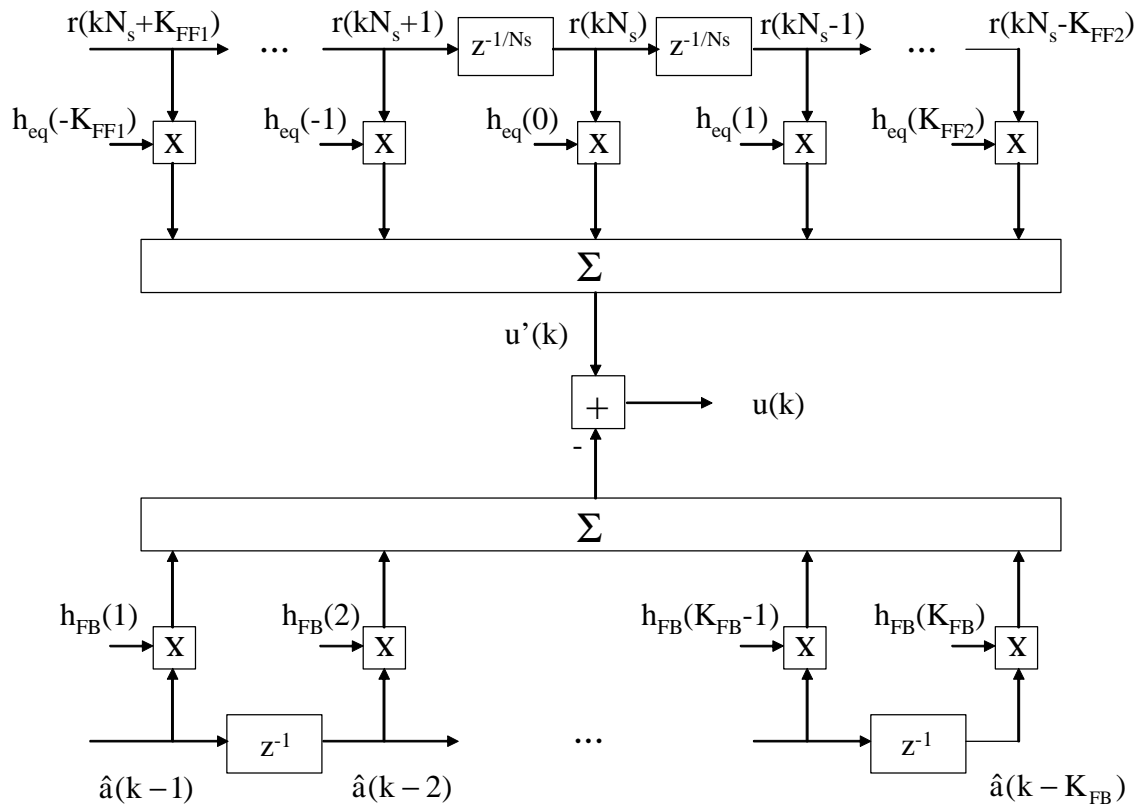


Fig. 6-34 : detail of the filters of the fractionally-spaced DFE  
( $z^{-1}$  : delay of  $T$ ;  $z^{-1/N_s}$  : delay of  $T_s$ )

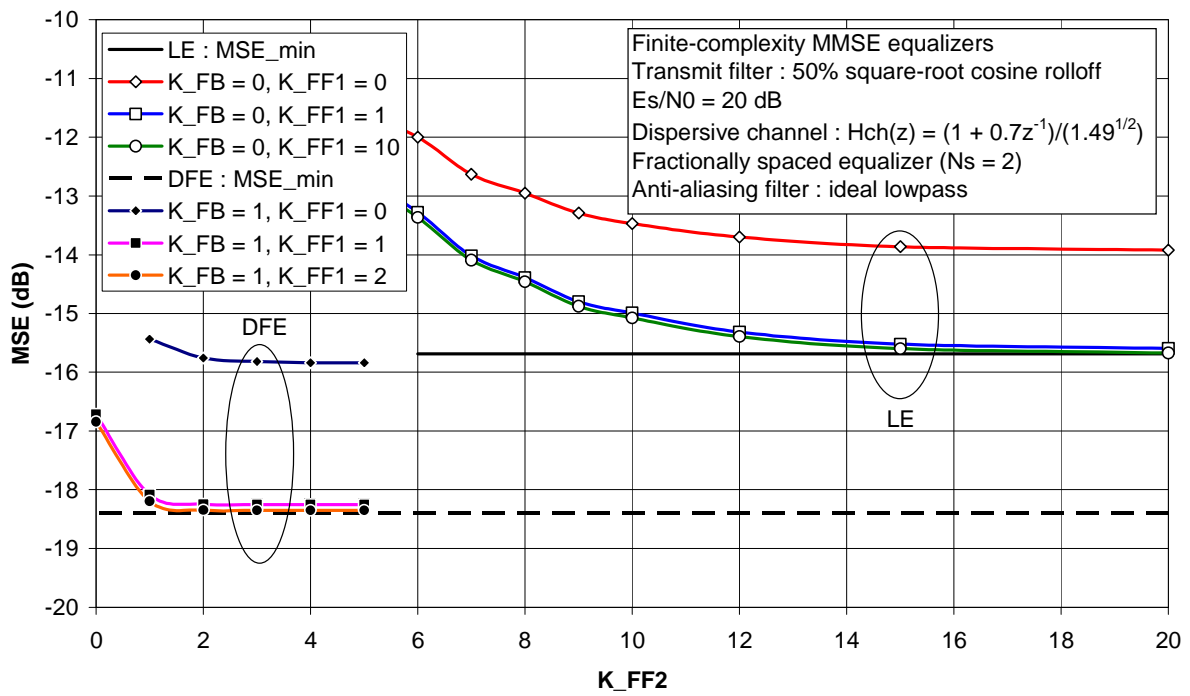


Fig. 6-35 : MSE performance of fractionally-spaced equalizers

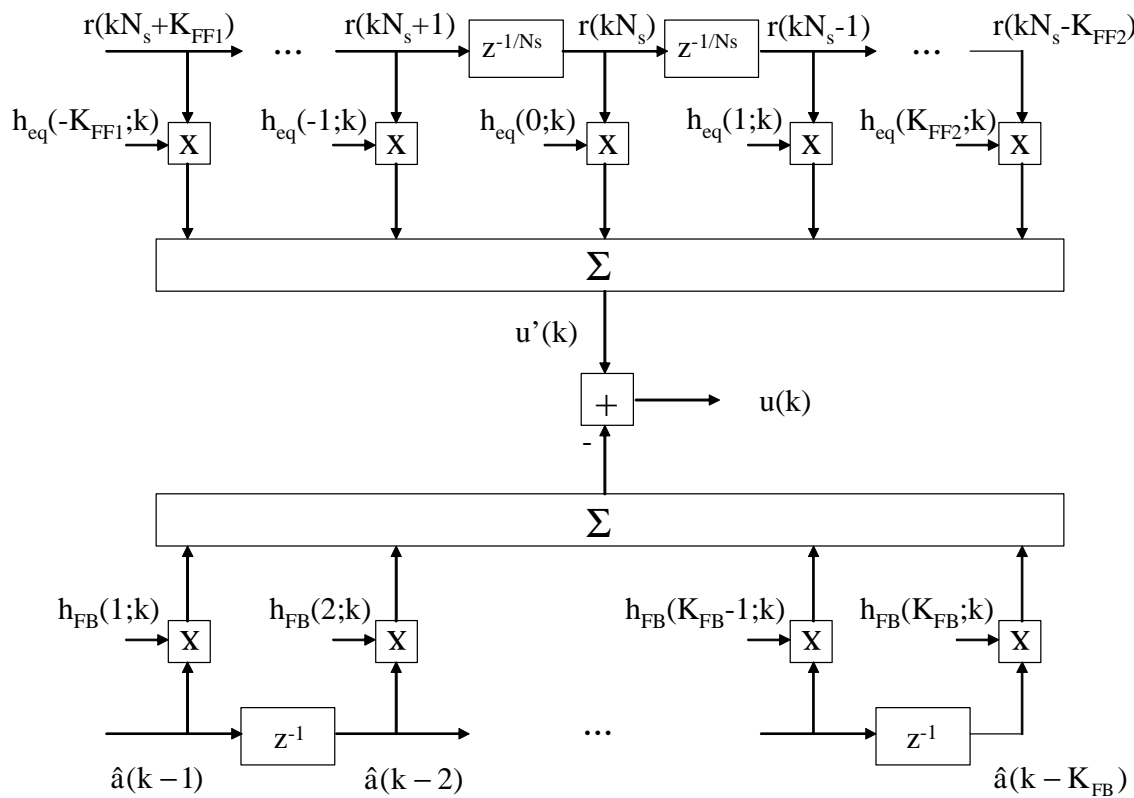


Fig. 6-36 : fractionally-spaced DFE with time-varying filters

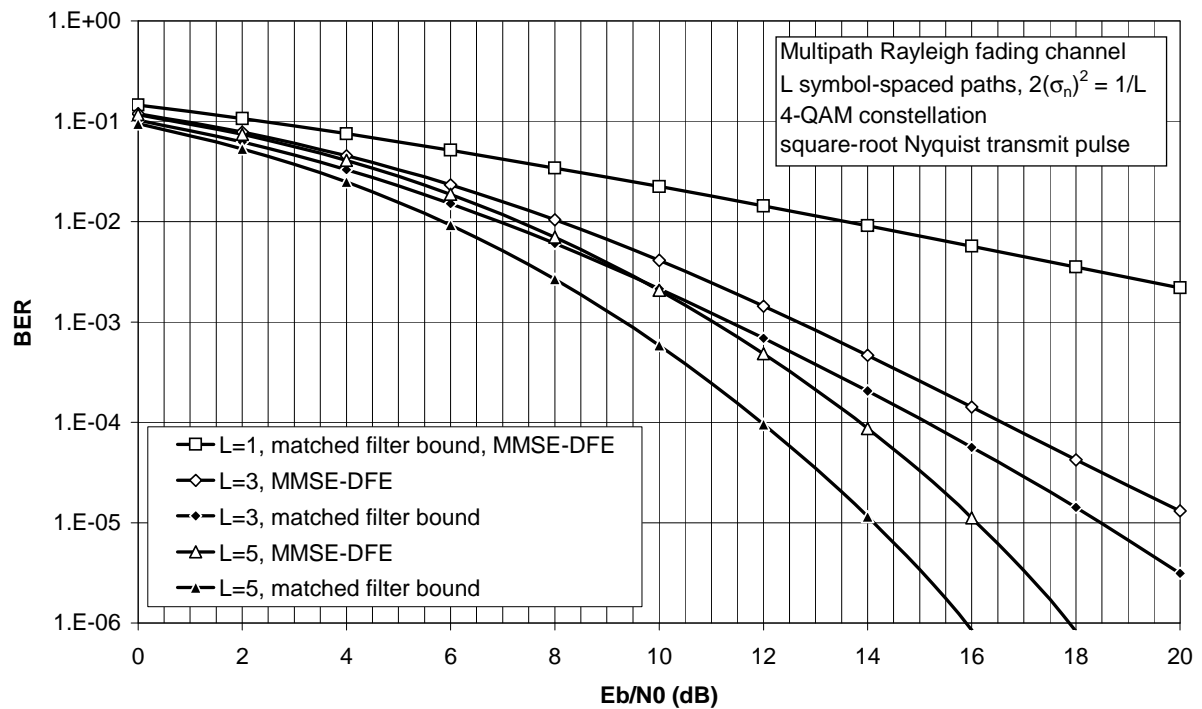


Fig. 6-37 : BER performance on multipath fading channels

# **Modulation and detection**

## **Chapter 7 : Spread-spectrum communication and CDMA**

---

Chapter 7 : Spread-spectrum communication and CDMA

1

### **Spread-spectrum point-to-point communication**

- AWGN channel
- Low detectability of signal presence
- Robustness against jamming
- Frequency-selective (fading) channel

### **Spread-spectrum multiuser communication : CDM(A)**

- AWGN channel, orthogonal CDM(A)
- Frequency-selective (fading) channel, multi-user interference
- Comparison of CDM(A) and TDM(A)

---

Chapter 7 : Spread-spectrum communication and CDMA

2

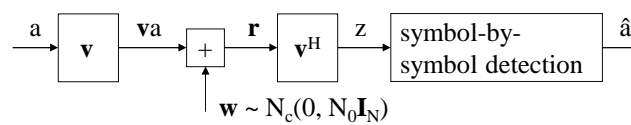


## Spread-spectrum / CDMA : Basic principles

Chapter 7 : Spread-spectrum communication and CDMA

3

### AWGN channel



Observation :  $\mathbf{r} = \mathbf{v}a + \mathbf{w}$

$$E[|a|^2] = E_s$$

$$\mathbf{v} = (v_1, \dots, v_N)^T$$

$$v_n = \frac{e^{j\phi_n}}{\sqrt{N}} \Rightarrow |v_n|^2 = 1/N \Rightarrow |\mathbf{v}|^2 = \mathbf{v}^H \mathbf{v} = 1$$

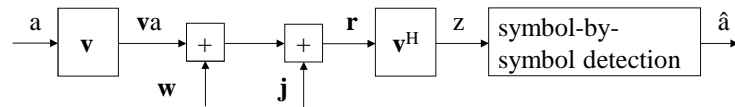
Sufficient statistic :  $z = \mathbf{v}^H \mathbf{r} = a + n$      $n = \mathbf{v}^H \mathbf{w} \sim N_c(0, N_0)$

SNR at input detector :  $\text{SNR} = E_s/N_0$

Chapter 7 : Spread-spectrum communication and CDMA

4

## AWGN channel + jamming



Observation :  $\mathbf{r} = \mathbf{v}a + \mathbf{w} + \mathbf{j}$

$\mathbf{j}$  : fixed-energy jamming signal,  $|\mathbf{j}|^2 = \mathbf{j}^H \mathbf{j} = E_j$

Suppose same receiver as for no jamming

Decision variable :  $z = \mathbf{v}^H \mathbf{r} = a + n + \mathbf{v}^H \mathbf{j}$      $n \sim N_c(0, N_0)$

## AWGN channel + jamming

Decision variable :  $z = \mathbf{v}^H \mathbf{r} = a + n + \mathbf{v}^H \mathbf{j}$      $n \sim N_c(0, N_0)$

BER performance depends on  $\mathbf{v}^H \mathbf{j}$  :

- best case :  $\mathbf{v}$  and  $\mathbf{j}$  orthogonal ( $\mathbf{v}^H \mathbf{j} = 0$ ) :  
jammer has no effect on  $z$
- worst case :  $\mathbf{v}$  and  $\mathbf{j}$  are parallel vectors  
 $\mathbf{j} = \sqrt{E_j} e^{j\theta} \mathbf{v}$      $\mathbf{v}^H \mathbf{j} = \sqrt{E_j} e^{j\theta}$   
 $\mathbf{v}^H \mathbf{j}$  has maximum possible energy  $E_j$  ( $|\mathbf{v}^H \mathbf{j}|^2 = E_j$ )  
 $z$  is affected by full jammer energy  $E_j$

## AWGN channel + jamming

Decision variable :  $z = \mathbf{v}^H \mathbf{r} = a + n + \mathbf{v}^H \mathbf{j}$      $n \sim N_c(0, N_0)$

Select  $\mathbf{v}$  *randomly* : components of  $\mathbf{v}$  are i.i.d. zero-mean RVs

with  $|\mathbf{v}_n|^2 = 1/N$ ,  $n = 1, \dots, N \Rightarrow E[\mathbf{v}\mathbf{v}^H] = (1/N)\mathbf{I}_N$

Suppose random  $\mathbf{v}$  is known to transmitter and receiver, but not to jammer

For given  $\mathbf{j}$ ,  $\mathbf{v}^H \mathbf{j}$  is a zero-mean RV, with

$$E[|\mathbf{v}^H \mathbf{j}|^2] = \mathbf{j}^H E[\mathbf{v}\mathbf{v}^H] \mathbf{j} = \frac{1}{N} \mathbf{j}^H \mathbf{j} = \frac{E_j}{N} \quad \text{inversely proportional to } N$$

SINR at detector input :

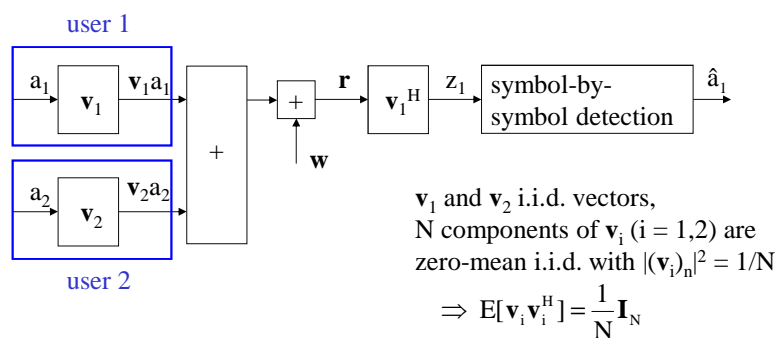
$$\text{SINR} = \frac{E_s}{N_0 + \frac{E_j}{N}} = \frac{1}{\frac{1}{\text{SNR}} + \frac{1}{N} \cdot \frac{1}{\text{SJR}}} \quad \begin{array}{l} \text{SNR} = E_s/N_0 \\ \text{SJR} = E_s/E_j \end{array} \quad \begin{array}{l} \text{signal-to-jammer} \\ \text{ratio} \end{array}$$

**Increasing  $N$  increases robustness against jamming !!**

Chapter 7 : Spread-spectrum communication and CDMA

7

## CDMA on AWGN channel



User 2 interferes with detection of user 1 (and vice versa)

Suppose same receiver as in the case where only user 1 is present

Detector input :  $z_1 = a_1 + \mathbf{v}_1^H \mathbf{v}_2 a_2 + n$     **multi-user interference**

Chapter 7 : Spread-spectrum communication and CDMA

8

## CDMA on AWGN channel

Detector input :  $z_1 = a_1 + \mathbf{v}_1^H \mathbf{v}_2 a_2 + n$

$\mathbf{v}_1^H \mathbf{v}_2 a_2$  is a zero-mean RV, with

$$\begin{aligned} E[|\mathbf{v}_1^H \mathbf{v}_2 a_2|^2] &= E[|a_2|^2 \mathbf{v}_1^H \mathbf{v}_2 \mathbf{v}_2^H \mathbf{v}_1] = E[|a_2|^2] E[\mathbf{v}_1^H \mathbf{v}_2 \mathbf{v}_2^H \mathbf{v}_1] \\ &= E_s E_{\mathbf{v}_1} [\mathbf{v}_1^H E_{\mathbf{v}_2} [\mathbf{v}_2 \mathbf{v}_2^H] \mathbf{v}_1] = \frac{E_s}{N} E_{\mathbf{v}_1} [\mathbf{v}_1^H \mathbf{v}_1] = \frac{E_s}{N} \end{aligned}$$

inversely proportional to N

SINR at detector input :

$$\text{SINR} = \frac{E_s}{N_0 + \frac{E_s}{N}} = \frac{1}{\frac{1}{\text{SNR}} + \frac{1}{N}}$$

increasing N increases robustness  
against multi-user interference

## CDMA on AWGN channel

Detector input :  $z_1 = a_1 + \mathbf{v}_1^H \mathbf{v}_2 a_2 + n$       interference =  $\mathbf{v}_1^H \mathbf{v}_2 a_2$

Example :

$$\mathbf{v}_1^H \mathbf{v}_2 a_2 = a_2 \sum_{n=1}^N (\mathbf{v}_1)_n^* (\mathbf{v}_2)_n$$

$a_2 \in \{-1, 1\}$  (2-PAM)

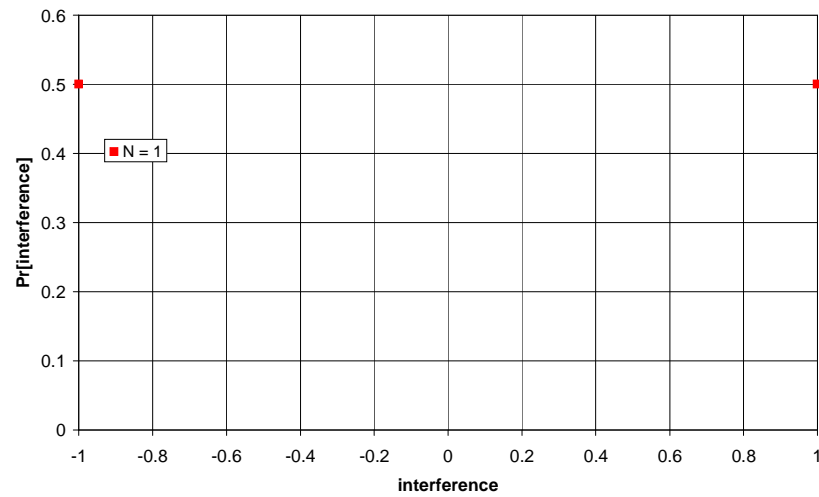
components of  $\mathbf{v}_1$  and  $\mathbf{v}_2$  are i.i.d., selected randomly from  $\{-1/\sqrt{N}, 1/\sqrt{N}\}$

when  $\mathbf{v}_1$  and  $\mathbf{v}_2$  differ in m components :  $\mathbf{v}_1^H \mathbf{v}_2 = (N - 2m)/N$

interference  $\mathbf{v}_1^H \mathbf{v}_2 a_2$  takes values from  $\{(N - 2m)/N; m = 0, \dots, N\}$

$$\Pr[\text{interference} = (N - 2m)/N] = \frac{2^{-N} N!}{m!(N - m)!} \quad (\text{binomial distribution})$$

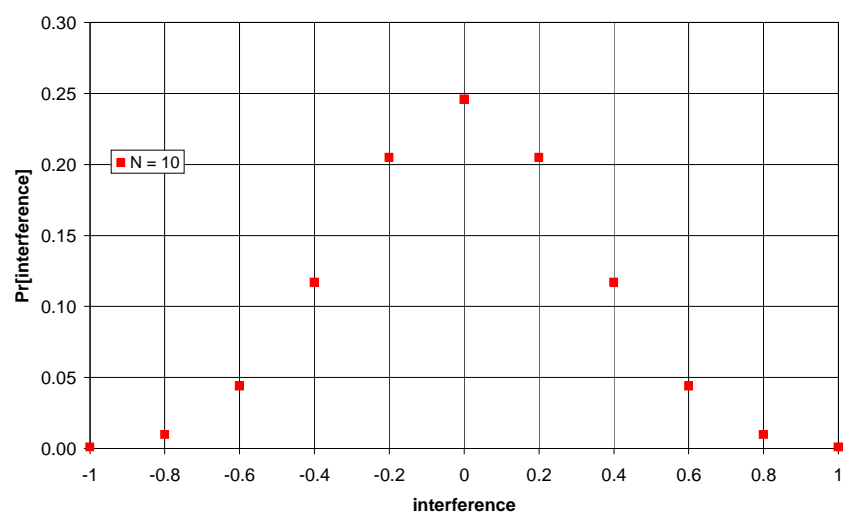
### CDMA on AWGN channel



Chapter 7 : Spread-spectrum communication and CDMA

11

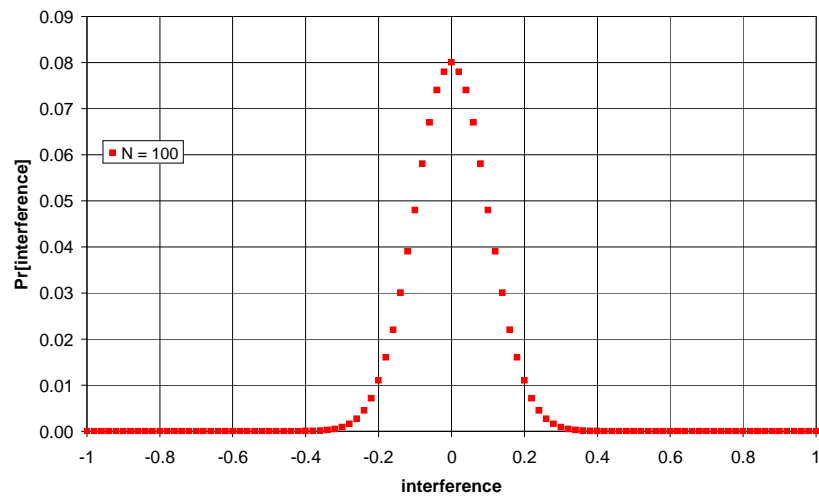
### CDMA on AWGN channel



Chapter 7 : Spread-spectrum communication and CDMA

12

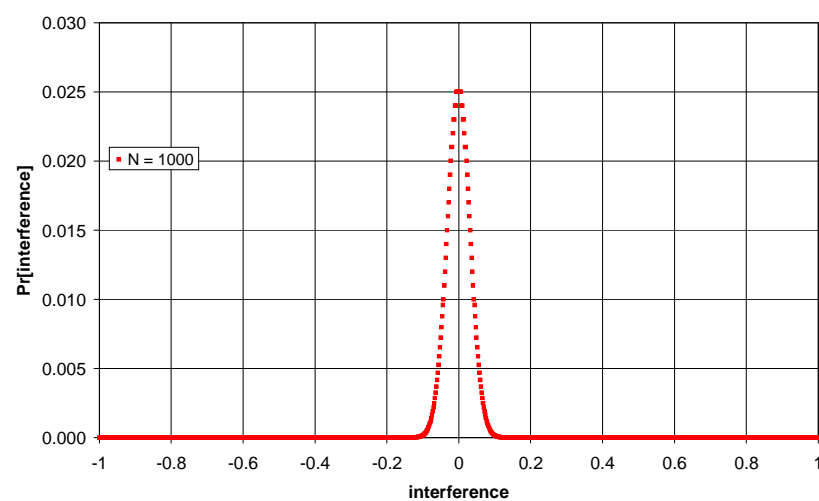
### CDMA on AWGN channel



Chapter 7 : Spread-spectrum communication and CDMA

13

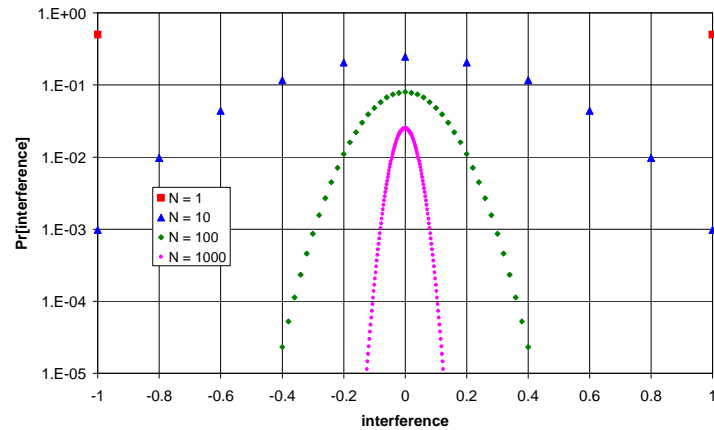
### CDMA on AWGN channel



Chapter 7 : Spread-spectrum communication and CDMA

14

## CDMA on AWGN channel



Large  $N$  :  $\log \Pr[\text{interference} = x] \approx A - Bx^2 \Rightarrow \Pr[\text{interference} = x] \approx C \cdot \exp(-Dx^2)$   
 $\Rightarrow$  interference approximately Gaussian

## Low detectability of signal presence

Signal presence detector based on *received energy* ( $\mathbf{v}$  is *not known* to detector)

**Signal present**  $\mathbf{r} = a\mathbf{v} + \mathbf{w}$   $\mathbf{w} \sim N_c(0, N_0 \mathbf{I}_N)$   $E[|a|^2] = E_s$   $|\mathbf{v}|^2 = 1$

received energy :  $E[|\mathbf{r}|^2] = E[|a|^2 |\mathbf{v}|^2] + E[|\mathbf{w}|^2] = E_s + N_0 N$

**Signal not present**  $\mathbf{r} = \mathbf{w}$  received energy :  $E[|\mathbf{r}|^2] = E[|\mathbf{w}|^2] = N_0 N$

**Energy ratio**  $\frac{E[|\mathbf{r}|^2]_{a \neq 0}}{E[|\mathbf{r}|^2]_{a=0}} = 1 + \frac{1}{N} \cdot \frac{E_s}{N_0} \approx 1$  when  $N \gg E_s/N_0$

If detector knows  $\mathbf{v}$ , signal presence detector is based on  $\mathbf{v}^H \mathbf{r}$

$\frac{E[|\mathbf{v}^H \mathbf{r}|^2]_{a \neq 0}}{E[|\mathbf{v}^H \mathbf{r}|^2]_{a=0}} = 1 + \frac{E_s}{N_0}$  much better performance than when  $\mathbf{v}$  is unknown

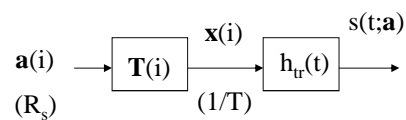
## Spread-spectrum transmitter

Chapter 7 : Spread-spectrum communication and CDMA

17

## Spread-spectrum modulation : special case of linear block modulation

### General linear block modulation



$$\begin{aligned} \mathbf{a}(i) &: N_s \times 1 \\ \mathbf{T}(i) &: N_t \times N_s \quad (N_t \geq N_s) \\ \mathbf{x}(i) &: N_t \times 1 \\ 1/T &= (N_t/N_s)R_s \geq R_s \end{aligned}$$

$$(\mathbf{x}(i))_m = x(iN_t + m) = \sum_{n=0}^{N_s-1} T_{m,n}(i) a_n(i) \quad m = 0, \dots, N_t-1$$

### Spread-spectrum modulation

$$N_s = 1$$

$$N_t = N \gg 1$$

$$\mathbf{a}(i) : \text{scalar} \quad \mathbf{T}(i) : N \times 1 \text{ (column vector)} \quad \mathbf{x}(i) : N \times 1 \quad 1/T = N \cdot R_s$$

$$\mathbf{T}(i) = \boldsymbol{\alpha}(i) = (\alpha(iN), \alpha(iN+1), \dots, \alpha(iN+N-1))^T \quad \{\alpha(k)\} : \text{chip sequence}$$

Chapter 7 : Spread-spectrum communication and CDMA

18



## Spread-spectrum modulation : special case of linear block modulation

$$\mathbf{x}(i) = \boldsymbol{\alpha}(i)\mathbf{a}(i) \quad \mathbf{x}(iN+m) = \boldsymbol{\alpha}(iN+m)\mathbf{a}(i) \quad m = 0, \dots, N-1 \quad i = 0, \dots, K-1$$

$$\mathbf{x} = (\dots, \mathbf{x}^T(i-1), \mathbf{x}^T(i), \mathbf{x}^T(i+1), \dots)^T \quad \mathbf{a} = (\dots, a(i-1), a(i), a(i+1), \dots)^T$$

$$\mathbf{x} = \mathbf{T}\mathbf{a} \quad \mathbf{x}(iN+m) = (\mathbf{T})_{iN+m,i}\mathbf{a}(i) \quad (\mathbf{T})_{iN+m,j} = \boldsymbol{\alpha}(iN+m)\delta_{i,j}$$

Example :  $N=2, I=3$

$$\begin{pmatrix} x(0) \\ x(1) \end{pmatrix} = \begin{pmatrix} \alpha(0) \\ \alpha(1) \end{pmatrix} a(0) = \boldsymbol{\alpha}(0)a(0)$$

$$\begin{pmatrix} x(2) \\ x(3) \end{pmatrix} = \begin{pmatrix} \alpha(2) \\ \alpha(3) \end{pmatrix} a(1) = \boldsymbol{\alpha}(1)a(1)$$

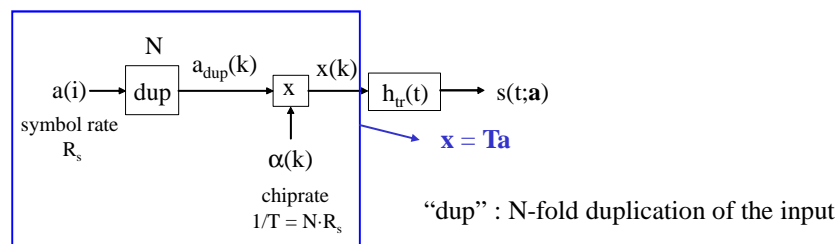
$$\begin{pmatrix} x(4) \\ x(5) \end{pmatrix} = \begin{pmatrix} \alpha(4) \\ \alpha(5) \end{pmatrix} a(2) = \boldsymbol{\alpha}(2)a(2)$$

$$\begin{pmatrix} x(0) \\ x(1) \\ x(2) \\ x(3) \\ x(4) \\ x(5) \end{pmatrix} = \underbrace{\begin{pmatrix} \alpha(0) & & & & & \\ \alpha(1) & & & & & \\ & \alpha(2) & & & & \\ & \alpha(3) & & & & \\ & & \alpha(4) & & & \\ & & \alpha(5) & & & \end{pmatrix}}_{\mathbf{T}} \begin{pmatrix} a(0) \\ a(1) \\ a(2) \end{pmatrix}$$

Chapter 7 : Spread-spectrum communication and CDMA

19

## Spread-spectrum transmitter



$$a_{\text{dup}}(k) = a(\lfloor k/N \rfloor) \quad \lfloor x \rfloor = \text{floor}(x) \quad a_{\text{dup}}(iN+m) = a(i) \quad m = 0, \dots, N-1$$

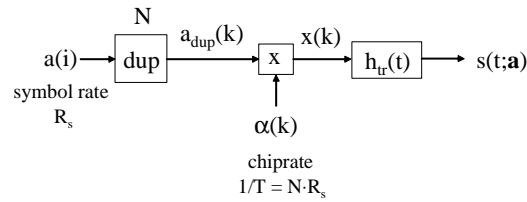
$$\mathbf{x}(iN+m) = \mathbf{a}(i)\boldsymbol{\alpha}(iN+m) \quad m = 0, \dots, N-1 \quad \mathbf{x}(k) = \mathbf{a}_{\text{dup}}(k)\boldsymbol{\alpha}(k)$$

$$\text{transmitted signal : } s(t; \mathbf{a}) = \sum_k \mathbf{x}(k)h_{tr}(t - kT)$$

Chapter 7 : Spread-spectrum communication and CDMA

20

## Spread-spectrum transmitter



$a(i)$  :  $i$ -th symbol ( $E[|a(i)|^2] = E_s$ )

$\alpha(iN+m)$  :  $m$ -th chip in  $i$ -th symbol interval ( $m = 0, \dots, N-1$ )

symbol rate :  $R_s$ , chip rate :  $1/T = N \cdot R_s$

$h_{tr}(t)$  : chip pulse

symbol  $a(i) \rightarrow N$  pulses  $\{x(iN+m)h_{tr}(t-(iN+m)T), m = 0, \dots, N-1\}$

## Chip sequence

$\{\alpha(k)\}$  consists of i.i.d. chips, known to both transmitter and receiver

Real-valued chips

values of  $\alpha(k)$  are equiprobable, taken from  $\{-1/\sqrt{N}, 1/\sqrt{N}\}$

$$\Rightarrow |\alpha(k)|^2 = 1/N, E[\alpha(k)] = 0, E[\alpha(k+m)\alpha(k)] = (1/N)\delta(m)$$

Complex-valued chips  $\alpha(k) = \alpha_R(k) + j\alpha_I(k)$

$\alpha_R(k)$  and  $\alpha_I(k)$  are i.i.d.

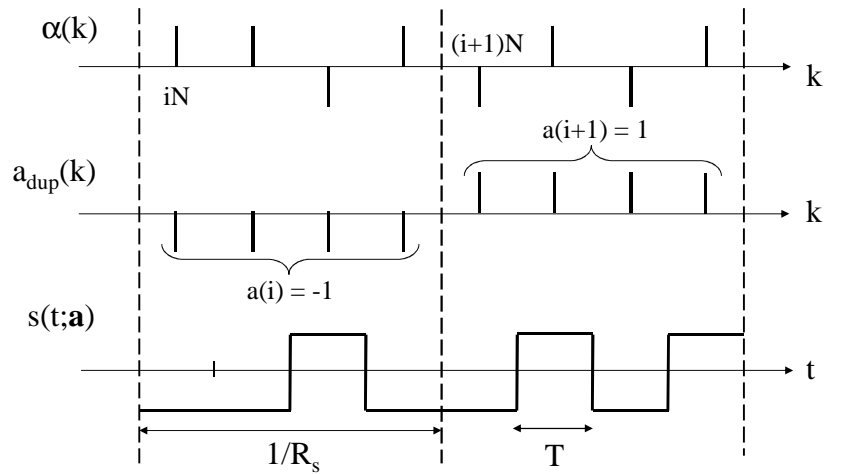
values of  $\alpha_R(k)$  and  $\alpha_I(k)$  are equiprobable, taken from  $\{-1/\sqrt{2N}, 1/\sqrt{2N}\}$

$$\Rightarrow |\alpha(k)|^2 = 1/N, E[\alpha(k)] = 0, E[\alpha(k+m)\alpha^*(k)] = (1/N)\delta(m)$$

$$\Rightarrow E[\alpha(k+m)\alpha(k)] = 0$$

### Example

$N = 4$ ,  $a(i) \in \{-1, 1\}$ ,  $\alpha(k) \in \{-1/\sqrt{N}, 1/\sqrt{N}\}$ , rectangular  $h_{tr}(t)$  of duration  $T$



Chapter 7 : Spread-spectrum communication and CDMA

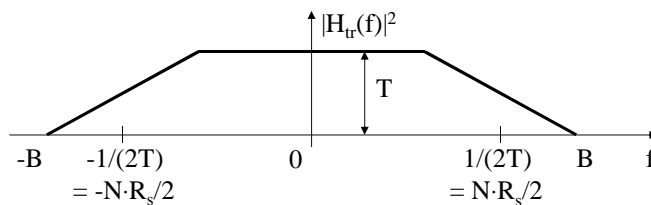
23

### Orthogonality condition on chip pulse

As in general linear block modulation, we impose orthogonality condition on chip pulse ( $h_{tr}(t)$  must be square-root Nyquist pulse) :

$$\int h_{tr}^*(t - kT) h_{tr}(t) dt = \delta(k) \Leftrightarrow \{|H_{tr}(f)|^2; 1/T\}_{fld} = 1$$

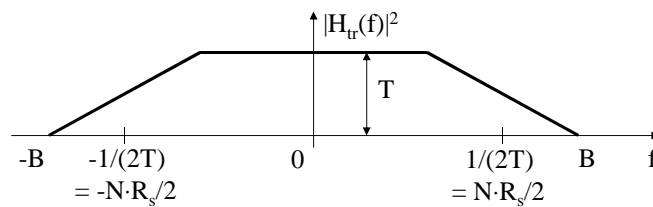
Assume  $H_{tr}(f) = 0$  for  $|f| > B \Rightarrow B \geq 1/(2T) = N \cdot R_s/2$   
 (necessary condition for orthogonality)



Chapter 7 : Spread-spectrum communication and CDMA

24

## Orthogonality condition on chip pulse



Assume  $N \gg 1 \Rightarrow B > N \cdot R_s/2 \gg R_s/2$  :

For given  $R_s$ , increasing  $N$  increases the bandwidth of the chip pulse

→ “**spread-spectrum**” modulation,

as opposed to bandwidth-efficient modulation ( $R_s/2 < B < R_s$ )

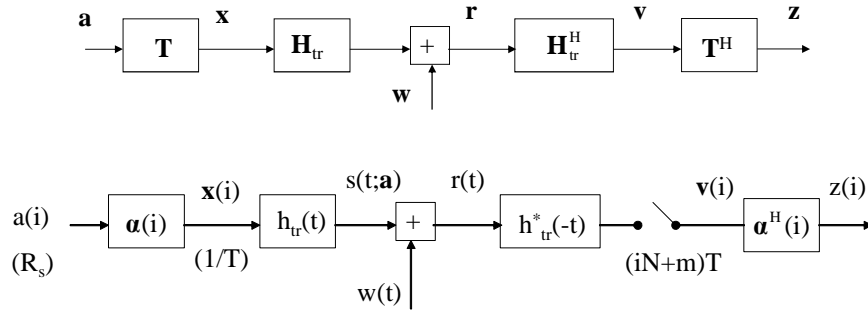
$N$  : spreading factor       $\{\alpha(k)\}$  : chip sequence, spreading sequence

Selecting  $N = 1$  and  $\alpha(k) = 1$  for all  $k$  yields conventional linear modulation :

$$s(t; \mathbf{a}) = \sum_i a(i) h_{tr}(t - iT) \quad R_s = 1/T \quad B > R_s/2$$

## Spread-spectrum communication on AWGN channel

### Sufficient statistic $\{z(i)\}$



$$(\alpha(i))_m = \alpha(iN + m) \quad (\mathbf{v}(i))_m = \mathbf{v}(iN + m)$$

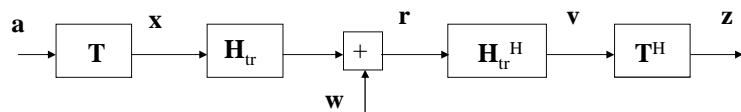
$$z(i) = \alpha^H(i) \mathbf{v}(i) = \sum_{m=0}^{N-1} \alpha^*(iN + m) v(iN + m) = \sum_{k=iN}^{iN+N-1} \alpha^*(k) v(k)$$

Chapter 7 : Spread-spectrum communication and CDMA

27

### Model for $\{z(i)\}$

General case of linear block modulation



$$\left. \begin{array}{l} \mathbf{H}_t^H \mathbf{H}_t = \mathbf{I} \text{ (orthogonal transmit pulses)} \\ \mathbf{T}^H \mathbf{T} = \mathbf{I} \end{array} \right\} \begin{array}{l} \mathbf{z} = \mathbf{a} + \mathbf{n} \\ \mathbf{n} = \mathbf{T}^H \mathbf{H}_t^H \mathbf{w} \sim N_c(0, N_0 \mathbf{I}) \end{array}$$

symbol-by-symbol decision is optimum

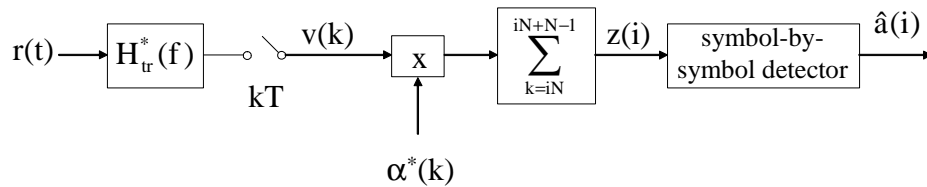
BER performance equals matched filter bound :

$$\text{BER} = \text{BER}_c \left( \frac{E_s}{N_0} \right) \quad \left( \begin{array}{l} \text{same as conventional modulation} \\ \text{with orthogonal pulses on AWGN channel} \end{array} \right)$$

Chapter 7 : Spread-spectrum communication and CDMA

28

## Spread spectrum : ML receiver

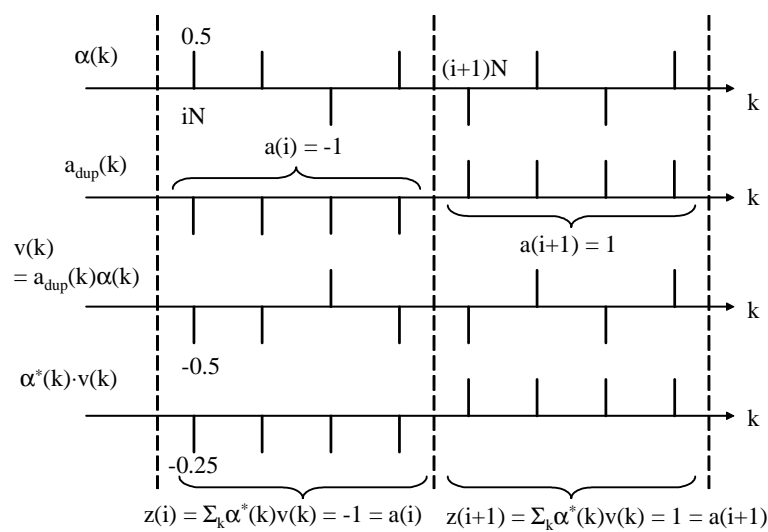


$H_{tr}^*(f)$  : filter matched to chip pulse  $h_{tr}(t)$

$$z(i) = \sum_{k=iN}^{(i+1)N-1} \alpha^*(k) v(k) \quad v(k) = \int r(t) h_{tr}^*(t - kT) dt$$

$$z(i) = a(i) + n(i) \quad n(i) \sim N_c(0, N_0 \delta(m)) \quad \text{irrespective of } N$$

## Example : $N = 4$ , no noise



## Benefits of spread-spectrum

Using spread-spectrum for point-to-point communication over the *AWGN channel* provides *no BER advantage* over conventional bandwidth-efficient modulation : the BER performance is the same, but for given symbol rate the occupied bandwidth is *much larger*.

Benefits of spread-spectrum (compared to bandwidth-efficient modulation) are :

- low detectability of the presence of a spread-spectrum signal by a receiver that does not know the spreading sequence
- robustness against narrowband interference and channel dispersion

These benefits are achieved when the spreading sequence behaves like a sequence of zero-mean i.i.d. chips (or “pseudo-noise” sequence, see later).

Several of these advantages are interesting mainly in a *military* context. Actually, the first applications of spread-spectrum were military.

## Low detectability of signal presence

We model the spreading sequence  $\{\alpha(k)\}$  as a sequence of i.i.d. zero-mean chips with variance  $1/N$ , statistically independent of the data symbols  $\{a(i)\}$ . Spreading sequence  $\{\alpha(k)\}$  is known to both transmitter and receiver.

Transmitted signal

$$s(t; \mathbf{a}) = \sum_k x(k) h_{tr}(t - kT) \quad x(k) = a_{dup}(k) \alpha(k)$$

$$\begin{aligned} E[x(k+m)x^*(k)] &= E[a_{dup}(k+m)a_{dup}^*(k)]E[\alpha(k+m)\alpha^*(k)] \\ &= E[|a_{dup}(k)|^2](1/N)\delta(m) \\ &= (E_s/N) \delta(m) \end{aligned}$$

$\Rightarrow$  quantities  $\{x(k)\}$  are uncorrelated

$\Rightarrow$  computation of power spectrum of  $s(t; \mathbf{a})$  is simple

$s(t; \mathbf{a})$  is a sum of uncorrelated terms

$\Rightarrow$  power spectrum of  $s(t; \mathbf{a})$  is  $1/T$  times the average energy spectrum of the individual terms

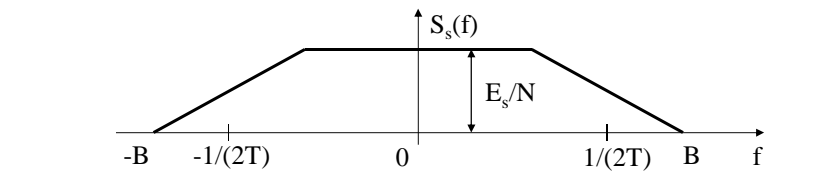
## Low detectability of signal presence

$$s(t; \mathbf{a}) = \sum_k x(k) h_{tr}(t - kT) \quad E[x(k+m)x^*(k)] = (E_s/N)\delta(m)$$

Energy spectrum of k-th term :  $E[|x(k)|^2]|H_{tr}(f)|^2 = (E_s/N) |H_{tr}(f)|^2$  (independent of k)

Power spectrum : 
$$S_s(f) = \frac{E_s |H_{tr}(f)|^2}{NT} \leq \frac{E_s}{N} \quad (|H_{tr}(f)|^2 \leq T)$$

Power : 
$$\int S_s(f) df = \frac{E_s}{N} \cdot \frac{1}{T} = E_s R_s$$



Chapter 7 : Spread-spectrum communication and CDMA

33

## Low detectability of signal presence

Enemy receiver (which does not know the spreading sequence) wants to detect the presence of  $s(t; \mathbf{a})$  by means of *power measurement*

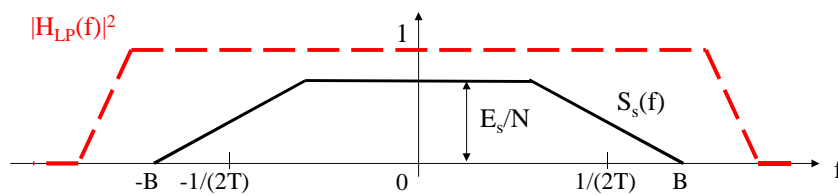
$$r(t) = s(t; \mathbf{a}) + w(t) \quad w(t) \sim N_c(0, N_0\delta(u))$$

- no signal present :

$$w(t) \longrightarrow \boxed{H_{LP}(f)} \longrightarrow \text{power}_0 = P_{\text{noise}} > 2N_0B$$

- signal present :

$$s(t; \mathbf{a}) + w(t) \longrightarrow \boxed{H_{LP}(f)} \longrightarrow \text{power}_1 = P_{\text{noise}} + E_s R_s$$



Chapter 7 : Spread-spectrum communication and CDMA

34



### Low detectability of signal presence

$$w(t) \longrightarrow \boxed{H_{LP}(f)} \longrightarrow \text{power}_0 = P_{\text{noise}} > 2N_0B$$

$$s(t;\mathbf{a}) + w(t) \longrightarrow \boxed{H_{LP}(f)} \longrightarrow \text{power}_1 = P_{\text{noise}} + E_s R_s$$

$$1 < \frac{\text{power}_1}{\text{power}_0} = 1 + \frac{E_s R_s}{P_{\text{noise}}} \leq 1 + \frac{E_s}{N_0} \cdot \frac{R_s}{2B} \leq 1 + \frac{1}{N} \left( \frac{E_s}{N_0} \right) \Rightarrow \frac{\text{power}_1}{\text{power}_0} \approx 1 \text{ when } N \gg E_s/N_0$$

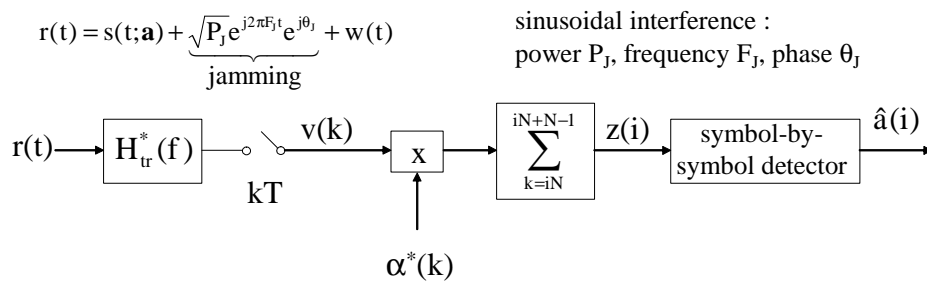
$(P_{\text{noise}} \geq 2N_0B)$

$(2B \geq N \cdot R_s)$

$\Rightarrow$  Presence of  $s(t;\mathbf{a})$  is hard to detect by simple power measurement when  $N \gg E_s/N_0$   
 Under the condition  $N \gg E_s/N_0$ , level of useful signal spectrum ( $E_s/N$ ) is far below noise spectrum ( $N_0$ ).

However, this low spectral density does **not** affect BER performance on AWGN channel (receiver knows spreading sequence), which depends only on  $E_s/N_0$  :  
 $\text{BER} = \text{BER}_C(E_s/N_0)$

### Robustness against narrowband interference (“jamming”)



$$v(k) = a_{\text{dup}}(k)\alpha(k) + J_v(k) + n_v(k) \quad J_v(k) = \sqrt{P_j} H_{tr}^*(F_j) e^{j\theta_j} e^{j2\pi F_j kT}$$

input symbol-by-symbol detector :  $z(i) = a(i) + J(i) + w(i)$

contribution from jammer :  $J(i) = \sqrt{P_j} H_{tr}^*(F_j) e^{j\theta_j} \sum_{k=iN}^{iN+N-1} \alpha^*(k) e^{j2\pi F_j kT}$

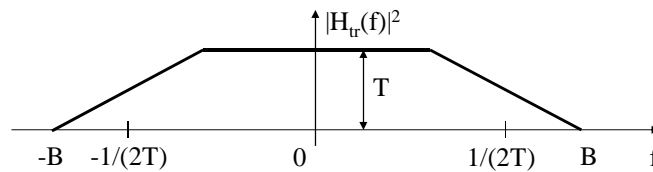
## Robustness against narrowband interference (“jamming”)

input symbol-by-symbol detector :  $z(i) = a(i) + J(i) + w(i)$

$$J(i) = \sqrt{P_j} H_{tr}^*(F_j) e^{j\theta_j} \sum_{k=iN}^{iN+N-1} \alpha^*(k) e^{j2\pi F_j k T} \quad \{\alpha(k)\} : \text{i.i.d. chips, } E[|\alpha(k)|^2] = 1/N$$

$J(i)$  : sum of statistically independent contributions

$$E[|J(i)|^2] = P_j |H_{tr}(F_j)|^2 \frac{N}{N} = P_j |H_{tr}(F_j)|^2 \leq P_j T = \frac{P_j}{NR_s}$$



Chapter 7 : Spread-spectrum communication and CDMA

37

## Robustness against narrowband interference (“jamming”)

input symbol-by-symbol detector :  $z(i) = a(i) + J(i) + w(i)$

$$E[|a(i)|^2] = E_s \quad E[|w(i)|^2] = N_0 \quad E[|J(i)|^2] \leq P_j T = \frac{P_j}{NR_s}$$

$$\text{SINR} \geq \frac{E_s}{N_0 + \frac{P_j}{NR_s}} = \left( \frac{N_0}{E_s} + \frac{P_j}{P_s} \cdot \frac{1}{N} \right)^{-1} \quad \begin{array}{l} P_s = E_s R_s \text{ (useful signal power in } r(t)) \\ P_j : \text{ jammer power in } r(t) \end{array}$$

Receiver is virtually unaffected by the sinusoidal interference when

$$N \gg \frac{E_s}{N_0} \cdot \frac{P_j}{P_s} = \frac{P_j}{N_0 R_s} \quad \Rightarrow \text{SINR} \approx E_s / N_0$$

Robustness against jamming increases with increasing spreading factor  $N$   
(at the expense of increasing signal bandwidth for given  $R_s$ )

Chapter 7 : Spread-spectrum communication and CDMA

38

## Real-valued or complex-valued chips ?

Assume jamming with  $F_j NT \ll 1$  (i.e.,  $F_j/R_s \ll 1$ )

$$J(i) = \sqrt{P_j} H_{tr}^*(F_j) e^{j\theta_j} \sum_{k=iN}^{iN+N-1} \alpha^*(k) e^{j2\pi F_j k T} \quad e^{j2\pi F_j k T} \approx e^{j2\pi(i+\frac{1}{2})F_j NT} \quad k = iN, \dots, iN + N - 1$$

$$\approx \sqrt{P_j T} e^{j\theta(i)} \sum_{k=iN}^{iN+N-1} \alpha^*(k) \quad \theta(i) = \theta_j + 2\pi(i + \frac{1}{2})F_j NT$$

We decompose  $J(i)$  into its real and imaginary parts :  $J(i) = J_R(i) + jJ_I(i)$

$$J_R(i) \approx \sqrt{P_j T} \left( \cos(\theta(i)) \sum_{k=iN}^{iN+N-1} \alpha_R(k) + \sin(\theta(i)) \sum_{k=iN}^{iN+N-1} \alpha_I(k) \right)$$

$$J_I(i) \approx \sqrt{P_j T} \left( \sin(\theta(i)) \sum_{k=iN}^{iN+N-1} \alpha_R(k) - \cos(\theta(i)) \sum_{k=iN}^{iN+N-1} \alpha_I(k) \right)$$

where  $\alpha(k) = \alpha_R(k) + j\alpha_I(k)$

## Real-valued or complex-valued chips ?

$$J_R(i) \approx \sqrt{P_j T} \left( \cos(\theta(i)) \sum_{k=iN}^{iN+N-1} \alpha_R(k) + \sin(\theta(i)) \sum_{k=iN}^{iN+N-1} \alpha_I(k) \right)$$

$$J_I(i) \approx \sqrt{P_j T} \left( \sin(\theta(i)) \sum_{k=iN}^{iN+N-1} \alpha_R(k) - \cos(\theta(i)) \sum_{k=iN}^{iN+N-1} \alpha_I(k) \right)$$

**Real-valued chips :**

$\alpha_I(k) = 0$ , all  $k$

$\{\alpha_R(k)\}$  : sequence of i.i.d. RVs with  $|\alpha_R(k)|^2 = 1/N$

For given  $i$  :  $E[J_R^2(i)] = P_j T \cos^2(\theta(i))$   $E[J_I^2(i)] = P_j T \sin^2(\theta(i))$

In-phase and quadrature interference powers each range between 0 and  $P_j T$ , depending on symbol index  $i$ .

Their sum equals  $P_j T$ , independently of symbol index  $i$ .

## Real-valued or complex-valued chips ?

$$J_R(i) \approx \sqrt{P_J T} \left( \cos(\theta(i)) \sum_{k=iN}^{iN+N-1} \alpha_R(k) + \sin(\theta(i)) \sum_{k=iN}^{iN+N-1} \alpha_I(k) \right)$$

$$J_I(i) \approx \sqrt{P_J T} \left( \sin(\theta(i)) \sum_{k=iN}^{iN+N-1} \alpha_R(k) - \cos(\theta(i)) \sum_{k=iN}^{iN+N-1} \alpha_I(k) \right)$$

### Complex-valued chips :

$\{\alpha_R(k)\}, \{\alpha_I(k)\}$  : independent sequences of i.i.d. RVs  
with  $|\alpha_R(k)|^2 = |\alpha_I(k)|^2 = 1/(2N)$

For given  $i$  :  $E[J_R^2(i)] = E[J_I^2(i)] = \frac{P_J T}{2}$        $E[J_R(i)J_I(i)] = 0$

In-phase and quadrature interference terms are uncorrelated,  
and both have power equal to  $P_J T/2$ , irrespective of symbol index  $i$

## Real-valued or complex-valued chips ? BER performance for 4-QAM

$$E_s = 2E_b$$

$$z_R(i) = a_R(i) + J_R(i) + w_R(i) \quad z_I(i) = a_I(i) + J_I(i) + w_I(i)$$

$$a_R(i), a_I(i) \in \{-\sqrt{E_b}, \sqrt{E_b}\} \quad E[|w_R(i)|^2] = E[|w_I(i)|^2] = N_0/2$$

$$\hat{a}_R(i) = \sqrt{E_b} \operatorname{sgn}(z_R(i)) \quad \hat{a}_I(i) = \sqrt{E_b} \operatorname{sgn}(z_I(i))$$

$$\text{BER}(i) = \frac{1}{2} \Pr[\hat{a}_R(i) \neq a_R(i)] + \frac{1}{2} \Pr[\hat{a}_I(i) \neq a_I(i)]$$

Assume  $J_R(i)$  and  $J_I(i)$  are Gaussian (sums of large number of i.i.d. terms)

$$\text{BER}(i) = \frac{1}{2} Q\left(\sqrt{\frac{E_b}{(N_0/2) + E[J_R^2(i)]}}\right) + \frac{1}{2} Q\left(\sqrt{\frac{E_b}{(N_0/2) + E[J_I^2(i)]}}\right)$$

### Real-valued or complex-valued chips ? BER performance for 4-QAM

$$\text{BER}(i) = \frac{1}{2} Q \left( \sqrt{\frac{E_b}{(N_0/2) + E[J_R^2(i)]}} \right) + \frac{1}{2} Q \left( \sqrt{\frac{E_b}{(N_0/2) + E[J_I^2(i)]}} \right)$$

**complex-valued chips :**  $E[J_R^2(i)] = E[J_I^2(i)] = \frac{P_J T}{2}$

$$\text{BER}(i) = Q \left( \sqrt{\left( \frac{N_0}{2E_b} + \frac{P_J}{NP_s} \right)^{-1}} \right) \quad P_s = E_s R_s = E_s / (NT) = 2E_b / (NT)$$

useful signal power at receiver input

BER(i) independent of symbol index i

Average BER (averaged over symbol index) :  $\text{BER} = Q \left( \sqrt{\left( \frac{N_0}{2E_b} + \frac{P_J}{NP_s} \right)^{-1}} \right)$

### Real-valued or complex-valued chips ? BER performance for 4-QAM

$$\text{BER}(i) = \frac{1}{2} Q \left( \sqrt{\frac{E_b}{(N_0/2) + E[J_R^2(i)]}} \right) + \frac{1}{2} Q \left( \sqrt{\frac{E_b}{(N_0/2) + E[J_I^2(i)]}} \right)$$

**real-valued chips :**  $E[J_R^2(i)] = P_J T \cos^2(\theta(i))$   $E[J_I^2(i)] = P_J T \sin^2(\theta(i))$

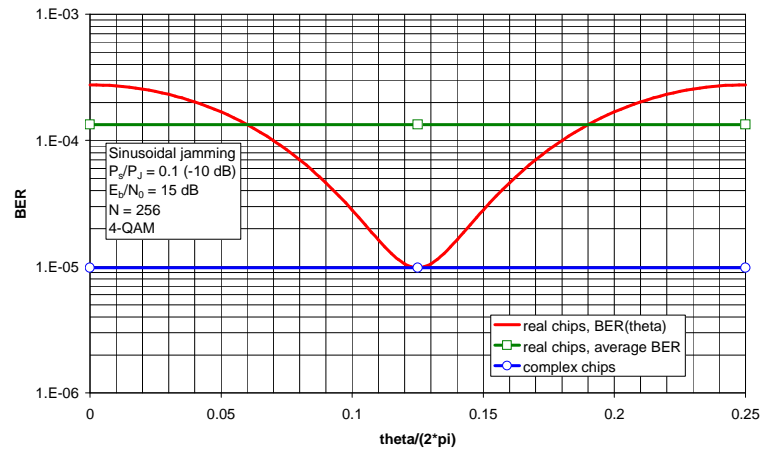
$$\text{BER}(i) = F(\theta(i)) = \frac{1}{2} Q \left( \sqrt{\left( \frac{N_0}{2E_b} + \frac{2P_J \cos^2(\theta(i))}{NP_s} \right)^{-1}} \right) + \frac{1}{2} Q \left( \sqrt{\left( \frac{N_0}{2E_b} + \frac{2P_J \sin^2(\theta(i))}{NP_s} \right)^{-1}} \right)$$

$P_s = E_s R_s = E_s / (NT) = 2E_b / (NT)$  (useful signal power at receiver input)

BER(i) depends on symbol index i through  $\theta(i)$

Average BER (averaged over symbol index) :  $\text{BER} = \frac{1}{2\pi} \int_{-\pi}^{\pi} F(\theta) d\theta$

## Real-valued or complex-valued chips ? BER performance for 4-QAM

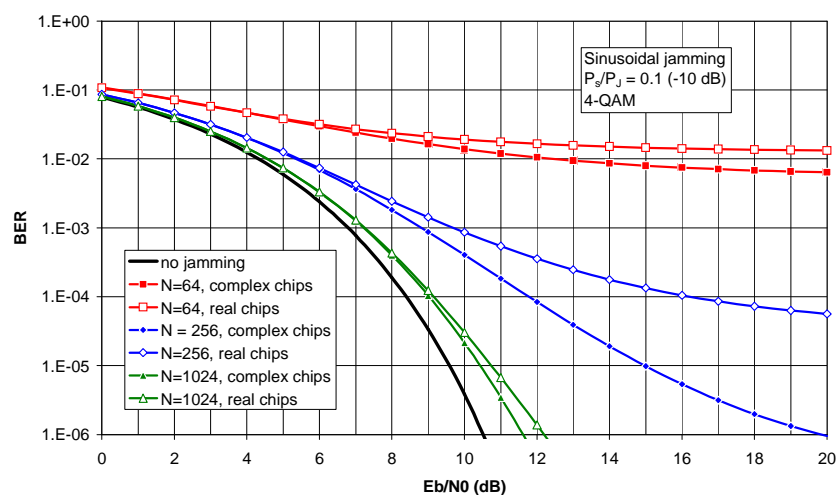


lower BER in presence of jamming when using complex-valued chips

Chapter 7 : Spread-spectrum communication and CDMA

45

## Real-valued or complex-valued chips ? BER performance for 4-QAM



Chapter 7 : Spread-spectrum communication and CDMA

46

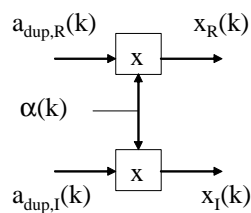
## Real-valued or complex-valued chips ? Implementation complexity

### Real-valued chips

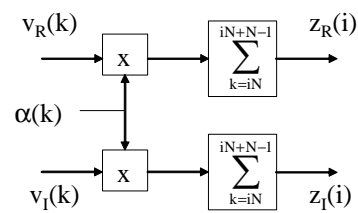
$$x_R(k) + jx_I(k) = (a_{\text{dup},R}(k) + ja_{\text{dup},I}(k))\alpha(k)$$

$$z_R(k) + jz_I(k) = \sum_{k=iN}^{iN+N-1} (v_R(k) + jv_I(k))\alpha(k)$$

#### Transmitter implementation



#### Receiver implementation



Chapter 7 : Spread-spectrum communication and CDMA

47

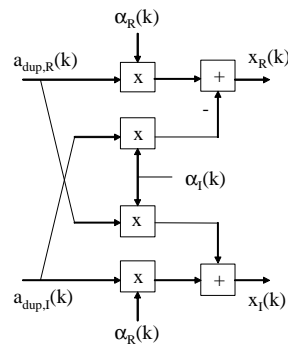
## Real-valued or complex-valued chips ? Implementation complexity

### Complex-valued chips

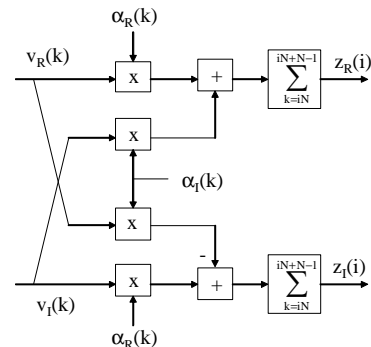
$$x_R(k) + jx_I(k) = (a_{\text{dup},R}(k) + ja_{\text{dup},I}(k))(\alpha_R(k) + j\alpha_I(k))$$

$$z_R(k) + jz_I(k) = \sum_{k=iN}^{iN+N-1} (v_R(k) + jv_I(k))(\alpha_R(k) - j\alpha_I(k))$$

#### Transmitter implementation



#### Receiver implementation

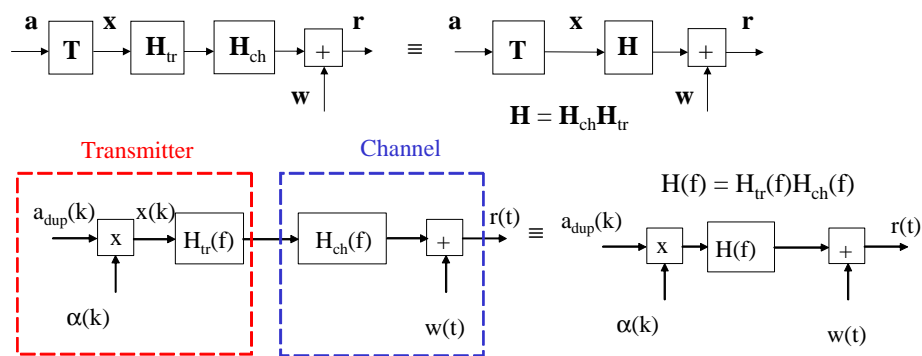


Chapter 7 : Spread-spectrum communication and CDMA

48

## Spread-spectrum on dispersive channel

### Transmitter and channel



$$a_{dup}(iN+m) = a(i)$$

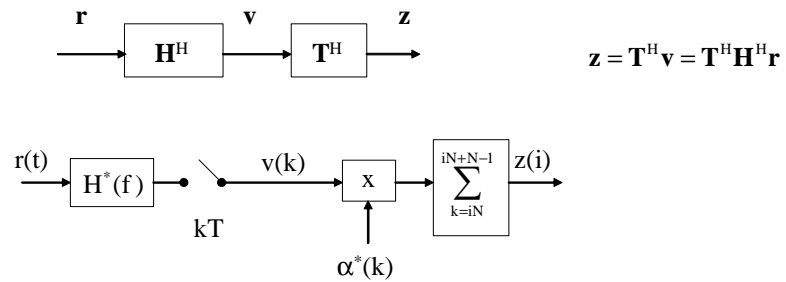
$$m = 0, \dots, N-1$$

We consider a given chiprate  $1/T$  and given transfer functions  $H_{tr}(f)$  and  $H_{ch}(f)$ .  
 $\Rightarrow$  modifying  $N$  affects the symbol rate  $R_s$  but not the filter transfer functions



## Computation of sufficient statistics

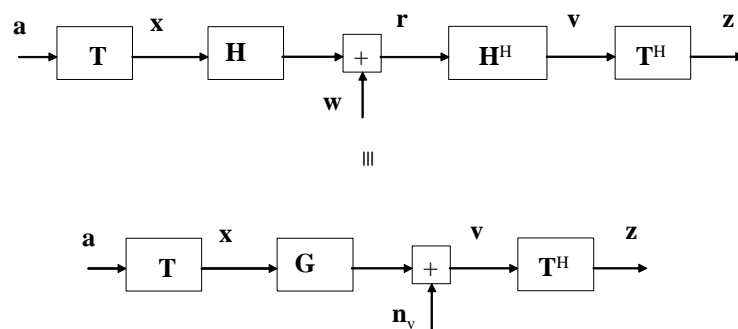
$\{z(i)\}$  : sufficient statistics for detecting  $\{a(i)\}$



Chapter 7 : Spread-spectrum communication and CDMA

51

## Discrete-time model for $\{z(i)\}$



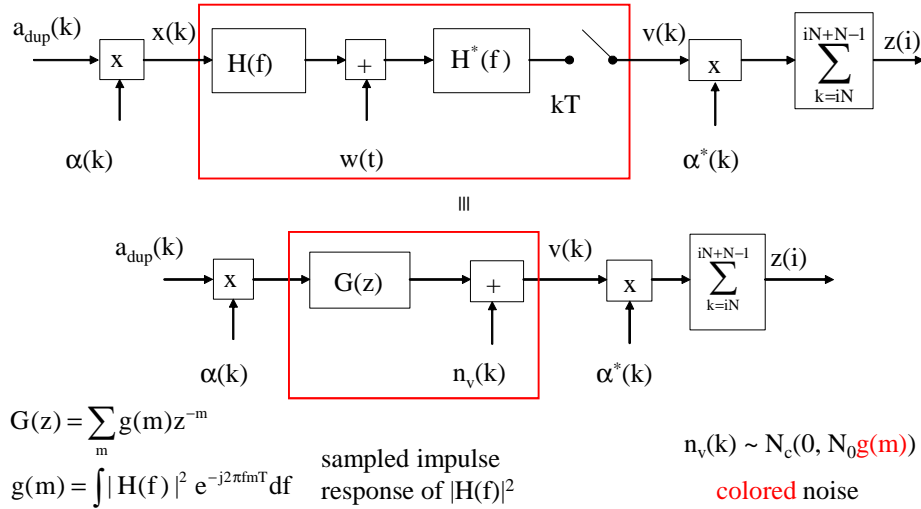
$$\mathbf{v} = \mathbf{H}^H \mathbf{H} \mathbf{x} + \mathbf{H}^H \mathbf{w} = \mathbf{G} \mathbf{x} + \mathbf{n}_v$$

$$E[\mathbf{n}_v \mathbf{n}_v^H] = N_0 \mathbf{H}^H \mathbf{H} = N_0 \mathbf{G} \quad \mathbf{G} = \mathbf{H}^H \mathbf{H}$$

Chapter 7 : Spread-spectrum communication and CDMA

52

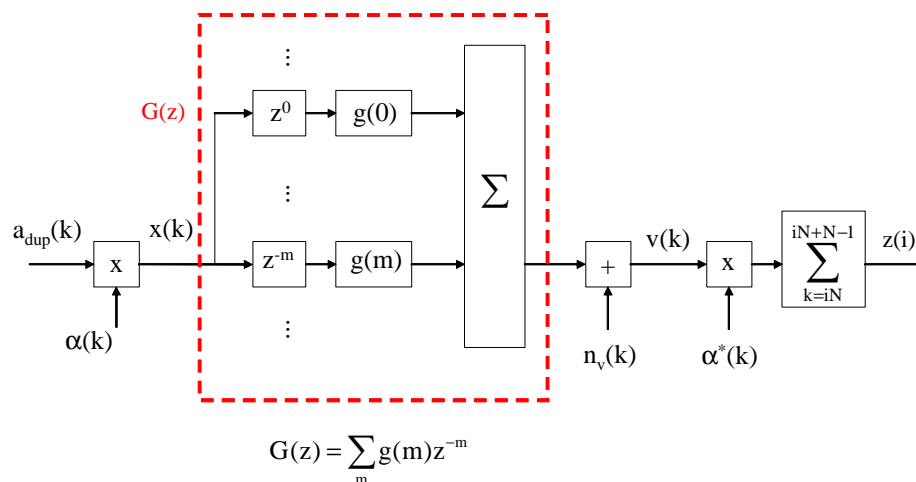
### Discrete-time model for $\{z(i)\}$



Chapter 7 : Spread-spectrum communication and CDMA

53

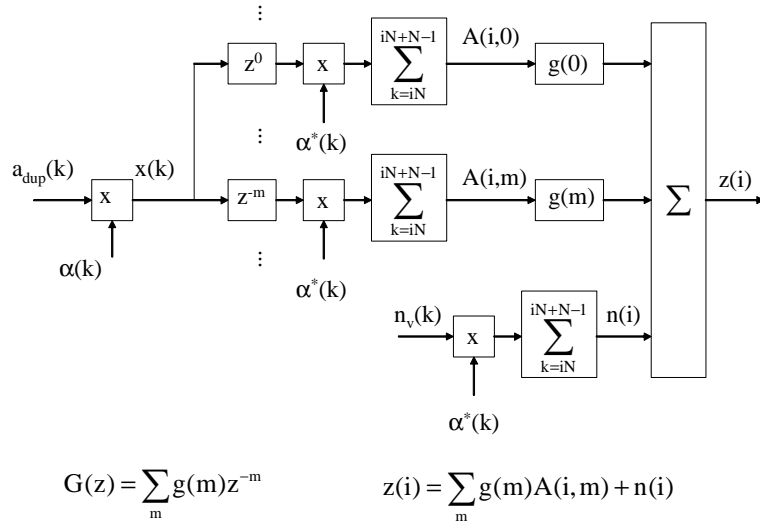
### Discrete-time model for $\{z(i)\}$



Chapter 7 : Spread-spectrum communication and CDMA

54

### Discrete-time model for $\{z(i)\}$

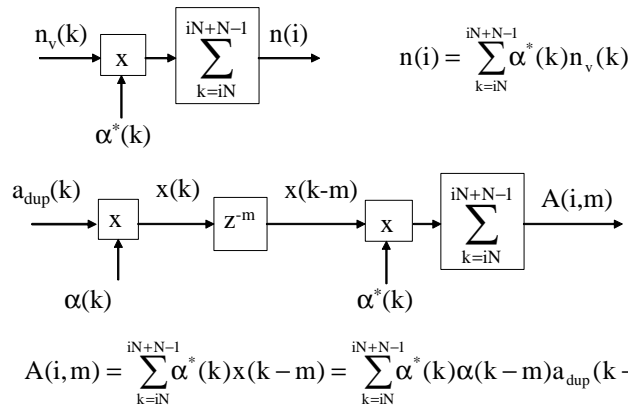


Chapter 7 : Spread-spectrum communication and CDMA

55

### Discrete-time model for $\{z(i)\}$

$$z(i) = \sum_m g(m) A(i, m) + n(i) = \underbrace{g(0) A(i, 0)}_{\text{useful}} + \underbrace{\sum_{m \neq 0} g(m) A(i, m)}_{\text{interference}} + \underbrace{n(i)}_{\text{noise}}$$



Chapter 7 : Spread-spectrum communication and CDMA

56

### Useful term in $z(i)$

$$z(i) = \underbrace{g(0)A(i,0)}_{\text{useful}} + \underbrace{\sum_{m \neq 0} g(m)A(i,m)}_{\text{interference}} + \underbrace{n(i)}_{\text{noise}} \quad A(i,m) = \sum_{k=iN}^{iN+N-1} \alpha^*(k) \alpha(k-m) a_{\text{dup}}(k-m)$$

$$\text{useful term} = g(0)A(i,0)$$

$$A(i,0) = \sum_{k=iN}^{iN+N-1} \alpha^*(k) \alpha(k) a_{\text{dup}}(k) = a(i) \sum_{k=iN}^{iN+N-1} |\alpha(k)|^2 = a(i) \quad |\alpha(k)|^2 = 1/N$$

$$\Rightarrow \text{useful term} = g(0)a(i)$$

### Interference term in $z(i)$

$$z(i) = \underbrace{g(0)A(i,0)}_{\text{useful}} + \underbrace{\sum_{m \neq 0} g(m)A(i,m)}_{\text{interference}} + \underbrace{n(i)}_{\text{noise}} \quad A(i,m) = \sum_{k=iN}^{iN+N-1} \alpha^*(k) \alpha(k-m) a_{\text{dup}}(k-m)$$

$$\text{interference term} : \sum_{m \neq 0} g(m)A(i,m) \quad A(i,m) = \sum_{k=iN}^{iN+N-1} \alpha^*(k) \alpha(k-m) a_{\text{dup}}(k-m)$$

$A(i,m)$  with  $m \neq 0$  contains  $N$  zero-mean *uncorrelated* terms.

Each term in  $A(i,m)$  has variance, equal to  $E_s/N^2$

$$\Rightarrow E[|A(i,m)|^2] = E_s/N \Rightarrow A(i,m) \rightarrow 0 \text{ for } N \rightarrow \infty$$

**interference term can be made arbitrarily small  
by making  $N$  sufficiently large**

$$\text{For complex-valued chips : } E \left[ \left| \sum_{m \neq 0} g(m)A(i,m) \right|^2 \right] = \frac{E_s}{N} \sum_{m \neq 0} |g(m)|^2$$

(more complicated expression in case of real-valued chips)

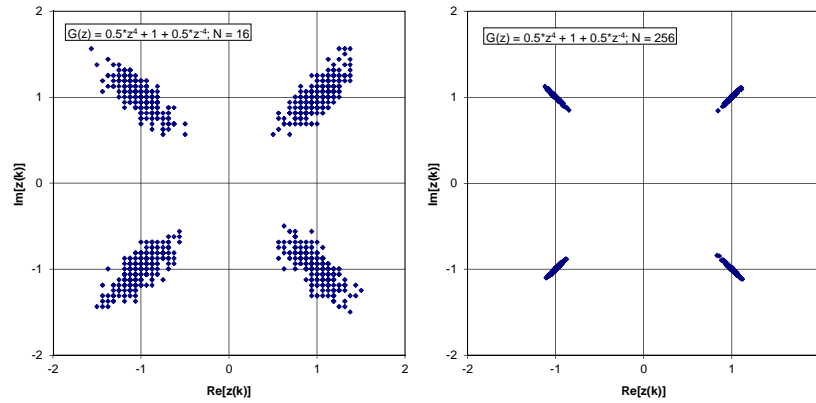
## Interference reduction : example

Scatter diagram (no noise) of  $z(i)$ , for  $N = 16, 256$ ;

4-QAM ( $\pm 1 \pm j$ ) data symbols, i.i.d. complex-valued chips

$H_{ch}(f) = 2^{-0.5}(1 + \exp(-j8\pi fT))$  : 2 paths, delay difference of 4 chip intervals

$$\Rightarrow G(z) = 0.5z^4 + 1 + 0.5z^{-4}$$



Chapter 7 : Spread-spectrum communication and CDMA

59

## Noise term in $z(i)$

$$n(i) = \sum_{k=iN}^{iN+N-1} \alpha^*(k) n_v(k) = \sum_{m=0}^{N-1} \alpha^*(iN+m) n_v(iN+m) \quad n_v(k) \sim N_c(0, N_0 g(0) \delta(m))$$

$$E[n(i+\ell) n^*(i)]$$

$$= N_0 \sum_{m,n=0}^{N-1} \underbrace{E[\alpha^*((i+\ell)N+m) \alpha(iN+n)]}_{(1/N) \delta(n-m) \delta(\ell)} g(\ell N + m - m)$$

$$= N_0 g(0) \delta(\ell) \sum_{n=0}^{N-1} (1/N) = N_0 g(0) \delta(\ell)$$

$$\{n(i)\} \text{ stationary and white : } n(i) \sim N_c(0, N_0 g(0) \delta(\ell))$$

Chapter 7 : Spread-spectrum communication and CDMA

60

## Asymptotic (large N) model for $\{z(i)\}$

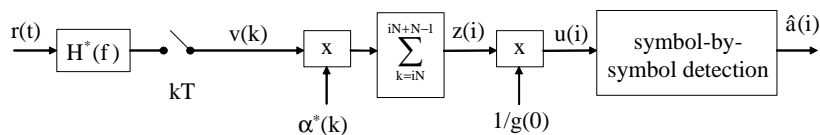
For large enough N : interference can be neglected as compared to noise

Assume large N :  $z(i) = g(0)a(i) + n(i)$        $n(i) \sim N_c(0, N_0g(0)\delta(\ell))$

Apply scaling :  $u(i) = z(i)/g(0)$   
 $\Rightarrow u(i) = a(i) + w(i)$        $w(i) \sim N_c(0, (N_0/g(0))\delta(\ell))$

In spite of channel dispersion, symbol-by-symbol decision on  $u(i)$  is (nearly) optimum for large N :

$$\hat{a}(i) = \arg \min_{\tilde{a}(i) \in C} |u(i) - \tilde{a}(i)|^2$$



Chapter 7 : Spread-spectrum communication and CDMA

61

## Symbol-by-symbol decision : BER performance for large N

$u(i) = z(i)/g(0)$        $u(i) \sim N_c(a(i), (N_0/g(0))\delta(\ell))$

Symbol-by-symbol decision on  $u(i)$  :

$$\text{BER} = \text{BER}_c \left( \frac{E_s g(0)}{N_0} \right) \quad \text{same BER as matched filter bound !}$$

(in spite of channel dispersion)

For large enough spreading factor N :

- symbol-by-symbol detection is essentially optimum (resulting BER equals matched filter lower bound when interference is negligible)
  - coefficients  $g(m)$  with  $m \neq 0$  do not affect BER performance
  - no noise enhancement (unlike conventional modulation using equalization)
- Price to pay : **symbol rate reduction by factor of  $1/N$  ( $N \gg 1$ ) for given  $1/T$**

Chapter 7 : Spread-spectrum communication and CDMA

62

## Multipath channel : RAKE filter

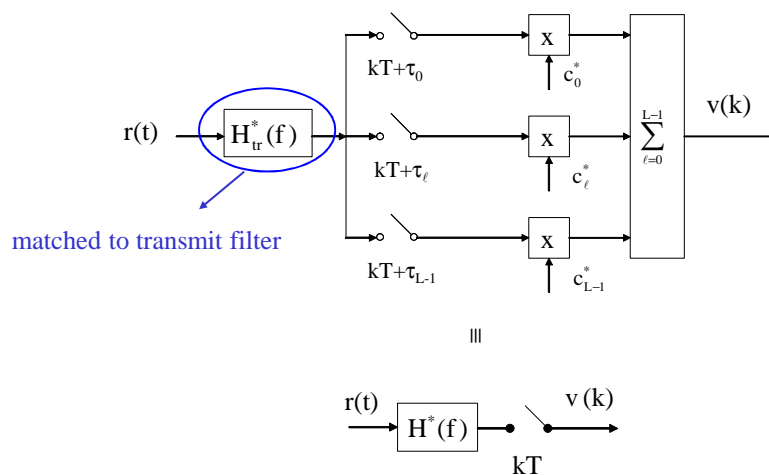
Matched filter implementation in case of *multipath channel* : *RAKE filter*

$$H_{ch}(f) = \sum_{\ell=0}^{L-1} c_{\ell} \exp(-j2\pi f \tau_{\ell}) \quad L \text{ paths}$$

$c_{\ell}, \tau_{\ell}$  : complex gain and delay of  $\ell$ -th path

$$\begin{aligned} \text{Matched filter outputs : } v(k) &= \int r(t) h^*(t - kT) dt \\ &= \int R(f) H^*(f) \exp(j2\pi f kT) df \\ &= \int R(f) H_{tr}^*(f) \sum_{\ell=0}^{L-1} c_{\ell}^* \exp(j2\pi f (kT + \tau_{\ell})) df \\ &= \sum_{\ell=0}^{L-1} c_{\ell}^* \int r(t) h_{tr}^*(t - kT - \tau_{\ell}) dt \end{aligned}$$

## Multipath channel : RAKE filter



## Multipath channel : BER

$$H_{\text{ch}}(f) = \sum_{\ell=0}^{L-1} c_{\ell} \exp(-j2\pi f \tau_{\ell}) \quad \text{BER} = \text{BER}_c \left( \frac{E_s g(0)}{N_0} \right)$$

$$g(0) = \int |H_{\text{tr}}(f)|^2 |H_{\text{ch}}(f)|^2 df = \sum_{\ell, \ell'=0}^{L-1} c_{\ell}^* c_{\ell'} g_{\text{tr}}(\tau_{\ell} - \tau_{\ell'})$$

$$g_{\text{tr}}(t) = \int |H_{\text{tr}}(f)|^2 \exp(j2\pi f t) df \quad \text{with } g_{\text{tr}}(kT) = \delta(k) \quad (\text{orthogonality condition on transmit pulse } h_{\text{tr}}(t))$$

Special (simple) case :  $\tau_{\ell} = \ell T$  ( $\ell = 0, \dots, L-1$ )

$$g(0) = \sum_{\ell=0}^{L-1} |c_{\ell}|^2 \quad \text{BER} = \text{BER}_c \left( \frac{E_s}{N_0} \sum_{\ell=0}^{L-1} |c_{\ell}|^2 \right)$$

## Reduced-complexity RAKE

$$\text{BER} = \text{BER}_c \left( \frac{E_s}{N_0} \sum_{\ell=0}^{L-1} |c_{\ell}|^2 \right)$$

weak paths do not contribute much to the reduction of the BER

$\Rightarrow$  RAKE filter considering only the  $L'$  strongest paths (instead of all  $L$  paths) gives rise to

$$\text{BER} = \text{BER}_c \left( \frac{E_s}{N_0} \sum_{\ell=0}^{L'-1} |c_{\ell}|^2 \right)$$

(small) SNR degradation (in dB) equal to

$$10 \log \left( \sum_{\ell=0}^{L-1} |c_{\ell}|^2 / \sum_{\ell=0}^{L'-1} |c_{\ell}|^2 \right)$$



## Multipath Rayleigh fading channel

$$H_{\text{ch}}(f) = \sum_{\ell=0}^{L-1} c_{\ell} \exp(-j2\pi f \tau_{\ell}) \quad c_{\ell} \sim N_c(0, 2\sigma_{\ell}^2) \quad c_{\ell} \text{ and } c_{\ell'} \text{ independent when } \ell \neq \ell'$$

$$g(0) = \int |H_{\text{tr}}(f)|^2 |H_{\text{ch}}(f)|^2 df \quad g_{\text{tr}}(t) = \int |H_{\text{tr}}(f)|^2 \exp(j2\pi f t) df$$

$$= \sum_{\ell, \ell'=0}^{L-1} c_{\ell}^* c_{\ell'} g_{\text{tr}}(\tau_{\ell} - \tau_{\ell'}) \quad \text{with } g_{\text{tr}}(kT) = \delta(k) \quad (\text{orthogonality condition on transmit pulse } h_{\text{tr}}(t))$$

$$\text{BER} = E \left[ \text{BER}_c \left( \frac{E_s g(0)}{N_0} \right) \right] \quad (\text{averaging over independent channel gains } \{c_{\ell}\})$$

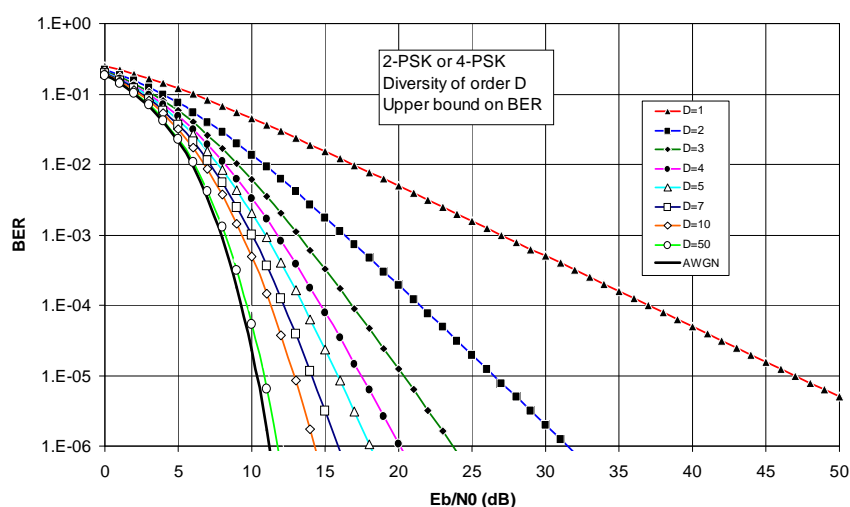
$$\text{Special (simple) case : } \tau_{\ell} = \ell T \quad (\ell = 0, \dots, L-1) \Rightarrow g(0) = \sum_{\ell=0}^{L-1} |c_{\ell}|^2$$

$\Rightarrow$  same BER as for transmission of  $s(t; \mathbf{a})$  over  $L$  parallel flat Rayleigh fading channels with gains  $\{c_{\ell}\}$ , yielding diversity of order  $L$  ("multipath diversity")

Chapter 7 : Spread-spectrum communication and CDMA

67

## Example : D equal-strength independently Rayleigh fading paths



Chapter 7 : Spread-spectrum communication and CDMA

68

## Spread-spectrum multi-user communication : CDMA, CDM

## CDMA, CDM

Point-to-point spread-spectrum communication has very low bandwidth efficiency when the spreading factor  $N$  is large. To increase bandwidth efficiency, several spread-spectrum signals are *simultaneously* transmitted in the *same* bandwidth.

**CDMA :**  $N_u$  user terminals (UTs) simultaneously transmit spread-spectrum signals in the same upstream bandwidth.

**CDM :** Base station (BS) transmits the sum of  $N_u$  simultaneous spread-spectrum signals in the same downstream bandwidth

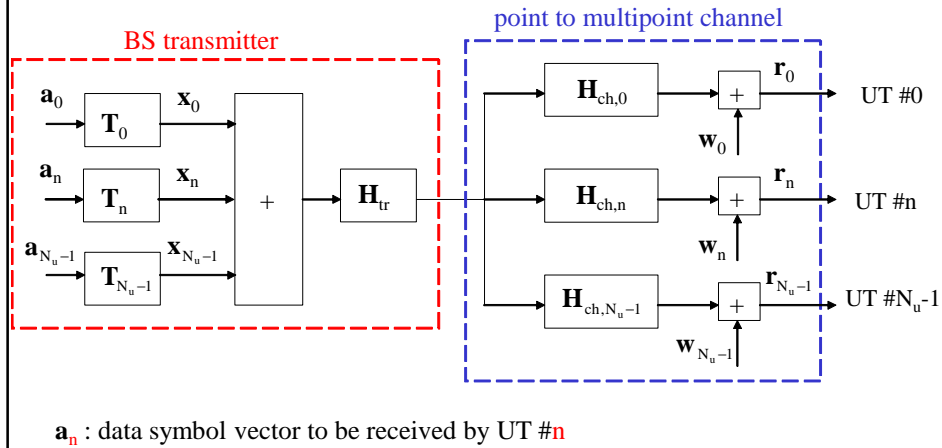
(assumption : upstream and downstream signals separated by FDD)

All spread-spectrum signals have :

- the same square-root Nyquist chip pulse  $h_{tr}(t)$
- the same upstream or downstream carrier frequency, the same symbol rate  $R_s$
- $N$  chips per symbol
- *different* spreading sequences :  $\{\alpha_n(k)\}$  is spreading sequence of  $n$ -th user signal

CDM(A) can be formulated in terms of block transform modulation

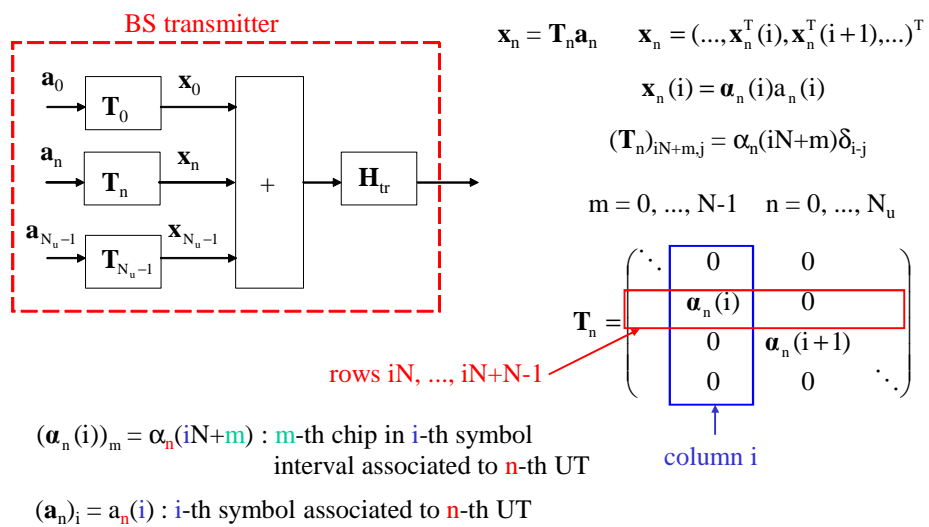
## Downstream communication : CDM



Chapter 7 : Spread-spectrum communication and CDMA

71

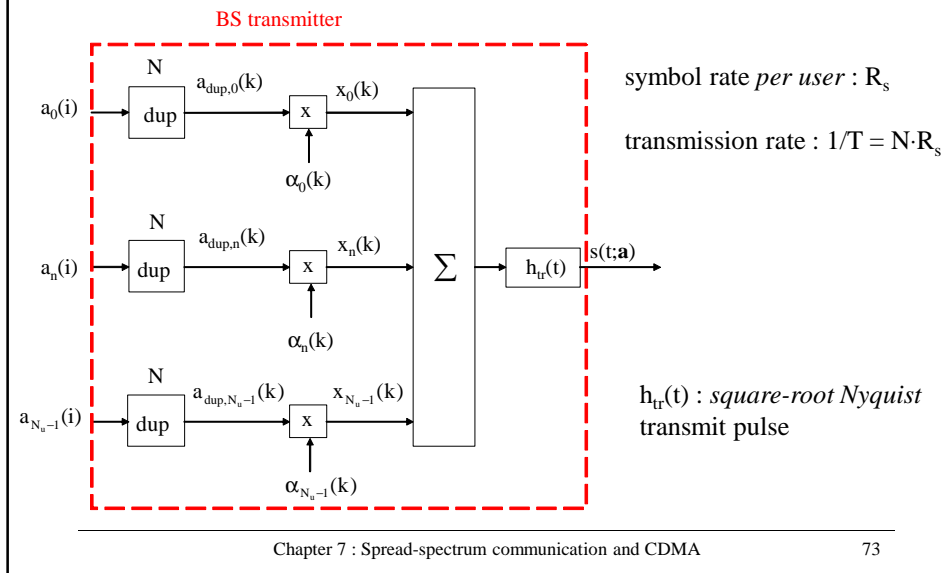
## Downstream communication : CDM



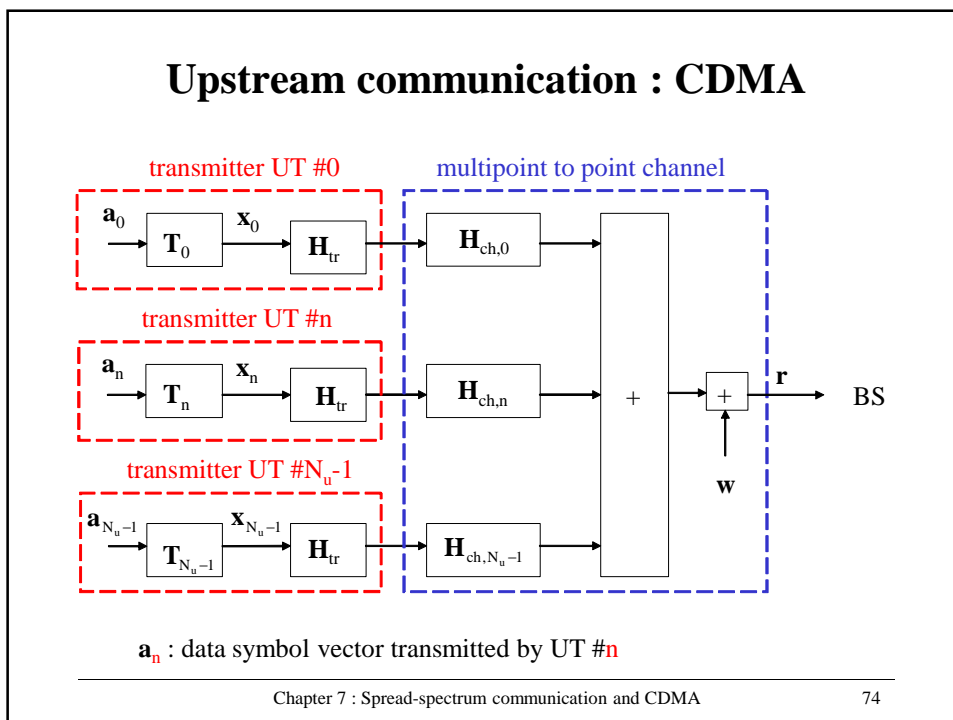
Chapter 7 : Spread-spectrum communication and CDMA

72

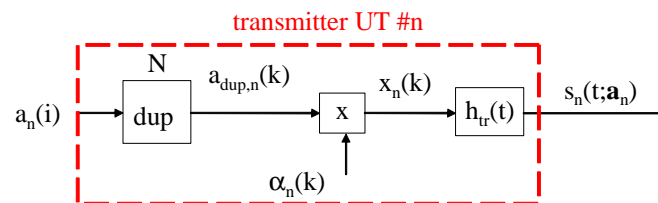
## Downstream communication : CDM



## Upstream communication : CDMA



## Upstream communication : CDMA



symbol rate *per user* :  $R_s$        $h_{tr}(t)$  : *square-root Nyquist* transmit pulse

transmission rate :  $1/T = N \cdot R_s$

## CDM(A) on AWGN channel

## CDM(A) on AWGN channel

AWGN channel :  $\mathbf{H}_{ch,n} = \mathbf{I}$

transmit filter :  $\mathbf{H}_{tr}^H \mathbf{H}_{tr} = \mathbf{I}$

Signal at BS receiver or UT receiver :

$$\mathbf{r} = \mathbf{H}_{tr} \mathbf{T} \mathbf{a} + \mathbf{w} \quad \mathbf{T} = (\mathbf{T}_0, \dots, \mathbf{T}_{N_u-1}) \quad \mathbf{a} = (\mathbf{a}_0^T, \dots, \mathbf{a}_{N_u-1}^T)^T \quad \mathbf{T} \mathbf{a} = \sum_{n=0}^{N_u-1} \mathbf{T}_n \mathbf{a}_n$$

$$\mathbf{a}_n : K \times 1, \mathbf{a} : N_u K \times 1, \mathbf{T}_n : NK \times K, \mathbf{T} : NK \times N_u K$$

Sufficient statistic  $\mathbf{z}$  ( $N_u K \times 1$ ) :

$$\mathbf{z} = \mathbf{T}^H \mathbf{H}_{tr}^H \mathbf{r} = \mathbf{T}^H \mathbf{v} \quad \mathbf{v} = \mathbf{H}_{tr}^H \mathbf{r} \quad \mathbf{z}_n = \mathbf{T}_n^H \mathbf{v} \quad \mathbf{z} = (\dots, \mathbf{z}_n^T, \mathbf{z}_{n+1}^T, \dots)^T$$

Model for  $\mathbf{z}$  :

$$\mathbf{z} = \mathbf{T}^H \mathbf{H}_{tr}^H (\mathbf{H}_{tr} \mathbf{T} \mathbf{a} + \mathbf{w}) = \mathbf{T}^H \mathbf{T} \mathbf{a} + \mathbf{n} \quad \mathbf{n} = \mathbf{T}^H \mathbf{H}_{tr}^H \mathbf{w} \sim N_c(0, N_0 \mathbf{T}^H \mathbf{T})$$

When  $\mathbf{T}^H \mathbf{T} = \mathbf{I}$ , we get :  $\mathbf{z} = \mathbf{a} + \mathbf{n} \quad \mathbf{n} \sim N_c(0, N_0 \mathbf{I})$

$\Rightarrow$  symbol-by-symbol detection is optimum; BER = matched filter bound

## Orthogonal CDM(A) (O-CDM(A))

$$\mathbf{T} = (\mathbf{T}_0, \dots, \mathbf{T}_{N_u-1}) \quad \Rightarrow \quad \mathbf{T}^H \mathbf{T} = \begin{pmatrix} \mathbf{T}_0^H \mathbf{T}_0 & \dots & \mathbf{T}_0^H \mathbf{T}_{N_u-1} \\ \vdots & & \vdots \\ \mathbf{T}_{N_u-1}^H \mathbf{T}_0 & \dots & \mathbf{T}_{N_u-1}^H \mathbf{T}_{N_u-1} \end{pmatrix}$$

$$(\mathbf{T}_n)_{iN+m,j} = \alpha_n(iN+m) \delta_{i-j}$$

$$(\mathbf{T}_n^H \mathbf{T}_{n'})_{i,j} = \sum_{k=0}^{K/N-1} (\mathbf{T}_n)_{k,i}^* (\mathbf{T}_{n'})_{k,j}$$

$$\mathbf{T}_n = \begin{pmatrix} \ddots & 0 & 0 \\ & \mathbf{a}_n(i) & 0 \\ & 0 & \mathbf{a}_n(i+1) \\ & 0 & 0 & \ddots \end{pmatrix}$$

$$= \delta_{i-j} \sum_{m=0}^{N-1} \alpha_n^*(iN+m) \alpha_{n'}(iN+m)$$

$$= \delta_{i-j} \mathbf{a}_n^H(i) \mathbf{a}_{n'}(i)$$

$$\mathbf{T}_n^H \mathbf{T}_{n'} \text{ diagonal}$$

## Orthogonal CDM(A) (O-CDM(A))

Orthogonal CDM(A) : the chip sequences associated to the  $N_u$  UTs are *orthogonal* over a symbol interval

Select  $\mathbf{a}_n^H(i)\mathbf{a}_{n'}(i) = \sum_{k=iN}^{iN+N-1} \alpha_n^*(k)\alpha_{n'}(k) = \delta_{n-n'}$  (all  $i$ )  $n, n'$  : indices of UTs

Because of the orthogonality of the chip sequences, we get

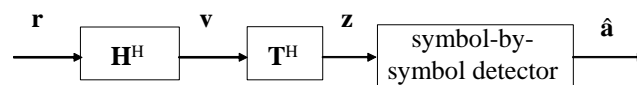
$$(\mathbf{T}_n^H \mathbf{T}_{n'})_{i,j} = \delta_{i-j} \mathbf{a}_n^H(i) \mathbf{a}_{n'}(i) = \delta_{i-j} \delta_{n-n'} \Rightarrow \mathbf{T}_n^H \mathbf{T}_{n'} = \mathbf{I}_K \delta_{n-n'}$$

$$\Rightarrow \mathbf{T}^H \mathbf{T} = (\mathbf{T}_0, \dots, \mathbf{T}_{N_u-1})^H (\mathbf{T}_0, \dots, \mathbf{T}_{N_u-1}) = \mathbf{I}_{N_u K}$$

## O-CDM(A) on AWGN channel

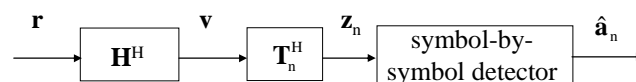
### O-CDMA

BS receiver : detects *all* symbols  $\mathbf{a}$



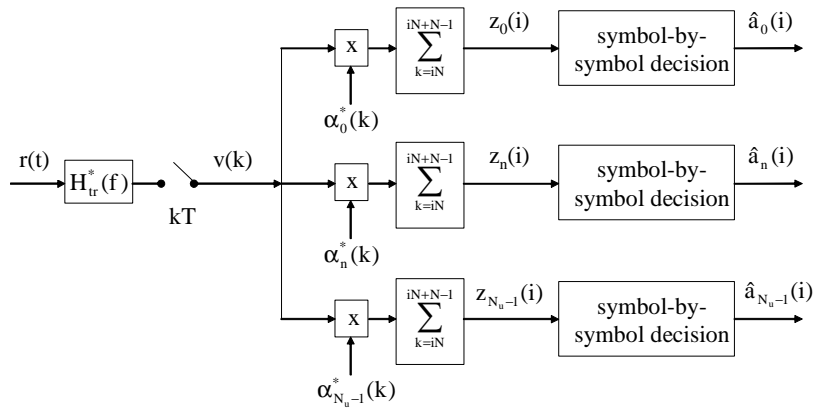
### O-CDM

Receiver of  $n$ -th UT : detects  $\mathbf{a}_n$  only



## O-CDMA : BS receiver (AWGN channel)

BS receiver details

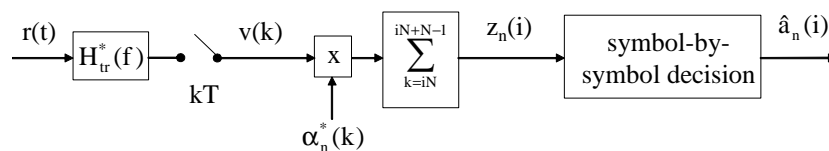


Chapter 7 : Spread-spectrum communication and CDMA

81

## O-CDM : UT receiver (AWGN channel)

n-th UT receiver details



(same as one branch of BS receiver)

Chapter 7 : Spread-spectrum communication and CDMA

82



## O-CDMA on AWGN channel : WH spreading sequences

N chips per symbol  $\Rightarrow$  a maximum of N orthogonal sequences of length N  
 $\Rightarrow$  a maximum of N users can be accommodated ( $N_u \leq N$ )

Walsh-Hadamard (WH) sequences :  $\alpha_n(iN+m) = WH_n(m)$

- binary orthogonal sequences are (scaled) columns of  $N \times N$  Hadamard matrix
- for given user, the *same* sequence of N chips is used in every symbol interval

Assume N power of 2

Recursive computation of  $N \times N$  Hadamard matrix  $\mathbf{H}_N$

$$\mathbf{H}_{2N} = \begin{pmatrix} \mathbf{H}_N & \mathbf{H}_N \\ \mathbf{H}_N & -\mathbf{H}_N \end{pmatrix} \quad \mathbf{H}_2 = \begin{pmatrix} 1 & 1 \\ 1 & -1 \end{pmatrix}$$

$$WH_n(m) = \frac{1}{\sqrt{N}} (\mathbf{H}_N)_{m,n} \quad \text{for spreading factor } N$$

## O-CDMA on AWGN channel : WH spreading sequences

WH spreading sequences do *not* appear random

E.g., the following are (unnormalized) WH sequences of length N (N : power of 2)

- period 1 : 1, 1, ...
- period 2 : (1, -1), (1, -1), ...
- period 4 : (1, 1, -1, -1), (1, 1, -1, -1), ... and (1, -1, -1, 1), (1, -1, -1, 1), ...

In order to obtain orthogonal spreading sequences that appear random, the user-dependent WH sequences are often multiplied with a common *user-independent* random chip sequence (*scrambling sequence*)  $\{\alpha_{scr}(k)\}$

$$\alpha_n(iN+m) = WH_n(m) \alpha_{scr}(iN+m) \quad WH_n(m) \in \{-1/\sqrt{N}, 1/\sqrt{N}\}, |\alpha_{scr}(k)|^2 = 1$$

$\Rightarrow$  orthogonality still preserved :

$$\alpha_n^H(i) \alpha_{n'}(i) = \sum_{m=0}^{N-1} \alpha_n^*(iN+m) \alpha_{n'}(iN+m) = \sum_{m=0}^{N-1} WH_n(m) WH_{n'}(m) = \delta(n-n')$$

## O-CDMA on AWGN channel : receiver operation

**Example** :  $N = 4$ , no noise, 2 UTs

$$\mathbf{H}_4 = \begin{pmatrix} 1 & 1 & 1 & 1 \\ 1 & -1 & 1 & -1 \\ 1 & 1 & -1 & -1 \\ 1 & -1 & -1 & 1 \end{pmatrix}$$

$\alpha_0(i)$	$0.5 \cdot (1, -1, -1, 1)^T$
$\alpha_n(i)$	$0.5 \cdot (1, 1, -1, -1)^T$
$a_0(i)\alpha_0(i)$ ( $a_0(i) = -1$ )	$0.5 \cdot (-1, 1, 1, -1)^T$
$a_n(i)\alpha_n(k)$ ( $a_n(i) = 1$ )	$0.5 \cdot (1, 1, -1, -1)^T$
$\mathbf{v}(i) = a_0(i)\alpha_0(i) +$ $a_n(i)\alpha_n(k)$	$(0, 1, 0, -1)^T$
$z_0(i) = \alpha_0^H(i)\mathbf{v}(i)$	$0.5 \cdot (1 \cdot 0 - 1 \cdot 1 - 1 \cdot 0 - 1 \cdot 1)$ $= -1 = a_0(i)$
$z_n(i) = \alpha_n^H(i)\mathbf{v}(i)$	$0.5 \cdot (1 \cdot 0 + 1 \cdot 1 - 1 \cdot 0 + 1 \cdot 1)$ $= 1 = a_n(i)$

## O-CDM(A) on AWGN channel : conclusions

- Chip pulse : square-root Nyquist, relative excess bandwidth  $\beta$
- Chip sequences associated to the UTs are orthogonal over symbol interval, e.g. based on WH sequences
- When the spreading factor is  $N$ , the number of users  $N_u$  is at most equal to  $N$
- Optimum detection reduces to symbol-by-symbol detection
- Resulting BER equals matched filter lower bound, which depends only on  $E_s/N_0$  and on the constellation considered

Total RF bandwidth (upstream+downstream) :  $B_{RF} = 2(1+\beta)N \cdot R_s$

Total symbol rate (upstream+downstream) :  $R_{s,tot} = 2N_u R_s$

$$\frac{R_{s,tot}}{B_{RF}} = \frac{1}{1+\beta} \cdot \frac{N_u}{N} \leq \frac{1}{1+\beta} \quad (\text{equality for } N_u = N)$$

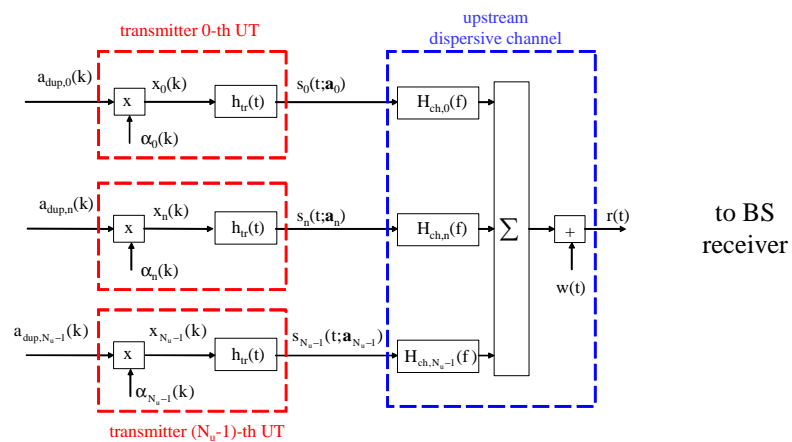
FDMA, TDMA :  $R_{s,tot}/B_{RF} \approx 1/(1+\beta)$  when all time/frequency slots are occupied

## CDM(A) on dispersive channels

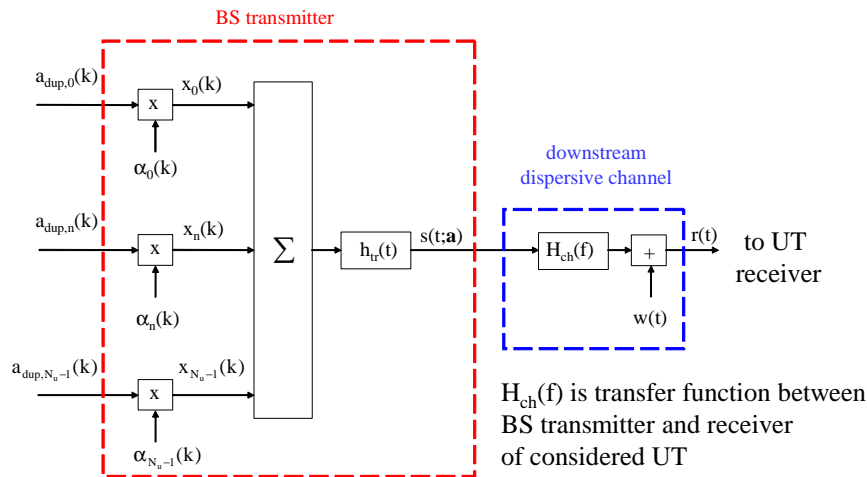
## CDMA on dispersive channels : upstream communication

$h_{tr}(t)$  : transmitted square-root Nyquist chip pulse

$h_{ch,n}(t)$  : impulse response of channel between n-th UT and BS



## CDM on dispersive channels : downstream communication



downstream model = upstream model with  $H_{ch,n}(f) = H_{ch}(f)$  for  $n = 0, \dots, N_u - 1$

Chapter 7 : Spread-spectrum communication and CDMA

89

## ML receiver for CDMA on dispersive upstream channels

Signal received by basestation :

$$\mathbf{H}_n = \mathbf{H}_{ch,n} \mathbf{H}_{tr}$$

$$\mathbf{r} = \sum_{n=0}^{N_u-1} \mathbf{H}_n \mathbf{T}_n \mathbf{a}_n + \mathbf{w} = \mathbf{M} \mathbf{a} + \mathbf{w} \quad \mathbf{M} = (\mathbf{H}_0 \mathbf{T}_0, \dots, \mathbf{H}_{N_u-1} \mathbf{T}_{N_u-1}) \quad \mathbf{a} = (\mathbf{a}_0^T, \dots, \mathbf{a}_{N_u-1}^T)^T$$

Because of channel dispersion, we get non-diagonal  $\mathbf{H}_n^H \mathbf{H}_n$ ,

$\Rightarrow \mathbf{M}^H \mathbf{M}$  is non-diagonal

$\Rightarrow$  complexity of ML receiver is *exponential* in  $K \cdot N_u$

( $K$  : number of symbols per user signal)

$\Rightarrow$  we will consider suboptimum receiver with complexity that is *linear* in  $K \cdot N_u$

Sufficient statistic :

$$\mathbf{z} = \mathbf{M}^H \mathbf{r} = (\mathbf{H}_0 \mathbf{T}_0, \dots, \mathbf{H}_{N_u-1} \mathbf{T}_{N_u-1})^H \mathbf{r} = (\mathbf{z}_0^T, \dots, \mathbf{z}_{N_u-1}^T)^T$$

$$\text{with} \quad \mathbf{z}_n = \mathbf{T}_n^H \mathbf{H}_n^H \mathbf{r} = \mathbf{T}_n^H \mathbf{v}_n \quad \mathbf{v}_n = \mathbf{H}_n^H \mathbf{r}$$

Chapter 7 : Spread-spectrum communication and CDMA

90

## Single-user receiver for CDMA on dispersive upstream channels

“Single-user” receiver allows to detect the  $N_u$  symbol vectors  $\{\mathbf{a}_n, n = 1, \dots, N_u-1\}$  independently. For detecting  $\mathbf{a}_n$ , the receiver assumes that only  $\mathbf{H}_n \mathbf{T}_n \mathbf{a}_n$  has been transmitted (i.e., the user signals  $\mathbf{H}_{n'} \mathbf{T}_{n'} \mathbf{a}_{n'}$  with  $n' \neq n$  are assumed to be zero) :

$$\mathbf{r} = \mathbf{H}_n \mathbf{T}_n \mathbf{a}_n + \mathbf{w} \quad (\text{other } N_u-1 \text{ user signals ignored by receiver})$$

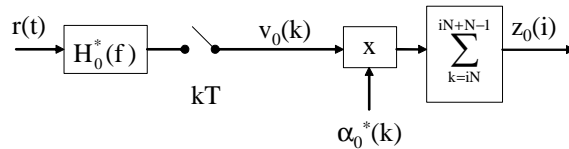
This corresponds to the observation model for *point-to-point* spread-spectrum communication on the dispersive channel. We have shown earlier that, for large spreading factor  $N$ , symbol-by-symbol detection is essentially optimum for point-to-point spread-spectrum communication. The resulting receiver for detecting  $\mathbf{a}_n$  has a complexity that is linear in  $K$ . The detection of all vectors  $\{\mathbf{a}_n\}$  involves  $N_u$  single-user receivers, yielding a total complexity that is *linear* (rather than exponential) in  $K \cdot N_u$ .

As the single-user receiver ignores the presence of  $N_u-1$  user signals, these signals act as *multiuser interference* (MUI). This will result in a BER degradation as compared to the case where only one user signal is present.

## Single-user receiver for CDM(A) on dispersive channels

We consider upstream transmission; results for downstream transmission are obtained by setting  $H_{ch,n}(f) = H_{ch}(f)$ ,  $n = 0, \dots, N_u-1$

Front-end of single-user receiver that detects  $\mathbf{a}_0$  :



$H_n(f) = H_{tr}(f)H_{ch,n}(f)$  : FT of chip pulse from  $n$ -th UT, received at BS

receive filter matched to *received* chip pulse from reference UT ( $n = 0$ )

$\{z_0(i)\}$  is sufficient statistic for detecting the data  $\{a_0(i)\}$  from reference UT, provided that other UTs are *not* active (single-user scenario)

## Single-user receiver for CDMA : model for $z_0(i)$

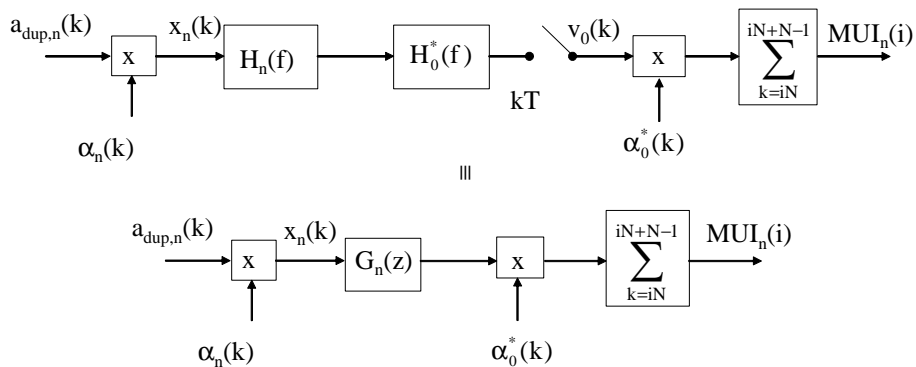
The contributions from the reference user symbols  $\mathbf{a}_0$  and the channel noise  $w(t)$  are the same as in the point-to-point spread-spectrum scenario. If only the reference user signal  $s(t; \mathbf{a}_0)$  is transmitted, we get, for large spreading factor  $N$ ,

$$z_0(i) = g_0(0)a_0(i) + n_0(i) \quad n_0(i) \sim N_c(0, N_0 g_0(0) \delta(\ell))$$

$$\text{with } g_0(0) = \int |H_0(f)|^2 df = \int |H_{tr}(f)|^2 |H_{ch,0}(f)|^2 df$$

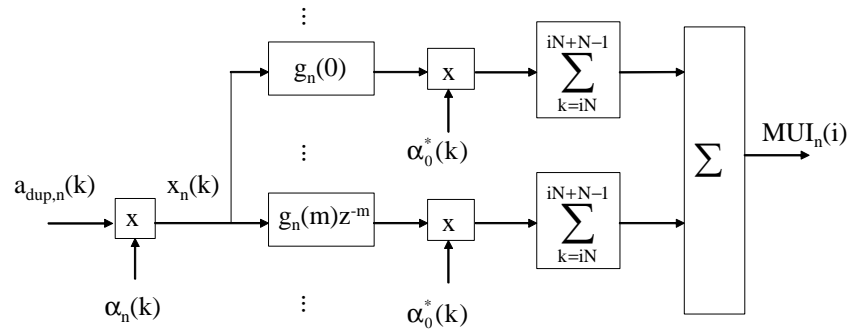
When also the user signals  $\{s_n(t; \mathbf{a}_n) \text{ with } n \neq 0\}$  are transmitted, we must add to  $z_0(i)$  a MUI term, which is a sum of contributions from the individual user signals. In the following we investigate the contribution  $MUI_n(i)$  from the user signal  $s_n(t; \mathbf{a}_n)$  to  $z_0(i)$ .

## Single-user receiver for CDMA : MUI contribution to $z_0(i)$



$$g_n(m) = \int H_0^*(f) H_n(f) \exp(j2\pi f m T) df \quad \text{sampled impulse response of } H_0^*(f) H_n(f)$$

### Single-user receiver for CDMA : MUI contribution to $z_0(i)$



$$MUI_n(i) = \sum_m g_n(m) A_n(i, m) \quad A_n(i, m) = \sum_{k=iN}^{iN+N-1} \alpha_0^*(k) \alpha_n(k-m) a_{\text{dup},n}(k-m)$$

Chapter 7 : Spread-spectrum communication and CDMA

95

### Single-user receiver for CDMA : MUI contribution to $z_0(i)$

$$MUI_n(i) = \sum_m g_n(m) \sum_{k=iN}^{iN+N-1} a_{\text{dup},n}(k-m) \alpha_n(k-m) \alpha_0^*(k)$$

Assume  $\{\alpha_0(k)\}$  and  $\{\alpha_n(k)\}$  are independent sequences of i.i.d. chips  
 $\Rightarrow$  all terms in  $MUI_n(i)$  are uncorrelated

$$E[MUI_n^*(i) MUI_n(i + \ell)] = \left( \frac{E_s}{N} \sum_m |g_n(m)|^2 \right) \delta(\ell)$$

$$\text{Total MUI : } MUI(i) = \sum_{n=1}^{N_u-1} MUI_n(i) \quad \text{sum of uncorrelated terms}$$

$$E[MUI^*(i) MUI(i + \ell)] = \left( \frac{E_s}{N} \sum_{n=1}^{N_u-1} \sum_m |g_n(m)|^2 \right) \delta(\ell) \quad \begin{array}{l} \text{MUI power } \uparrow \\ \text{when } N_u \uparrow \text{ and } N \downarrow \end{array}$$

Chapter 7 : Spread-spectrum communication and CDMA

96

### Single-user receiver for CDMA : MUI contribution to $z_0(i)$ for O-CDMA

In the case of O-CDMA, we have  $\alpha_n^H(i)\alpha_n(i) = \delta_{n-n}$ .

so that the MUI term proportional to  $g_n(0)$  is zero :

$$\text{MUI}_n(i) = g_n(0)a_n(i) \underbrace{\sum_{k=iN}^{iN+N-1} \alpha_n(k)\alpha_n^*(k)}_{=0} + \sum_{m \neq 0} g_n(m) \sum_{k=iN}^{iN+N-1} a_{\text{dup},n}(k-m)\alpha_n(k-m)\alpha_n^*(k)$$

$$E[\text{MUI}_n^*(i)\text{MUI}_n(i+\ell)] = \left( \frac{E_s}{N} \sum_{m \neq 0} |g_n(m)|^2 \right) \delta(\ell) \quad (\text{O-CDMA})$$

$$E[\text{MUI}^*(i)\text{MUI}(i+\ell)] = \left( \frac{E_s}{N} \sum_{n=1}^{N_u-1} \sum_{m \neq 0} |g_n(m)|^2 \right) \delta(\ell) \quad (\text{O-CDMA})$$

### MUI contribution to $z_0(i)$ for downstream communication (CDM)

The results for downstream communication are obtained from the results for upstream communication by simply substituting  $g(m)$  for  $g_n(m)$ , where

$$g(m) = \int |H(f)|^2 e^{j2\pi f m T} df \quad H(f) = H_{\text{tr}}(f)H_{\text{ch}}(f)$$

$$\Rightarrow E[\text{MUI}^*(i)\text{MUI}(i+\ell)] = \left( \frac{N_u-1}{N} E_s \sum_m |g(m)|^2 \right) \delta(\ell)$$

In the case of O-CDM we obtain :

$$E[\text{MUI}^*(i)\text{MUI}(i+\ell)] = \left( \frac{N_u-1}{N} E_s \sum_{m \neq 0} |g(m)|^2 \right) \delta(\ell)$$



## Single-user receiver for CDMA : model for $z_0(i)$

The total MUI power from  $N_u - 1$  interfering users increases with  $N_u$ , and *cannot* be neglected as compared to the noise power when  $N_u$  is large

$$z_0(i) = a_0(i)g_0(0) + n_0(i) + \text{MUI}(i)$$

$$E[|n_0(i)|^2] = N_0 g_0(0)$$

$\text{MUI}(i)$  : MUI from  $N_u - 1$  UTs in  $i$ -th symbol interval

$$E[|\text{MUI}(i)|^2] = E_s P_{\text{MUI}} \quad P_{\text{MUI}} = \frac{1}{N} \sum_{n=1}^{N_u-1} \sum_m |g_n(m)|^2$$

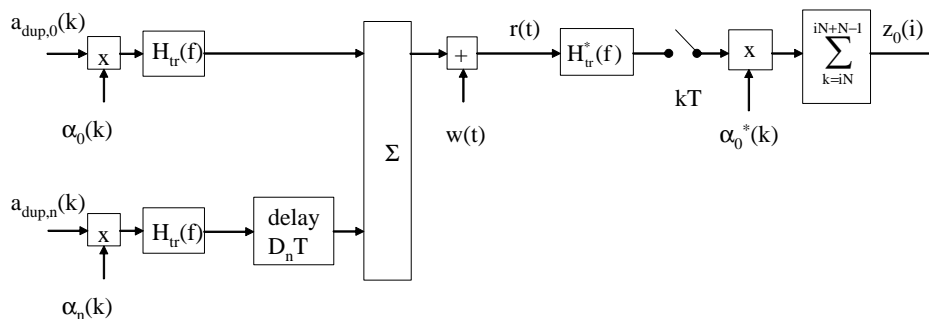
(terms with  $m=0$  in  $P_{\text{MUI}}$  must be dropped in case of O-CDMA)

$P_{\text{MUI}}$  : normalized MUI power, corresponding to  $E_s = 1$

## Example : CDMA on AWGN channel, **non-synchronized** UT transmissions

Assume synchronization errors between UTs are multiples of chip interval  $T$  :

$H_{\text{ch},n}(f) = \exp(-j2\pi f D_n T)$ , with  $D_0 = 0$  and  $D_n$  a nonzero integer for  $n \neq 0$



### Example : CDMA on AWGN channel, non-synchronized UT transmissions

$$g_n(m) = \int |H_{tr}(f)|^2 e^{-j2\pi f D_n T} e^{j2\pi f m T} df = \delta(m - D_n) \Rightarrow G_n(z) = z^{-D_n} \quad n = 0, \dots, N_u - 1$$

$$z_0(i) = a_0(i) + \text{MUI}(i) + n_0(i) \quad E[|a(i)|^2] = E_s \quad E[|n_0(i)|^2] = N_0$$

$$\text{MUI}(i) = \sum_{n=1}^{N_u-1} \text{MUI}_n(i) \quad \text{MUI}_n(i) = \sum_{k=iN}^{iN+N-1} \alpha_0^*(k) \alpha_n(k - D_n) a_{\text{dup},n}(k - D_n)$$

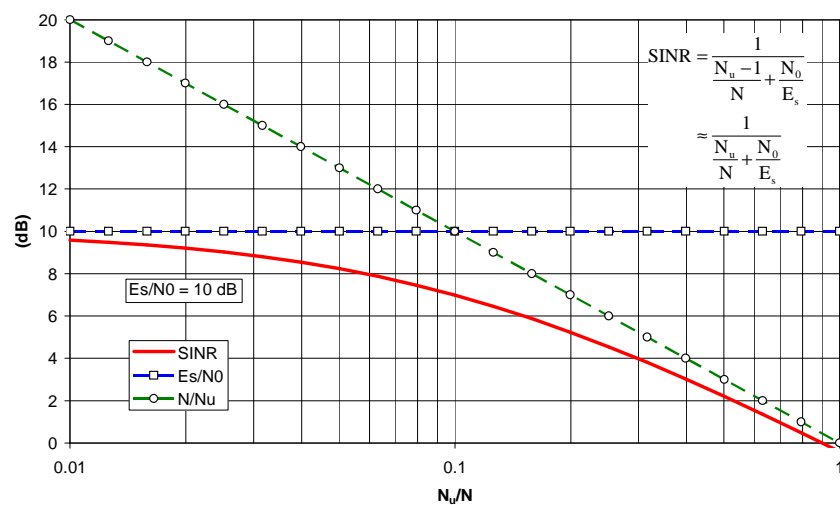
$$E[|\text{MUI}_n(i)|^2] = \frac{E_s}{N} \quad P_{\text{MUI}} = E[|\text{MUI}(i)|^2]/E_s = (N_u - 1)/N$$

$$\text{SINR} = \frac{1}{\frac{N_u - 1}{N} + \frac{N_0}{E_s}} \approx \frac{1}{\frac{N_u}{N} + \frac{N_0}{E_s}}$$

Chapter 7 : Spread-spectrum communication and CDMA

101

### Example : AWGN channel, CDMA, non-synchronized UT transmissions



Chapter 7 : Spread-spectrum communication and CDMA

102

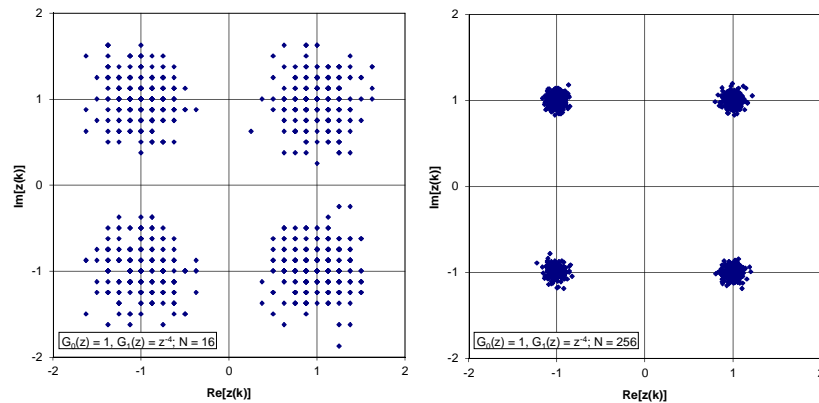
## Single-user receiver for CDMA : scatter diagrams

$N_u = 2$ , no noise, 4-QAM ( $\pm 1 \pm j$ ), i.i.d. complex-valued chips

$H_{ch,0}(f) = 1$ ,  $G_0(z) = 1$  (no distortion on received reference user signal)

$H_{ch,1}(f) = \exp(-j8\pi fT)$  : delay of 4 chip intervals,  $G_1(z) = z^{-4}$

Scatter diagram of  $z_0(i)$ , for  $N = 16, 256$



Chapter 7 : Spread-spectrum communication and CDMA

103

## Single-user receiver for CDMA : BER in the presence of MUI

1) Consider  $z(i) = a(i) + w(i)$       $w(i) \sim N_c(0, N_0\delta(m))$       $E[|a(i)|^2] = E_s$

$$\text{BER, no coding : } \text{BER}_{\text{uncoded}}\left(\frac{E_b}{N_0}\right) = \text{BER}_{\text{uncoded}}\left(\frac{E_s}{N_0} \cdot \frac{1}{\log_2(M)}\right) \quad \boxed{E_s = E_b \log_2(M)}$$

BER, coding (code rate  $r_c = k/n$ , coding gain CG):

coding :  $k$  info bits  $\rightarrow n$  coded bits  $\rightarrow n/\log_2(M)$  coded symbols

$$kE_b = nE_s/\log_2(M) \Rightarrow \boxed{E_s = E_b r_c \log_2(M)} \quad \begin{array}{l} E_b : \text{energy per} \\ \text{information bit} \end{array}$$

$$\text{BER}_{\text{coded}}\left(\frac{E_b}{N_0}\right) = \text{BER}_{\text{uncoded}}\left(\frac{E_b}{N_0} \text{CG}\right) = \text{BER}_{\text{uncoded}}\left(\frac{E_s}{N_0} \cdot \frac{\text{CG}}{r_c \log_2(M)}\right)$$

$10\log(\text{CG})$  : coding gain in dB

Chapter 7 : Spread-spectrum communication and CDMA

104

## Single-user receiver for CDMA : BER in the presence of MUI

2) Consider  $z_0(i) = a_0(i)g_0(0) + n_0(i) + \text{MUI}(i)$

Assumption :

$$\text{MUI}(i) \sim N_c(0, E_s P_{\text{MUI}} \delta(\ell)) \quad n_0(i) \sim N_c(0, N_0 g_0(0) \delta(\ell))$$

Detector operates at an “effective” SNR :

$$\left( \frac{E_s}{N_0} \right)_{\text{eff}} = \text{SINR} = \frac{g_0^2(0) E_s}{N_0 g_0(0) + E_s P_{\text{MUI}}}$$

$\Rightarrow$  computation of “effective”  $E_b/N_0$  for uncoded and coded transmission

## Single-user receiver for CDMA : BER in the presence of MUI

Uncoded transmission

$E_b$  : energy per bit (*transmitted*)

$E_b g(0)$  : energy per bit (*received*)

$$\begin{aligned} \left( \frac{E_b}{N_0} \right)_{\text{eff}} &= \frac{1}{\log_2(M)} \left( \frac{E_s}{N_0} \right)_{\text{eff}} \\ &= \frac{1}{\log_2(M)} \cdot \frac{g_0^2(0) E_s}{N_0 g_0(0) + E_s P_{\text{MUI}}} \\ &= \left( \frac{N_0}{g_0(0) E_b} + \frac{P_{\text{MUI}} \cdot \log_2(M)}{g_0^2(0)} \right)^{-1} \end{aligned} \quad E_s = E_b \log_2(M)$$

$$\text{BER} = \text{BER}_{\text{uncoded}} \left( \left( \frac{E_b}{N_0} \right)_{\text{eff}} \right)$$

## Single-user receiver for CDMA : BER in the presence of MUI

Coded transmission (code rate  $r_c = k/n$ )

$$\begin{aligned} \left(\frac{E_b}{N_0}\right)_{\text{eff}} &= \frac{1}{r_c \cdot \log_2(M)} \left(\frac{E_s}{N_0}\right)_{\text{eff}} & E_b : \text{energy per info bit (transmitted)} \\ & & E_{bg}(0) : \text{energy per info bit (received)} \\ &= \frac{1}{r_c \log_2(M)} \cdot \frac{g_0^2(0)E_s}{N_0 g_0(0) + E_s P_{\text{MUI}}} & E_s = E_b r_c \log_2(M) \\ &= \left( \frac{N_0}{g_0(0)E_b} + \frac{P_{\text{MUI}} r_c \log_2(M)}{g_0^2(0)} \right)^{-1} \end{aligned}$$

$$\text{BER} = \text{BER}_{\text{coded}} \left( \left( \frac{E_b}{N_0} \right)_{\text{eff}} \right) = \text{BER}_{\text{uncoded}} \left( \text{CG} \cdot \left( \frac{E_b}{N_0} \right)_{\text{eff}} \right)$$

## Single-user receiver for CDMA : BER in the presence of MUI

**Example :** 2-PSK,  $g_0(0) = 1$ ,  $P_{\text{MUI}} = (N_u - 1)/N$

1) BER, uncoded

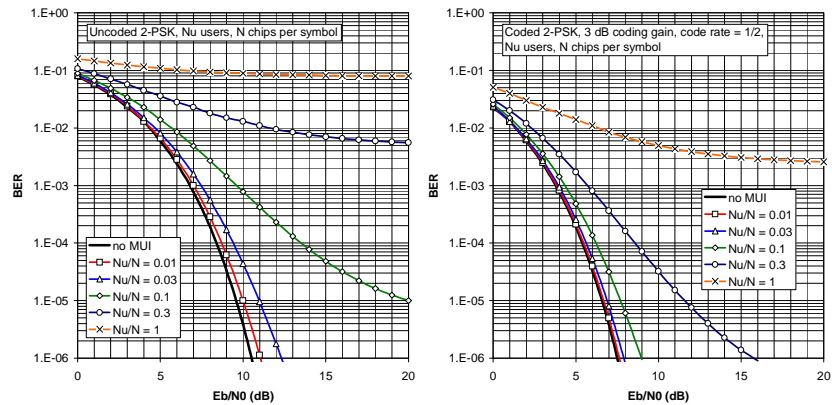
$$\text{BER}_{\text{uncoded}} = Q \left( \sqrt{\left( \frac{2E_b}{N_0} \right)_{\text{eff}}} \right) = Q \left( \sqrt{\left( \frac{N_0}{2E_b} + \frac{N_u - 1}{2N} \right)^{-1}} \right)$$

2) BER, coded (coding gain CG, code rate  $r_c$ )

$$\text{BER}_{\text{coded}} = Q \left( \sqrt{\text{CG} \cdot \left( \frac{2E_b}{N_0} \right)_{\text{eff}}} \right) = Q \left( \sqrt{\text{CG} \cdot \left( \frac{N_0}{2E_b} + r_c \frac{N_u - 1}{2N} \right)^{-1}} \right)$$

## Single-user receiver for CDMA : BER in the presence of MUI

MUI gives rise to “BER floor”, which can be lowered by means of coding.  
MUI limits the number of users that can be accommodated at given BER.



Chapter 7 : Spread-spectrum communication and CDMA

109

## Bandwidth (upstream + downstream) of uncoded/coded CDM(A)

Uncoded transmission

information bitrate  $R_b$ ,  $M$ -point constellation,  
relative excess bandwidth  $\beta$ ,  $N$  chips per symbol

$$B_{RF} = (1 + \beta) \frac{2N \cdot R_b}{\log_2(M)}$$

Coded transmission

information bitrate  $R_b$ ,  $M$ -point constellation,  
code rate  $r_c = k/n$ , relative excess bandwidth  $\beta$ ,  
 $N$  chips per symbol

$$B_{RF} = (1 + \beta) \frac{2N \cdot R_b}{r_c \log_2(M)}$$

$B_{RF}$  for uncoded and coded transmission are the same when taking  $N/r_c$  constant  
 $\Rightarrow$  coding does not necessarily increase bandwidth when using CDMA

Chapter 7 : Spread-spectrum communication and CDMA

110

## **CDM(A) on dispersive channels**

### **Conclusions**

- Because of channel dispersion, ML receiver has high computational complexity (exponential in  $K.N_u$ ).
- Single-user receiver is suboptimum receiver performing symbol-by-symbol decisions (complexity linear in  $K.N_u$ ).
- BER performance of single-user receiver is degraded by multi-user interference (MUI), caused by the presence of signals associated with other users.
- The MUI interference increases with the number of active users; the maximum degradation that one is prepared to accept puts a limit on the number of users that can be simultaneously active.

## **CDMA in cellular radio systems**

Examples : IS-95 (2nd generation mobile communications)  
W-CDMA in UMTS (3rd generation mobile communications)

## CDMA in cellular radio systems

Cellular CDMA uses  $N_{re} = 1$  : all cells use the *entire* system bandwidth  $B_{RF,tot}$  (this is unlike TDMA or FDMA, where each cell occupies a bandwidth  $B_{RF,tot}/N_{re}$ , with  $N_{re} = 3, 4$  or  $7$ , in order to reduce inter-cell interference).

In cellular CDMA, inter-cell multi-user interference adds to intra-cell multi-user interference.

A same spreading sequence can be used in different cells, provided that common sequences are shifted with respect to each other

⇒ power of inter-cell interference is  $\sim 1/N$  (as for intra-cell interference)

Taking into account the path loss, inter-cell interference is typically about 2 dB below intra-cell interference

## Bandwidth efficiency definition for cellular radio systems

$$\eta_{BW} = \frac{\text{total infobitrate in one cell}}{\text{total system bandwidth}} = \frac{2N_u R_b}{B_{RF,tot}} = \frac{2N_u R_s r_c \log_2(M)}{B_{RF,cell} N_{re}} \quad ((\text{bit/s})/\text{Hz})$$

total information bitrate : upstream + downstream

$N_u$  : number of UTs per cell

$R_b$  : information bitrate per user       $R_s$  : symbol rate per user

$M$  : constellation size

$r_c (= k/n)$  : code rate

$N_{re}$  : reuse factor (= 1 for CDM(A))

$B_{RF,tot}$  : total RF system bandwidth (upstream+downstream)

$B_{RF,cell}$  : RF bandwidth occupied by one cell (upstream+downstream)



### Bandwidth efficiency : CDM(A)

$$\eta_{BW} = \frac{2N_u R_s r_c \log_2(M)}{B_{RF,tot}}$$

**CDM(A)** : N chips per symbol

$$B_{RF,tot} = (1+\beta)2N \cdot R_s \quad (\beta : \text{rolloff factor})$$

$$\approx 2N \cdot R_s \quad (\text{small } \beta)$$

$$\Rightarrow \eta_{BW,CDMA} \approx \frac{N_u}{N} r_c \log_2(M)$$

bandwidth efficiency limited by ratio  $N_u/N$

### Bandwidth efficiency : TDM(A)

$$\eta_{BW} = \frac{2N_u R_s r_c \log_2(M)}{B_{RF,tot}}$$

**TDM(A)** :  $N_{slot}$  slots per frame

$$B_{RF,tot} = N_{re} B_{RF,cell} = (1+\beta)2N_{slot} N_{re} R_s \approx 2N_{slot} N_{re} R_s \quad (\text{small } \beta)$$

Assume fully loaded cell : all slots occupied  $\Rightarrow N_u = N_{slot}$   $B_{RF,tot} \approx 2N_u N_{re} R_s$

$$\Rightarrow \eta_{BW,TDMA} \approx \frac{1}{N_{re}} r_c \log_2(M) \quad \text{reuse factor } N_{re} \text{ reduces bandwidth efficiency}$$

same result for FDM(A) with fully loaded cell (all frequency slots occupied)

## BER considerations

Consider input decision device (decoder) :

$$u(k) = a(k) + w(k)$$

$$\text{with } E[|a(k)|^2] = E_s, w(k) \sim N_c(0, N_0\delta(m))$$

$$\text{coded transmission, code rate } r_c = k/n : E_s = E_b r_c \log_2(M)$$

$$\text{resulting BER : } \text{BER}_{\text{MF}} = f(E_b/N_0) \\ f(.) \text{ depends on constellation and code}$$

this is matched filter bound corresponding to observation model

$$r(t) = a(k)h(t) + w(t) \quad \int |h(t)|^2 dt = 1$$

$$w(t) \sim N_c(0, N_0\delta(u))$$

## BER considerations

Consider input decision device (decoder) :  $u(k) = \gamma a(k) + \text{INT}(k) + n(k)$

$\text{INT}(k)$  : interference (ISI, MUI, inter-cell, intra-cell, ...)

$n(k)$  : Gaussian noise

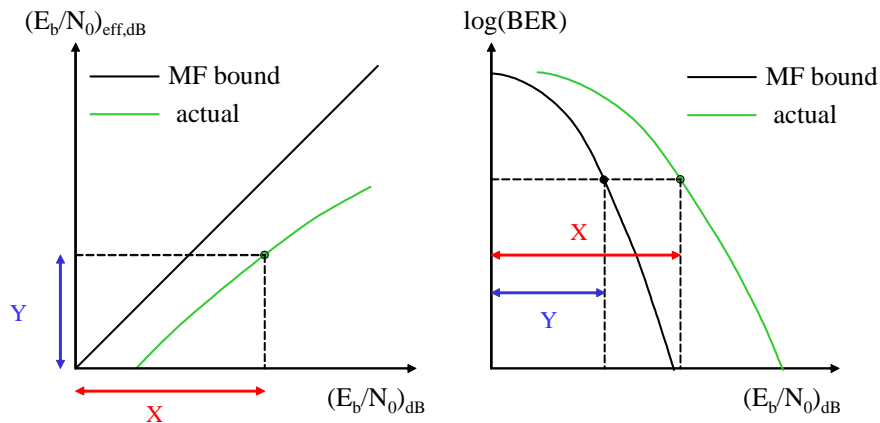
$a(k)$  : coded symbols with  $E[|a(k)|^2] = E_s$

$$(E_s/N_0)_{\text{eff}} = \text{SINR} \quad \text{SINR} = \frac{|\gamma|^2 E_s}{E[|\text{INT}(k)|^2] + E[|n(k)|^2]}$$

$$\left(\frac{E_b}{N_0}\right)_{\text{eff}} = \frac{1}{r_c \log_2(M)} \left(\frac{E_s}{N_0}\right)_{\text{eff}} = \frac{\text{SINR}}{r_c \log_2(M)}$$

actual BER :  $\text{BER}_{\text{act}} = f((E_b/N_0)_{\text{eff}})$  (assumes interference is Gaussian)

## BER considerations



Chapter 7 : Spread-spectrum communication and CDMA

119

## Simplifying assumptions for CDMA

Input decision device (decoder) :  $u(k) \approx a(k) + \text{MUI}(k) + w(k)$

large N

Contribution from reference user signal :

coefficient of  $a(k)$  equals 1 ( $g(0) = 1$ )

ISI caused by static dispersive channel is neglected

Contribution from noise :  $w(k) \sim N_c(0, N_0\delta(m))$

Interference

$\text{MUI}(k) \sim N_c(0, E_s P_{\text{MUI}})$ ,  $P_{\text{MUI}} \approx N_u/N$  (intra-cell interference)

Inter-cell interference is neglected (is smaller than intra-cell interference)

Chapter 7 : Spread-spectrum communication and CDMA

120

## Simplifying assumptions for TDMA

Input decision device (decoder) :  $u(k) \approx a(k) + n(k)$

Inter-cell interference is neglected (because of large  $N_{re}$ )

Negligible ISI because of equalization of the static dispersive channel

Equalizer yields noise enhancement at input decision device  
(amount of enhancement depends on channel transfer function  
and type of equalizer used)

$\Rightarrow E[n(k)^2] = \kappa N_0$ ,  
with noise enhancement (in dB) =  $10 \cdot \log(\kappa)$

## BER considerations : CDMA

Input decision device (decoder) :  $u(k) \approx a(k) + \text{MUI}(k) + w(k)$

$$\text{SINR} \approx \frac{E_s}{N_0 + E_s \frac{N_u}{N}} \quad \eta_{\text{BW,CDMA}} \approx \frac{N_u}{N} r_c \log_2(M)$$

$$\begin{aligned} \left( \frac{E_b}{N_0} \right)_{\text{eff,CDMA}} &= \frac{\text{SINR}}{r_c \log_2(M)} \approx \frac{1}{r_c \log_2(M)} \cdot \frac{E_s}{N_0 + \frac{N_u}{N} E_s} \\ &= \left( \left( \frac{E_b}{N_0} \right)^{-1} + \eta_{\text{BW,CDMA}} \right)^{-1} \end{aligned}$$

$\Rightarrow (E_b/N_0)_{\text{eff,CDMA}} \downarrow$  when  $\eta_{\text{BW,CDMA}} \uparrow$  (because of increase MUI)

$\Rightarrow \text{BER}_{\text{CDMA}} = f((E_b/N_0)_{\text{eff,CDMA}}) \uparrow$  when  $\eta_{\text{BW,CDMA}} \uparrow$

**BER performance traded for bandwidth efficiency**

## BER considerations : CDMA

$$\left( \left( \frac{E_b}{N_0} \right)_{\text{eff,CDMA}} \right)^{-1} = \left( \frac{E_b}{N_0} \right)^{-1} + \eta_{\text{BW,CDMA}}$$

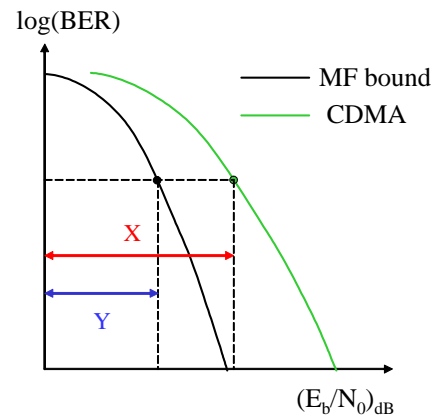
$$\eta_{\text{BW,CDMA}} = \left( 1 - \frac{1}{q} \right) \left( \frac{E_b}{N_0} \right)_{\text{eff,CDMA}}^{-1} \leq \left( \frac{E_b}{N_0} \right)_{\text{eff,CDMA}}^{-1}$$

$$\text{where } q = \frac{(E_b/N_0)}{(E_b/N_0)_{\text{eff}}} > 1$$

$$X - Y = 10 \cdot \log(q)$$

$$X = 10 \cdot \log(E_b/N_0)$$

$$Y = 10 \cdot \log((E_b/N_0)_{\text{eff,CDMA}})$$



Chapter 7 : Spread-spectrum communication and CDMA

123

## BER considerations : TDMA

Input decision device (decoder) :  $u(k) \approx a(k) + n(k)$

$$\text{SINR} \approx \frac{E_s}{\kappa N_0} \quad \kappa (\geq 1) : \text{noise enhancement (equalization of dispersive channel)}$$

$$\left( \frac{E_b}{N_0} \right)_{\text{eff,TDMA}} = \frac{\text{SINR}}{r_c \cdot \log_2(M)} \approx \frac{1}{\kappa} \cdot \frac{E_b}{N_0}$$

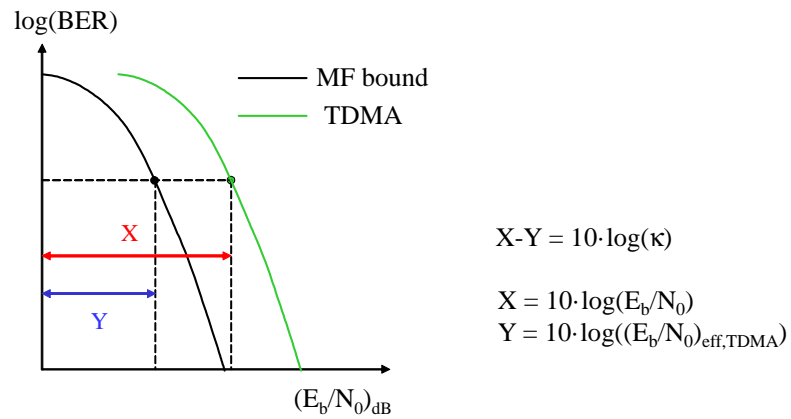
$$\text{BER}_{\text{TDMA}} = f((E_b/N_0)_{\text{eff,TDMA}})$$

$\Rightarrow (E_b/N_0)_{\text{eff,TDMA}}$  and  $\text{BER}_{\text{TDMA}}$  affected by  $\kappa$ , but *not* by number of users

Chapter 7 : Spread-spectrum communication and CDMA

124

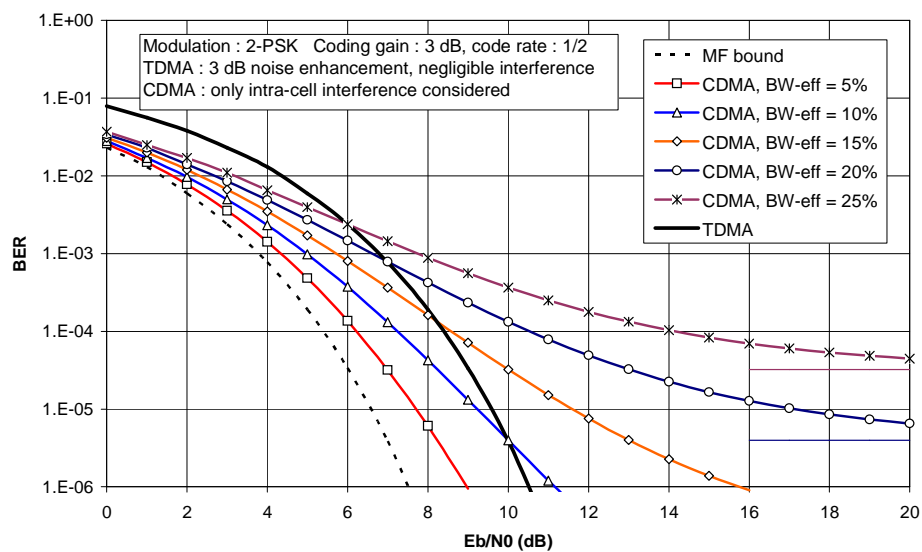
## BER considerations : TDMA



Chapter 7 : Spread-spectrum communication and CDMA

125

## BER : TDMA versus CDMA



Chapter 7 : Spread-spectrum communication and CDMA

126

## Bandwidth efficiency and BER

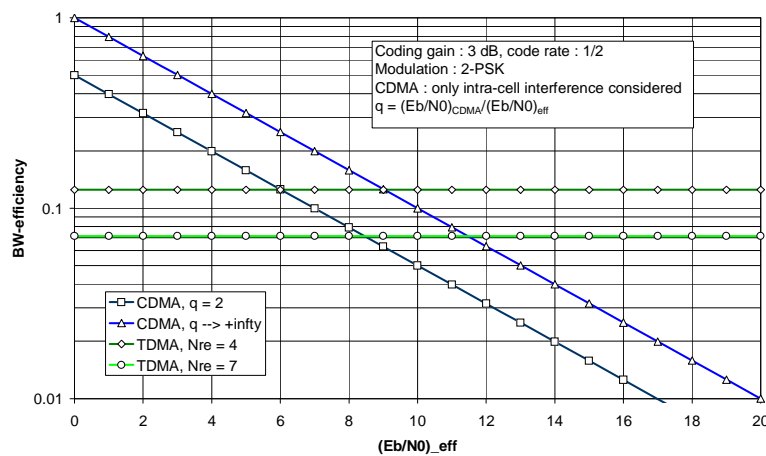
**TDMA :**  $\eta_{\text{BW,TDMA}} \approx \frac{1}{N_{\text{re}}} r_c \cdot \log_2(M)$  Reuse factor  $N_{\text{re}}$  reduces bandwidth efficiency

**CDMA :**  $\eta_{\text{BW,CDMA}} = \left(1 - \frac{1}{q}\right) \left(\frac{E_b}{N_0}\right)_{\text{eff}}^{-1} \leq \left(\frac{E_b}{N_0}\right)_{\text{eff}}^{-1}$  where  $q = \frac{(E_b/N_0)}{(E_b/N_0)_{\text{eff}}} > 1$

Bandwidth efficiency of CDMA is determined by  $(E_b/N_0)_{\text{eff}}$  corresponding to operating BER and by the amount of degradation ( $q$ ) one is willing to accept. For very large  $q$ , bandwidth efficiency is limited by operating BER : operating BER cannot be reached for BW efficiency larger than  $1/(E_b/N_0)_{\text{eff}}$ . Performance of CDMA system is **interference-limited**.

## BW efficiency : TDMA versus CDMA

for  $q = \kappa$ , TDMA and CDMA have same degradation w.r.t.  $\text{BER}_{\text{MF}}$



## Conclusions

### Point-to-point spread-spectrum communication

- Spread-spectrum with orthogonal chip pulses on the AWGN channel :
  - matched filter + symbol-by-symbol detection is optimum
  - same BER as for bandwidth-efficient modulation, which equals matched filter bound.
  - large spreading factor : low detection probability and high robustness against narrowband interference, at expense of large signal bandwidth
- Spread-spectrum with large spreading factor on dispersive channels :
  - matched filter (RAKE filter) + symbol-by-symbol detection close to optimum
  - effect of channel dispersion negligible
  - BER close to matched filter bound : no noise enhancement !
  - benefits from diversity on multipath fading channels

## Conclusions

### Multiuser spread-spectrum communication (CDM(A))

- O-CDMA (synchronized !) with orthogonal chip pulses on AWGN channel :
  - no interference between different user signals
  - single-user receiver with matched filter + symbol-by-symbol decisions is optimum.
  - same BER as for TDMA and FDMA, equal to matched filter bound
- CDMA with large spreading factor on dispersive channels :
  - optimum receiver very complicated (joint detection of all symbols from all users)
  - suboptimum single-user receiver with symbol-by-symbol detection : affected by MUI, not by distortion of reference user signal.
  - MUI increases with  $N_u/N$ , and degrades the BER as compared to matched filter bound
  - benefits from diversity on multipath fading channels



## Conclusions

### Cellular systems

- Cellular CDMA has reuse factor  $N_{re} = 1$ . Intercell interference is limited by using different chip sequences in different cells
- Bandwidth efficiency of cellular CDMA proportional to  $N_u/N$
- Ratio  $N_u/N$  determines MUI power, which in turn determines BER degradation as compared to matched filter bound
- Cellular TDMA (or FDMA) has reuse factor  $N_{re} > 1$ , to limit intercell interference
- Bandwidth efficiency of cellular TDMA (or FDMA) proportional to  $1/N_{re}$
- BER degradation as compared to matched filter bound caused by noise enhancement (equalization of dispersive channel)

## Spread-spectrum for localization : Global Positioning System (GPS)

## GPS : basic principle

- $N_{\text{sat}}$  synchronized satellites send (periodic) chip sequences to GPS receiver.
- GPS receiver measures propagation delays from each satellite to GPS receiver, and computes from these delays its distance to each satellite.
- GPS receiver spatial coordinates (x,y,z) are computed from known spatial coordinates of satellites

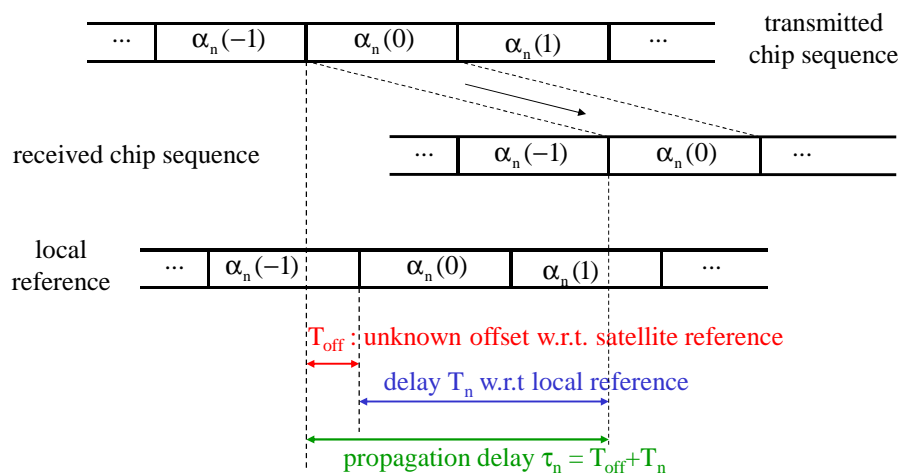
Satellites *synchronized* by means of atomic clock  
 $\Rightarrow$  transmissions from all satellites are *time-aligned*

transmitted chip sequences	...	$\alpha_1(-1)$	$\alpha_1(0)$	$\alpha_1(1)$	...
	...	$\alpha_n(-1)$	$\alpha_n(0)$	$\alpha_n(1)$	...
	...	$\alpha_{N_{\text{sat}}}(-1)$	$\alpha_{N_{\text{sat}}}(0)$	$\alpha_{N_{\text{sat}}-1}(1)$	...

Chapter 7 : Spread-spectrum communication and CDMA

133

## GPS : basic principle



Chapter 7 : Spread-spectrum communication and CDMA

134

## GPS : determining localization

4 unknowns : receiver coordinates  $(x,y,z)$  and timing offset  $T_{\text{off}}$

available :  $N_{\text{sat}}$  satellite coordinates  $\{(x_n, y_n, z_n)\}$ ,  $N_{\text{sat}}$  receiver measurements  $\{\hat{T}_n\}$

When  $N_{\text{sat}} = 4$  satellites are available, the 4 unknowns are computed from :

$$c \cdot (\hat{T}_n + T_{\text{off}}) = \sqrt{(x - x_n)^2 + (y - y_n)^2 + (z - z_n)^2} \quad (n = 1, 2, 3, 4)$$

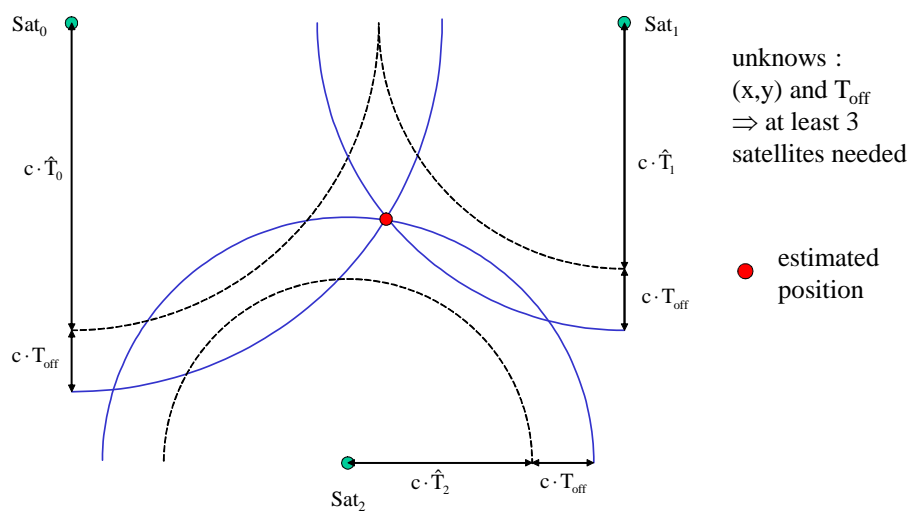
$c$  : speed of light

When more than 4 satellites are available,  $T_{\text{off}}$  and  $(x,y,z)$  are determined such that the following expression is minimized (*least squares fit*) :

$$\sum_{n=1}^{N_{\text{sat}}} \left( \sqrt{(x - x_n)^2 + (y - y_n)^2 + (z - z_n)^2} - c \cdot (\hat{T}_n + T_{\text{off}}) \right)^2$$

Having more than 4 satellites available reduces the effect of measurement errors.

## GPS : 2-D example



## GPS : delay estimation

Observation model :

$$r(t) = \sum_{n=1}^{N_{\text{sat}}} s_n(t - T_n) + w(t) \quad \text{signal at input GPS receiver}$$

$$\text{Signal transmitted by } n\text{-th satellite : } s_n(t) = \sqrt{P \cdot T} \sum_k \alpha_n(k) h_{tr}(t - kT)$$

$T_n$  : delay of signal received from  $n$ -th satellite,  
as compared to the local receiver clock

$$\text{orthogonality condition : } \int h_{tr}(t) h_{tr}^*(t - mT) dt = \delta(m)$$

$\{\alpha_n(k)\}$  and  $\{\alpha_{n'}(k)\}$  : independent sequences ( $n \neq n'$ ) of zero-mean i.i.d. chips  
with  $|\alpha_n(k)| = 1$

$P$  : signal power

## GPS : ML delay estimation

$$\text{ML estimate of delays : } (\hat{T}_1, \dots, \hat{T}_{N_{\text{sat}}}) = \arg \max_{\tilde{T}_1, \dots, \tilde{T}_{N_{\text{sat}}}} p(\mathbf{r} | \tilde{T}_1, \dots, \tilde{T}_{N_{\text{sat}}})$$

Log-likelihood function :

$$\begin{aligned} -N_0 \ln p(\mathbf{r} | \tilde{T}_1, \dots, \tilde{T}_{N_{\text{sat}}}) &= -2\sqrt{P \cdot T} \sum_{n=1}^{N_{\text{sat}}} \text{Re} \left[ \sum_k \alpha_n^*(k) v(k; \tilde{T}_n) \right] \\ &\quad + P \cdot T \sum_{n,n'=1}^{N_{\text{sat}}} \sum_{k,k'} \alpha_n^*(k) \alpha_{n'}(k') g(k - k'; \tilde{T}_n - \tilde{T}_{n'}) \end{aligned}$$

$$v(k; \tau) = \int r(t) h_{tr}^*(t - kT - \tau) dt \quad \text{matched filter output sample at } kT + \tau$$

$$g(m; \tau) = \int h_{tr}(t) h_{tr}^*(t - mT - \tau) dt$$

## GPS : ML delay estimation

$$-N_0 \ln p(\mathbf{r} | \tilde{T}_1, \dots, \tilde{T}_{N_{\text{sat}}}) = -2\sqrt{P \cdot T} \sum_{n=1}^{N_{\text{sat}}} \text{Re} \left[ \sum_k \alpha_n^*(k) v(k; \tilde{T}_n) \right] \\ + P \cdot T \sum_{n, n'=1}^{N_{\text{sat}}} \sum_{k, k'} \alpha_n^*(k) \alpha_{n'}(k') g(k - k'; \tilde{T}_n - \tilde{T}_{n'})$$

ML estimation involves the *joint* estimation of all  $N_{\text{sat}}$  delays

$\Rightarrow N_{\text{sat}}$ -dimensional search over  $N_{\text{sat}}$  continuous delay variables is required

$\Rightarrow$  very computationally intensive !

Reduce complexity by using *suboptimum* algorithm :

estimate the  $N_{\text{sat}}$  delays *separately* (instead of jointly)

$\Rightarrow$  ignore the presence of signals  $s_{n'}(t - T_{n'})$  with  $n' \neq n$  when estimating  $T_n$

$\Rightarrow N_{\text{sat}}$  one-dimensional searches (instead of one  $N_{\text{sat}}$ -dimensional search)

## GPS : suboptimum delay estimation

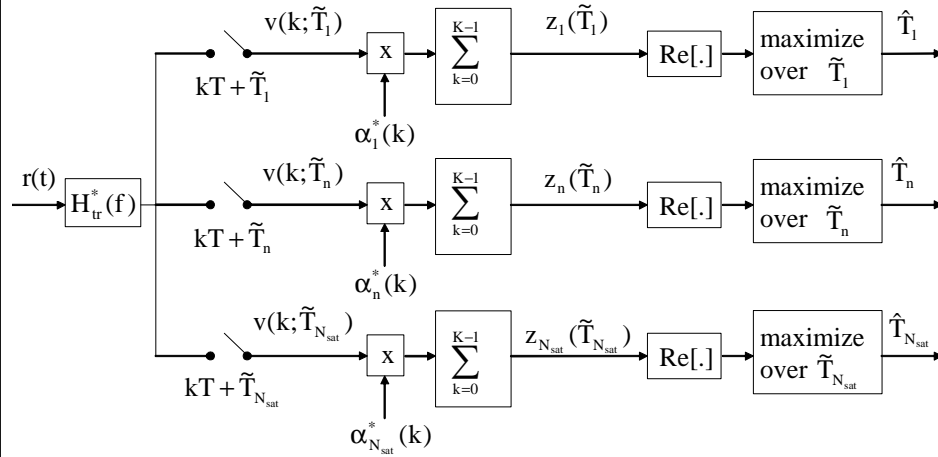
Simplified observation model for estimating  $T_n$  :

$$r(t) = s_n(t - T_n) + w(t) \quad (\text{ignores signals } s_{n'}(t - T_{n'}) \text{ with } n' \neq n)$$

Log-likelihood function :

$$-N_0 \ln p(\mathbf{r} | \tilde{T}_n) = -2\sqrt{P \cdot T} \text{Re} \left[ \sum_k \alpha_n^*(k) v(k; \tilde{T}_n) \right] \\ + P \cdot T \sum_{k, k'} \alpha_n^*(k) \alpha_n(k') g(k - k'; 0) \\ \propto -2\sqrt{P \cdot T} \text{Re}[z_n(\tilde{T}_n)] \\ = -2\sqrt{P \cdot T} z_{R,n}(\tilde{T}_n) \quad z_n(\tau) = \sum_{k=0}^{K-1} \alpha_n^*(k) v(k; \tau)$$

### GPS : suboptimum delay estimation



requires  $N_{\text{sat}}$  one-dimensional searches

Chapter 7 : Spread-spectrum communication and CDMA

141

### GPS : suboptimum delay estimation

$$\begin{aligned}
 z_n(\tilde{T}_n) &= \sum_{k=0}^{K-1} \alpha_n^*(k) v(k; \tilde{T}_n) \\
 &= \sqrt{PT} \sum_{k=0}^{K-1} \alpha_n^*(k) \sum_{n'=1}^{N_{\text{sat}}} \sum_m \alpha_{n'}(k-m) g(m; \tilde{T}_n - T_{n'}) + w_n(\tilde{T}_n) \\
 &= \underbrace{K\sqrt{PT}g(0; \tilde{T}_n - T_n)}_{\text{useful}} + \text{interference} + w_n(\tilde{T}_n)
 \end{aligned}$$

$$w_v(k; \tilde{T}_n) = \int h(t - kT - \tilde{T}_n) w(t) dt \sim N_c(0, N_0 \delta(m))$$

$$w_n(\tilde{T}_n) = \sum_{k=0}^{K-1} \alpha_n^*(k) w_v(k; \tilde{T}_n) \quad E[|w_n(\tilde{T}_n)|^2] = K \cdot N_0$$

$$\begin{aligned}
 \text{interference} &= \sqrt{PT} \sum_{m \neq 0} g(m; \tilde{T}_n - T_n) \sum_{k=0}^{K-1} \alpha_n^*(k) \alpha_n(k-m) \\
 &\quad + \sqrt{PT} \sum_{\substack{n'=1 \\ n' \neq n}}^{N_{\text{sat}}} \sum_m g(m; \tilde{T}_n - T_{n'}) \sum_{k=0}^{K-1} \alpha_n^*(k) \alpha_{n'}(k-m)
 \end{aligned}$$

Chapter 7 : Spread-spectrum communication and CDMA

142

## GPS : suboptimum delay estimation

$$z_n(\tilde{T}_n) = \underbrace{K\sqrt{PT}g(0; \tilde{T}_n - T_n)}_{\text{useful}} + \text{interference} + w_n(\tilde{T}_n)$$

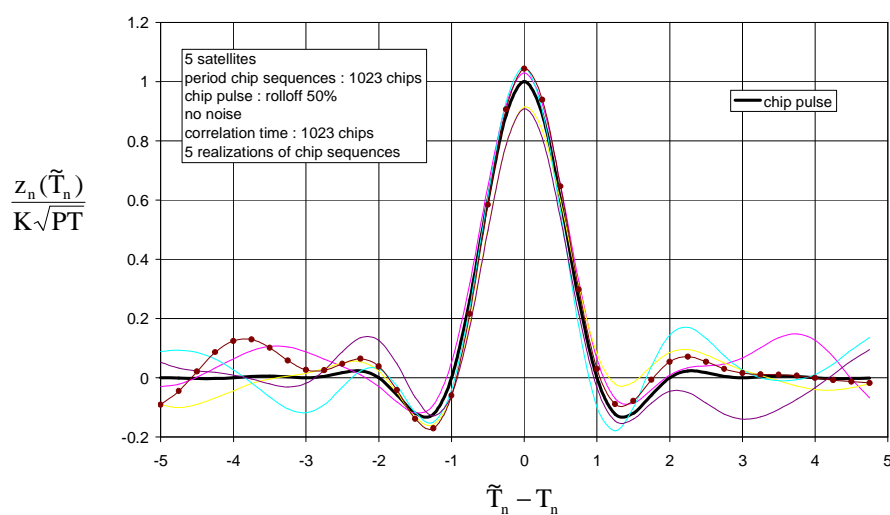
$$E[|\text{useful}|^2] = K^2 PT |g(0; \tilde{T}_n - T_n)|^2 \quad E[|w_n(\tilde{T}_n)|^2] = K \cdot N_0$$

$$E[|\text{interference}|^2] = K \cdot PT \sum_{m \neq 0} |g(m; \tilde{T}_n - T_n)|^2 + K \cdot PT \sum_{\substack{n'=1 \\ n' \neq n}}^{N_{\text{sat}}} \sum_m |g(m; \tilde{T}_n - T_{n'})|^2$$

$$\text{SINR}_n(\tilde{T}_n) = \frac{|g(0; \tilde{T}_n - T_n)|^2}{\frac{1}{K} \cdot \frac{N_0}{PT} + \frac{1}{K} \left( \sum_{m \neq 0} |g(m; \tilde{T}_n - T_n)|^2 + \sum_{\substack{n'=1 \\ n' \neq n}}^{N_{\text{sat}}} \sum_m |g(m; \tilde{T}_n - T_{n'})|^2 \right)}$$

$\Rightarrow$  increasing the summation range  $K$  reduces effect of noise and interference

## GPS : suboptimum delay estimation



## GPS : how to perform 1-D search ?

*Coarse search followed by fine search*

**Coarse search :**

delay estimate is restricted to be an integer multiple of (for example)  $T/2$

$$\tilde{T}_n = \tilde{m}_n T/2$$

$$\hat{m}_n = \arg \max_{\tilde{m}_n} z_{R,n}(\tilde{m}_n T/2)$$

**Fine search :** in vicinity of delay estimate resulting from coarse search

$$\tilde{T}_n = (\hat{m}_n + \tilde{\epsilon}_n) T/2$$

$$\hat{\epsilon}_n = \arg \max_{|\tilde{\epsilon}_n| \leq 1/2} z_{R,n}((\hat{m}_n + \tilde{\epsilon}_n) T/2)$$

**Final estimate :**  $\hat{T}_n = (\hat{m}_n + \hat{\epsilon}_n) T/2$

## GPS : coarse search

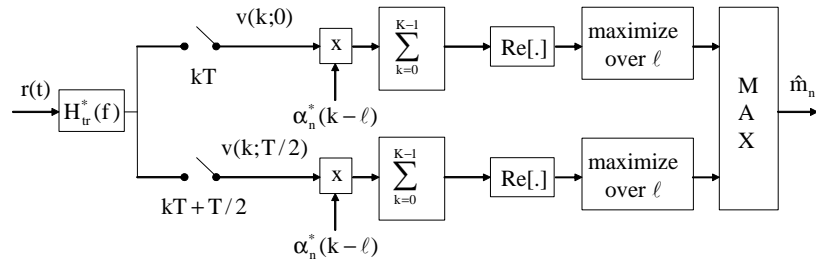
$$\tilde{T}_n = \tilde{m}_n T/2 \quad \hat{m}_n = \arg \max_{\tilde{m}_n} z_{R,n}(\tilde{m}_n T/2)$$

$$z_n(\tilde{m}_n T/2) = \sum_k \alpha_n^*(k) v(k; \tilde{m}_n T/2)$$

$$= \begin{cases} \sum_k \alpha_n^*(k) v(k; \ell T) = \sum_k \alpha_n^*(k - \ell) v(k; 0) & \tilde{m}_n = 2\ell \\ \sum_k \alpha_n^*(k) v(k; \ell T + T/2) = \sum_k \alpha_n^*(k - \ell) v(k; T/2) & \tilde{m}_n = 2\ell + 1 \end{cases}$$



## GPS : coarse search



Chapter 7 : Spread-spectrum communication and CDMA

147

## GPS : fine search

Fine search requires computation of  $z_{R,n}((\hat{m}_n + \tilde{\epsilon}_n)T/2)$  for  $|\tilde{\epsilon}_n| \leq 1/2$

This can be achieved by means of *interpolation*, based on the values

$$\{..., z_{R,n}((\hat{m}_n - 1)T/2), z_{R,n}(\hat{m}_n T/2), z_{R,n}((\hat{m}_n + 1)T/2), \dots\}$$

that have been computed during the coarse search.

When  $H_{tr}(f) = 0$  for  $|f| > B$  with  $B < 1/T$ , the samples  $z_{R,n}(mT/2)$  contain all information needed to compute  $z_{R,n}(\tau)$  for any  $\tau$  (sampling theorem) :

$$z_{R,n}((\hat{m}_n + \tilde{\epsilon}_n)T/2) = \sum_i z_{R,n}((\hat{m}_n - i)T/2) \frac{\sin(\pi((i + \tilde{\epsilon}_n)T/2))}{\pi((i + \tilde{\epsilon}_n)T/2)}$$

However, this exact interpolation requires an *infinite* number of samples. This problem can be circumvented by using interpolation based on a *limited* number of samples, but the result is approximate rather than exact.

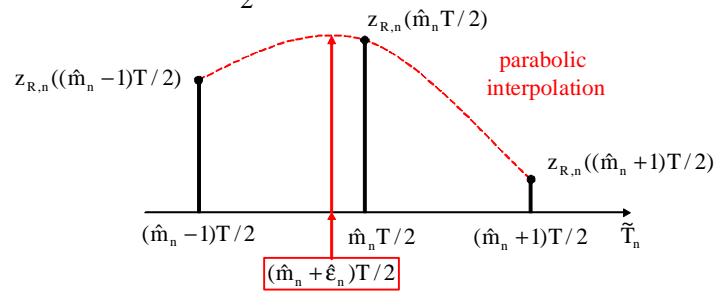
Chapter 7 : Spread-spectrum communication and CDMA

148

## GPS : fine search

When using *parabolic interpolation*, we get :

$$z_{R,n}((\hat{m}_n + \tilde{\epsilon}_n)T/2) \approx (1 - \tilde{\epsilon}_n^2)z_{R,n}(\hat{m}_n T/2) + \frac{\tilde{\epsilon}_n(1 + \tilde{\epsilon}_n)}{2}z_{R,n}((\hat{m}_n + 1)T/2) - \frac{\tilde{\epsilon}_n(1 - \tilde{\epsilon}_n)}{2}z_{R,n}((\hat{m}_n - 1)T/2)$$



which becomes  
maximum for

$$\tilde{\epsilon}_n = \hat{\epsilon}_n = \frac{z_R((\hat{m}_n + 1)T/2) - z_R((\hat{m}_n - 1)T/2)}{4z_R(\hat{m}_n T/2) - 2z_R((\hat{m}_n + 1)T/2) - 2z_R((\hat{m}_n - 1)T/2)}$$

## GPS : numerical data

GPS : developed by U.S. Dept. of Defense

At least 24 medium Earth orbit satellites, at least 6 satellites within line-of-sight

Chip sequence period : 1023 chips

Chiprate : 1.023 Mc/s  $\Rightarrow$  1023 chips in 1 ms

Delay estimation accuracy :  $\approx$  1% of chip interval  $\approx$  10 ns (= 3 m)

Position accuracy (incl. atmospheric, satellite, multipath ... errors) : about 15 m

Other positioning systems :

- Russian system : GLONASS (24 satellites)
- Future European system : Galileo (30 satellites)

## Generation of chip sequences

## Linear feedback shift register sequences

Shift register, I stages

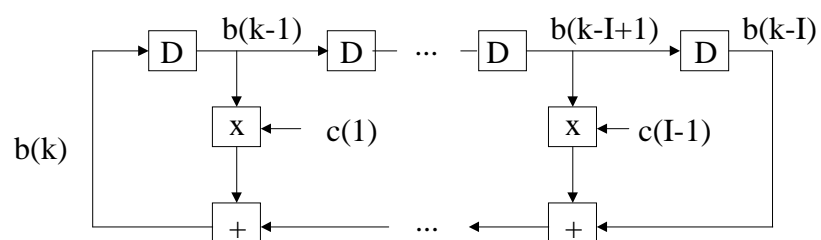
$b(n) \in \{0, 1\}$ ,  $c(i) \in \{0, 1\}$

$b(k)$  is linear combination of  $b(k-1)$ ,  $b(k-2)$ , ...,  $b(k-I)$

D : delay operator

$$b(k) = \sum_{i=1}^I c(i)b(k-i) \quad (\text{multiplication and addition are modulo-2})$$

with  $c(I) = 1$



## Linear feedback shift register sequences

State at instant  $k$  :  $S(k) = (b(k-1), \dots, b(k-I))$

State transitions are determined by *characteristic polynomial*  $c(D)$ , which describes the shift register connections

$$c(D) = \sum_{i=0}^I c(i)D^i \quad (c(0) = c(I) = 1)$$

Sequence  $\{b(n)\}$  is completely determined by polynomial  $c(D)$  and by initial state  $S(0) = (b(-1), \dots, b(-I))$

Sequence  $\{b(0), b(1), \dots\}$  is represented as a polynomial  $b(D)$  :

$$b(D) = \sum_{k=0}^{\infty} b(k)D^k$$

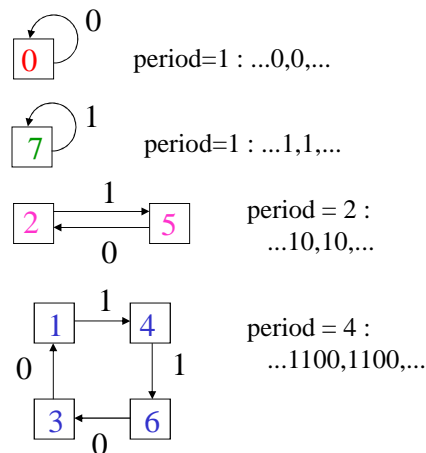
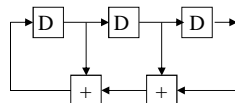
## LFSR sequences : examples

### Example 1

$$c(D) = 1 + D + D^2 + D^3$$

$$b(k) = b(k-1) + b(k-2) + b(k-3)$$

$S(k)$	$S(k+1)$	$b(k)$
000	000	0
001	100	1
010	101	1
011	001	0
100	110	1
101	010	0
110	011	0
111	111	1



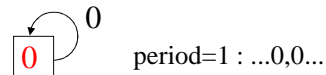
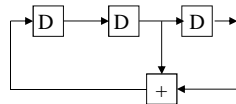
## LFSR sequences : examples

### Example 2

$$c(D) = 1 + D^2 + D^3$$

$$b(k) = b(k-2) + b(k-3)$$

S(k)	S(k+1)	b(k)
000	000	0
001	100	1
010	101	1
011	001	0
100	010	0
101	110	1
110	111	1
111	011	0



period=7 :  
...1011100,1011100...

## Linear feedback shift register sequences

$$b(k) = \sum_{i=1}^I c(i)b(k-i)$$

initial state :  $S(0) = (b(-1), \dots, b(-I))$

$D^0$	$b(0)$	$= c(1)b(-1) + c(2)b(-2) + \dots + c(I)b(-I)$
$D^1$	$b(1)$	$= c(1)b(0) + c(2)b(-1) + \dots + c(I)b(-I+1)$
$D^2$	$b(2)$	$= c(1)b(1) + c(2)b(0) + \dots + c(I)b(-I+2)$
$\vdots$	$\vdots$	$\vdots$
$D^{I-1}$	$b(I-1)$	$= c(1)b(I-2) + c(2)b(I-3) + \dots + c(I)b(-1)$
$D^I$	$b(I)$	$= c(1)b(I-1) + c(2)b(I-2) + \dots + c(I)b(0)$
$D^{I+1}$	$b(I+1)$	$= c(1)b(I) + c(2)b(I-1) + \dots + c(I)b(1)$
$\vdots$	$\vdots$	$\vdots$
$D^k$	$b(k)$	$= c(1)b(k-1) + c(2)b(k-2) + \dots + c(I)b(k-I)$
$\vdots$	$\vdots$	$\vdots$

$$\sum_k b(D) = (c(1)D + c(2)D^2 + \dots + c(I)D^I)b(D)$$

$$+ c(1)b(-1) + c(2)(b(-2) + b(-1)D) + \dots$$

$$+ c(I)(b(-I) + b(-I+1)D + \dots + b(-1)D^{I-1})$$

## Linear feedback shift register sequences

$$\begin{aligned} b(D) = & (c(1)D + c(2)D^2 + \dots + c(I)D^I)b(D) \\ & + c(1)b(-1) + c(2)(b(-2)+b(-1)D) + \dots \\ & + c(I)(b(-I)+b(-I+1)D+\dots+b(-1)D^{I-1}) \end{aligned}$$

$$\Rightarrow c(D)b(D) = p(D)$$

$$\begin{aligned} c(D) &= \sum_{i=0}^I c(i)D^i = 1 + \sum_{i=1}^I c(i)D^i \\ p(D) &= \sum_{i=0}^{I-1} \left( \sum_{j=i+1}^I c(j)b(i-j) \right) D^i \end{aligned}$$

degree(p(D)) ≤ I-1, degree(c(D)) = I

When initial state (b(-1), ..., b(-I)) is zero, we get p(D) = 0 and b(D) = 0, which yields the all-zero sequence for {b(k)}.

In the following we consider nonzero initial states only.

## Linear feedback shift register sequences

After removing all common polynomial factors (if any) of p(D) and c(D) :

$$\begin{aligned} c_0(D)b(D) &= p_0(D) & p_0(D) \text{ and } c_0(D) \text{ have no common factors} \\ \text{degree}(p_0(D)) &< \text{degree}(c_0(D)) \end{aligned}$$

Let P be the *smallest* integer such that c<sub>0</sub>(D) is a factor of 1-D<sup>P</sup> : 1-D<sup>P</sup> = q(D)c<sub>0</sub>(D)

$$q(D)c_0(D)b(D) = q(D)p_0(D)$$

$$\Rightarrow (1 - D^P)b(D) = b_0(D) \quad b_0(D) = q(D)p_0(D) \quad (\text{degree}(b_0(D)) < P)$$

$$\begin{aligned} \Rightarrow b(k) &= b_0(k) & k = 0, \dots, P-1 \\ b(k) - b(k-P) &= 0 & k = P, P+1, \dots \end{aligned}$$

$\Rightarrow b(k)$  periodic with period P,  
coefficients of b<sub>0</sub>(D) correspond to one period of {b(k)}

## LFSR sequences : example 1 revisited

$$\begin{aligned}
 c(D) &= 1+D+D^2+D^3 = (1+D)^3 & b(0) &= b(-1) + b(-2) + b(-3) \\
 (1+D)^3 b(D) &= (b(-1) + b(-2) + b(-3)) & b(1) &= b(0) + b(-1) + b(-2) \\
 &+ (b(-1) + b(-2))D + b(-1)D^2 & b(2) &= b(1) + b(0) + b(-1)
 \end{aligned}$$

a)  $(b(-1), b(-2), b(-3)) = (0,0,1)$       b)  $(b(-1), b(-2), b(-3)) = (0,1,0)$   
 $(1+D)^3 b(D) = 1$        $(1+D)^3 b(D) = 1+D$   
 $(1-D^4)b(D) = 1+D+0D^2+0D^3$        $(1-D^2)b(D) = 1+0D$   
 $P = 4 : 1100, 1100, \dots$        $P = 2 : 10, 10, \dots$

c)  $(b(-1), b(-2), b(-3)) = (1,1,1)$   
 $(1+D)^3 b(D) = 1+D^2$       We have made use of :  
 $(1-D)b(D) = 1$        $(1+D)^2 = 1 + D^2 = 1 - D^2$   
 $P = 1 : 1,1,\dots$        $(1+D)^4 = 1 + D^4 = 1 - D^4$

## Maximum length shift register sequences

When  $\text{degree}(c_0(D)) = d$ , then  $P \leq 2^d - 1$   
 Indeed,  $c_0(D)$  defines a shift register with  $d$  stages  
 $\Rightarrow$  maximum period when  $(S(0), \dots, S(P-1))$  contains all  $2^d - 1$  nonzero states

## Maximum length shift register sequences

When  $\text{degree}(c_0(D)) = d$ , then  $P \leq 2^d - 1$

Indeed,  $c_0(D)$  defines a shift register with  $d$  stages

$\Rightarrow$  maximum period when  $(S(0), \dots, S(P-1))$  contains all  $2^d - 1$  nonzero states

For an  $I$ -stage shift register and *irreducible*  $c(D)$ , we have  $c_0(D) = c(D)$  irrespective of the initial condition, so that  $P \leq 2^I - 1$ .

## Maximum length shift register sequences

When  $\text{degree}(c_0(D)) = d$ , then  $P \leq 2^d - 1$

Indeed,  $c_0(D)$  defines a shift register with  $d$  stages

$\Rightarrow$  maximum period when  $(S(0), \dots, S(P-1))$  contains all  $2^d - 1$  nonzero states

For an  $I$ -stage shift register and *irreducible*  $c(D)$ , we have  $c_0(D) = c(D)$  irrespective of the initial condition, so that  $P \leq 2^I - 1$ .

*Maximum length* shift register (MLSR) sequences have  $P = 2^I - 1$ .

The corresponding  $c(D)$  is a *primitive* polynomial of degree  $I$ , i.e. an irreducible polynomial of degree  $I$ , that is a factor of  $(1 - D^P)$  with  $P = 2^I - 1$ , but not of any other  $(1 - D^i)$  with  $i < P$ .

Primitive polynomials exist for any  $I$ , and are tabulated.

(e.g. [http://www.cs.umbc.edu/~lomonaco/f97/442/Peterson\\_Table.html](http://www.cs.umbc.edu/~lomonaco/f97/442/Peterson_Table.html))



## LFSR sequences : example 2 revisited

$c(D) = 1 + D^2 + D^3$  is primitive polynomial :  $1 - D^7 = (1 + D^2 + D^3)(1 + D + D^3)(1 + D)$

$$b(0) = b(-2) + b(-3)$$

$$b(1) = b(-1) + b(-2)$$

$$b(2) = b(0) + b(-1)$$

$$(1 + D^2 + D^3)b(D) = (b(-2) + b(-3)) + (b(-1) + b(-2))D + b(-1)D^2$$

$$(b(-1), b(-2), b(-3)) = (0, 0, 1)$$

$$(1 + D^2 + D^3)b(D) = 1$$

$$(1 - D^7)b(D) = 1 + 0D + D^2 + D^3 + D^4 + 0D^5 + 0D^6$$

$$P=7 : 1011100, 1011100$$

## Properties of MLSR sequences

When *sliding* a window of size  $r$  ( $r \leq I$ ) over a MLSR sequence with period  $2^I - 1$ , then the relative frequency of occurrence the  $2^r$  possible bit patterns of length  $r$  is :

$$\frac{2^{I-r}}{2^I - 1} \approx 2^{-r} \quad (\text{any nonzero pattern}) \qquad \frac{2^{I-r} - 1}{2^I - 1} \approx 2^{-r} \quad (\text{all-zero pattern})$$

Example :  $I = 3$ ,  $P = 2^I - 1 = 7$

MLSR sequence : 1011100, 1011100

$$r = 1 : 1011100$$

$$r = 2 : (10)(01)(11)(11)(10)(00)(01)$$

$$r = 3 : (101)(011)(111)(110)(100)(001)(010)$$

## Properties of MLSR sequences

When *sliding* a window of size  $r$  ( $r \leq I$ ) over a MLSR sequence with period  $2^I - 1$ , then the relative frequency of occurrence the  $2^r$  possible bit patterns of length  $r$  is :

$$\frac{2^{I-r}}{2^I - 1} \approx 2^{-r} \quad (\text{any nonzero pattern}) \qquad \frac{2^{I-r} - 1}{2^I - 1} \approx 2^{-r} \quad (\text{all-zero pattern})$$

The fraction of the positions where a MLSR sequence *agrees* with a shifted version (shift not a multiple of  $2^{I-1}$ ) of that MLSR sequence is :

$$\frac{2^{I-1} - 1}{2^I - 1} \approx \frac{1}{2}$$

Example :  $I = 3$ ,  $P = 2^I - 1 = 7$ , shift = 2

1 0 1 1 0 0, 1 0 1 1 0 0      3 agreements, 4 disagreements  
      1 0 1 1 0 0

## Properties of MLSR sequences

When *sliding* a window of size  $r$  ( $r \leq I$ ) over a MLSR sequence with period  $2^I - 1$ , then the relative frequency of occurrence the  $2^r$  possible bit patterns of length  $2^r$  is :

$$\frac{2^{I-r}}{2^I - 1} \approx 2^{-r} \quad (\text{any nonzero pattern}) \qquad \frac{2^{I-r} - 1}{2^I - 1} \approx 2^{-r} \quad (\text{all-zero pattern})$$

The fraction of the positions where a MLSR sequence *agrees* with a shifted version (shift not a multiple of  $2^{I-1}$ ) of that MLSR sequence is :

$$\frac{2^{I-1} - 1}{2^I - 1} \approx \frac{1}{2}$$

$\Rightarrow$  although they are completely deterministic, MLSR sequences behave (to some extent) like sequences of i.i.d. equiprobable bits

## Pseudo-noise (PN) sequences

Chip sequences derived from MLSR sequences are called PN-sequences. Although they are deterministic, PN-sequences behave (to some extent) as sequences of zero-mean i.i.d. chips

Real-valued chips :  $\alpha(i) \in \{-1, 1\}/\sqrt{N}$

- each bit of the MLSR sequence is mapped to a chip :  $b(i) \rightarrow \alpha(i)$
- select  $I$  such that  $(2^I - 1)$  and  $N$  are relative prime (e.g.,  $N$  is power of 2)
- $\Rightarrow$  Sequence of sets of  $N$  chips repeats after  $2^I - 1$  symbol intervals
- Each set of  $N$  chips has relative frequency of about  $2^{-N}$  (for  $I \gg N$ )

Complex-valued chips :  $\alpha(i) \in \{-1-j, -1+j, 1-j, 1+j\}/\sqrt{(2N)}$

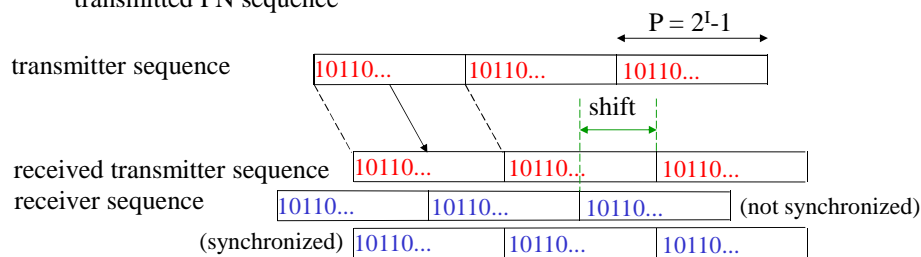
- each pair of bits of the MLSR sequence is mapped to a chip :  $b(i) \rightarrow \alpha(i)$
- select  $I$  such that  $(2^I - 1)$  and  $2N$  are relative prime (e.g.,  $N$  is power of 2)
- $\Rightarrow$  Sequence of sets of  $N$  chips repeats after  $2^I - 1$  symbol intervals
- Each set of  $N$  chips has relative frequency of about  $2^{-2N}$  (for  $I \gg 2N$ )

## Pseudo-noise (PN) synchronization

Transmitter and receiver both make use of  $I$ -stage shift register with the same feedback connections, and arbitrary (but nonzero) shift register states. The two registers generate delayed versions of the same MLSR sequence.

### PN synchronization

MLSR sequence generated at receiver must be properly delayed, until it is aligned with MLSR sequence received from transmitter. This way, each chip of receiver PN sequence will be multiplied with corresponding chip of transmitted PN sequence



## Conclusions

## Conclusions

### Point-to-point spread-spectrum communication

- Spread-spectrum with orthogonal chip pulses on the AWGN channel :
  - matched filter + symbol-by-symbol detection is optimum
  - same BER as for bandwidth-efficient modulation, which equals matched filter bound.
  - large spreading factor : low detection probability and high robustness against narrowband interference, at expense of large signal bandwidth
- Spread-spectrum with large spreading factor on dispersive channels :
  - matched filter (RAKE filter) + symbol-by-symbol detection close to optimum
  - effect of channel dispersion negligible
  - BER close to matched filter bound : no noise enhancement !
  - benefits from diversity on multipath fading channels

## Conclusions

### Multiuser spread-spectrum communication (CDM(A))

- O-CDMA (synchronized !) with orthogonal chip pulses on AWGN channel :
  - no interference between different user signals
  - single-user receiver with matched filter + symbol-by-symbol decisions is optimum.
  - same BER as for TDMA and FDMA, equal to matched filter bound
- CDMA with large spreading factor on dispersive channels :
  - optimum receiver very complicated (joint detection of all symbols from all users)
  - suboptimum single-user receiver with symbol-by-symbol detection : affected by MUI, not by distortion of reference user signal.
  - MUI increases with  $N_u/N$ , and degrades the BER as compared to matched filter bound
  - benefits from diversity on multipath fading channels

## Conclusions

### Cellular systems

- Cellular CDMA has reuse factor  $N_{re} = 1$ . Intercell interference is limited by using different chip sequences in different cells
- Bandwidth efficiency of cellular CDMA proportional to  $N_u/N$
- Ratio  $N_u/N$  determines MUI power, which in turn determines BER degradation as compared to matched filter bound
- Cellular TDMA (or FDMA) has reuse factor  $N_{re} > 1$ , to limit intercell interference
- Bandwidth efficiency of cellular TDMA (or FDMA) proportional to  $1/N_{re}$
- BER degradation as compared to matched filter bound caused by noise enhancement (equalization of dispersive channel)

## Conclusions

### Other applications of spread-spectrum signals

positioning, navigation (GPS, Galileo, ...)

### Generation of chip sequences

- PN-sequences from MLSR sequences
- Orthogonal (WH) sequences from Hadamard matrix
- Orthogonal sequences scrambled by common PN-sequence

# Modulation and detection

## Chapter 8 : Multicarrier modulation - Orthogonal frequency- division multiplexing (OFDM)

---

Chapter 8 : Multi-carrier modulation - OFDM

1

### Multicarrier modulation

**Multicarrier modulation** (orthogonal frequency-division multiplexing, OFDM) :

- Data symbol sequence is split into many (100 to 1000) low-rate sequences, that are modulated on different subcarriers and transmitted in parallel
- Symbol duration for each of the lower-rate sequences is much longer than the impulse response duration of the channel.  
⇒ robust against ISI caused by dispersive channel
- Although frequency bands of neighboring subcarriers have some overlap (unlike traditional FDM), subcarriers remain orthogonal
- Applications :
  - ADSL (twisted-pair cable)
  - Digital audio broadcast (DAB)
  - Terrestrial digital video broadcast (DVB-T)
  - Wireless local-area networks (W-LAN)
  - Proposals for future mobile radio systems

---

Chapter 8 : Multi-carrier modulation - OFDM

2

## Orthogonality of complex exponentials

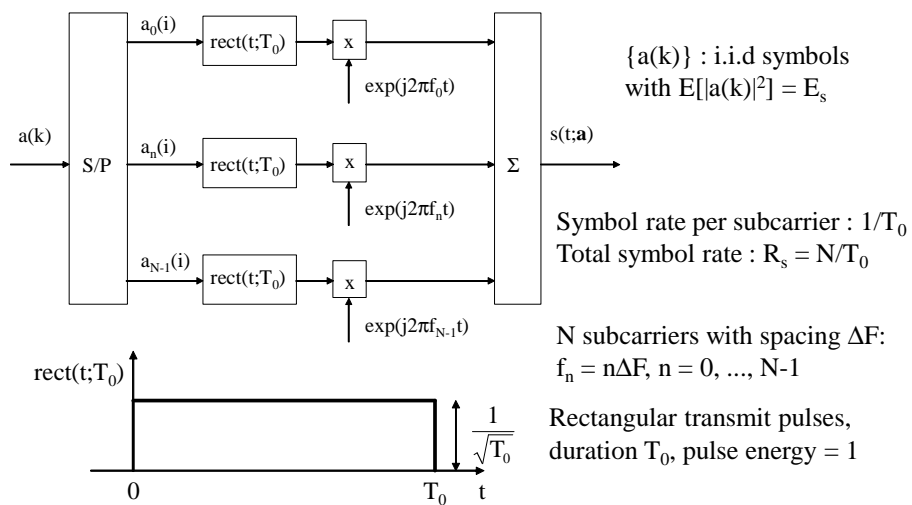
Complex exponentials  $\exp(j2\pi f_{n1}t)$  and  $\exp(j2\pi f_{n2}t)$  are orthogonal over an interval of duration  $T_0$  when  $f_{n1}-f_{n2}$  is a nonzero integer multiple of  $1/T_0$

Indeed,

$$\int_{t_0 - \frac{T_0}{2}}^{t_0 + \frac{T_0}{2}} \exp(j2\pi f_{n1}t) \exp(-j2\pi f_{n2}t) dt = T_0 \exp(j2\pi(f_{n1} - f_{n2})t_0) \frac{\sin(\pi(f_{n1} - f_{n2})T_0)}{\pi(f_{n1} - f_{n2})T_0}$$

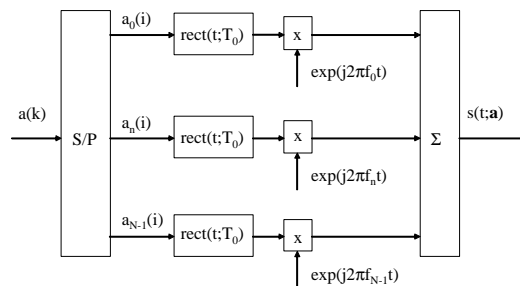
which becomes zero when  $(f_{n1}-f_{n2})T_0$  is a nonzero integer

## Multicarrier transmitter





## Multicarrier transmitter



$$\text{transmitted signal : } s(t; \mathbf{a}) = \sum_i \sum_{n=0}^{N-1} a_n(i) \text{rect}(t - iT_0; T_0) \exp(j2\pi n \Delta F t)$$

$a_n(i)$  :  $i$ -th symbol on  $n$ -th subcarrier

$\mathbf{a}(i) = (a_0(i), \dots, a_{N-1}(i))^T$  :  $i$ -th symbol block ( $N$  symbols)

$\mathbf{a} = (\dots, \mathbf{a}^T(i-1), \mathbf{a}^T(i), \mathbf{a}^T(i+1), \dots)^T$  :  
symbol vector containing all symbols from all blocks

## Multicarrier transmission on AWGN channel

## Log-likelihood function

$$\mathbf{r}(t) = \mathbf{s}(t; \mathbf{a}) + \mathbf{w}(t) \quad \mathbf{w}(t) \sim N_c(0, N_0 \delta(u))$$

$$\begin{aligned} -N_0 \ln p(\mathbf{r} | \mathbf{a}) &\propto -2 \operatorname{Re} \left[ \int \mathbf{r}(t) \mathbf{s}^*(t; \mathbf{a}) dt \right] + \int |\mathbf{s}(t; \mathbf{a})|^2 dt \\ &= -2 \sum_i \sum_{n=0}^{N-1} \operatorname{Re} [a_n^*(i) z_n(i)] + \sum_{i,i'} \sum_{n,n'=0}^{N-1} a_n^*(i) a_{n'}(i') g(i, i'; n - n') \\ z_n(i) &= \int \mathbf{r}(t) \operatorname{rect}(t - iT_0; T_0) e^{-j2\pi f_n t} dt \\ &= \frac{1}{\sqrt{T_0}} \int_{iT_0}^{(i+1)T_0} \mathbf{r}(t) e^{-j2\pi f_n t} dt \\ g(i, i'; n - n') &= \int \operatorname{rect}(t - iT_0; T_0) \operatorname{rect}(t - i'T_0; T_0) e^{-j2\pi(n-n')\Delta F t} dt \end{aligned}$$

ML detection reduces to symbol-by-symbol detection if and only if  
 $g(i, i'; n - n') = \delta(i - i') \delta_{n-n'}$

## Log-likelihood function

$$g(i, i'; n - n') = \int \operatorname{rect}(t - iT_0; T_0) \operatorname{rect}(t - i'T_0; T_0) e^{-j2\pi(n-n')\Delta F t} dt$$

$\operatorname{rect}(t - iT_0)$  and  $\operatorname{rect}(t - i'T_0)$  do not overlap for  $i \neq i'$

$$\begin{aligned} \Rightarrow g(i, i'; n - n') &= \delta(i - i') \int \operatorname{rect}^2(t - iT_0; T_0) e^{-j2\pi(n-n')\Delta F t} dt \\ &= \delta(i - i') \frac{1}{T_0} \int_{iT_0}^{(i+1)T_0} e^{-j2\pi(n-n')\Delta F t} dt \end{aligned}$$

Selecting  $\Delta F = 1/T_0$  yields

$$g(i, i'; n - n') = \delta(i - i') \delta_{n-n'}$$

## Log-likelihood function

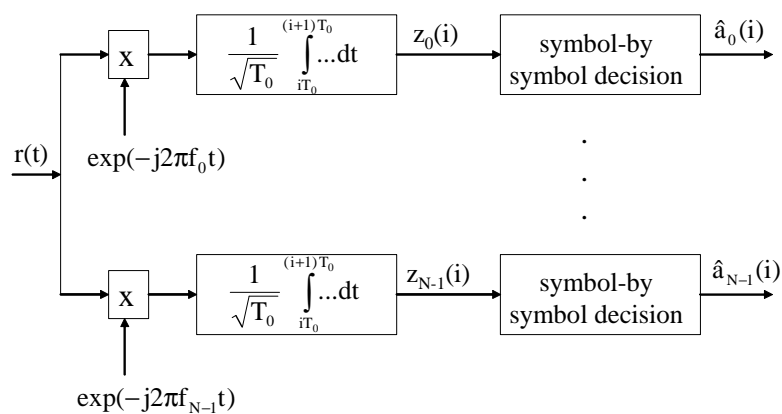
For  $\Delta F = 1/T_0$  :

$$\begin{aligned} -N_0 \ln p(\mathbf{r} | \mathbf{a}) &\propto -2 \sum_i \sum_{n=0}^{N-1} \operatorname{Re}[a_n^*(i) z_n(i)] + \sum_i \sum_{n=0}^{N-1} |a_n(i)|^2 \\ &\propto \sum_i \sum_{n=0}^{N-1} |z_n(i) - a_n(i)|^2 \end{aligned}$$

$\Rightarrow$  symbol-by-symbol detection is optimum

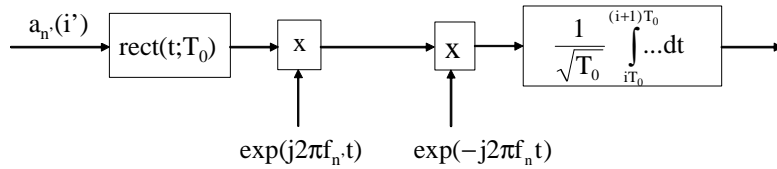
$\hat{a}_n(i)$  : constellation point that is closest to  $z_n(i)$

## ML receiver



## Discrete-time model for $z_n(i)$

Contribution from  $a_n(i')$  to  $z_n(i)$  :



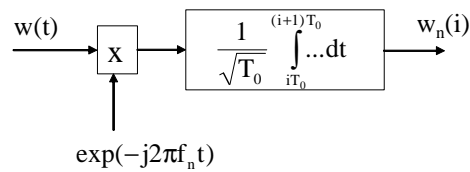
$$\begin{aligned}
 & \frac{1}{\sqrt{T_0}} \int_{iT_0}^{(i+1)T_0} a_n(i') \text{rect}(t - i'T_0; T_0) e^{-j2\pi(n-n')\Delta F t} dt \\
 &= a_n(i') \delta(i - i') \frac{1}{T_0} \int_{iT_0}^{(i+1)T_0} e^{-j2\pi(n-n')\Delta F t} dt \\
 &= a_n(i') \delta(i - i') \delta_{n-n'}
 \end{aligned}$$

Chapter 8 : Multi-carrier modulation - OFDM

11

## Discrete-time model for $z_n(i)$

Contribution from  $w(t)$  to  $z_n(i)$  :



$$\begin{aligned}
 E[w_n^*(i) w_n(i + \ell)] &= \frac{1}{T_0} \int_{iT_0}^{(i+1)T_0} dt \int_{(i+\ell)T_0}^{(i+\ell+1)T_0} dt' E[w^*(t) w(t')] e^{j2\pi(n-n')\Delta F} \\
 &= N_0 \frac{1}{T_0} \int_{iT_0}^{(i+1)T_0} dt \int_{(i+\ell)T_0}^{(i+\ell+1)T_0} dt' \delta(t - t') e^{j2\pi(n-n')\Delta F} \\
 &= N_0 \delta(\ell) \delta_{n-n'}
 \end{aligned}$$

Chapter 8 : Multi-carrier modulation - OFDM

12

### Discrete-time model for $z_n(i)$

$$z_n(i) = a_n(i) + w_n(i)$$

$$w_n(i) \sim N_c(0, N_0 \delta(\ell))$$

$w_n(i)$  and  $w_n(i+\ell)$  are statistically independent for  $n \neq n'$

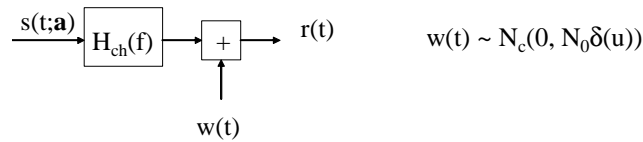
$\Rightarrow$  BER coincides with matched filter bound :

$$\text{BER} = \text{BER}_c \left( \frac{E_s}{N_0} \right) \quad \text{irrespective of symbol index } i \text{ or subcarrier index } n$$

same BER as for conventional modulation on AWGN channel

### Multicarrier transmission on dispersive channel

## Effect of channel dispersion



Contribution from  $a_n(i)$  to  $r(t)$

$$a_n(i) \int h_{ch}(u) \text{rect}(t - u - iT_0; T_0) e^{j2\pi f_n(t-u)} du$$

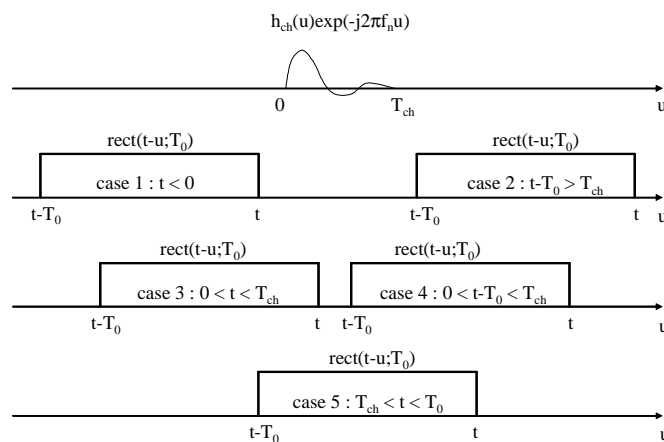
$$= a_n(i) e^{j2\pi f_n t} h_n(t - iT_0)$$

$$h_n(t) = \int \text{rect}(t - u; T_0) h_{ch}(u) e^{-j2\pi f_n u} du$$

## Effect of channel dispersion

$$h_n(t) = \int \text{rect}(t - u; T_0) h_{ch}(u) e^{-j2\pi f_n u} du \quad \text{assume : } h_{ch}(t) = 0 \text{ for } t \notin (0, T_{ch})$$

$$T_0 > T_{ch}$$



case 1, case 2 :  
 $h_n(t) = 0$

case 3, case 4 :  
transient in  $h_n(t)$

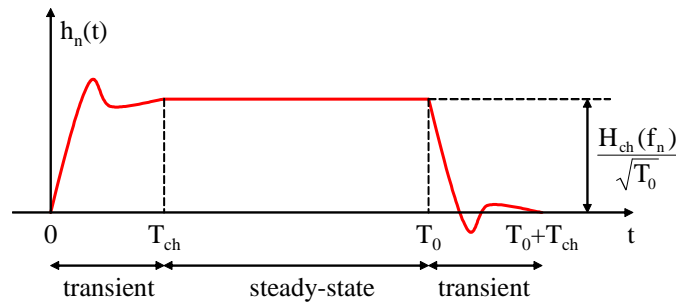
case 5 : steady-state  
value of  $h_n(t)$

## Effect of channel dispersion

Steady-state value of  $h_n(t)$  :

$$h_n(t) = \int \text{rect}(t-u; T_0) h_{ch}(u) e^{-j2\pi f_n u} du \quad T_{ch} < t < T_0$$

$$= \frac{1}{\sqrt{T_0}} \int h_{ch}(u) e^{-j2\pi f_n u} du = \frac{1}{\sqrt{T_0}} H_{ch}(f_n)$$



Chapter 8 : Multi-carrier modulation - OFDM

17

## Effect of channel dispersion : log-likelihood function

$$\text{Observation : } r(t) = \sum_i \sum_{n=0}^{N-1} a_n(i) h_n(t - iT_0) e^{j2\pi f_n t} + w(t)$$

Log-likelihood function :

$$-N_0 \ln p(\mathbf{r} | \mathbf{a}) \propto -2 \sum_i \sum_{n=0}^{N-1} \text{Re} \left[ a_n^*(i) \int r(t) e^{-j2\pi f_n t} h_n^*(t - iT_0) dt \right]$$

$$+ \sum_{i,i'} \sum_{n,n'=0}^{N-1} a_n^*(i) a_{n'}(i') \int e^{-j2\pi(f_n - f_{n'})t} h_n^*(t - iT_0) h_{n'}(t - i'T_0) dt$$

Chapter 8 : Multi-carrier modulation - OFDM

18

## Effect of channel dispersion : log-likelihood function

$h_n(t-iT_0)$  overlaps with  $h_{n'}(t-(i-1)T_0)$  and  $h_{n'}(t-(i+1)T_0)$ ,  $n' = 0, \dots, N-1$   
 $\Rightarrow$  interference between neighboring blocks (interblock interference, IBI)

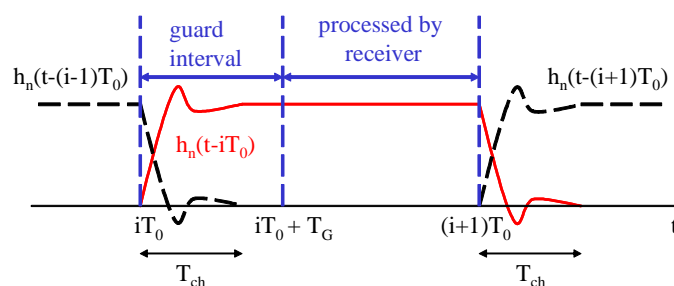
$h_n(t-iT_0)\exp(j2\pi f_n t)$  and  $h_{n'}(t-iT_0)\exp(j2\pi f_{n'} t)$  NOT orthogonal ( $n' \neq n$ )  
 $\Rightarrow$  interference between different subcarriers in same block  
 (intercarrier interference, ICI)

$\Rightarrow$  log-likelihood function contains crossterms involving symbols  $a_n(i)$  and  $a_{n'}(i')$

$\Rightarrow$  ML detection has high computational complexity, exponential in the total number of symbols transmitted

$\Rightarrow$  we consider a simple suboptimum receiver with symbol-by-symbol detection

## Simple suboptimum receiver



IBI occurs during transients of  $h_n(t-iT_0)$ , during interval  $(iT_0, iT_0+T_{ch})$

Suboptimum receiver uses only signal *segments* that are not affected by IBI.

Detection of  $a_n(i)$  with  $n = 0, \dots, N-1$  is based on  $r(t)$  in interval  $(iT_0+T_G, (i+1)T_0)$ , where  $T_G$  is a design parameter with  $T_G < T_0$ .

Guard interval  $(iT_0, iT_0+T_G)$  ignored by receiver.

Receiver can cope with channel impulse response durations  $T_{ch}$  not exceeding  $T_G$ .



### Simple suboptimum receiver : observation model

Observation model for suboptimum receiver (assuming  $T_{ch} \leq T_G$ ) :

$$r(t) = \frac{1}{\sqrt{T_0}} \sum_{n=0}^{N-1} a_n(i) H_{ch}(f_n) e^{j2\pi f_n t} + w(t) \quad i T_0 + T_G < t < (i+1) T_0$$

Resulting receiver is suboptimum because it makes use of a subset of the available observations only , i.e

$$r(t), t \in \bigcup_i (iT_0 + T_G, (i+1)T_0)$$

rather than  $r(t)$ ,  $-\infty < t < +\infty$ . Receiver performs ML detection based upon the subset of available observations.

### Simple suboptimum receiver : log-likelihood function

$$\begin{aligned} -N_0 \ln p(\mathbf{r} | \mathbf{a}) &\propto -2 \sum_i \sum_{n=0}^{N-1} \text{Re} [a_n^*(i) H_{ch}^*(f_n) z_n(i)] \\ &\quad + \sum_i \sum_{n,n'=0}^{N-1} a_n^*(i) a_{n'}(i) H_{ch}^*(f_n) H_{ch}(f_{n'}) g(i; n - n') \\ z_n(i) &= \frac{1}{\sqrt{T_0}} \int_{iT_0+T_G}^{(i+1)T_0} r(t) e^{-j2\pi f_n t} dt \quad g(i; n - n') = \frac{1}{T_0} \int_{iT_0+T_G}^{(i+1)T_0} e^{-j2\pi(n-n')\Delta F t} dt \end{aligned}$$

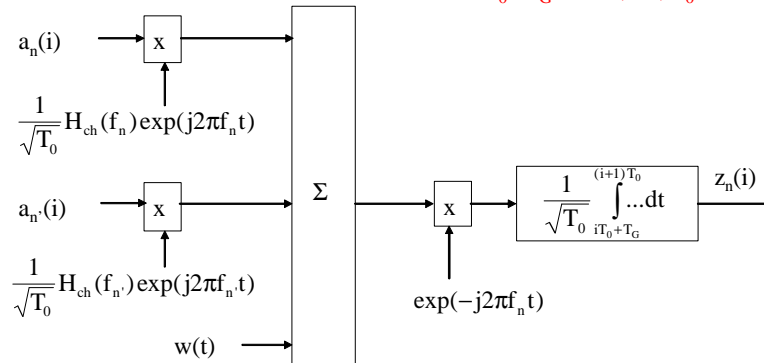
In order to avoid crossterms, we require  $g(i; n - n') = 0$  for  $n' \neq n$ . This is achieved by selecting  $\Delta F = 1/(T_0 - T_G)$ , which yields  $g(i; n - n') = ((T_0 - T_G)/T_0) \delta_{n-n'}$ .

$$-N_0 \ln p(\mathbf{r} | \mathbf{a}) \propto -2 \sum_i \sum_{n=0}^{N-1} \text{Re} [a_n^*(i) H_{ch}^*(f_n) z_n(i)] + \frac{T_0 - T_G}{T_0} \sum_i \sum_{n=0}^{N-1} |a_n(i)|^2 |H_{ch}(f_n)|^2$$

### Simple suboptimum receiver : discrete-time model for $z_n(i)$

$$z_n(i) = (z(i))_n = \frac{1}{\sqrt{T_0}} \int_{iT_0+T_G}^{(i+1)T_0} r(t) e^{-j2\pi f_n t} dt \quad r(t) = \frac{1}{\sqrt{T_0}} \sum_{n=0}^{N-1} a_n(i) H_{ch}(f_n) e^{j2\pi f_n t} + w(t)$$

$$iT_0 + T_G < t < (i+1)T_0$$



Chapter 8 : Multi-carrier modulation - OFDM

23

### Simple suboptimum receiver : discrete-time model for $z_n(i)$

$$z_n(i) = (z(i))_n = \frac{1}{\sqrt{T_0}} \int_{iT_0+T_G}^{(i+1)T_0} r(t) e^{-j2\pi f_n t} dt$$

Contribution from  $a_n(i)$  :  $\frac{T_0 - T_G}{T_0} H_{ch}(f_n) a_n(i)$

Contribution from  $a_{n'}(i)$  with  $n' \neq n$  :

$$a_{n'}(i) H_{ch}(f_{n'}) \frac{1}{T_0} \int_{iT_0+T_G}^{(i+1)T_0} \underbrace{e^{-j2\pi(n-n')\Delta F t}}_{=0} dt = 0$$

Channel dispersion does not give rise to ISI  
(provided that  $T_{ch} \leq T_G$  and  $\Delta F(T_0 - T_G) = 1$ )

Chapter 8 : Multi-carrier modulation - OFDM

24

### Simple suboptimum receiver : discrete-time model for $z_n(i)$

$$z_n(i) = \frac{T_0 - T_G}{T_0} H_{ch}(f_n) a_n(i) + w_{z,n}(i)$$

$$\text{Noise contribution : } w_{z,n}(i) = \frac{1}{\sqrt{T_0}} \int_{iT_0+T_G}^{(i+1)T_0} w(t) e^{-j2\pi n \Delta F t} dt$$

$$\begin{aligned} E[w_{z,n}(i+\ell) w_{z,n}^*(i)] &= \frac{1}{T_0} \int_{iT_0+T_G}^{(i+1)T_0} dt \int_{(i+\ell)T_0+T_G}^{(i+\ell+1)T_0} N_0 \delta(t-t') e^{-j2\pi n \Delta F (nt-n't')} dt' \\ &= \frac{T_0 - T_G}{T_0} N_0 \delta(\ell) \delta_{n-n'} \end{aligned}$$

noise contributions corresponding to different subcarrier indices  
and/or different block indices are statistically independent

### Simple suboptimum receiver : ML detection

$$z_n(i) = \frac{T_0 - T_G}{T_0} H_{ch}(f_n) a_n(i) + w_{z,n}(i)$$

$$\text{Scaling of } z_n(i) : u_n(i) = \frac{T_0}{T_0 - T_G} \cdot \frac{z_n(i)}{H_{ch}(f_n)}$$

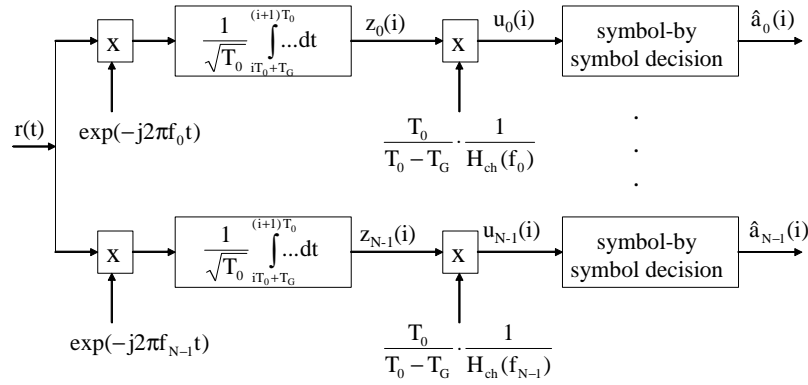
$$u_n(i) = a_n(i) + w_n(i) \quad E[w_n(i+\ell) w_n^*(i)] = \frac{T_0}{T_0 - T_G} \cdot \frac{N_0}{|H_{ch}(f_n)|^2} \delta_{n-n'} \delta(\ell)$$

$$\Rightarrow \ln p(\mathbf{u} | \mathbf{a}) = \sum_i \sum_{n=0}^{N-1} \ln p(u_n(i) | a_n(i))$$

$$\frac{-N_0}{|H_{ch}(f_n)|^2} \cdot \frac{T_0}{T_0 - T_G} \cdot \ln p(u_n(i) | a_n(i)) = |u_n(i) - a_n(i)|^2$$

$$\Rightarrow \hat{a}_n(i) : \text{constellation point closest to } u_n(i)$$

### Simple suboptimum receiver : ML detection



Chapter 8 : Multi-carrier modulation - OFDM

27

### Simple suboptimum receiver : BER performance

$$u_n(i) = a_n(i) + w_n(i) \quad E[w_n(i + \ell)w_n^*(i)] = \frac{T_0}{T_0 - T_G} \cdot \frac{N_0}{|H_{ch}(f_n)|^2} \delta_{n-n} \delta(\ell)$$

$$BER_n = BER_C(SNR_n)$$

$$SNR_n = \frac{E[|a_n(i)|^2]}{E[|w_n(i)|^2]} = \frac{E_s}{N_0} \cdot \frac{T_0 - T_G}{T_0} |H_{ch}(f_n)|^2$$

BER depends on subcarrier index  $n$ , through channel transfer function  $|H_{ch}(f_n)|^2$  :  
BER is large for subcarrier indices that correspond to small  $|H_{ch}(f_n)|^2$ .

The factor  $(T_0 - T_G)/T_0$  represents a loss of useful power, caused by not exploiting the received signal during the guard interval. This loss can be kept small by selecting  $T_0 \gg T_G$

Chapter 8 : Multi-carrier modulation - OFDM

28

## Matched filter bound for optimum receiver

Observation for optimum receiver :

$$r(t) = \sum_i \sum_{n=0}^{N-1} a_n(i) h_n(t - iT_0) e^{j2\pi f_n t} + w(t) \quad -\infty < t < +\infty$$

“Genie” receiver knows all symbols, except  $a_n(i)$ . Subtracting from  $r(t)$  the contributions from the known symbols yields the following observation :

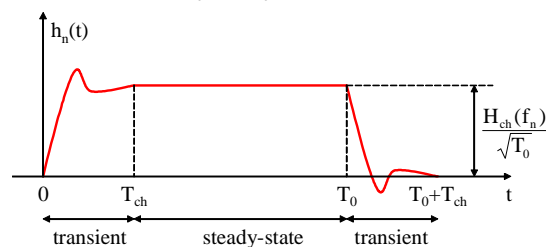
$$r'(t) = a_n(i) h_n(t - iT_0) e^{j2\pi f_n t} + w(t) \quad -\infty < t < +\infty$$

$$\Rightarrow \text{BER}_{\text{MF},n} = \text{BER}_C(\text{SNR}_{\text{MF},n})$$

$$\text{SNR}_{\text{MF},n} = \frac{E_s}{N_0} \int |h_n(t)|^2 dt$$

## Matched filter bound for optimum receiver

$$\begin{aligned} \text{SNR}_{\text{MF},n} &= \frac{E_s}{N_0} \int |h_n(t)|^2 dt = \frac{E_s}{N_0} \cdot \left( \int_0^{T_G} |h_n(t)|^2 dt + \int_{T_G}^{T_0} |h_n(t)|^2 dt + \int_{T_0}^{T_0+T_{ch}} |h_n(t)|^2 dt \right) \\ &\geq \frac{E_s}{N_0} \cdot \frac{T_0 - T_G}{T_0} \cdot |H_{ch}(f_n)|^2 = \text{SNR}_n \end{aligned}$$



When  $T_0 \gg T_G$ , we get  $\text{SNR}_{\text{MF},n} \approx \text{SNR}_n$  : suboptimum receiver is close to optimum

## Spectral properties

## Power spectrum

$$s(t; \mathbf{a}) = \sum_i \sum_{n=0}^{N-1} a_n(i) \text{rect}(t - iT_0; T_0) \exp(j2\pi n\Delta F t)$$

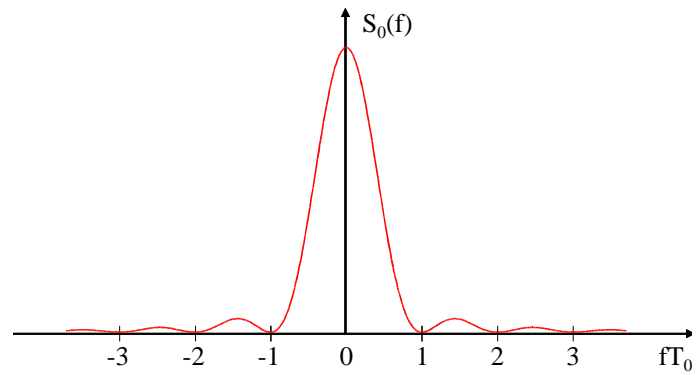
$$\text{Power spectrum : } S_s(f) = \sum_{n=0}^{N-1} S_n(f) = \sum_{n=0}^{N-1} S_0(f - n\Delta F)$$

$S_n(f) = S_0(f - n\Delta F)$  : power spectrum from n-th subcarrier

$$S_0(f) = \frac{E_s}{T_0} |\text{RECT}(f)|^2 = E_s \left( \frac{\sin(\pi f T_0)}{\pi f T_0} \right)^2$$

## Power spectrum

Mainlobe width of  $S_0(f)$  equals  $2/T_0$



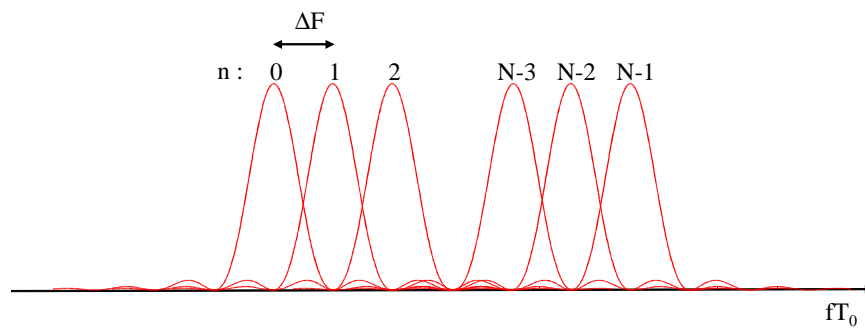
Chapter 8 : Multi-carrier modulation - OFDM

33

## Power spectrum

$$S_s(f) = \sum_{n=0}^{N-1} S_n(f) = \sum_{n=0}^{N-1} S_0(f - n\Delta F)$$

Spectra from neighboring subcarriers overlap (this is unlike traditional FDM)  
 $\Rightarrow$  high spectral efficiency

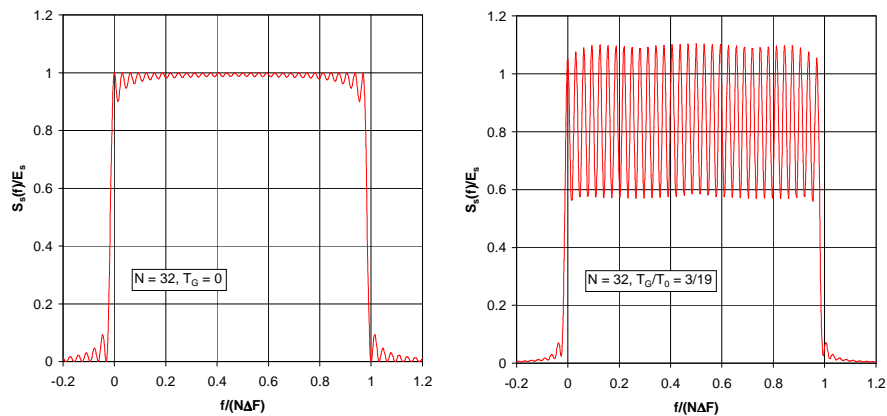


Chapter 8 : Multi-carrier modulation - OFDM

34

## Power spectrum

$T_G \neq 0$  gives rise to ripple in the power spectrum



Chapter 8 : Multi-carrier modulation - OFDM

35

## Spectral efficiency

theoretical limit for any linear modulation :  $R_s/B_{RF} \leq 1$

multicarrier system :

$$\frac{R_s}{B_{RF}} \approx \frac{R_s}{(N-1)\Delta F + 2/T_0} = \frac{N}{(N-1)T_0\Delta F + 2} \approx \frac{1}{T_0\Delta F} = \frac{T_0 - T_G}{T_0} \quad (N \text{ large})$$

spectral efficiency close to theoretical maximum when  $T_0 \gg T_G$

For conventional modulation we get :

$$\frac{R_s}{B_{RF}} = \frac{1}{1+\beta} \quad \text{where } \beta \text{ is the excess bandwidth factor (typically, } \beta > 0.2)$$

Chapter 8 : Multi-carrier modulation - OFDM

36



## Complexity considerations

## Complexity considerations

So far, modulation on subcarriers (transmitter) and demodulation of subcarriers (receiver) are carried out in continuous time, which requires analog multipliers. As the number ( $N$ ) of subcarriers is often quite large, this yields very high hardware complexity.

Hardware complexity can be substantially reduced by using digital FFT processors, which allow to carry out the modulation and demodulation of the  $N$  subcarriers in discrete time.

Example :  $T_G = 20 \mu s$      $R_s = 1 \text{ Mbaud}$

(channel impulse response duration can be up to 20 symbol intervals)

We select  $T_0 = 10T_G$ , which yields  $(T_0 - T_G)/T_0 = 0.9$  (or 0.5 dB power loss)

The symbol rate per carrier is  $1/T_0 = 5 \text{ kbaud} \Rightarrow N = 200$  subcarriers needed

## Complexity reduction by means of digital signal processing

## Complexity reduction by DFT/IDFT processing

### **Transmitter :**

Filtering (rectangular impulse response) and modulation in continuous time are replaced by IDFT (size  $N$ ) of symbol block  $\mathbf{a}(k)$ . Output of IDFT is applied to transmit filter.

### **Receiver :**

Demodulation and integration in continuous time are replaced by DFT (size  $N$ ) of receive filter output samples.

Replacing continuous-time operations (analog hardware) by discrete-time operations (digital hardware) yields considerable savings in hardware. When  $N$  is power of 2, DFT and IDFT are carried out by means of efficient FFT and IFFT processors.

## Transmitter : continuous-time implementation

$$s(t; \mathbf{a}) = \sum_i \sum_{n=0}^{N-1} a_n(i) \text{rect}(t - iT_0; T_0) \exp(j2\pi f_n t)$$

$$\Rightarrow s(t; \mathbf{a}) = \frac{1}{\sqrt{T_0}} \sum_{n=0}^{N-1} a_n(i) e^{j2\pi f_n t} \quad iT_0 \leq t < (i+1)T_0$$

$$\begin{aligned} s(iT_0 + T_G + u; \mathbf{a}) &= \frac{1}{\sqrt{T_0}} \sum_{n=0}^{N-1} a_n(i) e^{j\theta_n(i)} e^{j2\pi f_n u} \\ &= \frac{1}{\sqrt{T_0}} \sum_{n=0}^{N-1} a_n(i) e^{j\theta_n(i)} e^{j2\pi \frac{n}{T_0 - T_G} u} \end{aligned} \quad -T_G \leq u < T_0 - T_G$$

$$\theta_n(i) = 2\pi f_n (iT_0 + T_G)$$

## Transmitter : discrete-time implementation

transmitter produces samples of (scaled and time-shifted version of)  $s(t; \mathbf{a})$  at rate  $1/T$ , but without the phase rotation  $\theta_n(i)$

$$T_0 = (N + v)T \quad T_G = vT \quad T_0 - T_G = N \cdot T$$

$$s(iT_0 + T_G + u; \mathbf{a}) = \frac{1}{\sqrt{T_0}} \sum_{n=0}^{N-1} a_n(i) e^{j\theta_n(i)} e^{j2\pi \frac{n}{T_0 - T_G} u} \quad -T_G \leq u < T_0 - T_G$$

$$\text{Define : } s'(iT_0 + u; \mathbf{a}) = \frac{1}{\sqrt{T_0}} \sum_{n=0}^{N-1} a_n(i) e^{j2\pi \frac{n}{T_0 - T_G} u} \quad -T_G \leq u < T_0 - T_G$$

$\Downarrow$

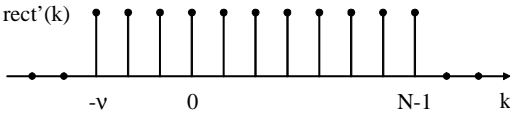
$$x(i(N + v) + m) = s'(iT_0 + mT) = \frac{1}{\sqrt{N + v}} \sum_{n=0}^{N-1} a_n(i) \exp(j2\pi \frac{mn}{N}) \quad -v \leq m < N-1$$

## Transmitter : discrete-time implementation

Equivalent representation :

$$x(k) = \sum_i \sum_{n=0}^{N-1} a_n(i) \text{rect}'(k - i(N+v)) e^{j2\pi \frac{n}{N}(k - i(N+v))}$$

$$\text{rect}'(k) = \sqrt{T} \text{rect}(kT + T_G)$$

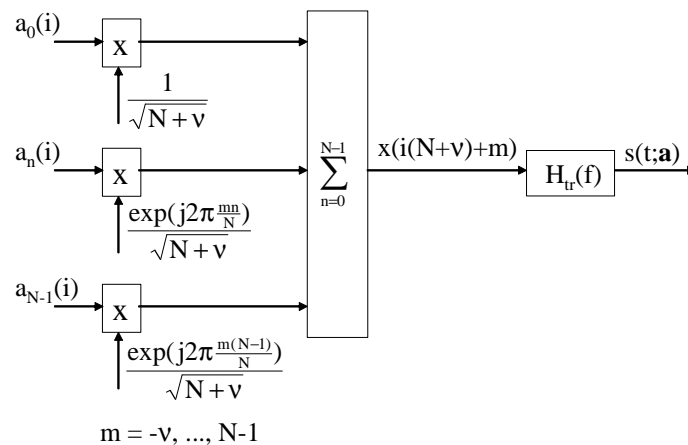
$$= \begin{cases} \frac{1}{\sqrt{N+v}} & k = -v, \dots, N-1 \\ 0 & \text{otherwise} \end{cases}$$


Verification :

$$x(i(N+v) + m) = \sum_{i'} \sum_{n=0}^{N-1} a_n(i') \text{rect}'((i-i')(N+v) + m) e^{j2\pi \frac{n}{N}((i-i')(N+v) + m)} \quad -v \leq m < N-1$$

$$= \frac{1}{\sqrt{N+v}} \sum_{n=0}^{N-1} a_n(i) \exp(j2\pi \frac{mn}{N})$$

## Transmitter : discrete-time implementation

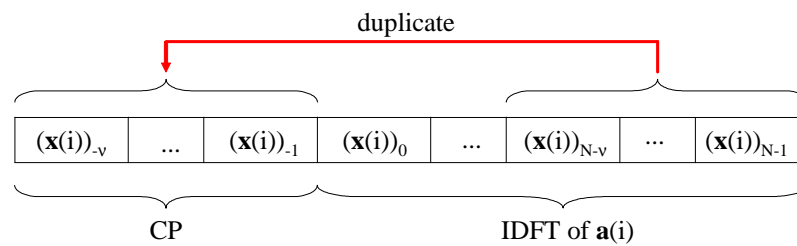


## Transmitter : IDFT implementation

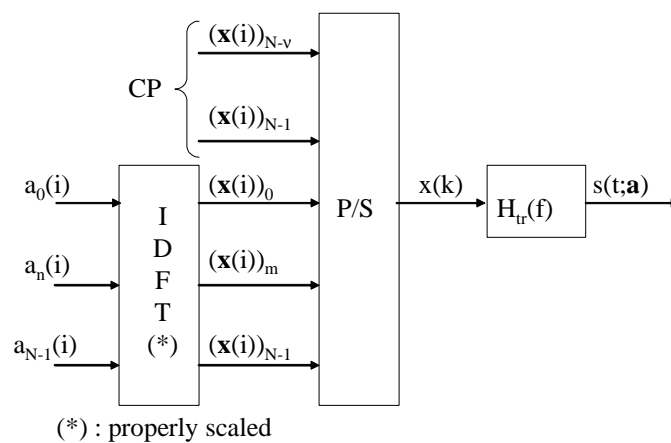
$$x(i(N+v)+m) = (\mathbf{x}(i))_m = \frac{1}{\sqrt{N+v}} \sum_{n=0}^{N-1} a_n(i) \exp(j2\pi \frac{mn}{N}) \quad m = -v, \dots, N-1$$

$(\mathbf{x}(i))_m$ ,  $m = 0, \dots, N-1$  : (scaled) **IDFT** of symbol block  $\mathbf{a}(i)$

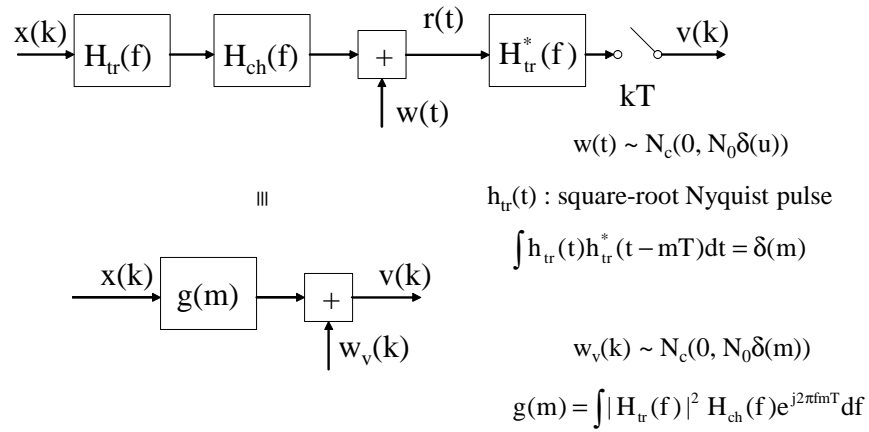
$(\mathbf{x}(i))_m = (\mathbf{x}(i))_{m+N}$ ,  $m = -v, \dots, -1$  : **cyclic prefix (CP)**



## Transmitter : IDFT implementation



## Transmit filter + Channel + Receive filter



Chapter 8 : Multi-carrier modulation - OFDM

47

## Receiver : continuous-time implementation

$$\begin{aligned}
 z_n(i) &= \frac{1}{\sqrt{T_0}} \int_{iT_0+T_G}^{(i+1)T_0} r(t) e^{-j2\pi f_n t} dt \\
 &= \frac{1}{\sqrt{T_0}} e^{-j\theta_n(i)} \int_0^{T_0-T_G} r(iT_0 + T_G + u) e^{-j2\pi f_n u} du \\
 &= \frac{1}{\sqrt{T_0}} e^{-j\theta_n(i)} \int_0^{T_0-T_G} r(iT_0 + T_G + u) e^{-j2\pi \frac{n}{T_0-T_G} u} du
 \end{aligned}$$

Chapter 8 : Multi-carrier modulation - OFDM

48

## Receiver : discrete-time implementation

Approximates (scaled version of) integral, without the phase rotation  $-\theta_n(i)$ , by a sum over receive filter output samples, taken at rate  $1/T$

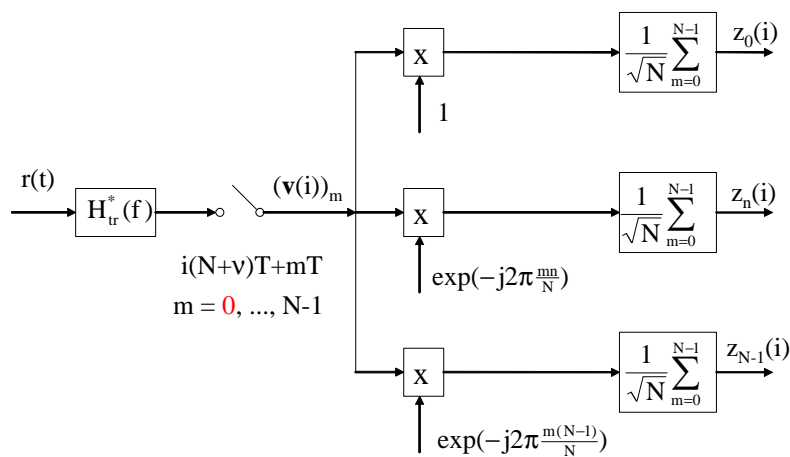
$$z_n(i) = \frac{1}{\sqrt{T_0}} e^{-j\theta_n(i)} \int_0^{T_0-T_G} r(iT_0 + T_G + u) e^{-j2\pi \frac{n}{T_0-T_G} u} dt$$

$$\Downarrow$$

$$z_n(i) = \frac{1}{\sqrt{N}} \sum_{m=0}^{N-1} v(i(N+v)+m) e^{-j2\pi \frac{mn}{N}}$$

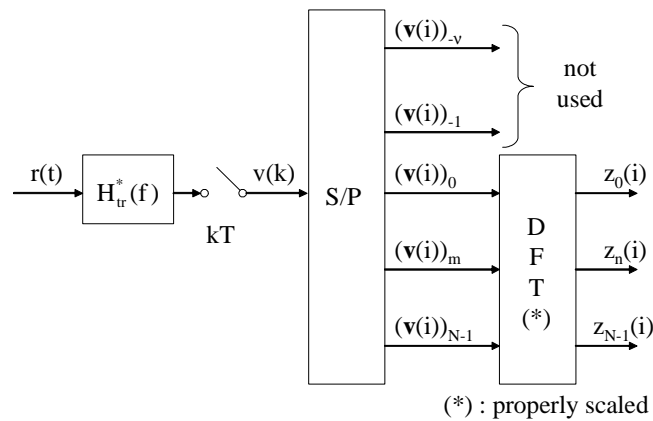
$$= \frac{1}{\sqrt{N}} \sum_{m=0}^{N-1} (\mathbf{v}(i))_m e^{-j2\pi \frac{mn}{N}} \quad (\mathbf{v}(i))_m = v(i(N+v)+m)$$

## Receiver : discrete-time implementation



## Receiver : DFT implementation

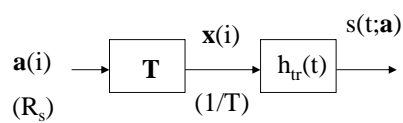
$$z_n(i) = \frac{1}{\sqrt{N}} \sum_{m=0}^{N-1} (v(i))_m \exp(-j2\pi \frac{mn}{N}) \quad : \text{ (scaled) DFT of } ((v(i))_0, \dots, (v(i))_{N-1})$$



Chapter 8 : Multi-carrier modulation - OFDM

51

## Multicarrier modulation viewed as linear block modulation



$\mathbf{a}(i) : N \times 1$   
 $\mathbf{T} : (N+v) \times N$   
 $\mathbf{s}(i) : (N+v) \times 1$   
 $1/T = ((N+v)/N)R_s$

$$(\mathbf{x}(i))_m = x(i(N+v) + m) = \sum_{n=0}^{N-1} T_{m,n} a_n(i)$$

$$= \frac{1}{\sqrt{N+v}} \sum_{n=0}^{N-1} a_n(i) \exp(j2\pi \frac{mn}{N})$$

 $m = -v, \dots, N-1$ 

$$T_{m,n} = \frac{\exp(j2\pi mn / N)}{\sqrt{N+v}}$$

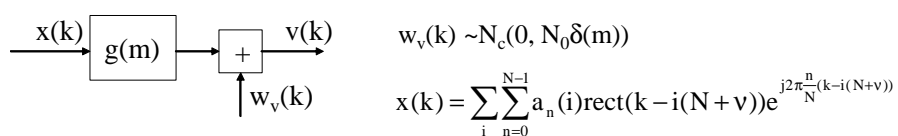
Chapter 8 : Multi-carrier modulation - OFDM

52



## Performance of discrete-time multicarrier modulation

### Model for $v(k)$



Contribution from  $a_n(i)$  to  $v(k)$  :

$$\begin{aligned}
 & a_n(i) \sum_m g(m) \text{rect}(k - m - i(N+v)) e^{j2\pi \frac{n}{N} (k - m - i(N+v))} \\
 &= a_n(i) e^{j2\pi \frac{n}{N} (k - i(N+v))} h_n(k - i(N+v))
 \end{aligned}$$

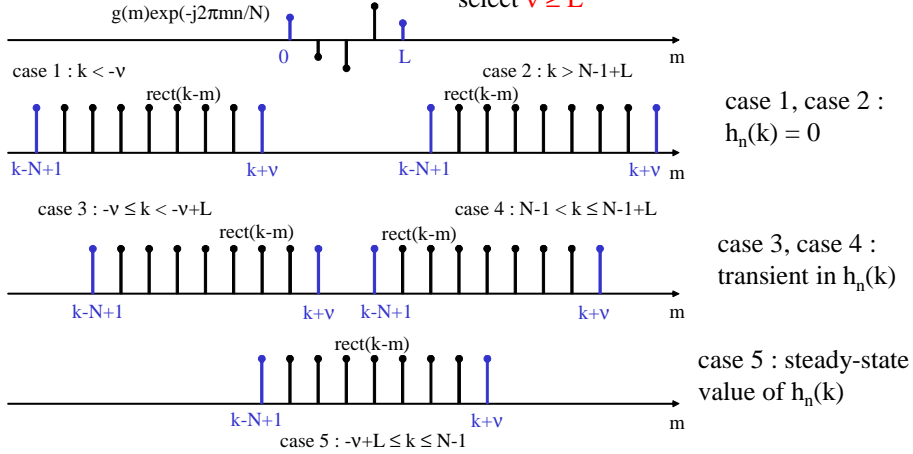
$$\text{with } h_n(k) = \sum_m g(m) e^{-j2\pi \frac{nm}{N}} \text{rect}(k - m)$$

### Model for $v(k)$

$$h_n(k) = \sum_m g(m) e^{-j2\pi \frac{nm}{N}} \text{rect}(k-m)$$

assume :  $g(m) = 0$  for  $m \notin \{0, \dots, L\}$   
 $g(m)$  has  $L+1$  nonzero samples

select  $v \geq L$



Chapter 8 : Multi-carrier modulation - OFDM

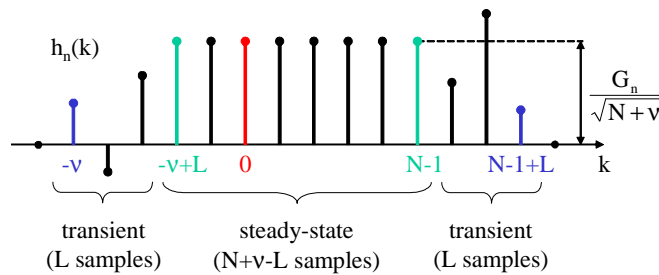
55

### Model for $v(k)$

Steady-state value of  $h_n(k)$  :

$$h_n(k) = \sum_m g(m) e^{-j2\pi \frac{nm}{N}} \text{rect}(k-m) = \frac{1}{\sqrt{N+v}} \sum_m g(m) e^{-j2\pi \frac{nm}{N}} = \frac{G_n}{\sqrt{N+v}}$$

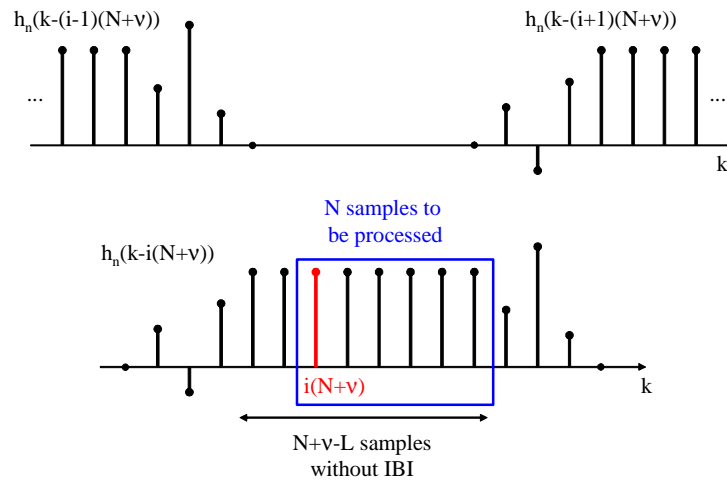
$$G_n = G(e^{j2\pi n/N}) = \frac{1}{T} \sum_{\ell} H_{ch}\left(\frac{n}{NT} - \frac{\ell}{T}\right) \left| H_{tr}\left(\frac{n}{NT} - \frac{\ell}{T}\right) \right|^2$$



Chapter 8 : Multi-carrier modulation - OFDM

56

### Model for $v(k)$



$k = i(N+v) + m, m = 0, \dots, N-1 : h_n(k-i'(N+v))$  contributes only when  $i' = i$   
 (contribution = steady-state value)

### Model for $v(k)$

$$v(k) = \sum_{i'=0}^{N-1} \sum_{n=0}^{N-1} a_n(i') e^{j2\pi \frac{n}{N}(k-i'(N+v))} h_n(k-i'(N+v)) + w_v(k) \quad \text{any } k$$

$$h_n(k) = \frac{G_n}{\sqrt{N+v}} \quad 0 \leq k \leq N-1$$

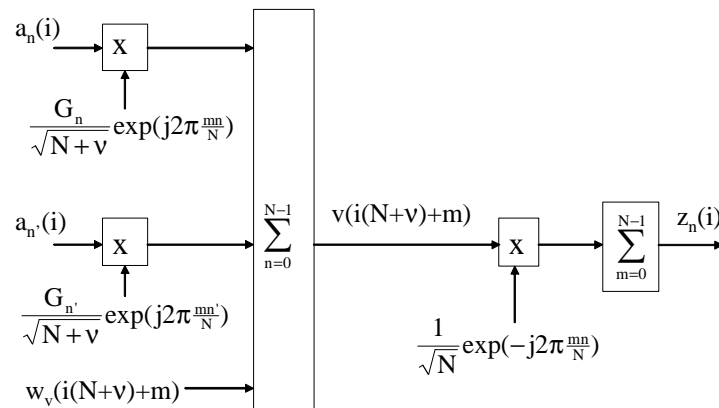
$$h_n(k) = 0 \text{ for } k < -v \text{ or } k > N-1+L \quad v \geq L$$

$$\Rightarrow v(i(N+v) + m) = \sum_{n=0}^{N-1} a_n(i) \frac{G_n}{\sqrt{N+v}} e^{j2\pi \frac{nm}{N}} + w_v(i(N+v) + m)$$

for  $m = 0, \dots, N-1$

### Model for $z_n(i)$

$$z_n(i) = \frac{1}{\sqrt{N}} \sum_{m=0}^{N-1} v(i(N+v)+m) \exp(-j2\pi \frac{mn}{N}) \quad n = 0, \dots, N-1$$

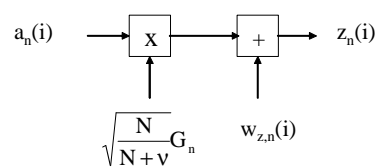


Chapter 8 : Multi-carrier modulation - OFDM

59

### Model for $z_n(i)$

$$z_n(i) = \sqrt{\frac{N}{N+v}} a_n(i) G_n + w_{z,n}(i) \quad E[w_{z,n}(i+\ell)w_{z,n'}^*(i)] = N_0 \delta(\ell) \delta_{n-n'}$$



$z_n(i)$  contains no interference from other symbols, provided that  $v \geq L$

We made use of orthogonality of discrete-time complex exponentials  $\exp(j2\pi mn/N)$  with  $n = 0, \dots, N-1$  over interval of  $N$  samples :

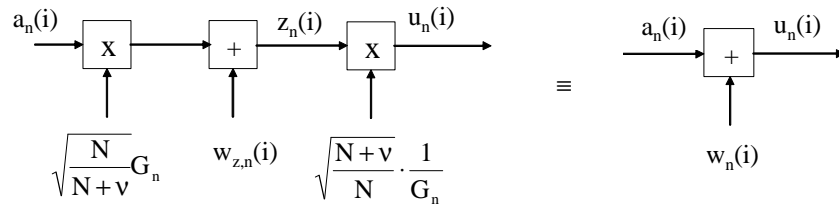
$$\sum_{m=0}^{N-1} e^{j2\pi \frac{(n-n')m}{N}} = N \delta_{n-n'} \quad \text{for } n, n' = 0, \dots, N-1$$

Chapter 8 : Multi-carrier modulation - OFDM

60

### Model for $u_n(i)$

Scaling of  $z_n(i)$  :  $u_n(i) = \sqrt{\frac{N+v}{N}} \cdot \frac{z_n(i)}{G_n}$



$$u_n(i) = a_n(i) + w_n(i) \quad E[w_n(i+\ell)w_n^*(i)] = \frac{N+v}{N} \cdot \frac{N_0}{|G_n|^2} \delta(\ell) \delta_{n-n'}$$

### BER performance

$$u_n(i) = a_n(i) + w_n(i) \quad E[w_n(i+\ell)w_n^*(i)] = \frac{N+v}{N} \cdot \frac{N_0}{|G_n|^2} \delta(\ell) \delta_{n-n'}$$

symbol-by-symbol detection :  $\hat{a}_n(i)$  is constellation point closest to  $u_n(i)$

$$\text{SNR}_n = \frac{N}{N+v} \cdot |G_n|^2 \cdot \frac{E_s}{N_0} \Rightarrow \text{BER}_n = \text{BER}_c \left( \frac{E_s}{N_0} \cdot \frac{N}{N+v} |G_n|^2 \right)$$

$10 \log \left( \frac{N+v}{N} \right)$  power loss (dB) caused by not exploiting the  $v$  samples that are contained in the CP

BER depends on subcarrier index  $n$  through  $|G_n|^2$ .  
Strongly attenuated subcarriers (small  $|G_n|$ ) give rise to large  $\text{BER}_n$ .

## Multicarrier modulation on AWGN channel

Chapter 8 : Multi-carrier modulation - OFDM

63

## AWGN channel

$$\text{AWGN channel : } H_{\text{ch}}(f) = 1 \Rightarrow g(m) = \int |H_{\text{tr}}(f)|^2 e^{j2\pi f m T} df = \delta(m) \Rightarrow \mathbf{L = 0}$$

(assuming that  $h_{\text{tr}}(t)$  is square-root Nyquist)

$$G_n = \frac{1}{T} \sum_{i=-\infty}^{+\infty} |H_{\text{tr}}(\frac{n}{NT} - \frac{i}{T})|^2 = 1$$

$$\Rightarrow z_n(i) = \sqrt{\frac{N}{N+v}} a_n(i) + w_n(i) \quad E[|w_n(i)|^2] = N_0$$

$$\text{SNR}_n = \frac{E_s}{N_0} \cdot \frac{N}{N+v} \quad \text{independent of subcarrier index } n$$

$$\text{BER}_n = \text{BER}_c \left( \frac{E_s}{N_0} \cdot \frac{N}{N+v} \right) \quad \text{independent of subcarrier index } n$$

Chapter 8 : Multi-carrier modulation - OFDM

64

## AWGN channel

Multicarrier modulation :

$$\text{SNR}_n = \frac{E_s}{N_0} \cdot \frac{N}{N+v} \qquad \text{BER}_n = \text{BER}_c \left( \frac{E_s}{N_0} \cdot \frac{N}{N+v} \right)$$

For conventional linear modulation with square-root Nyquist pulse, or  
block transform modulation with square-root Nyquist pulse and  $\mathbf{T}^H(i)\mathbf{T}(i) = \mathbf{I}_N$  :

$$\text{SNR} = \frac{E_s}{N_0} \qquad \text{BER} = \text{BER}_c \left( \frac{E_s}{N_0} \right)$$

With multicarrier modulation, SNR is reduced by a factor  $N/(N+v)$ .  
This loss is caused by using only  $N$  samples from a block of  $N+v$  samples.  
No loss occurs when taking  $v = 0$  (no CP), which is allowed on the AWGN  
channel because  $v = 0$  satisfies the condition  $v \geq L=0$

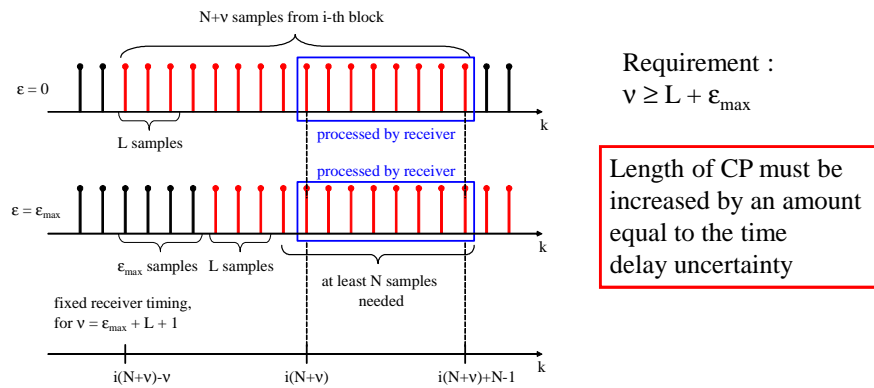
## Effect of time delay uncertainty

## Time delay uncertainty

Fixed sampling at receiver :

detection of  $\mathbf{a}(i)$  based on samples at instants  $i(N+v)T + mT$ ,  $m = 0, \dots, N-1$

Uncertainty about time delay  $\epsilon T$  of received signal :  $0 \leq \epsilon \leq \epsilon_{\max}$  ( $\epsilon_{\max}$  integer)



Chapter 8 : Multi-carrier modulation - OFDM

67

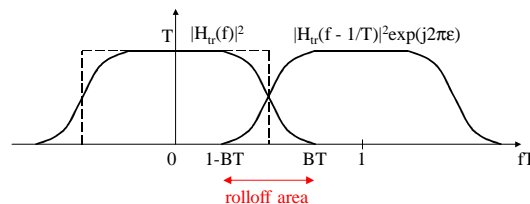
## Time delay uncertainty

assume  $H_{ch}(f) = \exp(-j2\pi f\epsilon T)$  : AWGN channel with delay  $\epsilon T$

$1/2 < BT < 1$

$$G_n = \exp\left(-j2\pi \frac{n\epsilon}{N}\right) \frac{1}{T} \sum_{\ell=-\infty}^{+\infty} H_{tr}\left(\frac{n}{NT} - \frac{\ell}{T}\right)^2 \exp(j2\pi \ell \epsilon)$$

- $n/N \in (0, 1-BT)$  : contribution from term with  $\ell=0$  only  
 $G_n = \exp(-j2\pi n\epsilon/N)$  : phase rotation depending on subcarrier index  $n$
- $n/N \in (BT, 1)$  : contribution from term with  $\ell=1$  only  
 $G_n = \exp(-j2\pi(n-N)\epsilon/N)$  : phase rotation depending on subcarrier index  $n$
- $n/N \in (1-BT, BT)$  : contribution from terms with  $\ell=0$  and  $\ell=1$  :  
 phase rotation + **attenuation**



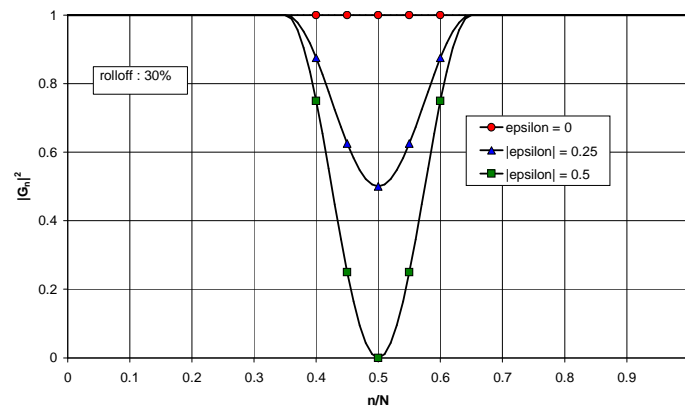
Chapter 8 : Multi-carrier modulation - OFDM

68



## Time delay uncertainty

30% rolloff  $\Rightarrow BT = 0.5 \cdot (1 + 0.3) = 0.65$ ,  $1 - BT = 0.35$



Chapter 8 : Multi-carrier modulation - OFDM

69

## Time delay uncertainty

On the AWGN channel, delay uncertainty can cause strong attenuation when  $n/N$  is in the rolloff area ( $1-BT$ ,  $BT$ ).

For this reason, we might decide *not to use* the corresponding subcarriers at the transmitter. In this case, only  $N_c = 2(1-BT)N$  subcarriers are used

When  $n/N$  is not in the rolloff area,  $G(n)$  causes only a rotation of the symbol  $a_n(i)$ , which does not affect the SNR (because  $|G_n| = 1$ )

### Conclusion :

When the CP is sufficiently long and the subcarriers in the rolloff area are not used, the timing of the sampling instants at the receiver is not very critical. A timing delay gives rise to an additional (subcarrier dependent) rotation of the data symbols, which is compensated at the DFT output without affecting  $SNR_n$ .

Chapter 8 : Multi-carrier modulation - OFDM

70

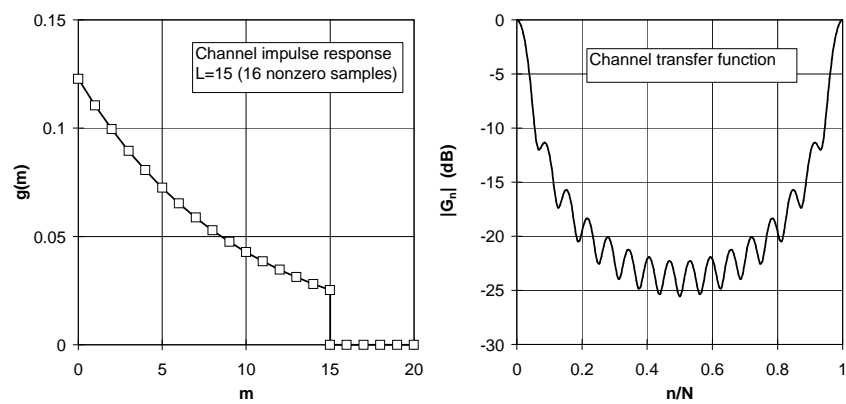
## Multicarrier modulation on dispersive channels

Chapter 8 : Multi-carrier modulation - OFDM

71

## Dispersive channel

Example : channel with  $L = 15$



Chapter 8 : Multi-carrier modulation - OFDM

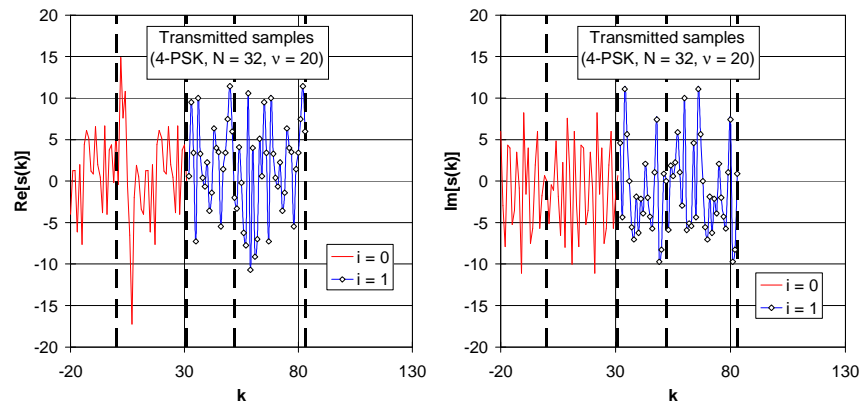
72

## Dispersive channel

Transmitted samples : 2 consecutive blocks ( $i = 0, 1$ ),  $N = 32$ ,  $v = 20 > L$

$i=0$  : CP :  $k = -20, \dots, -1$ ; useful :  $k = 0, \dots, 31$

$i=1$  : CP :  $k = 32, \dots, 51$ ; useful :  $k = 52, \dots, 83$



Chapter 8 : Multi-carrier modulation - OFDM

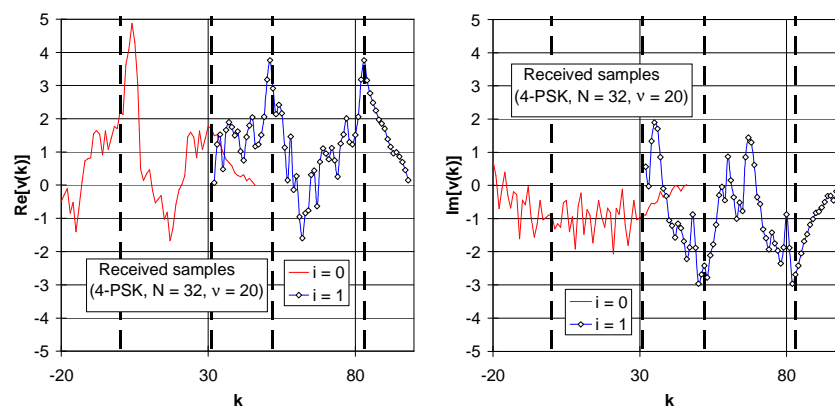
73

## Dispersive channel

Received samples : 2 consecutive blocks ( $i = 0, 1$ )

$i=0$  : CP :  $k = -20, \dots, -1$ ; useful :  $k = 0, \dots, 31$

$i=1$  : CP :  $k = 32, \dots, 51$ ; useful :  $k = 52, \dots, 83$

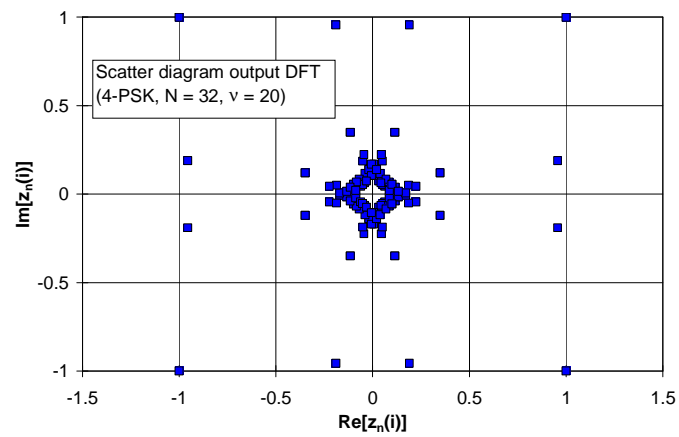


Chapter 8 : Multi-carrier modulation - OFDM

74

## Dispersive channel

Scatter diagram DFT output

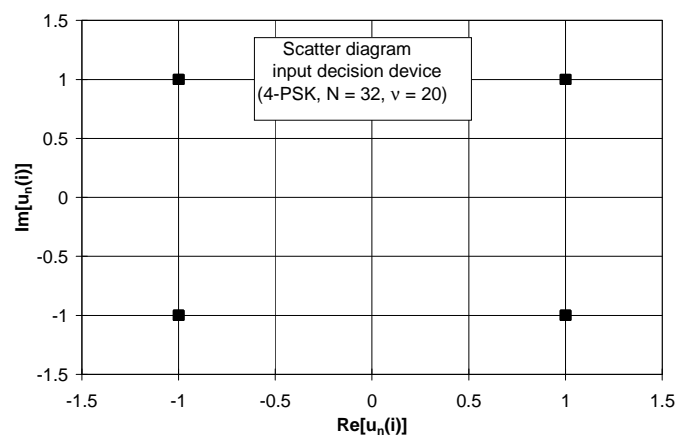


Chapter 8 : Multi-carrier modulation - OFDM

75

## Dispersive channel

Scatter diagram detector input



Chapter 8 : Multi-carrier modulation - OFDM

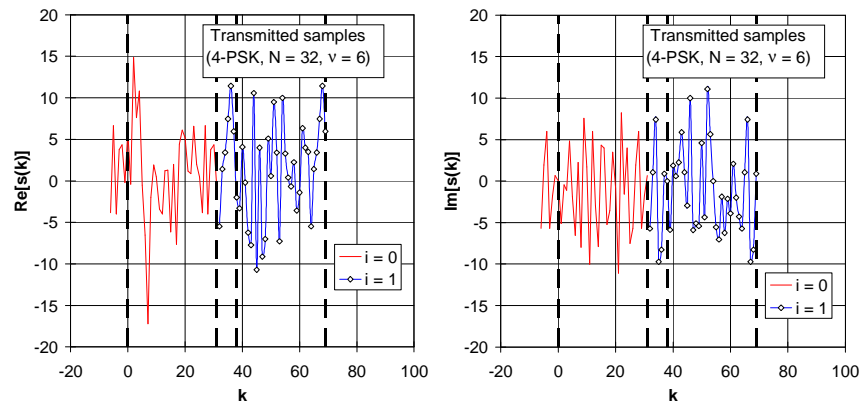
76

## Dispersive channel

Transmitted samples : 2 consecutive blocks ( $i = 0, 1$ ),  $N = 32$ ,  $v = 6 < L$

$i=0$  : CP :  $k = -6, \dots, -1$ ; useful :  $k = 0, \dots, 31$

$i=1$  : CP :  $k = 32, \dots, 37$ ; useful :  $k = 38, \dots, 69$



Chapter 8 : Multi-carrier modulation - OFDM

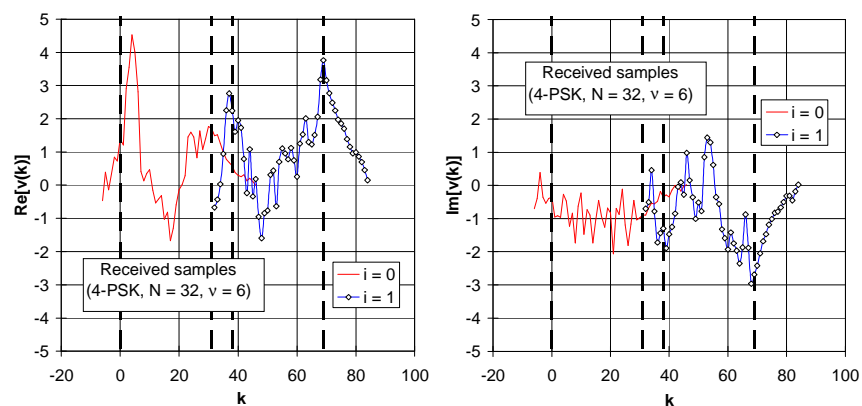
77

## Dispersive channel

Received samples : 2 consecutive blocks ( $i = 0, 1$ )

$i=0$  : CP :  $k = -6, \dots, -1$ ; useful :  $k = 0, \dots, 31$

$i=1$  : CP :  $k = 32, \dots, 37$ ; useful :  $k = 38, \dots, 69$

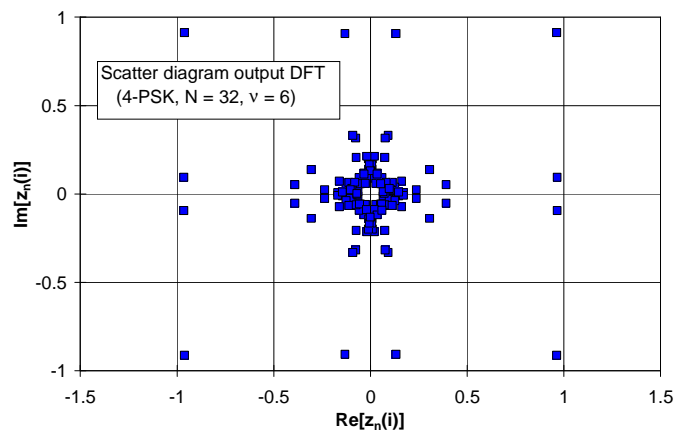


Chapter 8 : Multi-carrier modulation - OFDM

78

## Dispersive channel

Scatter diagram DFT output

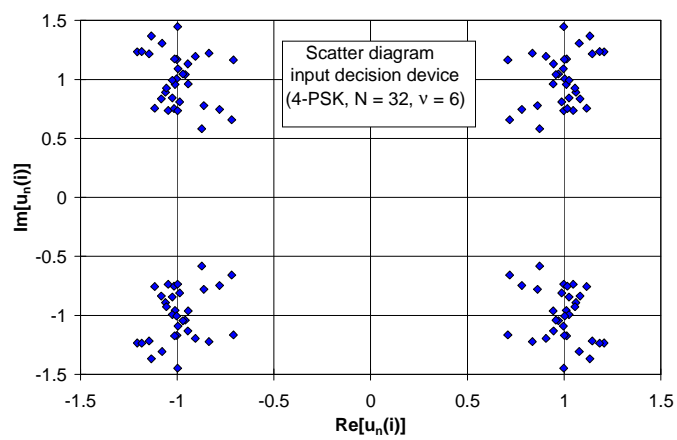


Chapter 8 : Multi-carrier modulation - OFDM

79

## Dispersive channel

Scatter diagram detector input : IBI+ICI



Chapter 8 : Multi-carrier modulation - OFDM

80

## BER on dispersive channel

dispersive channel :  $\text{SNR}_n = \frac{N}{N+\nu} \cdot |G_n|^2 \cdot \frac{E_s}{N_0}$

$$\text{BER}_n = \text{BER}_c \left( \frac{N}{N+\nu} \cdot |G_n|^2 \cdot \frac{E_s}{N_0} \right) \quad (\text{depends on carrier index } n)$$

Average BER (average over all carriers) :

$$\text{BER} = \frac{1}{N} \sum_{n=0}^{N-1} \text{BER}_n = \frac{1}{N} \sum_{n=0}^{N-1} \text{BER}_c \left( \frac{N}{N+\nu} \cdot |G_n|^2 \cdot \frac{E_s}{N_0} \right)$$

BER dominated by carriers with smallest  $|G_n|^2$

## BER on dispersive channel

Example :  $H_{\text{ch}}(f) = A + B \cdot \exp(-j2\pi fT)$  (2-tap channel)

$$\Rightarrow g(0) = A, g(1) = B, g(m) = 0 \text{ for } m \notin \{0,1\}$$

$$|G_n|^2 = |A|^2 + |B|^2 + 2|AB|\cos(2\pi n/N - \theta) : \text{periodic in } n \text{ with period } N$$

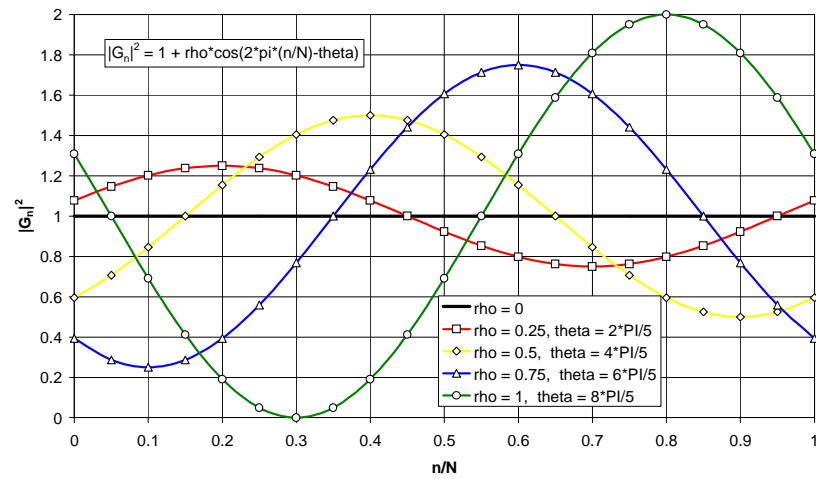
$$\theta = \arg(AB^*)$$

Define :  $\rho = \frac{2|AB|}{|A|^2 + |B|^2} \quad 0 \leq \rho \leq 1$       Normalization :  $A^2 + B^2 = 1$

$$\max |G_n|^2 = 1 + \rho \quad \text{at } n/N = \theta/(2\pi)$$

$$\min |G_n|^2 = 1 - \rho \quad \text{at } n/N = (\theta + \pi)/(2\pi)$$

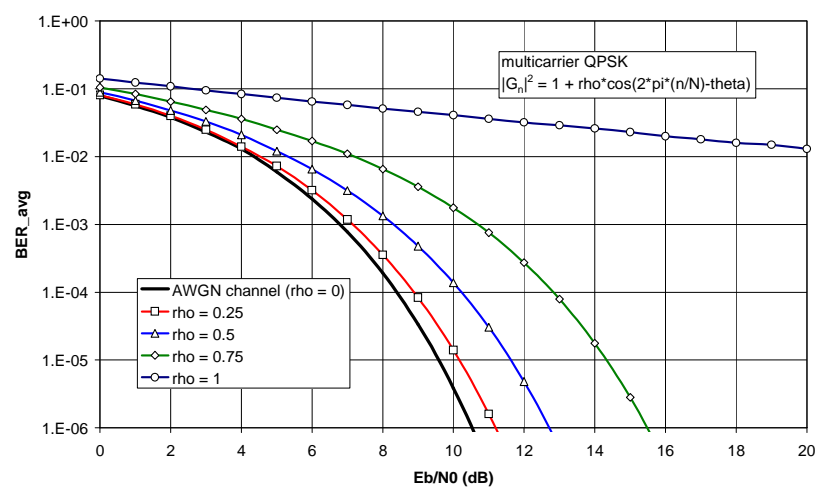
## BER on dispersive channel



Chapter 8 : Multi-carrier modulation - OFDM

83

## BER on dispersive channel

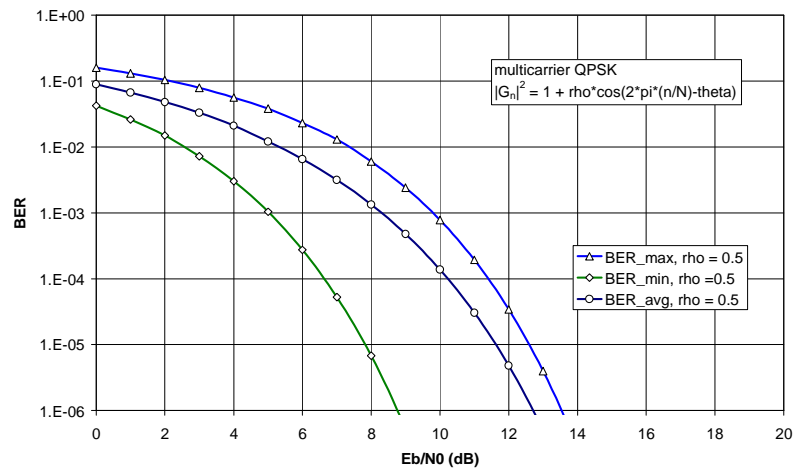


Chapter 8 : Multi-carrier modulation - OFDM

84



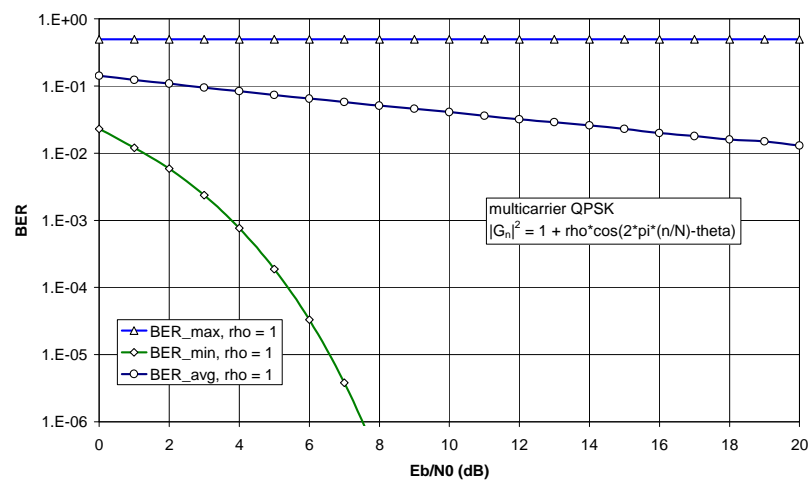
## BER on dispersive channel



Chapter 8 : Multi-carrier modulation - OFDM

85

## BER on dispersive channel



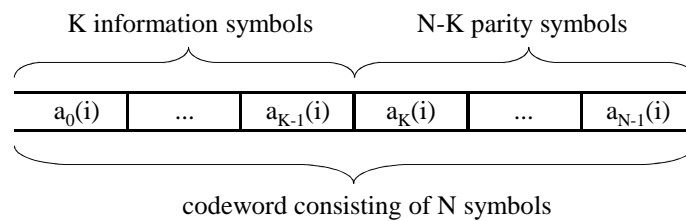
Chapter 8 : Multi-carrier modulation - OFDM

86

## BER on dispersive channel

When for some subcarriers  $|G_n|^2$  is very small, the data transmitted on these subcarriers cannot be reliably detected (high BER), although on other subcarriers the BER can be very small. As a result, the average (over all subcarriers) BER is high.

This problem can be solved by applying **channel coding** for error correction. The symbols belonging to the same codeword are put on different subcarriers : when only a few subcarriers are unreliable, the data on these subcarriers can be recovered from the data on reliable subcarriers.



## Multicarrier modulation on time-varying channels

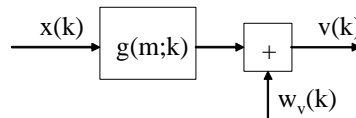
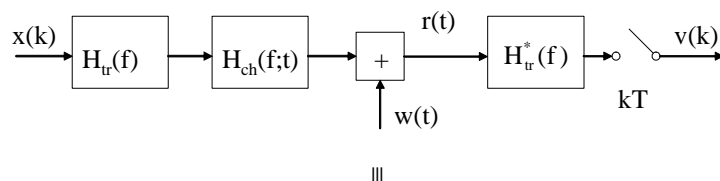
## Time-varying channels

The duration  $\nu T$  of the cyclic prefix (CP) in a multicarrier system is selected to be larger than the duration of the impulse response of the cascade of the transmit filter, channel filter and receive filter, in order to avoid interference between adjacent blocks.

As the receiver does not exploit the signal energy in the CP, useful signal power (and also the bandwidth efficiency) is reduced by a factor  $N/(N+\nu)$ . In principle, this degradation can be made arbitrarily small by taking  $N$  very large, yielding very long blocks of duration  $(N+\nu)T$ .

However, we will show that when the blocks are so long that the channel cannot be considered as time-invariant over one block, intercarrier interference (ICI) arises. To avoid ICI, the duration of a block should be much less than the coherence time of the channel. Equivalently, the subcarrier spacing should be much larger than the channel Doppler spread.

## Time-varying channels



$$g(m;k) = \int |H_{tr}(f)|^2 H_{ch}(f;kT) e^{j2\pi f m T} df \quad w_v(k) \sim N_c(0, N_0 \delta(m))$$

(assuming channel coherence time much larger than matched filter impulse response duration)

## Time-varying channels

$$x(i(N+v)+m) = \frac{1}{\sqrt{N+v}} \sum_{n=0}^{N-1} a_n(i) e^{j2\pi \frac{mn}{N}} \quad m = -v, \dots, N-1$$

$$\Rightarrow v(i(N+v)+m) = \frac{1}{\sqrt{N+v}} \sum_{n=0}^{N-1} a_n(i) G_n(i(N+v)+m) e^{j2\pi \frac{mn}{N}} + w_v(i(N+v)+m)$$

for  $m = 0, \dots, N-1$

$$\text{where } G_n(k) = \sum_{m=0}^L g(m;k) e^{-j2\pi \frac{mn}{N}} = \sum_{\ell} \left| H_u\left(\frac{n}{NT} - \frac{\ell}{T}\right) \right|^2 H_{ch}\left(\frac{n}{NT} - \frac{\ell}{T}; kT\right)$$

## Time-varying channels

$$z_n(i) = \frac{1}{\sqrt{N}} \sum_{m=0}^{N-1} v(i(N+v)+m) \exp(-j2\pi \frac{mn}{N})$$

$$\Rightarrow z_n(i) = \underbrace{\sqrt{\frac{N}{N+v}} a_n(i) A_{n,n}(i)}_{\text{useful}} + \underbrace{\sqrt{\frac{N}{N+v}} \sum_{\substack{n'=0 \\ n' \neq n}}^{N-1} a_{n'}(i) A_{n,n'}(i)}_{\text{ICI}} + \underbrace{w_{z,n}(i)}_{\text{noise}}$$

$$\text{where } A_{n,n'}(i) = \frac{1}{N} \sum_{m=0}^{N-1} G_{n'}(i(N+v)+m) \exp(-j2\pi \frac{(n-n')m}{N})$$

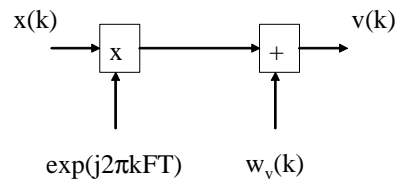
In general,  $A_{n,n'}(i) \neq 0$  for  $n \neq n' \Rightarrow$  **occurrence of ICI**

Time-varying channels affect orthogonality between subcarrier signals

When channel coherence time much larger than block length, we get :

$$\begin{aligned} H_{ch}((i(N+v)+m)T) &= H_{ch}(i(N+v)T) \Rightarrow G_n(i(N+v)+m) = G_n(i(N+v)) \\ m = 0, \dots, N-1 &\Rightarrow A_{n,n'}(i) = G_n(i(N+v)) \delta(n-n') \Rightarrow \text{no ICI} \end{aligned}$$

### Example 1 : carrier frequency offset F



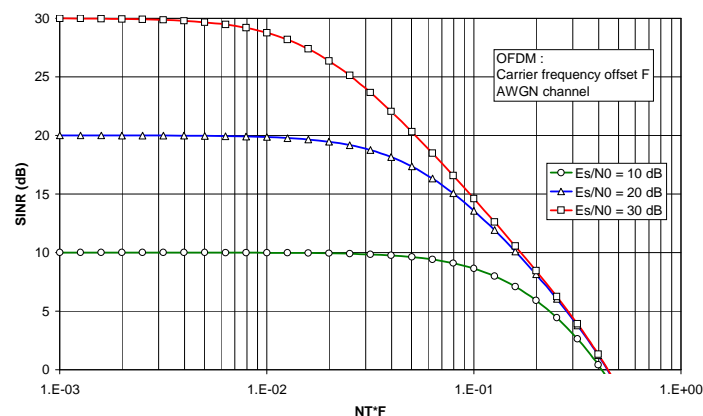
channel impulse response has only one nonzero coefficient :

$$g(m;k) = \delta(m)\exp(j2\pi kFT)$$

$$\Rightarrow G_n(k) = \exp(j2\pi kFT) \quad \text{independent of } n$$

### Example 1 : carrier frequency offset F

carrier frequency offset causes ICI  $\Rightarrow$  degradation of SINR



Frequency offset F should be limited to **small fraction** of subcarrier spacing  $1/(NT)$  to keep reduction of SINR within reasonable limits

## Example 2 : very slow multipath fading

We consider the case of a multipath Rayleigh fading channel.

We assume that fading is **very slow** : the channel coherence time is much larger than the duration of one block. Hence, the channel is static over at least one block.

To simplify computations, the path delay differences are assumed to be multiples of the sampling interval  $T$ .

$$H_{ch}(f; kT) = \sum_{\ell=0}^L c_{\ell}(k) \exp(-j2\pi f \ell T)$$

$$\text{This yields : } G_n(i(N+v) + m) = \sum_{\ell=0}^L c_{\ell}(i(N+v) + m) \exp(-j2\pi \frac{\ell n}{N})$$

$$m = 0, \dots, N-1$$

$$\approx \sum_{\ell=0}^L c_{\ell}(i(N+v)) \exp(-j2\pi \frac{\ell n}{N}) = G_n^{(i)}$$

independent  
of  $m$

$$\Rightarrow z_n(i) = \sqrt{\frac{N}{N+v}} G_n^{(i)} a_n(i) + w_{z,n}(i) \quad \text{no ICI}$$

## Example 2 : very slow multipath fading

$$z_n(i) = \sqrt{\frac{N}{N+v}} G_n^{(i)} a_n(i) + w_{z,n}(i) \quad E[|w_{z,n}(i)|^2] = N_0$$

BER (uncoded 2-PAM, 2-PSK, 4-PSK, 4-QAM) :

$$\text{BER}_n(i) = Q\left(\sqrt{\frac{N}{N+v}} \cdot |G_n^{(i)}|^2 \cdot \frac{2E_b}{N_0}\right) \quad \text{instantaneous BER depends on } (n, i)$$

$c_{\ell}(k)$  and  $c_{\ell'}(k)$  : zero-mean, Gaussian, independent for  $\ell \neq \ell'$ , and  $E[|c_{\ell}(k)|^2] = 2\sigma_{\ell}^2$

$$G_n^{(i)} = \sum_{\ell=0}^L c_{\ell}(i(N+v)) \exp(-j2\pi \frac{\ell n}{N}) \sim N_c(0, 2\sigma^2) \quad \sigma^2 = \sum_{\ell=0}^L \sigma_{\ell}^2$$

statistics of  $G_n^{(i)}$  do not depend on  $(n, i)$

## BER on multipath fading channels

Average BER :

$$E[\text{BER}_n(i)] = E \left[ Q \left( \sqrt{\frac{N}{N+v}} \cdot |G_n^{(i)}|^2 \cdot \frac{2E_b}{N_0} \right) \right]$$

$$\approx \frac{1}{2} \left( 1 + \frac{N}{N+v} \cdot \frac{E_b}{N_0} \right)^{-1}$$

$$G_n^{(i)} \sim N_c(0, 2\sigma^2) \quad (\text{assume } 2\sigma^2 = 1)$$

diversity of (only) order 1

Unlike conventional modulation (+ equalization) or spread-spectrum modulation (+ RAKE filter), multicarrier modulation is **not able to exploit multipath diversity**, because symbol  $a_n(i)$  “sees” a frequency-flat fading channel with complex gain  $G_n^{(i)}$

It is necessary to improve BER performance by means of coding  
or by increasing diversity (frequency diversity, time diversity, antenna diversity)

## Applications

## Applications

Multicarrier modulation (OFDM) is included in various standards :

- Twisted pair telephone line : ADSL, VDSL (“discrete multitone” (DMT))
- Wireless LAN/MAN : IEEE 802.11a/g, WiMAX
- Terrestrial Broadcasting : DAB, DVB-T  
(allows the use of **single-frequency networks**)

## Broadcasting : single-frequency networks

### Conventional broadcasting :

Carrier frequencies used in a geographical area are not reused in adjacent area, in order to avoid interference (similar situation as in cellular radio)

⇒ carrier frequency of given station depends on geographical area

⇒ available bandwidth not efficiently used, complicated frequency planning

### Single-frequency networks :

Carrier frequency of a given station is the **same** in **all** geographical areas.

Interference between transmissions of a same channel is equivalent to multipath, which can be dealt with by taking a sufficiently long CP

⇒ available bandwidth efficiently used, simple frequency planning



## Conclusions

## Conclusions

### Advantages of multicarrier modulation

- The multicarrier signal consists of a (very) large number of subcarriers. Adjacent subcarrier signals overlap in frequency, which yields a high bandwidth efficiency.
- Multicarrier modulation is robust against channel dispersion. Interblock interference (IBI) is avoided by prepending to each block a cyclic prefix (CP) that is longer than the impulse response of the cascade of the transmit filter, channel filter and receive filter. Intercarrier interference (ICI) is avoided by selecting the subcarrier spacing such that the subcarrier signals are orthogonal over the useful part of the block (i.e., after disregarding the CP)
- Efficient implementation makes use of IDFT (transmitter) and DFT (receiver)

## Conclusions

### Drawbacks of multicarrier modulation

- Because of the small bandwidth of a subcarrier signal, each symbol “sees” a frequency-flat channel. Hence, multicarrier modulation cannot exploit multipath diversity. BER performance should be improved by using coding or additional diversity (time, frequency or antenna diversity)
- Time-varying channels (carrier frequency offset, Doppler spread, ...) give rise to ICI. This sets a limit to the block length, which should be much less than the channel coherence time. This limit might be critical in high-mobility scenarios.
- As a large number of subcarrier signals are simultaneously active, the instantaneous power of a multicarrier signal can be much larger than its average signal power (high peak-to-average power ratio). This affects hardware design (A/D and D/A conversion, amplifiers, ...).

## Appendix

### A.1. Definitions related to matrices and vectors

- We make use of bold characters to denote matrices (upper case) and column vectors (lower case). The (generally complex-valued) elements of a matrix  $\mathbf{A}$  are denoted  $(\mathbf{A})_{i,j}$ ,  $A_{i,j}$  or  $A(i,j)$ , where  $i$  and  $j$  refer to the row and column index, respectively; a matrix with  $M$  rows and  $N$  columns has dimension  $M \times N$ . The components of a vector  $\mathbf{v}$  are denoted  $(\mathbf{v})_i$ ,  $v_i$  or  $v(i)$ ; when  $\mathbf{v}$  has  $N$  components, it has dimension  $N$  (a column vector of dimension  $N$  is in fact an  $N \times 1$  matrix). The notations  $A(i,j)$  and  $v(i)$  will be used mainly when  $i$  and  $j$  represent discrete time.
- The transpose of an  $M \times N$  matrix  $\mathbf{A}$  is an  $N \times M$  matrix  $\mathbf{A}^T$ , defined by  $(\mathbf{A}^T)_{i,j} = \mathbf{A}_{j,i}$ . A square matrix  $\mathbf{A}$  is symmetric when  $\mathbf{A}^T = \mathbf{A}$ . Transposing the column vector  $\mathbf{v}$  yields the row vector  $\mathbf{v}^T$ .
- The Hermitian conjugates of  $\mathbf{A}$  and  $\mathbf{v}$  are denoted  $\mathbf{A}^H$  and  $\mathbf{v}^H$ ; the Hermitian conjugate (or complex conjugate transpose) of a matrix  $\mathbf{A}$  or a vector  $\mathbf{v}$  are defined as  $\mathbf{A}^H = (\mathbf{A}^T)^* = (\mathbf{A}^*)^T$ ,  $\mathbf{v}^H = (\mathbf{v}^T)^* = (\mathbf{v}^*)^T$ , with  $(\cdot)^*$  denoting complex conjugate. A square matrix  $\mathbf{A}$  is Hermitian when  $\mathbf{A}^H = \mathbf{A}$ . When  $\mathbf{A}$  or  $\mathbf{v}$  have real-valued elements, their Hermitian conjugate equals their transpose.
- The inverse of a nonsingular square  $N \times N$  matrix  $\mathbf{A}$  is denoted  $\mathbf{A}^{-1}$  :  $\mathbf{A}\mathbf{A}^{-1} = \mathbf{A}^{-1}\mathbf{A} = \mathbf{I}_N$ , with  $\mathbf{I}_N$  representing the  $N \times N$  identity matrix.
- The norm of a vector  $\mathbf{v}$  is a nonnegative number denoted  $|\mathbf{v}|$ , defined through  $|\mathbf{v}|^2 = \mathbf{v}^H \mathbf{v}$ .
- The vectors  $\mathbf{v}_1$  and  $\mathbf{v}_2$  are orthogonal when  $\mathbf{v}_1^H \mathbf{v}_2 = 0$  (evidently, then also  $\mathbf{v}_2^H \mathbf{v}_1 = 0$  holds). Row vectors  $\mathbf{v}_1^T$  and  $\mathbf{v}_2^T$  are orthogonal when the corresponding column vectors  $\mathbf{v}_1$  and  $\mathbf{v}_2$  are orthogonal.
- When  $\mathbf{u}$  has unit norm ( $|\mathbf{u}| = 1$ ), then  $\mathbf{u}^H \mathbf{v}$  denotes the projection of  $\mathbf{v}$  on  $\mathbf{u}$ .
- An  $N \times N$  matrix  $\mathbf{A}$  is unitary, when  $\mathbf{A}^{-1} = \mathbf{A}^H$ . In this case we have  $\mathbf{A}\mathbf{A}^H = \mathbf{A}^H \mathbf{A} = \mathbf{I}_N$ . The equality  $\mathbf{A}^H \mathbf{A} = \mathbf{I}_N$  indicates that the columns of  $\mathbf{A}$  are orthogonal and have unit norm. Hence, the columns of  $\mathbf{A}$  form an orthonormal basis for the  $N$ -dimensional vector space. Any  $N$ -dimensional column vector  $\mathbf{v}$  can be uniquely decomposed as a linear combination of the columns of  $\mathbf{A}$ , with coefficients equal to the projections of  $\mathbf{v}$  on the columns of  $\mathbf{A}$  :

$$\mathbf{v} = \sum_{n=1}^N (\mathbf{a}_n^H \mathbf{v}) \mathbf{a}_n \quad (\text{A.1-1})$$

where  $\mathbf{a}_n$  is the  $n$ -th column of  $\mathbf{A}$ , and  $\mathbf{a}_n^H \mathbf{v}$  is the projection of  $\mathbf{v}$  on  $\mathbf{a}_n$ . Similarly,  $\mathbf{A} \mathbf{A}^H = \mathbf{I}_N$  indicates that the rows of the unitary matrix  $\mathbf{A}$  are orthogonal. When  $\mathbf{A}$  is real-valued, then  $\mathbf{A}^H = \mathbf{A}^T$ ; when  $\mathbf{A}^{-1} = \mathbf{A}^T$ ,  $\mathbf{A}$  is called an orthogonal matrix. In this case,  $\mathbf{A} \mathbf{A}^T = \mathbf{A}^T \mathbf{A} = \mathbf{I}_N$ , so that the real-valued columns of  $\mathbf{A}$  (and also the real-valued rows of  $\mathbf{A}$ ) form an orthonormal basis for the  $N$ -dimensional space of vectors with real-valued or complex-valued components.

## A.2. Gaussian random variables and processes

When a *real-valued* vector  $\mathbf{x}$  is Gaussian with zero mean and covariance matrix  $\mathbf{R}$ , this will be noted as  $\mathbf{x} \sim N(0, \mathbf{R})$ , where  $E[\mathbf{x}\mathbf{x}^T] = \mathbf{R}$ ; note that  $\mathbf{R}$  is a symmetrical matrix. The pdf  $p(\mathbf{x})$  of  $\mathbf{x}$  is completely determined by  $\mathbf{R}$ . The second-order moments of the individual components of  $\mathbf{x}$  are obtained as  $E[x_m x_n] = (\mathbf{R})_{m,n}$ . The diagonal element  $(\mathbf{R})_{m,m}$  equals the variance  $\sigma_m^2 = E[x_m^2]$  of  $x_m$ . When  $\mathbf{w}$  is a vector of  $K$  zero-mean independent identically distributed (i.i.d.) Gaussian random variables with variance  $\sigma^2$ , we have :  $\mathbf{w} \sim N(0, \sigma^2 \mathbf{I}_K)$ .

A real-valued Gaussian vector  $\mathbf{x}$  with mean  $\boldsymbol{\mu}$  and covariance matrix  $\mathbf{R}$  can be viewed as the sum of a constant  $\boldsymbol{\mu}$  and a zero-mean Gaussian vector with covariance matrix  $\mathbf{R}$ . We write  $\mathbf{x} \sim N(\boldsymbol{\mu}, \mathbf{R})$ . When  $\mathbf{x} \sim N(\boldsymbol{\mu}, \sigma^2 \mathbf{I}_K)$ , the corresponding pdf  $p(\mathbf{x})$  can be written as

$$p(\mathbf{x}) = \prod_{m=1}^K \frac{1}{\sqrt{2\pi}\sigma} \exp\left(-\frac{(x_m - \mu_m)^2}{2\sigma^2}\right) = \left(\frac{1}{\sqrt{2\pi}\sigma}\right)^K \exp\left(-\frac{|\mathbf{x} - \boldsymbol{\mu}|^2}{2\sigma^2}\right) \quad (\text{A.2-1})$$

which depends only on the Euclidean distance  $|\mathbf{x} - \boldsymbol{\mu}|$  between  $\mathbf{x}$  and  $\boldsymbol{\mu}$ .

A linear transformation  $\mathbf{x}_2 = \mathbf{M}\mathbf{x}_1$  of a Gaussian vector  $\mathbf{x}_1$  gives rise to a vector  $\mathbf{x}_2$  that has also a Gaussian distribution. When  $\mathbf{x}_1 \sim N(\boldsymbol{\mu}_1, \mathbf{R}_1)$ , then  $\mathbf{x}_2 \sim N(\boldsymbol{\mu}_2, \mathbf{R}_2)$ , with  $\boldsymbol{\mu}_2 = \mathbf{M}\boldsymbol{\mu}_1$  and  $\mathbf{R}_2 = \mathbf{M}\mathbf{R}_1\mathbf{M}^T$ .

Considering two zero-mean real-valued Gaussian vectors  $\mathbf{x}$  and  $\mathbf{y}$ , we can construct the *complex-valued* zero-mean Gaussian vector  $\mathbf{z} = \mathbf{x} + j\mathbf{y}$ . The pdf  $p(\mathbf{z})$  of  $\mathbf{z}$  is defined as the joint pdf  $p(\mathbf{x}, \mathbf{y})$ , which is completely determined by the covariance matrices  $\mathbf{R}_x = E[\mathbf{x}\mathbf{x}^T]$ ,  $\mathbf{R}_y = E[\mathbf{y}\mathbf{y}^T]$  and  $\mathbf{R}_{x,y} = E[\mathbf{x}\mathbf{y}^T]$ . The covariance matrix  $\mathbf{R}_z$  of  $\mathbf{z}$  is defined as  $\mathbf{R}_z = E[\mathbf{z}\mathbf{z}^H]$ ; note that  $\mathbf{R}_z$  is a Hermitian matrix.

We will restrict our attention to *circular* complex-valued Gaussian vectors :  $\mathbf{z}$  and  $\mathbf{z}' = \mathbf{z} \cdot \exp(j\theta)$  have the same Gaussian distribution, irrespective of  $\theta$ . Let us denote by  $\mathbf{x}' = \mathbf{x} \cdot \cos(\theta) - \mathbf{y} \cdot \sin(\theta)$  and  $\mathbf{y}' = \mathbf{x} \cdot \sin(\theta) + \mathbf{y} \cdot \cos(\theta)$  the real and imaginary parts of  $\mathbf{z}'$ . For the circular property to hold,  $(\mathbf{x}, \mathbf{y})$  and  $(\mathbf{x}', \mathbf{y}')$  must have the same pdf, or, equivalently, they must have

the same covariance matrices. This yields the following conditions, that must hold irrespective of  $\theta$  :

$$\begin{aligned}\mathbf{R}_x &= \mathbf{R}_x \cos^2 \theta + \mathbf{R}_y \sin^2 \theta - (\mathbf{R}_{x,y} + \mathbf{R}_{y,x}) \cos \theta \sin \theta \\ \mathbf{R}_y &= \mathbf{R}_x \sin^2 \theta + \mathbf{R}_y \cos^2 \theta + (\mathbf{R}_{x,y} + \mathbf{R}_{y,x}) \cos \theta \sin \theta \\ \mathbf{R}_{x,y} &= (\mathbf{R}_x - \mathbf{R}_y) \cos \theta \sin \theta + \mathbf{R}_{x,y} \cos^2 \theta - \mathbf{R}_{y,x} \sin^2 \theta\end{aligned}\tag{A.2-2}$$

The equations (A.2-2) are satisfied only when

$$\mathbf{R}_x = \mathbf{R}_y \quad \mathbf{R}_{x,y} = -\mathbf{R}_{y,x}.\tag{A.2-3}$$

A statement equivalent to (A.2-3) is  $E[\mathbf{z}\mathbf{z}^T] = \mathbf{0}$ . Indeed,

$$E[\mathbf{z}\mathbf{z}^T] = E[(\mathbf{x} + j\mathbf{y})(\mathbf{x} + j\mathbf{y})^T] = (\mathbf{R}_x - \mathbf{R}_y) + j(\mathbf{R}_{x,y} + \mathbf{R}_{y,x}) = \mathbf{0}\tag{A.2-4}$$

When the circularity condition (A.2-3) holds, the covariance matrix of  $\mathbf{z}$  reduces to

$$\mathbf{R}_z = E[\mathbf{z}\mathbf{z}^H] = E[(\mathbf{x} + j\mathbf{y})(\mathbf{x} - j\mathbf{y})^T] = (\mathbf{R}_x + \mathbf{R}_y) - j(\mathbf{R}_{x,y} - \mathbf{R}_{y,x}) = 2(\mathbf{R}_x - j\mathbf{R}_{x,y})\tag{A.2-5}$$

We write  $\mathbf{z} \sim N_c(0, \mathbf{R}_z)$ , where the subscript C refers to circularity. Taking (A.2-3) into account, the covariance matrices of  $\mathbf{x}$  and  $\mathbf{y}$  can easily be computed from  $\mathbf{R}_z$  :

$$\mathbf{R}_x = \mathbf{R}_y = \text{Re}[\mathbf{R}_z]/2 \quad \mathbf{R}_{x,y} = -\text{Im}[\mathbf{R}_z]/2.\tag{A.2-6}$$

Taking into account that the diagonal elements of  $\mathbf{R}_z$  are real-valued because  $\mathbf{R}_z$  is Hermitian, we obtain from (A.2-6) :

$$(\mathbf{R}_x)_{mm} = (\mathbf{R}_y)_{mm} = (\mathbf{R}_z)_{mm}/2 \quad (\mathbf{R}_{x,y})_{mm} = 0.\tag{A.2-7}$$

Hence, for given  $m$ , the real and imaginary parts  $x_m$  and  $y_m$  are i.i.d. zero-mean Gaussian with variance  $E[|z_m|^2]/2$ .

When  $\mathbf{w} = \mathbf{w}_R + j\mathbf{w}_I$  where  $\mathbf{w}_R$  and  $\mathbf{w}_I$  are statistically independent with  $\mathbf{w}_R \sim N(0, \sigma^2 \mathbf{I}_K)$  and  $\mathbf{w}_I \sim N(0, \sigma^2 \mathbf{I}_K)$ , we have :  $\mathbf{w} \sim N_c(0, 2\sigma^2 \mathbf{I}_K)$

A complex-valued circular Gaussian vector  $\mathbf{z}$  with mean  $\boldsymbol{\mu}$  and covariance matrix  $\mathbf{R}$  can be viewed as the sum of a constant  $\boldsymbol{\mu}$  and a zero-mean circular Gaussian vector with covariance matrix  $\mathbf{R}$ . We write  $\mathbf{z} \sim N_c(\boldsymbol{\mu}, \mathbf{R})$ . The vectors  $\mathbf{z} - \boldsymbol{\mu}$  and  $(\mathbf{z} - \boldsymbol{\mu})\exp(j\theta)$  have the same statistics, irrespective of  $\theta$ . When  $\mathbf{z} \sim N_c(\boldsymbol{\mu}, 2\sigma^2 \mathbf{I}_K)$  with  $\boldsymbol{\mu} = \boldsymbol{\mu}_R + j\boldsymbol{\mu}_I$ , the corresponding pdf  $p(\mathbf{z})$  is given by

$$\begin{aligned}p(\mathbf{z}) &= p(\mathbf{x}, \mathbf{y}) = \left(\frac{1}{\sqrt{2\pi}\sigma}\right)^{2K} \exp\left(\frac{-|\mathbf{x} - \boldsymbol{\mu}_x|^2}{2\sigma^2}\right) \exp\left(\frac{-|\mathbf{y} - \boldsymbol{\mu}_y|^2}{2\sigma^2}\right) \\ &= \left(\frac{1}{2\pi\sigma^2}\right)^K \exp\left(\frac{-|\mathbf{z} - \boldsymbol{\mu}|^2}{2\sigma^2}\right)\end{aligned}\tag{A.2-8}$$

which depends only on the Euclidean distance  $|\mathbf{z} - \boldsymbol{\mu}|$  between  $\mathbf{z}$  and  $\boldsymbol{\mu}$ .

When applying a linear transformation to a zero-mean circular Gaussian vector, the circular property is preserved. Indeed, defining  $\mathbf{z}_2 = \mathbf{M}\mathbf{z}_1$  with  $\mathbf{z}_1 \sim N_c(0, \mathbf{R}_1)$ , we obtain

$$\mathbf{E}[\mathbf{z}_2 \mathbf{z}_2^T] = \mathbf{M} \mathbf{E}[\mathbf{z}_1 \mathbf{z}_1^T] \mathbf{M}^T = \mathbf{0} \quad (\text{A.2-9})$$

$$\mathbf{R}_2 = \mathbf{E}[\mathbf{z}_2 \mathbf{z}_2^H] = \mathbf{M} \mathbf{E}[\mathbf{z}_1 \mathbf{z}_1^H] \mathbf{M}^H = \mathbf{M} \mathbf{R}_1 \mathbf{M}^H \quad (\text{A.2-10})$$

When  $\mathbf{z}_1 \sim N_c(\boldsymbol{\mu}_1, \mathbf{R}_1)$ , then  $\mathbf{z}_2 = \mathbf{M} \mathbf{z}_1$  yields  $\mathbf{z}_2 \sim N_c(\boldsymbol{\mu}_2, \mathbf{R}_2)$ , with  $\boldsymbol{\mu}_2 = \mathbf{M} \boldsymbol{\mu}_1$  and  $\mathbf{R}_2 = \mathbf{M} \mathbf{R}_1 \mathbf{M}^H$ .

The above notation related to vectors of Gaussian random variables can be straightforwardly extended to discrete-time and continuous-time Gaussian processes. First we consider discrete-time processes.

- For a real-valued Gaussian discrete-time process with mean  $\mathbf{E}[x(k)] = \mu(k)$  and covariance function  $\mathbf{E}[(x(k) - \mu(k))(x(k+m) - \mu(k+m))] = R(m, k)$  we write  $\{x(k)\} \sim N(\mu(k), R(m, k))$ . For a zero-mean real-valued stationary Gaussian white-noise process  $\{w(k)\}$  with variance  $\sigma^2$ , we write  $\{w(k)\} \sim N(0, \sigma^2 \delta(m))$ .
- Consider two real-valued discrete-time Gaussian processes  $\{x(k)\} \sim N(\mu_x(k), R_x(m, k))$  and  $\{y(k)\} \sim N(\mu_y(k), R_y(m, k))$ . When  $R_x(m, k) = R_y(m, k)$  and  $R_{x,y}(m, k) = -R_{x,y}(m, k)$ , the process  $\{z(k)\}$ , defined as  $z(k) = x(k) + jy(k)$ , is circular and Gaussian :  $\{z(k)\} \sim N_c(\mu(k), R(m, k))$ , with  $\mu(k) = \mathbf{E}[z(k)]$  and  $R(m, k) = \mathbf{E}[(x(k+m) - \mu(k+m))(x(k) - \mu(k))^*]$ . The moments  $\mu(k)$  and  $R(m, k)$  are given by  $\mu(k) = \mu_x(k) + j\mu_y(k)$  and  $R(m, k) = 2R_x(m, k) - 2jR_{x,y}(m, k)$ . For a zero-mean complex-valued circular stationary Gaussian white-noise process  $\{w(k)\}$ , we write  $\{w(k)\} \sim N_c(0, 2\sigma^2 \delta(m))$ , with  $\sigma^2$  equal to the variance of the real and imaginary parts of  $w(k)$ .

The same applies to continuous-time processes, with the discrete-time indices  $(k, m)$  replaced by continuous-time instants  $(t, u)$ . For a zero-mean real-valued stationary Gaussian white-noise process  $w(t)$  with power spectral density  $N_0/2$ , we write  $w(t) \sim N(0, (N_0/2)\delta(u))$ . The notation  $w(t) \sim N_c(0, N_0\delta(u))$  refers to a zero-mean complex-valued circular stationary Gaussian white-noise process, with the power spectral density of the real part and imaginary part of  $w(t)$  equal to  $N_0/2$ .

As for circular Gaussian vectors, it can be shown that a linear filtering operation on a discrete-time or continuous-time circular Gaussian process yields again a circular Gaussian process.

### A.3. Dimensionality of complex baseband signals that are essentially time- and frequency-limited

Let us consider complex-valued signals  $x_k(t)$  of finite duration  $T_0$ , that are zero for  $t$  outside the interval  $(t_0, t_0+T_0)$ . Such signals can be represented as a Fourier series :

$$x_k(t) = \sum_m X_{k,m} \psi_m(t) \quad t \in (t_0, t_0+T_0) \quad (\text{A.3-1})$$

where the complex-valued functions  $\psi_m(t)$  are defined on the interval  $(t_0, t_0+T_0)$  :

$$\psi_m(t) = \sqrt{\frac{1}{T_0}} \exp\left(\frac{j2\pi mt}{T_0}\right) \quad (\text{A.3-2})$$

and the Fourier coefficients are given by

$$X_{k,m} = \int_{t_0}^{t_0+T_0} x_k(t) \psi_m^*(t) dt \quad (\text{A.3-3})$$

It is easily verified that the functions  $\psi_m(t)$  form an orthonormal basis :

$$\int_{t_0}^{t_0+T_0} \psi_m(t) \psi_n^*(t) dt = \delta_{m-n} \quad (\text{A.3-4})$$

When the summation in (A.3-1) consists of  $D$  terms, the dimensionality of the corresponding signal space equals  $D$  : the maximum number of *linearly independent* functions  $x_k(t)$  that can be constructed as a linear combination of  $D$  orthonormal basis functions  $\psi_m(t)$  is equal to  $D$ .

Let us compute  $|\Psi_m(f)|^2$ , with  $\Psi_m(f)$  denoting the FT of  $\psi_m(t)$  :

$$|\Psi_m(f)|^2 = T_0 \left( \frac{\sin(\pi(fT_0 - m))}{\pi(fT_0 - m)} \right)^2 = |\Psi_0(f - \frac{m}{T_0})|^2 \quad (\text{A.3-5})$$

Keeping  $f_m = m/T_0$  fixed, the frequency components of  $\psi_m(t)$  become concentrated near  $f = f_m$  when  $T_0$  increases (see Fig. A-1).

We now consider the case where the summation index  $m$  in (A.3-1) ranges from  $-m_0$  to  $m_0$ . We define  $B = m_0/T_0$ . When  $2BT_0 \gg 1$ , the corresponding functions  $x_k(t)$  are essentially bandlimited to the frequency interval  $(-B, B)$ , and the number of terms in (A.3-1) is given by  $D = 2BT_0$ . Hence, the dimensionality  $D$  of the signal space, consisting of complex baseband signals that are essentially limited in time (duration  $T_0$ ) and frequency (bandwidth  $B$ ) is given by  $D = 2BT_0$ .

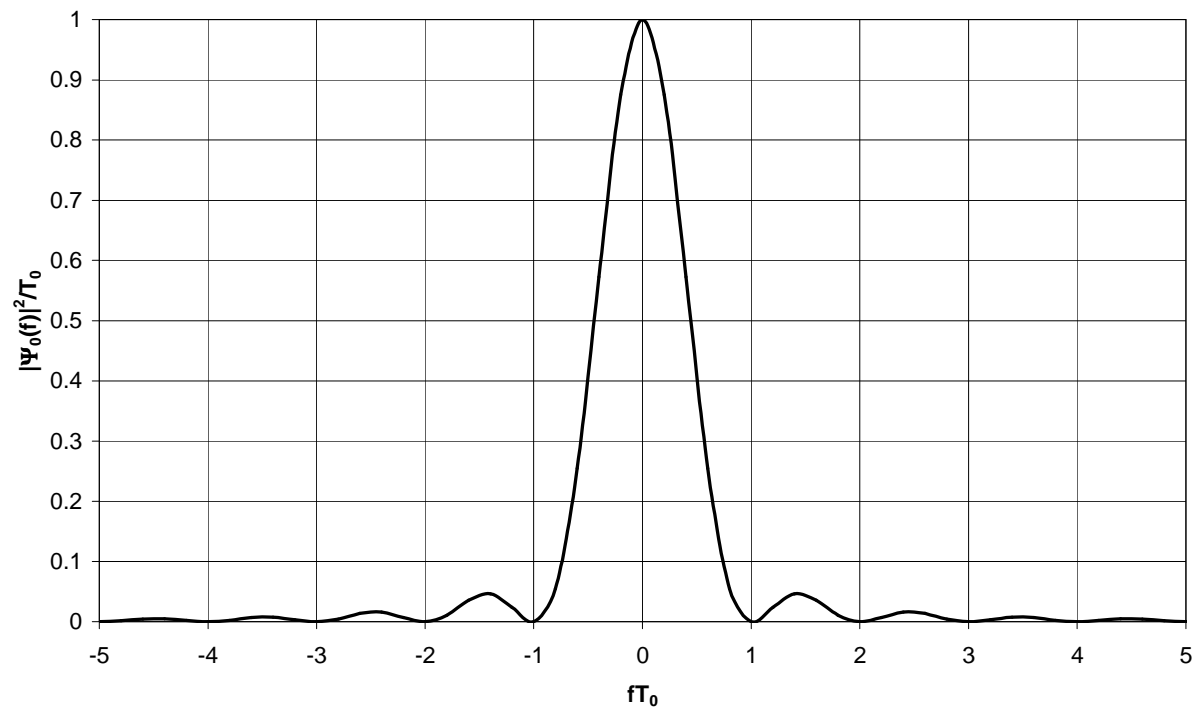


Fig. A-1 : shape of  $|\Psi_0(f)|^2$